TRANSPORTATION RESEARCH

RECORD

No. 1454

Materials and Construction

Asphalt Concrete Mixture Design and Performance

A peer-reviewed publication of the Transportation Research Board

TRANSPORTATION RESEARCH BOARD
NATIONAL RESEARCH COUNCIL

NATIONAL ACADEMY PRESS
WASHINGTON, D.C. 1994

Transportation Research Record 1454
ISSN 0361-1981
ISBN 0-309-06062-1
Price: $45.00

Subscriber Category
IIIB materials and construction

Printed in the United States of America

Sponsorship of Transportation Research Record 1454

GROUP 2—DESIGN AND CONSTRUCTION OF TRANSPORTATION FACILITIES
Chairman: Charles T. Edson, Greenman Pederson, Inc.

Bituminous Section
Chairman: Harold R. Paul, Louisiana Transportation Research Center

Committee on Characteristics of Bituminous-Aggregate Combinations To Meet Surface Requirements
Chairman: Rebecca S. McDaniel, Indiana Department of Transportation
John F. Adam, Imadi L. Al-Qadi, Alan C. Brooker, Yves Brosseaud, Samuel H. Carpenter, Benjamin Colucci, John A. D'Angelo, John J. Emery, Cindy K. Estakhri, Dimitrios Goulias, Dennis C. Jackson, Prithvi S. Kandhal, Paul E. Krugler, Dah-Yinn Lee, Dale B. Mellott, James S. Moulthrop, James A. Scherocman, Ali A. Selim, Anne Stonex, Mary Stroup-Gardiner, Nader Tabatabaee, Kai K. Tam, H. Fred Waller, Jr., Donald E. Watson, Jia Yu, Ludo Zanzotto

Committee on Characteristics of Bituminous Paving Mixtures To Meet Structural Requirements
Chairman: Dallas N. Little, Texas A&M University
Secretary: Robert N. Jester
Benjamin Colucci, Dale S. Decker, Jim Gee, R. G. Hicks, Richard J. Holmgreen, Jr., Darrel V. Holmquist, Vincent C. Janoo, Rudolf A. Jimenez, Y. Richard Kim, Kang-Won Wayne Lee, Jean-Marie Machet, Kamyar Mahboub, Michael S. Mamlouk, Harold R. Paul, R. D. Pavlovich, Reynaldo Roque, Anthony Frederick Stock, Walter J. Tappeiner, Ronald L. Terrel, Bernard A. Vallerga, Harold L. Von Quintus, James P. Walter, Gary C. Whited, John S. Youtcheff

Transportation Research Board Staff
Robert E. Spicher, Director, Technical Activities
Frederick D. Hejl, Engineer of Materials and Construction
Nancy A. Ackerman, Director, Reports and Editorial Services
Marianna Rigamer, Oversight Editor

Sponsorship is indicated by a footnote at the end of each paper. The organizational units, officers, and members are as of December 31, 1993.

Transportation Research Record 1454

Contents

Foreword

The papers in this volume deal with various facets of asphalt concrete mixtures and should be of interest to state and local engineers who are responsible for construction, design, materials, maintenance, or research as well as to contractors and material producers.

Mercer et al. report the results of a series of road trials to evaluate two French thin-surfacing materials (SAFEPAVE and UL-M) that are proposed for use in the United Kingdom. Estakhri and Button report on the initial field performance of a French ultrathin friction course (NOVACHIP) on two highways in Texas. Litzka et al. discuss experiences with thin bituminous layers in Austria; they point out that one of the principal applications to date has been the filling of ruts in concrete surfaces caused by studded tires. Reed reports on the 7-year performance of single-pass, thin-lift bituminous concrete overlays on rural highways in Illinois. She reports that the overlays are a cost-effective method for reducing the number of highway kilometers needing rehabilitation.

Fwa and Ong describe a study conducted in Singapore that examines the effects of using granite aggregates with initial absorbed moisture on the performance of asphalt mixtures. Kandhal presents a state-of-the-art report on the field and laboratory investigation of stripping in asphalt pavements.

Stuart and Malmquist report on a study that evaluates the effects of using different stabilizers in a stone matrix asphalt mix on draindown, rutting, low-temperature cracking, and aging. Mogawer and Stuart describe a study to compare the performance of stone matrix asphalt pavements to dense-graded mixture pavements. The two types of pavements were compared in terms of their resistance to rutting, moisture damage, low-temperature cracking, and aging.

Aschenbrener compares the rutting prediction capabilities of the French Laboratoire Central des Ponts et Chaussées (LCPC) rutting tester with various pavements of known field performance in Colorado. He states that the results from the LCPC rutting tester had excellent correlation with actual rutting depths when temperature and traffic levels were considered. Mohamed and Yue present the results of an investigation conducted in Canada aimed at developing a criterion for rutting potential using the repetitive uniaxial compression test. Kim et al. describe a study to evaluate the effect of moisture on low-temperature asphalt mixture properties and thermal cracking performance of asphalt pavements. Kim et al. report on their study that focused on microcrack healing of asphalt concrete. They present laboratory and field experimental approaches to evaluate this mechanism.

Deacon et al. discuss their study to develop and demonstrate techniques for incorporating the effects of in situ temperature in the Strategic Highway Research Program (SHRP) mixture design process without adding significantly to the complexity of testing and analysis. Harvey et al. describe their investigation of the effects of different laboratory compaction devices (rolling wheel, gyratory, and kneading) on aggregate orientation, air voids, and repetitive simple shear test results. Harvey et al. present the results of an evaluation of fatigue and permanent deformation properties of stone matrix asphalt, recycled asphalt pavement, asphalt-rubber concrete, and large stone gradation asphalt concrete, as well as conventional asphalt-concrete mixes, using the equipment and analysis procedures developed by the SHRP A-003A contract. Hanson et al. report on the first phase of a study to evaluate the process of densification in hot mix asphalt pavements and its effect on laboratory properties. They discuss the changes in properties of hot mix asphalt with time on the basis of analyses of data collected from 5-year-old pavements. Blankenship et al. present a rational method for laboratory compaction of hot mix asphalt developed as a part of the SHRP A-001 contract. McRae provides a discussion of the paper, which is followed by a closure by the authors. Sousa et al. discuss the first application of SHRP asphalt mix performance-based specifications based on results of fatigue tests and repetitive simple shear tests at constant height. Buttlar and Roque report the development and evaluation of the SHRP measurement and analysis system for indirect tensile testing at low temperatures. The system has been incorporated into the SUPERPAVE software.

Kamel and Miller present the results of a comprehensive laboratory comparison of asphalt pavement mixes containing conventional and engineered paving binders. Zhou et al. present a comprehensive

evaluation of the materials and their field performance up to June 1993 used on an Oregon Department of Transportation research study to evaluate three polymer-modified asphalts. Button et al. discuss the results of a study to determine which of four laboratory compaction methods—Exxon rolling wheel, Texas gyratory, rotating base Marshall hammer, and the ELF linear kneading compactor—most nearly simulate field compaction. The authors conclude that from an overall statistical standpoint, it cannot be stated with confidence that any one compaction method more closely simulated field compaction.

Thin Surfacing Material Trials in the United Kingdom

JOHN MERCER, J. CLIFFORD NICHOLLS, AND JOHN F. POTTER

Thin surfacings have been developed in France that are considered a cross between conventional thin-wearing course surfaces and thick surface dressings. Two of these materials, Safepave (or Euroduit) and UL-M, are now being offered in the United Kingdom. A series of road trials are under way to assess their benefits and any possible negative aspects. The trials have two main objectives: to compare the performance of these thin surfacings with existing materials of known performance and to assess their effectiveness as resurfacing materials. To compare their performance, the first aim, the surfacings were laid in sections alongside sections of rolled asphalt wearing course, racked-in surface dressing, and slurry surfacing. To assess their effectiveness, the second aim, Safepave was laid over concrete highways using different treatments at the joints to delay reflective cracking. Trials were conducted on various types of road, including a motorway, major-trunk dual carriageway, rural-trunk and urban dual carriageway. Measurements made on the surfacings included visual assessment, skid resistance (Sideway-force Coefficient Routine Investigation Machine and rake-force trailer), texture depth (sand patch and sensor-measured), rutting, longitudinal profile, and noise. Use of thin surfacings in the United Kingdom is discussed and results of the trials to date are reported. Usefulness of these materials, as well as the conditions under which they should prove effective compared with other currently available materials surfacing is also considered.

As the volume and loading of road traffic has risen and the disruption costs of making repairs has increased, new surfacing materials are being developed in many parts of the world that enable roads to remain maintenance free longer or that can be applied to roads in a manner that minimizes traffic disruption. New materials include thin surfacings, several of which have been developed and approved in France through the Avis Technique system. Some of France's thin surfacings are being brought to the United Kingdom through licensing agreements with U.K. contractors.

Thin surfacings are classified as a single layer of material, laid and compacted using paving machines and rollers. Such surfacings are considered a cross between thin wearing courses and thick surface dressings. Their typical thicknesses range between 15 mm and 30 mm, and it is possible to apply greater thicknesses in localized areas. The advantages to using thin surfacings are that they provide the appropriate level of skid resistance and also regulate the profile (to a limited extent) while minimizing the loss of headroom at overbridges and the need to raise ironwork. As with veneer surfacings, such as surface dressing and slurry seals, thin surfacings should be used only where supporting pavement is structurally adequate. The surfacings have all the advantages of a surface dressing, without the disadvantage of the after-care service that is required for surface dressing. They also are able to make uneven surfaces regular and can be laid under weather conditions that surface dressing cannot.

J. Mercer, Highways Engineering Division, Department of Transport, St. Christopher House, Southwark Street, London, SE1 0TE, United Kingdom; J. C. Nicholls and J. F. Potter, Transport Research Laboratory, Old Wokingham Road, Crowthorne, Berkshire RG11 6AU, United Kingdom.

In France, thin-surfacing systems have been grouped into categories such as very thin surface layers (VTSL) (*1*) and ultra thin hot-mix asphalt layers (UTHMAL) (*1,2*). The thin surfacing systems currently available in the United Kingdom are the UTHMAL Safepave, and the VTSL UL-M. Safepave, the UTHMAL, was introduced first; there are now several U.K. sites where it has been used. Whereas UL-M, the VTSL, a later import, may have been laid on only one public road in the United Kingdom prior to 1993. Stone mastic asphalt (SMA) (*3*), developed in Germany, can also be laid in thin layers and is shortly to be evaluated for United Kingdom conditions as part of another research project at the Transport Research Laboratory (TRL).

MIX DESIGNS

UTHMAL's sprayed binder is a modified emulsion, containing approximately 70 percent solids, and it is sprayed at a rate of 1 L/m^2. The mixed material specification follows a French design; it is shown for the 10-mm grading in Table 1. The binder used in the mix is 100 penetration-grade bitumen. The aggregates used are of high quality and have a high PSV, in order to provide good skid resistance. The binder content is 4.9 $\pm$ 0.3 percent.

The 10-mm size aggregate for VTSL is in accordance with the U.K. standard BS 63 (Part 2: 1987), and the fine/filler proportion should be within the limits shown in Table 1. The total mix, excluding the binder, should be within the grading envelope also indicated in Table 1. The bitumen is either a 70 pen or 100 pen, modified with an ethylene vinyl acetate, for which the grade and dosage rate were not identified. The binder content is within the range of 4.5 to 7.0 percent, depending on the mix.

TRIAL SITES

Thin surfacings have been laid at six sites; one of jointed concrete and the remaining five with asphalt surfacings. The sites are

- A47 Thorney, Cambridgeshire. An undulating two-lane single carriageway road built over marshy ground with transverse and longitudinal cracking and general deterioration of the original surface. UTHMAL was laid along a 3.6-km length on both sides of the road in September 1991; a racked-in surface dressing had been laid at one end of this section the previous week and rolled asphalt was laid adjacent to the other end about 3 months later during the winter. The surface dressing required remedial work the following season.
- A1 Eaton Socon, Cambridgeshire. Dual two-lane trunk road of jointed concrete with poor ride characteristics and a loss of texture. An overlay of UTHMAL was laid along a 1.2-km length of the

TABLE 1 Aggregate Gradings for 10-mm Nominal Mixes

BS Sieve	Per cent passing		
	UTHMAL Combined aggregate	VTSL Fine aggregate	VTSL Combined aggregate
14 mm	100		100
10 mm	55 - 100		80 - 100
6.3 mm	30 - 65	100	25 - 60
5.0 mm	20 - 55	85 - 100	-
2.36 mm	15 - 45	55 - 100	20 - 40
1.18 mm	10 - 35	40 - 70	15 - 35
600 μm	7 - 30	-	10 - 30
300 μm	5 - 25	15 - 35	7 - 25
75 μm	0 - 15	0 - 20	6 - 13

southbound carriageway in September 1991. The trial also incorporated a proprietary reflective crack reduction treatment and saw-cut-and-seal joint treatments at the joints of the concrete.

- A1033 Hull. Four-lane, single carriageway, heavily trafficked road in poor repair leading to the docks. UTHMAL was laid along a 1.35-km length on all lanes, and a length with slurry surfacing was laid to the east in October 1991.
- A31 Romsey, Hampshire. Two-lane single carriageway the original surface of which had poor texture, with transverse cracking and general deterioration. UTHMAL was laid on both sides of the road for a length of 1.06 km in October 1991.
- A34 Stafford. Dual two-lane urban ring road for which the local authority was interested in potentially noise-reducing surfaces. To evaluate VTSL and UTHMAL's properties, 800 m of the northbound carriageway was surfaced with VTSL and the same distance along the southbound carriageway was surfaced with UTHMAL in September 1992.
- M5, Avon, Dual three-lane motorway whose existing surface-dressing was stripping. UTHMAL was laid on 2.8 km of the southbound carriageway in October 1992. Control sections of rolled asphalt were constructed to compare the rolled asphalt with the UTHMAL.

MONITORING

Unevenness

At Romsey, measurements were made with TRL's High-Speed Survey Vehicle (HSV) on the original surface and repeated immediately after the UTHMAL had been laid; measurements were taken again after various periods of trafficking. The results in Table 2 give average unevenness in terms of 3-m, 10-m and 30-m longitudinal profile variance values. The 3-m variance gives a good indication of overall evenness and ride quality. The initial reading on the new UTHMAL surface appears a little high, probably because of the laser pulses' absorption effect, which sometimes occurs on new, very black surfaces and results in a slight increase in the average variance value. Results clearly show, however, that evenness was significantly improved by applying UTHMAL, and evenness has been maintained at a good standard. The regulating effect of UTHMAL and the improvement in the longitudinal profile after resurfacing at Romsey is illustrated in Figure 1, which shows the 3-m profile on a section of the site.

At Thorney, UTHMAL's regulating ability could be observed during the laying operation, as undulations in the existing surface were effectively filled in. The thickness of the mat being laid varied from 20 to 45 mm in order to accommodate unevenness. The thickness provided a good even finish, in compliance with Department of Transport specifications. The surface regularity measured at the other sites also complied with the specification requirements.

Surface Texture

Initial Texture

Both sand-patch texture depth and sensor measured texture depth measurements were made at Thorney. The latter measurement was made using the Mini-Texture Meter (MTM), at locations on the surface dressing, and on the UTHMAL sections soon after they were laid. The results are shown in Table 3.

At Eaton Socon, the sand-patch texture depth of the UTHMAL measured before the road was reopened to traffic was between 1.20 and 3.83 mm, with a mean value of 2.1 mm in the lane carrying most heavy vehicles, and between 1.32 and 3.25 mm (with a mean value of 2.0 mm) in the overtaking lane.

At Hull, sand-patch measurements were made at 14 locations on UTHMAL, indicating a mean value of 1.5 mm for texture depth. At 10 locations, the slurry-surfacing section's texture depth had a mean value of 3.2 mm. Because roads with the slurry surfacing appeared to lose aggregate as soon as they were opened to traffic, measure-

TABLE 2 HSV Uneveness Measurements at Romsey

Age (months)	Unevenness - Profile variance (mm^2) East b/d			West b/d			Wheel-path rutting (mm) East b/d	West b/d
	3 m	10 m	30 m	3 m	10 m	30 m	Average	Average
Original	1.82	19.94	697.45	1.22	5.93	23.69	-3.5	-2.6
1	1.10	16.50	666.61	0.61	3.51	18.05	-3.4	-1.8
9	0.72	15.62	673.39	0.50	3.31	17.72	-3.9	-2.1
12	0.77	16.05	666.59	0.45	3.31	18.20	-3.5	-2.5
16	0.73	16.04	670.34	0.46	3.35	17.89	-4.8	-3.7

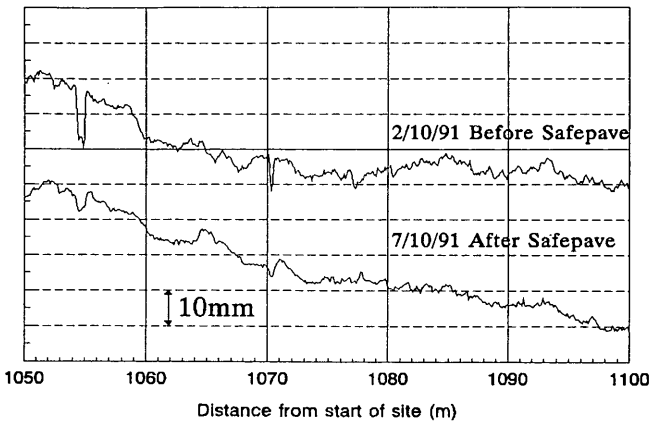

FIGURE 1 Improvement in longitudinal profile at Romsey.

ments were repeated after traffic had been on the surface for 1 hr. The texture depth, after trafficking, had decreased by 35 percent, down to 2.0 mm. However, this still is considered to be a relatively coarse texture.

At Stafford, a set of 10 sand-patch measurements were taken that indicated a mean of 1.4 mm on a 50-m length of VTSL that had not been opened to traffic. Measurements were made again in the inner wheel-track after 7 months of trafficking. By then the texture depth had to decreased slightly—to 1.3 mm.

Maintained Texture

The SMTD on all sites was monitored by the HSV soon after surfacing material had been laid. The absorption effect of the laser pulses was higher on the new UTHMAL surfacing than normally would be expected from conventional rolled asphalt surfacing. As a result, the SMTD for the new surfacing was slightly underestimated (by less than 10 percent). After a surface is trafficked for 3 to 4 months, the absorption effect decreases to levels comparable to those of conventional surfacings and does not affect the measured SMTD value. Results from all sites except Avon are given in Table 4. Average results for each surfacing material tested at Thorney are illustrated in Figure 2. The surface texture of UTHMAL is within current U.K. specification limits when laid but decreases with trafficking, much like surface dressings lose their thickness (Figure 2).

Surface texture is more easily explained for surface dressing, for which design allows embedment of chippings into the substrate. The UTHMAL layer provides less point loads on the existing substrate. Assuming that secondary compaction occurs under traffic, this reduces the texture depth. There is less reduction in texture depth than occurs with surface dressing. The SMTD of UTHMAL decreases about 40 percent during the first year, at which time the compaction appears to be complete. Therefore, the as-laid specification limits may need to be increased to compensate for reduction. The results from Stafford on VTSL are, as yet, insufficient to determine whether a reduction in SMTD occurs. The VTSL was laid on a site which was not classified as a high-speed road and therefore it was not a requirement to have an initial 1.5 mm sand-patch texture depth.

For roads with bituminous surfacings, a texture depth of 1.5 mm is required; whereas for concrete roads, a lower texture depth of 0.65 mm is specified. On the site at Eaton Socon, the original brushed concrete had a lower SMTD, averaging about 0.4 mm. This was improved by the application of UTHMAL, increasing the SMTD to about 1.0 mm. However, the SMTD decreased with time; measured values now approach 0.7 mm, the level of macro-texture for in-service roads (4). The risk of accidents begins to increase significantly on roads with a lower SMTD than that.

Skid-Resistance

The sideway-force coefficient (SFC) of the various surfacings were measured at 50 km/h, using the Sideway-Force Coefficient Routine Investigation Machine (SCRIM). Results from all the sites are given in Table 5, and the mean values for Thorney and Hull shown in Figures 3 and 4.

Skid-resistance of all surfacing materials increases during the first few months, as the binder on the surface is worn off by traffic. The UTHMAL surfaces had the best skid-resistance of all the surfaces for vehicles accelerating at 50 km/h in the comparative trials at Thorney and Hull. On the basis of the Stafford results, the UTHMAL has a marginally higher SFC than does the VTSL.

High-Speed Skid Resistance

In June 1992, a brake-force coefficient (BFC) trailer was used to measure high-speed skid resistance on the Thorney site at two speeds, 50 km/h and 130 km/h. Measurements were taken along a

TABLE 3 Initial Texture Depths at Thorney

	Surface dressing			UTHMAL			
	East b/d		West b/d	East b/d		West b/d	
	Location 1	Location 2	Location 3	Location 4	Location 5	Location 6	Location 7
Sand-patch							
Mean	3.2	3.4	3.0	3.2	1.6	1.5	2.3
Range	2.65-4.21	2.91-4.07	2.76-3.25	1.88-5.77	1.13-2.53	0.93-1.88	1.63-2.95
MTM*							
Mean	1.8	1.7	1.6	-#	0.7#	0.7#	0.9#
Range	1.75-1.76	1.68-1.74	1.59-1.65	0.00-1.10	0.73-0.73	0.70-0.73	0.93-0.96

* = '*Texture - Other Readings*' scale used
\# = Results with high absorption of laser pulses
\- = missing mean resulting from high absorption of laser pulses

TABLE 4 SMTD Results

THORNEY Date	Surface dressing East b/d	Surface dressing West b/d	UTHMAL East b/d	UTHMAL West b/d	Rolled asphalt East b/d	Rolled asphalt West b/d
25/ 9/91	1.98	1.85	1.33	1.13	1.34*	1.10*
8/11/91	1.70	1.51	0.88	0.98	1.30*	1.06*
21/ 7/92	1.28	0.98	0.71	0.75	1.21	1.30
7/10/92	1.22†	0.87†	0.74	0.85	1.44	1.26
20/ 1/93‡	0.99†	0.84†	0.59	0.61	1.04	0.98
9/ 2/93	1.15†	0.90†	0.70	0.76	1.33	1.14
30/ 4/93	1.09†#	0.89†	0.62#	0.88	1.11#	1.21
20/ 7/93	1.07†	0.62†	0.72	0.83	1.24	1.17

EATON SOCON Date	UTHMAL - Southbound S2	S3	S4	S5	S6	S7	S8
25/ 9/91*	0.41	0.40	0.48	0.74	0.42	0.38	0.43
3/10/91	0.88	1.03	0.96	1.18	0.91	0.73	0.78
8/11/91	0.83	0.96	0.85	1.07	0.80	0.68	0.66
20/ 7/92	0.81	0.92	0.92	0.85	0.78	0.60	0.57
8/10/92	0.77	0.88	0.94	0.82	0.76	0.60	0.57
9/ 2/93	0.65	0.75	0.80	0.73	0.70	0.59	0.58

HULL Date	Slurry surfacing East b/d n/s	o/s	West b/d o/s	n/s	UTHMAL East b/d n/s	o/s	West b/d o/s	n/s	Existing rolled asphalt East b/d n/s	o/s	West b/d o/s	n/s
27/ 6/93	0.37	0.55	0.61	0.39	0.91	1.07	1.05	0.87	0.48	0.65	0.48	0.49

ROMSEY Date	UTHMAL Eastbound S1	Eastbound S2	Westbound S3	Westbound S4
2/10/91*	0.90	1.07	0.91	1.14
7/11/91	1.35	1.33	1.10	1.12
17/ 7/92	0.88	0.89	0.78	0.83
8/10/92	0.93	0.91	0.85	0.95
10/ 2/93	0.88	0.86	0.82	0.87

STAFFORD Date	UTHMAL	VTSL
16/ 6/93	0.85#	0.85
12/ 7/93	1.04	0.95

† = after repairs * = prior to resurfacing
‡ = survey with 45° laser angle; other surveys with 60° angle giving 'deeper' readings
# = high absorption of laser pulses, tending to underestimate result

NOTE: Measurements are in millimeters.

70-m length at one location on the rolled asphalt section and at two locations on both the UTHMAL and surface-dressed sections. Three runs of the BFC trailer were made at each speed over the three sections, and a mean value of the BFC was calculated for each measurement location and test speed. The results are given in Table 6.

At Location 1 on the surface dressing section, the measured BFC was low at the higher speed, although there is no obvious explanation. It is possible that the test line at Location 1 might have a lower texture than the test line at Location 2, although this is not reflected by the sand-patch measurements shown in Table 3. Perhaps the line had been contaminated when the new test tire abraded away on an earlier run; however, the operator could not find any evidence of surface contamination.

Measurements of high-speed skid resistance at Thorney indicate that skid resistance drops with speed by slightly more on UTHMAL than on rolled asphalt or surface dressing between 50 km/h and 130 km/h. Nevertheless, the skid resistance at 130 km/h is still greater for the UTHMAL than the rolled asphalt, although not as great as that for the surface dressing (ignoring the result from location 1). Hence, the greater drop in BFC should be noted, although the UTHMAL material is still performing better than the rolled asphalt at these locations, that is, up to a speed above the legal limit for this type of road in the United Kingdom. The change in skid resistance with speed is being measured at other sites, and modifications to the UTHMAL material are being investigated in order to alleviate concerns.

Hydraulic Conductivity

To examine claims that UTHMAL is able to reduce spray on wet roads similarly to porous asphalt, a series of hydraulic conductivity measurements were taken on the material laid at Hull. The values measured implied that UTHMAL possesses a capacity to remove water from the tire/road interface that might reduce spray. To confirm that the measurements reflected this capacity and were not influenced by the surface texture, the corrected outflow times *(5)* at each location were analyzed to see if there were any relationship

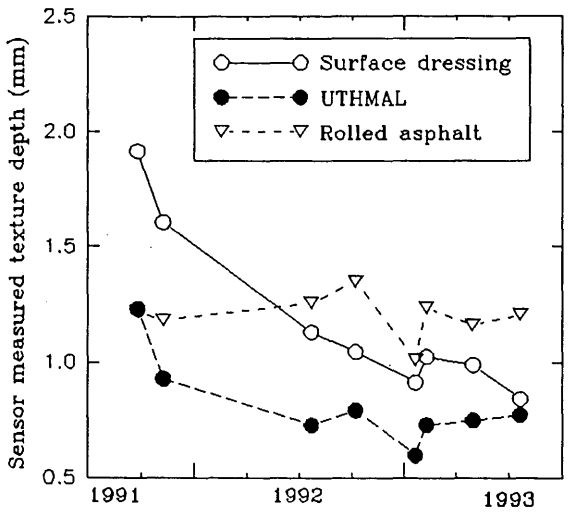

FIGURE 2 SMTD results from Thorney.

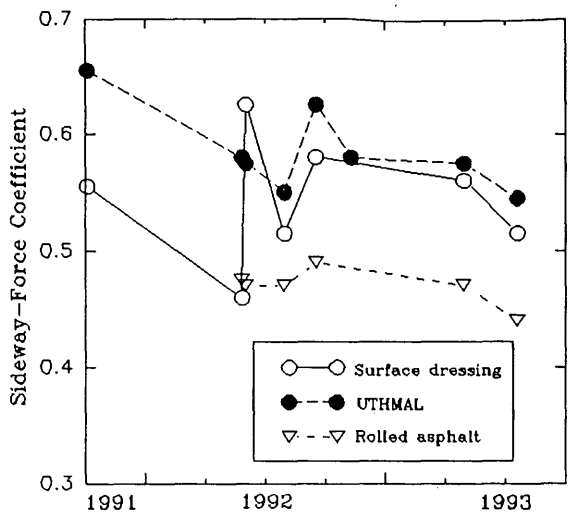

FIGURE 3 SFC results from Thorney.

TABLE 5 SFC Results

THORNEY

Date	Surface dressing East b/d	Surface dressing West b/d	UTHMAL East b/d	UTHMAL West b/d	Rolled asphalt East b/d	Rolled asphalt West b/d
4/10/91	0.55	0.56	0.67	0.64	-	-
27/ 5/92	0.52	0.40	0.60	0.56	0.47	0.48
2/ 6/92	0.65	0.60	0.58	0.57	0.48	0.46
30/ 7/92	0.53	0.50	0.56	0.54	0.48	0.46
18/ 9/92	0.57	0.59	0.65	0.60	0.50	0.48
11/ 2/93	-	-	0.58	0.58	-	-
30/ 4/93	0.57	0.55	0.58	0.57	0.47	0.47
20/ 7/93	0.54	0.49	0.55	0.54	0.44	0.44

EATON SOCON

Date	UTHMAL	Date	UTHMAL	Date	UTHMAL
8/10/91	0.69	6/ 7/92	0.55	10/ 2/93	0.59
1/ 6/92	0.61	7/ 9/92	0.56		

HULL

Date	Slurry surfacing East b/d n/s	Slurry surfacing East b/d o/s	Slurry surfacing West b/d o/s	Slurry surfacing West b/d n/s	UTHMAL East b/d n/s	UTHMAL East b/d o/s	UTHMAL West b/d o/s	UTHMAL West b/d n/s	Existing rolled asphalt East b/d n/s	Existing rolled asphalt East b/d o/s	Existing rolled asphalt West b/d o/s	Existing rolled asphalt West b/d n/s
16/ 7/92	0.39	-	-	0.38	0.53	-	-	0.48	0.39	-	-	0.34
27/ 8/92	0.49	-	-	0.52	0.56	-	-	0.58	0.44	-	-	0.48
16/ 5/93	0.44	0.46	0.47	0.44	0.57	0.57	0.58	0.57	0.41	0.45	0.42	0.37
27/ 6/93	0.41	0.43	0.43	0.38	0.56	0.57	0.57	0.55	0.38	0.45	0.42	0.36

ROMSEY

Date	UTHMAL Eastbound S1	UTHMAL Eastbound S2	Westbound S3	Westbound S4
28/ 5/92	0.57	0.57	0.57	0.57
14/ 7/92	0.63	0.63	0.61	0.64
4/ 9/92	0.62	0.61	0.66	0.69
12/ 2/93	0.58	0.59	0.60	0.60

STAFFORD

Date	UTHMAL	VTSL
16/ 6/93	0.58	0.52
12/ 7/93	0.55	0.51

AVON

Date	Section 1 Surface dressing	Section 2 UTHMAL	Section 3 Surface dressing	Section 3 Rolled asphalt	Section 4 UTHMAL	Section 5 Surface dressing	Section 5 Rolled asphalt
11/11/92	0.48	0.61	0.47	n/a	0.60	0.49	n/a
5/ 3/93	0.44	0.55	n/a	0.51	0.57	n/a	0.52

- = Section not surveyed

n/a = Surface not existing for that survey

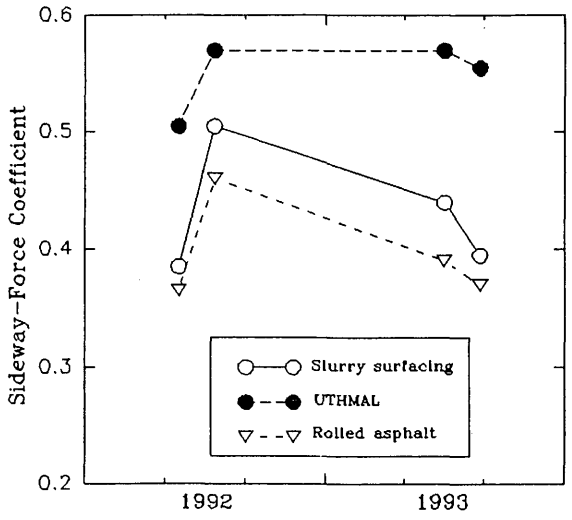

FIGURE 4 SFC results from Hull (north and south lanes).

between outflow time and texture, as indicated by sand-patch measurements.

Regression analysis showed that there was a relationship between texture depth and hydraulic conductivity, with a correlation coefficient of 0.85. The relationship, shown in Figure 5, suggests that water flow between interconnecting surface channels result from high texture levels and that texture is most likely a factor in the measured value of hydraulic conductivity. Locally, however, where the material had been laid thicker to even out the original surface, interconnecting voids within the material might have produced the increased levels of hydraulic conductivity, even though the voids were not sufficiently uniform to describe the material as genuinely porous. Because the basic structure of UTHMAL is a single aggregate layer, any interconnecting voids are likely to be open to the surface for much of their length rather than completely submerged. This assumption is consistent with the relationship found between texture depth and hydraulic conductivity.

Nevertheless, the surface texture and the ability to make it more even should help reduce ponding. Motorists have the perception that UTHMAL is a spray-reducing material. Compared with 20-mm porous asphalt, the hydraulic conductivity of UTHMAL is low, with only one point in Figure 5 attaining the minimum value (0.06 s^{-1}) specified in the U.K. standards for an individual measurement on porous asphalt. At 0.01 s^{-1}, the material can be considered to be closed up. However, if water is able to drain into the UTHMAL surfacing, then there is the likelihood of water being retained in the wheel ruts at the interface with the old underlying road surface, which in time, might cause problems within the new UTHMAL surfacing.

Noise

Vehicle noise was measured using the statistical pass-by method (*6*) on the UTHMAL and rolled asphalt sections at Thorney, and on the UTHMAL and brushed concrete sections at Eaton Socon. Results are given in Table 7.

For a broad range of conventional nonporous road surfaces, the maximum noise level relates to the skidding performance measure, or BFC, derived from the sand-patch texture depth. Recorded values of noise and BFC on the rolled asphalt and UTHMAL surfacings from Thorney lie below the "best-fit" line of the relationship determined from many measurements on conventional bituminous surfacings. The measurements taken at Eaton Socon are closer to the mean line of the relationship.

Although the results indicate that UTHMAL was quieter than either rolled asphalt or concrete surfacings at these sites, the noise levels from the UTHMAL surface were within the expected range for conventional surfaces for the same skid resistance, as derived from texture depth. However, the relationships between texture depth and BFC were derived from surfacings that differ from UTHMAL and so may not be valid.

Use of UTHMAL on Jointed Concrete

To examine ways of minimizing reflective cracking above joints, a number of joint treatments were applied before resurfacing with UTHMAL. The trial used a proprietary rubberized anticracking treatment, as an inlay and an overlay. The saw-cut-and-seal technique was also used. Sealing grooves were sawn in the final running surface directly above the transverse joints in the concrete to control the reflective cracking that resulted from thermal movements of the underlying slabs. For comparison, a length with no joint treatments was included as a control.

Anticracking treatments (ACT) were associated with bleeding through into the UTHMAL. Why the two materials were incompatible is unclear, but the result was that smooth bands appeared in the UTHMAL surface, giving it a patchy appearance—both at the joints and where longitudinal cracks were treated similarly. When used as an overlay treatment, in which the ACT was not recessed into the concrete, the bleed-through was more pronounced, and cracking reappeared in the UTHMAL above the joints in the concrete at both edges of the treatment. The inlay treatment/UTHMAL combination produced a better result, but the surface texture was still poor because of the bleeding. Therefore, this type of ACT is not considered suitable for use with UTHMAL.

TABLE 6 BFC Trailer Results (Thorney)

	Surface dressing		UTHMAL		Rolled
	1	2	1	2	asphalt
50 km/h	55.2	52.3	54.0	52.8	41.3
130 km/h	17.0*	41.0*	36.0	35.0	29.3
ΔBFC #	-	22 %	33 %	32 %	29 %

Drop in BFC from 50 km/h to 130 km/h
* Shredded tire on first run (of three)
- = Result not given as 130 km/h value suspect

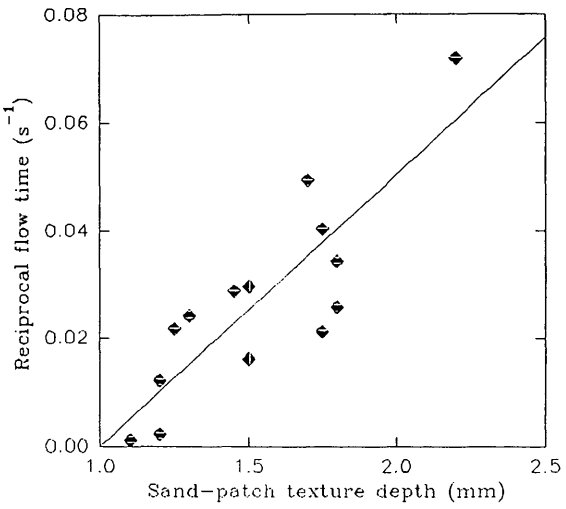

FIGURE 5 Relationship between hydraulic conductivity and texture depth.

On the control section, with no joint treatments, cracks reappeared at all expansion joints but not at contraction joints, indicating that only expansion joints may need to be treated. The majority of the saw-cut-and-seal joints are in very good condition, with seals intact. One or two seals have a fine parallel crack running alongside, probably caused by lack of precision when joint grooves were sawn. Accurate joint location, together with thorough cleansing before application of sealant, should ensure the effectiveness of this technique. Saw-cut-and-seal joints appear to be the best option if jointed concrete is to be resurfaced with UTHMAL.

General Condition

UTHMAL provides a visually acceptable surface when new, including no loose chippings and an even finish of good-riding quality. After the surface is trafficked for a few months, however, secondary compaction in the wheel-paths is noticeable, as is some closing-up of the surface texture, which might be caused by embedment of the aggregate, "fatting-up" of the binder-rich material, or a combination of both. Reasons for the closing up are being investigated.

A certain amount of wheel-path rutting is also evident at each site and, although not severe, is noticeable under wet conditions. Table 2 shows the average depth of rutting at Romsey to be about 2 to 5 mm, as measured by the HSV. However, as well as having an adverse effect on texture and skidding resistance, the combination of compaction/consolidation and wheel-path rutting could cause increased noise and spray.

Visual condition surveys were carried out before the application of UTHMAL and periodically for 16 months. The UTHMAL is generally in good condition at the first 3 sites to be treated and shows good integrity and adhesion, although a little scuffing and loss of material has been caused by vehicles turning at junctions at the Thorney and Hull sites. Where heavy vehicles turned on the control sections at Hull, similar scuffing and loss of aggregate occurred. Elsewhere at these sites, there are only a few localized areas of material loss. Reflective cracking has occurred at Thorney and Romsey where cracks and other defects were not pretreated. At Thorney, the majority of the transverse cracks in the original surface reappeared during the first 12 months, and, at Romsey, the more severe cracks observed in the original surface have now reappeared. This indicates that the behavior of UTHMAL is similar to that of other conventional bituminous materials in terms of minimizing reflective cracking, that is, cracks that would be expected to reappear within a year in an overlay thickness of 20 mm.

At Stafford, the UTHMAL was replaced before it was in service one year, because of of severe fretting. A noticeable loss of material occurred on the M5 Avon motorway site, in some areas, after only 6 months of trafficking. The contractor suggested the deterioration was due to the cold, wet weather conditions at the time the UTHMAL was laid at both sites. Poor bonding to the original surface was thought to be a contributing factor to the deterioration. At the M5 Avon site, the original surface dressing was in poor condition; there was severe stripping in some areas which was the reason for its resurfacing. Removal of this stripped surface dressing before application of UTHMAL, while adding to cost, might have been the better long-term solution.

The limited use of VTSL means that any conclusions about it have to be tentative. Using it to replace the UTHMAL at Stafford illustrates that it has its limitations, as have other materials, demonstrated by the need for repairs on the surface dressing section at Thorney.

COSTS

The cost per square meter of these thin surfacing ranges between £2.30 and £3.50, depending on the site and other local considera-

TABLE 7 Vehicle Noise and Surface Parameters

		THORNEY		EATON SOCON		
		UTHMAL	Rolled asphalt	UTHMAL 1	UTHMAL 2	Brushed concrete
Vehicle Noise* (dB(A))	Light	79.8	81.0	81.1	81.8	82.9
	Heavy	85.5	85.5	85.5	86.2	87.9
SP† (mm)		1.42	2.05	1.37	1.71	0.52
ΔBFC‡ (per cent)		+1.0	-11.6	-12.6	-5.8	-23.2

* Vehicle noise at 7.5 m and vehicle speed of 90 km/h
† Sand-patch texture depth
‡ Estimated change in skidding resistance calculated from:
ΔBFC = (20 x SP - 40)% for bituminous surfacings;
and ΔBFC = (90 x SP - 70)% for concrete surfacings

tions. The average cost for 10-mm of nominal size UTHMAL is about £2.60. For the sake of comparison, a 40-mm-thick layer of rolled asphalt costs between £3.50 and £4.00/m^2, whereas surface dressing can vary from 70p/m^2 for some unmodified single dressings to £3.00/m^2 for some modified racked-in systems.

CONCLUSIONS

The conclusions that can be drawn to date from this study are as follows:

- UTHMAL and VTSL materials are less expensive than conventional rolled asphalt but more expensive than surface dressing. They can be laid at a faster rate than rolled asphalt and do not require the high degree of aftercare needed for conventional surface dressing. Use of the materials is also less disruptive to traffic because the new surface can be put into service soon after it is laid down.
- Surfacings are laid using different application techniques, but no major problems occurred during laying, even when the job was done by contractors who had little experience with UTHMAL materials.
- Although the thin surfacing materials have not been in service for sufficient time to fully assess their durability and hence their life-cycle costs, nevertheless, when new, UTHMAL provides an effective regulating layer, improves evenness, and provides a good surface finish and standard of riding quality. At three of the five sites studied, UTHMAL generally is in good condition after 16 months, except at junctions where turning vehicles have caused scuffing and some loss of material. Poor weather conditions during construction appear to have caused loss of material from the surface during the initial months of trafficking at one site, resulting in the need to replace the new surface.
- Skid resistance, as measured by SCRIM, is good for UTHMAL materials; however, there is some concern about the reduction in skid resistance with increasing speed.
- Initial texture depth of UTHMAL is above the 1.5-mm sand-patch value required for high-speed roads within the United Kingdom, but the SMTD fell by about 40 percent during the first year of trafficking; after that texture depth maintained a steady level. The initial texture depth on the one VTSL test section (not a high-speed location) gave a sand-patch value of 1.4 mm.
- Spray- and noise-reducing properties of UTHMAL are at least as good as those of conventional rolled asphalt and surface-dressing surfacings.
- Where UTHMAL has been used over jointed concrete, the most effective solution for minimizing reflective cracking at transverse joints appears to be the technique of saw-cut-and-seal. However, the degree of success with this method relies on the accurate positioning of the sawn groove above the transverse joint in the concrete slabs. Observations also suggest that saw-cut-and-seal may only be necessary above expansion joints in the concrete and not at construction joints. A combination method, that is, using a proprietary anticrack treatment and UTHMAL for minimizing reflective cracking over concrete joints, was not satisfactory.

ACKNOWLEDGMENTS

The work described in this paper forms part of a Highways Engineering Division funded research program conducted by TRL. The paper is published by permission of the Deputy Secretary, Safety Highways and Traffic of the Department of Transport and the Chief Executive of TRL.

REFERENCES

1. Bellanger, J., Y. Brosseaud, and J. L. Gourdon. Thinner and Thinner Asphalt Layers for Maintenance of French Roads. In *Transportation Research Record 1334*, TRB, National Research Council, Washington, D.C., 1992, pp. 9–11.
2. Serfass, J. P., P. Bense, J. Bonnot, and J. Samanos. New Type of Ultrathin Friction Course. In *Transportation Research Record 1304*, TRB, National Research Council, Washington, D.C., 1992, pp. 66–71.
3. Kast, O. E. Long Term Experience with Splittmastixasphalt in the Federal Republic of Germany. *Proc., Third Eurobitume Symposium*, The Hague, Netherlands, Vol. 1, pp. 174–177.
4. Roe, P. G., D. C. Webster, and G. West. *The Relation Between the Surface Texture of Roads and Accidents.* TRRL Report RR 296. Department of Transport, Transport and Road Research Laboratory, Crowthorne, Berkshire, United Kingdom, 1991.
5. Daines, M. E. *Trials of Porous Asphalt and Rolled Asphalt on the A38 at Burton.* TRRL Report RR 323 Department of Transport. Transport and Road Research Laboratory, Crowthorne, Berkshire, United Kingdom, 1992.
6. Franklin, R. E., D. G. Harland, and P. M. Nelson. *Road Surfaces and Traffic Noise.* TRRL Report LR 896. Department of the Environment and Department of Transport, Transport and Road Research Laboratory, Crowthorne. Berkshire, United Kingdom, 1979.

The views expressed in this publication are not necessarily those of the Department of Transport.

Publication of this paper sponsored by committee on Characteristics of Bituminous-Aggregate Combinations To Meet Surface Requirements.

Evaluation of Ultrathin Friction Course

CINDY K. ESTAKHRI AND JOE W. BUTTON

The French process, NOVACHIP, sometimes known as ultrathin friction course, is a new technology in the United States. NOVACHIP was successfully constructed on two highways in the San Antonio District of Texas. A research study was conducted by the FHWA, in cooperation with the Texas Department of Transportation to evaluate and document the NOVACHIP process and its performance. After 10 months of service, the NOVACHIP pavement surfaces are in excellent condition. They appear to be in essentially the same condition they were immediately after construction and will be monitored for 3 years and their performance documented. In general, NOVACHIP appears to have promise as a preventive maintenance treatment or surface rehabilitation technique for asphalt concrete pavements. It should offer engineers an alternative to chip seals, microsurfacing, open-graded friction courses, or thin asphalt concrete overlays.

The San Antonio District of the Texas Department of Transportation (TxDOT) used the NOVACHIP process on a surface-rehabilitation project in Comal County (US 281 and SH 46) during October 1992. The experimental installation was one of three in the United States; others were constructed by the state departments of transportation in Mississippi and Alabama. Because NOVACHIP is a new technology in Texas and the United States, this research study was initiated to evaluate and document the process and its performance.

BACKGROUND

The NOVACHIP process was developed in France in 1986 by Screg Routes and Travaux Publics and is currently marketed by that company. NOVACHIP has been used successfully in Europe. (*1*) NOVACHIP, sometimes called "ultrathin friction course," was developed for use in preventive maintenance or surface rehabilitation (*2*). Its primary function is to restore skid resistance and surface impermeability. The process appears promising for pavement surface rehabilitation and provides engineers with alternatives to chip seals, microsurfacings, plant-mix seals, or thin overlays.

Some of the advantages of NOVACHIP™, as indicated by the manufacturer, are

- Excellent adhesion (no chip loss),
- Reduced rolling noise (particularly for urban use),
- Rapid application,
- Quick reopening to traffic, and
- Reshaping of existing pavement (to improve drainage, ride quality).

NOVACHIP can be used as a surface seal for bituminous pavements to reduce deterioration caused by weathering, ravelling, traffic, and oxidation. It seals small, "nonworking" cracks and provides a wearing surface with excellent skid resistance. NOVACHIP also can be used to restore pavement-surface smoothness to a limited extent, for examples, to fill ruts and smooth corrugations and other surface irregularities. NOVACHIP does not increase the structural capacity of the pavement, however.

Texas Transportation Institute, TTI/CE Building, Suite 508, Texas A&M University, College Station, Tex. 77843–3135.

Description of NOVACHIP

A NOVACHIP friction course consists of a layer of hot-mix material placed over a heavy tack coat. The course thickness ranges from ⅜ to ¾-in. (10 to 20 mm), depending on the maximum size of the stone. Layer thickness is generally about 1½ times the diameter of the largest stone (*2*).

The hot-mix material is a gap-graded mixture that includes a large portion (70 to 80 percent) of single-sized crushed aggregate, bound with a mastic composed of sand, filler (if needed), and binder (*2*). The mixture is sometimes described as "hot, coated chippings."

The binder content ranges from 5.3 to 6.0 percent, depending on the traffic, climate, and peculiarities of the existing pavement, as determined by engineers at Screg Routes.

The heavy tack coat is generally a polymer-modified, emulsified asphalt, and the application rate commonly varies between 0.15 and 0.22 gal/yd^2 (0.7 and 1.0 L/m^2).

NOVACHIP is placed with a specially designed paving machine that combines the functions of an asphalt distributor and a laydown machine. The paver applies the tack coat and the hot asphalt mixture in a single pass. This heavy application of tack helps to ensure adhesion of the friction course to the underlying pavement and to reduce the possibility of surface water intruding into the pavement structure.

Description of Paving Equipment

Application equipment for the NOVACHIP process was designed to accommodate these operations (*1*):

- Collection of the mixture from the transport trucks,
- Storage of the mixture,
- Storage of sufficient tack emulsion for at least 3 hr of operation,
- Distribution of the tack coat with servo-controlled application rate,
- Immediate covering of the tack with the mixture,
- Smoothing of the applied mixture into a virtual monogranular layer, in relation to the two or three highest points of the existing pavement surface.

The NOVACHIP paving machine, as it was developed, includes the following components (*1*):

- Hopper for the collection of the mix and a coupling for attaching it to the hook of the truck supplying the mixture. The hopper's design was changed several times to prevent hot, coated chippings from sticking in the mixture. Because the chippings tend to stick to each other, their manipulation, storage, and collection is not easy. The hopper is fitted with two transfer screws.
- Screw or rake conveyor that lifts and feeds the mix into a hopper.
- Heated compartment to store the mixture, which has a total capacity of about 4 to 6.5 yd^3 (3 to 5 m^3).
- Heated tank for the tack binder (16 yd^3 or 12 m^3).
- Conveyor to transfer the mixture to the forward part of the smoothing assembly, where the mixture is deposited on the road surface.
- Spray bar to distribute the tack coat. Nozzles on the spray bar are at a large distribution angle and closely spaced. The transverse displacement of the spray bar is servo-controlled to ensure that the spray lines up with the boundary of the hot mix.
- Heated assembly for screeding the hot mix layer. The width of the screed can be varied from 8 to 15 ft (2.5 to 4.6 m^3).

PRECONSTRUCTION INFORMATION

Existing Pavement Cross Sections

Before construction, the pavement surface of US 281 consisted of a 7-year-old double chip seal: Grade 5 (No. 4 or 4.75 mm) over Grade 3 (½ in. or 12.5 mm). Underneath the double chip seal, most of US 281 is a 3-in. (75-mm) layer of hot-mix asphalt concrete on top of a Grade 3 (½ in. or 12.5 mm) surface treatment over 8 in. of flexible base, constructed in 1972.

SH 46 had been surfaced with a 1-in. (25-mm) thick layer of asphalt concrete pavement (ACP); it was about 8 years old at the time of the construction project. Cracks in the pavement surface had been sealed with asphalt-rubber crack sealant the previous spring. Under the ACP surface was a series of chip seals over a 1-in. thick layer of ACP. The lower layer of ACP had been constructed in about 1958. Under the lower ACP layer was the original pavement, laid in the mid 1930s and thought to be a double-surface treatment on a limestone base.

Limestone bedrock is at or very near the surface in this part of Texas; therefore, the subgrade for much of the region's pavement is a limestone bedrock, which provides excellent support.

Traffic Data

Traffic data on US 281 and SH 46 near the time of construction was provided by TxDOT as follows:

- US 281: weighted average daily traffic (ADT) = 20,300 vehicles per day (vpd), 6.0 percent trucks;
- SH 46: weighted ADT = 4,200 vpd, 6.4 percent trucks.

Precondition Surveys

Before construction, precondition surveys were performed on US 281 and SH 46. An index of pavement condition was used that quantifies all forms and levels of pavement distress (*3*). Based on maintenance costs, this index, or pavement rating score (PRS), allows numerical comparison of pavement conditions. A PRS value of 100 describes a pavement with no distress. Progressively lower PRS values describe pavement conditions that include more severe types of distress.

US 281 was in good condition before construction. PRSs were obtained at several stations along the highway and are illustrated in Table 1. US 281 had an overall PRS value of 93 before construction began. Its surface was a double-chip seal that was in relatively good condition. Primary types of distress observed included some slight to moderate bleeding in various places and slight ravelling.

SH 46 had an overall PRS of 85; its scores are shown in Table 2. Its primary surface distress was longitudinal cracking and some slight ravelling. Cracks had been sealed the previous spring; however, at the time of the survey, they were partially sealed.

US 281 Pavement Test Sections

For the NOVACHIP study, eight test sections were designated along US 281. The sections were 120-ft (36-m) long and chosen for more detailed pavement evaluation. Data collected on test sections

TABLE 1 US 281 Preconstruction Pavement Rating Scores

Station	Northbound Lanes		Southbound Lanes	
	Inside	Outside	Inside	Outside
730 + 00	95	85	93	90
710 + 00	95	95	95	90
690 + 00	100	92	100	92
670 + 00	95	95	95	85
640 + 00	100	95	95	85
620 + 00	100	88	100	85
600 + 00	100	85	100	92
580 + 00	100	85	100	85
560 + 00	100	88	100	85
540 + 00	100	88	100	88
526 + 85	100	88	100	88
AVG.	99	89	98	88

Grand Average 93

TABLE 2 SH 46 Preconstruction Pavement Rating Scores

Station	Eastbound Lane	Westbound Lane
1060 + 00	88	88
1030 + 00	88	88
1000 + 00	83	83
970 + 00	83	73
940 + 00	83	88
910 + 00	88	88
880 + 00	88	92
850 + 00	88	78
820 + 00	88	85
790 + 00	89	81
760 + 00	90	83
730 + 00	90	83
700 + 00	90	90
670 + 00	90	93
640 + 00	90	90
610 + 00	88	88
580 + 00	88	90
AVG.	88	86

Grand Average 87

before construction of the NOVACHIP surface consisted of visual evaluations, photographs, rutting measurements, and surface-texture measurements.

A 2-mi (3.2-km) section of US 281, beginning at the south end of the NOVACHIP project site, served as a control section; it received no treatment and was monitored throughout the process. The pavement surface and cross section at the control site was in essentially the same condition as pavement that would be constructed with the NOVACHIP surface.

SH 46 Pavement Test Sections

Seven 120-ft (36-m) test sections were designated on SH 46 within the scope of the NOVACHIP project. In addition to the types of data collected on US 281, crack maps of the SH 46 test sections were prepared. Crack maps were unnecessary for US 281, because no cracking had been observed.

Ride-Quality Data

One of the claims to be investigated was that NOVACHIP could be used to restore pavement-surface smoothness to a limited extent, that is used for rut-filling and to smooth corrugations and other surface irregularities. TxDOT used a SIometer to measure the ride quality of the pavement surface both before and after NOVACHIP was applied. A SIometer has an accelerometer, processing computer, and data-storage computer mounted in one vehicle. The SIometer's data are converted into a ride score on the basis of a user-panel rating that ranges from 0.1 (very rough) to 5.0 (very smooth). Ride score classifications are shown in the in-text table. A road with a ride score below 3.0 is experienced as a rough one by the average person.

Ride Score	*Description*
4.0–5.0	Very Smooth
3.0–3.9	Smooth
2.0–2.9	Medium Rough
1.0–1.9	Rough
0.1–0.9	Very Rough

Before construction, US 281 had an overall ride score of 4.5, and SH 46 had an average ride score of 4.0.

CONSTRUCTION

Construction of the NOVACHIP pavement surface on US 281 began October 15, 1992, and the SH 46 job was completed on October 31, 1992. Weather was favorable during construction; morning temperatures usually were around 65°F (18°C), and afternoon highs of about 85°F (30°C). Skies were clear to partly cloudy, and the wind was calm at about 20 mph (32 km/hr).

Specifications

Certain specification requirements for the NOVACHIP mixture are somewhat more stringent than what is normally required in Texas for hot-mix asphalt concrete.

Materials

The NOVACHIP process requires that coarse aggregate in the mix be a high-quality, 100 percent crushed material. Coarse aggregate (plus No. 10 or 2.0 mm) must have a polish value of more than 35. This requirement eliminates many of the aggregate sources in

Texas. The Los Angeles Abrasion Test loss must be less than 35 percent, and the magnesium-sulfate soundness test loss must not exceed 25 percent.

The fine aggregate (minus No. 10 or 2.0 mm) must also be 100 percent crushed material. It must be supplied from a source where coarse aggregate meets the Los Angeles abrasion and magnesium sulfate soundness loss requirements just detailed. It must also have a sand-equivalent value of 60 or more.

Asphalt material used for the paving mixture must meet TxDOT standard specifications for AC-20.

Paving Mixture

A NOVACHIP contractor must provide the mixture design for the project.

Specification Changes Before Construction

At a preconstruction conference, October 13, 1992, it was revealed that the aggregate that was to be used for the mixture did not meet the specifications. The aggregate did not meet specification on the No. 4 (4.75 mm) and No. 40 (425 μm) sieve and was very close to the lower end of the specification limits on other screens. Its sand equivalent value, also out of specification, was measured at 54 instead of 60 or below, as required.

Screg Routes engineers at the meeting stated that it was paramount that the percent retained on the No. 10 (2.0 mm) sieve be below 75 and the percent passing the No. 200 (75μm) sieve be a minimum of 5.5. They said that the above gradation and the sand equivalent value of 54 were acceptable for the NOVACHIP process.

A fundamental objective was to provide an opportunity for Screg Routes to showcase the NOVACHIP pavement in the United States; therefore, TxDOT engineers decided that if the material properties of the aggregate were acceptable to Screg Routes, specifications would be changed to reflect this. Their changes to the mixture gradation specifications are shown in Figure 1. The sand-equivalent specification was changed from a minimum value of 60 to a minimum value of 50.

Job Materials

US 281

The coarse aggregate for US 281 was a traprock (basalt) provided by Vulcan Materials from its plant in Knippa, Texas. The traprock is a very hard, durable, dark-colored aggregate with a polish value of 38. The fine aggregate used on the job consisted of dry, limestone screenings from Gifford Hill. The aggregate portion of the NOVACHIP mix was made up of 68 percent of the coarse traprock aggregate and 32 percent of the dry, limestone screenings.

The design asphalt content was 5.0 percent of an AC-20 grade. A liquid antistripping agent (PERMATAC) was also used at a rate of 0.5 percent by weight of the binder.

SH 46

TxDOT engineers, material suppliers, and contractors decided that the existing supply and projected production rate of the traprock was insufficient to yield enough mix to keep up with the paving machine for construction on SH 46. According to the rock supplier, the gradation was difficult to produce and cut production rates 50 percent.

For SH 46, a new design mixture was developed by Screg Routes engineers, which contained 34 percent traprock, 34 percent limestone from Helotes, and 32 percent dry limestone screenings. The asphalt content was increased to 5.3 percent.

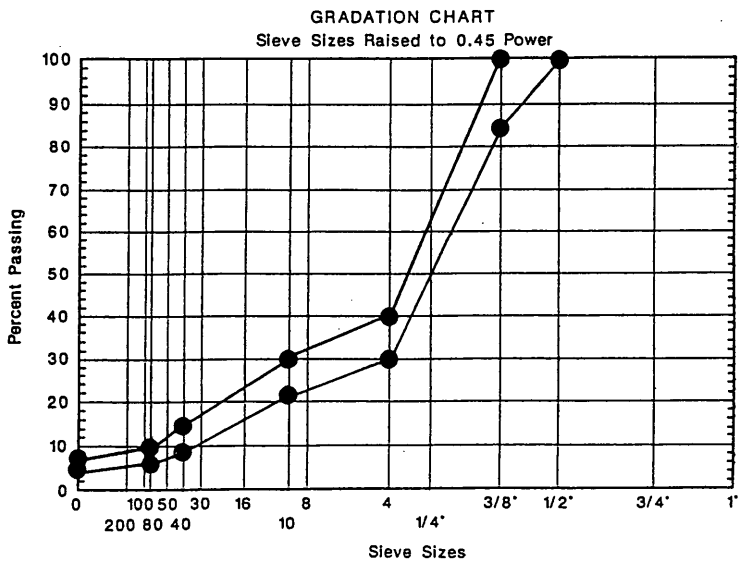

FIGURE 1 NOVACHIP aggregate gradation job specification limits.

Tack Coat

The tack coat was a polymer-modified emulsion designated CRS-2p. It was to be applied at a design-application rate of 0.20 gal/yd ^{2}.

Construction Sequence (US 281 and SH 46)

Before placement of the NOVACHIP, traffic buttons were removed from the existing pavement and the pavement surface was broomed. The NOVACHIP paving machine is capable of applying the tack coat and the paving mixture in one pass, and a nurse truck was used to periodically fill the NOVACHIP emulsion tank with the CRS-2p. Trucks transported hot-mix material from the drum-mix plant, which was approximately 10 mi (16 km) from the US 281 job and 20 mi (32 km) from the SH 46 job. Trucks backed up to the paving machine and dumped the mix into the hopper located at the front of the NOVACHIP paver, and the hopper augured the mixture to the back of the paver from which it was released onto the pavement. The tack coat was applied to the pavement about 2 sec before the mix was placed.

Two 10-ton (9-metric ton), steel-wheel rollers (66 in. or 1.7 m wide, and 54 in. or 1.4 m wide) made a total of 4 passes. The first roller ran immediately behind the paver. Traffic resumed on US 281 about 4 hr after construction, and on SH 46 it resumed about 2 hr after completion.

During construction on US 281, lanes were closed. On SH 46, pilot vehicles were used to control traffic.

The hot-mix plant operated at a temperature of 315°F (157°C), although Screg Routes engineers preferred that it operate at 330°F (165°C). Whereas the higher temperature improves workability of this harsh mixture, it was not possible to operate the plant at 330°F (165°C) and stay within the U.S. air-quality limits.

Construction Notes: US 281

US 281 is a four-lane, divided highway. Construction of US 281 began on Thursday, October 15, 1992, and included approximately 4 mi (6.5 km) of highway, or a total of 16 lane mi (26 km). Construction was completed in four working days. Production rates and job yields are shown in Table 3.

Construction of US 281 went very well, with the exception of a few minor problems. The most notable can be attributed to the equipment. Whenever the paving machine was stopped for any length of time on the pavement, the distributor nozzles continued to leak emulsion, causing excessive puddling. Sometimes the excess emulsion was washed off the pavement but often it was paved over. TxDOT engineers were concerned that the excess emulsion would eventually lead to a flushed surface in these areas. After the second day, the equipment was repaired.

Another problem occurs when the paver is stopped for an extended time period. Generally, there are two reasons to stop a paver during construction: to wait for a new load of hot-mix or to refill the emulsion tank on the paver with tack material. Where the paver was stopped for an extended period on US 281, there are very slight humps in the NOVACHIP surface that are noticeable when one passes over them at normal driving speed. When the paver was stopped, apparently the mix in front of the screed cooled excessively, which caused the screed to ride up over the mix, leaving a slight hump in the mat.

Construction Notes: SH 46

SH 46 is a two-lane highway. Construction of SH 46 began in the eastbound lane on Wednesday, October 21, 1992, and included approximately 9.5 mi (15 km), or a total of 19 lane mi (30 km), plus several climbing lanes dispersed along that length. Its main travel lanes SH 46 were constructed in six working days, and another three days were devoted to constructing the climbing lanes. Production rates and job yields for the main travel lanes are shown in Table 4.

The eastbound lane of SH 46 was constructed without incident; however, problems began to develop with the mix during the construction of the westbound lane, including excessive tearing of the mat. Material appeared to be building up in front of the screed and then dragging along the pavement, causing tears in the mat from 6 in. (150 mm) wide to 4 ft (1.2 m) wide. A significant amount of handwork was necessary to repair the mat. Because the NOVACHIP mixture is 100 percent crushed material and lacks workability, it does not lend itself to handwork.

The problem of tearing in the mat persisted for two days, before the problem was resolved. The problem was attributed to the variability of the dry screenings. Only a half-day's supply of screenings were on hand throughout this period, so the stockpile was changing constantly, making quality-control testing of the stockpile difficult.

Screg Routes engineers redesigned the mixture, replacing the dry screenings, 32 percent of the aggregate portion, with 22 percent dry screenings and 10 percent washed screenings. This adjustment solved the tearing problem, and the remainder of the job was completed without difficulty.

In numerous places where the mat had required handwork, however, an unattractive blemish remained visible on the pavement

TABLE 3 US 281 Job Production Rates

Date	CRS-2p Tack Rate, l/m^2	Mix Produced, metric tons	Area Paved, m^2	Yield, kg/m^2
10/15/92 Th.	0.91	754	21,529	34.9
10/16/92 Fr.	0.82	1133	33,722	33.3
10/19/92 Mn.	0.73	983	27,376	35.7
10/20/92 Tu.	0.82	740	21,372	34.5

1 l/m^2 = 0.22 gsy
1 kg/m^2 = 1.83 lb/yd^2
1 m^2 = 1.2 yd^2
1 kg/m^2 = 1.83 lb/yd^2

TABLE 4 SH 46 Job Production Rates

Date	CRS-2p Tack Rate, l/m^2	Mix Produced, metric tons	Area Paved, m^2	Yield, kg/m^2
10/21/92 W.	0.77	523	17,503	29.7
10/22/92 Th.	0.82	753	21,658	34.6
10/23/92 Fr.	0.82	770	25,179	30.5
10/26/92 Mn.	0.96	670	19,228	35.9
10/27/92 Tu.	0.21	443	12,558	35.1
10/28/92 W.	0.19	728	16,900	35.7

1 l/m^2 = 0.22 gsy
1 kg/m^2 = 1.83 lb/yd^2

1 m^2 = 1.2 yd^2
1 kg/m^2 = 1.83 lb/yd^2

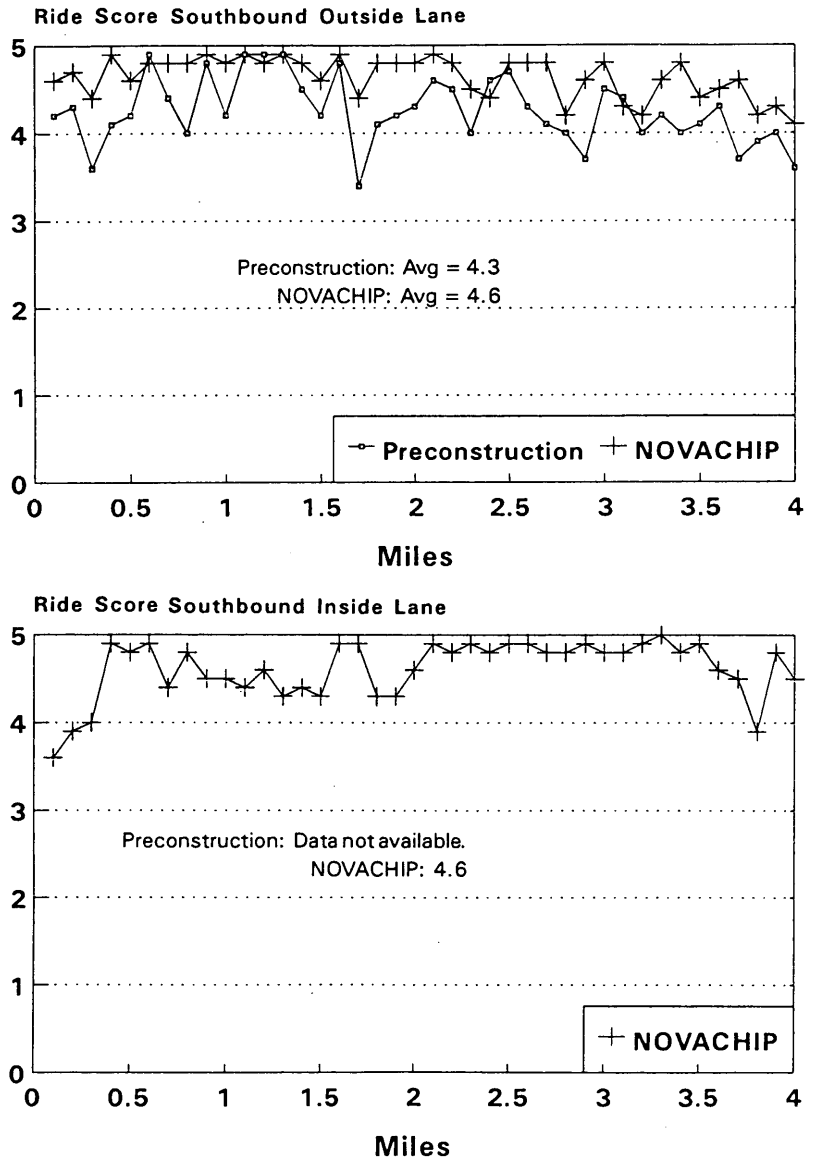

FIGURE 2 US 281 ride quality data for southbound lanes.

surface and was also noticeable from slightly rougher ride quality in these areas. Although the engineers hoped that these blemishes would fade with time and as the road was trafficked 10 months after construction, the blemishes were still evident.

Comments and Opinions of Engineers on Site

Comments of engineers visiting the construction site follow:

TxDOT Area Engineer: "For a pavement where I am very concerned about sealing the surface from the intrusion of water, the NOVACHIP pavement appears to be a good choice."

FHWA Engineer: "I am pleased with the way the NOVACHIP pavement looks, but the real issue is life-cycle cost. It has its place, but I'm not yet sure where—maybe in urban areas. I would like for NOVACHIP to be a success in this country, so that we have more paving options available to us."

FHWA Engineer: "NOVACHIP pavement looks very good—it's a very tough-looking mix. The NOVACHIP paving operation appears to be a lot quicker than a laydown machine. NOVACHIP may be a good alternative to microsurfacing, as there is no waiting time to allow traffic on surface. This pavement surface would be good to use anywhere ride quality and frictional characteristics need improvement."

EARLY PERFORMANCE

In August 1993 the NOVACHIP pavement surfaces on US 281 and SH 46 were evaluated for performance. They appeared to be in excellent condition—essentially the same condition as immediately after construction.

Ride Quality

Ride-quality measurements were made at the project sites before construction began and again 3 weeks later. The data for US 281 are shown in Figures 2 and 3. Before construction, US 281 had an ex-

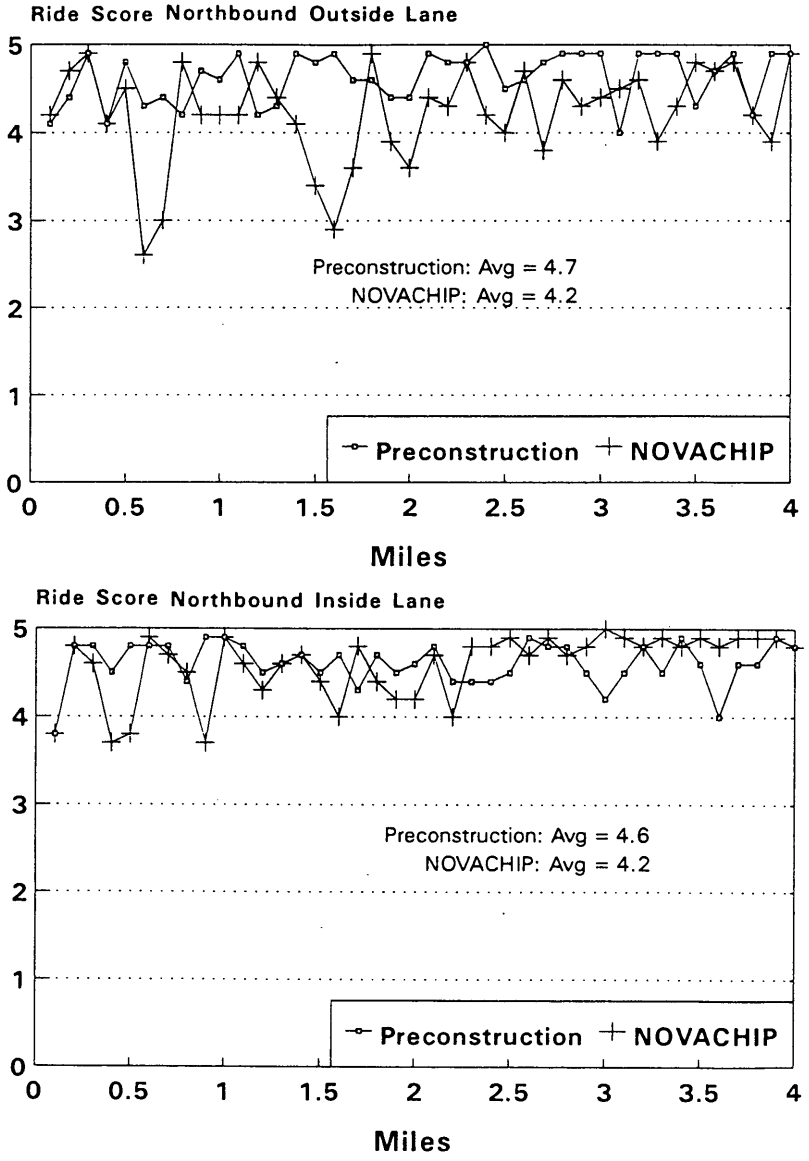

FIGURE 3 US 281 ride quality data for northbound lanes.

cellent overall average ride score of 4.5. After NOVACHIP surface construction, the overall average ride score again was 4.5, that is, no additional improvement in ride quality was detected.

Ride quality data for SH 46 is shown in Figure 4. The average ride score for SH 46 before construction was 4.0. After the NOVACHIP surface was laid the ride score improved; it measured 4.4.

Frictional Characteristics

Skid resistance data were collected using TxDOT's locked-wheel skid trailer (ASTM E274, ribbed tire). The skid unit travels at a constant speed, with the left trailer wheel locking at periodic intervals on a wetted surface. Classes of skid numbers (as described by TxDOT as part of their Pavement Management System) are shown in the in-text Table

Skid Number	*Description*
50–100	Very good
40–49	Good
30–39	Fair
20–29	Poor
1–19	Very poor

Skid resistance data also were obtained from the district site before construction of the NOVACHIP surfaces in May 1992. The average skid number for both US 281 and SH 46 was 31. (See Figures 5 and 6.)

After NOVACHIP construction, skid data were collected again on November 17, 1992. The skid number for US 281 increased to 40 and for SH 46 the number increased to 46.

When skid data were collected again on March 17, 1993, the NOVACHIP surface of US 281 had a skid number of 48 and SH 46

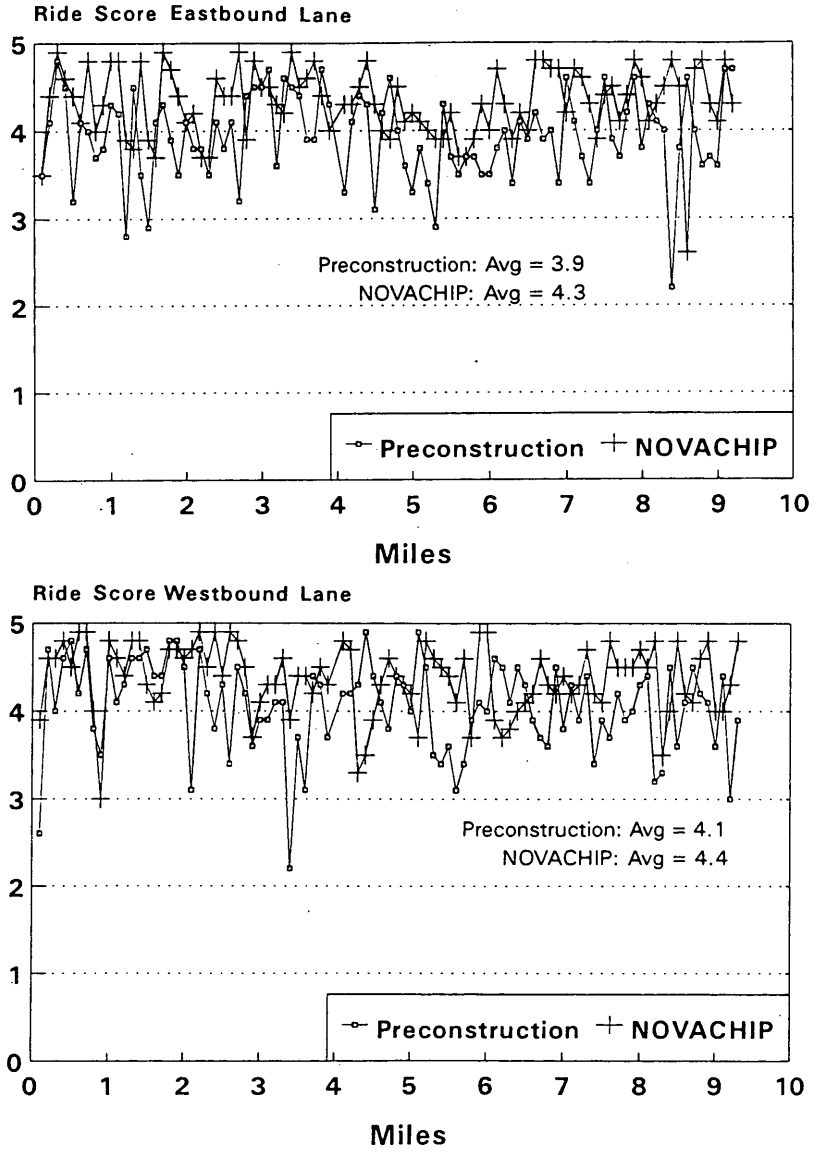

FIGURE 4 SH 46 ride quality data.

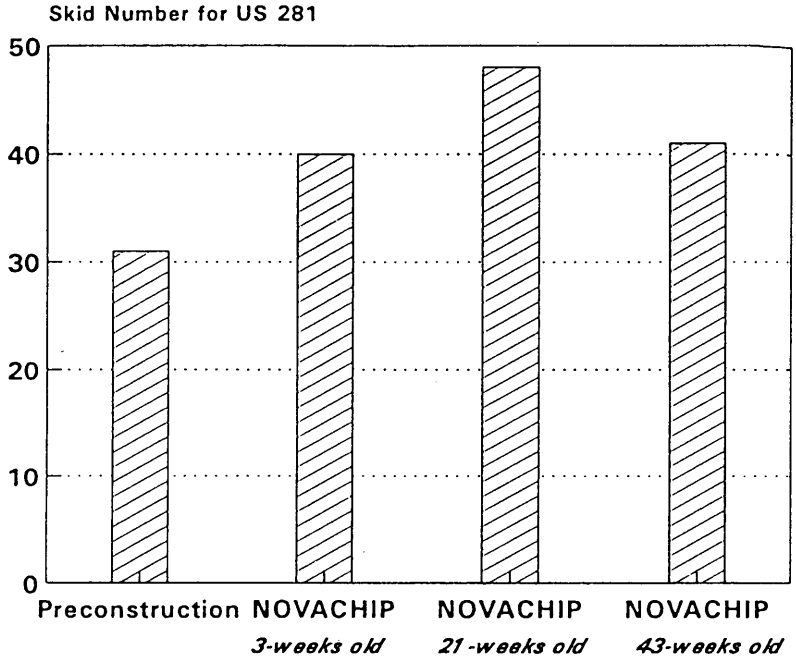

FIGURE 5 US 281 skid resistance data.

had a skid number of 53. The increase in skid resistance soon after construction probably results from traffic and weather wearing away or eroding the asphalt binder on the aggregate surface.

SUMMARY AND GENERAL COMMENTS

NOVACHIP was constructed successfully on two highways, US 281 and SH 46 in Bexar County, in the San Antonio District of TxDOT. The French process, NOVACHIP, is a new technology for the United States, and this research study was conducted to evaluate and document the process and its performance.

After one year of service, the NOVACHIP pavement surfaces are in excellent condition. The pavements appear to be in essentially the same condition they were immediately after construction. The pavements will be monitored for 3 years and their performance will be documented.

Because so few NOVACHIP jobs are constructed in the United States, the cost of the two projects was excessive. Equipment had to be transported to the United States from France to perform the two

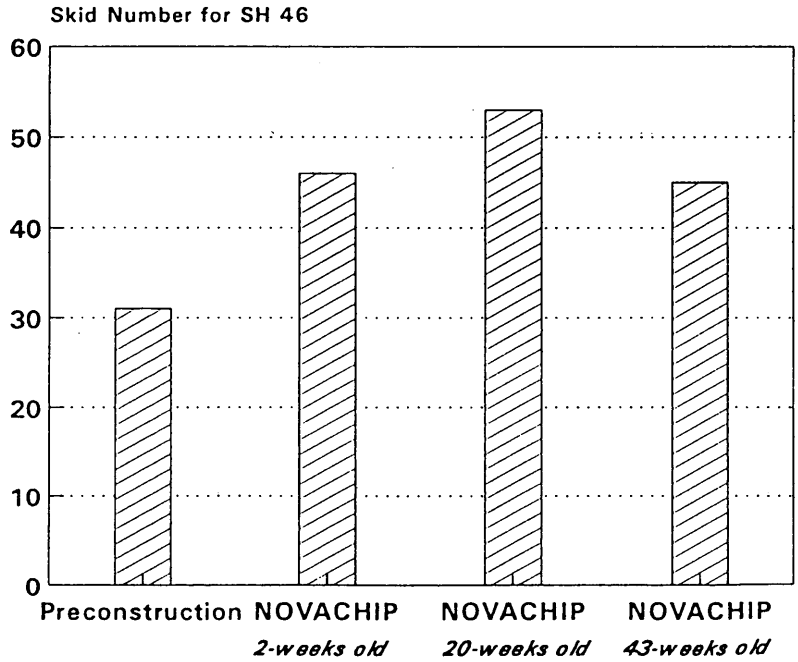

FIGURE 6 SH 46 skid resistance data.

jobs on a demonstration basis. In France NOVACHIP is reported to cost the same as microsurfacing and just a little more than a polymer-modified-asphalt chip seal.

In general, NOVACHIP appears to have promise as a preventive-maintenance treatment or surface rehabilitation technique for asphalt concrete pavements. It should provide the maintenance engineer with an alternative to chip seals, microsurfacing, plant-mix seals, or thin asphalt concrete overlays. This study cannot directly compare NOVACHIP with other maintenance treatments, because no comparable test sections were constructed using other maintenance treatments. Some advantages NOVACHIP may have over these maintenance treatments were determined subjectively by the authors although they are not quantified in the study.

- Advantages Over Chip Seal
  - –Excellent chip retention,
  - –Ability to reshape existing pavement to a limited degree by filling ruts and smoothing minor surface irregularities,
  - –Less rolling noise (a factor not measured in this study),
  - –Suitability for use on roads with high traffic volumes, and
  - –Greater resistance to surface damage caused by vehicles turning and stopping.
- Advantages Over Microsurfacing
  - –Quick reopening of the constructed road to traffic,
  - –Better adhesion to underlying surface with use of heavy tack coat,
  - –Greater surface macrotexture, and
  - –Better drainage—reduced splash and spray with the open surface texture.
- Advantages Over Open-Graded Friction Courses
  - –Better adhesion to underlying surface with use of heavy tack coat, and
  - –Better protection of underlying pavement from surface water, a typical problem with open-graded friction courses.
- Advantages Over Dense-Graded Thin Overlay
  - –Better adhesion to underlying surface with use of heavy tack coat,
  - –Rut-resistance with use of high-quality crushed materials,
  - –Greater surface macrotexture,
  - –Improved surface drainage, and
  - –Better protection of underlying pavement from surface water.

Some preliminary conclusions regarding NOVACHIP from on-site observation and early performance data follow.

- NOVACHIP is a high-quality mixture, consisting of 100 percent crushed materials. The type of mixture, however, does not lend itself to a significant amount of handwork and raking.
- It is important that the mixture be at 280°F (138°C) or above when it is placed. Because of the openness of the aggregate gradation, the mixture loses heat quickly. If the mixture gets too cool, the paver must operate at a slower speed than is optimal. Excess mixture may also back up in front of the screed, causing tears in the mat that are not as easy to repair with this mix as with dense-graded hot mix. The plant temperature should be 315°F (157°C) or more. Trucks that are transporting the mix should be covered with tarps, if possible.
- NOVACHIP significantly increased the skid resistance of the treated pavement.
- No improvement in ride quality was measured on US 281 after NOVACHIP construction; however, existing pavement already had a very good ride score. However, ride quality was improved on SH 46; its ride score increased from 4.0 to 4.4.
- Quality-control procedures used for conventional hot-mix asphalt concrete jobs may not be acceptable for NOVACHIP. The mixture is noticeably sensitive to changes in mixture proportions. Instead, a performance-based specification on workmanship quality might be appropriate for NOVACHIP surfacing.
- NOVACHIP provides a uniform, attractive appearance but the mixture lacks workability. Therefore, excessive handwork and raking of the mix is very noticeable and detracts from the pavement's appearance and sometimes the ride quality. However, raking is necessary when the paving proceeds as it should.

REFERENCES

1. NOVACHIP™, A New Type of Pavement Surfacing. Screg Routes.
2. Serfass, J.P., P. Bense, and J. Samanos. Performance Assessment of Ultrathin Friction Courses. Preprint of paper presented at 71st Transportation Research Board meeting, Washington, D.C., January 1993.
3. Epps, J.A., A.H. Meyer, I.E. Larrimore, Jr., and H.L. Jones. Roadway Maintenance Evaluation User's Manual. Research Report 151–2, Texas Transportation Institute, Sept. 1974.

Publication of this paper sponsored by Committee on Characteristics of Bituminous-Aggregate Combinations To Meet Surface Requirements.

Experiences with Thin Bituminous Layers in Austria

JOHANN H. LITZKA, FRIEDRICH PASS, AND EDUARD ZIRKLER

Thin bituminous layers have been used successfully for road maintenance in Austria for several years. Such thin layers are constructed by laying hot-, warm- or cold-mixed material in a thickness of approximately 20 mm on existing asphalt or concrete surfaces. One of the principal applications to date has been the filling of ruts in concrete surfaces caused by studded tires. Technical requirements for thin layers are laid down in an Austrian code of standards. Those standard specifications applicable to the binder, the aggregates, the mixture and the finished layer are discussed and notes on these layers' preparation and application are provided. Recent experiences with thin layers are reported, as is current development work on noise-reducing thin layers. Austria's primary (federal) road network, with a total length of about 12,000 km, includes approximately 5 million m^2 of roadway covered by thin bituminous layers. Of these layers, about 90 percent are hot-mixed layers. Construction costs average about $4.50/sqm. Thin bituminous layers' average service life is an estimated 8 to 10 years.

Thin bituminous layers are wearing courses with thicknesses of up to 20 mm that are applied to bituminous structures or concrete pavements. Their purpose is to increase skid resistance, seal poor bituminous surfaces, and improve transverse evenness, the most important application to date. Structural load-bearing capacity is not increased by such surfacing.

Cold-mixed thin layers, so-called slurry seals, were first applied in Austria in the late 1960s, using cationic emulsions with 200-pen standard bitumen. The results achieved varied, depending on weather conditions, mainly (*1*). This variability is the main reason why slurry seals are not applied extensively on heavily trafficked roads.

First tests with hot-mixed thin layers, based on experiences in Switzerland, date back to the late 1970s. It had become necessary to repair rutting in asphalt and concrete surfaces that was resulting from the use of studded tires. Initially, coated materials containing conventional binders were used, but these did not bond sufficiently to the layer below. At first, some sections of the thin layers peeled extensively after relatively short exposure to traffic. Finally, by using polymer-modified binders in the tack coat and the bituminous mixture, satisfactory results were achieved. In the early 1980s, these results encouraged the use of thin bituminous layers on concrete highways as well. The process has developed on the basis of practical, on-site experiences. The technique was used to repair most of the rutting on Austria's West Autobahn (federal highway A1 from Vienna to Salzburg) and Süd Autobahn (A2 from Vienna to the south). Some of these first maintenance sections are still under traffic today.

J.H. Litzka, Vienna University of Technology, Gusshausstrasse 28, A-1040 Vienna, Austria; F. Pass and E. Zirkler, Central Laboratory, Teerag-Asdag AG 7 Haidequerstrasse 1, A-1110 Vienna, Austria.

SPECIFICATIONS FOR THIN LAYERS

Specifications to which such thin bituminous layers are constructed in Austria have been derived from practical experience gained during the past 10 years (*2*) and compiled in a code of standards (*3*) to which all federal roads and highways must conform. The code of standards contains specifications for the binder, chippings, grading, mixture, and finished layer as well as details concerning preparation, transportation, and laying of the material.

Binders

For hot-mixed thin layers, only polymer-modified binders may be used; for cold-mixed layers use of these binders is recommended. In Austria, such binders are primarily SBS-modified binders. The need to use polymer-modified binders arises from the more stringent requirements regarding adhesion (adhesion to the chippings) as well as cohesion (a binder's ability to withstand and resist the impact of heavy vehicle trafficking).

Two types of binders are used: hot binders (whereby the mixture is prepared in a mixing plant) and bitumen emulsions (whereby the material is mixed on site). In the latter case, special modified emulsions must be used, to which chemicals are added to extend breaking time.

Use of cut-back bitumen in thin layers, applied in the warm state (100 to 120°C), is in principle permissible, but the practice is decreasing for environmental reasons.

To be suitable for use in thin layers binders must exhibit a broad range between softening- and breaking-point temperatures, high elasticity, and good low-temperature characteristics. Specifications for such binders are summarized in Table 1.

As thin layers may contain a higher proportion of binder than asphalt concrete, there is the risk of a binder draining off hot mixture at higher temperatures. To prevent this, binder carriers are sometimes used that have proved effective at high temperatures and shown to have no detrimental effect on asphalt performance at service temperatures. In Austria, cellulose fibers normally are used; fibers possible alternatives include special fillers, mineral and synthetic fibers.

Aggregates

Aggregates used must also conform to strict requirements. An aggregate's grain shape should be as close to cubic as possible. Badly shaped grains (those with a length-to-width ratio of greater than 3) must not account for more than 10 percent of the total. Edge-holding power must be high, and the Los Angeles coefficient (*5*) not

TABLE 1 Binder Specifications for Thin Bituminous Layers

Parameter	unit	hot mix	cold mix
Softening point (R & B)	°C	> 55	> 43
Penetration at 25°C	1/10 mm	60 to 90	130 to 150
Elastic recovery at 25°C	%	> 70	> 40
Ductility at 25°C (*10*)	cm	> 100	> 100
Breaking point (Fraass)	°C	< -20	< -20
Adhesion between binders and aggregates in water (*4*)	%	> 95	> 95

exceed 18 to 25, depending on the traffic load. Polishability of the aggregates must be low (PSV >50) (*6*). The maximum grain size to be used depends on the application; it will lie between 4 mm and 11 mm. In Austria, most thin layers are built with a maximum grain size of 8 mm.

Grading

The surface of a thin layer must be homogenous and show good skid resistance. It must be even, free from mastic patches, and slightly open graded. This is achieved by reducing fine components in the filler and sand ranges while, at the same time, increasing the proportion of chippings, in particular, that of coarse chippings. A typical mixture might be

	Percent by Weight
Filler (<0.09 mm)	7–9
Sand (0.09 to 2 mm)	18–28
Chippings (> 2 mm)	63–75

Figure 1 shows a typical grading curve for a thin bituminous layer with a maximum grain size of 8 mm. With such mixes, the voids content in the finished layer will lie between 8 percent and 11 percent by volume.

Mix design

Mix composition is determined by tests with different binder contents. For mixtures with an 8-mm maximum grain size, the binder content is approximately 6 percent to 6.5 percent by weight. Optimum binder content is assessed in terms of voids content and marshall stability.

PREPARING AND PLACING THE MIXTURE

When preparing the hot mixture, it is important to ensure that mixing does not take place at temperatures above 180°C. Otherwise the binder will be irreparably damaged, adversely affecting its adhesion to the aggregates. If fibers are added, mixing time will be prolonged by 10 percent to 15 percent, reducing plant capacity.

The hot mixture must be transported in covered trucks in order to prevent excessive cooling of the material. Delivery must be continuous to avoid idle time on the road finisher.

The support to which the thin layer is applied must be clean and dry and have sufficient load-bearing capacity. Any existing cracks must be repaired before the thin layer is applied. Major unevenness must be remedied by a leveling course. Milled areas must be cleaned by a compressed-air or high-pressure water jet.

With such thin layers, good adhesion to the support is especially important to enable the absorption of shear forces and prevent the surface layer from peeling off. The base should be tack-coated before the hot, thin layer is applied in order to secure uniform bonding. The bitumen emulsions used should be modified by the same means used in the preparation of the hot mixture. When the emulsion has broken, the thin bituminous layer is applied by a road finisher working at moderate speed.

If possible, the finisher should not be idle at any time during application. The working speed of the finisher should be coordinated with the deliveries of the hot mix. Compaction preferably is carried out by rubber-wheel rollers. The temperature of the material should lie between 150°C and 170°C during application, and between 120°C and 150°C during compaction. As thin layers cool down very

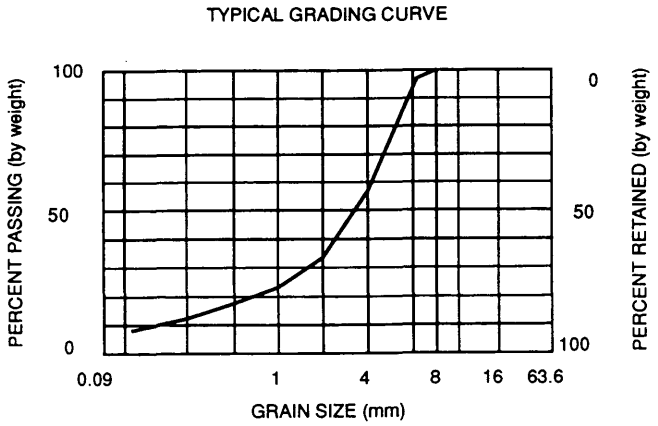

FIGURE 1 Typical grading curve for hot-mixed thin layers with a maximum grain size of 8 mm.

rapidly, efficient rolling is possible only for a few minutes, so rollers must operate immediately behind the finisher. Usually it is not possible to achieve compaction rates of more than 96 percent, but the essential goal is to ensure that the rollers press the layer onto the base in time to secure both good bonding and a good internal structure within the layer.

Final acceptance tests should examine the quality of the raw materials, mixture, thickness of the layer, longitudinal evenness, and bonding of the layer to the support.

Bonding to the support is tested with a special pull-off device (for example, the Schenck-Trebel) that is attached to ring-groove bore holes with a diameter of 50 mm (Figure 2). In the laboratory, it can be attached using cores with a diameter of 100 mm at a temperature of 0°C. The mean value that results from three tests must not be below 1 MPa (*7*).

The warranty period for thin layers made with polymer-modified binders is 3 years. This means that any defects caused by faulty construction that appear during this period must be corrected by the contractor.

Cold application (slurry seals) is carried out with the technique developed in the United States and adopted in Austria. The warranty terms are the same as for hot-mixed thin layers.

EXPERIENCE AND ONGOING DEVELOPMENTS

In Austria's relatively wet climate, applying thin layers by the cold process (slurry seals) is more difficult than laying the hot-mixed material. Furthermore, slurries whose maximum grain size is bigger than 4 mm are rarely used in Austria. For these reasons, cold-mixed thin layers are limited mostly to the secondary highways.

Originally, hot-mixed thin layers were used to rehabilitate old asphalt surface courses in urban areas, as the technique does not require milling the existing surfaces or raising the sidewalks. Hot-mixed thin layers also have been used successfully in overlaying block pavements, provided that a minimum layer thickness of 20 mm over the highest block is ensured and blocks are embedded well enough so that they cannot move. As early as 1980, hot-mixed thin layers were applied to old concrete paved highways on a trial basis. During this time, the entire width of the highway in one direction was overlaid with a thin bituminous layer (*8*).

However, because the need for repairs was limited—rutting in the right-hand lane—a technique was developed in the mid-1980s whereby hot-mixed thin layers could be applied to just one single lane, as had been done previously with slurry seals. The technique uses pavers whose screed can be angled in three sections, making it possible to obtain a "zero" thickness at the edges of a lane. From the hopper and the bar feeders, 0/8-mm material is fed into the middle section of the paver. At the same time, 0/4-mm material is fed into the spreading screws supplying the edge sections of the paver. This action minimizes the step between the new layer on the right lane and the adjacent untreated lane, which prevents damage to the newly laid surface from snow ploughs and ensures adequate transverse drainage, as shown in Figure 3.

Another method used to provide a level transition to untreated lanes consists of laying the thin layer into a bed previously milled to a depth of about 1 to 2 cm, (as shown in Figure 3). This procedure, however, is extremely costly, as milling tools wear out very quickly when used on concrete surfaces made of hard chippings. In addition, milling dust affects the thin layers' bonding to the support layer.

Thin bituminous layers that substantially reduce tire noise have been developed. The so-called "noise-reducing thin surface layers" could be developed because the surface texture of a layer with an 8-mm maximum grain size reduces tire deformation and therefore the vibration of tire casings. In addition, air can escape both through the tire tread and the surface layer without much resistance because the layer's voids content is about 15 percent by volume. In effect, the air-pumping effect is minimized. This development makes hot-mixed thin layers specially suited for use in built-up areas, where the use of thicker noise-reducing surface layers (for example, drainage asphalt) can frequently cause problems.

Overall, an estimated 5 million m^2 of thin bituminous layers have been applied to 12,000 km of Austria's primary (federal) road network. Of these layers, about 50 percent were laid on concrete pavements and 50 percent onto asphalt surfaces. About 90 percent of the layers were hot-mixed, 10 percent cold-mixed.

The extent to which thin layers are used on the secondary road network (provincial and local roads) is very hard to estimate. It may be assumed, though, that hot-mixed layers account for only about 75 percent of the total.

Use of warm-mixed thin layers has been confined to roads in rural areas; however, relevant data are not available.

Estimated mean cost of material per ton laid are as follows:

- AC11 (conventional mix)—$55.00 (100 percent),
- Hot-mixed DDH 8—$75.00 (130 percent), and
- Cold-mixed DDK 8—$175.00 (310 percent).

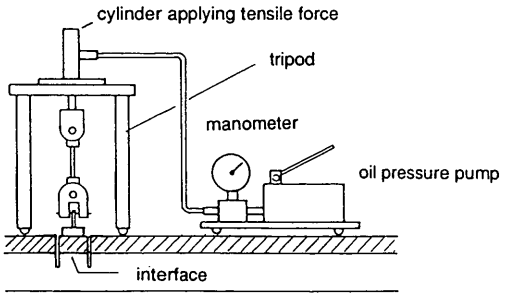

FIGURE 2 Special pull-off device used to test the bonding of layers (field test on ring-groove drilling holes).

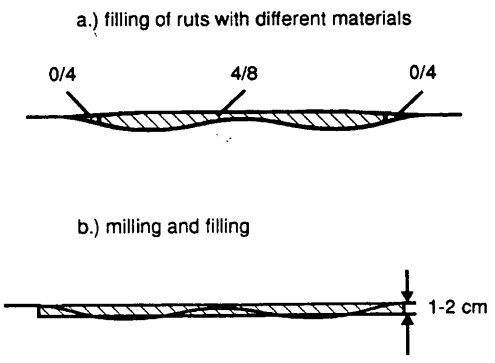

FIGURE 3 Techniques for placing thin layers on the right-hand lane only. One (top) ensures transverse drainage; a second (bottom) provides a level transition to untreated lanes.

Estimated mean cost of finished layer per m^2 of finished layer, including cleaning and tack-coating of the underlying pavement, are as follows:

- Hot-mixed DDH8—$4.50 (100 percent) and
- Cold-mixed DDK 8—$8.00 (190 percent).

Taking into account that, as a rule, cold-mixed thin layers are applied to only one lane, namely the right-hand lane, the cost-per-meter for dual carriageways (motorways) in one direction is the same as for construction of a hot-mixed thin layer covering both lanes.

As mentioned before, to ensure satisfactory performance under traffic it is critical that layers adequately bond with underlying pavement. Therefore, tack coating with a bituminous binder is particularly important.

On cracked pavements, thin layers should be applied only if the cracking was caused by something other than inadequate load-bearing capacity, and if the cracking is confined to the surface course (such as hardening of binder or low-temperature cracking). Experience shows that to successfully use thin bituminous layers on concrete pavements, joints also must be sawn in the overlay and sealed.

In Austria, rutting from abrasion is no longer a significant problem. Even though studded tires are allowed in Austria, their use has declined substantially because of a ban in effect in Germany and a speed limit in Austria.

Experience gained so far suggests the service life of properly constructed thin bituminous layers on a primary road network can be estimated thus:

	Cold-Mixed	*Hot-Mixed*
On asphalt	$\leq$ 10 years	$\geq$ 10 years
On concrete	$\leq$ 8 years	$\geq$ 8 years

The service life of thin bituminous layers on asphalt on a secondary road network can be estimated to be 10 years or longer.

SUMMARY

Austria's experience with thin bituminous layers to date indicates that this method of road maintenance is universally applicable (*9*). Use of high-quality aggregates and suitable binders is a fundamental prerequisite to constructing durable thin layers with an adequate service life, as are careful construction and special attention to ensure their permanent bonding to the supporting layer.

Austria's specification for thin bituminous layers (*3*) is being revised on the basis of the experience gained so far. It is expected that minimum requirements for bonding between the layers will be increased in order to secure good long-term performance.

REFERENCES

1. Zirkler, E. Grundlagen und Erfahrungen auf dem Gebiet der kationischen Emulsionsschlämmen (Slurry-Seal-Verfahren) (Principles and experiences in the field of cationic emulsion slurries [slurry-seal techniques]), *Bitumen* magazine. July 1967.
2. Fenz, G., H. Gregori, E. Hintsteiner, H. Holiczki, M. Khazai, R. Krzemien, G. Nievelt, and E. Zirkler. Asphalte als Dünnschichtbeläge (Asphalt Mixtures as Thin Layers). *Schriftenreihe Strassenforschung* (Road Research), Vol. 298, Federal Ministry of Construction and Technology, Vienna, Austria, 1986.
3. RVS 8.06.25. Bituminöse Decken, Dünnschichtdecken (Bituminous Surfaces, Thin Layers), Forschungsgesellschaft für das Verkehrs- und Strassenwesen (Standards and Specifications for Road Construction), *Richtlinien und Vorschriften für den Strassenbau,* Österr. (Austrian Research Society for Transport and Roads), Vienna, 1990.
4. ÖNORM B 3682. Technische Asphalte für den Strassenbau und verwandte Gebiete; Prüfung des Haftverhaltens zwischen Bindemittel und Gestein bei Wasserlagerung (Technical Asphalts for Road Construction and Related Areas; Testing Adhesion Between Binders and Aggregates in Water). Austrian Standardization Institute, Vienna, 1991.
5. ÖNORM B 3128. Prüfung von Naturstein und anorganischen Baustoffen, Prüfung von Körnungen in der Los-Angeles-Trommel (Testing Natural Stone and Anorganic Building Materials, Testing of Aggregates in a Los Angeles Drum). Austrian Standardization Institute, Vienna, 1986.
6. RVS 11.062. Prüfverfahren; Steinmaterial, Pkt. 4: Polierversuch (Testing procedures; Stone Material, Point 4: Polishing test), Forschungsgesellschaft für das Verkehrs- und Strassenwesen, (*Standards and Specifications for Road Construction). Richtlinien und Vorschriften für den Strassenbau,* Österr. Austrian Research Society for Transport and Roads), Vienna, 1986.
7. RVS 11.065. Prüfverfahren, Haftverbund von Asphaltschichten (Testing Procedures, Bonding of Asphalt Courses). Forschungsgesellschaft für das Verkehrs- und Strassenwesen, (*Standards and Specifications for Road Construction.) Richtlinien und Vorschriften für den Strassenbau,* Österr. (Austrian Research Society for Transport and Roads), Vienna, 1991.
8. Fenz, G., H. Gregori, R. Krzemien, and H. Waldhans. Spurrinnensanierung auf Betondecken (Repairing Ruts in Concrete Surfaces). *Schriftenreihe Strassenforschung (Road Research)* Vol. 360, Federal Ministry of Economic Affairs, Vienna, 1988.
9. Pass. F. Erhaltung mit Asphalt (Maintenance with Asphalt Mixtures). Presented at *Gestrata Construction Seminar,* Vienna, 1993.
10. ÖNORM C 9219. Bitumen und Steinkohlenteerpech, Prüfung, Elastische Rückformung von polymermodifiziertem Bitumen (Duktilometermethode) [Bitumen and Hard Coal Tar Pitch, Testing, Elastic Recovering of Modified Bitumen (Ductilometermethod)]. Austrian Standardization Institute, Vienna, 1990.

Publication of this paper sponsored by Committee on Characteristics of Bituminous-Aggregate Combinations To Meet Surface Requirements.

Seven-Year Performance Evaluation of Single Pass, Thin Lift Bituminous Concrete Overlays

CHRISTINE M. REED

In the mid-1980s, the Illinois Department of Transportation (IDOT) faced the challenge of maintaining an aging highway network at an acceptable level of service with limited finances. Programming rehabilitation for rural highways was difficult under the existing rehabilitation policies. To minimize the required maintenance effort on these highways, and maximize the available rehabilitation dollars, IDOT initiated a single pass, thin lift bituminous concrete overlay policy. The new rehabilitation strategy, Surface Maintenance at the Right Time (SMART) was designed for rural highways with low levels of traffic, which otherwise probably would not be rehabilitated under the current rehabilitation policy. Pavements chosen for rehabilitation under SMART ideally would have age-related distresses, with few indications of structural failure. Project rehabilitation consists of pavement patching, milling, and reflective crack control treatments where necessary, followed by a 30- to 40-mm (1.25- to 1.50-in.) bituminous concrete overlay. The SMART program has been very successful. Performance is high: rehabilitations are expected to last 7 to 10 years. Through proper project selection and construction, this program is a cost-effective method for reducing the number of highway kilometers needing rehabilitation.

In 1986, the Illinois Department of Transportation (IDOT) initiated a single pass, thin lift bituminous concrete overlay rehabilitation strategy for rural highways with low volumes of traffic. It was anticipated that the new policy would minimize the required maintenance effort on these highways, as well as maximize the available rehabilitation dollars. The new policy was titled Surface Maintenance at the Right Time (SMART). Performance of projects rehabilitated under the SMART Program has been monitored for 7 years.

PROJECT SELECTION CRITERIA

For a single pass, thin bituminous overlay to perform well, it must be applied in a timely manner (*1*). Therefore, pavement selection is crucial to the project's success. If the pavement has deteriorated to a low level of service, a thin bituminous overlay will fail quickly because it cannot correct significant structural deficiencies. Conversely, it would not be cost-effective to overlay before rehabilitation is necessary (*2*). To ensure proper project selection for the SMART program, selection guidelines were developed that focus on pavement type, traffic levels, and pavement condition.

Pavement Type

The SMART program is limited to rehabilitating pavements with an existing bituminous concrete surface. IDOT experience has shown that thin bituminous concrete overlays on bare concrete pavements are likely to develop bonding problems. In addition, there is concern within IDOT that a thin bituminous concrete overlay would not survive structurally on a rigid platform.

Illinois Department of Transportation, Bureau of Materials and Physical Research, 126 East Ash Street, Springfield, Ill. 62704-4766.

Traffic Levels

For a pavement section to qualify for the SMART program, multiple-unit truck traffic must be less than 500 units per day if required patching is less than 6 percent of a section's surface area. If required patching is between 6 and 10 percent of the section, multiple-unit truck traffic is limited to 250 units per day or less. Pavements requiring patching on more than 10 percent of their surface are not eligible for the SMART program.

Pavement Condition

Every 2 years IDOT performs a condition rating survey (CRS) of all highway kilometers maintained by the state. CRS involves the visual inspection of pavements by a trained panel of raters. Existing distresses, including severity and quantity, are noted for each pavement section. In addition, each pavement section is assigned a CRS value, which represents its current condition. Each panel member selects a CRS value for the pavement condition, and these values are then averaged to obtain the CRS value that is assigned to the pavement section. CRS values can range from 1.0 for a failed pavement to 9.0 for a new pavement surface (*3*). Table 1 gives a complete description of the ranges of CRS values. The project selection guidelines require that all projects selected for rehabilitation through the SMART program have a CRS value of 4.0 to 6.0 for marked routes and 3.8 to 5.4 for unmarked routes. Marked routes include any route with an Illinois or U.S. designation, such as IL 67 or US 30.

In addition to falling within the designated CRS range, all potential SMART projects should have less than 4 percent alligator cracking that requires patching. Alligator or fatigue cracking can be seen as a series of interconnecting cracks and is a positive indication of base and structural failures in bituminous concrete pavements (*3*).

CONSTRUCTION GUIDELINES

IDOT defines the SMART overlay thickness as 30 to 40 mm (1.25 to 1.50 in.) of bituminous concrete. The IDOT standard bituminous-concrete surface mix most commonly used contains between 5 and

TABLE 1 Ranges of CRS Values

Numerical Range	Adjective Rating	Description
1.0 - 4.5	Poor	Pavement is critically deficient, in need of immediate repair.
4.6 - 6.0	Fair	Pavement is approaching a condition that will necessitate repair over the short term.
6.1 - 7.5	Good	Pavement is in acceptable to good condition.
7.6 - 9.0	Excellent	Pavement is in excellent condition.

6 percent asphalt cement, has a void in the mineral aggregate (VMA) near 14, and has 3 to 5 percent air voids. It contains a coarse aggregate with a top size of 9.5 to 12.5 mm (⅜ to ½ in.). Overlays are placed in accordance with standard IDOT practices (*4*).

Most pavement sections selected for rehabilitation were overlaid several years ago and are failing because of the age of the overlay instead of structural inadequacies. Age-related pavement distresses are surface distresses, such as block cracking, weathering, and raveling. To eliminate these surface distresses and to remove any rutting problems, milling is usually recommended on SMART projects.

Strip-reflective crack control treatments that have been tested and approved for use in Illinois (*5*) are also recommended whenever the distress level of a widening or centerline crack is significant. If the widening crack's width is greater than 15 mm (0.5 in.) or it is moderately to severely spalled, a strip-reflective control treatment should be used. Strip-reflective crack control treatments should be used at the centerline whenever the centerline is spalled frequently and severely. Field checks of SMART projects indicate that both milling and strip-reflective crack control treatments improve the performance of a SMART overlay (*6*).

Because the SMART program is intended to be a single pass, thin lift bituminous concrete overlay for pavement sections that might not be rehabilitated under standard policies, the use of a leveling binder before overlaying is strongly discouraged. The percentage of projects for which a leveling binder was used over 50 percent or more of the project's surface area was calculated for each fiscal year. The percentage of projects for which reflective crack-control treatments and milling were used over at least 50 percent of the surface area was determined. From these statistics (Figure 1), it is clear that SMART construction guidelines usually are followed.

PERFORMANCE MONITORING

Long-Term Performance of Early Projects

The first SMART projects were constructed in late summer 1986, during fiscal year 1987. As Figure 2 shows, 346.98 km (215.61 mi) were rehabilitated during fiscal year 1987. CRS values for these projects were recorded in 1986, 1988, 1990, and 1992. CRS ratings indicated all of the projects were excellent in 1986. By 1990, 317.71 km (197.42 mi) of the 346.98 km (215.61 mi) rated in the good to excellent range, as shown in Figure 3. Figure 3 also shows that in 1992, 6 years after construction, 200.60 km (124.65 mi) of the 346.98 km (215.61 mi) still rated in the good to excellent range. It was hoped originally that five or more years after rehabilitation the CRS value of a selected project would be no lower than it had been before rehabilitation. CRS values compiled in Table 1 and Figure 3 indicate that 136.95 km (85.10 mi) had a low enough CRS value to qualify for rehabilitation a second time. Only 0.48 km (0.30 mi) was rated critically deficient and in need of immediate repairs. Although there is not enough data at this time to conduct a thorough long-term performance evaluation, these historical CRS values provide an indication of the average life of a SMART overlay.

Average CRS values evaluated in this paper were weighted by the individual project's pavement length. For fiscal year 1987 pro-

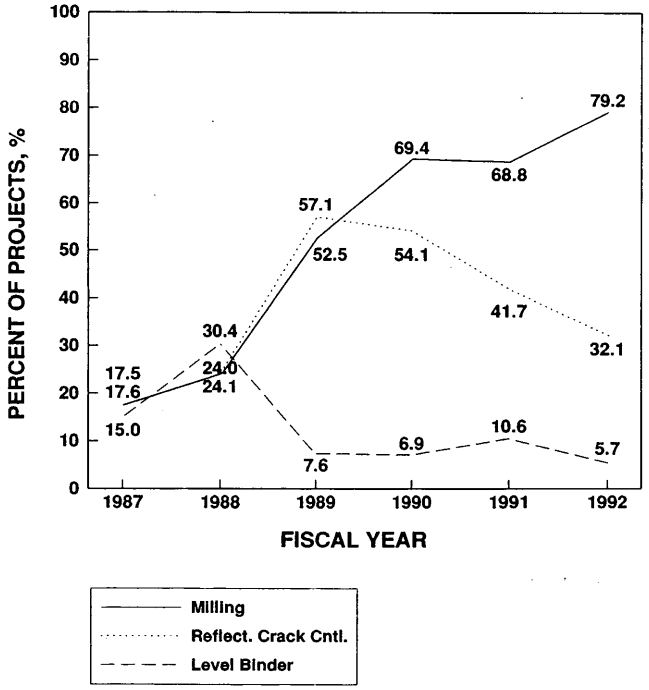

FIGURE 1 Percentage of projects using level binder, reflective crack control treatments, or milling.

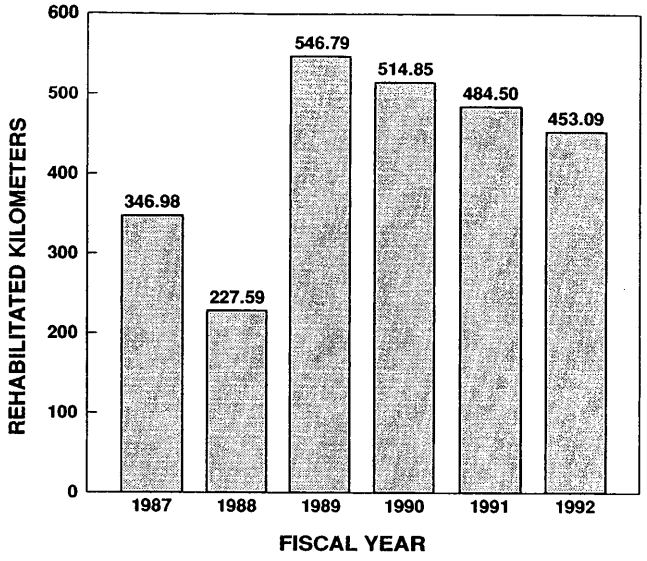

FIGURE 2 Kilometers rehabilitated under SMART program.

jects, weighted average CRS values from 1986, 1988, 1990, and 1992 are shown in Figure 4. The average decrease in CRS value per 2-year interval was 0.9. Projecting a decrease of 0.9 in CRS values for 2 years, Figure 4 shows that the average SMART project will not reach a critically deficient CRS of 4.5 or less for at least 10 years. However, after 7 years, the average SMART project will have a CRS value of 6.0, which is low enough to qualify for a second rehabilitation under the SMART program.

Average 1992 CRS Value Evaluation

Perhaps a better method of predicting the expected life of a SMART project is to compare the weighted average 1992 CRS values of pro-

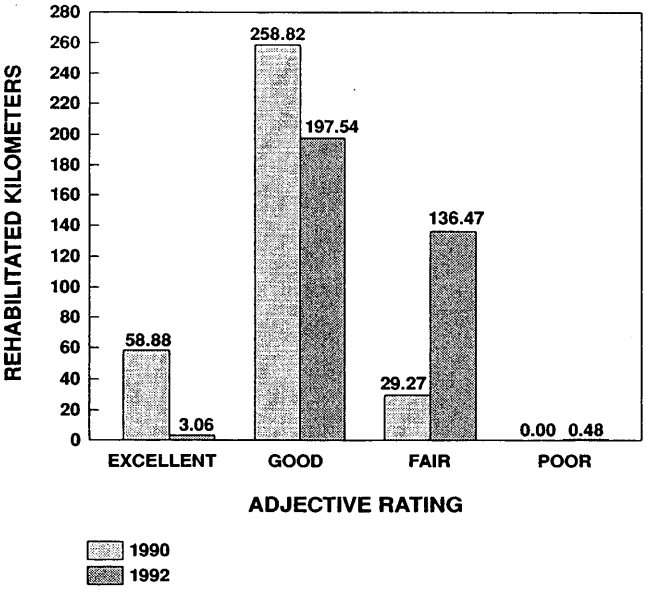

FIGURE 3 1990 and 1992 CRS adjective ratings for SMART projects constructed in fiscal year 1987.

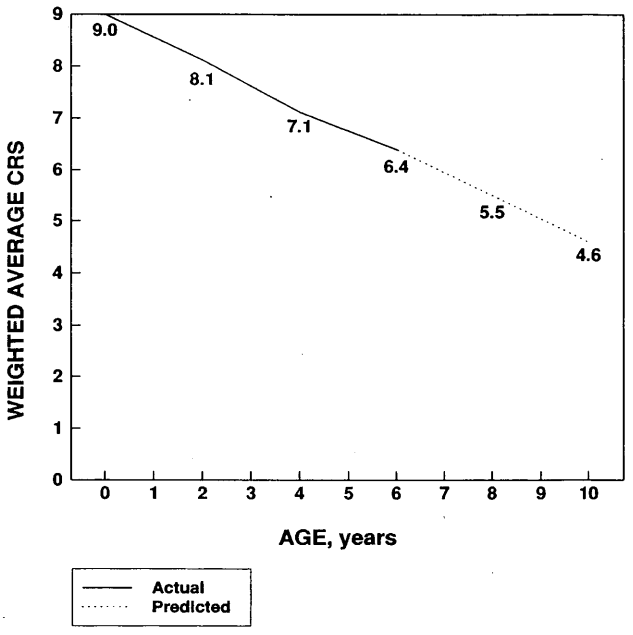

FIGURE 4 CRS values for SMART projects constructed in fiscal year 1987.

jects constructed in different years. The average 1992 CRS value for each fiscal year of construction is shown in Figure 5. The average decrease in CRS values per year is 0.4. Projecting a decrease of 0.4 per year, the average SMART project will not reach a critical CRS value of 4.5 for over 10 years. The average SMART project will reach a CRS value of 6.0 or less in 7 years, qualifying it for a second SMART rehabilitation.

Hence, both methods for predicting the average life of a SMART project indicate that a SMART rehabilitation should last 7 to 10

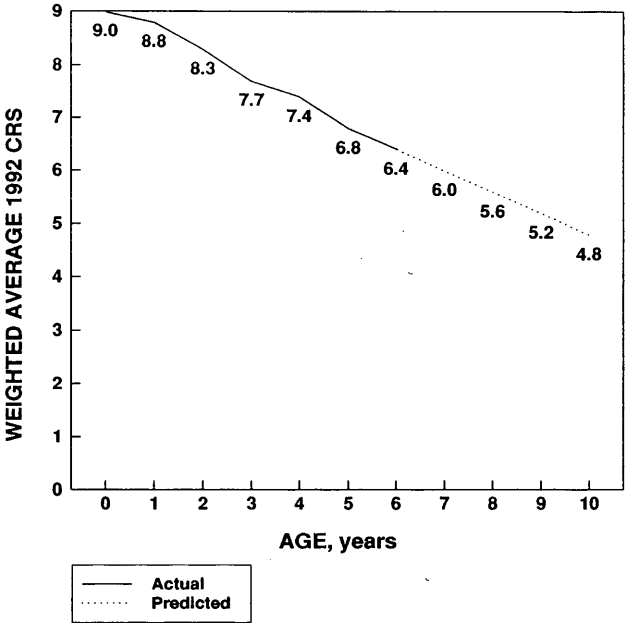

FIGURE 5 Weighted average 1992 CRS ratings for all SMART projects.

years. A project's life expectancy therefore exceeds IDOT's original expectation of 5 years. As more data become available, better estimates of long-term project performance will be made. It is clear at the present time, however, that the average SMART project is lasting longer than was anticipated.

Ride Quality

In addition to CRS values, ride quality, measured in International Roughness Indexes (IRI) and rut-depth measurements, can be used to evaluate the performance of the SMART projects.

In 1992, a report detailing the ride quality and rutting histories of selected SMART projects was published (*6*). Because IRI and rut-depths are now collected every other year, there were no new data to include at this time. No ride-quality data on these projects before rehabilitation are available either.

Figures 6 and 7, published in the 1992 report (*6*), are reproduced here. Figure 6 indicates that the IRI for SMART projects is not diminishing with age at this time. Figure 7 shows that increased rutting with age is minimal. As with the CRS values, the IRI and rut-depth measurement averages for projects were weighted by the length of road involved.

CONSTRUCTION COSTS

Bituminous-concrete overlay thicknesses on routes maintained by IDOT are determined by policy instead of structural design. Typically, a standard second-generation bituminous concrete overlay is 65 mm (2.5 in.) thick and the average cost per two-lane kilometer is approximately $110,000 ($175,000 per two-lane mile). It follows that a SMART overlay should cost significantly less than a standard overlay because the SMART overlay is thinner, requires minimal preparation work, and does not require any safety features, such as guardrails and shoulder improvements. At the start of the SMART program, it was expected that the average cost per two-lane kilometer would be $50,000 or less ($80,000 per two-lane mile).

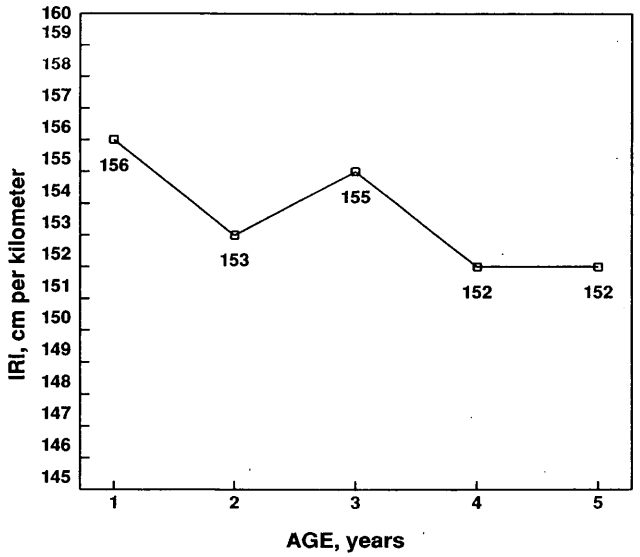

FIGURE 6 International roughness indexes of selected SMART projects.

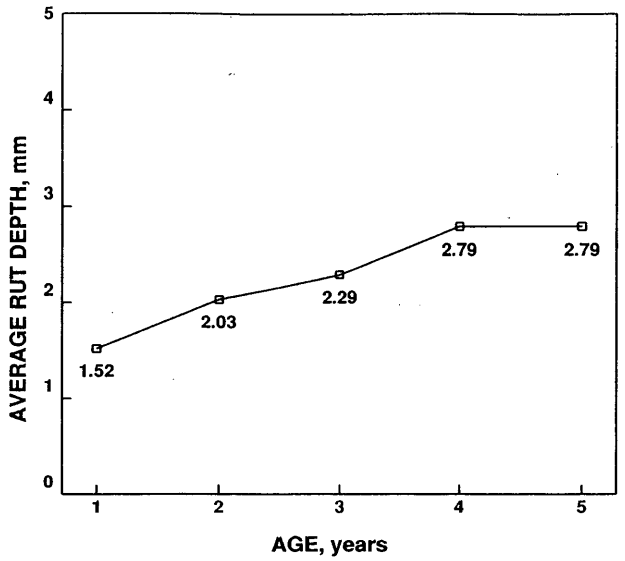

FIGURE 7 Average rut depths of selected SMART projects.

The average cost per two-lane kilometer has been calculated for each SMART project for the past 6 years. Each project's total cost was divided by surface length to determine the average project cost per two-lane kilometer. If a project had four lanes, the total project was divided by two times the length of the project. The statewide project cost for each fiscal year was then calculated by averaging all of the project costs. Figure 8 shows the average project costs for the past 6 fiscal years. Project costs for fiscal year 1993 are not included, because many of the projects were not yet complete when this paper was written.

Some fluctuation in the yearly averages was expected, but not to the extent shown in Figure 8. Further evaluation revealed that some of the average project costs were as high as $185,000 per two-lane kilometer ($300,000 per two-lane mile). Most of the projects that

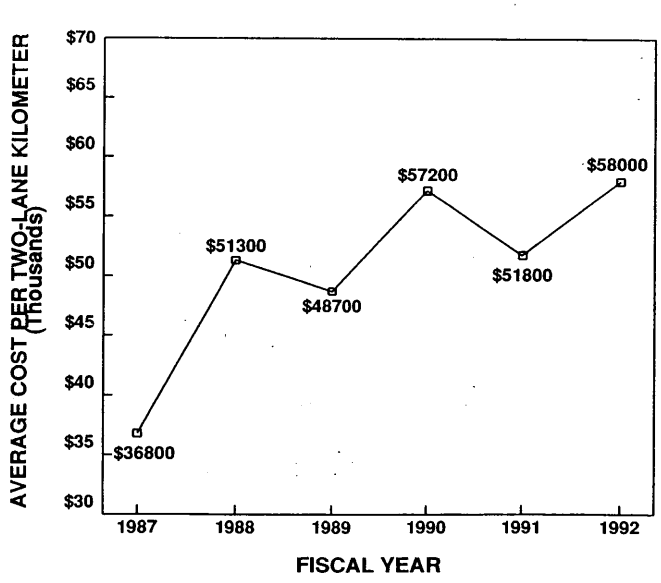

FIGURE 8 Average SMART project costs.

had high costs per two-lane kilometer were rehabilitations that included intersection work or patching of more than 10 percent of the surface area.

Originally, SMART was to include only rural highways that were structurally sound. In 1990 and 1992, however, several urban projects that required significant additional work were rehabilitated under the SMART program, and that is reflected in the high average project cost for both years. These types of projects should not be rehabilitated through the SMART program, but should be rehabilitated through standard rehabilitation policies. Figure 8 clearly illustrates why proper project selection is critical to a successful, cost-effective SMART program.

CONCLUSIONS

As Figure 2 indicates, more than 2,400 km (1,500 mi) of highway has been rehabilitated through the SMART program. Many of these kilometers probably would not have been rehabilitated under standard rehabilitation policies. Yet they have been rehabilitated under the SMART program at a minimal cost to IDOT, and the rehabilitations are lasting longer than was anticipated.

The highest average cost per two-lane kilometer is $58,000 ($93,000 per two-lane mile). For a standard second generation 65 mm (2.5 in.) thick overlay, the cost per two-lane kilometer is approximately $110,000 ($175,000 per two-lane mile). Through the SMART program, IDOT has realized a significant cost savings while not sacrificing the quality of the entire highway network.

Early success of the SMART program can be attributed to selection criteria and construction guidelines. Construction data collected to date indicate that construction guidelines are usually followed. Performance monitoring of the projects indicates that they are performing better than was expected: the average SMART project can be expected to last 7 to 10 years.

SMART is a cost-effective rehabilitation strategy for rural highways with low levels of traffic. It is not cost-effective for pavements that contain intersections, require extensive patching, or involve excessive secondary costs related to shoulder or drainage improvements, or thermoplastic paint striping.

RECOMMENDATIONS

On the basis of 7 years' experience with the SMART program, these recommendations are made:

- Only rural highways with multiple-unit truck traffic levels less than 500 should be considered for rehabilitation through the SMART program.
- Selection criteria should be followed when identifying projects for the SMART program.
- Construction guidelines should be followed to ensure a project's optimal performance.
- SMART should be continued because it is a viable rehabilitation alternative.

REFERENCES

1. Rajagopal, A. S., and K. P. George. Pavement Maintenance Evaluation. In *Transportation Research Record 1276,* TRB, National Research Council, Washington, D.C., 1990, pp. 62–68.
2. Hellnegel, E. J. *Second Generation Pavement Overlays. Final Report.* FHWA/NJ-86-013-7778. New Jersey Department of Transportation and FHWA, U.S. Department of Transportation, July 1987.
3. *Pavement Condition Rating Survey Distress Guide.* Illinois Department of Transportation, Office of Planning and Programming, Springfield, May 1988.
4. *Standard Specifications for Road and Bridge Construction.* Illinois Department of Transportation, Springfield, Oct. 1, 1983.
5. Mascunana, I. *An Evaluation of Engineering Fabric in Pavement Rehabilitation.* Report PRR-88. Illinois Department of Transportation, Bureau of Materials and Physical Research, Springfield, March 1981.
6. Reed, C. M. *Performance Evaluation of Single Pass Thin Lift Bituminous Overlays.* Report PRR-110. Illinois Department of Transportation, Bureau of Materials and Physical Research, Springfield, June 1992.

Publication of this paper sponsored by Committee on Characteristics of Bituminous-Aggregate Combinations To Meet Surface Requirements.

Effect of Moisture in Aggregates on Performance of Asphalt Mixtures

T. F. FWA AND B. K. ONG

A study was conducted to examine the effects of using aggregates with initial absorbed moisture during asphalt mixture production. On the basis of the moisture-absorption capacity of the granite aggregate studied, asphalt mixtures were prepared by using aggregates with five different initial moisture contents: 0 percent (oven-dried condition), 0.3 percent (corresponding to a so-called "air-dried" condition), 1.0 percent, 2.0 percent, and 3.5 percent (approximately saturated-surface-dry condition). Specimens were subjected to two different laboratory weathering treatments, namely a wetting-drying treatment and a heating-cooling treatment. Initial aggregate moisture contents were found harmful to the moisture-damage resistance of the mixture, but they did not significantly affect the performance of the mixtures exposed to the heating-cooling treatment in the absence of externally applied water. The addition of hydrated lime to the five mixtures substantially improved their moisture-damage resistance when subjected to the wetting-drying treatment, and its effectiveness was affected only marginally by the level of initial moisture content in the aggregate.

Moisture-related damage in asphalt pavements is a major distress form in Southeast Asian countries such as Indonesia, Malaysia, and Singapore. Problems with stripping and related moisture-induced damage have led to increasingly wider use of antistripping agents in the region since the early 1980s (*1–3*). Occurrence of moisture-induced distress during the initial years of pavement life, as well as in some newly constructed pavements, concerns the region's highway agencies. A possible contributing factor to the problem is the presence of damp aggregates during mixing. This paper presents the results of a laboratory study that examined how the performance of asphalt mixture would be affected by different levels of moisture present in the aggregates.

SCOPE OF STUDY

The study was conducted in three major parts. Part 1, an investigation of the moisture-absorption characteristics of the aggregates studied, established the range of moisture content to be considered. Part 2 was a test program involving five asphalt mixtures, each prepared with aggregates containing a different moisture content. The objective was to evaluate the effect of aggregate moisture content on the performance of asphalt mixtures. In Part 3, hydrated lime was added in the preparation of asphalt mixtures to study whether the effectiveness of antistripping additives would be affected by the use of damp aggregates.

In Part 2 and 3, the effects on the performance of asphalt mixtures were evaluated by examining the response of compacted specimens after two types of weathering treatment: a wetting-drying treatment to examine the moisture-damage resistance of different specimen types and a heating-cooling treatment to examine how moisture within the aggregates would affect the compacted specimens of asphalt mixture.

Crushed granite stones are practically the only source of aggregate used in asphalt pavement construction in Indonesia, Malaysia, and Singapore (*4*). It is the aggregate type investigated in this study. The asphalt mixtures specified for the wearing course of asphalt pavement in the three countries are basically the same: all are dense-graded mixtures with a nominal top aggregate size of 19 mm (3/4 in.). Penetration grade of the asphalt was 60/70. The binder content was 5.5 percent—the optimum asphalt content by weight of total mix as determined using the Marshall method of mix design (*5*). Aggregate gradation is presented in the following table.

Sieve Size (mm)	*Percent Passing*
19	100
13	95
9.5	90
6.4	77
3.2	58
1.2	37
0.3	19
0.075	6

PART 1: AGGREGATE MOISTURE STUDY

Most of the asphalt mixing plants in Southeast Asia use drum mixers (*6*). Practically all the plants in the region store aggregates (except for fillers) in open stockpiles before feeding them to cold feed bins. Characteristics of moisture condition of aggregates in the cold-feed bins of a mixing plant were evaluated.

Aggregate Moisture Contents at Mixing Plants

An assessment of the moisture condition of cold-feed aggregates for asphalt mixture production was made by sampling aggregates directly from the cold-feed bins of a mixing plant. The sampling for moisture determination was carried out twice per month for a period of 10 months. Figure 1 shows the time history of moisture-content variations for aggregates from four cold feed bins. Bin I contained aggregates smaller than 5 mm (3/16 in.). The sizes of aggregates in Bin II, III, and IV ranged from 5 to 14 mm (3/16 to 9/16 in.), from 14 to 20 mm (9/16 to 3/4 in.), and from 20 to 28 mm (3/4 to 1.125 in.), respectively.

In general, Figure 1 suggests that moisture content of cold-feed aggregates increases as aggregate size decreases. The moisture content of aggregates in Bin I was significantly higher than those in other bins. The higher moisture content could be attributed to the

Center for Transportation Research and Department of Civil Engineering, National University of Singapore, 10 Kent Ridge Crescent, Singapore 0511.

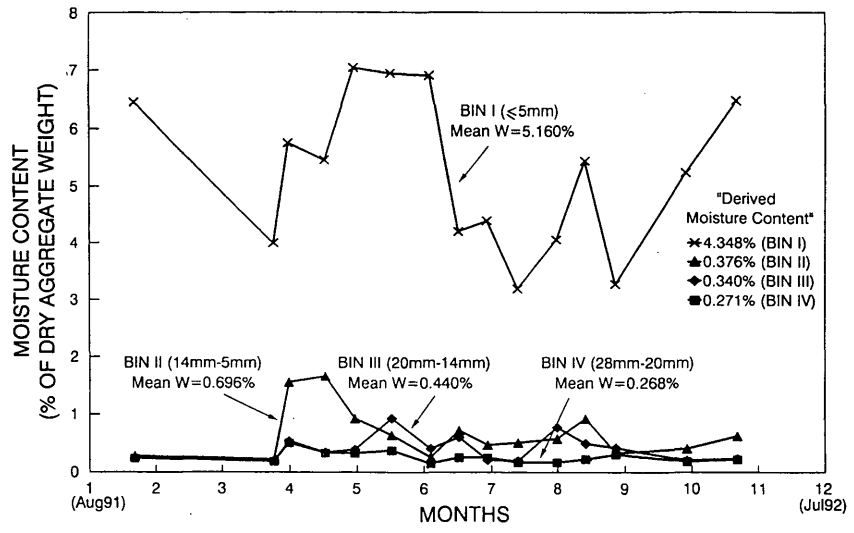

FIGURE 1 Moisture contents of cold-feed aggregates at mixing plant over 10 months.

ability of the particles of smaller aggregates to attract moisture to their surface because of their relatively high surface-area/volume ratios.

Also indicated in Figure 1 is the so-called "derived moisture content" of the aggregates in each bin. Derived moisture contents were computed in the following manner: (a) the moisture content at full saturation of aggregate for each of the size designations shown in Table 1 was first determined in accordance with ASTM test method C566 (*7*); (b) the size distribution of the aggregates in each bin was determined; (c) the derived moisture content of the aggregates in each bin was computed on the basis of the size distribution and assumption that all aggregate particles were fully saturated. Comparison of the computed derived moisture contents with the actual moisture contents suggests that the cold-feed aggregates were close to full saturation most of the time. The larger difference between the computed and actual moisture contents for smaller aggregate sizes was likely the result of trapped surface water.

Drying Characteristics of Aggregates

No attempt was made to simulate the drying process of aggregates in a mixing plant. A simple drying experiment, however, was useful in illustrating the differences in drying characteristics of aggregates of different sizes. Aggregates of size designations 25 mm, 9.5 mm, and 1.2 mm (see Table 1) were studied. The aggregates, in quantities as required by the ASTM test method C566 (*7*), were first soaked in water for 24 hr to achieve full saturation. The saturated-surface-dry aggregates were next placed in an oven maintained at 110°C. The loss of moisture with time was monitored and the results plotted (see Figure 2).

The drying curves in Figure 2 highlight that the larger the size of an aggregate, the longer it took to dry the aggregate. It can be seen from the figure that complete drying of 1.2-mm aggregates (sieve size number 16) was achieved in slightly less than an hour, 9.5-mm (3/8-in.) aggregates in about 7 hr, and 25-mm aggregates in about 15 hr. This finding concurs with Lottman's observation (*8*), "If the dryer retention time is too short, the internal temperature of large particles will remain relatively cool and the moisture in deep pores will not be vaporized."

Choice of Moisture-Content Range for Study

To cover the complete range of possible aggregate moisture contents in mixing, aggregate moisture conditions varying from oven dried to saturated-surface-dry were included. The saturated-surface-dry state was achieved by soaking in water for 24 hr. Particles finer

TABLE 1 Aggregate Sizes for Moisture Content Determination

Size Designation	Size Grouping		Minimum Quantity Needed (kg)
	Passing Sieve Size	Retained on Sieve Size	
25 mm	38 mm	25 mm	4.0
19 mm	25 mm	19 mm	3.0
13 mm	19 mm	13 mm	2.0
9.5 mm	13 mm	9.5 mm	1.5
6.4 mm	9.5 mm	6.4 mm	1.0
3.2 mm	6.4 mm	3.2 mm	0.5
1.2 mm	3.2 mm	1.2 mm	0.5
Fines	1.2 mm	--	0.5

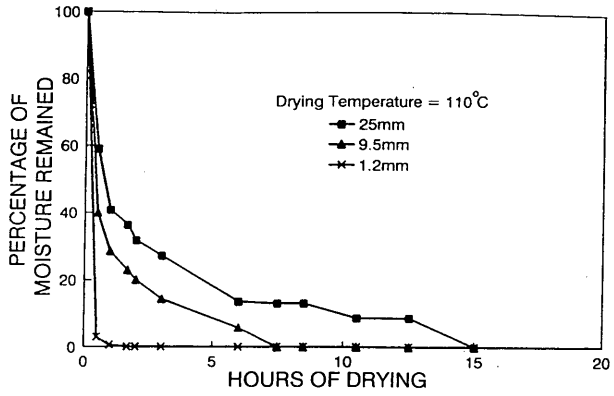

FIGURE 2 Drying characteristics of fully saturated granite aggregates.

than 0.15 mm were not included in the soaking treatment because of difficulty in handling them and the need to prevent loss of dust. Therefore the scope of study was restricted to the moisture effects of particles larger than 0.15 mm. Because fine particles dry much more rapidly than coarser aggregates, this limitation is not a major shortcoming.

There was a need to determine the moisture content at or close to saturated-surface-dry condition so that the same moisture content was used for repeated specimens. The moisture content was determined after soaking, for 24 hr. First, aggregates with sizes proportioned according to Table 1 were surface dried with a piece of absorbent cloth to bring about a resultant moisture content slightly more than 3.5 percent (expressed as percent of total dry-aggregate weight, including the fines not soaked). By drying the aggregate under a fan, the moisture content could be brought to 3.5 percent, which was selected as the convenient upper moisture limit for this study. Moisture contents of 2 percent and 1 percent were achieved by subjecting the aggregates to longer periods of drying after soaking for 24 hr.

Oven-dried aggregates, a standard requirement in laboratory preparation of asphalt mixtures, were used to produce specimens for purpose of comparison. In addition, specimens were also prepared by using aggregates that were stored in the laboratory for more than 3 months and had reached a stable air-dried moisture condition. These aggregates gave a total moisture content of 0.3 percent for the blend of aggregate mix specified in the in-text table.

PART 2: STUDY OF ASPHALT MIXTURES WITHOUT ANTI-STRIPPING AGENT

Specimen Preparation

Five sets of 18 Marshall-size specimens were prepared, each 102 mm (4 in.) in diameter and approximately 64 mm (2.5 in.) in height. The first set of 18 specimens was prepared using oven-dried aggregates and was mixed and compacted in accordance with the ASTM test method D1559 (*9*). The remaining four sets of specimens were prepared using the same mixing and compaction procedure, except that the overall aggregate moisture content at mixing was 0.3 percent (air-dried condition), 1 percent, 2 percent, and 3.5 percent, respectively.

Weathering Treatments

Two types of weathering treatment were used. The first type subjected the test specimens to alternating wetting and drying in a "weathering chamber." Operating features of the chamber are detailed elsewhere (*10*). It is essentially a moisture treatment to induce moisture damage in the specimens treated; its objective is to compare the moisture-damage resistance of specimens prepared with aggregates of different moisture contents. Wetting of the specimens was achieved by spraying tap water, at about 28°C, through shower heads positioned in the chamber. Drying was effected by heat from ceramic heaters once the spraying water was cut off. Previous experience with the chamber (10) has indicated that a moisture treatment consisting of 150 cycles of 4 hr each (2 hr of wetting and 2 hr of drying per cycle) produces the best results for assessing moisture damage. The recommendation was followed for this study.

The second type of treatment subjected test specimens to alternating heating and cooling in an oven. This test was conducted to examine how different sets of specimens respond to thermal treatment in the absence of externally applied moisture. Figure 3 shows the temperature range of thermal cycles applied in the heating-cooling treatment. A total of 150 cycles was applied per treatment.

Methods of Evaluation

The resilient modulus M_r and the indirect tensile strength T_s were adopted as the basis for assessing the relative performance of the five sets of specimens. M_r was determined according to the procedure outlined in ASTM test method D4123 (*11*) using a load of 1.6 kN (0.36 kip) applied at a frequency of 1 Hz and with loading duration equal to 400 msec. T_s was determined by using a rate of loading of 50.8 mm/min (2 in./min).

Figure 4 gives the sequence of tests in the experimental program. Each set of 18 specimens was first tested for resilient modulus. They were arranged in either decreasing or increasing order by their magnitudes of resilient modulus. The first three specimens were randomly assigned one each to groups A, B, and C. The next three specimens were randomly assigned to the three groups, and so on. The random assignment was repeated until all 18 specimens were assigned. This process represented an effort to distribute the specimens to achieve a fair comparison of $(T_s)'_B$ or $(T_s)'_C$ with $(T_s)'_A$.

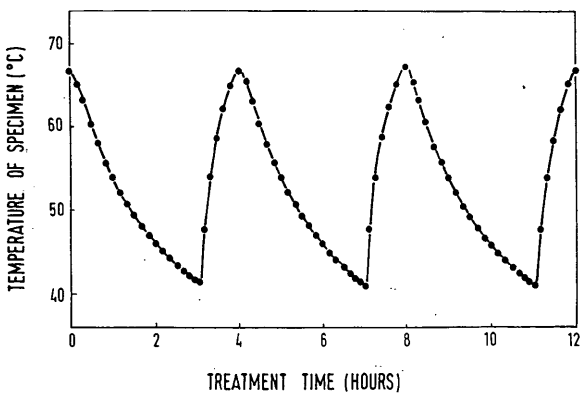

FIGURE 3 Specimen surface temperature variations during heating-cooling treatment.

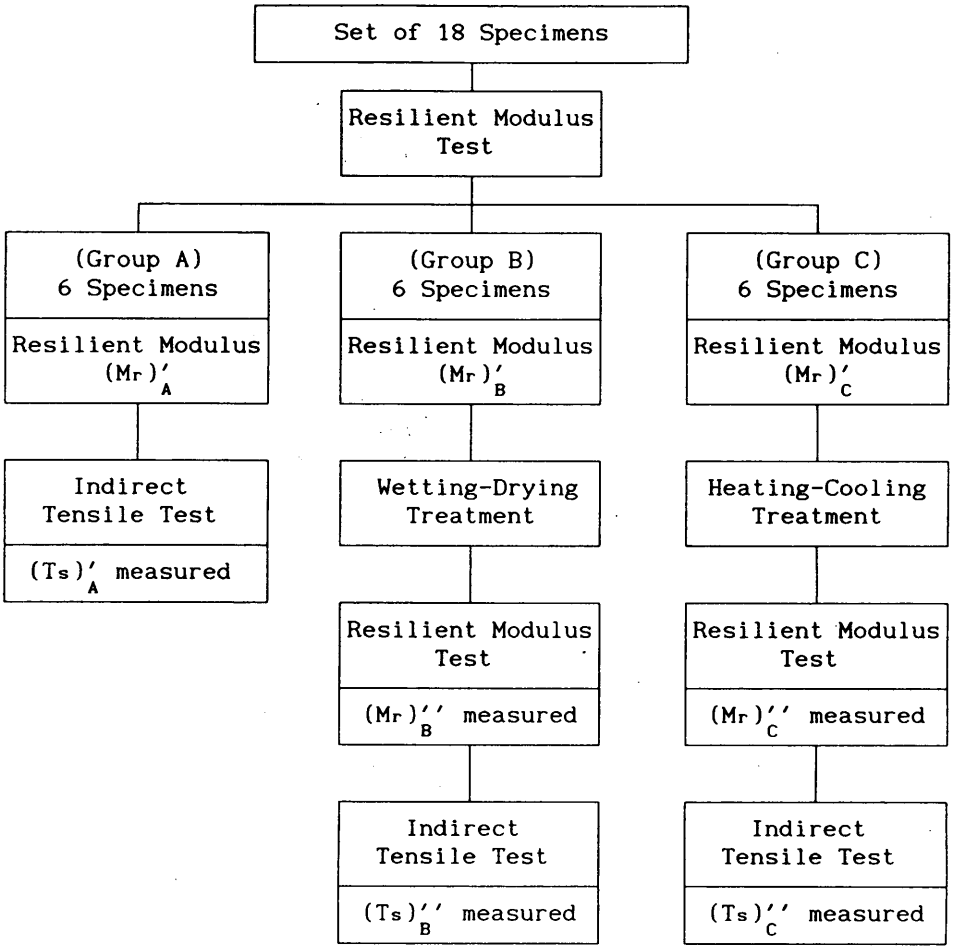

FIGURE 4 Test program for each set of 18 specimens.

After the assignment process, Group A specimens were tested for their indirect strength. The other two groups of specimens were subjected to a weathering treatment each, the wetting-drying treatment for Group B and the heating-cooling treatment for Group C. After the respective weathering treatments, all specimens of the two groups were tested for resilient modulus before their indirect tensile strength was measured.

Analysis of Test Results

Basis of Comparison

The performance of test specimens was evaluated by means of the following three procedures: (a) comparison based on compacted density d, resilient modulus M_r, and indirect tensile strength T_s of specimens without any weathering treatment; (b) comparison based on changes in M_r and T_s of specimens after wetting-drying treatment; and (c) comparison based on changes in M_r and T_s after heating-cooling treatment.

For procedures (b) and (c), comparisons were made using after-to-before ratios of M_r or T_s defined as:

$$\text{Percentage resilient modulus retained, } R(M) = \frac{\text{Resilient modulus of specimen after weathering treatment}}{\text{Resilient modulus of specimen before weathering treatment}} \times 100\% \quad (1)$$

$$\text{Percentage indirect tensile strength retained, } R(T) = \frac{\text{Average } T_s \text{ of 6 specimens after weathering treatment}}{\text{Average } T_s \text{ of 6 specimens without weathering treatment}} \times 100\% \quad (2)$$

$R(M)$ as defined in Equation 1 applies to $(M_r)'_B$ and $(M_r)''_B$, or $(M_r)'_A$ and $(M_r)''_A$. $R(T)$ as defined in Equation 2 applies to $(T_s)'_A$ and $(T_s)''_B$, or $(T_s)'_A$ and $(T_s)''_C$ (see Figure 4).

Effect on Properties of Compacted Specimens

Test results shown in Figure 5 compare the mean density, resilient modulus, and indirect tensile strength of different specimens. Each mean density or resilient modulus represents the mean of 18 specimens, whereas each mean indirect tensile strength represents the mean of 6 specimens.

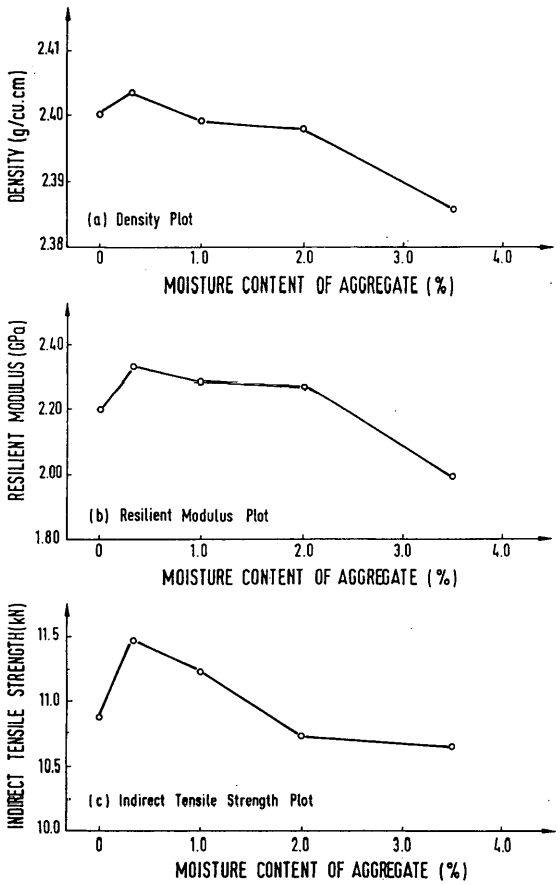

FIGURE 5 Effect of aggregate moisture content on properties of compacted specimens.

Density of Compacted Specimens Figure 5(a) shows that only marginal differences were found among the mean compacted densities of the five different specimen types. Although the air-dried specimens had the highest mean compacted density, and the specimens with moisture content w 5 3.5 percent had the lowest, these differences were not statistically significant at a 95 percent confidence level.

Resilient Modulus of Compacted Specimens The M_r values in Figure 5 (b) have an interesting trend, showing a peak at aggregate moisture content close to the air-dried condition of 0.3 percent. The difference in resilient modulus values between the air-dried and oven-dried conditions or between the air-dried and 3.5-percent moisture condition was statistically significant at a 95 percent confidence level. For aggregate moisture content exceeding the optimal value, resilient modulus shows a decreasing trend as aggregate moisture increased.

Indirect Tensile Strength of Compacted Specimens As illustrated in Figure 5(c), the plot of mean T_s exhibits the same trend as that observed for M_r. An optimal aggregate moisture content close to the air-dried condition of 0.3 percent was again observed. Statistically, the difference between the peak strength and that at oven-dried or 3.5 percent moisture condition was significant at a 95 percent confidence level.

Effect on Performance of Mixtures Subjected to Wetting-Drying Treatment

Figure 6(a) summarizes the test results in terms of $R(M)$ and $R(T)$ defined in Equations 1 and 2, respectively.

It can be seen from Figure 6(a) that the five mixture types tested were affected to different extents by the treatment. In terms of $R(M)$, specimens of the oven-dried condition were the least affected, followed by those of the air-dried condition. There was a sharp drop in the percentage M_r retained for specimens with aggregate moisture content higher than the air-dried condition. The percentage M_r retained was only 55 percent when the aggregate moisture content was 3.5 percent.

Figure 6(a) plots the test results in terms of $R(T)$. The results display essentially the same pattern of changes as observed for $R(M)$. Similar conclusions as those made in the preceding paragraph can be drawn.

Effect on Performance of Mixtures Subjected to Heating-Cooling Treatment

Figure 6(b) shows that with the heating-cooling treatment, the response of specimens in terms of $R(M)$ and $R(T)$ exhibited a different trend from that shown in Figure 6(a). The treatment led to gains in both resilient modulus and indirect tensile strength. Specimens prepared with aggregates of higher moisture content were found to register higher percentage gains. This trend was especially pro-

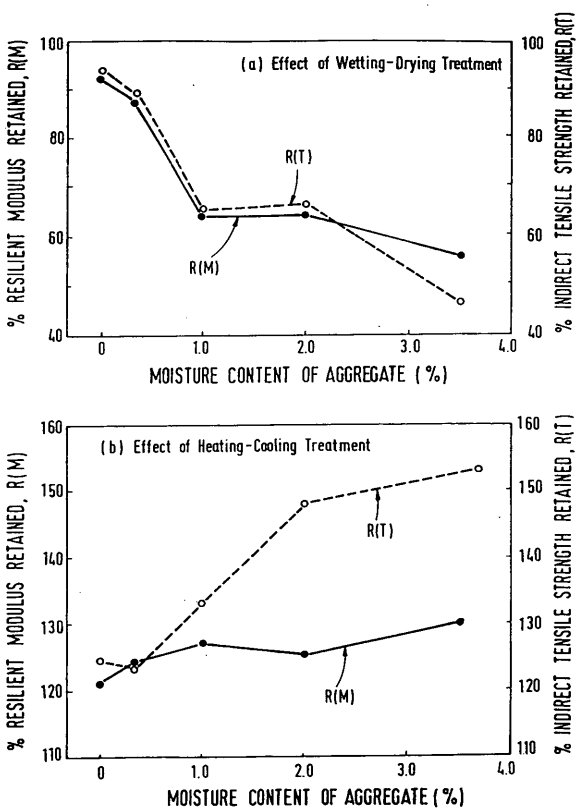

FIGURE 6 Effects of laboratory weathering treatments on specimens without lime.

nounced in the case of $R(T)$, the percentage of indirect tensile strength retained.

PART 3: EFFECT ON ASPHALT MIXTURE WITH HYDRATED LIME ADDED

Hydrated lime was selected as the additive for the simple reason that it was easily available and that it had been widely recognized as an effective agent to increase the resistance of asphalt mixtures to moisture damage (*12–14*). Being in powder form instead of in liquid or slurry form, it suited the purpose of the present study by not altering the moisture content of the aggregates, thus allowing easier interpretation of the test results. On the basis of previous work on the use of hydrated lime (*3,14,15*), a dosage equal to 1.5 percent by weight of total aggregate was adopted.

Specimen Preparation

Five sets of 18 Marshall-size specimens were needed, and the aggregates were treated in the same manner as in Part 2 of the study to produce the following five different moisture conditions: 0 percent (oven-dried condition), 0.3 percent (air-dried condition), 1 percent, 2 percent, and 3.5 percent of total aggregate by weight. Specimens were next prepared by mixing the correct amount of hydrated lime with aggregates before asphalt was added. The subsequent mixing and compaction procedure was identical to that performed in Part 2 of the study.

Weathering Treatments

As in Part 2, wetting-drying and heating-cooling treatments were applied to test specimens according to the experimental program shown in Figure 4. The objective of the wetting-drying treatment was to study how different initial moisture contents of aggregates would affect the effectiveness of the anti-moisture-damage action of hydrated lime. The objective of the heating-cooling treatment was to examine how the performance of asphalt mixtures with hydrated lime, when subjected to thermal treatment in the absence of water, would be affected by the initial moisture content of aggregates.

Methods of Evaluation

The resilient modulus test and indirect tensile test were again used to provide the quantitative basis for evaluation. The comparison of before- and after-treatment properties is again made in terms of $R(M)$ and $R(T)$, as is illustrated in Figure 4.

Analysis of Test Results

Effect on Properties of Compacted Specimens

The properties of compacted specimens with hydrated lime added are plotted in Figure 7. Comparison of the plots in this figure with those in Figure 5 shows that the shapes of corresponding curves are similar. The compacted specimen density peaked at moisture content close to the air-dried condition of 0.3 percent and decreased as the moisture content of the aggregate increased. This trend of variation was also repeated when resilient modulus or indirect tensile strength was considered as shown in Figure 7. Little difference existed between the corresponding properties of specimens with and without hydrated lime; any difference was statistically insignificant at a 95 percent confidence level.

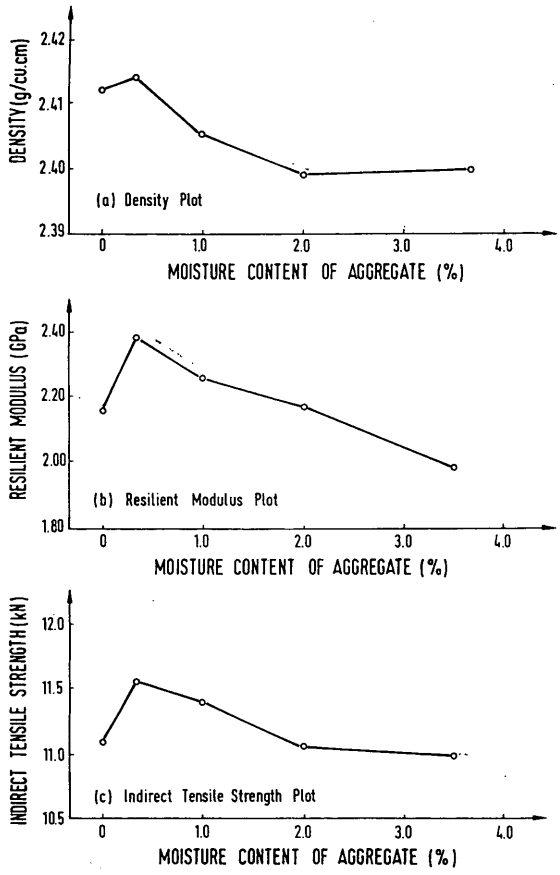

FIGURE 7 Effect of aggregate moisture content on properties of compacted specimens with lime added.

Effect on Performance of Hydrated Lime-Treated Mixtures Subjected to Wetting-Drying Treatment

Tests carried out in Part 2 indicated that the wetting-drying treatment caused deterioration of both M_r and T_s of test specimens. Figure 8(a) shows a distinctly different response from hydrated lime-treated specimens. Instead of some reductions in the values of M_r and T_s, addition of hydrated lime had in fact led to increases in both properties. These results verify the antistripping property of hydrated lime as an additive to asphalt mixtures. Considering the effect of the moisture content of aggregate in terms of $R(M)$ and $R(T)$, it is interesting to note that the trends observed in Figure 6(a) are also found in Figure 8(a)—that is, $R(M)$ and $R(T)$ of the specimens subjected to the wetting-drying treatment decreased as the moisture content of aggregate increased. In short, the effectiveness of hydrated lime as an antistripping agent was reduced when moisture existed in the aggregate.

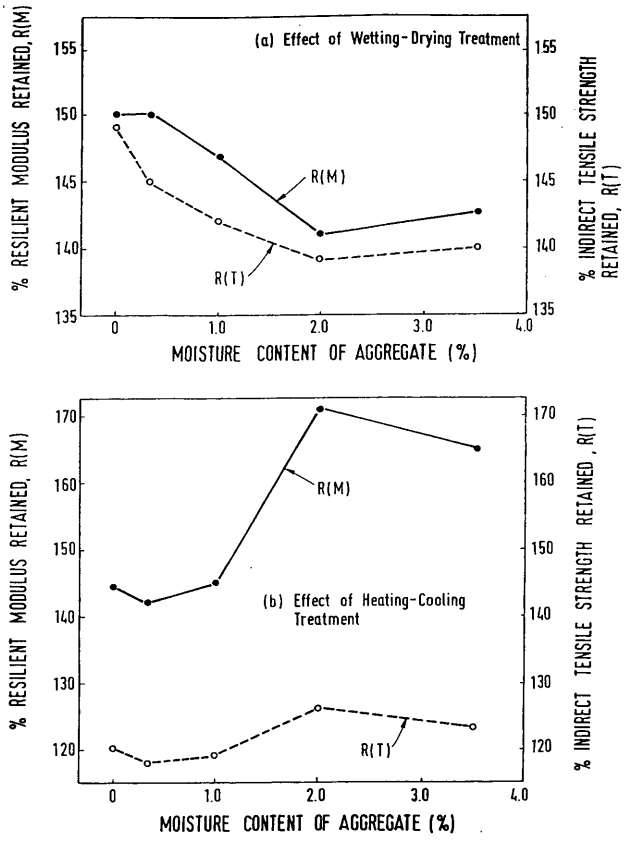

FIGURE 8 Effect of laboratory weathering treatments on specimens with lime added.

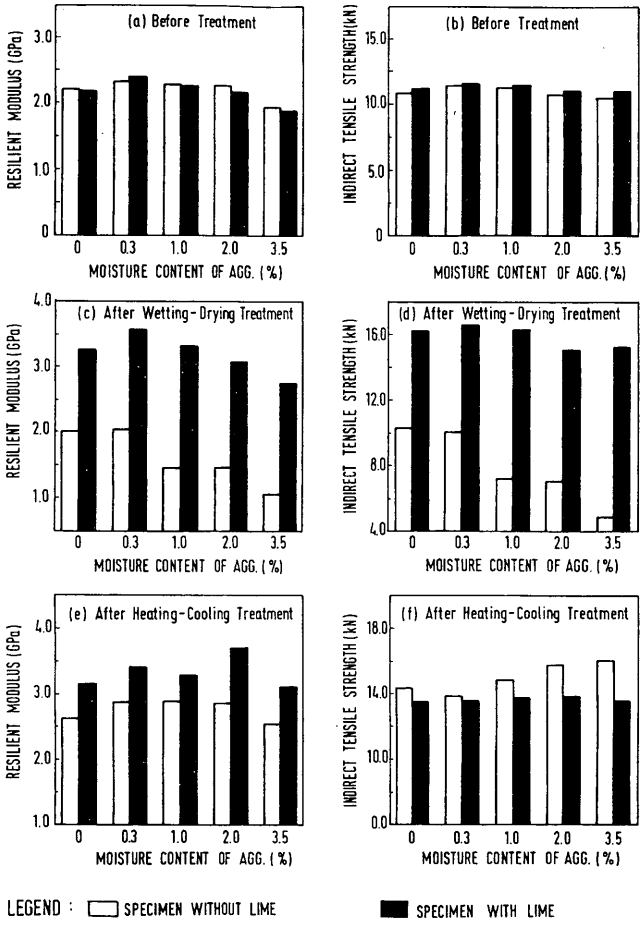

FIGURE 9 Comparison of performance of specimens with and without hydrated lime added.

Effect on Performance of Hydrated Lime-Treated Mixtures Subjected to Heating-Cooling Treatment

The heating-cooling treatment used in Part 2 was found to improve M_r and T_s of test specimens (Figure 6), and the percentage gain increased with the moisture content of aggregate. Figure 8(b) shows that these trends were retained for hydrated lime-added specimens. One difference, however, can be observed: $R(T)$ was considerably higher than $R(M)$ for specimens without lime, whereas the reverse was true for specimens with hydrated lime.

RESPONSE COMPARISON OF SPECIMENS WITH AND WITHOUT HYDRATED LIME

Figure 9 presents a comparison of the performance of specimens with and without hydrated lime to highlight the effect of hydrated-lime addition, and the influence of aggregate moisture. Figure 9 (a) and (b) illustrate an earlier conclusion that there were no significant differences in resilient modulus M_r and indirect tensile strength T_s between the as-compacted specimens of the two types of asphalt mixtures. For both types of specimens, the use of aggregates with moisture content exceeding the air-dried condition appeared to have caused some loss in M_r and T_s.

Figure 9 (*c*) and (*d*) highlight several aspects of specimen behavior with respect to moisture damage. The superiority of the anti-moisture damage property of the hydrated lime-added specimens was clearly demonstrated. The plots show that, regardless of the type of specimen, higher moisture content of aggregate resulted in lower M_r and T_s. However, the effect of excess moisture content in aggregate appeared to be more severe in specimens without hydrated lime than in specimens with hydrated lime.

For specimens subjected to the heating-cooling treatment, the effects of hydrated lime and aggregate moisture were less easily understood. Figure 9(*e*) shows that hydrated lime-added specimens achieved higher gains in M_r than specimens without hydrated lime, but Figure 9(*f*) indicates that this was not the case for T_s. Figure 9(*f*) also indicates that after receiving the heating-cooling treatment, specimens with higher aggregate moisture ended up with higher T_s, a trend that was not found in Figure 9 (*e*) for M_r.

SUMMARY OF FINDINGS

Fed from open stockpiles, cold-feed bin aggregates in Southeast Asia had moisture contents very close to full saturation, practically throughout the year. The moisture content of aggregates increased as the size of aggregate decreased.

Although higher in moisture content, smaller-size aggregates lost their absorbed moisture faster than bigger size aggregates upon

heating. Residue-absorbed moisture is a more likely problem with bigger-size aggregates.

For the crushed granite aggregate studied, an aggregate moisture content close to the air-dried moisture content of 0.3 percent was optimal for producing the highest compacted density, resilient modulus M_r and indirect tensile strength T_s of the dense-graded mixture tested. Beyond this moisture level, lower values of the three properties were obtained as aggregate moisture content increased.

Adding hydrated lime to aggregates had insignificant effects on the as-compacted density, resilient modulus, and indirect tensile strength of the dense-graded mixture.

The positive effect of adding hydrated lime was most pronounced with respect to moisture-induced damage. Whereas specimens without hydrated lime deteriorated in terms of M_r and T_s after wetting-drying treatment, all test specimens with hydrated lime gained in both M_r and T_s after the same treatment. This beneficial effect of hydrated lime, however, tended to decrease as the aggregate moisture content increased.

Heating-and-cooling treatment had the effect of increasing the M_r and T_s of test specimens, whether or not hydrated lime was added. For both types of specimens, those prepared from aggregates with higher moisture content achieved a higher percentage increase in M_r and T_s.

CONCLUSIONS

On the basis of the findings of this study, the following conclusions may be drawn with respect to the effect of residue moisture in the aggregate:

- A small amount of residue moisture content in the aggregate, close to the aggregate's equilibrium moisture content in the operating ambient condition in the present study, was found to produce enhanced performance as compared with the asphalt mixtures prepared using oven-dried aggregate. This applied to specimens with or without hydrated lime.
- Aggregates with high residue moisture (more than 0.3 percent for the granite aggregate studied) significantly weakened the moisture damage resistance of the asphalt mixture. The moisture damage resistance of the mixture dropped as the residue aggregate moisture content increased.
- Adding hydrated lime was effective in improving the moisture damage resistance of the asphalt mixtures studied. The effectiveness of the antistripping agent was only marginally affected by the presence of excess residue moisture content in the aggregate.
- Use of aggregates with residue moisture did not appear to impair the performance of the asphalt mixture when subjected to heating-cooling treatment without the presence of externally applied water.

REFERENCES

1. Lee, S. K., and K. T. Lim. The Effect of Anti-Stripping Additives on the Properties of Bituminous Mixes. Project Report T2-83/84. Department of Civil Engineering, National University of Singapore, 1984.
2. Ramaswamy, S. D. Durability of Flexible Road Surfacings. *Proc., International Seminar on Transportation Engineering and Management for Developing Countries,* Singapore, April 23–25, 1987, pp. 135–142.
3. Wong, S. W. A Study on the Performance of Bitumen Blended with Hydrated Lime. Project Report T1-84/85. Department of Civil Engineering, National University of Singapore, 1985.
4. Fwa, T. F. Asphalt Hot-Mix Production Practice in Four ASEAN Countries. *Proc., Symposium on Pavement Construction and Maintenance Practice,* Singapore, March 31–April 1, 1993, pp. 2.1–2.13.
5. *Mix Design Methods for Asphalt Concrete and Other Hot-Mix Types,* Manual Series MS-1, 5th ed., Asphalt Institute, 1983.
6. Cham, T. S. Characteristics of Asphalt Mixing Plants in Four ASEAN Countries. *Proc., Symposium on Pavement Construction and Maintenance Practice,* Singapore, March 31–April 1, 1993, pp. 3.1–2.14.
7. ASTM Test Method C566, Standard Test Method for Total Moisture Content of Aggregate by Drying. *Annual Book of ASTM Standards,* Vol. 04.02, ASTM, 1991.
8. Lottman, R. P. Aggregate Heating and Drying Variations in Asphalt Plants. *Proc., Association of Asphalt Paving Technologists,* Vol. 30, 1961, pp. 120–131.
9. ASTM Test Method D1559, Standard Test Method for Resistance to Plastic Flow of Bituminous Mixtures Using Marshall Apparatus. *Annual Book of ASTM Standards,* Vol. 04.03, ASTM, 1991.
10. Fwa, T. F., and T. S. Ang. Effects of Moisture on Properties of Asphalt Mixes in Wet Tropical Climate—A Laboratory Study. In *Transportation Research Record 1417,* TRB, National Research Council, Washington, D.C., 1993.
11. ASTM Test Method 4123, Test Method for Indirect Tensile Test for Resilient Modulus of Bituminous Mixtures. *Annual Book of ASTM Standards,* Vol. 04.03, ASTM, Philadelphia, Pa., 1991.
12. Taylor, M. A., and N. P. Khosla. Stripping of Asphalt Pavements: State of the Art. In *Transportation Research Record 911,* TRB, National Research Council, Washington, D.C., 1983, pp. 150–158.
13. Kennedy, T. W. Prevention of Water Damage in Asphalt Mixtures. ASTM Special Technical Publication STP 899, ASTM, Philadelphia, Pa., 1985, pp. 119–133.
14. Button, J. W. Maximizing the Beneficial Effects of Lime in Asphalt Paving Mixtures. ASTM Special Technical Publication STP No. 899, ASTM, Philadelphia, Pa., 1985, pp. 134–146.
15. Gardiner, M. S., and J. Epps. Four Variables Affecting the Performance of Lime in Asphalt-Aggregate Mixtures. Presented at the 70th Annual Meeting of the Transportation Research Board, Washington D.C., 1992.

Publication of this paper sponsored by Committee on Characteristics of Bituminous-Aggregate Combinations To Meet Surface Requirements.

Field and Laboratory Investigation of Stripping in Asphalt Pavements: State of the Art Report

PRITHVI S. KANDHAL

Stripping of hot mix asphalt (HMA) pavements appears to have become a major problem in recent years. More and more states are specifying the use of antistripping agents. There is a need to investigate and identify the problem properly so that decisions are not made solely on the basis of observation of isolated distress areas. External factors and in-place properties of HMA pavements can induce their premature stripping. Contributing factors, such as inadequate pavement drainage, inadequate compaction of HMA pavement, excessive dust coating on aggregate, inadequate drying of aggregate, and overlays on concrete pavements, are described. Suggestions for alleviating the problems associated with these factors are given, and an investigative methodology based on forensic experience is recommended for use by the specifying agencies and industry that want to establish whether stripping is a problem either on a specific project or statewide. Current practices of using laboratory moisture-susceptibility tests across the United States are reviewed and the AASHTO T283 (Modified Lottman) test method is recommended for use until more suitable and reliable tests are developed and validated.

Stripping of hot mix asphalt (HMA) pavements appears to have become a major problem in recent years. Stripping can result prematurely from poor subsurface drainage (causing excessive moisture in the pavement structural layers), use of weak and friable aggregates (fracturing during construction and subsequently in service exposing uncoated surfaces), excessive dust coating around the aggregates, and very poor compaction of the HMA mat during construction.

Every year more and more states are specifying the use of antistripping (AS) agents. There is a need to investigate and identify the problem properly so that decisions are not made simply on the basis of observation of isolated distress areas. Within states that have started to specify AS agents, the proliferation of specifications and test methods is great. Different test methods, such as immersion-compression, boiling water, Texas pedestal, Lottman, modified Lottman, and Tunnicliff-Root, are specified, usually with some variations. Different acceptance criteria are used for the same test method. This study was undertaken, in part, to make recommendations for a viable, common strategy.

OBJECTIVES

- List and discuss factors that can induce premature stripping in HMA pavements;
- Recommend a field investigative methodology that can be used by the specifying agencies and industry to establish stripping as a problem on a specific project or statewide;
- Review current laboratory test methods used by various agencies for determining the stripping potential of HMA mixtures and make recommendations for a common strategy on test methods and criteria.

National Center for Asphalt Technology, 211 Ramsay Hall, Auburn University, Ala. 36849–5354.

FACTORS RESPONSIBLE FOR INDUCING PREMATURE STRIPPING

Figure 1 shows the estimated percentage of HMA pavements experiencing moisture related distress in the United States according to a 1989 survey of state departments of transportation (*1*). Research conducted at the National Center for Asphalt Technology (NCAT) under the SHRP A-003B Project has shown that physico-chemical surface properties of mineral aggregates are more important to moisture-induced stripping than the properties of asphalt cement binder. Some mineral aggregates are inherently very susceptible to stripping. However, in many cases, external factors or in-place properties of HMA pavements induce stripping prematurely in HMA pavements. Knowledge of these factors is essential to investigating and solving the stripping problem. A discussion of these factors follows.

Inadequate Pavement Drainage

Inadequate surface or subsurface drainage produces water or moisture vapor, the necessary catalyst to induce stripping. If excessive water or moisture is present in the pavement system, HMA pavement can strip prematurely. Kandhal et al. (*2*) have reported case histories in which stripping was not a general phenomenon occurring on an entire project but instead a localized phenomenon in areas of the project that were over-saturated with water or water vapor because of inadequate subsurface drainage.

Water can enter HMA pavement layers in different ways. It can enter as run-off through the road surface, particularly through surface cracks. It can enter from the sides and bottom as seepage from ditches or a high water table in the cut areas.

Water commonly moves upward by capillarity from under a pavement. Above the capillary fringe, water moves as a vapor. Many subbases or subgrades in the existing highway system lack the desired permeability and, therefore, are saturated with capillary moisture. The construction of multilane highways, the widening of existing roads, in addition to gentler slopes and milder curves in all kinds of terrain, compound the subsurface-drainage problem. Doubling a road's width, for example, makes drainage about four times as difficult as before (*3*). Quite often, a four-lane highway is

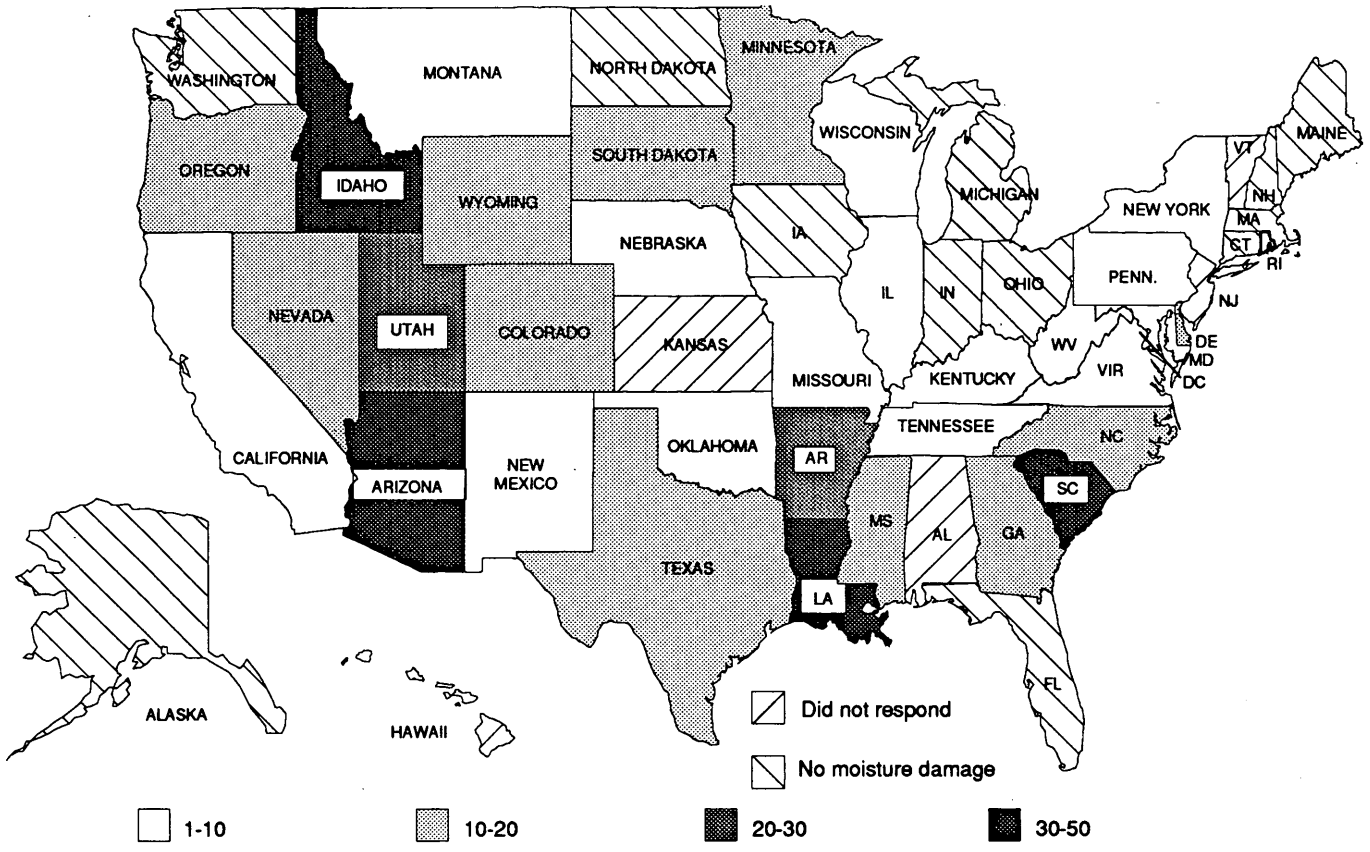

FIGURE 1 Estimated percentage of pavements experiencing moisture-related distress (*1*).

rehabilitated by paving the median and shoulders with HMA, resulting in a fully paved width of 72 to 78 ft. The new surface is equivalent to that of a six-lane highway, without any increase in subsurface drainage capacity (*2*).

Extensive research conducted at the University of Idaho (*4*) on the mechanism of asphalt stripping indicates "air voids in asphalt concrete may become saturated with water, even from vapor condensation due to water in the subgrade or subbase. A temperature rise after this saturation can cause expansion of the water trapped in the mixture voids, resulting in significant void pressure when the voids are saturated. It was found that void water pressure may develop to 138 kPa (20 psi) under differential thermal expansion of the compacted asphalt mixture and could exceed the adhesive strength of the binder-aggregate surface. If asphalt concrete is permeable, water could flow out of the void spaces under the pressure developed by the temperature rise and, in time, relieve the pressure developed. If not, then the tensile stress resulting form the pressure may break adhesive bonds and the water could flow around the aggregates causing stripping. The stripping damage due to void water pressure and external cyclic stress (by traffic) mechanism is internal in the specimens, the exterior sides of the specimens do not show stripping damage unless opened up for visual examination."

Majidzadeh and Brovold (*5*) also have stated that pore pressure from stresses induced by traffic can cause the failure of the binder-aggregate bond. Initially, traffic stresses may further compact the mixture and trap or greatly reduce the internal water drainage. Therefore, the internal water is in frequent motion (cyclic), and considerable pore pressure is built up under traffic action.

Halberg (*6*) has reported "the required internal water pressure causing an asphaltic mixture to have adhesive or interfacial tension failure (stripping) is inversely proportional to the diameter of the pores." Binder-course mixtures generally strip more than wearing course mixtures do, possibly because of large diameter pores in the binder course. Moreover, the wearing course is exposed repeatedly to high temperature drying periods as the pavement heals. Asphalt films that debond from the aggregate attach themselves again, and the mix regains its strength and water resistance. Humid periods are longer in the underlying binder course and, therefore, the self-healing forces during warm periods have much less influence.

Lovering and Cedergren (*7*) have reported that "with insufficient drainage, water may flood the base and rise through the pavement. Many drainage problems and deteriorated pavements can be attributed to water that enters the structural section from below." Apparently the deterioration is caused by premature stripping in many cases.

Telltale signs of water damage to HMA overlays (over concrete pavements) have been described by Kandhal et al. (*2*), who observed wet spots on HMA overlay surface scattered throughout a project. Usually, at these wet spots, water oozed out during hot afternoons. Some of the wet spots contained fines suspended in the water, which were tracked on the pavement by the traffic and appeared as white spots. Most white spots turned into fatty areas (from asphalt stripping and migration to the surface), which usually preceded the formation of potholes. Figures 2 and 3 show all three stages: white spots, fatty areas, and potholes on a four-lane highway. Figure 4 shows severely stripped aggregate particles in a pot-

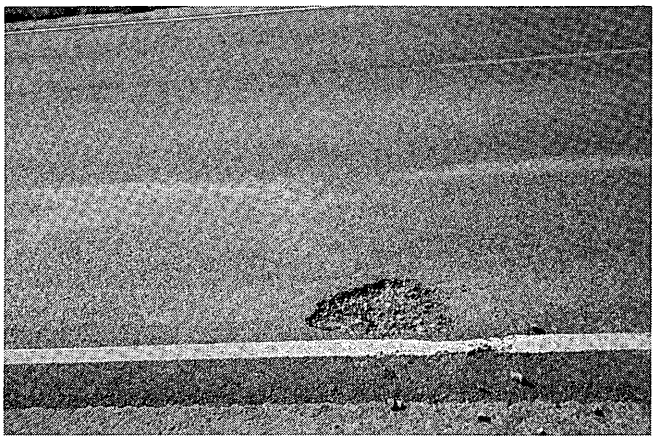

FIGURE 2 Three stages of stripping: white spots, fatty area, and pothole (close up).

FIGURE 4 Close up of pothole showing severely stripped aggregate.

hole. Small and large blisters caused by entrapped moisture were also observed. Sometimes blisters occurred with asphaltic globules at the surface (*8*).

Usually stripping in a four-lane highway facility occurs first in the slow traffic lane, as evident in Figure 3, because that lane carries more and heavier traffic compared with the passing lane. Typically stripping starts at the bottom of an HMA layer and progresses upward.

In sum, inadequate subsurface drainage is one of the primary factors inducing premature stripping in HMA pavements. Subsurface drainage problems can be alleviated in different ways, depending on local conditions (*9,10*); Kandhal et al. (*2*) have reported some such cases in detail.

Inadequate Compaction

Inadequate compaction of HMA mat is probably the most common construction-related factor to cause premature stripping. Studies indicate that at less than 4 to 5 percent air-void content in the HMA, the voids generally are not interconnected and thus are almost impervious to water. Most HMA mixes are designed to have 3 to 5 percent air-void contents. When constructed, a maximum air-void content of 8 percent (at least 92 percent of the theoretical maximum specific gravity) is specified by most agencies. It is assumed that the pavement will become densified to the design air-void content after 2 to 3 years of traffic use. However, some agencies do not exercise good compaction control, resulting in HMA's with air-voids contents higher than 8 percent at the time of construction. This can cause premature surface ravelling, because the mix does not possess adequate cohesion (*11*). Quite often, stripping is blamed for this type of premature raveling although the mixture is not examined closely. However, if the HMA pavement remains pervious for an extended time, stripping is likely to occur because of the ingress of water and hydraulic pore pressures induced by the traffic.

Terrel and Shute (*12*) have advanced the concept of "Pessimum" voids content for stripping. Figure 5 shows the general relationship

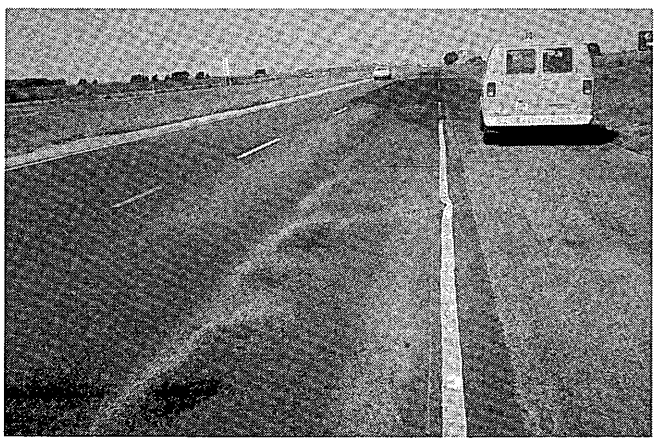

FIGURE 3 Slow traffic lane showing three stages of stripping.

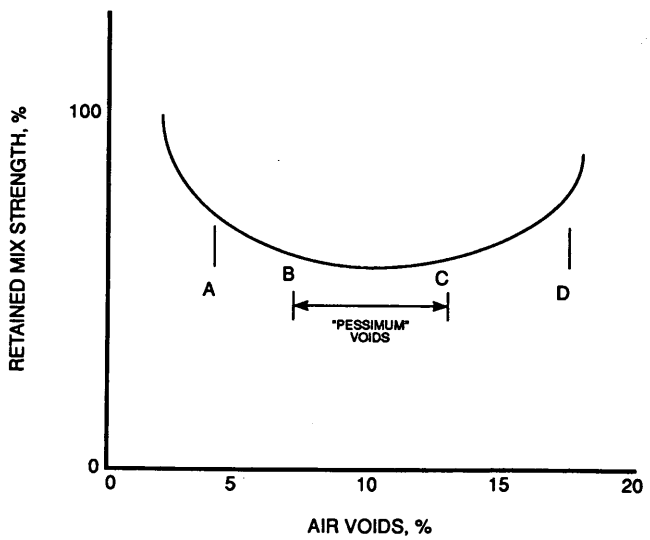

FIGURE 5 Air-void content versus retained mix strength, region of pessimum voids (*12*).

between air voids and relative strength of HMA mixtures following water conditioning. The amount of strength loss depends on the amount and nature of the voids. As shown in Figure 5, at less than 4 percent voids (Region A), the mixture is virtually impermeable to water, so it is essentially unaffected. Unfortunately, many pavements get constructed between Region B and C. As the voids increase to Region D and beyond, the mix strength becomes less affected by water, because the mixture is now free draining. Region B to C in Figure 5 is termed "Pessimum" void content because voids within its range are the opposite of optimum. The objective is to stay out of the "Pessimum" void range in order to minimize stripping problems. This can be done through proper mix design and compaction control procedures.

Excessive Dust Coating on Aggregate

The presence of dust and clay coatings on the aggregate can inhibit an intimate contact between the asphalt cement and aggregate and provide channels for penetrating water (*13*). The asphalt cement coats the dust coating and is not in contact with the aggregate surface. Some very fine clayey material may cause stripping by emulsifying the asphalt cement binder in presence of water.

The author is aware of one project in which stripping occurred by the mechanism of hydraulic scouring, which is applicable only to surface courses. Unlike typical stripping, this scouring starts at the surface and progresses downward, and it results from the action of vehicle tires on a saturated pavement surface. The water gets pressed down into the pavement in front of the tire and is immediately sucked away from the pavement behind the tire. This compression-tension cycle contributes to the stripping of the asphalt film from the aggregate (*14*). The aggregate used on the project had excessive amounts of a very fine dust coating. When the aggregate was washed in the quarry and used again the problem went away. Laboratory studies (*15*) also have shown improved adhesion characteristics of some dust-contaminated coarse aggregates when washed.

Use of Open-Graded Asphalt Friction Course

Several states in the southeastern United States experienced stripping in the HMA course underlying open-graded asphalt friction course (OGFC) during the late 1970s. It has been hypothesized that the OGFC retains moisture for a longer time and does not dry out after rain as fast as a conventional, dense-graded HMA surface. The water in OGFC is also pressed into the underlying course by the truck tires initiating the stripping action, which can also cause flushing, rutting, or shoving at the surface. Several states suspended the use of OGFC in the early 1980s. In South Carolina the statewide average stripping frequency was determined to be 18.7 percent under OGFC compared with a statewide average of 8.5 percent for all pavement layers (*16*). Some studies also have indicated that the stripping in the layers underlying OGFC resulted from the layers' high air-void content (lack of adequate compaction). Evidently, to minimize stripping, it is all the more desirable to have an impervious HMA course below the OGFC. It is recommended that the air-void content of the underlying HMA course should not exceed 4 to 5 percent when OGFC is placed to minimize stripping in the underlying course. Quite often, the air-void content in the HMA course can be as much as 8 percent just after construction. The construction of OGFC in such cases should be delayed until the traffic densifies the HMA course to an air-void of 4 to 5 percent.

Inadequate Drying of Aggregates

Laboratory studies (*17*) indicate that high residual-moisture content in the mineral aggregate before mixing with asphalt cement binder increases the potential for stripping. When drum-mix facilities were introduced to HMA production in the 1970s, low mixing temperatures (and high moisture content in the HMA) were encouraged to facilitate compaction. Now it is hypothesized that this might have caused some of the stripping problems. However, most states have now increased the mix-temperature requirements for drum-mix facilities to those required for batch-mix facilities. Undoubtedly, a dry aggregate surface will better adhere to the asphalt cement than a moist or wet aggregate surface.

Weak and Friable Aggregate

If weak and friable aggregates are used in the HMA mix, degradation takes place during rolling and later under heavy traffic. Degradation or delamination exposes new uncoated aggregate surfaces that can absorb water readily and initiates the stripping phenomenon in the mix. Also, if not observed carefully, these uncoated aggregate surfaces can mistakenly be deemed as stripped aggregate particles. Obviously, use of sound, durable aggregate in the HMA is recommended.

Overlays on Deteriorated Concrete Pavements

Many concrete pavements on interstate and primary highways are deteriorating before their design life. In recent years, HMA overlays have increasingly been put over existing concrete pavements, some of which have faulted, spalled, cracked, and water-pumping slabs. Dense-graded subbase material under concrete pavements can hold considerable water, which can escape through cracks or longitudinal and transverse joints. Once the concrete pavement is overlaid with an impervious HMA course, the water is trapped underneath. Excessive pore pressure builds under the traffic, initiating stripping, and then potholes form at the worst spots. Whenever a concrete pavement is due to be overlaid for the first time, it is necessary to evaluate existing drainage conditions. It may be necessary for the project to include installation of a positive drainage system, especially in troubled spots. Unless this is done, the problem of stripping and potholing will persist forever.

Usually edge drains are not sufficient to drain the entire roadway width. Transverse (lateral) drains are necessary, especially on steppe grades where water tends to flow longitudinally rather than toward the edge drain. Lateral drains can be installed at or near the existing transverse joints of concrete pavements before overlay and connected to the edge drain.

If an existing concrete pavement is badly deteriorated, cracked, and pumping were because of inadequate subsurface drainage, putting a 4-in. drainage layer of open-graded asphalt-treated permeable material (ATPM) directly above it before placing the dense-graded HMA overlay is recommended. The drainage layer should be connected to the edge drain(s). The ATPM will not only drain the water very efficiently, it will prevent any moisture-vapor

buildup in the pavement system. The ATPM has been used successfully in such applications. It will also help to minimize reflection cracking emanating from the concrete pavement. If required, the ATPM can also be placed over concrete pavements that have been subjected to crack and seat, break and seat, and rubblizing operations. Details on the design and use of ATPM are provided elsewhere (*9,10*).

Waterproofing Membranes and Seal Coats

If the source of moisture is from beneath the pavement, which is usually the case, then sealing of the road surface can be detrimental. Use of some waterproofing membranes (such as stress-absorbing membranes to minimize reflection cracking) and seal coats between the pavement courses or at the surface, acts like a vapor seal or a vapor barrier. McKesson (*18*) has observed that "ground water and water entering the roadbed from the shoulders, ditches and other surface sources, is carried upward by capillarity under a pavement. Above the capillary fringe water moves as a vapor and, if unimpeded at the surface, it passes to the atmosphere. This method of reduction of moisture has been termed Drainage by Evaporation, and it is the considered opinion of [McKesson] that the Drainage by Evaporation is usually as important as drainage downward by gravitation. If the pavement or seal coat constitutes a vapor seal or a vapor barrier, the moisture during cool nights and in cool weather condenses beneath the surface. When the pavement absorbs solar heat, the water is again vaporized and, if not free to escape, substantial vapor pressure results because water as vapor has more than a thousand times the volume of water in liquid form. Vapor pressure forces the moisture up into the pavement and through the surface. Blistering in bituminous pavements is a well known example of the effect of entrapped moisture and moisture vapor."

Many asphalt-paving technologists have observed this phenomenon of induced stripping in the pavement layers underlying waterproofing membranes and seal coats. The potential for stripping should, therefore, be considered whenever such sealing systems are used.

FIELD INVESTIGATIVE METHODOLOGY

It is necessary to apply an investigative methodology based on forensic experience with HMA pavements is to establish whether stripping is a problem either on a specific project or statewide. Surface distresses such as ravelling, flushing, and rutting can be caused by factors other than stripping. Visual investigation of the road surface alone is often inconclusive; it should not be used as the sole basis for determining whether stripping has occurred. The following field methodology is suggested.

Sampling

Inspect the whole project and select a 152.5-m (500-ft) long section that represents the "distressed area." Most projects also will have relatively better areas, with minimal or no distress. Select another 152.5-m (500-ft) long section from the same project that can be termed a relatively "good area." Document the type and extent of the observed distress (such as ravelling, flushing, rutting, and potholing) in both areas.

Obtain at least seven cores 102-mm (4-in.) in diameter at random locations in each area. A minimum sample size of seven for each area is necessary for reasonable statistical analysis of the data and to represent the sampled population with an acceptable degree of confidence. If it is a four-lane highway, obtain all cores from the inside wheel track of the slow-traffic (outside) lane. If it is a two-lane highway, obtain all cores from the outside wheel track of the lane. Stripping usually occurs first at these locations, across the roadway pavement. Cores 4-in. in diameter are recommended so that an indirect tensile test can be conducted. An additional eighth core also can be obtained, if the aged asphalt cement binder is to be recovered and tested for penetration and viscosity.

It is necessary to drill the cores without using water as a coolant, so that the in-situ moisture contents can be determined. Compressed air and CO_2 can be introduced under pressure to cool the inside of the core drill. The advance rate of the gas-cooled core drill is usually slower than that of the water-cooled core drill, but valuable information on moisture content cannot be obtained from wet coring. Similar procedures have been used by Chevron Research Company in studies of asphalt emulsion mixtures in California (*19*) and by the South Carolina Department of Highways and Public Transportation (SCDHPT) in an investigation of stripping of HMA in the state (*16*). Cores should be sealed in air-tight containers so that the in-situ moisture content can be determined later in the laboratory. Seasonal variations of the in-situ moisture content in HMA layers must be taken into account.

If dry coring cannot be done, then additional pavement layer samples should be obtained adjacent to the wet coring sites using a jack hammer. The HMA chunk samples loosened by the jack hammer from each layer should also be sealed in air-tight containers so that the in situ moisture content can be determined in the laboratory later. Kandhal et al (*2*) used a jack hammer in investigating stripped pavements on the Pennsylvania Turnpike.

Testing

The recommended testing plan is shown in Figure 6. The in situ moisture content should be determined by weighing the cores before and after drying to constant weight. It is preferable to dry the cores at ambient temperatures with a fan. Measure the thickness of all layers in the core. Observe the condition of the core, especially an evidence of stripping in the layer(s) or at the interface between the layers; it is not always possible to see the stripping on the outside of cores.

Saw the cores to separate the HMA layers so that the individual layer(s) can be tested. Measure the average thickness of each layer specimen after sawing.

Determine the bulk specific gravity of all specimens using the specification AASHTO T166. Determine the indirect tensile strength of the dry specimens at 25°C (77°F) using AASHTO T283 (Sections 10 and 11) or ASTM D4867 (Sections 8 and 9).

Examine the split exposed surfaces of the tested core specimens for stripping. Disregard the fractured and crushed aggregate particles. Heat the specimen just enough to push it apart by hand and observe the extent of stripping. A visual rating of the stripping on the exposed surface should be made and documented. A rating system developed by the Georgia Department of Transportation (DOT) and used by SCDHPT in their statewide stripping survey (*16*) is recommended. This visual stripping rating is based on broad, easily assessed range estimates of stripping. The rating system considers the

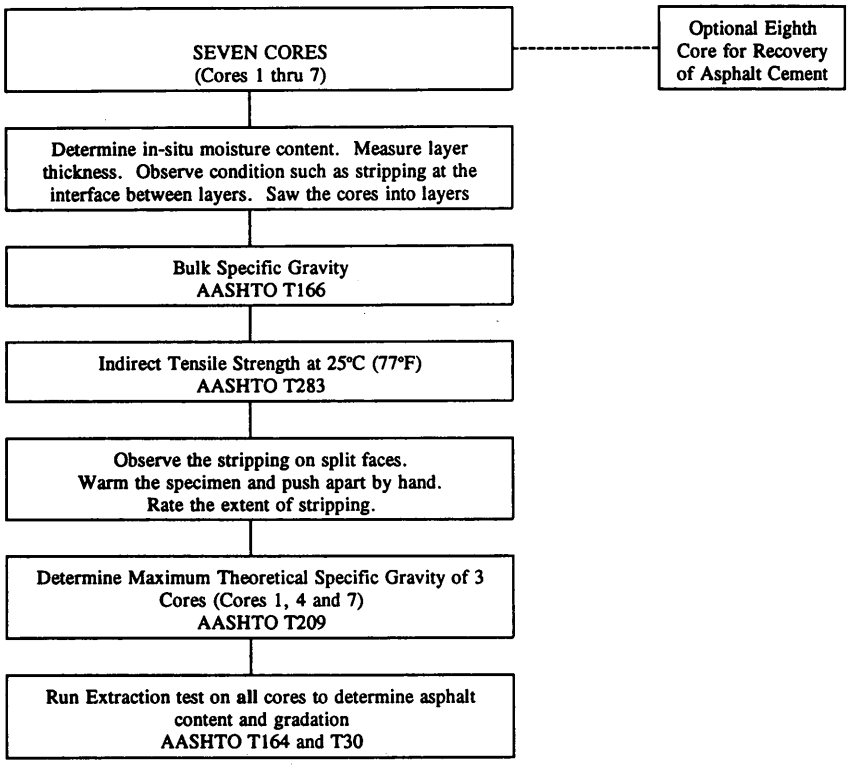

FIGURE 6 Testing plan.

stripping of the fine aggregate matrix and the coarse aggregate fraction separately. Stripping of the fine aggregate matrix is considered more critical than a comparable percentage of stripping in the coarse aggregate fraction. The procedure, however, does require some training for consistent interpretation of observations.

The Georgia DOT stripping rating, *S,* is calculated by assigning values to *C* and *F* in the expression $S = (C + F)/2$, where the values of *C* and *F* are as follows:

Values of C	*Values of* F
C = Coarse Aggregate Stripping	*F* = Fine Aggregate Stripping
1 = less than 10 percent	1 = less than 10 percent
2 = 10–40 percent	2 = 10–25 percent
3 = more than 40 percent	3 = more than 25 percent

If possible, have at least three evaluators note the stripping in each core and then calculate the average stripping rating.

An average stripping rating of 2.5 and 3.0 was used by SCDHPT to identify pavements for which stripping was considered severe. After all seven cores from an area have been rated for stripping, determine the maximum theoretical specific gravity (AASHTO T209) of the paving mixtures from three cores (Cores 1, 4, and 7 are recommended because in combination they encompass most of the representative area).

Conduct an extraction test (AASHTO T164) and gradation of extracted aggregate (AASHTO T30) on all seven cores to determine the mix composition (asphalt content and gradation).

Calculations and Tabulation

Figure 7 shows the flow diagram for calculations. The effective specific gravity of aggregates in Cores 1, 4 and 7 should be calculated using their maximum theoretical specific gravity values and their respective asphalt-content values. Calculate the average, effective specific gravity of the aggregate from these three values. Calculate the maximum, theoretical specific gravity values for each of the seven cores using the average effective specific gravity and the cores' respective asphalt contents obtained by extraction. Calculate the air void content in each core from its bulk specific gravity and its maximum theoretical specific gravity.

Calculate the percentage of in situ water saturation by the following formula:

$$\text{Percent saturation} = \frac{\text{Percent moisture in core} \times \text{bulk specific gravity of core}}{\text{Percent air void content in core}} \times 100$$

Tabulate all calculated and observed data separately for "good" and for "distressed" areas. Calculate the mean, standard deviation, and 95-percent confidence limits for each parameter. A high standard deviation would indicate lack of uniformity (or consistency) for that test parameter.

Compare the mean and standard deviation of each test parameter obtained in "good" and "distressed" areas to identify the differences, if any. In a majority of cases, the deficiencies in the "distressed" area will stand out by this comparison.

Example

Tables 1 and 2 show some hypothetical data from a 3-year old distressed project. Table 1 represents test data obtained by this investigative methodology from a "good" area whereas Table 2 has data

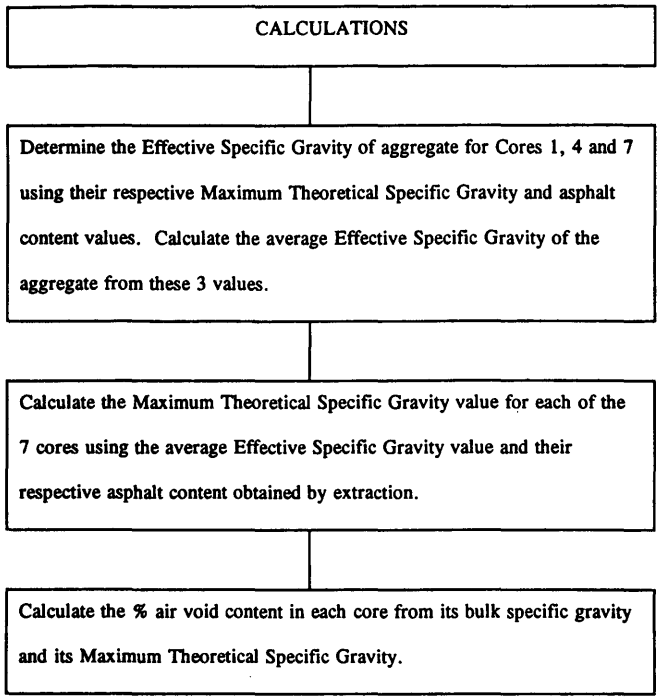

FIGURE 7 Calculation of air-void content.

from a representative "distressed" area of the project. The hypothetical data in Table 2 has been presented purposely to illustrate most of the HMA-related factors (or deficiencies) that are likely to induce stripping. Therefore, this can be considered the worst-case scenario. The "distressed" area in this example has the following problems:

- Very high and inconsistent air void content,
- Deficient and inconsistent asphalt content,
- Excessive and inconsistent minus-200 material, and
- Very high in situ moisture contents or saturation levels.

These problems can be identified easily by comparing the data from Table 2 with that of Table 1. In this example, severe stripping was observed in the "distressed" area, which was also indicated by lower tensile strengths compared with those in the good area.

When data such as those in Table 2 are obtained, one should not immediately presume that an antistripping agent is needed; instead, remedial measures should be taken to remove the cause(s). For example, the data in Table 2 indicate the following needs:

- Adequate compaction level at the time of construction. An average air-void content of 8.9 percent after 3 years' service is unacceptable. The HMA pavement should have achieved its design air-void content (3 to 5 percent) in 3 years.
- Quality control of mix composition. The average asphalt content of 6.4 percent is deficient by 0.5 percent from the job-mix formula, and the standard deviation of 0.45 percent is too high. The average minus-200 content is excessive by 1.9 percent from the job mix formula and is also especially variable considering the standard deviation of 1.97 percent.
- Positive drainage system. The project has a water-drainage problem in the distressed area; saturation is as high as 100 percent.

If test data such as those in Table 1 are obtained throughout a project, and there still is evidence of stripping, most likely the HMA mix is sensitive to moisture damage. In such cases, a suitable antistripping agent should be considered.

Statewide Survey

Before specifying antistripping agents or moisture-susceptibility test methods statewide, it is prudent first to establish whether stripping is a statewide problem or only occurring in isolated cases. Georgia and South Carolina have each completed a statewide survey and evaluation of the stripping problem through an extensive coring program. South Carolina sampled 805 km (500 mi) of pavements, coring 1,324 cores and testing 4,503 pavement layers(*16*). A random sample, consisting of two pavement cores, was taken from every 3.2-km (2-mi) segment for each highway section sampled. Two-lane and multilane highways, and HMA pavements with and

TABLE 1 Core Test Data—Good Area

Test	Job-Mix Formula	Core No.							$\bar{X}$	Std. Dev.	95% Confidence Limits
		1	2	3	4	5	6	7			
Bulk Specific Gravity	2.290	2.286	2.287	2.285	2.271	2.256	2.293	2.260	2.277	0.0145	2.248 - 2.306
Max. Specific Gravity	2.385	2.394	2.380	2.398	2.371	2.380	2.389	2.394	2.386	0.0098	---
% Voids	4.0	4.5	3.9	4.7	4.2	5.2	4.0	5.6	4.6	0.63	3.3 - 5.9
Tensile Strength, psi	---	118	130	110	128	98	121	90	114	15.1	84 - 144
% Asphalt Content	6.9	6.7	7.0	6.6	7.2	7.0	6.8	6.7	6.8	0.21	6.4 - 7.2
% Minus 200	5.2	5.8	6.1	5.3	4.3	4.8	6.0	4.5	5.3	0.74	2.6 - 8.0
% in-situ Moisture in core	---	0.3	0.2	0.3	0.2	0.3	0.2	0.4	0.27	0.076	0.1 - 0.4
% in-situ Saturation	---	15.2	11.7	14.6	10.8	13.0	11.5	16.1	13.3	2.05	9.2 - 17.4
Stripping Rating	---	1.0	1.0	1.0	1.0	1.5	1.0	1.5	1.14	---	---

TABLE 2 Core Test Data—Distressed Area

Test	Job-Mix Formula	Core No.							$\bar{X}$	Std. Dev.	95% Confidence Limits
		1	2	3	4	5	6	7			
Bulk Specific Gravity	2.290	2.154	2.213	2.213	2.212	2.135	2.211	2.205	2.192	0.0329	2.126 - 2.258
Max. Specific Gravity	2.385	2.434	2.411	2.380	2.407	2.429	2.385	2.407	2.408	0.0202	---
% Voids	4.0	11.5	8.2	7.0	8.1	12.1	7.3	8.4	8.9	2.02	4.9 - 12.9
Tensile Strength, psi	---	76	52	107	83	72	97	56	78	20.1	38 - 118
% Asphalt Content	6.9	5.8	6.3	7.0	6.4	5.9	6.9	6.4	6.4	0.45	5.5 - 7.3
% Minus 200	5.2	4.5	7.2	9.6	9.2	7.1	4.7	7.3	7.1	1.97	3.2 - 11.0
% in-situ Moisture in core	---	5.2	4.5	0.8	3.5	5.1	1.1	5.8	3.7	2.02	0.3 - 7.7
% in-situ Saturation	---	97.4	121.4*	25.3	95.6	90.0	33.3	152.2 *	87.9	45.30	0 - 178.5*
Stripping Rating	---	2.5	3.0	2.0	2.5	2.5	2.0	3.0	2.5	---	---

*Calculated saturation can exceed 100% because part of the water has been absorbed by the stripped aggregate particles.

without open-graded friction courses (OGFC), were sampled. A similarly unbiased, statewide testing program is recommended for others. Ideally, however, one would obtain at least three 102-mm (4-in.) diameter cores randomly from each project to obtain preliminary data on in-situ moisture content, air-void content, mix composition, tensile strength, and the extent of stripping, if any. If 100 projects were selected across the state, testing would involve 300 cores; that does not appear to be an unreasonable number to establish whether or not stripping is a statewide problem.

Data from 100 projects would not only help assess the average frequency for severe stripping (that is, visual ratings of 2.5 and 3.0) within a state, it would also indicate whether there were other problems to be addressed statewide, such as inadequate compaction, lack of HMA-production quality control, or inefficient subsurface drainage systems.

Selected projects could be revisited, sampled, and tested every year to assess increasing moisture-induced damage, if any. Georgia DOT has such a program, which has been successful.

Since materials, mix design, construction practices, maintenance procedures, and climatological conditions vary from state to state, it is essential that each state conduct its own statewide survey to assess and quantify the "stripping" problem, as recommended. Calling for antistripping agents as "insurance" against stripping, without establishing the extent or cause of the problem is not justified. Not only is such a policy uneconomical, it may be ineffective if underlying causes responsible for stripping are not addressed adequately.

LABORATORY INVESTIGATIVE TESTING METHODS

Test Methods

Numerous test methods have been developed and used in the past to predict the moisture susceptibility of HMA mixes. However, no test has gained wide acceptance because they have low reliability and lack a satisfactory relationship between laboratory and field conditions. Selected test methods, only those commonly used by certain agencies, are discussed briefly.

Qualitative or Subjective Tests

- Boiling Water Test (ASTM D3625 or a variation): Loose HMA mix is added to boiling water. Although the current ASTM D3625-83 specifies 1 min. of boiling, most agencies use a 10-min. boiling period. The percentage of the total visible area of the aggregate that retains its original coating after boiling is estimated as either above or below 95 percent. This test can be used for initial screening of HMA mixes. Some agencies use it for quality control during production to determine the presence of antistripping agent. This test method does not involve any strength analysis. Also, determining the stripping of fine aggregate is very difficult.
- Static-Immersion Test (AASHTO T182): A sample of HMA mix is immersed in distilled water at 25°C (77°F) for 16 to 18 hours. The sample is then observed through water to estimate the percentage of total visible area of the aggregate that remains coated as above or below 95 percent. Again, this method does not involve any strength test.

Quantitative Strength Tests

- Lottman Test (NCHRP 246): This method was developed by Lottman (*20*) under the National Cooperative Highway Research Program 246. Nine specimens (102-mm or 4-in. in diameter and 64-mm or 2½ in. high) are compacted to expected field air-void content. Specimens are divided into three groups of three specimens each. Group 1 is treated as a control, without any conditioning. Group 2 specimens are vacuum saturated (660 mm or 26 in. Hg) with water for 30 min. Group 3 specimens are vacuum saturated like those in Group 2 and then subjected to a freeze (−18°C or 0°F for 15 hr) and a thaw (60°C or 140°F for 24 hr) cycle. All nine specimens are tested for resilient modulus (M_R) and indirect tensile strength (ITS) at 13°C (55°F) or 23°C (73°F). A loading rate of 1.65 mm/min. (0.065 in.) is used for the ITS test. Group 2 reflects field

performance up to 4 years. Group 3 reflects field performance from 4 to 12 years. Retained tensile strength (TSR) is calculated for Group 2 and Group 3 specimens as follows:

$$TSR = \frac{\text{ITS of conditioned specimens}}{\text{ITS of control specimens}}$$

A minimum TSR of 0.70 is recommended by Lottman (*20*) and Maupin (*21*), who reported values between 0.70 and 0.75, differentiated between stripping and nonstripping HMA mixtures. It has been argued that the Lottman procedure is too severe because the warm-water soak of the vacuum-saturated and frozen specimen can develop internal water pressure. However, Stuart (*22*) and Parker and Gharaybeh (*23*) generally found a good correlation between the laboratory and field results. Oregon has successfully used this test with modulus ratio in lieu of tensile strength ratio (TSR).

- Tunnicliff and Root Conditioning (NCHRP 274): This method was proposed by Tunnicliff and Root under the NCHRP Project 274 (*24*). They proposed that six specimens be compacted to a 6 to 8 percent air-void content and then divided into two groups of three specimens each. Group 1 specimens are treated as a control, without any conditioning. Group 2 specimens are vacuum-saturated (508 mm or 20 in. Hg for about 5 min.) with water to attain a saturation level of 55 to 80 percent. Specimens attaining more than 80 percent saturation are discarded. The saturated specimens are then soaked in water at 60°C (140°F) for 24 hours. All specimens are tested for ITS at 25°C (77°F) using a loading rate of 51 mm/min. (2 in)/min. A minimum TSR of 0.7 to 0.8 usually is specified. Evidently, the use of a freeze-thaw cycle is not incorporated into ASTM D4867-88, which is based on this method. The freeze-thaw cycle is optional. The primary emphasis is on saturation of the specimen, which for a short duration of about 24 hours has been reported to be insufficient to induce moisture-related damage (*25*).
- Modified Lottman Test (AASHTO T283): This method was proposed by Kandhal and was adopted by AASHTO in 1985 (*26*). It combines the good features of the Lottman test (NCHRP 246) and Tunnicliff and Root test (NCHRP 274). Six specimens are compacted to a 6 to 8 percent air-void content. Group 1 (three specimens) is used as a control. Group 2 specimens are vacuum saturated (55 to 80 percent saturation) with water and then subjected to one freeze and one thaw cycle as proposed by Lottman. All specimens are tested for ITS at 25°C (77°F) using a loading rate of 51 mm/min. (2 in)/min., and the TSR is determined. A minimum TSR of 0.7 is usually specified. This method is gaining acceptance by the specifying agencies.
- Immersion-Compression Test (AASHTO T165): Six specimens (102-mm or 4-in. diameter times 102-mm or 4-in. high) are compacted with a double plunger at a pressure of 20.7 MPa (3,000 psi) for 2 min. to about 6 percent air-void content. Group 1 (three specimens) is treated as control. Group 2 specimens are placed in water at 49°C (120°F) for 4 days or at 60°C (140°F) for 1 day. All specimens are tested for unconfined compressive strength at 25°C (77°F) using a 5.1 mm/min. (0.2 in/minute) loading rate. The retained compressive strength is determined. Many agencies specify at least 70 percent retained strength. This test has produced retained strengths near 100 percent, even when stripping is evident. Stuart (*13*) has attributed this to the internal pore water pressure and insensitivity of the compression test in measuring the moisture-induced damage. Lack of precision is a major problem with this test.
- Other Tests: Moisture-vapor susceptibility, a swell test, and a film stripping test are used by Caltrans. Retained Marshall stability is used in Puerto Rico and some other states.

Survey of Test Methods Used

A survey of test methods used in the United States and their effectiveness in predicting moisture susceptibility was conducted in 1989 by Hicks for NCHRP Topic 19-09 (*1*). Figure 8 shows the relative effectiveness of different test methods on a zero to nine scale, according to this survey. Zero means "not effective" and 9 means "100-percent effective." The results are given in Table 3.

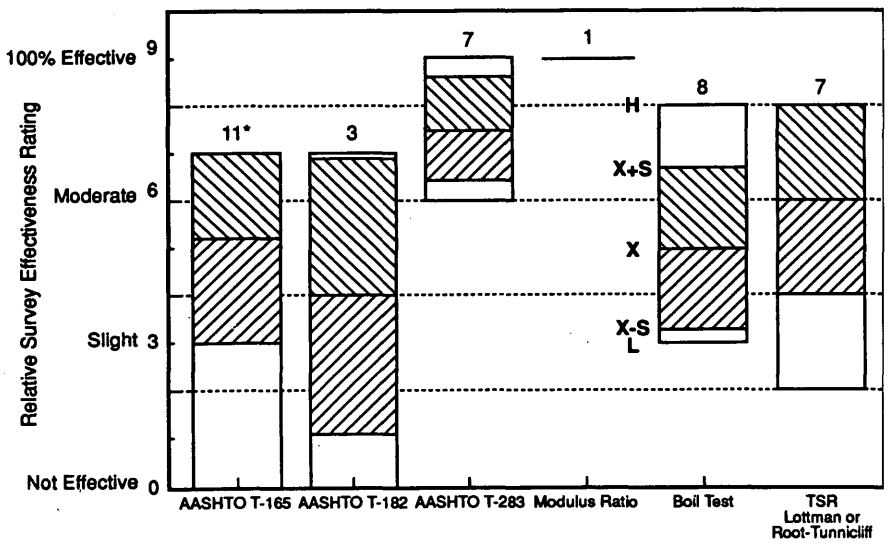

FIGURE 8 Relative effectiveness of mixture test procedures to identify moisture-related problems (*1*).

TABLE 3 Survey of Test Methods and Their Effectiveness

Test Method	No. of Agencies Using	Average Rating	
		Number	Description of Effectiveness
Boiling Water	9	5	Slight to moderate
Static-Immersion (AASHTO T182)	3	4	Slight
Lottman (NCHRP 246)	3	7.5	High
Tunnicliff and Root (ASTM D4867)	9	5	Slight to moderate
Modified Lottman (AASHTO T283)	9	7.5	High
Immersion-Compression (AASHTO T165)	11	5	Slight to moderate

Although the Tunnicliff and Root procedure is used by nine agencies, only four rated its effectiveness (range of 2 to 8 with an average value of 5), apparently from lack of sufficient experience.

Evidently, a wide variety of test methods are being used by various agencies. However, no test has proven "superior" at correctly identifying a moisture-susceptible mix in all cases. Kiggundu and Roberts (*27*) quantified the success rate of several tests, based on test data available from various research reports and papers, as given in Table 4.

Data on success rates indicate that many HMA mixes that might otherwise perform satisfactorily in the field, are likely to be unacceptable if these tests and criteria are used. Use of these tests has encouraged the increased use of antistripping agents in many states.

Many concerns and requirements related to the test methods still need to be addressed:

- Proliferation of test procedures and criteria.
- Unsatisfactory reproducibility of most test methods. For example, small variations in air-void content of the specimens can significantly affect the TSR results.
- Sole reliance on the TSR value instead of considering minimum wet strength (if the desired value can be established) of the conditioned specimens. For example, some additives increase both dry and wet strengths but might have a low TSR value.
- Lack of satisfactory correlation between laboratory and field performance.

However, based on the preceding discussion, it appears that at the present time the Modified Lottman Test (AASHTO T283) is the most appropriate test method available to detect moisture damage in HMA mixes. A minimum TSR of 0.70 is recommended when using this test method; the criterion should be applied to the field-produced rather than laboratory produced mixes.

Strategic Highway Research Program (SHRP) had two research contracts dealing with moisture susceptibility of HMA mixes. SHRP project A-003A "Performance Related Testing and Measuring of Asphalt-Aggregate Interactions and Mixtures" was needed to develop an improved test method to evaluate moisture susceptibility. A second contract, SHRP project A-003B "Fundamental Properties of Asphalt-Aggregate Interactions Including Adhesion and Adsorption," studied the fundamental aspects of asphalt-aggregate bond.

A Net Adsorption Test (NAT) was developed under SHRP A-003B and completed by the National Center for Asphalt Technology. It is a preliminary screening test for matching mineral aggregates and asphalt cement (*28*) and is based on the principles of adsorption and desorption. A solution of asphalt cement and toluene is introduced and circulated in a reaction column containing the aggregate sample. Once the solution temperature has been stabilized, 4 ml of solution is removed and the absorbance is determined with a spectrophotometer. Fifty grams of minus No. 4 aggregate is then added to the column, and the solution is circulated through the aggregate bed for 6.5 hours. A second 4-ml sample of the solution then is removed from the column and the absorbance is again determined. The difference in the absorbance readings is used to determine the amount of asphalt that has been removed from the solution (adsorption) because of the chemical attraction of the aggregate for the molecular components of the asphalt cement. Immediately after the second solution sample is taken, 575 μm of water is added to the column. The solution is then circulated through the system for an-

TABLE 4 Success Rates of Test Methods

Test Method	Minimum Test Criteria	% Success
Modified Lottman (AASHTO T283)	TSR = 70% TSR = 80%	67 76
Tunnicliff-Root (ASTM D4867)	TSR = 70% TSR = 80% TSR = 70-80%	60 67 67
10-Minute Boil Test	Retained Coating 85-90%	58
Immersion-Compression (AASHTO T165)	Retained Strength 75%	47

other 2 hr. A final 4 ml of solution is taken from the column at the end of this time. The increase in the absorptivity is a measure of the amount of asphalt cement that is displaced by water molecules (desorption). Additional validation data are needed for the NAT.

An Environmental Conditioning System (ECS) was developed in SHRP A-003A (*29*) in which HMA samples are exposed to wetting and accelerated hot-cold cycling to represent actual field exposure, including repeated loading to simulate traffic. The modulus of the HMA specimen and change in air and water permeability are monitored during the conditioning after each cycle, and tensile strength and stripping are measured at the conclusion of conditioning. Both warm- and cold-climate conditioning can be performed. Modulus ratio and water permeability ratio are calculated after completing each conditioning cycle. A provisional AASHTO standard, Designation TP34, "Standard Test Method for Determining Moisture Sensitivity Characteristics of Compacted Bituminous Mixtures Subjected to Hot and Cold Climate Conditions," is available. The ECS system is expensive but versatile; however, sufficient field-validation data are not available to warrant its use in lieu of AASHTO T283.

SUMMARY, CONCLUSIONS, AND RECOMMENDATIONS

Stripping of hot mix asphalt (HMA) pavements appears to have become a major problem in recent years. More and more states are specifying the use of antistripping (AS) agents. Moisture susceptibility of HMA mixes were reviewed in this paper, especially field investigation of the problem and laboratory test methods. The following conclusions and recommendations are warranted:

- External factors and in-place properties of the HMA pavements can induce premature stripping in HMA pavements. A proper knowledge of these factors is essential to identifying and solving the stripping problem.

Some factors were discussed in detail: inadequate pavement drainage (especially subsurface drainage); inadequate compaction of HMA pavement; excessive dust coating on aggregate; inadequate drying of aggregates before mixing with asphalt cement; use of weak and friable aggregates in HMA; overlays on deteriorated concrete pavements; use of waterproofing layers and seal coats when the source of the moisture is from beneath the pavement; and the possible use of open-graded asphalt friction courses. Suggestions for alleviating problems associated with these factors were offered.

- An investigative field methodology based on forensic experience is recommended for use by the specifying agencies and industry in establishing whether stripping is a problem either on a specific project or statewide. [Details of sampling, testing, and interpretation of test results (along with examples) were included.] The recommended methodology will help to determine the causes of stripping, if present, take remedial measures to remove the causes, and specify antistripping agents only when absolutely necessary.
- [Current practices of specifying laboratory moisture-susceptibility test procedures (and acceptance criteria) were reviewed.] Until more suitable test procedures are developed and validated with field performance, Modified Lottman test (AASHTO T283) is recommended to determine potential moisture susceptibility of HMA mixes. Furthermore, a minimum TSR of 0.70 is recommended when using the test. The criterion should be applied to field-produced instead of the laboratory-produced HMA mixes.
- AS agents (both liquid and lime additives) should not be specified across the board in all HMA mixes or from an approved list of sources as "insurance." Some agents are aggregate and asphalt specific and, therefore, may not be effective in all mixes; they could even be detrimental at times. The practice also is uneconomical because some HMA mixes are inherently resistant to moisture damage and do not need an AS agent.
- A thorough and fundamental understanding of mechanisms (especially asphalt cement-aggregate interactions) involved in moisture-induced damage is necessary to develop improved and more reliable laboratory test methods and criteria to predict the moisture susceptibility of HMA mixes.

REFERENCES

1. Hicks, R. Gary. *NCHRP Synthesis of Highway Practice 175: Moisture Damage in Asphalt Concrete.* TRB, National Research Council, Washington, D.C., Oct. 1991. 90 pp.
2. Kandhal, P. S., C. E. Lubold, and F. L. Roberts. Water Damage to Asphalt Overlays: Case Histories. *Proc., Association of Asphalt Paving Technologists,* Vol. 58, Association of Asphalt Paving Technologists, St. Paul, Minn., 1989.
3. Cedergren, H. R., and W. R. Lovering. The Economics and Practicality of Layered Drains for Road Beds. *Highway Research Record 215,* HRB, National Research Council, Washington, D.C., 1968.
4. Lottman, R. P. *The Moisture Mechanism that Causes Asphalt Stripping in Asphalt Pavement Mixtures.* Final Report Research Project R-47. University of Idaho, Moscow, Idaho, Feb. 1971.
5. Majidzadeh, K., and F. N. Brovold. *Effect of Water on Bitumen-Aggregate Mixtures.* Report CE-1. University of Florida, Gainesville, Sept. 1966.
6. Hallberg, S. The Adhesion of Bituminous Binders and Aggregates in the Presence of Water. Statens Vaginstitut, Stockholm, Meddeland, Sweden 1950.
7. Lovering, W. R., and H. R. Cedergren. Structural Section Drainage. *Proc., International Conference on the Structural Design of Asphalt Pavements,* Ann Arbor, Mich., 1962.
8. Acott, S. M., and C. Crawford. *Blistering in Asphalt Pavements: Causes and Cures.* IS 97. National Asphalt Pavement Association, 1987.
9. Cedergren, H. R., J. A. Arman, and K. H. O'Brien. *Development of Guidelines for the Design of Subsurface Drainage Systems.* Report RD-73-14. FHWA, U.S. Department of Transportation, Feb. 1973.
10. Forsyth, R. A. *Asphalt Treated Permeable Material: Its Evolution and Application.* QIP series 117. National Asphalt Pavement Association, Lanham, Md., 1991.
11. Kandhal, P. S., and W. C. Koehler. *Pennsylvania's Experience in the Compaction of Asphalt Pavements.* Special Technical Publication 829. ASTM, Philadelphia, Pa., 1984.
12. Terrel, R. L., and J. W. Shute. Summary Report on Water Sensitivity. Report SHRP-A/IR 89–003. Strategic Highway Research Program, National Research Council, Washington, D.C., Nov. 1989.
13. Stuart, K. D. *Moisture Damage in Asphalt Mixtures: State of the Art.* Report FHWA-RD-90-019. FHWA, U.S. Department of Transportation, Aug. 1990.
14. Taylor, M. A., and N. P. Khosla. Stripping of Asphalt Pavements: State of the Art. In *Transportation Research Record 911,* TRB, National Research Council, Washington, D.C., 1983, 178 pp.
15. Balghunaim, F. Improving the Adhesion Characteristics of Bituminous Mixes by Washing Dust Contaminated Coarse Aggregates. Paper submitted to TRB, Aug. 1990.
16. Busching, H. W., J. L Burti, and S. N. Amirkanian. An Investigation of Stripping in Asphalt Concrete in South Carolina. Report FHWA-SC-86-02. South Carolina Department of Highways and Public Transportation, Columbia, S.C., July 1986.
17. Parker, F. Field Study of Stripping Potential of Asphalt Concrete Mixtures. Report ST 2019-6. Alabama Highway Department, Montgomery, Ala., Aug. 1989.

18. McKesson, C. L. Slippery Pavements-Causes and Treatments. *Proc., Association of Asphalt Paving Technologists,* Vol. 18, Association of Asphalt Paving Technologists, St. Paul, Minn., 1949.
19. Lottman, R. P. Laboratory Test Method for Predicting Moisture-Induced Damage to Asphalt Concrete. In *Transportation Research Record 843,* TRB, National Research Council, Washington, D.C., 1982, 126 pp.
20. Lottman, R. P. *NCHRP Report 246: Predicting Moisture-Induced Damage to Asphaltic Concrete: Field Evaluation.* TRB, National Research Council, Washington, D.C., 1982, 50 pp.
21. Maupin, G. W. The Use of Antistripping Additives in Virginia. *Proc., Association of Asphalt Paving Technologists,* Vol. 51, Association of Asphalt Paving Technologists, St. Paul, Minn., 1982.
22. Stuart, K. D. *Evaluation of Procedures Used To Predict Moisture Damage in Asphalt Mixtures.* Report FHWA/RD-86/091. FHWA, U.S. Department of Transportation, 1986.
23. Parker, F., and F. Gharaybeh. Evaluation of Indirect Tensile Tests for Assessing Stripping of Alabama Asphalt Concrete Mixtures. In *Transportation Research Record 1115,* TRB, National Research Council, Washington, D.C., 1987.
24. Tunnicliff, D. G., and R. E. Root. *NCHRP Report 274: Use of Antistripping Additives in Asphaltic Concrete Mixtures: Laboratory Phase.* TRB, National Research Council, Washington, D.C., 1984, 50 pp.
25. Coplantz, J. S., and D. E. Newcomb. Water Sensitivity Test Methods for Asphalt Concrete Mixtures: A Laboratory Comparison. In *Transportation Research Record 1171,* TRB, National Research Council, Washington, D.C., 1988, pp. 44–50.
26. Resistance of Compacted Bituminous Mixture to Moisture Induced Damage. Test Method T283-85. Part II: Methods of Sampling and Testing, AASHTO, Washington, D.C., Aug. 1986.
27. Kiggundu, B. M., and F. L. Roberts. Stripping in HMA Mixtures: State-of-the-Art Report. *Research Report,* National Center for Asphalt Technology, Auburn University, Ala., Sept. 1988.
28. Curtis, C. W., K. Ensley, and Jon Epps. Fundamental Properties of Asphalt-Aggregate Interactions Including Adhesion and Absorption. A-003B, Draft Final Report, Strategic Highway Research Program, 1991.
29. Al-Swailmi, S., and R. L. Terrel. Evaluation of Water Damage of Asphalt Concrete Mixtures Using the Environmental Conditioning System (ECS). *Journal of the Association of Asphalt Paving Technologists,* Vol. 61, 1992.

The opinions, findings, and conclusions expressed here are those of the author and not necessarily those of the National Center for Asphalt Technology or Auburn University.

Publication of this paper sponsored by Committee on Characteristics of Bituminous-Aggregate Combinations To Meet Surface Requirements.

Evaluation of Using Different Stabilizers in the U.S. Route 15 (Maryland) Stone Matrix Asphalt

KEVIN D. STUART AND PETER MALMQUIST

Stone matrix asphalt (SMA) is a gap-graded hot mix that maximizes the binder and coarse-aggregate contents. A stabilizing additive, such as cellulose fiber, rock wool fiber, or polymer, is added to prevent the binder and aggregate dust from draining when the mixture is hot. Stabilizers should reduce the amount of draindown without decreasing the performance of the mixture. The effects of using different stabilizers in an SMA on draindown, rutting, low temperature cracking, and aging are evaluated. Stabilizers had no significant effect on rutting or low temperature properties. The two polymers were not as effective as the four fibers for preventing draindown, although they were better at reducing age hardening.

Stone matrix asphalt (SMA) is a gap-graded hot mix that maximizes the binder and coarse-aggregate contents. SMA technology was developed in Europe more than 20 years ago, although the characteristics of the mixture have been refined over the years. On the basis of European experience, SMAs perform better under heavy traffic loads and are more cost-effective than dense-graded mixtures. They are primarily used as surface-course mixtures in Europe (*1*).

The higher percentage of coarse aggregate in an SMA, as compared with that in a dense-graded mixture, the more contact points between coarse aggregate particles (*1*). Such contacts provide a high resistance to rutting and should reduce the influence of the type and amount of binder on rutting. An SMA has a high proportion of high quality, manufactured, coarse aggregate; a high proportion of binder and mineral filler; and a low proportion of middle-sized aggregate as compared with dense-graded mixtures.

More than 20 SMA pavements have been built in the United States, and additional SMA projects have been proposed. Construction aspects and the performances of these pavements are being evaluated. Laboratory studies also are needed to improve the definitions of the components of an SMA, and to develop tests for their design and analysis.

Gap gradation of an SMA may allow the binder and the aggregate dust to drain when the mixture is hot during storage, hauling, and placement. Hence, a stabilizing additive is used to prevent draindown. Cellulose and mineral fibers are used as stabilizers in Europe; polymers are used to a lesser degree (*1*). Fibers stiffen a binder through absorption and the resulting fiber network. Some suppliers claim there are other benefits, such as the mixture's improved resistance cracking.

Polymers stiffen a binder through various mechanisms that depend on the polymer and the method of addition. These mechanisms are not sufficiently documented in the literature. One of the more common mechanisms is to form a rubbery network, which may also reduce the temperature susceptibility of the binder and increase the elastic strain.

Stabilizers should reduce draindown without decreasing the performance of the mixture. Different stabilizers have provided different optimum binder contents in a given mixture at equal design air voids (*1*). This could indicate that stabilizers can affect how a mixture compacts. If a stabilizer excessively stiffens a binder to the point that the SMA is more difficult to compact, the mixture will require more asphalt to meet the target air-void level. This could decrease the degree of contact between aggregate particles.

K. D. Stuart, FHWA, Turner-Fairbank Highway Research Center, 6300 Georgetown Pike, McLean, Va. 22101–2296. P. Malmquist, University of Maryland, College Park, Md. 20742.

OBJECTIVE

The objective of this study was to evaluate the effects of using different stabilizers in an SMA, in terms of draindown and the resistance of the SMA to rutting, low temperature cracking, aging, and moisture susceptibility.

MATERIALS

Six primary SMAs were tested in this study. These contained the same aggregates and gradation, but they used different stabilizers. The aggregate, asphalt, and three of the stabilizers were used in an SMA pavement built in 1992 as part of a resurfacing project on U.S. Route 15, south of Frederick, Maryland (*2*).

One additional SMA was also tested. The gradation used in the six SMAs was altered to reduce the gap. This gradation was added to the study when we learned that the polymer stabilizers did not prevent draindown. The objective was to determine the effects of the change in gradation on draindown and other mixture properties and thereby provide preliminary information for a planned FHWA study under which the effects of gradation on SMA properties would be examined.

Stabilizers

The stabilizers included two loose cellulose fibers named Custom Fiber CF 31500 and Interfibe 230; a pelletized cellulose fiber named Arbocel BG 50/50; a loose-rock wool fiber named Inorphil; and two polymers named Vestoplast-S and Styrelf 1-D. Arbocel, Vestoplast, and Styrelf were used in the Route 15 pavement (*2*). Custom Fiber and Interfibe were included in our study in order to investigate the

use of domestic cellulose fibers. (The other two fibers, Arbocel and Inorphil, have European origins. Inorphil was included in the study because it has been used in other SMA pavements built in the United States.)

Stabilizers were added based on those quantities used in the pavement sections and according to the recommendations of the suppliers (*2*). Custom Fiber and Interfibe were added at 0.3 percent by mixture weight. The Arbocel pellets, which are 50-percent binder, were added at 0.6 percent by mixture weight; Inorphil was added at 0.5 percent by mixture weight; and the Vestoplast pellets were added at 7.0 percent by asphalt weight. Styrelf is an asphalt, modified with polymer by the supplier, and is received in bulk form. The amount of polymer in the binder is not reported by the supplier.

Asphalt

Properties of the AC-20 asphalt and the two modified binders are given in Table 1. The base asphalt for the Vestoplast binder was the AC-20 asphalt. A different AC-20 asphalt was used in the Styrelf binder. Both polymer-modified binders were significantly stiffer than the AC-20 asphalt, according to the capillary viscosities and penetrations. The data for the Vestoplast binder assume that the pellets and the asphalt homogeneously blend; that may not be true. When performing a mixture design, the pellets are mixed with the hot aggregate and melted before the asphalt is added.

Aggregates

The aggregates were a blend of No. 68 and No. 8 diabase from Leesburg, Virginia; a No. 10 limestone called "Bird Eye" from Frederick, Maryland; and a mineral filler called "Aglime" from Texas, Maryland. Properties of the aggregates, target gradation based on the average gradation of the pavement sections, and actual gradation of the blend used in this study are shown in Table 2.

The Los Angeles Abrasions of the coarse fraction of each aggregate were below the maximum allowable loss of 30 percent for aggregates used in SMAs (*3*).

The coarse fractions of the No. 68 diabase and Bird Eye aggregates passed the German test for flat and elongated particles, and the data for the No. 8 diabase aggregate was right at the specification. SMA specifications reject aggregates in which more than 20 percent of the particles by mass have a length-to-thickness ratio greater than 3 to 1 (*3*).

The altered gradation is also shown in Table 2. The 41-percent aggregate passing the 4.75-mm sieve is estimated to be the maximum allowable according to German gradation specifications (*1*). Styrelf was used with this gradation.

MIXTURE TESTING PROGRAM

The following mixture tests were performed:

TABLE 1 Physical Properties of the Binders

Physical Properties	Virgin Binder	Binder After Thin-Film Oven Test
AC-20		
Thin-Film Oven Test, percent loss		0.02
Penetration, 25 °C (100 g, 5 s), 0.1 mm	72	49
Absolute Viscosity, 60 °C, dPa-s	2 420	6 382
Kinematic Viscosity, 135 °C, mm^2/s	478	746
Specific Gravity, 25/25 °C	1.032	
Solubility in Trichloroethylene, percent	100.00	
Inorganic Material or Ash, percent	0.00	
Flash Point, COC, °C	322	
AC-20 with 7-Percent Vestoplast by Weight		
Thin-Film Oven Test, percent loss		0.06
Penetration, 25 °C (100 g, 5 s), 0.1 mm	54	48
Absolute Viscosity, 60 °C, dPa-s	10 619	14 493
Kinematic Viscosity, 135 °C, mm^2/s	1 179	1 687
Specific Gravity, 25/25 °C	1.020	
Solubility in Trichloroethylene, percent	99.96	
Inorganic Material or Ash, percent	0.02	
Flash Point, COC, °C	346	
Styrelf 1-D		
Thin-Film Oven Test, percent loss		0.26
Penetration, 25 °C (100 g, 5 s), 0.1 mm	59	43
Absolute Viscosity, 60 °C, dPa-s	33 122	90 995
Kinematic Viscosity, 135 °C, mm^2/s	2 345	3 178
Specific Gravity, 25/25 °C	1.026	
Solubility in Trichloroethylene, percent	99.61	
Inorganic Material or Ash, percent	0.02	
Flash Point, COC, °C	316	

TABLE 2 Aggregate Properties

Sieve Size (mm)	Leesburg, Virginia Traprock No. 68	Leesburg, Virginia Traprock No. 8	Frederick, Maryland Bird Eye Limestone No. 10	Texas, Maryland Aglime Mineral Filler	40 % No. 68, 34 % No. 8, 12 % Bird Eye, 14 % Aglime Target Blend	40 % No. 68, 34 % No. 8, 12 % Bird Eye, 14 % Aglime Actual Blend	Altered Blend
Aggregate Gradations, Percent Passing:							
19.0	100.0				100.0	100.0	100.0
12.5	75.0	100.0		100.0	90.0	91.8	92.0
9.5	41.4	87.9	100.0	99.7	72.4	74.2	74.0
4.75	7.3	22.1	62.1	99.4	31.8	33.8	41.0
2.36	2.0	6.2	14.8	98.1	18.8	18.9	23.0
1.18	1.6	3.6	4.3	96.4	15.6	15.6	15.9
0.600	1.4	2.8	3.2	95.7	14.6	14.7	15.3
0.300	1.2	2.3	2.9	91.6	14.0	14.0	14.4
0.150	0.9	1.9	2.6	85.0	12.9	13.0	13.2
0.075	0.6	1.4	2.2	65.0	10.1	10.1	10.1
Specific Gravities and Percent Absorption:							
Bulk Dry	2.946	2.964	2.692			2.899	2.895
Bulk SSD	2.964	2.980	2.707			2.914	2.912
Apparent	2.998	3.012	2.734	2.813		2.941	2.941
Abs (%)	0.59	0.54	0.28			0.55	0.56
Los Angeles Abrasion of the Particles in the Predominant Size Fractions above the 2.36-mm Sieve, Percent Loss by Mass:							
	14.6	20.4	27.3				
Flat and Elongated Particles in Size Fractions above the 4.75-mm Sieve, Percent by Mass:							
	17.5	20.3	14.2				

Bulk Dry = Bulk-Dry Specific Gravity.
Bulk SSD = Bulk-Saturated-Surface-Dry Specific Gravity.
Apparent = Apparent Specific Gravity.
Abs (%) = Percent Absorption.

- Marshall mixture design at 60°C, using 50 blows per side.
- Draindown:
  - –German,
  - –FHWA 2.36-mm sieve test, and
  - –Open-graded friction course (pie plate test).
- Resistance to rutting
  - –Georgia loaded-wheel tester (GLWT) at 40.6°C
  - –French pavement rutting tester at 60°C
  - –Gyratory testing machine (GTM) at 60°C
- Resistance to low temperature cracking
  - –Diametral modulus (M_d) at −32, −24, −16, −8, and 0°C
  - –Indirect tensile test at −16, −8, and 0°C
- Resistance to Aging (Strategic Highway Research Program Method M-007)
  - –Short-term Oven Aging with Diametral Modulus (M_d) at 25°C
  - –Long-term Oven Aging with M_d and Indirect Tensile Strength at 25°C
- Resistance to Moisture Damage
  - –Tensile Strength Ratio (TSR)
  - –Diametral Modulus Ratio (M_dR)
  - –Percent Visual Stripping

MIXTURE TEST DESCRIPTIONS

Mixture Design

Mixtures were designed by the 50-blow Marshall method, using binder contents of 5.5, 6.0, 6.5, and 7.0 percent by mixture weight. Optimum binder contents were based on a 3.5-percent air-void level. The target mixing and compaction temperatures were 154°C and 143°C, respectively.

Draindown

A German test, an FHWA test developed at the Turner-Fairbank Highway Research Center (TFHRC), and an FHWA test for open-graded friction courses (OGFC) were used to determine the efficiency of the stabilizers in preventing draindown in loose mixtures.

German Test (Schellenberg Institute, Germany)

Approximately 1 kg of mixture is placed into a dried, tared, 800-ml glass beaker immediately after mixing and weighed to the nearest

0.1 g (*1,3*). The beaker is then covered with aluminum foil and stored for 60 ± 1 min at the compaction temperature. (In Germany, the typical hot-mix plant discharge temperature of 170°C is used.) After storage, the mixture is placed into a tared bowl by quickly turning the beaker upside down without shaking. The final mass of the mixture is then recorded. The loss resulting from draindown is calculated as

$$\text{Loss, percent} = \frac{100(\text{original mass of mixture} - \text{final mass of mixture})}{\text{original mass of mixture}}$$

Losses up to 0.3 percent are allowable. Losses greater than 0.3 percent indicate that draindown may be a problem.

FHWA 2.36-mm Sieve Test

A dried circular bowl is weighed to the nearest 0.1 g. A dried 2.36-mm sieve of similar diameter is then placed on top of this bowl. The sieve and bowl are tared. Approximately 1 kg of asphalt mixture is placed on the sieve immediately after mixing and weighed to the nearest 0.1 g. The bowl, sieve, and mixture are covered with aluminum foil and stored for 60 ± 1 min at the compaction temperature. After storage, the sieve is removed and the final mass of the bowl is obtained, which includes the mass of the drained binder and fines. The percent loss resulting from draindown is calculated as

$$\text{Loss, percent} = \frac{100(\text{final bowl mass} - \text{initial bowl mass})}{\text{original mass of mixture}}$$

Because this test has not been correlated to problems in the field, there is no pass-fail criteria for it. It was developed as a potential replacement for the German test. Several suppliers of polymers have indicated that the German test is biased against polymers because the increase in tackiness provided by many polymers can cause more aggregate particles to stick to the bottom of the beaker.

FHWA Open-Graded Friction Course (OGFC)

The OGFC draindown test uses a 203.2- to 228.6-mm diameter clear pyrex pie plate to determine draindown (*4*). The quantity of mixture, storage time, and storage temperature used in the previous two draindown tests were again used. The loose mixture is spread across the pie plate and placed in the oven. After removal from the oven, the mixture is allowed to cool. The pie plate with mixture is then turned upside down. The degree of draindown is determined visually by comparing the amount of drained binder to five standard pictures of draindown, representing, on a scale of 1 to 5, no draindown to excessive draindown. For OGFC, draindown levels of 3 or 4 are desirable because the amount of drained binder that these levels provide is used to tack the mixture to the underlying layer. For SMAs, it was assumed that the degree of draindown should be less than or equal to a level of 3.

Resistance to Rutting

Georgia Loaded-Wheel Tester (GLWT)

The GLWT tests a beam for permanent deformation at 40.6°C. Each beam is 76.2 mm in width and thickness, and 381 mm in length. Beams are compacted by compression. The mixtures were tested at the 3.5-percent design air-void level.

The sides of a beam are confined by steel plates during testing except for the top 12.7 mm. A 690-kPa pressurized, stiff rubber hose is positioned across the top of the beam, and a loaded steel wheel runs back and forth on top of this hose for 8,000 cycles to create a rut. One cycle is defined as two passes of the wheel.

The load on the beam changes with the direction of travel. When the wheel is moving from right to left, the load is approximately 740 N at the center of the beam, while it is 630 N when moving left to right. Across the central region of the beam where the deformations are recorded, each of these loads has a variation of less then 5 percent.

Deformations are measured at the center of the beam, 51 mm left of center, and 51 mm right of center. If the average rut depth for three replicate beams exceeds 7.6 mm, the mixture is considered susceptible to rutting.

French Pavement Rutting Tester

The French (Laboratoires des Ponts et Chaussees) Pavement Rutting Tester tests a slab for permanent deformation at 60°C. Each slab is 500 mm in length, 180 mm in width, and 50 mm in thickness. The French Plate Compactor was used to fabricate the slabs. Mixtures are compacted in a steel mold using a smooth, reciprocating, pneumatic rubber tire having a diameter of 415 mm and a width of 109 mm.

Various sequences of different compaction efforts, tire pressures, and positions of the tire relative to the width of a slab are used to compact a slab. These parameters depend on the thickness of the slab and the required air-void level. The manufacturer verbally stated that the sequence used in this study should provide an air-void level close to the low end of the air-void range that can be obtained in the field after compaction by the rollers. This range varies with the type of mixture. Air voids in this study were approximately 3.5 percent, except for the Styrelf specimens that were at a 6-percent air-void level.

The French Pavement Rutting Tester tests two slabs at a time using two reciprocating tires. The tires are always at a fixed elevation. Hydraulic jacks underneath the slabs push them upward to create the load, normally 5000 ± 50 N. Each tire is inflated to 600 ± 30 kPa. The same type of tire used by the Plate Compactor is also used by this tester. Approximately 67 cycles are applied per minute. One cycle is defined as two passes of the tire. Slabs are tested in their molds.

Initially, 1,000 cycles are applied at 25°C to densify the mixture and to provide a smoother surface. The height of each slab is then calculated by averaging measurements taken at 15 positions using a depth gauge with a resolution of 0.1 mm. This average height is considered the initial height, or point-of-zero rut depth.

The slabs are then heated to 60°C for 6 hr, and the average rut depths are measured at 30, 100, 300, 1,000, and 3,000 cycles. A mixture is acceptable if the average rut depths at 1,000 and 3,000 cycles are less than or equal to 10 and 20 percent of the thickness of the slab, respectively. Slopes for different mixtures taken from log rut depth versus log cycles plots can also be compared. Rut-susceptible mixtures generally have higher slopes.

Gyratory Testing Machine (GTM)

Shear susceptibility was measured using the static shear strength (Sg), gyratory stability index (GSI), and gyratory elasto-plastic

index (GEPI) provided by the U.S. Corps of Engineers GTM, Model 8A6B4C. The GTM is a combination compaction and plane strain-shear testing machine that applies stresses simulating pavement conditions. The FHWA GTM is completely automated; it monitors and calculates all parameters.

The GTM was operated in accordance with the 1993 proposed version of American Society for Testing and Materials (ASTM) D 3387, "Compaction and Shear Properties of Bituminous Mixtures by Means of the U.S. Corps of Engineers Gyratory Testing Machine (GTM)." A vertical pressure of 0.827 MPa and a 0.014-radian gyratory angle were used. Specimens were compacted to their refusal density, which is defined as the point where the change in density becomes less than 16 kg/m^3 per 100 revolutions. It required 260 to 300 revolutions to reach this density.

Mixtures were tested at binder contents of 5.6, 6.2, and 6.8 percent, which bracketed the Marshall optimum-binder contents. By doing this, the GTM data at the optimum binder contents could be evaluated and whether the GTM provided different optimum binder contents determined. Compacted specimens had a diameter of 101.6 mm and a height of 63.5 mm.

The 0.014-radian angle of compaction is set by the operator using two rollers that circle around a flange that is part of the mold chuck. The two rollers, which are 3.14159-radians apart, are offset in vertical elevation, causing the mold chuck and specimen mold to tilt. A kneading action is applied to the mixture as the rollers circle around the mold chuck. One roller compresses an oil-filled pressure gauge that is used to calculate the Sg. The GTM continuously monitors the Sg of the mixture with revolutions, but the current procedure only evaluates the Sg at the refusal density.

A mixture can shear in the mold, causing the mold and mold chuck to tilt sideways to an angle that is larger than the angle on the axis of the rollers. This angle is a measure of the shear strain in the mixture. The GTM continuously monitors this angle to the nearest 0.0017 radian. The GSI is the ratio of the maximum angle that occurs at the end of the test to the minimum intermediate angle. It is a measure of shear susceptibility at the refusal density. The minimum intermediate angle is the smallest angle that occurs after the compaction process has started. It can be greater than the angle set by the operator. The GSI at 300 revolutions is close to 1.0 for a stable mixture and is significantly above 1.1 for an unstable mixture (*5*). (A more definitive criteria for the GSI has not been established.) When designing a mixture, the manufacturer states that the optimum binder content should be less than the binder content when the GSI begins to exceed 1.0.

The GEPI is the ratio of the minimum intermediate angle to the initial angle. A GEPI of 1.0 indicates high internal friction. A GEPI significantly above 1.0 indicates lower internal friction, from the use of rounded aggregates or moisture damage. A GEPI below 1.0 indicates that the aggregate is deteriorating. (More definitive criteria for the GEPI have not been established. The manufacturer suggests using an acceptable range of 1.0 to 1.5.)

Resistance to Low-Temperature Cracking

The majority of low-temperature cracking studies use stiffness to compare the performances of binders or mixtures. High stiffnesses at cold temperatures are equated to low flexibility and to increased susceptibility to cracking. In this study, the diametral modulus test and the indirect tensile strength test were used to evaluate low-temperature cracking. Specimens were tested at the design air-void level of 3.5 percent.

Diametral Modulus, M_d

The M_d's were measured at −32, −24, −16, −8, and 0 °C using an apparatus manufactured by the Retsina Company of Oakland, California. The apparatus provides a total diametral modulus at a loading time of 0.1 s by applying a load on the vertical diameter of a specimen and measuring the total, horizontal, tensile deformation. It is marketed for measuring the resilient (mainly elastic) modulus of a specimen, but it actually measures a total modulus that consists of elastic, viscoelastic, and permanent deformations. The equation used by ASTM D 4123 to calculate M_d is as follows:

$$M_d = \frac{P\,(u + 0.2734)}{t\,H_t}$$

where

M_d = diametral modulus (MPa),
P = load (N),
u = Poisson's ratio (assumed as 0.35),
t = specimen thickness (mm), and
H_t = total horizontal deformation (mm).

The deformations were maintained within a range of 76 to 200 E-05 mm by varying the load. The test is virtually nondestructive in this range, and the same specimens can be tested at all temperatures. Specimens were tested at the lowest temperature first, and specimens were maintained at each temperature for 24 hr. A lower M_d generally means better resistance to low-temperature cracking, although this generalization may not be true for all modified binders.

Indirect Tensile Test

Indirect tensile tests were performed at −16, −8, and 0°C with a loading rate of 1.27 mm/min. Indirect tensile strength, tensile strain at failure (horizontal strain), and the amount of work needed to cause tensile failure were evaluated. The work is the area under the stress-strain curve from the beginning of the test until failure. Higher strains at failure and higher amounts of work are associated with increased resistance to low-temperature cracking. These increases are usually accompanied by lower tensile strengths, although this may not be true for all modified binders.

The equation used by ASTM D 4123 to compute the indirect tensile strength of a 101.6-mm diameter specimen is as follows:

$$S_t = \frac{6.27\,P}{t}$$

where

S_t = indirect tensile strength (kPa),
P = load (N), and
t = thickness (mm).

The equation used to compute the strain at failure, assuming a Poisson's ratio of 0.35, is

$$e_t = 0.0205\,H_t$$

where e_t is the indirect tensile strain at failure and H_t is the total horizontal deformation (mm).

Resistance to Aging

The mixtures were oven-aged according to Strategic Highway Research Program (SHRP) Method M-007 (*6*). The method stated that short-term aging produces the average amount of aging that occurs during production and placement of the paving mixture. Long-term aging produces the average amount of aging that occurs between placement and approximately 10 years of service life.

Standard practice for preparing specimens at TFHRC did not include ovenaging when this study was performed. Thus, all mixtures tested under the other parts of this study were not subjected to the SHRP aging methods. The properties of mixtures not subjected to these methods are termed "unaged" properties in this section of the study, although some aging does occur during mixing and compaction.

To simulate short-term aging, the loose mixture is placed in a forced draft oven for 4 h at 135°C. The mixture is then compacted to an air-void level typically obtained after construction. A 5- to 6-percent level is typical for SMA, and 5.5 percent was used in this study. To simulate long-term aging, the compacted specimens are placed in a forced draft oven for 5 days at 85°C.

M_d and indirect tensile strengths were measured at 25°C on the unaged and long-term aged specimens. The specimens subjected to short-term aging were only tested for M_d so that they could also be used for long-term aging. Surface-course mixtures with lower M_d and tensile strengths are more flexible and therefore more resistant to fatigue cracking, although these generalizations may not be true for all modified binders.

Resistance to Moisture Damage

Both the AC-20 asphalt and the Styrelf binder had been treated with liquid antistripping additives before being used in the pavement. Therefore, it was decided to determine the moisture susceptibilities of the Arbocel and Styrelf mixtures using ASTM D 4867 "Effect of Moisture on Asphalt Concrete Paving Mixtures," and to test the other mixtures later if appropriate. Specimens were compacted to a 5- to 6-percent air-void level. Both the diametral modulus-retained ratio (M_dR) and TSR ratio were computed in terms of percentages.

RESULTS AND DISCUSSION

An analysis of variance and Fisher's Least Significant Difference statistical procedures at a 95-percent confidence level were used to analyze the test results. Fisher's analysis places sample averages into groups by determining which averages are statistically equal. Groups are designated by letters starting with A. Averages in group A are statistically equal and higher than those in group B. Averages in group B are statistically equal and higher than those in group C, and so forth. Averages can fall into more than one group. For example, a designation of AB shows that the average can be put into group A or B.

Mixture Design

Properties at optimum binder contents are given in Table 3. The optimum binder contents were 6.5 percent for the mixtures with Interfibe, Vestoplast, and Styrelf; 6.4 percent for Arbocel; 6.2 percent for Inorphil; 5.9 percent for Custom Fiber; and 5.8 percent for the Styrelf mixture with altered gradation. The average binder contents used in the pavement sections based on quality-control testing were 6.5 ± 0.2 percent for the Styrelf and Arbocel sections, and 6.2 ± 0.3 percent for the Vestoplast sections.

It was expected that the mixture with Custom Fiber would have an optimum binder content closer to those for the other cellulose fibers. Also, a representative for Vestoplast stated that the optimum binder content for the Vestoplast mixture should have been lower than those for fibers. These mixtures were retested, but the same data were obtained.

Table 3 shows that the Styrelf mixtures had the highest Marshall stabilities and flows. The other mixtures had statistically equal stabilities and flows; one reason for this equality was that the data were highly variable. Altering the gradation lowered the void in the mineral aggregate (VMA) by approximately 1.6 percent.

The VMA versus binder-content relationships (not given in this paper) showed that the optimum binder contents for the Custom Fiber mixture and Styrelf mixture with altered gradation were at the point of minimum VMA. The VMAs were starting to increase at the optimum binder contents for the other stabilizers, indicating they

TABLE 3 Marshall Mixture Design Properties

Type of Stabilizer	Optimum Binder Content (%)	MSG	Density (kg/m³)	Stability (N)	Flow (0.25-mm)	Air Voids (%)	VMA (%)	VFA (%)
Custom Fibers	5.9	2.623	2527	6 623	14	3.5	18.2	87.3
Inorphil	6.2	2.628	2531	6 303	12	3.5	18.2	79.9
Arbocel	6.4	2.615	2519	7 422	13	3.5	18.6	84.0
Interfibe	6.5	2.600	2500	7 406	10	3.5	19.3	80.5
Vestoplast	6.5	2.606	2520	7 504	16	3.5	18.7	82.8
Styrelf	6.5	2.606	2514	9 933	27	3.5	18.9	81.7
Styrelf with Altered Gradation	5.8	2.638	2545	10 721	30	3.5	17.3	79.2

Marshall Design Blows = 50
Mixing Temperature = 154 °C
Compaction Temperature = 143 °C

MSG = Maximum Specific Gravity of the Mixture.
VMA = Voids in the Mineral Aggregate.
VFA = Voids Filled with Asphalt.

may have been slightly high for obtaining maximum resistance to rutting.

Draindown

Table 4 shows that the mixtures with Vestoplast and Styrelf and an AC-20 control mixture had the highest amounts of draindown for all three methods, and all failed the German and OGFC tests. The four mixtures with fibers had low amounts of draindown and passed these tests. (An AC-20 control mixture with no stabilizer at a binder content of 6.5 percent was included for comparative purposes. This mixture was not included in the other parts of this study because the asphalt drained during compaction. This did not occur when using Vestoplast or Styrelf.)

Altering the gradation significantly reduced the amount of draindown. The mixture passed the OGFC test; the loss of 0.05 percent in the 2.36-mm sieve method is very low compared to the binder content of 5.8 percent. (This is a low amount of draindown even if it is assumed that all of the drained material was binder.) The mixture did fail the German test.

The German test provided one discrepancy. The loss of 3.86 percent for the Styrelf mixture was greater than the loss of 2.88 percent for the AC-20 control mixture. Middle-sized and coarse aggregate particles had stuck to the bottom of the beakers when testing these two mixtures, as they did when testing the mixture with Vestoplast. Therefore, the discrepancy may have been related to differing amounts of aggregate stuck to the beaker. When aggregates other than dust are left in the beaker, the test does not measure draindown accurately.

The 2.36-mm sieve method provided a similar discrepancy. The losses of 0.89 and 0.84 percent for the Styrelf and Vestoplast mixtures, respectively, were greater than the loss of 0.19 percent for the AC-20 control mixture. A reason for this discrepancy was not apparent. It was hypothesized that the control mixture had a higher loose density, which provided fewer channels for draindown.

Because the Marshall design and draindown results were similar for the mixtures with fibers, it was decided not to test the Interfibe and Inorphil fibers any further unless the data for the other stabilizers provided a reason for testing them. For example, if the mixtures with the other four stabilizers showed significant differences in rutting potential, then the mixtures with the Interfibe and Inorphil fibers would be tested for rutting.

Resistance to Rutting

GLWT

The GLWT results are given in Table 5. All rut depths were statistically equal and less than the specification level of 7.6 mm.

French Pavement Rutting Tester

The French Pavement Rutting Tester results are presented in Table 5. All rut depths and slopes were statistically equal, and none of the rut depths exceeded the maximum allowable levels.

GTM

The GTM data at the optimum binder contents provided by the Marshall designs are indicated in Table 5. The static shear strengths, GSIs, GEPIs, and refusal air-void levels were statistically equal from mixture to mixture; all were in the acceptable range. (This testing was added at the end of the study. Only three stabilizers were tested because of insufficient aggregate.)

The static shear strengths, GSIs, and GEPIs at all three binder contents tested, namely, 5.6, 6.2, and 6.8 percent, were equal. These data indicate that binder contents higher than the Marshall optimums could be used without detrimentally affecting rutting resistance.

Extractions were performed to determine whether the GTM breaks coarse aggregate. Table 6 shows that aggregate did break even though the Los Angeles Abrasions were within the specification. The cumulative percent passing the 4.75-mm sieve increased more than 5 percent. Extractions were also performed on Custom Fiber specimens compacted with the Marshall hammer. The two compaction methods broke an equal amount of aggregate. The Mar-

TABLE 4 Draindown Test Results

Type of Stabilizer	Binder Content, Percent by Mix Weight	German Method, Percent Weight Loss	2.36-mm Sieve Method, Percent Weight Loss	Open-Graded Friction Course Drainage Test
Custom Fibers	5.9	0.07	0.00	2.5
Inorphil	6.2	0.11	0.00	2.5
Arbocel	6.4	0.27	0.00	2.5
Interfibe	6.5	0.25	0.00	2.5
Vestoplast	6.5	1.58	0.84	5
Styrelf	6.5	3.86	0.89	5
AC-20 Control	6.5	2.88	0.19	5
Styrelf with Altered Gradation	5.8	0.40	0.05	2.5
Specification, maximum		0.30	Not Established	3

TABLE 5 GLWT, French Pavement Rutting Tester (PRT), and GTM Results

Type of Stabilizer	GWLT Rut Depth (mm)	French PRT: Percent Rut Depth at 3000 Cycles	French PRT: Slope	Gyratory Testing Machine: Static Shear Strength, Sg (kPa)	GSI	GEPI	Refusal Air Voids (%)
Custom Fibers	5.8	4.5	0.12	430	0.89	1.24	2.7
Arbocel	6.5	6.5	0.11	430	0.93	1.21	2.4
Vestoplast	4.0	6.1	0.17	NT	NT	NT	NT
Styrelf	3.2	7.7	0.14	480	0.92	1.23	2.4
Styrelf with Altered Gradation	4.3	4.3	0.16	NT	NT	NT	NT

NT = Not Tested.

TABLE 6 Aggregate Gradations (Percent Passing) Before and After Compaction

Sieve Size (mm)	Before Compaction	After Gyratory Compaction: Custom Fiber	After Gyratory Compaction: Arbocel	After Gyratory Compaction: Styrelf	After Marshall Hammer Compaction: Custom Fibers
19.0	100.0	100.0	100.0	100.0	100.0
12.5	91.8	91.2	91.3	91.9	90.6
9.5	74.2	74.3	73.4	73.6	74.0
4.75	33.8	39.2	39.8	39.6	39.6
2.36	18.9	23.8	23.6	24.0	23.2
1.18	15.6	19.2	19.1	19.2	18.2
0.600	14.7	17.7	17.3	17.5	16.5
0.300	14.0	16.4	16.1	16.3	15.2
0.150	13.0	14.9	14.7	14.9	13.7
0.075	10.1	11.7	11.7	11.7	10.5

shall hammer produced less material passing the 0.075-mm sieve, but in other concurrent FHWA studies, the two compaction methods have provided equal amounts of broken aggregate and equal increases in dust. Additional extractions showed that the aggregate broke during compaction and not during mixing.

Resistance to Low-Temperature Cracking

Diametral Modulus, M_d

The M_d in Table 7 do not show conclusively that any SMA was better than another. The data were close at a given temperature. Mixtures with better low-temperature properties have a designation of *B*.

Indirect Tensile Test

The tensile test data in Table 7 also, do not indicate that any SMA was better than another. Mixtures with better low-temperature properties have a designation of A for strain at failure and for work. All mixtures had statistically equal strains at the two lowest temperatures. One reason for this was that the data were highly variable. This also caused the works to be highly variable, especially at the lowest temperature. The two mixtures with Styrelf had higher strains and works at 0°C, possibly indicating improved resistance to fatigue cracking at higher temperatures. Mixtures with the highest strains or works did not necessarily have the lowest tensile strengths, as it is often assumed.

Resistance to Aging

Table 8 shows that how the mixtures grouped together varied with the test and the degree of aging. The Styrelf mixture had the best (lowest) properties after long-term aging. This binder did contain a different base asphalt.

The unknown consequence of having different rankings for unaged properties complicated the analyses; thus, the resistance to aging was related to changes in the moduli and strengths. These changes, also shown in Table 8, were computed from the averages for each mixture. Therefore, replicate measurements needed for statistical analyses were not available. (Averages had to be used because different specimens had to be tested to obtain the unaged and aged properties.) The two polymer-modified mixtures had the lowest changes; therefore, these mixtures aged less. Altering the gradation had a negative effect on aging.

Resistance to Moisture Damage

All retained ratios were above 90 percent, and visual stripping was less than 10 percent. These data indicated little susceptibility to

TABLE 7 Low Temperature Test Results

Diametral Modulus, MPa

Type of Stabilizer	Temperature (°C) 0	-8	-16	-24	-32
Custom Fiber	22 505 (B)	34 475 (A)	43 273 (A)	46 376 (A)	57 670 (A)
Arbocel	26 580 (A)	34 382 (A)	42 749 (A)	48 272 (A)	53 202 (AB)
Vestoplast	20 092 (B)	32 062 (A)	41 860 (A)	44 500 (A)	51 540 (B)
Styrelf	21 340 (B)	32 710 (A)	37 474 (B)	48 555 (A)	53 154 (AB)
Styrelf with Altered Gradation	26 049 (A)	33 937 (A)	41 949 (A)	50 389 (A)	52 754 (AB)

Indirect Tensile Test

	Temperature (°C)								
	0	-8	-16	0	-8	-16	0	-8	-16
Type of Stabilizer	Tensile Strength (kPa)			Failure Strain ($\times 10^{-6}$ mm/mm)			Work for Failure, (Pa or J/m^3)		
Custom Fiber	1 769 (B)	2 310 (B)	3 314 (AB)	389 (B)	328 (A)	196 (A)	4 777 (B)	5 659 (AB)	4 882 (A)
Arbocel	2 054 (AB)	2 353 (B)	3 294 (AB)	363 (B)	273 (A)	284 (A)	5 610 (B)	4 767 (B)	4 925 (A)
Vestoplast	2 186 (A)	2 722 (AB)	3 070 (B)	393 (B)	268 (A)	240 (A)	6 147 (B)	4 668 (B)	5 104 (A)
Styrelf	2 297 (A)	2 648 (AB)	3 594 (AB)	715 (A)	425 (A)	238 (A)	12 597 (A)	7 742 (A)	5 383 (A)
Styrelf with Altered Gradation	2 282 (A)	2 936 (A)	3 779 (A)	793 (A)	303 (A)	304 (A)	14 423 (A)	6 350 (A)	6 297 (A)

moisture damage. The effects of the stabilizers on moisture damage, if any, could not be determined because antistripping additives had been used.

CONCLUSIONS

- The stabilizers had no significant effect on rutting susceptibility or low-temperature properties, even though the optimum binder contents varied from 5.9 to 6.5 percent. Therefore, small changes in the composition of the mastic also had no effect. All mixtures had a low susceptibility to rutting.
- The two mixtures containing the polymer stabilizers were better at controlling age hardening than the mixtures with fibers. This means they should provide more resistance to cracking after a pavement ages, including resistance to low-temperature cracking.
- The two polymers did not control draindown in the 1-hr draindown tests; whereas, the four fibers reduced the amount of drained material to acceptable levels. Fibers retain their structure with changes in temperature. The two polymers are thermoplastic.
- Reducing the optimum binder content by altering the gradation decreased the amount of draindown, but it also increased the susceptibility to age hardening. It had no effect on rutting susceptibility and low-temperature properties.
- The Marshall hammer and the GTM broke equal amounts of coarse aggregate.

RECOMMENDATIONS

- Further studies of draindown tests are needed. The current tests produce discrepancies that are difficult to explain. Draindown tests need to be performed when pavements are constructed to evaluate the tests' usefulness. No draindown problems were reported during construction on U.S. Route 15, although the tests only provide a propensity for draindown.

TABLE 8 Aging Test Results

Type of Stabilizer	Dynamic Modulus, M_d at 25 °C (MPa)			Change in Dynamic Modulus[a]		
	Unaged	Short-Term Aging	Long-Term Aging	Short-Term to Unaged	Long-Term to Short-Term	Total Aging
Custom Fiber	1518 (A)	3410 (A)	5157 (AB)	1892	1747	3639
Arbocel	1095 (B)	3814 (A)	5701 (A)	2719	1887	4607
Vestoplast	1545 (A)	3644 (A)	4405 (B)	2099	761	2860
Styrelf	814 (C)	1975 (B)	2435 (C)	1161	460	1621
Styrelf with Altered Gradation	1170 (B)	3778 (A)	4979 (AB)	2608	1201	3809

Type of Stabilizer	Tensile Strength at 25 °C (kPa)		Change in Tensile Strength[a]
	Unaged	Long-Term Aging	Total Aging
Custom Fiber	478 (C)	982 (AB)	504
Arbocel	519 (B)	1001 (A)	482
Vestoplast	594 (AB)	905 (AB)	311
Styrelf	582 (AB)	835 (B)	253
Styrelf with Altered Gradation	661 (A)	1022 (A)	361

[a]Obtained by subtraction.

- Additional mixtures need to be tested to verify the conclusions of this study.
- The consequences of aggregate being broken during mixture design need to be determined.
- The results from this study need to be compared to field performance. After 1.5 years, all three SMA pavement sections have no distress.

REFERENCES

1. Stuart, K. D. *Stone Mastic Asphalt (SMA) Mixture Design,* FHWA-RD-92-006. FHWA, U.S. Department of Transportation, March 1992.
2. Harmon, T. P., C. A. Gordon, K. M. Headrick, C. Harris Jr., J. R. Bukowski, and J. A. D'Angelo. *Mix Design Support & Field Production Testing.* Demonstration Project #90, Project #9202. FHWA, U.S. Department of Transportation, June 1992.
3. SMA Technical Working Group. *SMA Material and Construction Model Specification,* FHWA, U.S. Department of Transportation, Oct. 9, 1992.
4. Smith, R. W., J. M. Rice, and S. R. Spelman. *Design of Open-Graded Asphalt Friction Courses.* FHWA-RD-74-2. FHWA, U.S. Department of Transportation, January 1974 and July 1975 (supplement).
5. Roberts, F. L., P. S. Kandhal, E. R. Brown, D. Y. Lee, and T. W. Kennedy. *Hot Mix Asphalt Materials, Mixture Design, and Construction.* National Asphalt Pavement Association (NAPA) Education Foundation, Lanham, Md., 1991.
6. *Short and Long-Term Aging,* Method M-007. Strategic Highway Research Program, National Research Council, Washington, D.C., Sept. 25, 1992.

Publication of this paper sponsored by Committee on Characteristics of Bituminous Paving Mixtures To Meet Structural Requirements.

Evaluation of Stone Matrix Asphalt Versus Dense-Graded Mixtures

WALAA S. MOGAWER AND KEVIN D. STUART

Since 1991, several states in the United States have built stone matrix asphalt (SMA) pavements in order to evaluate the performance of SMA mixtures in terms of their durability and resistance to rutting. Two such SMA mixtures and two dense-graded mixtures are compared in terms of their resistance to rutting, moisture damage, low-temperature cracking, and aging, and the effect of using a polymer instead of a fiber in SMA mixtures is examined. SMA performance are evaluated using existing tests, to determine which are applicable to SMAs. U.S. Army Corps of Engineers Gyratory Testing Machine (GTM), confined and unconfined repeated load tests, diametral resilient modulus tests, the indirect tensile strength tests, and two wheel-tracking devices, the French Pavement Rutting Tester and the Georgia Loaded Wheel Tester are applied and their results analyzed. Both wheel-tracking devices and the GTM indicate that none of the mixtures is susceptible to rutting. The confined and the unconfined repeated load and diametral resilient modulus tests, however, predict more rutting in the SMAs than in the dense-graded mixtures, which contradicts the results from the wheel-tracking devices and the GTM. The SMAs had less potential for moisture damage and age hardening. When using a polymer instead of a fiber as the stabilizer in the SMAs, the amount of drained binder and mineral filler increased.

Stone matrix asphalt (SMA) was developed in Europe approximately 20 years ago. Field experience in Europe has shown SMAs to be durable and more resistant to rutting than dense-graded mixtures. Recently, the SMA technology has been implemented in the United States. Several states built SMA pavements in 1991, 1992, and 1993 to evaluate the performances of these mixtures in terms of their durability and resistance to rutting.

In principle, an SMA is to have a higher percentage of coarse aggregate in its mixture compared with that of a dense-graded mixture with a given maximum aggregate size (*1*). An SMA mixture thus provides greater stone-on-stone contact, which gives it a high resistance to rutting and should reduce the dependency of the distress on the type and amount of binder. An SMA includes a large proportion of high-quality coarse, crushed aggregate (stone); a large proportion of binder and mineral filler, including minus No. 0.075 mm dust (mastic); a small proportion of middle-sized aggregate; and, generally, a stabilizing additive to prevent drainage of the binder and mineral filler before the mixture is placed and can cool. Cellulose fibers, mineral fibers, and polymers have been used as stabilizers (*1*).

SMAs have higher binder contents than dense-graded mixtures do. An SMA's higher binder content should produce a durable mixture that is resistant to cracking, moisture damage, and age-hardening.

Several tests, available to measure the durability and rutting resistance of dense-graded mixtures, were examined to determine whether they could be used to evaluate the performances of SMAs. The objectives of the study were to

- Compare SMAs to dense-graded mixtures in terms of their resistance to rutting, moisture damage, low-temperature cracking, and aging.
- Determine which mechanical tests can be used to measure the rutting susceptibility of SMAs.

W. S. Mogawer, Civil Engineering Department, University of Massachusetts Dartmouth, North Dartmouth, Mass. 02747. K. D. Stuart, FHWA, Turner-Fairbank Highway Research Center, 6300 Georgetown Pike, McLean, Va. 22101-2627.

EXPERIMENTAL PROGRAM

To achieve the study's objectives, a dense gradation and an SMA gradation with a nominal maximum size of 9.5 mm (3/8 in.) and a dense gradation and an SMA gradation with a nominal maximum size of 12.5 mm (1/2 in.) were used. These mixtures were designated as D 9.5, SMA 9.5, D 12.5, and SMA 12.5. The asphalt and aggregate were the same materials used in constructing pavement sections tested by the Accelerated Loading Facility (ALF) at the Turner-Fairbank Highway Research Center (TFHRC). The asphalt was an AC-20, and the aggregate was a crushed diabase. The aggregate gradation of each mixture is presented in Table 1 and illustrated in Figure 1. For the SMAs, the aggregates were blended according to gradations presented in an FHWA report on SMAs that were developed based on German specifications (*1*). The SMA 12.5 also met the target gradation ranges recommended by the FHWA plan for the test and evaluation of SMA (*2*). The D 9.5 gradation was prepared to meet the Virginia Department of Transportation S-5 specifications for surface mixtures.

The four mixtures were evaluated in terms of their resistance to rutting, moisture damage, low-temperature cracking, and aging. The two SMAs were prepared using Arbocel 50/50 (i.e., pellet composed of 50 percent cellulose fiber and 50 percent asphalt) as the stabilizer, at 0.6 percent by total weight of the mixture.

A polymer stabilizer called Vestoplast was also used at 7 percent by weight of the asphalt in order to investigate the effect of using a polymer instead of a fiber. The SMAs with Vestoplast were compared with the other mixtures in terms of their resistance to rutting and drainage potential only. The SMAs with Vestoplast resistances to rutting were evaluated using two-wheel-tracking devices only.

Mix Design

Marshall mix designs were performed to determine the optimum asphalt contents (OAC). The mixtures were designed to sustain heavy traffic. The SMAs were compacted using 50 blows, whereas the dense-graded mixtures were compacted using 75 blows.

SMAs are designed in Europe for heavy traffic using 50 blows. Increasing the number of blows is not recommended because it

TABLE 1 Aggregate Gradations of Mixtures Tested (Percent Passing)

Sieve Size mm	in	D 9.5 (1)	SMA 9.5 (2)	(3)	(4)	D 12.5 (1)	SMA 12.5 (2)	(3)	(4)
19.0	(3/4 in)					100.0	100.0	100.0	100.0
12.5	(1/2 in)	100.0	100.0	100.0	100.0	95.0	95.0	95.5	94.6
9.5	(3/8 in)	95.0	95.0	95.1	94.5	82.0	71.0	74.5	76.1
4.75	(No. 4)	66.0	46.0	50.8	52.9	56.0	25.0	33.4	34.4
2.36	(No. 8)	48.7	25.0	29.6	31.0	39.0	20.0	24.1	24.2
1.18	(No. 16)	37.2	20.0	23.4	23.4	29.0	18.0	20.7	20.5
0.600	(No. 30)	26.9	16.0	19.0	18.8	21.0	16.0	18.1	17.9
0.300	(No. 50)	16.0	13.0	15.6	15.4	13.8	13.0	15.2	14.9
0.150	(No. 100)	8.7	12.0	13.7	13.6	9.1	12.0	13.3	13.3
0.075	(No. 200)	6.7	10.0	11.4	11.2	6.3	10.0	10.9	11.1

(1) and (2): Design Gradations.
(3): Extraction results of samples prepared using the GTM.
(4): Extraction results of samples prepared using the Marshall hammer.

could increase the number of fractured aggregates without increasing density (*1*).

The design air-void contents were 4 percent for the dense-graded mixtures and 3 percent for the SMA's. These are typical average design contents. The greater stone-on-stone contact in an SMA allows the use of lower air voids.

Rutting Evaluation

The French Laboratoire des Ponts et Chaussées (LCPC) Pavement Rutting Tester, the Georgia Loaded Wheel Tester (GLWT), the U.S. Army Corps of Engineers Gyratory Testing Machine (GTM), and a confined and unconfined repeated load test were used to measure the resistance to rutting.

French Pavement Rutting Tester

The French Pavement Rutting Tester tests slabs that are 500 by 180 by 50 mm thick (19.7 by 7.1 by 1.97 in.) using a smooth, reciprocating, pneumatic rubber tire at 0.61 MPa (87 lbf/in.^{2}) and loaded at 5000 ± 50 N (1124 lbf). The tire is 415 mm (16.3 in.) in diameter and 109 mm (4.3 in.) wide. A hydraulic jack underneath the slab pushes the slab upward to create the load. The machine has two reciprocating tire assemblies and tests two slabs at a time. The slabs were fabricated using the French Plate Compactor and were cured at room temperature for 2 days.

An initial densification of 1,000 cycles at 25°C (77°F) is first applied. A cycle is two passes of the tire. The deformations in the slabs are measured at the end of the initial densification. These readings are the zero readings. The slabs are then heated to the test tempera-

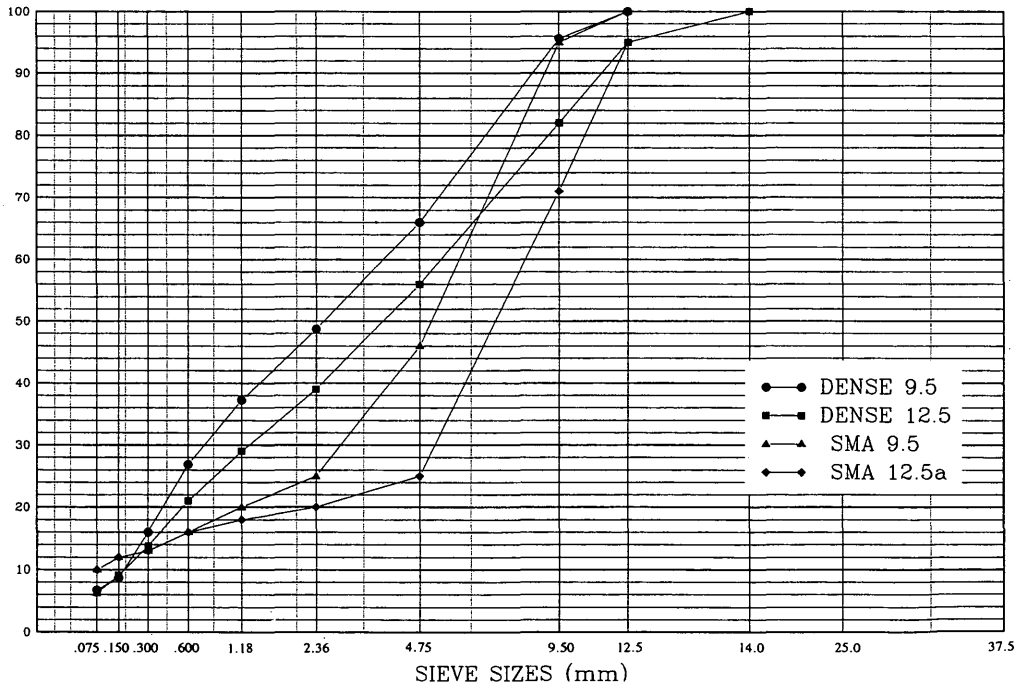

FIGURE 1 Aggregate gradations used in preparing dense and SMA mixtures.

ture of 60°C (140°F) for 3 hr before the test begins. The average rut depths at 30, 100, 300, 1,000, and 3,000 cycles are measured. To measure the rut depth, the machine is stopped and 15 measurements on the slab are taken to calculate the average rut depth: 5 locations along the length times three locations along the width. The test is stopped if the average rut depth is more than 20 percent of the slab thickness (*3*). Three slabs were fabricated at the OAC for each mixture.

Before testing, each slab's air voids were calculated using the slab density and the maximum specific gravity of the mixture. After testing, each slab was cut into three pieces along the length of the slab, two pieces out of the wheel path, and one piece in the wheel path. The air voids in each piece were measured. The voids before testing and the voids out of the wheel path after testing were expected to be close; however, the voids out of the wheel path were higher. This means that the voids in the wheel path must be measured before testing using trial slabs.

Georgia Loaded Wheel Tester

GLWT tests a 381-mm by 76.2-mm by 76.2-mm (15-in. by 3-in. by 3-in.) beam for rutting at 40.6°C (105°F). The beams are prepared by compression. Densities within 97 percent of the mix design density are recommended (*4*).

To achieve the recommended density, a 444.8-kN (100-kip) load was applied rapidly four times and then applied for 6 min. A load of 266.9 kN (60 kip) was used instead for the Vestoplast mixtures because binder squeezed out of the beams using 444.8 kN (100 kip). Nevertheless, the required air-void level of 3 percent was still met.

Before testing, beams were cured at room temperature for 7 days, then cured for 24 hr at 40.6°C (105°F). After curing, each beam was loaded into the testing frame of the GLWT; an initial reading was taken at the beam's center, at 50.8 mm (2 in.) left of the center, and at 50.8 mm (2 in.) right of the center, across the length of the beam. A 0.69-MPa (100-lbf/in.^{2}) inflated rubber hose was positioned across the sample and a loaded wheel ran back and forth on the top of the rubber hose. When the wheel moved from right to left, the load was approximately 740 N (166.3 lbf) at the center of the beam, whereas it was 630 N (141.6 lbf) when moving left to right.

The test was performed for 8,000 cycles, and final readings were taken at the same positions at which initial readings were taken. If the average rut depth for the three beams exceeded 7.6 mm (0.30 in.), the mixture was considered to have failed (*4*). Three beams were fabricated at the OAC for each mixture.

GTM

The GTM was used to evaluate rutting resistance, using the gyratory stability index (GSI) and the refusal densities.

The refusal density is where there is no reduction in air voids with additional gyrations. The GSI is the ratio of the maximum gyratory angle to the minimum gyratory angle that occurs during the test. Typically, for stable mixtures, the GSI value is close to 1.0; for unstable mixtures, the GSI is significantly above 1.1 (*5*). A more definitive failing GSI has not been established.

The mixtures were tested at 60°C (140°F) in accordance with the National Cooperative Highway Research Program (NCHRP) Asphalt-Aggregate Mixture Analysis System (AAMAS) procedure (*6*). Three specimens were fabricated at the OAC for each mixture. All specimens were tested with a vertical pressure of 0.83 MPa (120 lbf/in.^{2}) and a 0.0175-rad (1°) gyratory angle. The GTM oil-filled roller was used. Samples were compacted to 300 revolutions. Extraction tests and sieve analyses were performed on the SMA specimens to determine whether the GTM fractured any aggregate.

Compressive Repeated Load Test

Unconfined repeated load tests were performed under compression to determine the dynamic modulus and permanent deformation of each mixture. The specimens had a diameter of 101.6 mm (4.0 in.) and a height of 203.2 mm (8.0 in.) and were compacted to the design air-void levels using kneading compaction. Testing was performed at 40°C (104°F) using a closed-loop servohydraulic MTS Materials Testing System. Vertical compressive strains were measured by averaging the outputs of two linear variable differential transducers (LVDT), each having a gauge length of 101.6 mm (4.0 in.).

A repeated load consisting of a 0.1-sec sinusoidal wave followed by a 0.9-sec rest period was applied to each specimen. The vertical stress was 0.45 MPa (65 lbf/in.^{2}). The dynamic modulus and its associated permanent deformation at the hundredth cycle were used to evaluate the mixtures.

Also, two confined repeated load tests were performed on the SMA 12.5. One test consisted of a 0.59-MPa (85-lbf/in.^{2}) vertical stress and a 0.14-MPa (20-lbf/in.^{2}) confining pressure, which provided a deviator stress of 0.45 MPa (65 lbf/in.^{2}). The other test consisted of a 0.45-MPa (65-lbf/in.^{2}) vertical stress and a 0.14-MPa (20- lbf/in.^{2}) confining pressure, which provided a deviator stress of 0.31 MPa (45 lbf/in.^{2}).

Moisture Damage Evaluation

The resistance to moisture damage was evaluated by determining the diametral modulus (M_d) and static indirect tensile strength (S_t) of specimens before and after exposure to water (*7*). Six specimens per mixture were compacted using the Marshall hammer to air-void levels expected in the field after construction. Dense-graded mixtures were compacted to 6- to 8-percent air voids. The Swedes and Germans report that, for SMAs, field air-void levels are typically 3 to 5 percent and are specified to be less than 6 percent (*1*). Thus, the SMAs were compacted to a 5 to 6-percent air-void range. The six specimens were then divided into two sets. One set was maintained in a dry state; the other was vacuum saturated with distilled water so that 55 to 80 percent of the air voids were (*a*) filled with water, (*b*) subjected to freezing for 15 h at -18 ± 2.0°C (-0.4 ± 3.6°F), then (*c*) moisture conditioned by soaking the specimens in distilled water at 60°C (140°F) for 24 hr, and (*d*) soaked in distilled water at 25°C (77°F).

Moisture damage is presented as the ratio of the wet M_d to the dry M_d (M_dR) as well as the ratio of the wet S_t to the dry S_t (TSR). Mixtures with a TSR less than 0.8 or an M_dR less than 0.7 have a moisture-damage potential (*7*).

Visual stripping was also estimated; Above 10 percent, it was considered excessive (*7*).

Low-Temperature Cracking Evaluation

High stiffnesses, or moduli, of asphalt mixtures at cold temperatures are equated with low flexibility and an increased susceptibility to

cracking. In this study, three Marshall specimens per mixture were prepared and tested for M_d at −32, −24, −16, −8, 0, 5, 16, 25, 32, and 40°C (i.e., −25.6, 11.2, 3.2, 17.6, 32, 41, 60.8, 77, 89.6, and 104°F).

Drainage

The German drainage test, the FHWA drainage test for open-graded friction courses (OGFC), and a proposed drainage test developed in the Bituminous Mixtures Laboratory at TFHRC were included in this study to determine the efficiency of the two stabilizers used to prevent drainage of the binder and mineral filler.

For the German drainage test, 1 kg (2.2 lbm) of mixture is prepared at the mixing temperature. The mixture is then placed into a dried 800-ml glass beaker and weighted to the nearest 0.1 g (0.00022 lbm). The beaker is covered and stored for 60 ± 1 min at 170°C (338°F). After storage, the mixture is removed from the beaker and placed into a tared bowl by quickly turning the beaker upside down without shaking. The final weight of the mixture is measured, and the percent drainage is calculated as

$$\text{Loss (percent)} = \frac{100\ (\text{original weight} - \text{final weight})}{\text{original weight}}$$

Losses of less than 0.2 percent indicate that drainage should not occur, although losses of up to 0.3 percent are still acceptable. Losses greater than 0.3 percent indicate that drainage may be a problem (*1*). The storage temperature used in Germany is the hot-mix discharge temperature, which is much higher than those used in the United States. Hence, the procedure was modified so that the compaction temperature of 143°C (290°F) could be used.

The FHWA's OGFC drainage test uses a clear pyrex pie plate, 203.2- to 228.6-mm (8- to 9-in.) in diameter, instead of a beaker. The amount of drainage is observed on the bottom of the plate and compared to standard pictures of drainage, ranging from no drainage to excessive drainage.

In the proposed drainage test, called the 2.36-mm (No. 8) sieve drainage test, a dried mixing bowl is weighed to the nearest 0.1 g (0.00022 lbm). A 2.36-mm (No. 8) sieve of similar diameter is placed on top of the bowl, and 1 kg (2.2 lbm) of mixture is placed on the sieve immediately after mixing. The bowl, sieve, and mixture are then covered with aluminum foil and stored for 60 ± 1 min at 143°C (290°F). After storage, the sieve is removed and the final weight of the bowl is obtained. The percent loss resulting from drainage is calculated as

$$\text{Loss (percent)} = \frac{100\ (\text{final bowl weight} - \text{initial bowl weight})}{\text{original weight of mixture}}$$

The German test criteria (i.e., losses less than 0.2 percent indicate no drainage problem) was also applied to this test.

Aging

The effect of aging on the mixtures was examined according to Strategic Highway Research Program (SHRP) Method M-007 (*8*). The procedure consists of determining the effects of short- and long-term aging on asphalt mixture stiffness. For short-term aging, loose mixtures were aged in a forced draft oven for 4 hr at 135°C(275°F) and then compacted using the Marshall hammer to an air-void level expected in the field. Dense-graded mixtures were compacted to 6- to 8-percent air voids. SMAs were compacted to 5- to 6-percent air voids. The M_d of each compacted mixtures was measured at 25°C (77°F). For long-term aging, the compacted mixtures were aged in a forced draft oven for 5 days at 85°C (185°F). Each mixture's M_d and tensile strength were then measured.

RESULTS AND ANALYSIS

Mix Design

The Marshall-mix design results are presented in Table 2. Dense-graded mixtures had higher stabilities and lower flows than the SMAs. This could be because of the higher binder contents of SMAs. The D 12.5 had lower voids in mineral aggregate (VMA) than the D 9.5, resulting in a lower binder content for the D 12.5 mixture—the typical relationship. The reverse was true for SMAs. Both SMAs 12.5 had slightly higher VMAs than the SMAs 9.5, resulting in higher binder contents for the SMAs 12.5. This is proba-

TABLE 2 Mixture Design Properties and Materials

Mixture Type	OAC (%)	Stability (N)	Flow (0.25 mm)	Air Voids (%)	VMA (%)
D 9.5	5.2	15 450	11.0	4.0	14.8
SMA 9.5 Arbocel	6.3	9 510	12.5	3.0	16.3
SMA 9.5 Vestoplast	6.5	9 483	14.5	3.0	16.8
D 12.5	4.5	17 066	10.7	4.0	13.7
SMA 12.5 Arbocel	6.7	7 116	14.3	3.0	17.5
SMA 12.5 Vestoplast	6.8	8 286	18.2	3.0	17.7

1 lbf = 224.72 kN
1 in = 25.64 mm.

bly related to the choice of the gradation. Opening up the gradation of the SMA 9.5 by reducing the percent passing the 4.75-mm (No. 4) and 2.36-mm (No. 8) sieves might provide a higher VMA. The VMAs of each SMA did not vary with binder content, and the air voids versus binder content relationships were generally linear. The only exception was for the SMA 9.5 with Vestoplast, for which the air voids versus binder content relationship was curvilinear, as air voids less than 3 percent could not be obtained. Only three binder contents were used in designing the SMA mixtures.

Rutting Evaluation

French Pavement Rutting Tester

Percent rut depths are presented in Table 3. The percent rut depth in all mixtures at the different number of passes was less than 20 percent of the specimens' thickness. Hence, all of the mixtures passed. A statistical comparison of the percent rut depths, both between the D 9.5 and two SMAs 9.5 and between the D 12.5 and two SMAs 12.5 (at a level of significance $\alpha = 0.05$ using a *t*-test) revealed no significant difference for the various numbers of passes. If 3,000 cycles represents pavement service life, then all six mixtures will not have a rutting problem in the field.

Georgia Loaded Wheel Tester (GLWT)

The rut depths and air voids are presented in Table 4. All six mixtures had rut depth less than 7.6 mm (0.30 in.). The SMAs as well as the dense-graded mixtures were not rut susceptible. Statistical comparisons of the rut depths between the D 9.5 and the SMAs 9.5 and between the D 12.5 and the SMAs 12.5 (at a level of significance $\alpha = 0.50$ using a *t*-test) revealed no significant difference between the mixtures.

Gyratory Testing Machine Results (GTM)

The results from the GTM are presented in Table 4. The GSIs of the mixtures were not significantly different and indicated that none of the mixtures should rut. This result agrees with the results from the wheel-tracking devices. Extractions were performed on the SMAs with Arbocel before and after testing. The results are presented in Table 1. The results show a significant increase in the percentage of aggregate passing the 4.75-mm (No. 4) and 2.36-mm (No. 8) sieves. Hence, the GTM fractured the aggregate. Based on this result, it was decided that the effect of the Marshall compaction process on the SMA gradations should also be examined. Therefore, the SMAs with Arbocel were compacted using the Marshall hammer and extractions were performed. The extraction results are also presented in Table 1. Marshall compaction had the same effect on gradation. Because aggregate gradation is an important factor in designing SMAs, the GTM and Marshall hammer compaction methods used in this study may be affecting the mixture design adversely.

Compressive Repeated Load Test

Moduli and permanent deformations are presented in Table 5. Because of the stone-on-stone contact that occurs in SMAs, they were expected to have lower permanent deformations than dense-graded mixtures. However, the unconfined repeated load test showed that both SMAs had significantly higher average permanent deformations than the dense-graded mixtures tested. Applying a 0.14-MPa (20-lbf/in.^{2}) confining pressure and a 0.59-MPa (85-lbf/in.^{2}) or 0.45-

TABLE 3 French Pavement Rutting Tester Results—Percent Rut Depth

Number of Cycles	D 9.5	SMA 9.5 Arbocel	SMA 9.5 Vesto-plast	D 12.5	SMA 12.5 Arbocel	SMA 12.5 Vesto-plast
30	0.4	0.6	4.5	0.3	2.3	4.0
100	1.3	1.8	5.7	0.9	3.2	5.3
300	1.6	2.4	7.1	1.4	3.8	5.8
1000	3.0	2.9	7.7	2.3	4.3	6.5
3000	4.0	3.3	8.5	3.4	5.3	7.3

TABLE 4 Georgia Loaded Wheel Tester and GTM Results

Mixture Type	GLWT		GTM	
	Rut (mm)	Air Voids (%)	GSI	Refusal Air Voids (%)
D 9.5	4.67	4.26	1.02	3.90
SMA 9.5 with Arbocel	4.04	2.82	1.02	2.04
SMA 9.5 with Vestoplast	4.06	2.89	NT	NT
D 12.5	3.20	3.69	1.04	3.30
SMA 12.5 with Arbocel	3.96	2.76	1.01	2.10
SMA 12.5 with Vestoplast	3.47	2.68	NT	NT

NT: Not tested.

1 in = 25.64 mm.

TABLE 5 Compressive Repeated Load Test Results

	D 9.5	SMA 9.5 Arbocel	D 12.5	SMA 12.5 Arbocel		
				Unconfined	Confined (1)	Confined (2)
Modulus (MPa)	1020	885	791	742	845	1062
Permanent deformation ($\times 10^{-2}$ mm)	5.3	14.4	6.3	17.6	14.1	10.4
% Air Voids	3.5	3.3	4.3	3.4	2.1	2.1

(1): 0.45-MPa (65-lbf/in^2) deviator stress.
(2): 0.31-MPa (45-lbf/in^2) deviator stress.

lbf/in^2 = 145.03 MPa.
1 in = 25.64 mm.

MPa (65-lbf/in.^{2}) vertical pressure did not improve the data (i.e., permanent deformations for SMA 12.5 did not drop). A test using 101.6-mm (4.0-in.) by 203.2-mm (8.0-in.) specimens might not apply to an SMA.

Moisture Damage Evaluation

Visual Stripping

Average percentages of visual stripping are presented in Table 6. Both SMAs with Arbocel had less visual stripping than the dense-graded mixtures. The D 9.5 and the D 12.5 had visually stripped areas of 30 and 25 percent, respectively. The SMA 9.5 and the SMA 12.5 had visually stripped areas of 15 and 10 percent, respectively. The lower percentage of visual stripping in the SMAs could be related to their higher binder contents, which increase the asphalt film around the aggregates.

Tensile Strength Ratio (TSR)

Tensile strengths and TSRs of the mixtures are summarized in Table 6. Statistically, there was no significant reduction in the tensile strength of either SMA from moisture conditioning. Both SMAs had a TSR close to 100 percent. Statistically, the tensile strengths of the dense-graded mixtures were significantly reduced by moisture conditioning. This reduction resulted in TSRs below 80 percent. Testing indicates that the SMAs are more resistant to moisture damage than are dense-graded mixtures.

Diametral Modulus Ratio

The dense-graded mixtures each had a diametral modulus ratio (M_dR) of less than 70 percent, whereas the SMAs tested each had an M_dR that was greater than 70 percent. Thus, testing indicates that the SMAs were less susceptible to moisture damage than were the

TABLE 6 Resistance to Moisture Damage Results

	D 9.5	SMA 9.5 Arbocel	D 12.5	SMA 12.5 Arbocel
Tensile Strength, 25 °C (77 °F)				
Average Dry, kPa	628.1	504.7	632.3	422.0
Average Wet, kPa	358.5	502.6	450.9	400.6
Retained Ratio (TSR), percent	57.1	99.6	71.3	95.0
Diametral Modulus, 25 °C (77 °F)				
Average Dry, MPa	1125.9	1165.9	1350.7	1048.0
Average Wet, MPa	456.4	913.6	692.9	748.1
Retained Ratio (M_dR), percent	40.5	78.4	51.3	71.4
Average Visual Stripping, percent	30.0	15.0	25.0	10.0
Average Swell, percent by volume	0.6	0.3	0.2	0.1
Average Air Voids, percent	7.0	5.5	6.9	5.5

lbf/in^2 = 145.03 MPa.

TABLE 7 Diametral Modulus Results (MPa) for Low-Temperature Cracking

Temperature °C (°F)	D 9.5	SMA 9.5 Arbocel	D 12.5	SMA 12.5 Arbocel
-32 (-25.6)	45 640	43 208	51 450	43 580
-24 (-11.2)	43 550	42 670	45 470	36 300
-16 (3.2)	38 850	36 230	43 420	32 710
-8 (17.6)	34 040	30 830	36 690	26 940
0 (32.0)	17 670	16 030	21 620	15 420
5 (41.0)	12 300	10 610	14 390	9 870
16 (60.8)	4 160	3 890	4 900	3 310
25 (77.0)	1 480	1 410	1 870	1 240
32 (89.6)	650	660	860	550
40 (104.0)	340	320	430	260

lbf/in^2 = 145.03 MPa.

dense-graded mixtures. A *t*-test was performed at a level of significance $\alpha = 0.05$ to compare the wet and dry M_d of each mixture. These analyses revealed that the wet M_d of the dense-graded mixtures was significantly lower than mixtures dry M_d.

A *t*-test showed there was not a significant difference between the wet M_d and the dry M_d of SMA 9.5. However, SMA 12.5 had a significantly lower wet M_d than dry M_d and it had a borderline M_dR. Therefore, for this mixture, the M_d test measured susceptibility to moisture damage better than the TSR test.

Low-Temperature Cracking Evaluation

Results of the low-temperature cracking evaluation are tabulated in Table 7. A *t*-test statistical comparison of the M_d data for the SMA 12.5 and D 12.5 (at a level of significance $\alpha = 0.05$) revealed that the stiffnesses of the SMA 12.5 were significantly lower than that of the D 12.5 mixture. This implies that the SMA will be less susceptible to low-temperature fracture but more susceptible to rutting at high temperatures. Test results at the high temperature contradict the French Pavement Rutting Tester, GLWT, and GTM results, however; they showed no significant difference in the rutting susceptibility. Hence, diametral configuration may not be a good method for determining the rutting susceptibility of SMA mixtures. There was no significant difference in M_d between the D 9.5 and the SMA 9.5.

Drainage

Drainage test results are presented in Table 8. The three drainage tests showed that the SMA 12.5 with Vestoplast had a high amount of drainage. The gradation may have to be altered to reduce the amount of drainage. The other three mixtures passed all tests, including the SMA 9.5 with Vestoplast.

Aging

Aging results are presented in Table 9. Increases in stiffness for the dense-graded mixtures related to short- and long-term aging were significantly higher than the increases for the SMAs. Also, the increases in tensile strength for the dense-graded mixtures after long-term aging were significantly higher than the increases for SMAs indicating that dense-graded mixtures might be more susceptible to cracking than the SMAs after they are age hardened.

CONCLUSIONS

Rutting Evaluation

- The SMAs with Arbocel and the dense-graded mixtures passed the French Pavement Rutting Tester, GLWT, and GTM. The SMA's with Vestoplast passed the two tests performed on them, namely, the French Pavement Rutting Tester and the GLWT. This means that none of the mixtures were susceptible to rutting.
- The unconfined, compressive, repeated load test showed more permanent deformation for SMAs than for dense-graded mixtures, and applying a confined pressure did not improve the results.
- The diametral configuration may not be a good method for determining the rutting susceptibility of SMAs at high temperatures.

TABLE 8 Drainage Test Results

Test Type	SMA 9.5 Arbocel	SMA 9.5 Vestoplast	SMA 12.5 Arbocel	SMA 12.5 Vestoplast
German Test, % loss	0.10	0.31	0.08	3.21
FHWA Open-Graded Friction Course Test, drainage level	Slight	Slight	Slight	Excessive
2.36-mm (No. 8) Sieve Drainage Test, % Loss	0.00	0.02	0.11	2.13

TABLE 9 Aging Test Results

Type of Mix	Dynamic Modulus, M_d at 25 °C, MPa			Change in M_d		
	Unaged	Short-Term Aging	Long-Term Aging	Short-Term to Unaged	Long-Term to Short-Term	Total Aging
D 9.5	1126	2570	3943	1444	1373	2817
SMA 9.5 Arbocel	1166	2283	3094	1177	811	1928
D 12.5	1351	2981	4625	1630	1644	3274
SMA 12.5 Arbocel	1048	1555	2133	507	578	1085

	Tensile Strength at 25 °C, kPa		Change in Tensile Strength
	Unaged	Long-Term Aging	Total Aging
D 9.5	628	1314	686
SMA 9.5 Arbocel	505	960	455
D 12.5	632	1267	635
SMA 12.5 Arbocel	422	671	249

1.8(°C) + 32 = °F
lbf/in^2 = 145.03 MPa

Moisture Damage Evaluation

- The SMAs had lower percentages of visual stripping than the dense-graded mixtures. This could be because of high binder contents in SMAs, which increase the asphalt film around the aggregates.
- The TSR and M_dR indicated that the SMAs had less potential for moisture damage than the dense-graded mixtures.

Low-Temperature Cracking Evaluation

- There was no significant difference in the resistance to low-temperature cracking between the D 9.5 and the SMA 9.5 with Arbocel.
- The SMA 12.5 with Arbocel had a significantly lower stiffness than the D 12.5. This implies that the SMA 12.5 will be less susceptible to low-temperature cracking.

Drainage

- All three drainage tests performed in this study showed that the SMA 12.5 with Vestoplast has an unacceptable level of drainage.

Aging

- The increase in stiffness and tensile strength from aging was significantly higher in dense-graded mixtures than in SMAs. This indicates that dense-graded mixtures might be more susceptible to cracking than SMAs after they age harden.

Note that both the GTM and the Marshall hammer fractured the aggregates of the SMA mixtures, as evidenced by the extraction test results.

ACKNOWLEDGMENT

This study was funded by FHWA and was performed at the FHWA Turner-Fairbank Highway Research Center in McLean, Virginia.

REFERENCES

1. Stuart, K. D. *Stone Mastic Asphalt (SMA) Mixture Design.* Report FHWA-RD-92-006. FHWA, U.S. Department of Transportation, March 1992.
2. SMA Technical Working Group. *SMA Material and Construction Model Specification.* FHWA, Office of Technology Applications. U.S. Department of Transportation, March 1, 1992.
3. Brosseaud, Y., J. L. Delorme, and R. Hiernaux. Use of LPC Wheel-Tracking Rutting Tester To Select Asphalt Pavements Resistant to Rutting. In *Transportation Research Record 1384.* TRB, National Research Council, Washington, D.C., 1993.
4. Lai, J. S. *Development of a Laboratory Rutting Resistance Testing Method for Asphalt Mixtures.* Research Project No. 8716. Final Report. Georgia Department of Transportation. Atlanta, Aug. 1989.
5. Roberts, F. L. P. S. Kandhal, E. R. Brown, D. Y. Lee, and T. W. Kennedy. *Hot Asphalt Materials, Mixtures Design, and Construction.* National Asphalt Pavement Association Education Foundation, Lanham, Md. 1991.
6. Von Quintus, H. L., J. A. Scherocman, C. S. Hughes, and T. W. Kennedy. *NCHRP Report 338: Asphalt-Aggregate Mixture Analysis System.* TRB, National Research Council, Washington, D.C., 1991.
7. Stuart, K. D. *Evaluation of Procedures Used to Predict Moisture Damage in Asphalt Mixtures.* Report FHWA-RD-86-090. FHWA, U.S. Department of Transportation, Sept. 1986.
8. "Short- and Long-Term Aging," Method M-007. Strategic Highway Research Program. National Research Council, Washington, D.C. Sept. 25, 1992.

Publication of this paper sponsored by Committee on Characteristics of Bituminous Paving Mixtures To Meet Structural Requirements.

Comparison of Results Obtained from the LCPC Rutting Tester with Pavements of Known Field Performance

TIM ASCHENBRENER

In France the Laboratoire Central des Ponts et Chaussees (LCPC) rutting tester has been used successfully for 15 years to prevent rutting. The Colorado Department of Transportation and the FHWA's Turner-Fairbank Highway Research Center were selected to demonstrate this equipment in the United States. Thirty-three sites across Colorado, with either good or poor rutting performance and various temperature and traffic conditions, were selected. Test results indicated that applying the French specification and the LCPC rutting tester was proved too severe for many of the temperature and environmental conditions in Colorado. However, once the testing temperature was adjusted to match the highest on-site temperature, the LCPC rutting tester did an excellent job of predicting pavement performance. The results from the LCPC rutting tester also had excellent correlation with actual rutting depths when temperature and traffic levels were considered.

In September 1990, a group of individuals representing AASHTO, FHWA, National Asphalt Pavement Association, Strategic Highway Research Program, Asphalt Institute, and TRB participated in a 2-week tour of 6 European countries. Information concerning the tour has been published in the "Report on the 1990 European Asphalt Study Tour" (*1*). Several potential improvements of asphalt pavement technology were identified on tour, including adoption of the performance-related testing equipment used in several European countries. French equipment was distributed commercially and marketed, so it was a natural choice for demonstration in the United States. The Colorado Department of Transportation and the FHWA Turner-Fairbank Highway Research Center were selected to demonstrate the testing equipment.

The Laboratoire Central des Ponts et Chaussees (LCPC) rutting tester has been used successfully to prevent rutting in France for 15 years (*2*). However, traffic and terrain in France are extremely different than they are in Colorado. Therefore, first priority was to verify the predictive capabilities of the LCPC equipment by performing tests on mixtures of known field performance in Colorado. Samples of hot mix asphalt pavements, with either a history of rutting or of good performance, were identified and tested with the LCPC rutting tester. An analysis of the LCPC rutting tester's results for pavements with known performance is presented in a detailed report by Aschenbrener (*3*).

EQUIPMENT DESCRIPTION

A full description of the French hot mix asphalt (HMA) design methodology and equipment operation, as followed by the LCPC, is provided by Bonnot (*4*). A brief description of the LCPC rutting tester, its operation, and typical results is provided here.

Colorado Department of Transportation, 4340 East Louisiana Avenue, Denver, Colo. 80222.

Testing Equipment and Procedure

To evaluate resistance to permanent deformation, the LCPC rutting tester (Figure 1) is used on a confined slab. The slab is 50 by 18 cm (19.7 by 7.1 in.) and can be 50 to 100 mm (2.0 to 3.9 in.) thick. A 100-mm thick slab has a mass of 20 kg (44 lb).

Two slabs can be tested simultaneously. The slabs are loaded with 5000 N (1,124 lb) by a pneumatic tire inflated to 600 kPa (87 psi). The tire loads the slab at 1 cycle per second; one cycle is two passes. The chamber is typically heated to an air temperature of 60°C (140°F) but can be set to any temperature between 35°C and 60°C (95°F and 140°F).

When a test is performed on a laboratory compacted slab, the slab is aged at room temperature for as long as 7 days. It then is placed in the LCPC rutting tester and loaded with 1,000 cycles at room temperature. The deformations recorded after the initial loading are the "zero" readings. The sample is then heated to the test temperature for 12 hr before the test begins. Rutting depths are measured after 100; 300; 1,000; 3,000; 10,000; 30,000; and possibly 100,000 cycles. The rutting depth is reported as a percentage of the slab thickness. The percentage is calculated as the average of 15 measurements (five locations along the length times three along the width) divided by the slab's original thickness. A pair of slabs can be tested in about 9 hr.

Test Results

The results are plotted as rutting depth over cycles on log-log graph paper. The slope and intercept (at 1,000 cycles) are calculated using linear regression:

$$Y = A\left(\frac{X}{1{,}000}\right)^{B} \quad (1)$$

where

Y = rutting depth in percent,
X = cycles,
A = intercept of rutting depth at 1000 cycles, and
B = slope of curve.

French Specifications

French specifications for the test are reported in detail elsewhere (*2*). In France, a successful test typically will have a rutting depth

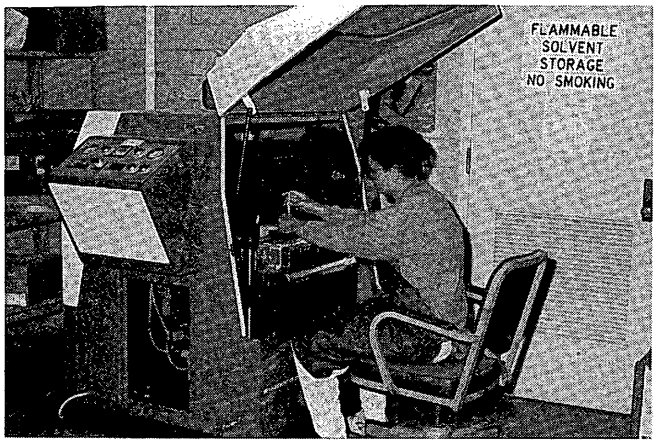

FIGURE 1 Measuring rutting depths on LCPC rutting tester.

that is less than or equal to 10 percent of the slab thickness after 30,000 cycles. The test always is performed at 60°C. The thickness of the slab tested is controlled by the thickness of the overlay.

The French indicate that there are no reports of rutting on highways in which the HMA has passed the test (*2*). In the few cases where rutting did occur, problems were identified that included the following: the HMA failed the original design, an improper test procedure was used with the LCPC rutting tester, or the HMA placed on the project varied from the HMA used in the design during production.

STUDY APPROACH

Three options were considered for comparing the LCPC rutting tester results to pavements of known field performance. One was selected to provide initial field performance validation, it is Option 2, reported in this study.

Option 1

Option 1 would be to design and build pavements that would either pass or fail the LCPC rutting tester and then monitor their performance. Whereas this method will be performed and will be the primary method of validating the LCPC rutting tester, results may not be available for 5 years.

Option 2

Option 2, like the third option that follows, involves testing HMA that was placed in the past but has a known performance. Option 2 would test field cores and slabs and would involve testing HMA with an aged asphalt cement. The primary cause of rutting in Colorado is not the asphalt cement stiffness but the change in properties that occurs between the time of HMA design and construction (*5*). The error in using Option 2 was considered minimal; it is reported in this study.

Option 3

Option 3 would involve obtaining the original raw materials and blending them to match the original job mix formula of pavements of known field performance. Option 3 would not reflect changes that could have occurred during actual production or changes in aggregate sources and asphalt cements during the past 5 to 10 years. Because most rutting in Colorado is considered to involve HMA that was constructed with different properties than were designed, the error would be large. The third option was not investigated.

SITE SELECTION

Temperature

High-temperature environment was defined as the highest monthly mean maximum temperature (HMMMT), i.e. the average of the daily high temperatures in the hottest month of the year. Three high-temperature environments exist in Colorado.

Traffic

The levels of traffic are commonly defined according to the number of equivalent 18-kip single-axle loads (ESALs) during the design life of the pavement. Six levels of traffic were selected. The traffic levels used in this report were determined from the network level pavement-management data that report the equivalent daily 18-kip load applications (EDLAs). Traffic measurement is highly variable, so just EDLA was used since there is confidence in the current values. EDLA was selected to provide a relative comparison of traffic loading for each site analyzed.

Performance

Well performing pavements and pavements exhibiting rutting were selected. Pavements rutting less than 5 mm (0.2 in.) were considered good. Rutting depths reported by Colorado's network level pavement management program are from the ARAN system that measures ruts with a laser beam. Ruts were also measured with a 2-m straight edge.

Only those sites that exhibited rutting from plastic flow were used. Sites that had rutting because of subgrade failure, stripping, or improper compaction were eliminated from the study. Additionally, sites at intersections or which included climbing lanes for trucks on steep grades also were eliminated. In short, the study was confined to sites that had rutted from plastic flow under normal highway speeds, 73 to 105 km/hr (45 to 65 mph).

Colorado experience suggests that pavements typically rut within the first 3 to 5 years after construction. Further, there is a high probability that pavements that do not rut in the first 3 to 5 years will not rut throughout their service life. The well performing pavements selected for this study were over 6 years old.

Final Site Selection

At least one rutting and non-rutting site from most traffic levels and temperature environments in Colorado were selected, as indicated in Table 1. Additional sites were selected that corresponded to a majority of Colorado's interstate conditions. A total of 33 sites was evaluated. They are listed in Table 2 and the vicinity of each test site is indicated in Figure 2.

TABLE 1 Summary of Sites by Traffic and Environmental Conditions

	Highest Mean Monthly Maximum Temperature		
EDLA	< 27°C	27° to 32°C	32° to 38°C
< 27	---	19, 20	25, 26
27 - 82	33	27, 28	23, 24
82 - 274	31, 32	5, 6	21
274 - 822	17, 18	7, 8	15, 34, 35
822 - 2740	36,37	3,4,11,12,13,14	9, 10
2740 - 8220	---	29, 30	---

SAMPLING AND TESTING

Cores and slabs were obtained from each site. Slabs were sawed between the wheel paths, and parallel to the direction of travel. Three slabs were obtained at each location. Five 100-mm (4-in.) diameter cores were obtained between the wheel paths, and three were obtained in the wheel paths. The thickness of lifts at each site was identified by observing and measuring the slabs.

The results of the forensic investigation are reported by Aschenbrener (*5*), including testing aggregate, asphalt cement, and HMA properties.

RESULTS AND DISCUSSION OF TESTING

Three slabs were obtained at each site for testing in the LCPC rutting tester. One slab was typically tested at 50° (122°F) and another at 60°C (140°F). The third slab was tested at either 40° or 45°C (104°or 113°F) for low temperature sites, and usually at 55°C (131°F) for moderate and high temperature sites.

Typically each slab tested had two to four layers. No attempt was made to separate the layers of the slabs. Each slab was tested as a multiple layer, just as it was in the field. If a lower lift had contributed to rutting, it was detected by the LCPC rutting tester (*6*).

TABLE 2 Site Descriptions

Site	Highway	M.P.	Location	Rut Depth	Temp.	EDLA
3	US-85	251	Platteville	0 mm	31°C	941
4	US-85	248	Platteville	25	31	864
5	SH-66	40	Longmont	0	31	250
6	SH-119	50	Niwot	10	31	221
7	SH-52	12	Dacona	3	31	358
8	SH-52	19	Fort Lupton	18	31	310
9	US-287	430	Lamar	3	36	878
10	US-287	430	Lamar	25	36	878
11	I-25	41	Walsenburg	0	29	1027
12	I-25	35	Walsenburg	20	29	1027
13	I-70	430	Burlington	3	32	1377
14	I-70	445	Burlington	20	32	1336
15	US-50	375	LaJunta	3	34	551
17	US-160	271	LaVeta Pass	13	24	493
18	US-160	278	LaVeta Pass	3	24	465
19	US-389	10	Branson	0	29	3
20	US-389	10	Branson	10	29	3
21	US-50	454	Granada	0	34	270
23	US-160	490	Walsh	3	33	48
24	US-160	486	Walsh	10	33	48
25	SH-55	2	Crook	3	33	20
26	SH-55	1	Crook	13	33	20
27	SH-71	219	Stoneham	0	31	56
28	SH-71	214	Stoneham	18	31	56
29	I-25	237	Denver	8	31	3127
30	I-25	243	Denver	15	31	3127
31	US-40	225	Fraser	10	24	169
32	US-40	216	Granby	3	24	171
33	US-34	2	Granby	13	24	53
34	I-70	15	Fruita	25	34	780
35	US-50	75	Delta	13	34	399
36	I-70	214	Eisenhower	20	22	1137
37	I-70	207	Silverthorne	3	22	1137

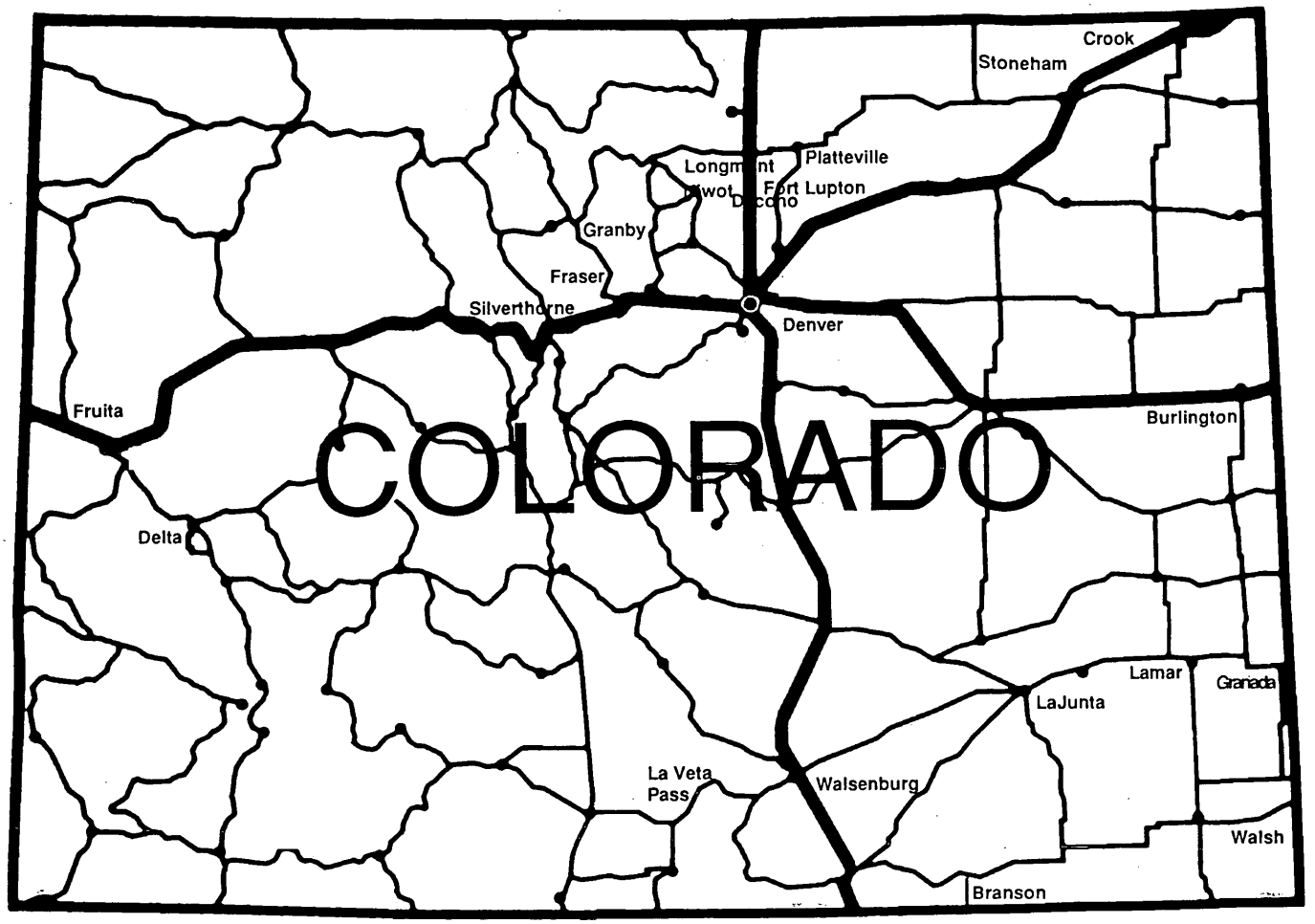

FIGURE 2 Test site locations.

Comparison to the French Specification

An acceptable mix for the pavements tested in this study using the French specification will have a rutting depth of less than or equal to 10 percent of the slab thickness after 30,000 cycles at 60°C. This is a "go, no-go" criteria.

For the 31 Colorado sites tested at 60°C, the comparison of the actual pavement performance versus the specification established by the French is shown in Table 3. Two sites (32 and 36) were not included because the slabs were not tested at 60°C.

The French specification is more severe than is necessary for conditions typically encountered in Colorado. Of the sites tested, there was no rutting in the field for those slabs that passed the test, and sites that had rutted in the field all failed the test. However, several pavements with good performance would have failed the French specification.

Temperature Adjustments

The French use one very severe temperature to perform the test. The method is appropriate to promote a high factor of safety against rutting. However, in order to make the test more representative of the conditions in Colorado, different test temperatures were examined. The testing temperature should simulate the actual pavement temperatures it was thought.

Tests were performed using different testing temperatures. The slope *B*, as defined in Equation 1, is reported along with results from the LCPC rutting tester in Tables 4–6. The rutting depth at 30,000 cycles was reported if the sample survived; those cycles at a 10-percent rutting depth were reported if the test had to be stopped.

High-Temperature Sites

Seven of the 10 high-temperature sites presented in Table 4 performed very well using the "go, no-go" criteria at a 60°C testing temperature. Site 23 at Walsh had very poor performance results from the rutting tester despite the good historical performance of the road. The results from Sites 23 and 24 were not distinguishable from each other, despite their having different performance histories. The sites were from the same project and within 4 mi of each other. It was assumed that this mix was marginal and that some site-specific situation during or after placement caused the difference in rutting in the field.

Site 15 in LaJunta did not meet the LCPC criteria despite good field performance. The pavement had 1.7 percent air voids in the wheel path, and at adjacent locations there is 13 mm (0.5 inches)

TABLE 3 Comparison of Actual Pavement Performance to French Specification Using a 60°C Test Temperature

LCPC Results	Actual Pavement Performance	
	No Rutting	Rutting
Pass	4	0
Fail	11	16

TABLE 4 Summary of Results for High-Temperature Sites

	60°C Test Temp.		55°C Test Temp.		50°C Test Temp.	
Site	Slope (B)	Rut @ 30,000 or cycles @ 10%	Slope (B)	Rut @ 30,000 or cycles @ 10%	Slope (B)	Rut @ 30,000 or cycles @ 10%
25	---	---	0.40	22,000 C	---	---
26	---	---	---	---	0.70	9,000 C
23	0.86	600 C	---	---	0.70	4,000 C
24	0.86	100 C	---	---	0.80	2,000 C
21	0.33	5.5%	---	---	0.35	4.1%
35	1.02	600 C	---	---	0.89	2,000 C
15	0.45	9,000 C	---	---	0.57	29,000 C
34	0.84	3,000 C	---	---	0.69	12,000 C
9	0.34	4.8%	---	---	0.36	7.1%
10	0.73	300 C	---	---	0.40	2,000 C

--- Not Tested
C Cycles to 10% rutting depth
% Rutting depth at 30,000 cycles

TABLE 5 Summary of Results for Moderate-Temperature Sites

	60°C Test Temp.		55°C Test Temp.		50°C Test Temp.	
Site	Slope (B)	Rut @ 30,000 or cycles @ 10%	Slope (B)	Rut @ 30,000 or cycles @ 10%	Slope (B)	Rut @ 30,000 or cycles @ 10%
19	0.37	12,000 C	0.36	7.8%	0.37	9.7%
20	0.96	400 C	*0.93	700 C	0.90	1,000 C
27	0.41	20,000 C	0.28	4.4%	0.31	3.7%
28	1.02	200 C	*1.03	1,000 C	1.03	2,000 C
5	0.71	7,000 C	0.26	3.1%	0.38	2.5%
6	0.74	300 C	*0.72	*1,000 C	0.70	2,000 C
7	0.49	4,000 C	---	---	0.37	6.4%
8	0.89	400 C	*0.82	*700 C	0.75	1,000 C
3	0.55	7,000 C	---	---	0.37	2.9%
4	0.73	500 C	*0.73	*2,000 C	0.74	5,000 C
13	0.41	7.9%	*0.32	*5.5%	0.24	3.0%
14	0.92	200 C	0.55	5,000 C	0.62	3,000 C
11	0.22	5.7%	*0.21	*5.1%	0.21	4.4%
12	1.06	800 C	*0.95	*2,000 C	0.85	3,000 C
C29	0.38	15,000 C	0.44	27,000 C	0.36	3.6%
30	0.60	4,000 C	0.55	6,000 C	0.59	12,000 C

* Estimated value
--- Not tested
C Cycles to 10% rutting depth
% Rutting depth at 30,000 cycles

TABLE 6 Summary of Results for Low-Temperature Sites

	50°C Test Temp.		45°C Test Temp.		40°C Test Temp.	
Site	Slope (B)	Rut @ 30,000 or cycles @ 10%	Slope (B)	Rut @ 30,000 or cycles @ 10%	Slope (B)	Rut @ 30,000 or cycles @ 10%
33	0.85	5,000 C	0.77	8,000 C	0.46	5.5%
32	0.33	4.7%	0.35	4.3%	0.44	4.1%
31	0.62	5,000 C	---	---	0.60	3.9%
18	0.66	8,000 C	0.53	17,000 C	---	---
17	0.79	3,000 C	0.71	9,000 C	0.75	9,000 C
37	0.37	3.8%	---	---	0.30	1.9%
36	0.29	6.1%	0.29	5.3%	0.30	4.3%

--- Not tested
C Cycles to 10% rutting depth
% Rutting depth at 30,000 cycles

rutting depths. Past research had indicated that pavements with less than 3 percent air voids in the wheel path have a high probability of rutting (*7–9*). Even though the pavement did not rut at the location of the sample, the material would not be desirable for use statewide. Results from the LCPC rutting tester indicated that the material was unacceptable.

Mechanical problems developed with the LCPC rutting tester while testing Sites 25 and 26. Therefore only one result from each site was obtained. Site 25 had very low traffic. For low traffic, 10,000 or 20,000 cycles possibly should be specified.

Moderate Temperature Sites

Moderate temperature sites correlated excellently with the LCPC rutting tester at temperatures lower than 60°C. Results are compiled in Table 5 from the pavements placed in moderate temperature areas; they were significantly affected by the testing temperature. By changing the testing temperature from 60°C to 50°C, six sites with good field performance (sites 3, 5, 7, 19, 27, and 29) went from failing to passing laboratory-test results, and no sites with poor performance went from failing to passing.

Site 29 in Denver had an 8 mm (0.3 in.) rutting depth; this is considered slightly unacceptable. At the 55°C testing temperature, the slab failed at 27,000 cycles, short of the required 30,000 cycles. A testing temperature of 55°C would closely represent the actual performance of this pavement.

Because there was no test performed at 55°C for several sites, values were estimated on the basis of results from 50°C and 60°C. No values were estimated for Sites 3 and 5 because there was a large change in results from the 10°C difference in testing temperature.

Low-Temperature Sites

Results for the low-temperature sites are compiled in Table 6. Correlating results with actual pavement performance was highly variable and is believed to be dependent on elevation. It was not always possible to obtain the temperature at the exact site location. The "standard" low-temperature sites (Sites 17, 31, 32, and 33) were below 2400 m (8,000 ft) in elevation and had good correlation at 50°C. Site 18 was at the top of LaVeta Pass at over 3000 m (9,800 ft). For a mix placed at this elevation, the testing temperature that models field performance, possibly 40°C, appears to be much lower than that of the "standard" sites.

Site 36 was in the Eisenhower Tunnel at an elevation of more than 3500 m (11,000 ft). Although the pavement rutted 15 mm (0.6 in.), it was not because of plastic flow; rutting likely occurred because of abrasion from studded tires and tire chains. The voids in the wheel path were 6.4 percent, and the pavement texture was very rough and potholed. This site was not analyzed further.

Comparison to the Modified French Specification

The French specification was modified so that the testing temperatures would match pavement temperatures in the field. The three highest testing temperatures that provided a correlation with the field results were 60°, 55°, and 50°C, respectively, for three different high-temperature areas in Colorado. Table 7 shows acceptable and unacceptable pavement performance as related to the test results, based upon the "go, no-go" specification.

Three sites were not included in Table 7: Sites 3 and 7 did not have a sample tested at the proposed specification temperature, and Site 36 did not rut because of plastic flow.

The four sites that had acceptable field performance but were not acceptable according to the specification and modified test temperatures were Sites 15, 18, 23, and 25. Sites 15 and 23 were discussed with the high-temperature sites and were considered marginally acceptable. Site 18 was at a very high elevation; it possibly should have been tested at 10 degrees Centigrade lower than the modified specification.

Site 25 had very low traffic. Consideration should be given to establishing a testing specification of 10,000 or 20,000 cycles for such low-volume roads. Although the 30,000-cycle criterion worked for Sites 19, 20, 23, 24, 25, 26, 27 and 28, which also had very low traffic, using the 10,000 or 20,000 cycle criterion also would have been appropriate.

Prediction of Rutting Depth

Additional analysis was performed in order to determine whether the LCPC rutting tester could be extended beyond a "go, no-go"

TABLE 7 Comparison of Actual Pavement Performance to French Specification Using Variable Test Temperatures

LCPC Results	Actual Pavement Performance	
	No Rutting	Rutting
Pass	10	0
Fail	4	16

device to forecast actual rutting depths. The results from the LCPC rutting tester used in the analysis were the slope of the rutting curve, B, as defined in Equation 1. The slopes were plotted versus actual pavement rutting depths.

Results indicated that there was a distinct difference between sites with high and low levels of traffic. In all cases, when traffic was divided into two categories, the coefficient of determination increased dramatically. Several entities use 1 million ESALs to differentiate between high and moderate traffic, and that is approximately an EDLA of 250 for 10 years. Regardless of test temperature, there seemed to be slightly better correlation when an EDLA of 400 was used that is approximately 1.5 million ESALs over 10 years.

Furthermore, the best correlations occurred when sites were divided into the different temperature groups. A testing temperature of 60°C was used for high-temperature sites, and 50°C was used for moderate-temperature sites.

On the basis of regression analysis, there was a correlation with the tests from the LCPC rutting tester and actual rutting depths. The forecasting capability was better when traffic volume and site temperatures were considered. The plot shown in Figure 3 is for traffic with an EDLA greater than 400 and a testing temperature of 60°C and 50°C for high- and moderate-temperature sites, respectively. A coefficient of determination, r^2, of 0.87 indicated good correlation. Figure 4 is a plot for traffic with an EDLA of less than 400, and a testing temperature of 60°C and 50°C. A coefficient of determination, r^2, of 0.68 indicated a positive correlation.

CONCLUSIONS

It is understood that the sites tested were old pavements, and that the air voids and asphalt cement had changed since the pavements' original construction. This study provides a preliminary indication of the ability of the LCPC rutting tester to forecast pavement performance.

1. The French specification for the LCPC rutting tester is too severe for many sites in Colorado. Eleven of 15 sites failed the criteria despite good pavement performance. However, no sites that passed the French specification rutted in the field, and all sites that rutted in the field failed the specification.
2. By making slight modifications to the testing temperature, the correlation between the French specification and field performance was greatly improved. Test temperatures of 50°C, 55°C or 60°C (122°F, 131°F or 140°F) for sites in low-, moderate- and high-temperature environments, respectively, were used. For pavements with good performance, 10 out of 14 sites met the French specification at the modified test temperature, and all rutted sites still failed.

Additional adjustments might be considered for extremely low traffic and extremely high altitudes. A requirement of 10,000 to 20,000 cycles might be considered for sites with very low volume. A testing temperature of 40°C (104°F) might be considered for sites at very high elevation.

3. Correlations of the results from the LCPC rutting tester with actual field rutting depths were excellent when the temperature and

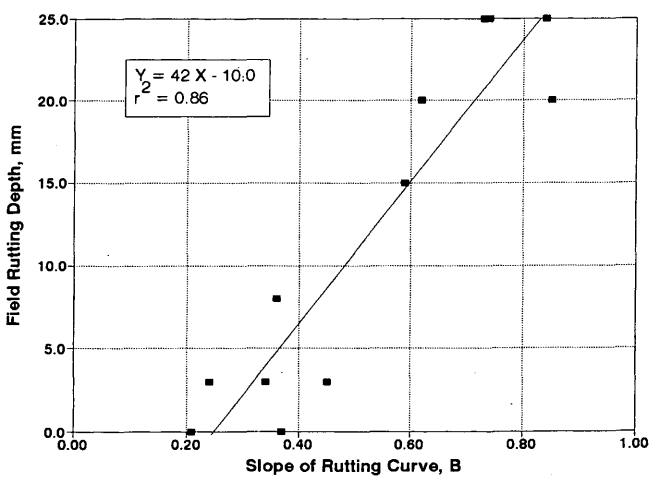

FIGURE 3 Slope from LCPC rutting tester versus actual rutting depths for high-traffic sites using variable test temperatures.

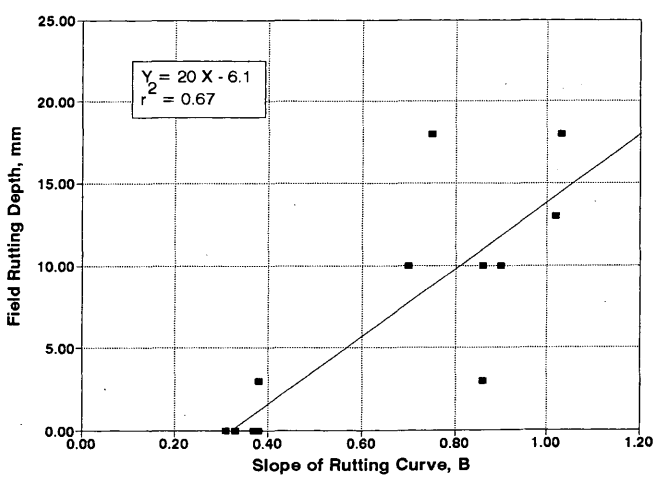

FIGURE 4 Slope from LCPC rutting tester versus actual rutting depths for low-traffic sites using variable test temperatures.

traffic at the site were considered. The best correlation for forecasting actual pavement rutting depths was obtained when two traffic levels (greater and less than an EDLA of 400) and three test temperatures (60°C and 50°C for sites with a Highest Monthly Mean Maximum Temperature of 32°C to 38°C and 27°C to 32°C, respectively) were used.

ACKNOWLEDGMENTS

The study was funded by Colorado's State Planning and Research and FHWA.

The author would like to express gratitude to the many people who assisted him in performing this study. Kevin Stuart of the FHWA's Turner Fairbank Highway Research Center, who provided numerous contributions throughout the sampling, testing, analysis, and report writing performed for this project. Werner Hutter performed the search of the network-level pavement management data used to identify the options for site selections. Donna Harmelink and Skip Outcalt performed scheduling and obtained all the samples used in this study. Kim Gilbert and Cindy Moya performed all the trimming, testing, tire changing, and troubleshooting to keep the rutting tester operating.

Special thanks to the expert panel of Colorado asphalt paving experts, who provided numerous ideas and suggestions that made this study more informational: Bud Brakey (BCE), Jim Fife (Western Colorado Testing), Darrel Holmquist (CTL/Thompson), Joe Proctor (Morton/Thiokol), and Eric West (Western Mobile, Inc.).

REFERENCES

1. Report on the 1990 *European Asphalt Study Tour.* AASHTO, Washington, D.C., June 1991, 115 pp.
2. Brosseaud, Y. *Assessment of the Use of the L.C.P.C. Rutting Tester.* Section des Materiaux de Chaussees, Laboratoire Central des Ponts et Chaussees, Nantes, France, 1992, 12 pp.
3. Aschenbrener, T. *Comparison of Results Obtained from the French Rutting Tester with Pavements of Known Field Performance.* CDOT-DTD-R-92-11. Colorado Department of Transportation, Denver, 1992, 73 pp.
4. Bonnot, J. Asphalt Aggregate Mixtures. In *Transportation Research Record 1096,* TRB, National Research Council, Washington, D.C., 1986, pp. 42–51.
5. Aschenbrener, T. *Investigation of the Rutting Performance of Pavements in Colorado.* CDOT-DTD-R-92-12. Colorado Department of Transportation, Denver, 1992, 63 pp.
6. Nievelt, G., and H. Thamfald. Evaluation of the Resistance to Deformation of Different Road Structures and Asphalt Mixtures Determined in the Pavement-Rutting Tester. *Proc., Association of Asphalt Paving Technologists,* Vol. 57, Association of Asphalt Paving Technologists, St. Paul, Minn., 1988, pp. 320–345.
7. Huber, G. A., and G. H. Heiman. Effect of Asphalt Concrete Parameters on Rutting Performance: A Field Investigation. *Proc., Association of Asphalt Paving Technologists,* Vol. 56, Association of Asphalt Paving Technologists, St. Paul, Minn., 1987, pp. 33–61.
8. Brown, E. R., and S. A. Cross. A National Study of Rutting in Asphalt Pavements. *Journal of the Association of Asphalt Paving Technologists,* Vol. 61, 1992, pp. 535–582.
9. Ford Jr., M. C. Asphalt Mix Characteristics and Related Pavement Performance. *Proc., Association of Asphalt Paving Technologists,* Vol. 57, Association of Asphalt Paving Technologists, St. Paul, Minn., 1988, pp. 519–544.

Publication of this paper sponsored by Committee on Characteristics of Bituminous Paving Mixtures To Meet Structural Requirements.

Criteria for Evaluation of Rutting Potential Based on Repetitive Uniaxial Compression Test

EL HUSSEIN H. MOHAMED AND ZHONGQI YUE

Tests conducted following the mix design stage, are unable to assess the rutting potential of asphalt concrete pavements. They range from moving a rubber tire on a slab and monitoring the rut depth to large-scale field tests using accelerated loading facilities. The Strategic Highway Research Program (SHRP) has proposed evaluating induced damage by determining the accumulated permanent shear strains based on a repetitive simple shear (constant height) test.

An investigation conducted at the Centre for Surface Transportation Technology of the National Research Council of Canada is aimed at developing a criteria for measuring rutting potential. A repetitive uniaxial compression test was used to determine accumulated permanent axial strain. Tests were conducted on cores recovered from the field and others compacted in the laboratory using a SHRP gyratory compactor. Test results indicate that the accumulated permanent axial strain undergoes three distinct stages: strain-hardening (volume change), shear flow, and, finally, fracture failure. During the secondary stage (shear flow) the rate of accumulation of permanent axial strain is constant and is sensitive to asphalt mix's resistance to rutting. Performance-related testing of the mix's resistance to potential rutting was carried out at different temperatures. Based on a proposed rutting criterion, one focused on the constant rate of permanent axial strain, the SHRP gyratory compactor simulates field compaction reasonably well. The influence of sample height, applied pressure, and compaction effort on the proposed rutting criterion also was investigated.

Rutting of asphalt pavements, primarily from high tire pressure and increased wheel loads of commercial vehicles, has increased in recent years. High stresses near the pavement surface induce high shear deformation and are considered responsible for rutting in asphalt concrete pavements. Difficulties associated with predicting the rutting susceptibility of asphalt concrete in the laboratory during the mix design stage have forced researchers to consider broad and expensive field testing (*1*). Disagreements about existing laboratory tests focus on the extent to which these tests simulate field conditions.

BACKGROUND

Many investigators consider rutting in asphalt concrete to be caused principally by shear deformations resulting from high shear stress near the surface. However, inadequate structural capacity as a result of improper designs and construction practices cannot be ruled out.

Recently, the Strategic Highway Research Program's (SHRP) asphalt research program described a series of tests for the evaluation of material properties related to permanent deformation (rutting) in asphalt concrete (*2*). In particular, a repetitive simple-shear test was recommended for determining the accumulated shear damage in asphalt concrete.

Centre for Surface Transportation Technology; National Research Council of Canada; Ottawa, Ontario, Canada K1A 0R6.

Reasons for Test Selection

In the authors' laboratory investigation, however, a repetitive uniaxial compression test was used to evaluate permanent deformation (rutting) of asphalt concrete. A repetitive uniaxial compressive load applied on the cylindrical samples of asphalt concrete can provide reasonable simulation of asphalt pavements subjected to repetitive heavy axle loads. Based on the test results of this study, a constant rate of accumulated permanent strain was found for all tested samples. This constant rate, which is unique for each mix, can be used as a criterion for evaluation of rutting potential of asphalt concrete.

Conventional mix-design procedures allow for additional densification of asphalt concrete under traffic loads. Compaction in the field seldom achieves densities specified in the laboratory. Therefore, any laboratory test designed for predicting rutting susceptibility of a new mix must account for permanent deformations following mix densification that are associated with changes in the mix microstructure. These factors influenced the selection of the appropriate test for this study. The uniaxial compression test can be used to determine reasonably the susceptibility of a mix to permanent deformations related to shear deformation as well as those associated with changes in the microstructure of asphalt concrete.

Uniaxial Compression Test

The components of the test, described in detail in an earlier publication (*3*), include the test set up (Figure 1), the choice of a load cycle, and a laboratory procedure for manufacturing samples. A SHRP gyratory compactor was chosen for sample preparation on the basis of results from a comprehensive investigation that compared many devices used to compact asphalt concrete in the laboratory (*4*). Gyratory compaction seems to produce compacted mixtures with engineering properties similar to those produced in the field. More evidence has been produced by the results of this investigation, further justifying the use of the SHRP gyratory compactor.

Repetitive compressive loading was used to simulate traffic loading on the basis of research conducted at Nottingham University, and a square wave load application was selected consistent with subsequent work. The square wave consisted of a constant loading period of 0.2 sec followed by a rest period of 1.8 sec. The axial pressure used was 690 kPa (100 psi), which was reduced to

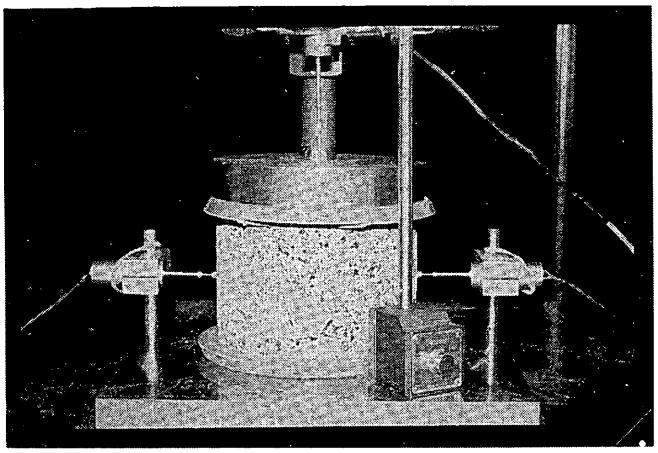

FIGURE 1 Repetitive uniaxial compression test setup.

2 percent of that level during the rest period to avoid separation of the loading head from the sample surface. The stress level was chosen on the basis of the tire pressure of commercial vehicles common to North American highways. Because plastic flow had been identified as the major cause of severe rutting, tests were conducted at 25°C and 40°C to account for the instability of asphalt cement at high temperatures.

EXPERIMENTAL INVESTIGATION

The testing program was designed to study the response of tested mixes to the repetitive uniaxial compression test, and to determine a performance indicator that could be adopted as a criterion for rutting. Factors influencing the rutting criterion were investigated:

- Height of the tested sample,
- Level of the applied pressure,
- Compaction effort,
- Laboratory compaction versus field compaction, and
- High-temperature environment.

Material

To determine the test's sensitivity to the type of mix, tests were conducted on two asphalt concrete mixes. These two mixes are known to exhibit significantly different rutting characteristics. One mix, a conventional dense hot asphalt mix, was designed following the Marshall mix design procedure. Details of the mix formula, referred to as HL4, are indicated in Table 1. The other mix (see Table 2) is a large aggregate asphalt mix developed at The Centre for Surface Transportation Technology of The National Research Council of Canada (CSTT/NRC) to provide high resistance to rutting (*5*). High resistance to rutting has been achieved with use of a stone-to-stone contact, which has offered higher resistance to traffic-induced stresses than have conventional mixes.

Sample Height

To study the influence of the sample height on accumulated permanent deformation, samples with heights ranging from 40 to 80 mm were manufactured from the conventional HL4 mix using a SHRP gyratory compactor. One set of samples was tested at 25°C

TABLE 1 H4 Mix Details

Sieve Designation	Percent Passing				
	Coarse Aggregate	Fine Agg. 1 (crusher screenings)	Fine Agg. 2 sand	Combined Agg. Mix	MTO[x] specifications
26.5	100	-	-	-	-
19.0	100	-	-	100	100
16.0	97.2	-	-	98.7	98-100
13.2	78.1	-	-	89.9	83-95
9.5	48.8	100	100	76.4	62-82
# 4	9.6	100	100	58.4	40-67
# 16	2.5	80.1	79.5	44.2	27-66
# 50	2.0	35.2	36	20.2	4-27
# 100	1.7	9.9	4.8	4.3	1-10
# 200	1.5	4.8	0.7	2	0-6

x MTO - Ministry of Transportation of Ontario, Canada

The job mix formula used:			
	coarse aggregate	=	43.8%
	crusher screenings	=	17.4%
	natural sand	=	33.6%
	asphalt cement (85/100)	=	5.2%

TABLE 2 Large Aggregate Mix Details

Sieve Size (mm)	37.5 mm	Percent Passing			
		HL 3	Crusher Screenings	Sand	Combined Agg. Mix
37.5	100	-	-	-	100
25.0	90	-	-	-	95
16.0	25	100	-	-	61
11.0	5	90	-	-	49
8.0	2	47	100	-	40
#4	2	4	93	100	31
#10	1	1	56	93	24
#20	-	-	34	80	19
#40	-	-	22	49	12
#60	-	-	15	21	6
#100	-	-	10	5	3
#200	-	-	5	1	1

The job mix formula used:

38 mm McFarland Stone	=	49.9%
HL3 stone	=	17.3%
Quarry screenings	=	11.5%
Field sand	=	17.3%
Asphalt cement content (85/100)	=	4.0%

and 690 kPa (100 psi). The minimum sample height was selected to satisfy requirements related to maximum aggregate size used in the tested mix. The maximum sample height was selected to represent maximum layer thicknesses used in stage construction. To account for the influence of temperature, a second set of samples was tested at 40°C.

Applied Pressure

Although a pressure of 690 kPa (100 psi) has been adopted to simulate tire pressure of commercial vehicles, a number of gyratory-compacted HL4 mix samples were tested using different uniaxial pressure levels. During the loading cycle pressure ranging from 345 kPa (50 psi) to 1034 kPa (150 psi) was changed from one sample to another.

Compaction Effort

Compaction specifications for laboratory tests to be used for quality control in the field are expected to adopt the number of gyrations used to achieve the required compaction quality. The relationship between the number of gyrations and compaction quality factor was studied in this investigation by compacting, varying the number of gyrations, testing samples that had the same initial uncompacted height, and using a SHRP gyratory compactor. Initial material weight was equivalent to that used earlier in order to achieve a sample height of 64 mm with 250 gyrations. These data illustrate that inadequate structural capacity resulting from improper construction practices contribute to rutting potential.

Laboratory Mix Versus Field Compaction

To investigate the ability of SHRP gyratory compaction to simulate field compaction, a number of cores representing the two mixes described earlier were recovered from full-scale, field-compacted test sections and were tested following the procedures used for laboratory-compacted samples. Unlike samples prepared in the laboratory, cores recovered from across the width of the experimental road sections showed high variation in physical properties, as reflected by bulk-specific gravity values. The average bulk-specific gravity of cores recovered from the road was determined according to ASTM D2726-90, on the basis of saturated surface dry specimens. The air-voids content for all samples used for comparison was determined according to ASTM D3203-88, using values of theoretical maximum-specific gravity as determined by ASTM D2041. Cores with average bulk-specific gravity close to that of laboratory-compacted samples were then selected for testing using the uniaxial compression test. Note that these samples were recovered from sections that were constructed 7 months apart; so to compare them with the laboratory results, one must consider the different aging periods and resulting difference in stiffness of the cores.

TEST RESULTS

Stages of Permanent Strain

Plots of the permanent axial strain accumulated under cyclic loading exhibit a readily identifiable trend. Figure 2 shows the typical relationship between accumulated permanent strain and the number

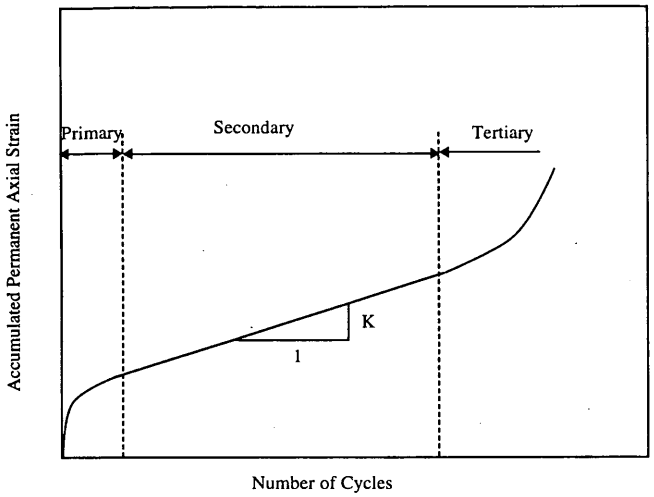

FIGURE 2 Typical relationship between permanent axial strain and number of cycles.

of cycles. The test results indicate that the accumulated permanent axial strain undergoes three distinct stages with increasing number of cycles. The three stages are referred to as primary, secondary and tertiary stages.

Primary Stage

Upon the initial load-application stage, large deformation occurs during a short period of time, indicating a very high rate of deformation (slope of the curve). This condition is followed by a rapid decrease in the rate of deformation with an increased number of cycles. Mechanisms that may act during this early stage of the test and lead to the observed behavior are summarized:

- The initial relatively high rate of deformation implies an immediate decrease in the sample height during the first few seconds that the load pulse is applied. One factor may be that the irregular surface of the sample leads to stress concentrations at relatively elevated points, resulting in the high deformations observed. Other mechanisms, such as densification of the mix as a result of reduced air voids, may lead to similar high rates of deformation.
- The rapid decrease in the rate of deformation within this primary stage may be the result of strain-hardening. The change in the microstructure of an asphalt concrete mix associated with aggregate reorientation leads to a dense mix with increased resistance to deformation.

Primary deformations could significantly contribute to rutting in the field under traffic loading. However, there are inadequate data from these tests to distinguish between deformation that is an artifact of the test procedure and true rutting deformation.

Secondary Stage

During the secondary stage, the rate of accumulation of permanent deformation remains constant. Surface irregularities are no longer a factor because load application during the primary stage flattened the surface. Also strain-hardening is balanced by the recovery process, as the controlling microstructure remains essentially unchanged. Aggregates are not expected to reorient more, because they probably have reached a preferred orientation for the particular energy level applied during the test. The permanent deformation during this stage is mainly caused by shear flow.

The rate of deformation during the secondary stage is essentially a constant, (K); This constant was selected for use in evaluating the rutting potential of different mixes. In this investigation, two mixes under different stress and temperature conditions provided uniquely different values of the constant K, indicative of their actual performance. High K values indicate high rutting susceptibility.

Tertiary Stage

In this final stage, the rate of deformation seems to accelerate until complete failure takes place. This stage is usually associated with the formation of cracks, suggesting that fatigue could be the primary cause of failure. However, other factors such as non-homogeneity of the mix, eccentricity of the loading plate, and surface inclination of the sample also may lead to premature failure.

Constant Rate of Deformation

Considering the uncertainties associated with the primary and tertiary stages, we concentrated on the secondary stage and investigated the constant rate of deformation (K) associated with this stage, considering it an indicator of rutting potential. The rest of the paper discusses the influence of various loading and temperature conditions on the value of K for different mixes.

The constant slope (K) was determined on the basis of the best fit of the straight line at the secondary stage. Test results obtained during the experimental investigation were processed by means of a computer program to determine:

- The accumulated permanent strain corresponding to the number of load cycles. This exercise includes eliminating the elastic portion of the deformation from the total deformation recorded during the test.
- The rate of permanent deformation, K, during the secondary stage using linear regression. The lowest correlation coefficient obtained, considering all samples reported in this study, was 0.993; the highest residual value was 0.34×10^{-3}

Influence of Sample Height

The relationship between accumulated permanent strain and the number of cycles for tests conducted at 25°C is plotted in Figure 3. Results of tests conducted at 40°C are plotted in Figure 4. The corresponding values of K that were determined for both temperature conditions are also indicated in the figures.

Clearly, sample height has little or no influence on accumulated deformations at either temperature. Variables related to compaction that seem to slightly influence the bulk-specific gravity of various samples, have no effect on the value of K determined at 25°C, (standard deviation $S = 0.01$). However, at the higher temperature, the difference between the bulk-specific gravity values seems to influence the determined values of K, as indicated by the relatively

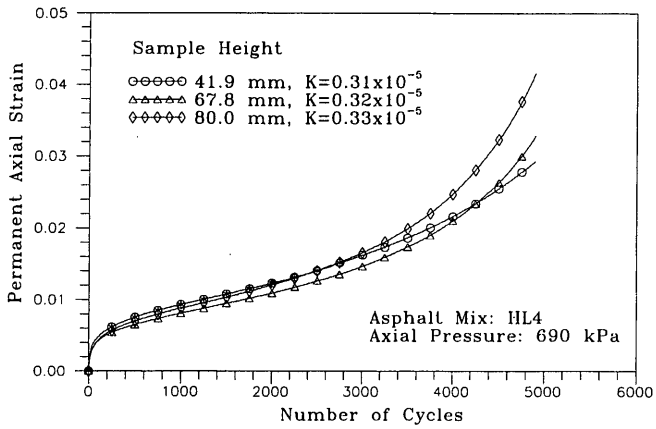

FIGURE 3 Effect of sample heights on accumulated permanent axial strain; tested at 25°C.

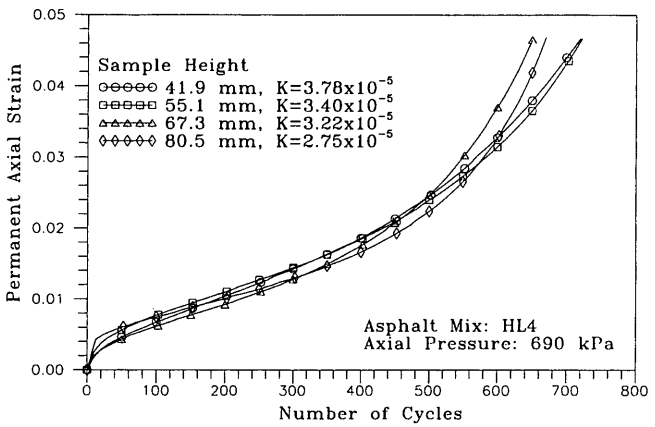

FIGURE 4 Effect of sample heights on accumulated permanent axial strain; tested at 40°C.

high standard deviation ($S = 0.42$). Another observation related to compaction deals with quality of compaction and is associated with the thickness of the sample. Compaction by the gyratory compactor of thinner samples proved less effective because there was little space for aggregate movement to a preferred orientation. The thickness is not a factor when the sample height is more than 60 mm.

Although the determined value of the rate of accumulated axial strain (K) is independent of the sample height, it is necessary to consider the difference in density that may have a direct link to the microstructure of the mix. Comparing results for the two test temperatures, we found the value of K increased by ten-fold on average when the temperature was increased from 25°C to 40°C. The increase is a natural result of more shear flow at low asphalt viscosity.

Another difference in performance related to temperature was observed at the transition from the secondary to tertiary stage. The number of cycles required to cause the transition from the secondary stage dropped approximately 10 times at high temperatures. Perhaps this transition point could be used in the future as another performance indicator. The decision whether to test rutting potential at an elevated temperature should be made based on the prevailing temperature of the region where the mix will be used.

Effect of Applied Pressure

The effect of varying the pressure levels applied during cyclic loading is illustrated in Figure 5. Accumulated permanent axial strain increased with increased pressure. The values of K determined for each pressure level are plotted in Figure 5.

Values of K are plotted against applied pressure in Figure 6. The plot of K against axial pressure suggests that this relationship may be represented by two linear functions with a transition pressure at 0.69 MPa.

$$10^5 K(\sigma) = \begin{cases} 0.52\sigma - 0.07, \text{ for } \sigma \leq 0.69 \text{ MPa} \\ 1.83\sigma - 0.98, \text{ for } \sigma \geq 0.69 \text{ MPa} \end{cases}$$

where K equals the rate of accumulated axial strain at secondary stage and σ equals the applied axial pressure (MPa).

From the equation it is apparent that there is a dramatic change (350 percent) in the rate of increase of K for axial pressures above 0.69 MPa. It is particularly interesting that this transition pressure is very close to the compaction pressure used to prepare the samples

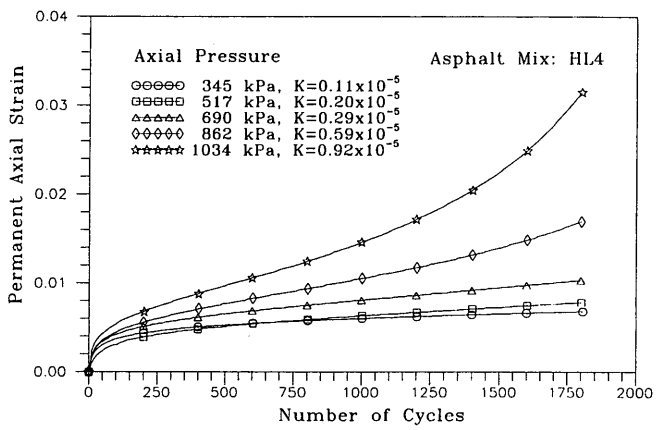

FIGURE 5 Effect of axial pressure on accumulated permanent axial strain; tested at 25°C.

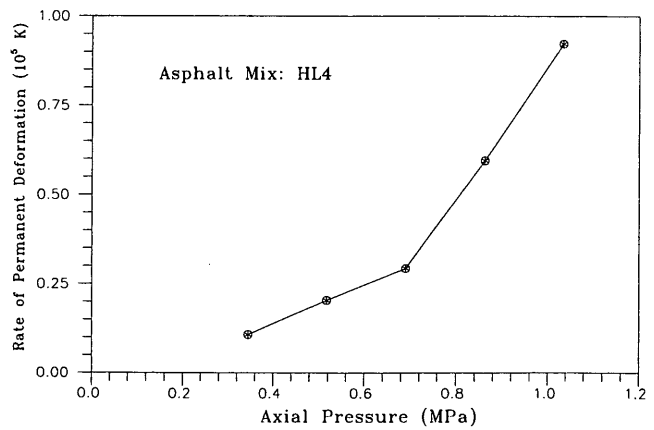

FIGURE 6 Effect of axial pressure on the constant rate (K) of accumulated permanent axial strain during the secondary stage; tested at 25°C.

(0.6 MP). In the future it will be interesting to determine whether a similar relationship exists between compaction pressure and increased value of K for different laboratory-compaction pressures.

Compaction Effort

Results of the repetitive uniaxial compression tests conducted on laboratory samples compacted by an SHRP gyratory compactor on basis of different numbers of gyrations are compiled in Figure 7. The results clearly demonstrate the effect of compaction effort on the mix's resistance to permanent deformation. Determined values of K for these samples, corresponding to the number of gyrations used during compaction, are also shown in Figure 7. The accumulated permanent strain decreased dramatically as the number of gyrations increased. After the number of gyrations reached 150, the rate of decrease in the K value dropped dramatically.

Larger accumulated deformation during the primary stage with a lower number of gyrations was expected because of the sample's probable restructuring. However, the values of the rate of accumulation of axial strain indicate that the value of K is also sensitive to the quality of compaction. The bulk-specific gravity values ranged from 2.290 after 30 gyrations to 2.394 after 250 gyrations. The bulk-specific gravity values clearly indicate that 200 gyrations bring the sample close to a refusal density for which the difference achieved at 250 gyrations is less than 1 percent. The small change in the values of K for the samples compacted to 200 gyrations as compared with samples compacted to 250 gyrations was an indication that shear flow will dominate close to refusal density.

Laboratory Compaction versus Field Compaction

This part of the experimental investigation was designed to confirm the suitability of the SHRP gyratory compactor to produce samples for laboratory evaluation of the rutting potential of various mixes using the uniaxial compression test. However, it is essential to consider the effect of variations in physical properties contributed by field compaction, when comparing them to test results for laboratory-compacted samples. In an effort to reduce the influence of properties such as bulk-specific gravity and air-void content on performance, cores from the field with properties close to that of laboratory samples were intentionally selected. The properties for the field-compacted samples listed are averages for the selected samples:

Mix Type	*Bulk-Specific Gravity*		*Air Void Percentage*	
	Laboratory	*Field*	*Laboratory*	*Field*
HL4	2.411* [0.006]	2.409	2.0* [0.006]	2.5
Large Aggregate Mix	2.401* [0.010]	2.395	3.0* [0.025]	2.0

** Value represents average of samples compacted by SHRP gyratory compactor; numbers in brackets represent standard deviation*

Both theoretical maximum-specific gravity and bulk-specific gravity differ for field and laboratory samples. As a result, laboratory samples for a large aggregate mix have more air voids than can be achieved by field compaction. The differences in physical properties between the field and laboratory samples are expected to slightly influence the resistance of the tested mixes to permanent deformation, which must be considered when reviewing the results described here.

Figure 8 shows the results of the repetitive uniaxial compression test (24°C) conducted on a laboratory-compacted sample and a core recovered from the field for the same mix (HL4). Whereas values of the total permanent axial strain were different for the two samples, the rate of deformation (K) was approximately the same (0.35×10^{-5}). The difference in the shape of the deformation curve between the two compaction types (field and gyratory compaction) was limited to the primary and tertiary stages. As dicsussed before, the primary stage is partially influenced by the nature of the sample surface. For cores recovered from the field, the surface was rough compared with the texture of the laboratory-prepared sample, which explains the high rates of accumulation of permanent strain. The transition from secondary to tertiary stage took place at lower numbers of cycles in the gyratory-compacted sample. The difference in performance at this stage between the two samples may be related to the difference in curing periods in this particular experiment. As mentioned earlier, the field cores were 7 months older than the laboratory-prepared samples.

Based on the suggested evaluation criterion for rutting, (K), gyratory compaction produced a mix that behaves quite similar to

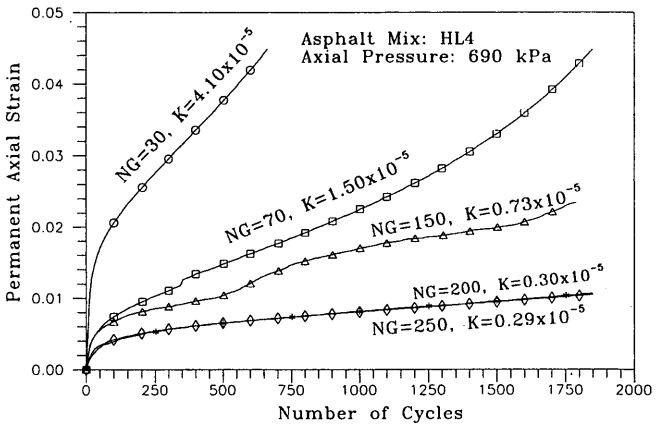

FIGURE 7 Effect of compaction effort on accumulated permanent axial strain: tested at 25°C.

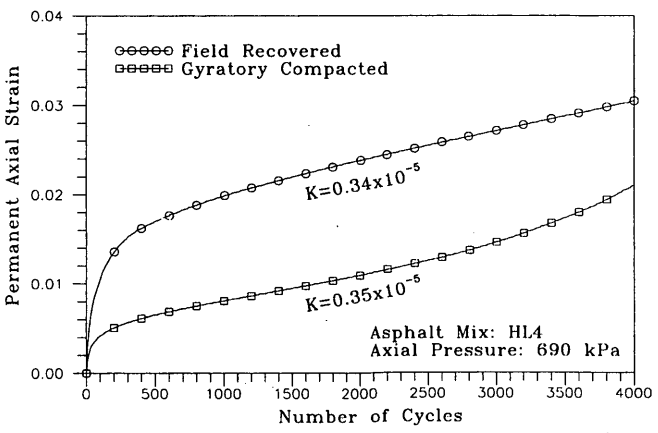

FIGURE 8 Comparison of accumulated permanent axial strains between (HL4) samples compacted by SHRP gyratory compactor and cores recovered from field; tested at 25°C.

that which is compacted in the field. A second test was conducted on similar samples at 40°C to study the effect of a high-temperature environment; the results are plotted in Figure 9. The values of K were found to be approximately equal (3-percent difference). The difference between the two compaction types at the primary and tertiary stage was magnified in the test conducted at the higher temperature. Behavior at the primary stage can be explained by the effect of differences in the sample's surface condition and in the compaction effort. There is no definite explanation for the considerable difference in the behavior of tested samples at the tertiary stage.

The same experiment was performed at 40°C on a large aggregate mix developed at CSTT/NRC. The test results are plotted in Figure 10. Similar to the above experiment, the gyratory compactor produced a mix with a K value equivalent to that of a core recovered from the field (1-percent difference). The deviations observed at the primary and tertiary stages in the HL4 mix were repeated with the large aggregate mix.

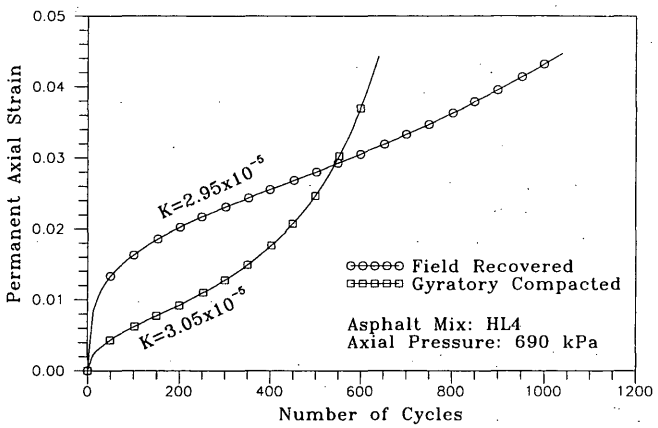

FIGURE 9 Comparison of accumulated permanent axial strains between (HL4) samples compacted by SHRP gyratory compactor and cores recovered from field; tested at 40°C.

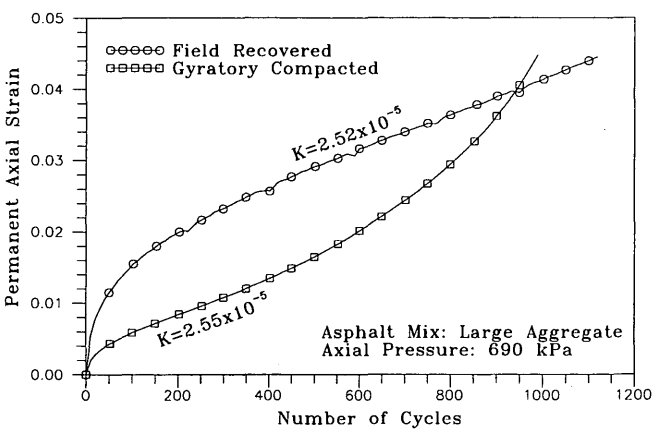

FIGURE 10 Comparison of accumulated permanent axial strains between samples (large aggregate mix) compacted by SHRP gyratory compactor and cores recovered from field; tested at 40°C.

Mix Rating

The ability of the defined rutting criteria (K) to rate various mixes can be demonstrated by comparing results of two uniquely different mixes with known resistance to rutting. Test results can be used to rate the performance of these two mixes with respect to each other of the HL4 and the large aggregate mixes shown earlier in Figures 9 and 10. As anticipated, the tests, conducted at 40°C, illustrated the high resistance to rutting offered by the large aggregate mixes—a direct consequence of the favorable microstructure of the large aggregate mix. Based on these results, the K value of the large aggregate mix is 17 percent less than that of the HL4 mix. The difference between the two mixes continued beyond the secondary state to the tertiary stage. The increased rate of deformation occurred much earlier in the HL4 mix. It is not yet possible to explain why this occurred based on the data available.

CONCLUSIONS AND RECOMMENDATIONS

This paper is a progress report on the ongoing effort at CSTT/NRC to develop a prediction procedure for rutting of asphalt concrete pavement. The authors acknowledge the need for sufficient replicates of the obtained test results to make statistically significant conclusions. The authors chose to investigate the large number of variables involved in developing a prediction procedure in order to identify areas that require additional effort. Further work is already in progress to determine the reproducibility of the test results and to expand analysis to the primary and tertiary stages of the test. The following are conclusions based on the test results presented in this paper:

1. The constant rate of deformation (K) within the secondary stage, as identified by this study, is a suitable criterion for rating the resistance to permanent deformation, for use in predicting rutting potential in the field.
2. The SHRP gyratory compactor produces samples with rutting characteristics equivalent to that of cores recovered from the field as far as the rate of deformation within the secondary stage is concerned.
3. The sample height has no effect on the value of K when tests are conducted at room temperature. However, the value of K determined by tests conducted at elevated temperatures (40°C) is influenced by variations in density associated with differences in the microstructure.
4. Increasing the applied pressure during test at elevated temperature that was used during compaction seems to result in a dramatic increase in the rate of permanent deformation. Data from more specimens at various applied pressure levels are needed to verify this finding and to establish a relationship between the two pressure types.
5. The selected criterion (K) has been proven sensitive to permanent deformation associated with the degree of laboratory compaction used to simulate the quality of field compaction during construction.
6. Distinguishing between factors that contribute to the accumulated permanent strain during the primary and the tertiary stage is necessary if the test is to be used for quantifying rutting potential. Additional work is underway at CSTT/NRC to determine these factors and to collect the necessary data on rutting from the field to support the findings of the laboratory evaluation procedure.

REFERENCES

1. Bonaquist, R. Summary of Pavement Performance Tests Using the Accelerated Loading Facility, 1986–1990. In *Transportation Research Record 1354,* TRB, National Research Council, Washington, D.C., 1992, pp. 74–85.
2. *Compaction Method and Accelerated Performance Tests for SUPERPAVE Mix Design System.* Technical Memorandum No. 7. Strategic Highway Research Program Asphalt Research Program, National Research Council, Washington, D.C., Aug. 1992.
3. El Hussein, H. M. and Z. Yue. Repetitive Uniaxial Compression Test for Evaluating Asphalt Concrete Resistance to Rutting. Proc., Canadian Technical Asphalt Association, Nov. 1993, pp. 98–110.
4. Consuegra, A., D. N. Little, H. Von Quintus, and J. Burati. Comparative Evaluation of Laboratory Compaction Devices Based on Their Ability To Produce Mixtures with Engineering Properties Similar to Those Produced in the Field. In *Transportation Research Record 1228,* TRB, National Research Council, Washington, D.C., 1989, pp. 80–87.
5. El Hussein, H. M., O. J. S. Svec, and L. Zanzotto. Performance of Asphalt Concrete Mixes Containing Large Size Mineral Aggregates. Proc., Canadian Society for Civil Engineering, Vol. IV, Fredericton, 1993, pp. 307–317.

Publication of this paper sponsored by Committee on Characteristics of Bituminous Paving Mixtures To Meet Structural Requirements.

Effect of Moisture on Low-Temperature Asphalt Mixture Properties and Thermal-Cracking Performance of Pavements

NAMHO KIM, REYNALDO ROQUE, AND DENNIS HILTUNEN

Effects of moisture on asphalt mixtures were evaluated by determining the fundamental low-temperature properties of field cores from 22 field test sections at two different levels of moisture, to get an indication of how much these properties may have changed during the pavements' service. The idea was to introduce moisture into the mixtures without causing significant breakdown of the mixtures from stripping or disintegration. The indirect tensile creep and failure test at low temperature, which was selected by the Strategic Highway Research Program (SHRP) to support the mixture specification for thermal cracking, was performed on field cores at two temperatures and two levels of moisture. Master compliance curves and fracture properties were generated and compared to evaluate changes in fundamental low-temperature properties at two different levels of moisture. The properties were input into a thermal-cracking model that was developed at Penn State and is now part of the SHRP SUPERPAVE software in order to determine whether the differences in properties had an effect on thermal-cracking performance in the field. The key finding was that changes in moisture condition within asphalt mixtures have a significant effect on the low-temperature properties of asphalt mixtures and may have a significant effect on the thermal-cracking performance of asphalt pavements. Changes in properties and performance occur even when moisture does not damage the mixture significantly.

Moisture damage of asphalt mixtures is a combined result of moisture-induced changes in mixture characteristics and induced stress in the mixture (*1*). Moisture damage resulting from these two effects, primarily stripping, has been a subject of much research. Even so, there is limited understanding of moisture-induced changes in asphalt mixtures in the absence of stress effects. Some evidence in the literature indicates that moisture changes in the mixture induce changes in mixture properties even when the moisture does not result in mixture damage or disintegration (*2,3,4*). Such moisture-induced property changes may significantly affect the field performance of pavements.

Accurate characterization of low-temperature properties of asphalt mixtures is important to evaluating the thermal-cracking performance of pavements. However, investigations into changes in fundamental low-temperature properties of asphalt mixtures induced by moisture have not been conducted. Therefore, this study was undertaken to evaluate the effects of moisture on the low-temperature properties of asphalt mixtures; the study is part of research being conducted at the Pennsylvania State University as part of a Strategic Highway Research Program (SHRP) research project titled, "Performance Models and Validation of Test Results." Objectives of the work presented in this paper are as follows:

N. Kim, 173–18 Nonhyun-Dong, Kangnam-Gu, Seoul, Korea. R. Roque and D. Hiltunen, Pennsylvania Transportation Institute, Pennsylvania State University, Research Office Building, University Park, Pa. 16802.

- To investigate the effects of moisture on the low-temperature creep compliance of asphalt mixtures;
- To investigate the effects of moisture on the low-temperature failure limits of asphalt mixtures; and
- To conduct a preliminary evaluation to determine the effects of these changes on thermal-cracking performance.

RESEARCH APPROACH

The study was based on the evaluation of 22 field-test sections that were selected as part of an SHRP thermal-cracking validation effort to provide data on a wide range of materials and environmental conditions in United States. Effects of moisture were evaluated by determining the fundamental low-temperature properties of the field cores from the test sections at two different levels of moisture to get an indication of how much these properties may have changed while the pavement has been in service. The idea was to introduce moisture into the mixtures without causing significant breakdown of the mixtures from stripping or disintegration. The goal was to determine how the presence (or lack) of moisture affected properties, not to cause damage to the mixtures. Visual observations of the field cores clearly indicated that the mixtures had not stripped or disintegrated in service.

Field cores were tested in two ways, either as dry specimens or wetted specimens.

- Dry specimens are those specimens that were tested in the-as-received condition, except that they were kept in a chamber at constant low, relative humidity (30 percent) for at least 3 days before testing.
- Wetted specimens are those specimens to which moisture was introduced by applying the wetting portion of Lottman moisture conditioning procedure AASHTO T-283, (i.e., they were vacuum saturated at 26 in. of mercury for 30 min, then left submerged for an additional 30 min.). The procedure was the most effective way of introducing moisture into the specimens without inducing damage in them. After wetting, the specimens were also placed in a 30 percent relative humidity chamber for at least three days before testing.

The following response variables were measured:

- Creep compliance;
- Tensile strength and strain at failure; and
- The *m*-value, which is the slope of the linear portion of the master creep compliance curve on a log-log scale and is related to the fracture parameters of viscoelastic materials (*5*).

The indirect tensile creep and failure test at low temperature (ITLT), developed by R. Roque and his coworkers at Penn State (*6,7*), was conducted at three temperatures (0°C, −10°C, and −20°C) for dry specimens, and at two temperatures (−5°C and −15°C) for wetted specimens. The creep portion of the test involved applying static compressive loads on the diametral specimens for 1,000 sec and measuring horizontal and vertical creep strains near the center of both flat faces. Loads were selected according to preestablished protocols in order to keep strains in the linear viscoelastic range. The strength portion of the test immediately followed the creep portion. Without releasing the creep load, the specimen was failed by applying loads at a constant rate of vertical displacement. Master compliance curves and fracture properties were generated for both of these sets of tests, as described elsewhere (*7*).

The results were compared to evaluate the changes in fundamental low-temperature properties between dry and wetted mixtures. The properties were input to the thermal-cracking model developed at Penn State as part of a research contract to determine the effect of the differences in properties on predicted thermal-cracking performance (*7*).

MATERIALS AND SAMPLE PREPARATION

Selection of Field Specimens Used in Testing

Thirty-six cores each 6 in. in diameter, from each of the 22 field sections, were included in the thermal-cracking validation study, which was conducted at the Pennsylvania Transportation Institute. Nine cores were randomly selected for testing in the dry condition and six cores for testing in the wetted condition. At each temperature, 69 tests were performed (23 sections times 3 replicates). The order at which each test was performed was selected at random.

Slicing of Field Core Specimens

The specimens, 6 inch diameter were sliced to a thickness of 2 in. with a water-cooled masonry saw equipped with a diamond-tipped blade. The cut provided the smooth surface necessary to mount gage points on a specimen's flat faces.

Specimen Humidity Conditioning

While making field core specimens for mechanical property tests moisture is introduced into the test specimen. A series of procedures is used, including coring, core slicing, and specific gravity measurement. Even though all the cores were stored in sealed plastic bags, the core storage period of the each test section before testing varied by as much as one year. As a result, there was high probability that different moisture effects were induced. A way to standardize the moisture effect throughout the test sections was needed.

A small-scale experiment was conducted to monitor the changes in moisture in specimens stored in the humidity-controlled chamber. Changes in moisture were monitored for laboratory-compacted specimens wetted using Lottman's short-term conditioning procedure (*8*). Changes in moisture were also monitored in field cores after they were submerged for specific gravity determination. Changes in sample weights are plotted in Figure 1. The weight of a saturated specimen changed rapidly for the first 2 days after wetting,

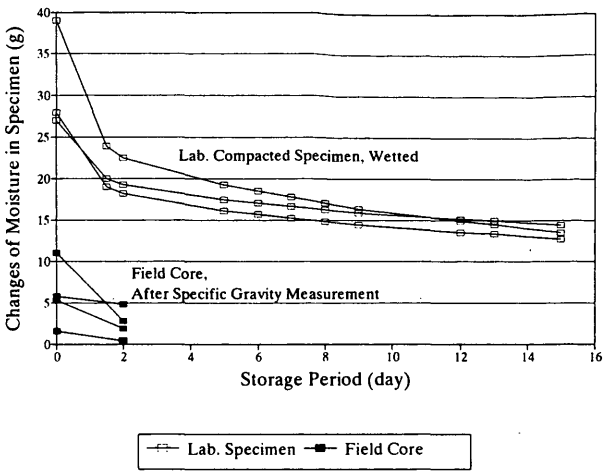

FIGURE 1 Changes of moisture in specimen during humidity conditioning.

after which a slow constant rate of weight change was observed through the 15th day. The weight of most field cores also changed rapidly for the first 2 days.

On the basis of results presented in Figure 1, it is expected that the moisture level at 3 days after a 5-minute soaking (as required for specific gravity measurement) will be very close to the moisture level before the 5-minute soaking. The fast change in weight during the first few days appears to be caused by evaporation of water entrapped in the surface region of the specimen, whereas the slow change in weight after the first few days appears to be related to permeability or the air-void structure of a specimen.

Therefore, after bulk specific gravity was measured, all specimens were placed in a constant-humidity environment for a minimum of 3 days before testing. Specimens were conditioned at 30 percent relative humidity and at room temperature (20°C).

Specimen Load Conditioning

In order to minimize specimen-seating effects during testing, a preconditioning load sequence was applied to each core during the humidity-conditioning period. The procedure consisted of 100 cycles of loading at 20°C. Each load cycle consisted of a 0.1 sec inverse haversine (compression) followed by a 0.9 sec rest period. The amplitude of the haversine pulse was set to the load corresponding to a horizontal tensile stress of 6.9 kPa (10 psi).

Specimen Temperature Conditioning

Specimens were kept at the constant test temperature for no less than 6 hr before testing. Because little is known about the effects of keeping mixture specimens at very low temperatures for extended periods of time [i.e., low-temperature physical hardening (−*9*)], extended deep-freeze periods were avoided.

TEST RESULTS AND ANALYSIS

Test results were compared in order to evaluate changes in fundamental low-temperature properties between dry and wetted mixtures. The effect of moisture on mixture properties is summarized in Table 1.

TABLE 1 Effect of Wetting on Mixture Properties

Sec No	Environment	Location	Effect of Wetting on Mixture Properties					
			Stiffness*		Shift Factor ($1/a_T$)	m*	Strength @ -10 C (kPa)	
			@10sec	@longer time			Dry	Wet
1	Dry Freeze Thaw	Chickasha,OK	Same	Dec	Dec	Inc	3878	4341
2		Hackberry,AZ	Same	Same	Mild Dec	Same	3660	4341
6		Oasis,NV	Same	Dec	Mild Dec	Inc	2369	2228
7		Ottawa,KS	Mild Inc	Dec	Same	Inc	2941	2958
11	Dry Hard Freeze	Idaho Falls,ID	Inc	Dec	Dec	Inc	3622	3176
12		Coeur d'Alene,ID	Same	Dec	Mild Dec	Inc	4462	4009
13		Edison,NE	Same	Same	Mild Dec	Same	3114	2892
16		Marysvale,UT	Mild Dec	Dec	Dec	Inc	2678	2315
17		Cody,WY	Mild Inc	Mild Dec	Mild Inc	Same	3427	2410
18		Rangely,CO	Dec	Dec	Mild Inc	Same	2632	1934
21	Wet Freeze Thaw	Glasgow,KY	Inc	Same	Inc	Same	3399	3455
22		Ponca City,OK	Same	Dec	Mild Dec	Inc	2708	2799
23		Berlin,MD	Inc	Inc	Inc	Same	2856	2898
26		Salem,SC	Same	Dec	Same	Inc	1789	1366
27		Trenton,NJ	Inc	Mild Inc	Same	Inc	3742	3221
28		Waynesville,MO	Same	Dec	Dec	Same	2126	1819
31	Wet Hard Freeze	Lawrenceville,PA	Same	Dec	Dec	Inc	2874	2671
32		Huntington,IN	Mild Inc	Dec	Dec	Inc	2153	2332
33		Farmington,ME	Inc	Same	Same	Same	3442	2933
36		Bonnville,IN	Inc	Inc	Inc	Same	2894	2599
37		Farmington,MN	Inc	Mild Dec	Mild Dec	Inc	2921	3405
38		Frazee, MN	Inc	Mild Dec	Mild Dec	Inc	2306	2211

*Same = no change; Dec = decrease; Inc = increase in property induced by moisture

Compliance

Comparisons of master stiffness (inverse of compliance) curves for dry and wetted specimens clearly indicated that the introduction of moisture had a significant effect on the low-temperature stiffness of the mixtures. Figures 2 through 7 show comparisons of master stiffness curves and shift-factor temperature relationships at a reference temperature of −15°C for three mixtures that characterize the types of changes observed to be induced by moisture. Actual measured data were plotted within the measured reduced time range. Outside the measured reduced time range, wetted stiffness was extrapolated using a hyperbolic model to cover the entire reduced time range corresponding to specimens tested in the dry condition.

Compared with dry stiffness curves, the stiffness of wetted mixtures changed very significantly for most mixtures (see Table 1). However, the effect of moisture appeared to be different for different mixtures; it was difficult to find trends among these data. In general, but not always, wetted-mixture stiffness at shorter reduced time (around 10 sec) was the same or greater than dry-mixture stiffness. On the other hand, wetted-mixture stiffness at longer reduced times (10^3 sec or greater) either was generally less than dry-mixtures stiffness or was decreasing more rapidly than dry mixture stiffness.

As indicated in Figures 3, 5, and 7, shift factor/temperature relationships also changed as a result of changes in moisture content in the mixture. Among more than half of the test sections, wetting reduced the shift factors, indicating that wetted rheological property was less temperature-dependent than dry.

It is nearly impossible to determine the effect of changes in the master compliance curve on thermal-stress development without actually performing thermal-stress computations. Thermal-stress development not only depends on the magnitude and shape of the compliance curve at a reference temperature but also on the characteristics of the shift factor/temperature relationship. For example,

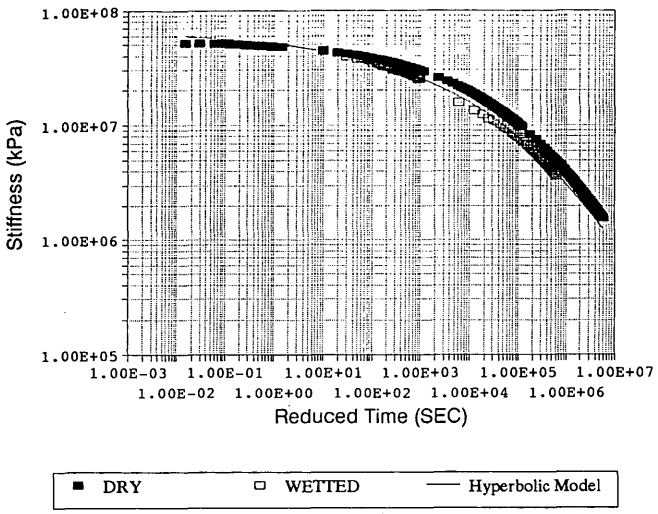

FIGURE 2 Comparison of dry and wetted master stiffness curves (Section 2).

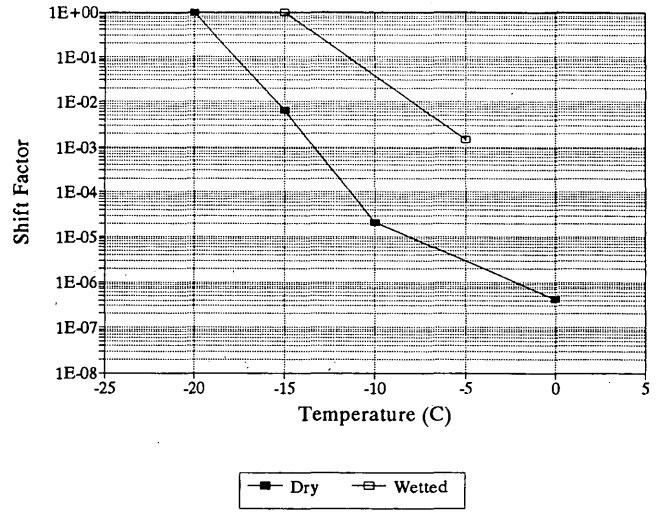

FIGURE 3 Comparison of dry and wetted shift factors (Section 2).

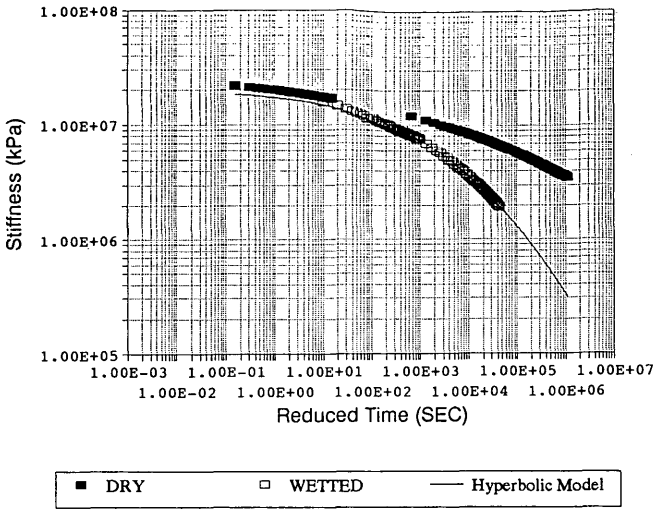

FIGURE 4 Comparison of dry and wetted master stiffness curves (Section 6).

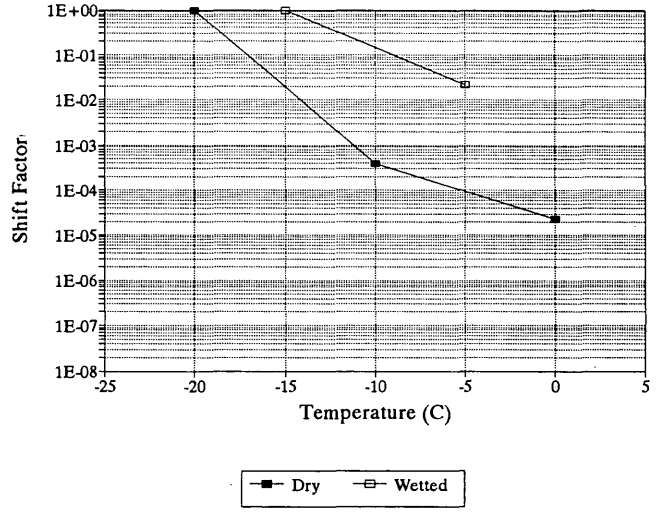

FIGURE 5 Comparison of dry and wetted shift factors (Section 6).

two materials may have identical compliance curves at a specified reference temperature, but their compliance at another temperature may be significantly different if their shift factor/temperature relationships are different. These complexities make it extremely difficult to assess the effect of moisture changes simply by looking at how the master compliance curve changed. Therefore, the effect of these changes was evaluated by predicting pavement performance using dry and wetted rheological properties. The results of this evaluation are presented later in this paper. More detailed research is under way that should provide explanations to the observed changes in rheological properties induced by moisture.

Failure Limits

Comparisons of strengths and *m*-values between dry and wetted specimens indicated that the introduction of moisture also had a significant effect on the fracture properties of the mixtures. Figure 8 through 10 indicates comparisons of strengths at different temperatures, whereas Figure 11 provides comparisons of *m*-values for the three sections presented earlier. Again, the *m*-value is defined as the slope of the linear portion of the master creep compliance curve on a log-log plot. It has been found to be an important fracture parameter in distinguishing between the thermal-cracking performance of different materials. Once again, the effect was different for different mixtures, and it was difficult to draw conclusions or trends from the data. In general, the strengths of wetted specimens were either lower or about the same as the dry specimens, while the *m*-values of wetted specimens were either higher or about the same as the *m*-values of dry specimens. Lower strengths result in less resistance to thermal cracking, whereas higher *m*-values result in better resistance to thermal cracking. As for compliance, it is nearly impossible to tell what the combined effect of these differences in properties might be on thermal-cracking performance simply by

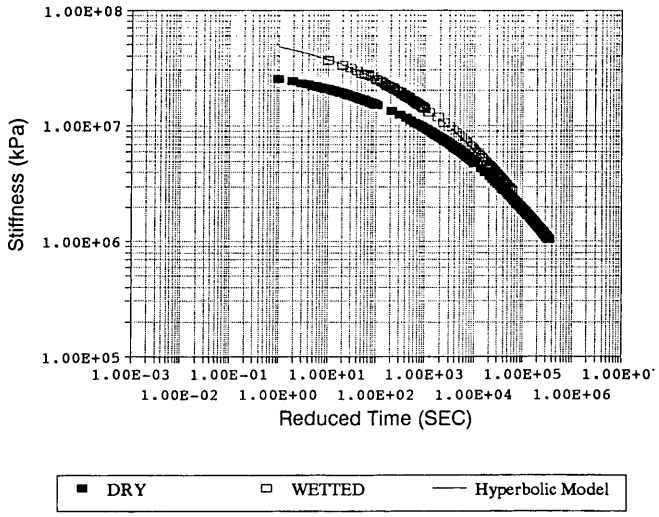

FIGURE 6 Comparison of dry and wetted master stiffness curves (Section 27).

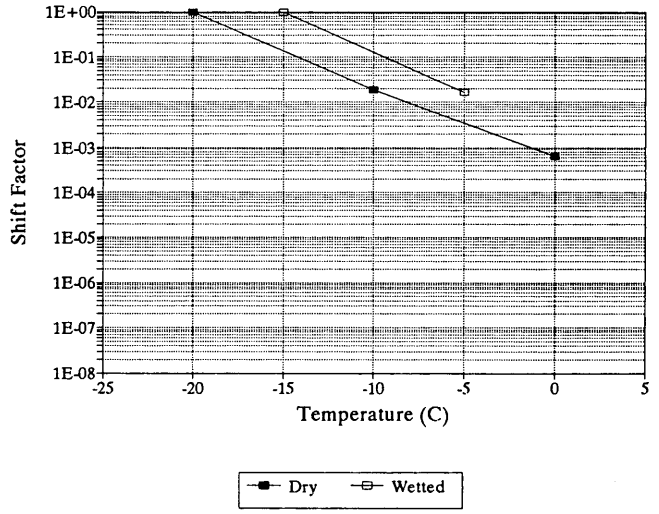

FIGURE 7 Comparison of dry and wetted shift factors (Section 27).

comparing the values. Again, performance predictions were made to evaluate the effects induced by moisture.

Stripping Observations

After the ITLT test at −5°C was conducted pictures were taken to monitor the stripping on split faces of test cores—for both dry and wetted cores—to monitor and compare the changes in stripping induced by moisture. In most cases, no changes in stripping or disintegration by wetting were observed which may imply that the wetting procedure used in this research was not severe enough to induce any moisture damage, as that was the intent of the study. As mentioned earlier, the basic idea was to introduce moisture into mixtures without causing significant breakdown of the mixtures.

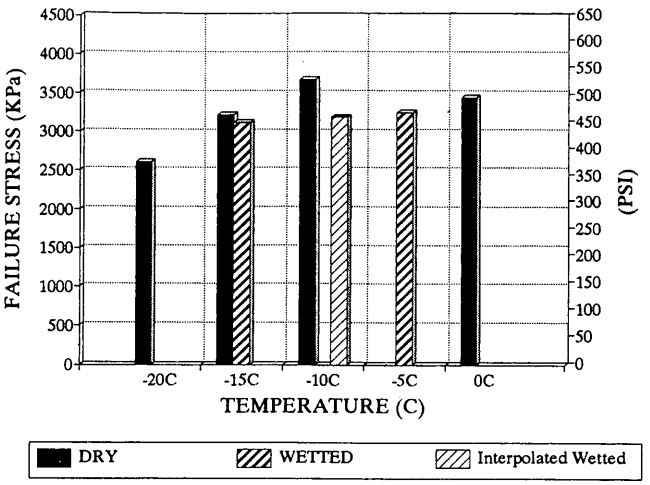

FIGURE 8 Comparison of dry and wetted strengths (Section 2).

Effect of Wetting on Thermal-Cracking Performance

Generally, but not always, moisture makes asphalt mixture less stiff and weaker in strength. As far as the thermal-cracking performance of pavement is concerned, an increase in mixture compliance (reduction in stiffness) reduces thermal stress, thereby reducing its thermal-cracking potential. On the other hand, a comparable decrease in strength increases thermal-cracking potential. A decrease in $1/a_T$ (shift factor/temperature relationship) results in higher stiffness at temperatures above the reference temperature, which consequently increases thermal-cracking potential for mixtures with identical compliance curves at a specific reference temperature. Moisture in a mixture generally increases the *m*-value, which results in better resistance to thermal cracking. Thus, as mentioned earlier, it is nearly impossible to tell what effect these changes will have on thermal-cracking performance without actually performing thermal-stress computations and performance predictions.

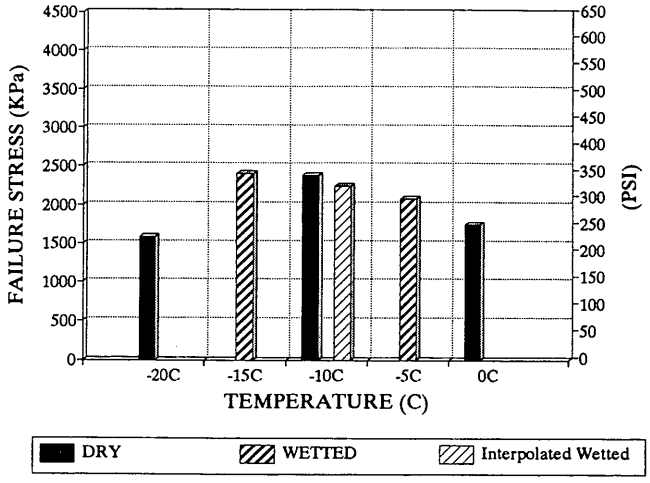

FIGURE 9 Comparison of dry and wetted strengths (Section 6).

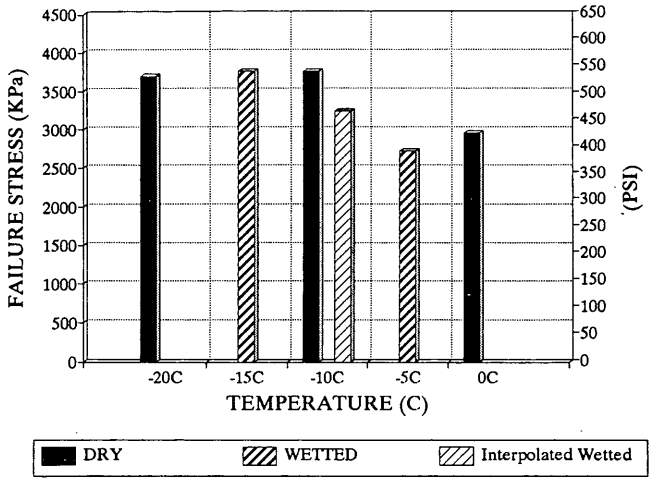

FIGURE 10 Comparison of dry and wetted strengths (Section 27).

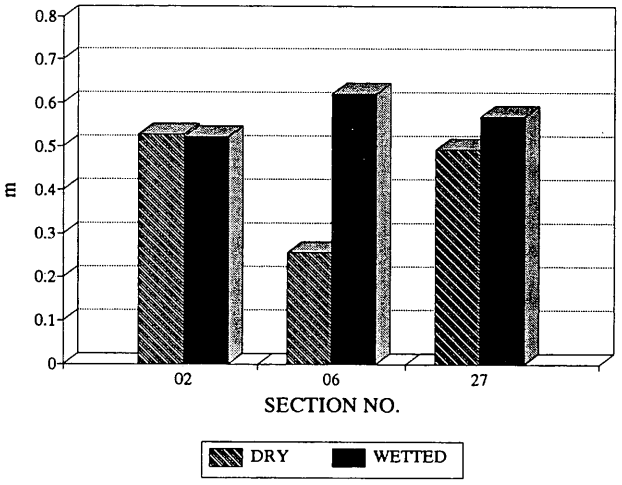

FIGURE 11 Comparison of dry and wetted *m*-values.

A mechanics-based thermal-cracking model developed at Penn State, which has been incorporated into the SHRP SUPERPAVE software, was used for this analysis. The model predicts the amount (or frequency) of thermal cracking as a function of time. Inputs to the model include: fundamental properties (master relaxation modulus curve and fracture parameters A and n) obtained from the ITLT, pavement structure, and site-specific weather data. The model predicts thermal stress as a function of pavement depth on an hourly basis throughout the analysis period. Thermal stresses are used to predict crack propagation and the amount of transverse thermal cracking as a function of time. Pavement temperatures used in these computations are predicted from daily air temperature data using the FHWA Environmental Effects Model (*10*). Thermal stresses are computed using an algorithm based on Boltzmann's superposition principle as it applies to viscoelastic materials. Viscoelastic mixture properties (i.e., the master relaxation modulus curve) as measured by the ITLT test are used for these computations. Thermal stresses are then used to determine stress intensity factors for use in the Paris law of crack propagation [$\Delta C = A\,(\Delta K)^n$].

Thus, the average depth of transverse cracks within the pavement is computed on a daily basis. A probabilistic approach is then used to determine the amount of cracking in the pavement. A detailed description of the model is presented elsewhere (7).

A generalized four-element Maxwell model was selected to represent the viscoelastic properties of the asphaltic concrete mixture. Mathematically, the generalized Maxwell model is expressed according to the following Prony series expansion:

$$E(\xi) = \sum_{i=1}^{4} E_i e^{-\xi/\lambda_i} \tag{1}$$

where $E(\xi)$ is the relaxation modulus at reduced time ξ, and E_i, λ_i are Prony series parameters for master relaxation modulus curve.

The Prony series was fit to the ITLT compliance data obtained from both the dry and wetted specimens for input into the thermal-cracking model. Details concerning the Prony series parameter fitting are presented elsewhere (*7*). Thermal-cracking predictions then were made for each test section, using both dry and wetted properties, to determine the difference in predicted performance. All other input data were the same for both sets of predictions.

The effect of moisture on mixture properties was reflected in the predicted thermal-cracking performance of the pavement sections. The results of thermal-cracking predictions for the three test sections for which properties were presented earlier in the paper, are presented in Figures 12 through 14. As expected, the effects of moisture on predicted performance varied significantly from mixture to mixture: very little difference in thermal-cracking performance was observed for some sections (e.g., PTI Section 2; Figure 12), whereas significant differences were observed in other sections (e.g., PTI Section 6; Figure 13). As mentioned earlier, moisture affects numerous mixture properties (i.e., compliance, strength, shift factor, and *m*-value each of which may contribute to the thermal-cracking performance of a particular mixture. The combined effect of such moisture-induced property changes determines whether moisture has been beneficial, harmful, or has had no effect on thermal-cracking performance.

In summary, the introduction of moisture resulted in little or no change in the thermal-cracking performance of 13 test sections,

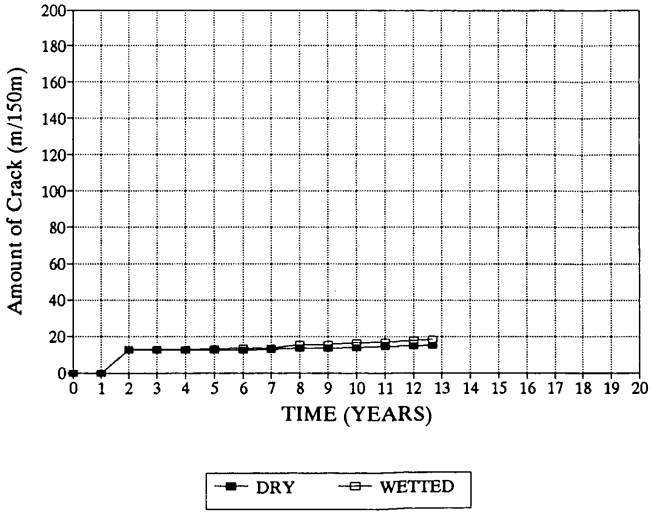

FIGURE 12 Effect of moisture on thermal cracking performance (Section 2).

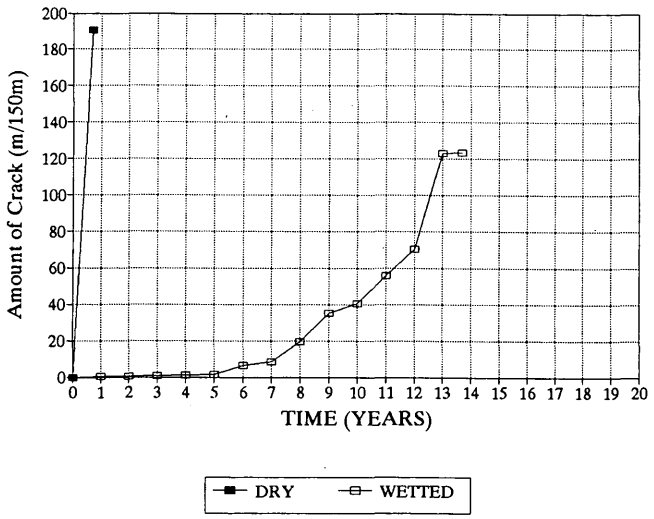

FIGURE 13 Effect of moisture on thermal cracking performance (Section 6).

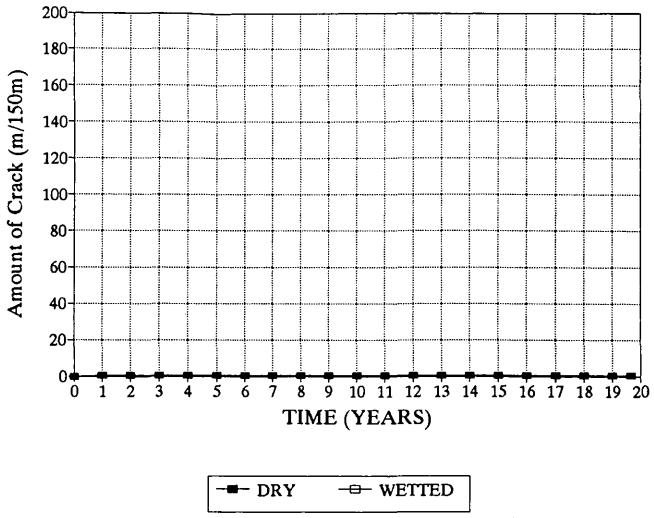

FIGURE 14 Effect of moisture on thermal cracking performance (Section 27).

significantly improved the performance of 6 test sections, and significantly reduced the performance of 2 test sections. It should be noted that the fact that no change in predicted performance was observed for a particular section in a particular environment does not mean that this same change in properties would not produce a significant change in performance in a different environment. It appears that the effects of moisture may be both mixture and environment dependent. At this point, it is not entirely clear why moisture had a different effect on different mixtures. It appears that these changes may be related to the pore structure of the mixture, whether or not the pore water froze, and the effect of freezing on the structure of the mixture. More research is being conducted to evaluate these effects.

CONCLUSIONS

Conclusions from this work may be summarized as follows:

- Changes in moisture condition within asphalt mixtures significantly affect the low-temperature properties of asphalt mixtures. Generally, but not always, the introduction of moisture into the mixture results in lower strength and higher compliance at longer reduced times. The magnitude of the moisture-induced changes in properties is highly mixture dependent.
- Changes in moisture condition within asphalt mixtures may have a significant effect on the thermal-cracking performance of asphalt pavements.
- Changes in properties and performance occur even when moisture does not damage the mixture significantly.

These results clearly indicate that great care must be exercised to bring field cores to standard moisture condition before laboratory testing for determination of fundamental low-temperature properties. Further research is recommended to identify mixture characteristics that lead to mixtures whose properties and performance are significantly affected by moisture changes.

ACKNOWLEDGMENT

Funding for the work presented in this paper was provided by SHRP.

REFERENCES

1. Graf P. E. Factors Affecting Moisture Susceptibility of Asphalt Concrete Mixes. *Proc., Association of Asphalt Paving Technologists,* Vol. 55, St. Paul, Minn. 1986, pp. 175–212.
2. Busching, W., S. N. Amirkhanian, J. L. Burati, J. M. Alewine, and M. O. Fletcher. Effects of Selected Asphalts and Antistrip Additives on Tensile Strength of Laboratory-Compacted Marshall Specimens: A Moisture Susceptibility Study. *Proc., Association of Asphalt Paving Technologists,* Vol. 55, 1986, St. Paul, Minn., pp. 120–148.
3. Coplantz, J. S. and D. E. Newcomb. Water Sensitivity Test Methods for Asphalt Concrete Mixtures: A Laboratory Comparison. In *Transportation Research Record* 1171, TRB, National Research Council, Washington, D.C., 1988, pp. 44–50.
4. Schmidt, J. and P. E. Graf. The Effect of Water on the Resilient Modulus of Asphalt Treated Mixes. *Proc., Association of Asphalt Paving Technologists,* Vol. 41, 1972, St. Paul, Minn., pp. 118–162
5. Schapery, R. A. *A Theory of Crack Growth in Viscoelastic Media:* Research Report MM2764-73-1. Mechanics and Materials Research Center, Texas A&M University, College Station, March 1973.
6. Roque, R. and W. Buttlar. Development of a Measurement and Analysis System to Accurately Determine Asphalt Concrete Properties Using the Indirect Tensile Mode. *Proc., Association of Asphalt Paving Technologists,* Vol. 61, 1992, St. Paul, Minn., pp. 304–342.
7. Lytton, R. L., R. Roque, J. Uzan, D. R. Hiltunen, E. Fernardo, and S. M. Stoffels. *Performance Models and Validation of Test Results.* Final Report to Strategic Highway Research Program; Asphalt Project A-005, July 1993.
8. Lottman, R. *NCHRP Report 246: Predicting Moisture-Induced Damage to Asphalt Concrete–Field Evaluation Phase.* TRB, National Research Council, Washington, D.C. 1982.
9. Bahia, H. *Low Temperature Physical Hardening of Asphalt Cements.* Ph.D. thesis. Pennsylvania State University, University Park, 1991
10. Lytton, R. L., D. E. Pufahl, C. H. Michalak, H. S. Liang, and B. J. Dempsey. *An Integrated Model of the Climatic Effects on Pavements.* Report FHWA-RD-90-033. FHWA, U.S. Department of Transportation, Nov. 1989.

Publication of this paper sponsored by Committee on Characteristics of Bituminous Paving Mixtures To Meet Structural Requirements.

Healing in Asphalt Concrete Pavements: Is it Real?

Y. R. KIM, S. L. WHITMOYER, AND D. N. LITTLE

Microcrack healing of asphalt concrete during rest periods is among the many variables influencing the lab-to-field fatigue shift factor. Experimental approaches to evaluating this mechanism, both in the laboratory and in the field are presented. Three techniques introduced in this paper include the nonlinear viscoelastic correspondence principle, the impact-resonance test method for the laboratory characterization, and the stress-wave testing method for in situ characterization of asphalt concrete pavements. When analyzing the change in stress-strain behavior of asphalt concrete during rest periods, one must consider both the relaxation and healing of microcracks. A nonlinear viscoelastic correspondence principle based on the pseudo-strain concept was successfully applied to both controlled-stress and controlled-strain uniaxial testing under varying test conditions. The principle enabled determination of the healing potential of asphaltic mixtures. The impact-resonance test method appeared to be an excellent means of evaluating the change in elastic properties of asphalt concrete resulting from damage growth or healing. Finally, 24-hr stress-wave testing of a pavement section demonstrated a decrease in the elastic modulus as temperature increased, and an increase in the elastic modulus after the rest period, possibly due to microcrack healing in asphalt concrete layers.

In mechanistic pavement design procedures, the progression of distresses is first modeled in the laboratory using simplified test methods and theoretical approaches, such as the mechanics of materials. The laboratory models are then calibrated by observed field-performance data. A number of researchers have shown that the power relationship between number of cycles to failure and tensile strain obtained from laboratory fatigue-test data grossly underpredicts field fatigue life. The discrepancy prompted development of the so-called "lab-to-field shift factor." The most widely used shift factor, presented by Finn et al. (*1*), resulted from evaluating AASHTO Road Test data.

The difference between fatigue lives predicted from the laboratory model and those observed from the in-service pavements can be attributed to the following factors, among others:

1. Difference in loading conditions, including rest periods, multi-level loading, sequence of multi-level loading;
2. Reactions or frictional forces between the asphalt layer and the base layer;
3. Residual stresses caused by the plasticity of the pavement layers;
4. Dilatancy stresses from the expansion of paving materials under load, which builds up large confining pressures under passing wheel loads; and
5. Complicated environmental conditions in the field.

Y. R. Kim and S. L. Whitmoyer, Department of Civil Engineering, North Carolina State University, Box 7908, Raleigh, N.C. 27695–7908; D. N. Little, Department of Civil Engineering, Texas A&M University, Room 508, CE/TTI Building, College Station, Tex. 77843–2473

Although it is quite difficult, if not impossible, to develop a shift factor based on sound mechanical theory that accounts for the effects of all the factors listed above, it is extremely important to determine how much of the shift factor is under the control of the designer. Being able to understand and evaluate the mechanisms governing the fatigue damage growth, one can improve materials and pavement design to extend the fatigue service life of pavements.

Of the numerous factors influencing fatigue life of asphalt pavement, this paper focuses on the microcrack healing of asphalt concrete layers during rest periods. Although the significance of rest periods on the fatigue performance of asphaltic mixtures has been recognized since the 1960s, only during the last 10 years has healing during rest periods been studied as a mechanism whereby asphalt concrete regains its strength. (*2,3*).

When an asphalt concrete pavement is subjected to repetitive applications of multi-level vehicular loads and various durations of rest periods, three major mechanisms take place: fatigue, which can be regarded as damage-accumulation during loading; time-dependent behavior related to the viscoelastic nature of asphalt concrete; and chemical healing across microcrack and macrocrack faces during rest periods. The difficulty of evaluating these mechanisms arises from the fact that they occur simultaneously in an asphalt concrete pavement; that is, during rest periods, relaxation and chemical healing take place together.

This paper presents three different approaches to evaluating the chemical healing of asphalt concrete: the elastic-viscoelastic correspondence principle, the impact-resonance testing method for the laboratory characterization, and the stress-wave testing for the field evaluation. Both laboratory and field data are presented with the following questions in mind:

- Is healing in asphalt concrete a real phenomenon both in the laboratory and the field?
- If so, how can we measure it in the laboratory and in the field?

EVALUATION OF HEALING VIA THE CORRESPONDENCE PRINCIPLE

The so-called elastic-viscoelastic correspondence principle (CP) is an excellent means of evaluating and modeling the hysteretic behavior of viscoelastic media. This principle simply states that one can reduce a viscoelastic (time-dependent) problem to an elastic (time-independent) problem merely by working in an appropriately transformed domain and substituting elastic moduli.

The nonlinear viscoelastic CP was developed by Schapery in 1984 (*4*). He suggested that the constitutive equations for certain nonlinear viscoelastic media are identical to those for the nonlinear elastic case, but stresses and strains are not necessarily physical

quantities in the viscoelastic body. Instead, they are "pseudo" parameters in the form of a convolution integral. For the uniaxial case with growing damage, pseudo strain in the following form is recommended:

$$\epsilon^R = \frac{1}{E_R} \int_0^t E(t - \tau) \frac{d\epsilon}{d\tau} d\tau \quad (1)$$

where

ϵ, ϵ^R = uniaxial strain and pseudo strain,
E_R = reference modulus which is an arbitrary constant, and
$E(t)$ = uniaxial relaxation modulus.

This principle's application to the hysteretic stress-strain behavior of asphalt concrete is illustrated using actual data. Repetitive uniaxial testing is performed under two completely different sets of testing conditions in order to demonstrate the applicability of the pseudo strain concept. The details of the testing conditions include the following:

Test 1	*Test 2*
Controlled-stress test	Controlled-strain test
Compressive loading	Tensile loading
Haversine wave form	Saw-tooth wave form
0.2 sec/cycle	1 sec/cycle
Short rest periods (1, 4, 8, 16 sec)	Long rest periods (5, 10, 20, 40 min)
Densely graded asphalt concrete (AC)	Sand-asphalt

A broad range of testing conditions are applied to cover most test conditions encountered in the characterization of asphalt concrete. All details in the materials, sample preparation methods, and testing and analysis methods are not presented here, however, because of space limitation; but they can be found elsewhere (Test 1, see Reference *5;* Test 2, see Reference *6*).

When cyclic loading is applied to asphaltic mixtures, hysteresis loops are usually observed from the stress-strain curves with changing dissipated energy (i.e., area inside the stress-strain curve) as cycling continues. Based on the control mode (controlled-stress versus controlled-strain), two different trends can be observed in the stress-strain behavior, as are illustrated in Figure 1. It is noted here that the stress and strain levels in Figure 1 are low enough not to induce any significant damage in the specimens. Relaxation moduli are determined from both the mixtures, and pseudo strains are calculated using Equation 1. The data presented in Figure 1 are replotted in Figure 2 using the pseudo strain instead of the physical strain on the abscissa. The figures indicate that regardless of the control mode, the hysteretic behavior from cyclic loading disappears when the pseudo strain is used, except for the first cycle, during which some minor adjustments occur in the specimen and test setup. It is also noted that the stress-pseudo strain behavior is linear.

The same approach is employed to investigate the ability of the CP to account for the relaxation effect during rest periods. Figure 3 presents the hysteresis loops observed in the controlled-strain and controlled-stress testing before and after rest periods. Again, the stress and strain levels are kept low so as not to induce any damage. A significant increase in the dissipated energy is observed after the rest period, irrespective of the control mode. Pseudo strains are calculated and plotted against the stress values in Figure 4. The use of pseudo strain successfully eliminates the effect of relaxation and results in a linear, elastic-like behavior between the stress and pseudo strain.

On the basis of the observations made from Figures 2 and 4, it can be concluded that, as long as the damage induced by the cyclic

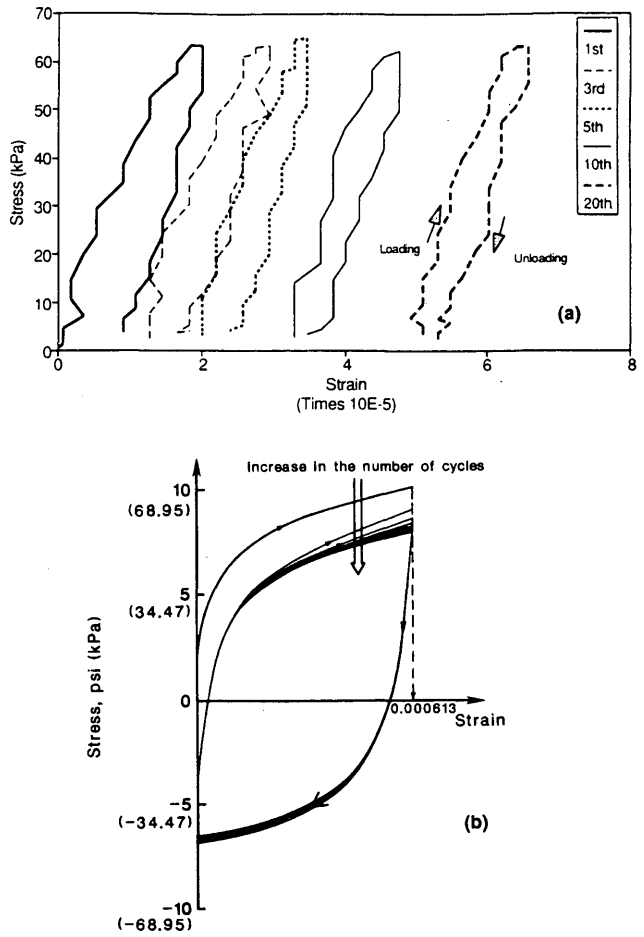

FIGURE 1 Hysteretic stress-strain behavior with negligible damage: (*a*) controlled-stress test; (*b*) controlled-strain test.

loading is negligible, the pseudo strain can be utilized to eliminate the time-dependence of asphaltic mixtures from the hysteretic behavior, irrespective of mode of control, loading type (tension versus compression), loading rate, wave form, or length of rest period. It is this use of pseudo strain that makes it possible to evaluate the healing mechanism during rest periods separately from the relaxation.

To evaluate fracture healing, the load amplitude is increased to a level at which significant damage growth can be expected during cyclic loading. Again a significant increase in the dissipated energy is observed by comparing the stress-strain diagrams before and after the rest periods that could be resulting from either relaxation or healing, or both. As mentioned previously, one cannot determine how much increase in the dissipated energy is related to healing merely by looking at stress-strain diagrams. Therefore, pseudo strains are calculated for both the controlled-stress and controlled-strain tests and plotted against the stresses in Figure 5. Different stress-pseudo strain behavior is observed in Figure 5 compared with that in Figure 4, where negligible damage occurred. Because the beneficial effect of the relaxation phenomenon now has been accounted for by using pseudo strain, changes in the stress-pseudo strain curves during the rest periods, as are observed in Figure 5, must result from the fracture healing of microcracks.

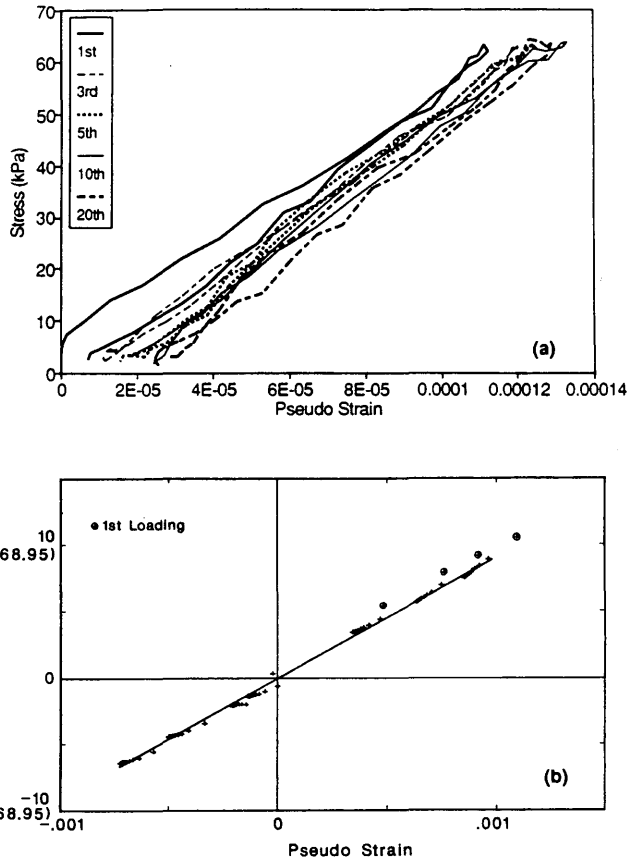

FIGURE 2 Application of CP to the data in Figure 1: (*a*) controlled-stress test; (*b*) controlled-strain test.

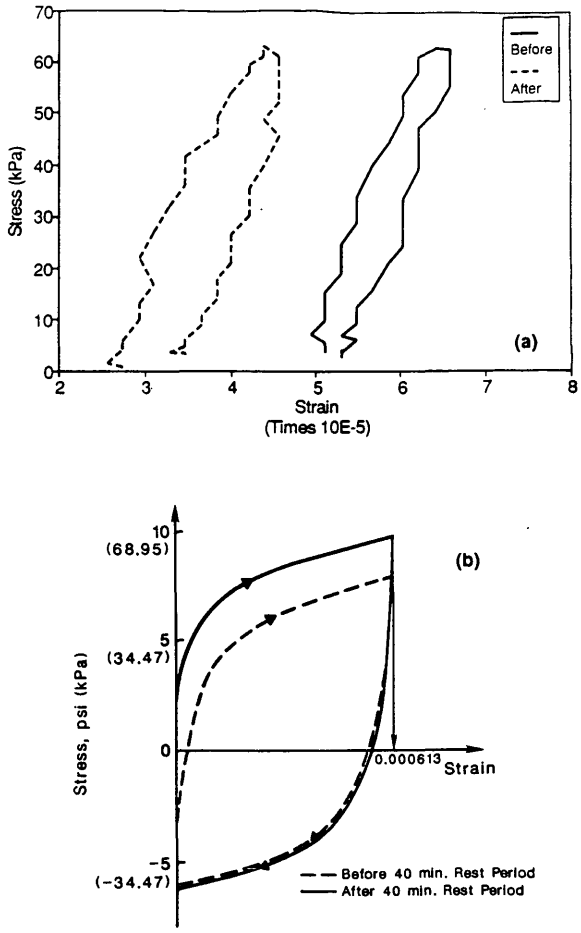

FIGURE 3 Effect of rest periods on stress-strain behavior (with negligible damage): (*a*) controlled-stress test; (*b*) controlled-strain test.

One can determine different mixtures' propensity for microcrack healing by measuring the difference in areas under the stress-pseudo strain curves before and after a rest period and normalizing it by the stress-pseudo strain area before the rest period. This method has been used successfully in differentiating the healing potentials of various binders (*3*).

LABORATORY EVALUATION OF HEALING VIA VIBRATIONAL TESTS

The impact-resonance method described in ASTM C 215 has been shown to produce very repetitive, consistent results for Portland cement concrete and for asphalt concrete (*7*). Low equipment costs and the small amount of time required to set up, conduct, and analyze results from the impact-resonance method are additional reasons to use this method as a standard.

In this study three modes of testing—longitudinal, transverse, and torsional—are performed on 10.2 cm (4 in.) by 20.3 cm (8 in.) cylindrical specimens. Test configurations, slightly modified from ASTM C 215, are illustrated in Figure 6. The impact was produced by a steel ball with a 0.64 cm (0.25 in.) diameter. A piezoelectric accelerometer with an operating frequency range of 100 to 10,000 Hz and a resonant frequency of 100,000 Hz is used, and the vibrational signal is sampled and processed by the Fast Fourier Transform (FFT) to determine the resonant frequency of the material under a specific testing mode. Elastic modulus is determined from both the longitudinal and transverse testing, and shear modulus is determined from the torsional testing. Detailed information on the impact resonance testing and analysis methods can be found elsewhere (*7*).

A set of specimens (H1, H2, and H3) are fabricated from the same mixture used in the uniaxial controlled-stress testing. Repetitive haversine tensile loads with an amplitude of 3114 newtons (700 lb) are applied to induce damage growth within the specimens. The tensile load consists of a 0.1-sec loading period followed by a 0.4-sec rest period. In order to determine whether the increase in moduli of the damaged specimens after exposure to heat was caused by healing or some type of aging phenomenon, the number of loading cycles is varied among the specimens. No tensile loads are applied to Specimen H1. Specimens H2 and H3 are subjected to 4,000 and 6,000 cycles of loading, respectively. The maximum axial strain resulting from the application of the tensile loadings is 0.57 percent for H2 and 0.59 percent for H3. After application of repetitive loads, the ends of the specimens are cut off with a circular stone saw in order to remove steel attachments and to conduct the impact-resonance tests.

Because a stone saw requires the application of water in the cutting process, the specimens are towel dried and permitted to air

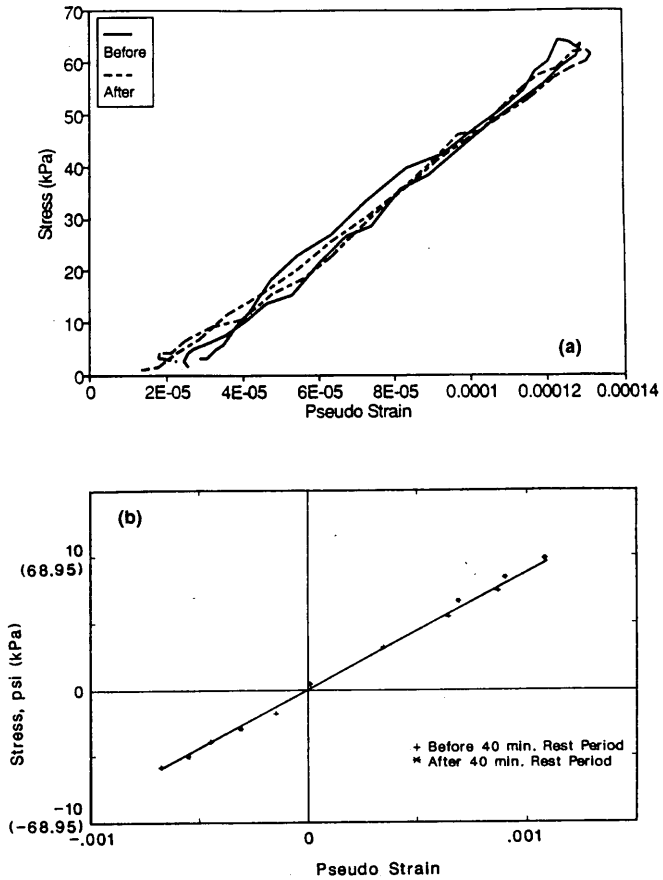

FIGURE 4 Application of CP to the data in Figure 3: (*a*) controlled-stress test; (*b*) controlled-strain test.

dry (laying on their long side) at 21°C (70°F) for 1 hr. Afterwards, the length and mass of the three H-specimens are measured. Then the longitudinal and torsional resonant frequencies are obtained at 21°C (70°F) by the impact-resonance method. The preheat experimental tests are completed within 3 hr after application of the tensile loads. Specimens then are conditioned to a temperature of 49°C (120°F) for 3 hr and permitted to cool, until post-heat frequencies are obtained at 21°C (70°F). Results are compared first to determine whether any change in moduli could be detected and, second, to evaluate whether specimens with more damage yield greater magnitudes of moduli increase after exposure to heat. Poisson's ratios are calculated to determine the accuracy of the experiment.

Experimental results obtained for the elastic and shear moduli along with Poisson's ratios are presented in Table 1. Because elastic and shear moduli were obtained independently, reasonable Poisson's ratios, obtained from the elastic and shear moduli confirmed the accuracy of the experimental test results. Healing ratios, defined as the ratio between the moduli obtained before and after exposure to heat, were calculated and are presented in Figure 7 for three specimens with varying levels of damage.

A comparison of the test results yielded the following conclusions:

1. There was a detectable increase in moduli for all three specimens after exposure to the high temperature.

2. The increase in moduli after 3 hr of exposure to 49°C (120°F) was different for each specimen. The specimen with more damage yielded a greater healing ratio, possibly indicating the presence of a reversible process at the microcracks.

Test results demonstrate that the impact-resonance test is able to determine varying magnitudes of structural regain of asphaltic mixtures after rest periods at higher temperatures.

FIELD EVALUATION OF HEALING VIA WAVE PROPAGATION TESTS

On May 20, 1993, wave propagation tests were initiated on the closed outer lane section of US 70 East outside Clayton, North Carolina. The pavement was about a year old with a 14-cm (5.5-in.) thick asphalt layer and 28-cm (11-in.) thick aggregate base course. Thermocouples were installed in the asphalt layer that allowed for temperature at various depths.

The test section was closed around 7:30 a.m. on May 20th and reopened to traffic at 8 a.m. the next day, constituting a 24-hr rest period. The wave propagation test was conducted immediately after closing the road and repeated hourly until the same time the next morning. Temperatures at different depths of the asphalt layer were measured at the time of wave propagation testing. The primary

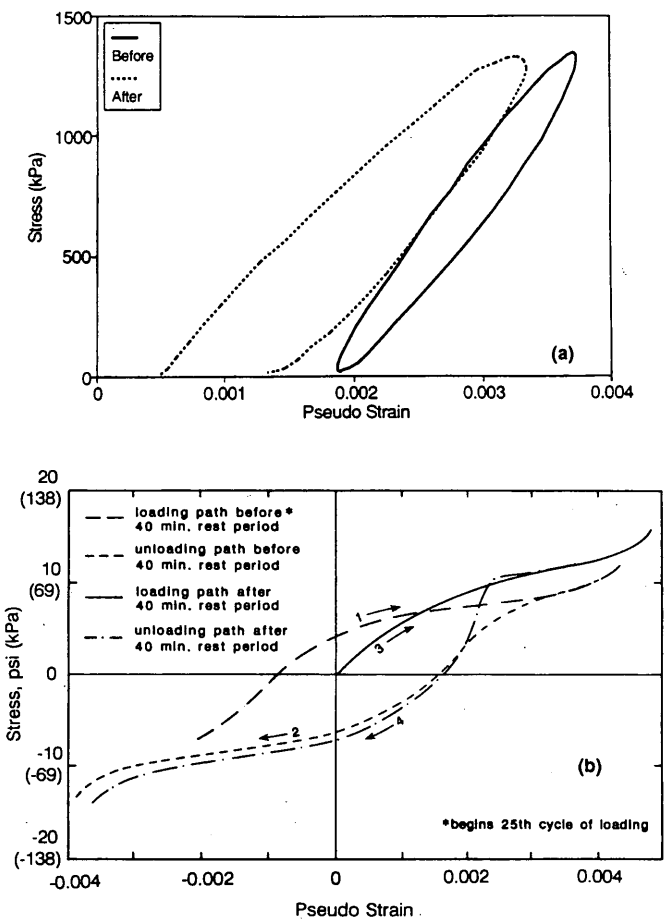

FIGURE 5 Stress-pseudo strain behavior before and after rest periods with significant damage: (*a*) controlled-stress test; (*b*) controlled-strain test.

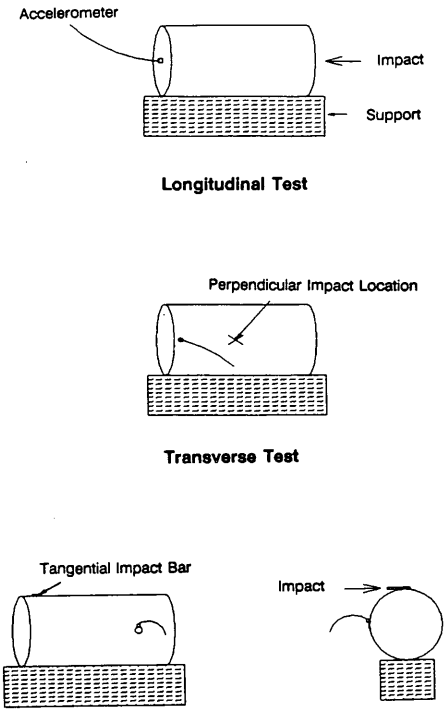

FIGURE 6 Three methods of the impact-resonance test (ASTM C 215).

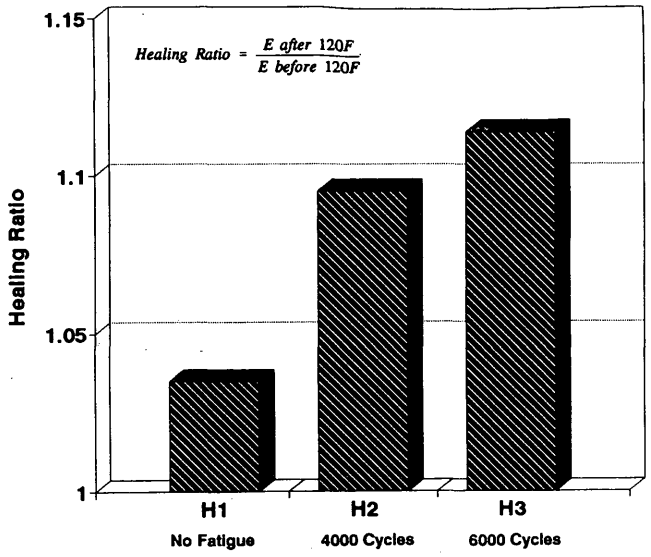

FIGURE 7 Effect of damage level on the healing ratio determined by the impact-resonance tests.

objective of the tests: to determine the change in the elastic modulus of asphalt layer as a function of temperature during a 24-hr cycle.

Stress Wave Theory

In an unbounded isotropic solid, only two types of waves (longitudinal and shear) can propagate. In an homogeneous, isotropic, linear elastic, solid half-space with a bounded surface (like the surface of a road), however, an elastic surface wave may also occur (as Lord J.W.S. Rayleigh determined in 1887). Surface waves are slightly slower than shear waves but contain vastly more energy. According to Douglas et al. (*8*), surface waves are nondispersive in the HILES half-space. However, when the half-space is a layered medium, surface waves are dispersive in nature; again, the surface wave will travel slightly slower than the shear wave, whose wavespeed is around 60 percent that of a longitudinal wave.

Given that all three of the wavespeeds are interrelated, determining one of them allows for the determination of the other two, given Poisson's ratio. In effect, the elastic modulus can be derived from the measurement of any one of the three waves by obtaining the longitudinal wavespeed from any measured wavespeed, squaring the longitudinal wavespeed, and multiplying the squared wavespeed by the density of the material through which the wave propagated.

Test Setup

Three PCB (Piezotronics, Inc.) 303A02 accelerometers were used along with a 482A05 series line power supply. The data were obtained via a Rapid Systems 4-Channel R1016 data-acquisition system attached to a 486 megabytes personal computer. At the field test section, 540 hexhead nuts were epoxied to the pavement at

TABLE 1 Impact Resonance Test Results for Evaluation of Healing Potentials as Function of Damage Level

		H1 (0 cycles)			H2 (4000 cycles)			H3 (6000 cycles)		
	Test	E[a]	G[a]	ν[b]	E	G	ν	E	G	ν
Preheating	1	19.7	7.52	0.31	18.8	7.24	0.30	19.3	7.45	0.30
	2	19.7	7.52	0.31	18.8	7.38	0.27	19.3	7.45	0.30
	3	19.7	7.52	0.31	19.0	7.45	0.28	19.3	7.45	0.30
Postheating	1	20.4	7.86	0.30	20.6	8.07	0.25	21.5	8.34	0.29
	2	20.4	7.79	0.31	20.6	8.14	0.27	21.5	8.34	0.29
	3	20.4	7.79	0.31	20.6	8.14	0.27	21.5	8.34	0.29

[a]Units are in 10^3 MPa (1 MPa = 6.89 ksi).
[b]Poisson's ratio calculated from the relationship between the elastic and shear moduli.

various locations between 7.6 cm (3 in.) and 61.0 cm (24 in.) away from the designated impact location (see Figure 8). The line of nuts extended parallel to and 1.2 m (4 ft) offset from the edge of pavement, which was the area with the most vehicular-wheel passes.

Field Testing

The initial test plan was to evaluate pavement using various accelerometer locations, in order to obtain the best possible resolution for determining the wavespeed. In order to accomplish the task, there had to be as much distance between accelerometers as possible and data had to be obtained at the highest allowable acquisition rate. On the basis of a series of experiments, we found that the most consistent data could be obtained with accelerometers placed at 7.6 cm (3 in.), 30.5 cm (12 in.), and 45.7 cm (18 in.) away from the impact. The energy of the impact dissipated so rapidly that an accelerometer 61.0 cm (24 in.) away was unable to obtain good data at test temperatures.

The experiments in this study were conducted using a 0.3 Kg (0.7 lb) steel claw hammer with a wooden handle, striking a 1.3-cm (0.5-in.) thick, 6.4-cm (2.5-in.) wide, 2.5-cm (1-in.) tall aluminum impact bar that was sitting on the surface of the road without any medium in between it and the road surface. As the temperature increased during the day, the amount of obtainable signal decreased.

Data Analysis and Results

Each signal data set was adjusted to a zero baseline, and amplitude was normalized by the maximum value. Every point in channel A (closest to the impact) was then multiplied by 100; in channel B (middle location) points were multiplied by 80, and in channel C (farthest from the impact) they were multiplied by 60. The rescaling of the amplitude allowed clearer analysis for the Short Kernel Method, which is described later. Figure 9 displays three data signals obtained from one of the tests.

FFT Analysis

The data signals were analyzed initially via an FFT to determine the frequency range that contained the largest amount of energy. Figure 10 presents the FFT amplitude versus frequency for all three data signals. The graph demonstrates that the resulting bulk of the energy of the signal resides in frequencies around 15,000–18,000 Hz. The FFT can also be used to determine wavespeeds via the phase change of a frequency between two data signals. This analysis is in fact a simple and straightforward technique, but it does have the serious drawback of not being able to accurately define the multiple wavespeeds of the dispersion field (*8*).

In an inverted, geologically layered system, such as asphalt concrete pavements, individual frequencies can travel at several different velocities if they penetrate into layers having different elastic properties. In this study the FFT was used to determine the dominant frequencies from the wave signals only.

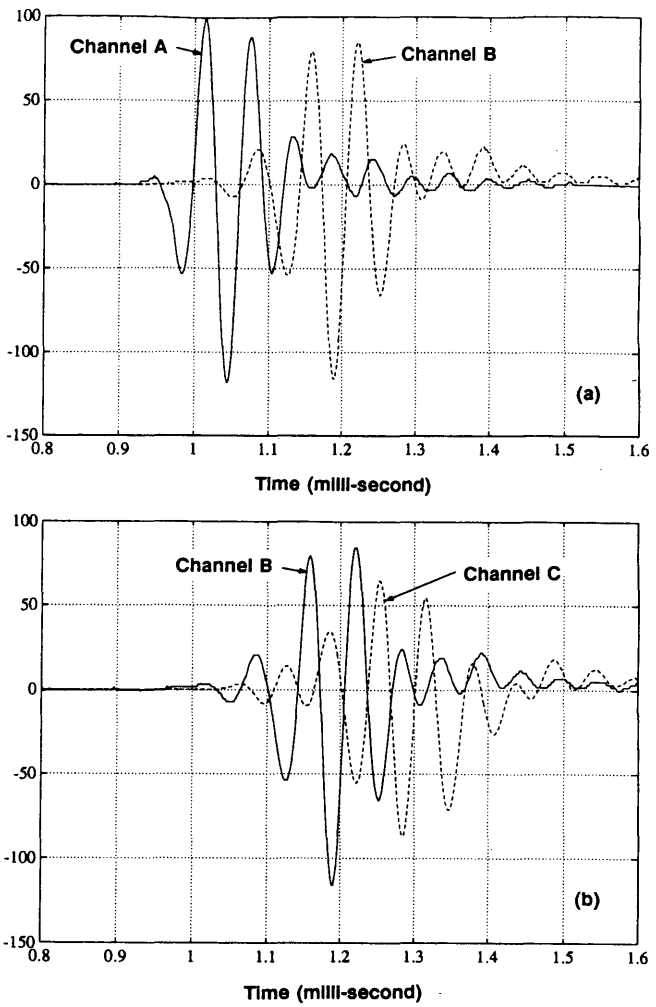

FIGURE 9 Stress wave signals from three accelerometers: (*a*) Channel A versus Channel B; (*b*) Channel B versus Channel C.

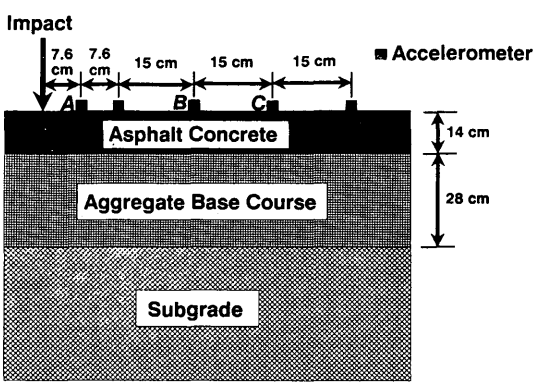

FIGURE 8 Various accelerometer locations tested in the initial testing.

Short Kernel Method

Signals are analyzed further using the Short Kernel Method (SKM) presented by Douglas et al. (*8*). The SKM is a frequency-dependent scanning operation that is based on the cross-correlation procedure. The SKM method amplifies a given frequency within the time domain of a signal to determine the time it took the wave to travel between the two gage points. Holt et al. (*9*) recently developed a

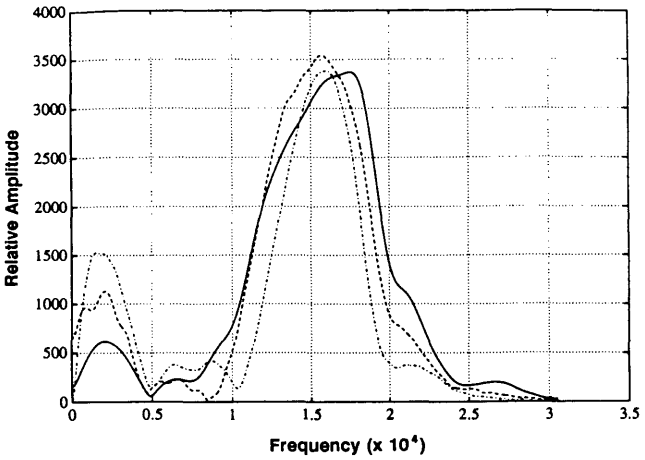

FIGURE 10 Fast Fourier Transform amplitude versus frequency for all three signals.

method of determining embedments of installed timber piles that applies SKM in analyzing bending-wave signals generated by striking a pile on its side transversely to its longitudinal axis. Detailed information on the SKM is found elsewhere (*8,9*).

Because the data signal from channel A contained the largest amount of energy, a one-cycle kernel of the maximum frequency from channel A was used for the SKM analysis. The SKM results for the given data signals are shown in Figure 11. The time distance is measured between the corresponding peaks of the two transformed signals.

The wavespeed are obtained, and elastic moduli are calculated. The results are plotted with respect to their corresponding measured mid-depth temperatures in Figure 12. The density of the road is obtained by measuring the density of some field cores removed from the pavement. Poisson's ratios used in the calculation were obtained from the Poisson's ratio versus the temperature relationship, which was determined in the laboratory using the impact-resonance test method. Maximum surface and mid-depth temperatures during the test period were 43°C (110°F) and 39°C (102°F), respectively. Adequate data was difficult to obtain above 32°C (90°F) because of significant damping in the asphaltic layer that was also observed from laboratory vibrational testing (*7*).

As illustrated in Figure 12, the elastic modulus of the asphalt concrete layer decreased as the pavement temperature increased. Also, the elastic modulus after the 24-hr rest period was greater than it was before the rest period for the same mid-depth pavement temperature. The stress-wave testing method measures the stiffness of asphalt concrete in a glassy (purely elastic) region, because of the impact nature of loading, so the modulus change is not affected by time-dependent relaxation. Therefore, this increase in the elastic modulus could be a result of microcrack healing in the asphalt concrete layer.

Although the field data presented in this paper are somewhat limited, on the basis of experience with stress-wave testing at North Carolina State University, this technique has strong potential as a means of nondestructively determining the properties of asphaltic surface layers as a function of various factors, such as binder viscosity, aggregate gradation, air voids, temperature, type of modifiers. In addition, the simple and inexpensive nature of the stress-wave testing technique as well as the inability of deflection-

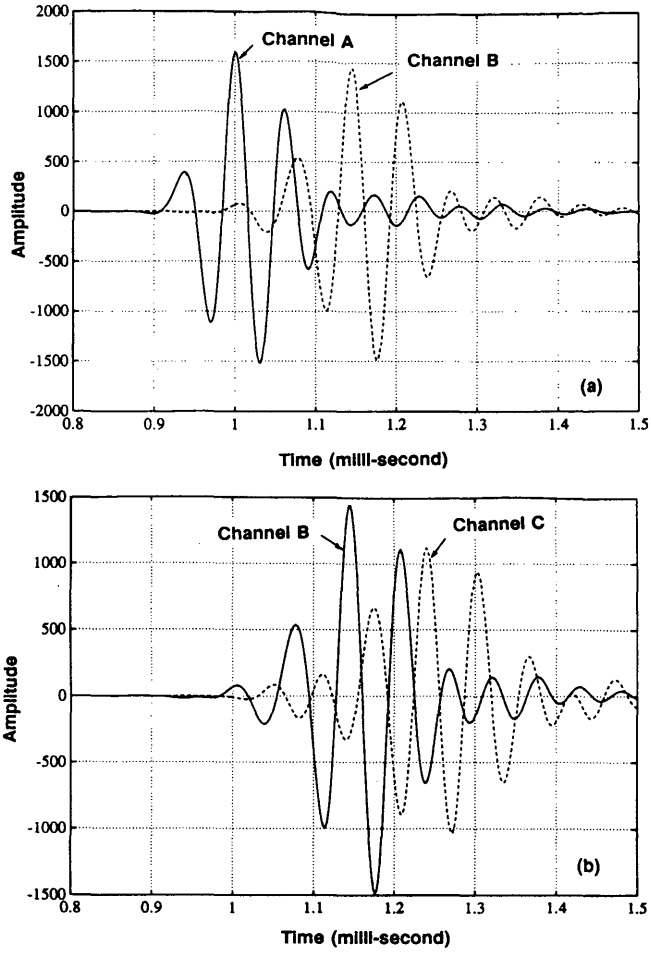

FIGURE 11 Short Kernal Method plot for all three signals: (*a*) Channel A versus Channel B; (*b*) Channel B versus Channel C.

based testing methods in determining the properties of thin surface layers make the stress-wave testing method more attractive.

CONCLUSIONS

Three different experimental approaches to evaluating microcrack healing of asphalt concrete during rest periods are presented in this paper: the elastic-viscoelastic correspondence principle to eliminate the effect of relaxation, the use of the impact-resonance testing methods in the laboratory, and the application of stress-wave testing to actual in-service pavements in order to determine change in elastic properties resulting from healing.

The nonlinear viscoelastic correspondence principle, applying the pseudo strain concept, was used successfully to eliminate time-dependence under various testing conditions, including control mode, loading type, wave form, loading rate, rest duration, and type of mixture. The principle proves to be an excellent method of modeling damage growth and healing in asphalt concrete under complex cyclic loading.

The impact-resonance method, a modified version of ASTM C 215, is also used successfully as a laboratory tool to evaluate modulus increase after rest periods at higher temperatures, that could result from microcrack healing of asphalt concrete. The

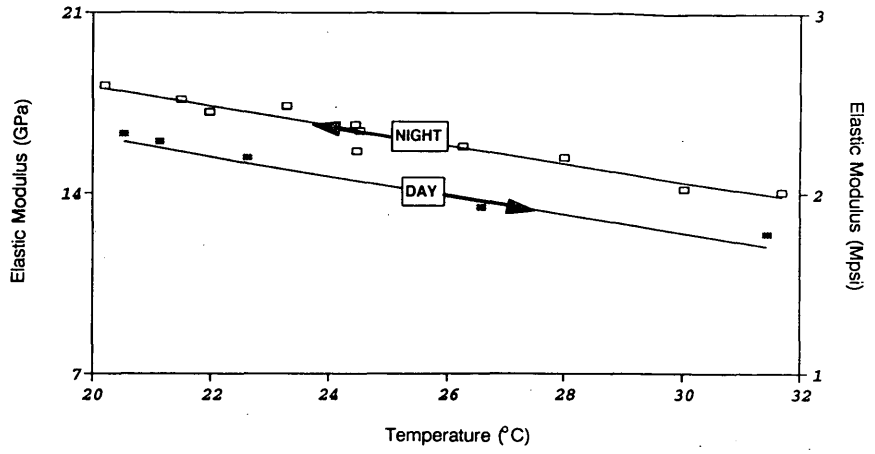

FIGURE 12 Elastic modulus versus pavement temperature from stress wave testing of a pavement in service.

testing method provides consistency of test results with simple and inexpensive equipment, making it an excellent and sensitive means for determining changes in material properties from damage growth or healing.

Stress-wave testing was performed hourly on an in situ pavement section for 24 hr. Elastic modulus of asphalt concrete decreased as pavement temperature increased. Also, an increase in elastic modulus was observed at a selected pavement temperature after a 24-hr rest period. This modulus increase is thought to result from microcrack healing in asphalt concrete pavements.

ACKNOWLEDGMENTS

Research projects sponsored by the following organizations provided the data presented in this paper: the National Science Foundation (controlled-strain data), the Air Force Office of Scientific Research (controlled-stress data), the North Carolina Department of Transportation (pavement temperature data), and the FHWA (wave field test results). The authors are grateful for these organizations' support.

REFERENCES

1. Finn, F., C. Saraf, K. Kulkarni, W. Smith, and A. Abdullah. The Use of Prediction Subsystems for the Design of Pavement Structures. *Proc., Fourth International Conference on Structural Design of Asphalt Pavements,* 1977.
2. Kim, Y. R. Evaluation of Healing and Constitutive Modeling of Asphalt Concrete by Means of the Theory of Nonlinear Viscoelasticity and Damage Mechanics. Ph.D. Dissertation, Texas A&M University, College Station, Tex., 1988.
3. Kim, Y. R., D. N. Little, and F. C. Benson. Chemical and Mechanical Evaluation on Healing Mechanism of Asphalt Concrete. *Proc., Association of Asphalt Paving Technologists,* Vol. 59, St. Paul, Minn., 1990.
4. Schapery, R. A. Correspondence principles and a generalized J-integral for large deformation and fracture analysis of viscoelastic media. *International Journal of Fracture,* 25, 1984.
5. Kim, Y. R. and D. N. Little. One-Dimensional Constitutive Modeling of Asphalt Concrete. ASCE *Journal of Engineering Mechanics,* Vol. 116, No. 4, April 1990.
6. Kim, Y. R., Y. Lee, and H. J. Lee. Application of Correspondence Principles to Testing of Asphalt Concrete. ASCE *Journal of Materials in Civil Engineering,* in preparation, 1994.
7. Whitmoyer, S. L. and Y. R. Kim. Determination of Elastic Properties of Asphalt Concrete Using Vibrational Analysis. ASTM *Journal of Testing and Evaluation,* Vol. 22, No. 2, March, 1994.
8. Douglas, R. A., J. L. Eddy, and H. E. Wahls. On Transforms and the Dispersion Computations Used for Evaluating Layer Properties. ASTM STP 1026. ASTM, Philadelphia, Pa., 1989.
9. Holt, J. D., S. Chen, and R. A. Douglas. Determining Lengths of Installed Timber Piles by Dispersive Wave Propagation. In *Transportation Research Record No. 1447,* TRB, National Research Council, Washington, D.C., 1994.

Publication of this paper sponsored by Committee on Characteristics of Bituminous Paving Mixtures To Meet Structural Requirements.

Temperature Considerations in Asphalt-Aggregate Mixture Analysis And Design

JOHN A. DEACON, JOHN S. COPLANTZ, AKHTARHUSEIN A. TAYEBALI, AND CARL L. MONISMITH

The objective was to develop and demonstrate techniques for incorporating the effects of in situ temperature in the mixture-design process without adding significantly to the complexity of testing and analysis. The recommended approach converts the expected traffic, expressed in terms of equivalent single axle loads (ESALs) according to conventional AASHTO practice, into its equivalent value at critical pavement temperature. For both fatigue and permanent deformation, acceptable mixtures are those that resist equivalent laboratory loading in cyclic tests conducted at the critical temperature. Critical temperatures, the points at which most damage occurs in situ, were developed for nine climatic regions throughout the United States using the FHWA's Integrated Climatic Model for determining in situ temperatures. For 20-cm (8-in.) pavements, more than 40 percent of the fatigue damage and more than 64 percent of the permanent-deformation damage occurred within a 5°C (9°F) range centered on the critical temperature. Temperature equivalency factors, used to convert ESALs at one temperature to their equivalent at the critical temperature, were found to depend on mode of distress, the pavement structure, and the asphalt mixture—but to be independent of climate. When multiple temperature laboratory testing is required, for example, when reliability must be unusually high, suitable temperature ranges are 15°C to 30°C (59°F to 86°F) for fatigue testing and 30°C to 45°C (86°F to 113°F) for permanent-deformation testing.

Objectives of the recently completed Strategic Highway Research Program (SHRP) Project A-003A included developing a series of accelerated performance-related tests for asphalt-aggregate mixtures, and systems for analyzing the effects of mixture properties on pavement performance. The hierarchical structure of the analytical process requires a minimum amount of testing and analysis for most routine mixture designs but permits, at the same time, a much more comprehensive approach for specialized requirements, including the evaluation of new types of mixtures and mixture designs for major paving projects. Regardless of the level of detail, however, the analysis seeks to assure, within a level of reliability selected by and suitable to the designer, that the mixture will perform satisfactorily in service. Mixture properties, traffic, temperature, and the pavement structure are among the factors considered in all analyses, regardless of the degree of sophistication.

Distress mechanisms considered in the evaluation process include fatigue cracking, permanent deformation or rutting, and thermal cracking. For both fatigue cracking and permanent deformation, the destructive effects of highway traffic are expressed in terms of equivalent single axle loads (ESALs). Load equivalency factors have proven to be indispensable for expressing the relative destructive effects of a wide variety of over-the-road axle loadings and for determining the number of repetitions of a standard, 80-kN (18,000-lb), single-axle load that is equivalent to the traffic volume anticipated in service (*1*).

Extending the equivalency concept into the temperature domain offers considerable promise for conveniently and accurately treating the complexity of the in situ temperature environment during mixture evaluation. Factors are needed to convert the design ESAL to its equivalent at a single temperature. Use of a single temperature significantly reduces the testing and analysis effort in evaluating mixture performance. Even routine mixture designs can accurately reflect the thermal environment anticipated in situ. Thus the temperature equivalency approach can simplify testing and analysis and thereby increase productivity, reduce costs, and improve predictive accuracy.

A process that has been included in the SHRP A-003A mixture analysis and design system for treating temperature conditions is described, as are the various factors necessary to implement that process.

APPROACH

As originally conceived, the investigation concentrated on the development of a set of temperature-equivalency factors, patterned after the AASHTO load-equivalency procedure, that could be used to easily account for traffic level and environmental temperatures in mixture fatigue and permanent-deformation analyses. The temperature equivalency factor is a multiplicative factor used to convert the number of load applications at one temperature, *i*, to an equivalent number of load applications at a standard reference temperature, *s*. Thus,

$$\sum \text{TEF}_i \times \text{ESAL}_i = \text{equivalent ESAL}_s \quad (1)$$

where TEF_i is the temperature equivalency factor for the *i*th temperature interval, and ESAL_i is the design ESALs accumulating during the *i*th temperature interval.

The temperature equivalency concept theoretically requires independence of the effects of both multiple temperature levels and the order in which they occur. Because such independence has not yet been validated, the temperature equivalency factors developed here only represent first-order approximations.

As illustrated by the following equation, the computation of temperature equivalency factors requires simulations of pavement life at different temperatures:

J.A. Deacon, University of Kentucky, 202B Transportation Research Building, Kentucky Transportation Center, Lexington, Ky. 40506–0043. J. Coplantz, Bowman and Williams, P.O. Box 1621, Santa Cruz, Calif., 95061. A. Tayebali, Institute of Transportation Studies, University of California at Berkeley, Richmond Field Station, Building 480, Richmond Calif. 94804. C.L. Monismith, Department of Civil Engineering/ITS, University of California at Berkeley, Room 115 McLaughlin Hall, Berkeley, Calif. 94720.

$$TEF_i = N_s/N_i \quad (2)$$

where N_s is the number of load repetitions to failure at the standard reference temperature, and N_i is the number of load repetitions to failure at the ith temperature. "Failure" is defined as initiation of cracking and a permanent surface deformation of 12.7 mm (0.5 in.) for fatigue and permanent deformation, respectively. Pavement life is modeled using multilayer elastic analysis (ELSYM) to estimate the stress and strain states within hypothetical pavement structures. For fatigue, the maximum principle tensile strain, (ϵ), at the bottom of the asphalt layer is converted to a pavement-life estimate using an $N-\epsilon$ relationship calibrated from laboratory controlled-strain fatigue tests. For permanent deformation, layered-strain procedures are used together with repeated-load triaxial compression test results to estimate the effect of load repetitions on permanent surface deformation. The simulated traffic load in each case was the standard AASHTO 80-kN (18,000-lb), single-axle load.

Temperature equivalency factors must be computed for a specific geographic location (that is, temperature environment) and a specific pavement structure. There are two primary tasks: the first is to estimate temperature profiles throughout the pavement structure; the second is to correlate pavement life (number of repetitions to failure) with the pavement temperature profile. FHWA's Integrated Climatic Model (2) was used to compute temperature profiles (depth increments of 5 cm, or 2 in.) for each of 4,380 hr in a typical year. Elimination of one-half the 8,760 hr in each year significantly reduced the computational effort without sacrificing accuracy. The temperature profile for each of the 4,380 hr was then characterized by two quantities, the temperature at the critical pavement location and a temperature gradient. For fatigue, the critical location was considered to be the bottom of the asphalt layer. For permanent deformation, the critical location, which is to be near the pavement surface, was selected somewhat arbitrarily to be a depth of 5 cm (2 in). In each case, the temperature gradient in °C per inch was defined as

$$(T_B - T_{2''})/D \quad (3)$$

in which T_B is the temperature at the bottom of the asphalt layer, $T_{2''}$ is the temperature at a 5-cm (2-in.) depth, and D is the thickness of the asphalt layer less 5 cm (2 in.).

The pavement-life computations sought to relate pavement life to temperature and temperature gradient. Approximately 10 temperature categories and 10 temperature-gradient categories were analyzed—approximately 100 combinations. For each of these combinations, the average temperature profile for those of the appropriate 4,380 hr was analyzed. All pavements were composed of two layers, an upper asphalt layer, and a uniform foundation that supported it. To properly account for temperature effects, the asphalt layer was further subdivided into four sublayers of varying temperatures and, hence, varying stiffnesses. For fatigue, the output variable of interest from the multilayer elastic simulations was the maximum principle tensile strain at the bottom of the asphalt layer. For permanent deformation, the deviator stress was computed at 1 in. deep increments throughout the asphalt layer. To ensure that the critical condition was examined, computations included locations at the center of the dual tire set, at the center of one tire of the dual set, and at an outer edge of one of the tires.

The estimation of pavement life in fatigue applied a laboratory-calibrated equation of the following type:

$$N_f = 10^{(K1+K2 \cdot T)} \cdot \epsilon^{(K3+K4 \cdot T)} \quad (4)$$

where

N_f = number of repetitions to initiate fatigue cracking under controlled-strain loading
ϵ = maximum principle tensile strain,
T = temperature, and
Ks = experimentally determined constants.

The estimation of pavement life in permanent deformation is slightly more involved. Using layered-strain procedures, permanent surface deformation is estimated as follows:

$$\sum \epsilon_p \cdot (\text{thickness}) \quad (5)$$

where

ϵ_p = vertical permanent strain in a layer increment,
thickness = thickness of the increment, and,
$\sum$ = summation over all the increments within the asphalt layer.

For all computations reported here, 1-in. thickness increments were used. The permanent strain was in turn calculated from a laboratory-calibrated expression of the following type:

$$\epsilon_p = C1 \cdot N_p^{C2} \cdot \sigma_d^{C3} \cdot T^{C4} \quad (6)$$

where

ϵ_p = permanent strain,
N_p = number of load repetitions,
σ_d = deviator stress,
T = temperature, and
Cs = experimentally determined constants.

Because failure is associated with a permanent surface deformation of 12.7 mm (0.5 in.), a trial-and-error process was necessary to determine the appropriate permanent-deformation life.

The objective of the computations is to develop generalized relationships between pavement life and both temperature and temperature gradient, so that a life corresponding to each of the 4,380 simulated hours could be estimated. For both fatigue and permanent deformation, the approximately 100 sets of calculations provided a suitable data base for calibrating regression equations in the following form:

$$Ln(N) = A_1 + A_2 \cdot T + A_3 \cdot G + A_4 \cdot T^2 + A_5 \cdot G^2 + A_6 \cdot T \cdot G \quad (7)$$

where

N = number of load repetitions to failure either for fatigue or permanent deformation,
T = temperature at the critical pavement location (bottom of asphalt layer for fatigue and at a 5-cm (2-in.) depth for permanent deformation),
G = temperature gradient as defined in Equation 3, and
As = regression estimates.

Finally, after determining appropriate temperature categories for which temperature equivalency factors were desired, pavement lives were estimated for each of the 4,380 hr using Equation 7. The 4,380 hr were grouped according to the preselected temperature

categories, average pavement lives were computed for each category, and temperature equivalency factors were computed by entering these average lives into Equation 2.

This process was repeated for nine climatic regions spanning the continental United States, for two pavement structures in the fatigue investigation: a "thin" 10-cm (4-in.) structure and a thicker 20-cm (8-in.) structure and also for one 20-cm (8-in. pavement structure in the permanent-deformation investigation. In the latter analysis the 20-cm (8-in.) thickness was considered sufficient to confine most of the rutting to the asphalt layer. A dual-tire load of 40 kN (9,000 lb) with a contact pressure of 585.7 kPa (85 psi) and a 30.5-cm (12-in.) center-to-center tire spacing was used throughout the study.

PAVEMENT TEMPERATURES

The approach taken herein required the simulation of pavement temperature profiles through the 10-cm and 20-cm (4-in. and 8-in.) asphalt surfaces every other hour throughout a typical year. FHWA's Integrated Model of the Climatic Effects on Pavements (2) was well suited to this task.

The FHWA model's computer program can simulate pavement temperatures for any time period up to 1 year. Necessary data for nine climatic regions are built into the program's data base so that, for many purposes, climatological data need not be independently collected and inputted. Unfortunately, output for a specific run is limited to one particular hour of each day. This required 12 runs to analyze a specific site and pavement-structure combination and, at 15 to 20 min per run on 486-based computers with processor speeds of 25 to 33 MHz, the time to complete the temperature simulations for each situation was about 4 hr.

Pavement profiles were produced for both 10-cm and 20-cm (4-in. and 8-in.) surfaces in each of the nine climatic regions. Default characteristics for both material properties and climatic conditions were used throughout. Minimum daily air temperature was assumed to occur at 6 a.m. and maximum daily air temperature at 3 p.m. For the simulations, a time step of 0.125 hr was used, and the node spacing (vertically) was 5 cm (2 in.) in the top 50 cm (20 in.) and 15 cm (6 in.) in the next 320 cm (126 in). Constant deep ground temperatures for the nine regions are shown in Table 1.

The ASCII output files from the temperature simulations served as the input to a series of simple BASIC-language programs that were used for data manipulations and summaries. Tables 2–4, illustrative of the kinds of possible summaries, show the frequency distributions of temperatures at critical locations within the pavement as a function of climatic region.

TEMPERATURE EFFECTS ON PAVEMENT LIFE

For the computations to be tractable, the models must relate pavement life to both temperature and temperature gradient. To develop such models, a number of "standard" temperature profiles, defined by temperature level and by temperature gradient, were developed. For the 10-cm (4-in.) pavement, 110 profiles were identified consisting of all possible combinations of 11 levels of temperature—ranging from −5°C to 45°C (23°F to 95°F) in 5°C (9°F) increments—and 10 levels of gradient—ranging from −1.8°C to 0.9°C/in. in 0.3°C/in. increments. For the 20-cm (8-in.) pavement, 72 profiles were identified consisting of all possible combinations of nine levels of temperature—ranging from −5°C to 35°C (23°F to 95°F) in 5°C (9°F) increments—and eight levels of gradient—ranging from −1.5°C to 0.6°C/in. in 0.3°C/in. increments. For each category of temperature and temperature gradient, the temperature profile to be analyzed was determined by averaging over the applicable 4,380 hr of data and the nine climatic regions. Multilayered elastic analysis was used to estimate the stress and strain conditions within the pavement structure under the 40-kN (9,000-lb) dual-tire load.

Fatigue

A series of laboratory, controlled-strain, flexural-fatigue tests was performed to provide data to support the development of temperature equivalency factors for fatigue. Testing was limited to a single mixture, selected to be representative of a normal paving mixture in the United States. The asphalt cement had a penetration index of approximately 1.0. The aggregate was a dense-graded, partially crushed Greywacke with a 1-in. maximum size. The asphalt content was 5.2 percent by weight of aggregate, and the air-voids content was targeted at 4 ± 1 percent. A total of 23 specimens was tested at four temperature levels ranging from 5°C to 25°C (41°F to 77°F). Test specimens, with dimensions of 6.4 cm by 5 cm by 38 cm (2.5

TABLE 1 Constant Deep Ground Temperatures

Region	Temperature (°C)
IA (Boston, MA, and Chicago, IL)	10.0
IB (Little Rock, AR, and Washington, D.C.)	15.6
IC (Atlanta, GA, and San Francisco, CA)	21.1
IIA (Fargo, ND, and Lincoln, NE)	10.0
IIB (Oklahoma City, OK)	18.3
IIC (Dallas, TX)	21.1
IIIA (Billings, MT, and Reno, NV)	7.2
IIIB (Las Vegas, NV, and San Angelo, TX)	18.3
IIIC (San Antonio, TX)	21.1

°F = (°C × 1.8) + 32

TABLE 2 Frequency Distribution of Temperatures at Bottom of 10-cm (4-in.) Pavement (Percent)

Mid-Range Temp. (°C)	Region								
	IA	IB	IC	IIA	IIB	IIC	IIIA	IIIB	IIIC
-12.5				1.19					
-10.0				3.56					
-7.5				5.18			0.04		
-5.0				6.55	0.02		1.30		
-2.5	7.62			7.24	0.55		4.54		
0.0	17.81	1.80		13.10	6.53		17.12		
2.5	2.88	4.50	0.36	2.81	3.45	0.68	5.73	0.84	
5.0	3.90	5.09	3.93	2.90	4.09	2.28	5.09	2.42	0.34
7.5	4.29	6.30	6.16	3.06	4.79	3.81	4.86	3.61	2.24
10.0	4.63	7.12	7.67	3.63	5.78	4.68	4.91	4.57	3.81
12.5	5.18	6.67	9.52	4.02	5.98	5.96	5.39	5.75	5.23
15.0	5.75	6.39	10.39	4.57	6.19	7.10	6.32	6.75	6.74
17.5	6.87	6.76	11.39	5.73	6.37	7.15	7.99	7.08	7.97
20.0	9.04	7.26	11.85	7.62	6.71	7.21	7.15	7.12	8.63
22.5	7.05	9.95	9.34	5.80	8.67	8.17	6.05	7.81	9.43
25.0	5.94	7.56	6.92	5.20	8.45	10.94	4.43	10.62	11.85
27.5	5.20	7.19	6.03	4.70	7.49	8.26	5.00	8.04	9.66
30.0	4.61	5.50	4.79	3.70	4.84	7.74	3.65	7.81	7.74
32.5	3.77	5.07	4.93	3.52	5.68	6.16	3.95	5.34	6.64
35.0	3.42	3.86	4.27	3.22	4.16	5.36	2.92	5.96	6.53
37.5	2.01	4.25	2.44	2.69	3.56	4.38	3.15	4.47	3.95
40.0		3.81			3.84	4.09	0.39	4.00	5.25
42.5		0.91			2.85	3.40		4.16	3.49
45.0						2.60		3.10	0.50
47.5								0.55	

$$°F = (°C \times 1.8) + 32$$

in. by 2.0 in. by 15 in.), were sawed from slabs prepared by rolling-wheel compaction. Initial flexural stiffness was measured at the fiftieth load cycle, and fatigue life was defined to be the number of repetitions to a 50 percent reduction in flexural stiffness. A work by Tayebali et al. (*3*) provides a detailed description of the test program and its results.

Initial flexural stiffness, serving to characterize the modulus of elasticity in the multilayered elastic analysis, was found to be acutely sensitive to temperature but independent of strain level. The regression equation quantifying the effect of temperature on stiffness is as follows:

$$S_o(mPa) = 1.491 \cdot 10^4 \cdot e^{-0.09385\,T}$$

$$S_o(psi) = 2.1621 \cdot 10^6 \cdot e^{-0.09385\,T} \qquad (R^2 = 0.92) \tag{8}$$

where

S_o = initial flexural stiffness after 50 load cycles at 10Hz,
e = base of the natural logarithms, and
T = temperature in °C.

As expected in controlled-strain testing, fatigue life decreased with increasing stiffness (decreasing temperature) and with in-

TABLE 3 Frequency Distribution of Temperatures at Bottom of 20-cm (8-in.) Pavement (Percent)

Mid-Range Temp. (°C)	Region								
	IA	IB	IC	IIA	IIB	IIC	IIIA	IIIB	IIIC
-10.0				3.01					
-7.5				8.08					
-5.0				6.76			0.11		
-2.5	2.08			5.02	0.07		1.32		
0.0	20.80	0.18		9.43	1.23		11.92		
2.5	3.38	2.94		2.90	3.33		7.40		
5.0	3.95	7.15	1.05	3.49	6.55	0.87	7.10	0.84	
7.5	4.63	8.40	6.39	4.15	7.76	3.65	6.76	3.54	0.41
10.0	5.41	6.98	10.98	4.41	6.78	6.87	6.44	6.37	3.56
12.5	5.80	6.58	10.00	4.86	6.30	7.19	6.46	7.40	6.96
15.0	6.19	6.32	9.52	5.23	6.07	6.99	6.78	6.92	8.58
17.5	6.83	6.48	9.68	5.68	6.12	6.96	7.15	6.87	8.20
20.0	7.65	7.05	11.39	6.60	6.60	7.24	8.86	6.87	8.38
22.5	10.80	8.04	15.50	9.38	7.53	7.69	10.41	7.42	8.81
25.0	9.43	10.52	10.80	8.04	9.13	8.84	7.42	8.29	10.30
27.5	7.15	11.07	9.11	6.60	12.08	12.03	6.32	10.43	14.29
30.0	5.64	8.70	5.57	5.36	8.33	11.55	5.18	12.62	12.44
32.5	0.27	6.53		0.98	7.33	9.36	0.36	8.97	8.97
35.0		3.04			4.54	6.74		8.06	7.74
37.5					0.23	4.02		5.25	1.35
40.0								0.14	

$$°F = (°C \times 1.8) + 32$$

creased tensile strain. The slope of the strain-life relationship was found to be highly temperature sensitive. The regression equation quantifying the effects of temperature and strain on fatigue life is as follows:

$$N_f = 10^{(20.0341 - 0.2261\,T)} \cdot \epsilon^{(-5.9138 + 0.1056\,T)} \qquad (R^2 = 0.94) \qquad (9)$$

where

N_f = number of cycles to a 50 percent reduction in flexural stiffness (that is, the fatigue life),
ϵ = maximum principal tensile strain in units of 10^{-6} mm/mm (in./in.), and
T = temperature in °C.

The two hypothetical pavement structures that we analyzed are described in Table 5. The asphalt surface was treated as four layers. Its modulus of elasticity of each layer was determined using Equation 8, based on its midpoint temperature. Fatigue life was calculated using Equation 9.

The computations are used to develop models relating fatigue life to both temperature and temperature gradient in the asphalt layer. Resulting models, containing only statistically significant terms, are summarized.

For the 8-in. pavement and all temperatures ($R^2 = 0.999$)

$$Ln(N_f) = 22.7019 - 0.55674\,T + 1.0481\,G + 0.0088228\,T^2 - 0.024482\,T\,G \qquad (10)$$

where

N_f = cycles to failure in fatigue,
T = temperature (T_B) at bottom of asphalt-bound layer in °C, and
G = temperature gradient in °C/in. [$(T_B - T_{2"})$/depth increment].

TABLE 4 Frequency Distribution of Temperatures at 5-cm (2-in.) Depth in 20-cm (8-in.) Pavement (Percent)

Mid-Range Temp. (°C)	Region								
	IA	IB	IC	IIA	IIB	IIC	IIIA	IIIB	IIIC
-12.5				2.24					
-10.0				3.58					
-7.5				5.68	0.02		0.04		
-5.0	1.96			6.46	0.04		1.10		
-2.5	4.47			4.95	0.11		3.31		
0.0	12.44	1.07		7.78	2.56		10.18		
2.5	5.39	4.63	0.20	3.95	4.45	0.43	7.21	0.55	
5.0	5.20	5.39	3.26	3.86	5.02	2.15	6.39	2.21	0.25
7.5	5.11	6.21	5.94	4.11	5.66	3.49	6.12	3.47	1.78
10.0	5.23	6.94	7.88	4.25	6.37	5.04	6.23	4.73	3.68
12.5	5.34	6.42	9.11	4.45	6.21	5.80	6.23	5.50	5.23
15.0	5.73	6.37	9.93	4.91	6.03	6.78	6.57	6.58	6.46
17.5	6.46	6.42	10.27	5.52	6.05	6.89	7.90	6.85	7.74
20.0	8.47	6.87	12.83	7.17	6.51	7.03	7.99	6.89	8.29
22.5	8.61	8.10	9.47	7.19	7.40	7.51	6.05	7.21	8.74
25.0	6.39	9.93	7.81	5.59	9.68	9.29	6.19	8.74	11.14
27.5	5.71	7.15	6.28	5.00	7.42	10.75	4.54	10.71	11.14
30.0	3.33	6.53	5.02	3.54	6.23	7.51	4.00	7.24	9.02
32.5	4.54	4.54	4.95	3.90	5.48	6.89	3.20	6.76	7.62
35.0	3.63	5.09	5.20	3.20	3.77	5.27	3.56	5.84	4.45
37.5	1.96	3.10	1.83	2.65	4.50	4.61	3.17	3.93	5.91
40.0		4.92			3.17	4.18		4.98	3.31
42.5		0.94			3.31	4.32		3.31	4.66
45.0						2.03		3.93	0.57
47.5								0.57	

$$°F = (°C \times 1.8) + 32$$

For the 10-cm (4-in.) pavement and temperatures at a depth of 10 cm (4 in.) less than 25°C (77°F) ($R^2 = 0.999$)

$$Ln(N_f) = 18.4110 - 0.39772\,T + 0.45151\,G + 0.0081376\,T^2 - 0.013477\,T\,G \quad (11)$$

For the 10-cm (4-in.) pavement and temperatures at a depth of 10 cm (4 in.) of 25°C (77°F) or more ($R^2 = 0.999$)

$$Ln(N_f) = 16.1578 - 0.21948\,T + 0.28405\,G + 0.0044294\,T^2 - 0.0064224\,T\,G \quad (12)$$

As indicated by the very large R^2s, all the calibrations were highly significant in the statistical sense. Figures 1 and 2 illustrate the relationship between regression estimates and fatigue-life estimates from the calculations described.

Permanent Deformation

The SHRP A-003A approach to calculating permanent deformation in pavement structures uses a finite-element analysis that incorporates nonlinear viscoelastic surface properties and requires a suite of laboratory tests, including constant-height simple shear, uniaxial

TABLE 5 Hypothetical Pavement Structures

Layer	Property	"Thin" Structure	"Thick" Structure
Asphalt Surface	Thickness	10 cm (4 in.)	20 cm (8 in.)
	Number of Layers	4	4
	Modulus of Elasticity	Varies with temperature and temperature gradient	Varies with temperature and temperature gradient
	Poisson's Ratio	0.35	0.35
Subgrade	Modulus of Elasticity	172.3 MPa (25,000 psi)	68.9 MPa(10,000 psi)
	Poisson's Ratio	0.40	0.40

strain, volumetric, and shear frequency sweeps. In lieu of this approach, which had neither been well tested nor sufficiently refined at the time of our investigation, a conventional layered-strain analysis was used to aid development of pavement life versus temperature and temperature gradient models.

Again, the necessary models were calibrated using a mixture that was considered typical of paving mixtures in the United States. Table 6 summarizes mixture properties that were selected as characteristic of typical mixtures. The dynamic modulus-temperature relationship was taken from work reported by Akhter and Witczak (*4*). After adjustment using the mixture properties of Table 6, this relationship is as follows:

$$E = 100{,}000 \cdot 10^{(1.691635 - 0.00815T - 0.0000618\,T^2)} \quad (13)$$

where E is the dynamic modulus of the asphalt mixture in psi and T is the temperature in degrees Fahrenheit.

Work by Leahy (*5*) provided the basis for relating permanent strain to number of load repetitions, temperature, and deviator stress. For the mixture properties of Table 6, this relationship is as follows:

$$\log \epsilon_p = -12.3469 + 0.408 \log N_p + 6.865 \log T + 1.107 \log \sigma_d \quad (14)$$

where

ϵ_p = permanent strain in in./in.,
N_p = number of load cycles,
T = temperature in °F, and
σ_d = deviator stress in psi (or 90 psi, whichever is greatest).

The basis for this relationship was repeated-load triaxial testing of 251 specimens, including two aggregate types and two asphalt types. Unfortunately, Leahy's testing was limited to temperatures of 35°C (95°F)) and below. Thus considerable extrapolation was required to reach some of the temperatures at which rutting occurs in hotter climates.

All analysis was limited to one pavement structure having an asphalt surface of sufficient thickness to minimize the likelihood of significant rutting within subsurface layers. The specific section that was evaluated is defined in Table 7. The asphalt surface was treated as four layers, and the modulus of elasticity of each layer was determined using Equation 13 on the basis of its midthickness temperature. Pavement life, the number of repetitions resulting in a permanent deformation at the surface of 1.3 cm (0.5 in.), was calculated using the layered-strain approach of Equation 5 combined with the permanent strain relationship of Equation 14. In this trial-and-error process, eight 2.5-cm (1-in.) layers were used to represent the 20-cm (8-in.) surface course and the midthickness deviator

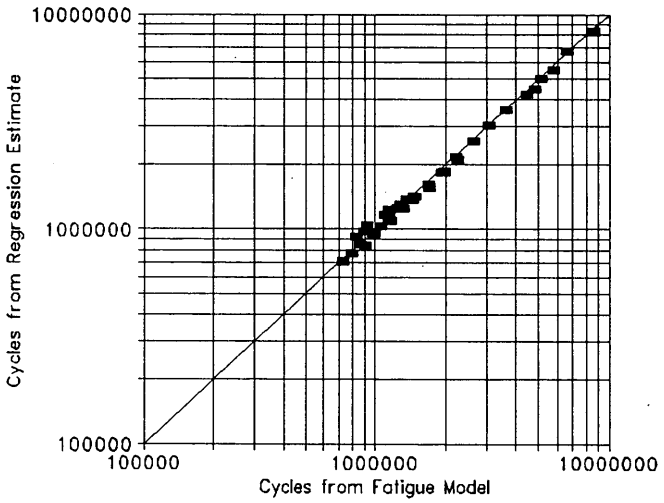

FIGURE 1 Accuracy of fatigue model for 20-cm (8-in) pavement.

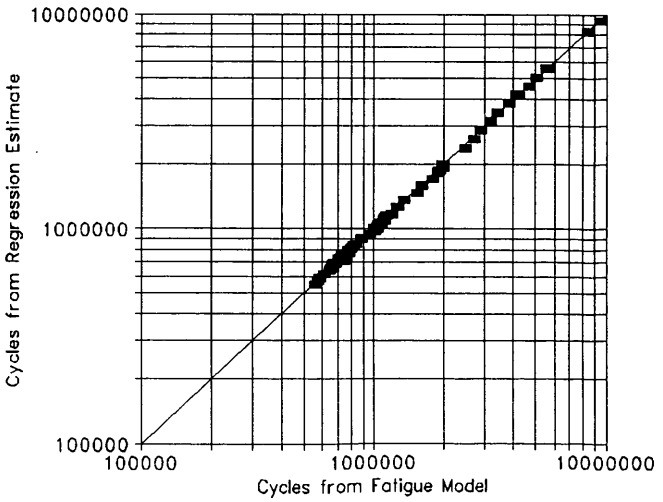

FIGURE 2 Accuracy of fatigue model for 10-cm (4-in.) pavement.

TABLE 6 Mixture Properties for Permanent-Deformation Investigation

Property	Value
f - frequency, Hz	10
Vis - viscosity @ 70°F, × 10^6 poise	1.5
Peff - percent effective asphalt by volume	12
Pair - percent air by volume	4
Pabs - percent of asphalt absorbed by weight of aggregate	0.5
PP200 - percent passing #200 sieve	5
PR4 - percent retained on #4 sieve	50
PR3/8 - percent retained on 3/8" sieve	30
PR3/4 - percent retained on 3/4" sieve	5

TABLE 7 Simulation Parameters

Layer	Property	Value
Asphalt Surface	Thickness	20 cm (8 in.)
	Number of Layers	4
	Modulus of Elasticity	Varies with temperature and temperature gradient
	Poisson's Ratio	0.35
Subgrade	Modulus of Elasticity	138 MPa (20,000 psi)
	Poisson's Ratio	0.40

stresses were calculated both directly and, as necessary, by interpolation.

The purpose of these computations was to develop models relating permanent-deformation life to both temperature and temperature gradient in the asphalt layer. The resulting models, containing only statistically significant terms, are summarized.

For temperatures at a depth of 5 cm (2 in.) less than 25°C (77°F) ($R^2 = 0.993$)

$$Ln(N_{0.5"}) = 28.0936 - 0.82261\,T - 5.0689\,G + 0.0099138\,T^2 + 0.10840\,T\,G \quad (15)$$

where

$N_{0.5"}$ = cycles to 0.5-in. permanent deformation,
T = temperature ($T_{2"}$) in °C at a 2-in. depth, and
G = temperature gradient in °C in. $[(T_{8"}-T_{2"})/6]$.

For temperatures at a depth of 2 inches of 25°C or more ($R^2 = 0.994$)

$$Ln(N_{0.5"}) = 26.6040 - 0.64020\,T - 4.2074\,G + 0.0046575\,T^2 + 0.069677\,T\,G \quad (16)$$

As indicated by the very large R^2s, all of the calibrations were highly significant in the statistical sense just as they were for the fatigue calibrations. Figure 3 illustrates the relationship between the regression estimate and the permanent-deformation–life estimates from the calculations described.

TEMPERATURE FACTORS

The primary attribute of the temperature equivalency approach is that both testing and the bulk of the routine analyses are limited to a single temperature. Mixture analysis and design are thus rather simple, given the proper choice of the testing temperature and the availability of applicable temperature equivalency factors. Atypical mixtures, however, particularly those with atypical temperature

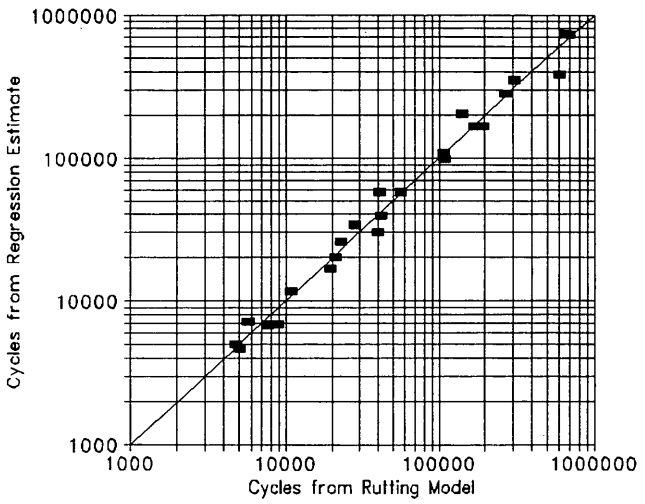

FIGURE 3 Accuracy of permanent-deformation model.

sensitivities, require a more complex routine and testing at multiple temperatures. Multiple-temperature testing also may be desired for large paving projects to increase the accuracy of evaluations.

Testing at a Single Temperature

Some of the factors to be considered by each mixture design agency in selecting the standard reference temperature for single-temperature testing include the following:

- Testing time will be minimized if the test temperature promotes early failure during laboratory testing,
- Accuracy will be maximized if the test temperature is near that to which in situ pavements are most vulnerable to damage,
- Efficiency will be maximized if a single test temperature can be used regardless of structural design and regardless of where the paving project is located within the design agency's jurisdiction, and
- Testing will be easier and less expensive if the test temperature affords comfortable working conditions and can be accurately controlled.

The ideal testing temperature would be one that could be used by any design agency without regard to distress mechanism, specific pavement structure, or project location. Available testing temperatures include, among others, effective temperature, critical temperature, and maximum temperature. Effective temperature is defined as that temperature at which loading damage accumulates at the same average rate in service as in the laboratory. Thus, when testing at the effective temperature, there is a one-to-one correspondence between laboratory and in-service loading cycles. The critical temperature is defined as that temperature at which the largest amount of damage occurs in service. For purposes of this investigation, the critical temperature was defined more specifically to be that temperature integer at the midpoint of a 5°C (9°F) temperature range, within which the largest amount of damage accumulates. Tables 8–10 summarize the effective, critical, and maximum temperatures for nine climatic regions within the continental United States. The tables indicate sizable differences between fatigue and permanent-deformation distress and much smaller but perhaps significant effects of climatic region and pavement structure (for fatigue only).

Critical temperature—or a standard temperature near critical temperature—is considered the optimal temperature for laboratory testing because it minimizes error associated with variations in mixture temperature sensitivity and because of its accelerated rate of damage accumulation. Remaining calculations focus on critical temperature but also include standard temperatures of 20°C (68°F) for fatigue and 35°C (95°F) for permanent deformation.

Temperature Equivalency Factors

Temperature equivalency factors, computed using Equation 2, are summarized in Tables 11–13. The reference temperature for fatigue is 20°C (68°F) (Tables 11 and 12) and, for permanent deformation, 35°C (95°F) (Table 13). Detailed examination of these tables reveals

- Temperature equivalency factors (TEFs) are a function of the type of distress. Regarding fatigue, maximum TEF occurs at an intermediate temperature level, whereas the TEFs increase monotonically with increases in temperature with respect to permanent deformation.
- Concerning fatigue, temperature equivalency factors are a function of the pavement structure. TEFs for thicker pavements are more sensitive to temperature than those for thinner pavements.
- Temperature equivalency factors are relatively independent of climate, especially regarding fatigue.

The apparently inconsequential effect of climate on temperature equivalency factors is of great interest, and potentially has considerable practical significance.

TABLE 8 Key Temperatures at 10-cm (4-in.) Depth for Fatigue Analysis, 10-cm (4-in.) Pavement

Region	Temperature in °C		
	Effective	Critical	Maximum
IA	15.2	22	37.7
IB	17.1	25	41.8
IC	17.9	21	37.6
IIA	14.1	27	38.6
IIB	17.0	26	43.7
IIC	18.9	28	45.6
IIIA	15.0	25	39.1
IIIB	18.6	27	46.5
IIIC	20.2	27	44.2
Mean	17.1	25.3	41.6

$°F = (°C \times 1.8) + 32$

TABLE 9 Key Temperatures at 20-cm (8-in.) Depth for Fatigue Analysis, 20-cm (8-in.) Pavement

Region	Temperature in °C		
	Effective	Critical	Maximum
IA	19.6	25	31.3
IB	21.8	28	34.9
IC	20.6	26	30.9
IIA	19.2	27	31.9
IIB	22.0	28	36.3
IIC	23.2	30	38.1
IIIA	19.3	27	31.4
IIIB	23.3	30	38.8
IIIC	23.7	29	37.0
Mean	21.4	27.8	34.5

°F = (°C × 1.8) + 32

TABLE 10 Key Temperatures at 5-cm (2-in.) Depth for Permanent-Deformation Analysis

Region	Temperature in °C		
	Effective	Critical	Maximum
IA	27.7	35	37.6
IB	33.0	40	41.8
IC	29.3	35	37.5
IIA	28.3	36	38.4
IIB	34.2	42	43.7
IIC	36.0	43	45.7
IIIA	30.1	36	38.6
IIIB	37.2	44	46.6
IIIC	35.1	42	44.3
Mean	32.3	39.2	41.6

°F = (°C × 1.8) + 32

Temperature Conversion Factors

Equation 1, using temperature equivalency factors such as those in Tables 11–13, is used to convert the design ESALs to their equivalent at the standard reference temperature. Before the computation can be performed, however, the designer must estimate the number (or proportion) of the design ESALs that accumulate during each temperature interval. In the absence of detailed frequency distribution data, it appears reasonable to assume that damaging truck traffic is distributed uniformly over time. Thus, in the context of mixture evaluation, this suggests that a daytime hour is reasonably similar to a nighttime hour in terms of truck traffic, that a wintertime hour is reasonably similar to a summertime hour, and so forth.

The assumption that truck traffic is uniformly distributed through time permits the computation of a temperature conversion factor as follows:

$$TCF = \sum f_i \times TEF_i \quad (17)$$

where

TCF = temperature conversion factor,
f_i = frequency associated with the ith temperature interval, and
TEF_i = temperature equivalency factor for the ith temperature interval.

TABLE 11 Temperature Equivalency Factors in Fatigue for 10-cm (4-in.) Pavement; Referenced to 20°C (68°F) at 10-cm (4-in.) Depth

Mid-Range Temp. (°C)	Region								
	IA	IB	IC	IIA	IIB	IIC	IIIA	IIIB	IIIC
-12.5				2.4e-05					
-10.0				7.2e-05					
-7.5				2.9e-04			4.9e-04		
-5.0				1.1e-03	1.2e-03		1.3e-03		
-2.5	3.4e-03			3.5e-03	4.6e-03		3.7e-03		
0.0	0.011	0.014		0.011	0.012		0.012		
2.5	0.029	0.027	0.039	0.029	0.026	0.034	0.028	0.033	
5.0	0.068	0.063	0.067	0.067	0.063	0.063	0.065	0.061	0.077
7.5	0.140	0.137	0.141	0.139	0.133	0.136	0.133	0.134	0.135
10.0	0.258	0.259	0.261	0.258	0.255	0.250	0.248	0.245	0.251
12.5	0.425	0.429	0.437	0.430	0.424	0.423	0.413	0.423	0.413
15.0	0.636	0.636	0.649	0.635	0.636	0.638	0.618	0.636	0.629
17.5	0.848	0.846	0.860	0.848	0.844	0.845	0.816	0.844	0.846
20.0	1.000	1.000	1.000	1.000	1.000	1.000	1.000	1.000	1.000
22.5	1.071	1.056	1.106	1.066	1.051	1.060	1.062	1.057	1.058
25.0	1.246	1.296	1.378	1.221	1.283	1.324	1.376	1.330	1.270
27.5	1.731	1.708	1.814	1.712	1.697	1.668	1.731	1.660	1.683
30.0	1.566	1.544	1.580	1.593	1.541	1.560	1.570	1.546	1.550
32.5	1.398	1.383	1.424	1.385	1.376	1.328	1.411	1.326	1.347
35.0	1.106	1.120	1.138	1.124	1.084	1.116	1.103	1.119	1.101
37.5	0.927	0.869	0.952	0.882	0.862	0.854	0.894	0.832	0.852
40.0		0.627			0.624	0.613	0.723	0.612	0.621
42.5		0.495			0.429	0.439		0.419	0.413
45.0						0.298		0.271	0.329
47.5								0.213	

$$°F = (°C \times 1.8) + 32$$

Computation of the equivalent ESALs at the standard reference temperature then requires only a single multiplication, as follows:

$$\text{equivalent ESAL}_s = TCF \times \text{design ESAL} \quad (18)$$

where equivalent ESAL_s is the equivalent number of ESALs at the standard reference temperature, s, and design ESAL is the design traffic loading.

Temperature conversion factors for the pavements evaluated herein are summarized in Tables 14–16. For comparative purposes, reference temperatures include both the critical temperature for each condition as well as standard temperatures of 20°C (68°F) for fatigue and 35°C (95°F) for permanent deformation. The percentage of damage that occurs within a range of 5°C (9°F) centered on the reference temperature is illustrated in Tables 14–16. A large percentage is desirable because it minimizes potential error associated with atypical mixture temperature sensitivities.

Examination of Tables 14–16 reveals that temperature conversion factors are affected by mode of distress, pavement structure (at least for fatigue), and climatic region. A mixture effect, although also ex-

TABLE 12 Temperature Equivalency Factors in Fatigue for 20-cm (8-in.) Pavement; Referenced to 20°C (68°F) at 20-cm (8-in.) Depth

Mid-Range Temp. (°C)	Region								
	IA	IB	IC	IIA	IIB	IIC	IIIA	IIIB	IIIC
-10.0				8.7e-07					
-7.5				3.4e-06					
-5.0				1.7e-05			2.9e-05		
-2.5	1.3e-04			9.0e-05	1.5e-04		1.4e-04		
0.0	3.4e-04	5.6e-04		3.4e-04	4.4e-04		4.0e-04		
2.5	1.6e-03	2.3e-03		1.6e-03	1.9e-03		1.6e-03		
5.0	5.7e-03	5.8e-03	9.7e-03	5.5e-03	5.6e-03	9.3e-03	5.4e-03	9.2e-03	
7.5	0.018	0.017	0.019	0.017	0.017	0.018	0.017	0.018	0.030
10.0	0.049	0.049	0.050	0.048	0.047	0.050	0.046	0.050	0.052
12.5	0.123	0.124	0.123	0.122	0.122	0.125	0.119	0.123	0.128
15.0	0.275	0.278	0.277	0.273	0.277	0.279	0.266	0.277	0.278
17.5	0.557	0.555	0.556	0.554	0.552	0.561	0.549	0.561	0.557
20.0	1.000	1.000	1.000	1.000	1.000	1.000	1.000	1.000	1.000
22.5	1.628	1.616	1.576	1.648	1.605	1.614	1.528	1.604	1.595
25.0	2.169	2.330	2.224	2.193	2.321	2.301	2.232	2.298	2.293
27.5	2.885	2.843	2.764	2.823	2.914	2.966	2.886	2.951	2.921
30.0	3.220	3.221	3.234	3.319	3.284	3.258	3.288	3.288	3.185
32.5	3.359	3.356		3.232	3.292	3.271	3.623	3.334	3.344
35.0		3.137			3.033	3.028		2.964	2.988
37.5					2.718	2.510		2.404	2.628
40.0								2.059	

$$°F = (°C \times 1.8) + 32$$

pected to be significant, was not among the variables investigated. Approximately 64 to 77 percent of the permanent-deformation damage occurs within a 5°C (9°F) interval centered on the critical temperature. The critical temperature is thus an effective temperature for permanent-deformation testing. For fatigue, approximately 26 to 46 percent of the damage occurs within a similar 5°C (9°F) interval. Choice of the test temperature thus seems to be somewhat less critical for fatigue than for permanent deformation.

Mode of distress, pavement structure, and climatic effects on the temperature conversion factor are similar for both the critical temperature and a standard reference temperature of 20°C (68°F) for fatigue, and 35°C (95°F) for permanent deformation. By definition, however, more damage is concentrated nearer the critical temperature than any other alternative. As a starting point for establishing testing norms on a nationwide basis, the average critical temperatures listed in Tables 8–10; that is, approximately 25°C (77°F) for fatigue and 40°C (104°F) for permanent deformation could be used. Other testing-temperature norms, reflecting more accurately the local climate, would likely be more appropriate than national norms for use by local and state design agencies.

Testing at Multiple Temperatures

Testing and analyzing mixtures at multiple temperatures are necessary when evaluating mixtures of atypical temperature sensitivity for which standard temperature equivalency and conversion factors are not applicable. It is also desirable for important paving projects, those designs demanding the utmost accuracy. The objective of such testing is to recalibrate Equations 8 and 9 for fatigue investi-

TABLE 13 Temperature Equivalency Factors in Permanent Deformation; Referenced to 35°C (95°F) at 5 cm (2-in.) Depth

Mid-Range Temp. (°C)	Region								
	IA	IB	IC	IIA	IIB	IIC	IIIA	IIIB	IIIC
-12.5				3.0e-11					
-10.0				1.2e-10					
-7.5				1.0e-10	1.3e-07		5.7e-09		
-5.0	4.8e-08			2.3e-10	4.4e-08		4.2e-08		
-2.5	6.5e-08			1.5e-09	5.0e-08		1.1e-07		
0.0	8.4e-08	6.3e-07		1.8e-08	3.1e-07		2.2e-07		
2.5	1.5e-07	2.6e-06	1.5e-05	1.3e-07	9.8e-07	1.3e-05	4.8e-07	1.5e-05	
5.0	3.1e-07	5.3e-06	3.3e-05	3.2e-07	2.1e-06	2.0e-05	1.2e-06	2.3e-05	9.4e-05
7.5	7.0e-07	9.9e-06	1.0e-04	7.3e-07	2.5e-06	6.5e-05	5.0e-06	7.2e-05	1.8e-04
10.0	1.5e-06	1.8e-05	1.2e-04	2.4e-06	1.6e-05	7.2e-05	2.1e-05	7.9e-05	3.5e-04
12.5	1.3e-05	7.4e-05	2.5e-04	7.5e-05	5.7e-05	1.7e-04	8.5e-05	1.9e-04	6.6e-04
15.0	4.4e-04	3.1e-04	5.6e-04	2.7e-04	2.6e-04	2.8e-04	3.3e-04	2.4e-04	1.2e-03
17.5	1.6e-03	1.1e-03	2.4e-03	1.1e-03	1.0e-03	1.1e-03	1.7e-03	7.9e-04	1.7e-03
20.0	7.0e-03	4.3e-03	9.1e-03	5.2e-03	3.9e-03	3.8e-03	4.9e-03	3.1e-03	4.8e-03
22.5	0.021	0.017	0.021	0.018	0.015	0.013	0.013	0.011	0.017
25.0	0.042	0.049	0.041	0.038	0.053	0.045	0.035	0.036	0.061
27.5	0.102	0.108	0.091	0.095	0.122	0.144	0.080	0.136	0.164
30.0	0.179	0.239	0.177	0.181	0.270	0.245	0.165	0.228	0.344
32.5	0.475	0.434	0.402	0.443	0.566	0.527	0.494	0.510	0.630
35.0	1.000	1.000	1.000	1.000	1.000	1.000	1.000	1.000	1.000
37.5	2.364	2.012	2.007	2.324	2.561	1.912	2.956	1.702	2.464
40.0		4.419			4.967	3.714		4.015	4.559
42.5		7.197			11.391	8.585		7.597	9.876
45.0						17.069		16.594	15.991
47.5								24.673	

$$°F = (°C \times 1.8) + 32$$

gations and Equations 13 and 14 for permanent-deformation investigations. Following these recalibrations, temperature equivalency or conversion factors could be determined by procedures such as those we've employed here.

Testing temperatures should be carefully chosen so that they are compatible with the capabilities of laboratory test equipment and so that they span the range within which much of the damage occurs in situ. The calculations reported in Table 17 suggest that most damage occurs within a temperature range as small as 15°C (59°F). An even smaller range may eventually prove sufficient for permanent deformation. At the present, however, it appears that testing in the ranges of 15°C to 30°C (59°F to 86°F) for fatigue and 30°C to 45°C (86°F to 113°F) for permanent deformation is likely to be sufficient for most locations in the continental United States. In any case, lower-temperature testing is unproductive for both fatigue and permanent-deformation investigations, because very little fatigue and permanent-deformation damage occurs at such temperatures.

TABLE 14 Temperature Conversion Factors for Fatigue; 10-cm (4-in.) Pavement

Region	Reference Temperature: 20°C		Reference Temperature: Critical	
	Temperature Conversion Factor	Percent Damage Within 5°C Range	Temperature Conversion Factor	Percent Damage Within 5°C Range
IA	0.6587	25.1	0.6234	26.4
IB	0.8261	17.9	0.6332	28.9
IC	0.8748	24.9	0.8507	25.8
IIA	0.5720	24.2	0.3288	26.2
IIB	0.8083	17.0	0.4750	29.6
IIC	0.9407	15.6	0.5740	31.8
IIIA	0.6215	22.0	0.4528	25.7
IIIB	0.9258	15.4	0.5502	31.0
IIIC	1.0091	17.0	0.6065	33.0
Mean	0.8041	19.9	0.5661	28.7
Coefficient of Variation (%)	18.0	19.4	24.1	9.2

°F = (°C × 1.8) + 32

TABLE 15 Temperature Conversion Factors for Fatigue; 20-cm (8-in.) Pavement

Region	Reference Temperature: 20°C		Reference Temperature: Critical	
	Temperature Conversion Factor	Percent Damage Within 5°C Range	Temperature Conversion Factor	Percent Damage Within 5°C Range
IA	0.9147	18.5	0.4036	45.8
IB	1.4254	10.5	0.4788	43.6
IC	1.1457	23.8	0.4374	45.5
IIA	0.8531	16.7	0.2883	44.3
IIB	1.4817	9.5	0.4987	42.1
IIC	1.7928	8.3	0.5519	41.4
IIIA	0.8586	22.6	0.3180	42.5
IIIB	1.8268	7.9	0.5563	40.1
IIIC	1.9276	9.1	0.6135	42.6
Mean	1.3585	14.1	0.4607	43.1
Coefficient of Variation (%)	30.0	42.5	22.5	4.1

°F = (°C × 1.8) + 32

APPLICATION OF TEMPERATURE FACTORS IN MIXTURE ANALYSIS AND DESIGN

Temperature equivalency or conversion factors are applied in the SHRP A-003A mixture analysis and design process to convert in-service traffic loading (expressed in ESALs) to its equivalent at the preselected reference temperature. These equivalent traffic loading cycles are compared with mixture resistance as measured by laboratory repeated-load testing at the same reference temperature to determine the acceptability of specific mixtures. The SHRP A-003A system uses controlled-strain, flexural beam testing for fatigue. For basic-level, permanent-deformation analysis, a constant-height, simple-shear device operated in a repeated-load mode is used. The laboratory environment is calibrated to in situ

TABLE 16 Temperature Conversion Factors for Permanent Deformation; 20-cm (8-in.) Pavement

Region	Reference Temperature: 35°C		Reference Temperature: Critical	
	Temperature Conversion Factor	Percent Damage Within 5°C Range	Temperature Conversion Factor	Percent Damage Within 5°C Range
IA	0.1262	70.2	0.1262	70.2
IB	0.4800	20.6	0.0993	69.8
IC	0.1517	74.2	0.1517	74.2
IIA	0.1466	56.2	0.1006	76.6
IIB	0.7486	16.4	0.0707	67.8
IIC	1.4443	9.4	0.1224	64.2
IIIA	0.1817	47.4	0.1218	76.2
IIIB	1.1627	7.0	0.1337	68.5
IIIC	1.0486	13.4	0.1162	67.3
Mean	0.6100	35.0	0.1158	70.5
Coefficient of Variation (%)	78.6	72.8	18.9	5.7

$°F = (°C \times 1.8) + 32$

conditions by applying an empirically determined shift factor, and a suitable multiplier is applied to satisfy reliability requirements. The procedure has been fully documented elsewhere (*6,7*).

SUMMARY AND CONCLUSIONS

The primary objective was to demonstrate the efficacy of the temperature equivalency concept for use in mixture analysis and design. For both fatigue and permanent-deformation investigations, techniques have been developed by which traffic loading in situ can be expressed in terms of its equivalent at a single reference temperature. This provides a simple effective way to accurately account for both traffic and environmental effects in mixture analysis and design. Specific conclusions include the following:

- Single-temperature testing is sufficient for routine mixture analysis of mixtures with typical temperature sensitivity. Setting the testing temperature to correspond with the critical temperature (appropriate to the geographical location and structural section) assures optimum results.

TABLE 17 Extent of Damage Accumulation in Suggested Temperature Ranges

Region	Percent Damage Within Indicated Temperature Range		
	Fatigue [15° through 30°C (59° through 86°F)]		Permanent Deformation [30° through 45°C (86° through 113°F)]
	10 cm (4-in.) Pavement	20-cm (8-in.) Pavement	
IA	71.6	92.4	89.6
IB	66.9	71.7	95.4
IC	71.5	95.1	89.3
IIA	70.3	88.6	91.3
IIB	65.8	67.3	97.4
IIC	67.8	61.2	92.3
IIIA	67.8	92.0	94.4
IIIB	66.3	56.5	78.7
IIIC	68.8	64.1	96.3
Mean	68.5	76.5	91.6

- Temperature equivalency factors are a function of the type of distress, pavement structure, and, presumably, mixture characteristics. However, equivalency factors appear to be relatively independent of climate especially for fatigue.
- Temperature conversion factors provide a simple, convenient way to convert traffic loading to its equivalent at a fixed temperature level. As a result, direct comparisons can be made between traffic loading in situ and single-temperature repeated-load testing in the laboratory.
- Particularly for permanent deformation, testing and analysis at the critical temperature are effective in reducing the influence of climatic variations throughout the continental United States.
- Test temperatures of 25°C (77°F) for fatigue and 40°C (104°F) for permanent deformation appear to be promising levels for establishment of national norms. Fatigue testing at 20°C (68°F) is an acceptable alternative if available testing equipment is unsuitable for testing at 25°C (77°F). However, other temperatures are likely to permit more accurate analyses by local and state design agencies.
- When multiple-temperature testing is necessary, the range of test temperatures can be reasonably small. On average, within nine climatic regions spanning the continental United States, temperatures in the range of 15°C to 30°C (59°F to 86°F) accommodate about 68 percent of the fatigue damage in 10-cm (4-in.) pavements and 76 percent in 20-cm (8-in.) pavements. Permanent-deformation testing from 30°C to 45°C (86°F to 113°F) encompasses the range within which an average of about 92 percent of the rutting occurs. These findings are expected to depend on mixture type, and they may be refined based on future work with a greater variety of mixture types.

The temperature equivalency and conversion factors reported here are considered to be first-order approximations that, if applied with care, provide an effective way to account for traffic and climatic effects in mixture analysis and design. They form an integral part of the system that has been developed by SHRP Project A-003A.

The next important requirement is to replace the layered-strain analysis with a more accurate model of permanent deformation, coupled with a range of appropriate laboratory test data to support its application. A more suitable permanent-deformation model also would allow investigation of the independence of the effects of multiple temperature levels, as well as the order in which they occur, and spur refinement if needed. Another objective would be to incorporate the effects of climate on subgrade support and to identify the variety of mixtures for which standard temperature equivalency and conversion factors are applicable. Finally, an investigation of the temporal (hourly, daily, and seasonally) variation in traffic loading is necessary to validate the assumption that damaging traffic loads are uniformly distributed through time.

ACKNOWLEDGMENTS

Research reported here was conducted as part of Project A-003A of the Strategic Highway Research Program, "Performance Related Testing and Measuring of Asphalt-Aggregate Interactions and Mixtures." The project was conducted by the Institute of Transportation Studies of the University of California, Berkeley.

REFERENCES

1. *AASHTO Guide for Design of Pavement Structures*—1986. AASHTO, Washington, D.C., 1986.
2. Lytton, R. L., D. E. Pufahl, C. H. Michalak, H. S. Liang, and B. J. Dempsey. *An Integrated Model of the Climatic Effects on Pavements.* FHWA-RD-90-033. Texas Transportation Institute, College Station, Tex., 1990.
3. Tayebali, A. A., J. A. Deacon, J. S. Coplantz, F. N. Finn, and C. L. Monismith. *Fatigue Response of Asphalt-Aggregate Mixtures: Part II—Extended Test Program.* SHRP Project A-003A, Institute of Transportation Studies, University of California, Berkeley, 1993.
4. Akhter, G. F., and M. W. Witczak. Sensitivity of Flexible Pavement Performance to Bituminous Mix Properties. In *Transportation Research Record 1034,* TRB, National Research Council, Washington, D.C., 1985, pp. 70–79.
5. Leahy, R. B. *Permanent Deformation Characteristics of Asphalt Concrete.* Ph.D. dissertation, University of Maryland, College Park, 1989.
6. Deacon, J. A., A. A. Tayebali, J. S. Coplantz, F. N. Finn, and C. L. Monismith. *Fatigue Response of Asphalt-Aggregate Mixtures: Part III—Mixture Design and Analysis.* SHRP Project A-003A, Institute of Transportation Studies, University of California, Berkeley, 1993.
7. Sousa, J. B., et al. *Permanent Deformation Response of Asphalt-Aggregate Mixtures: Part III—Mixture Design and Analysis.* SHRP Project A-003A, Institute of Transportation Studies, University of California, Berkeley, 1993.

This paper represents the views of the authors only and does not necessarily reflect the views of the National Research Council, SHRP, or SHRP's sponsor. The results reported here are not necessarily in agreement with the results of other SHRP research activities. They are reported to stimulate review and discussion within the research community.

Publication of this paper sponsored by Committee on Characteristics of Bituminous Paving Mixtures To Meet Structural Requirements.

Effects of Laboratory Specimen Preparation on Aggregate-Asphalt Structure, Air-Void Content Measurement, and Repetitive Simple Shear Test Results

JOHN HARVEY, KIRSTEN ERIKSEN, JORGE SOUSA, AND CARL L. MONISMITH

Effects of laboratory compaction devices (rolling wheel, gyratory, and kneading) on asphalt aggregate structure is investigated using image analysis of plane sections cut from specimens. Also investigated are the effects of specimen surface condition (both as-compacted and cut and cored) on air-void structure, air-void content measurement, and repetitive simple shear test-constant height (RSST-CH) results. Image analysis indicates that gyratory compaction produces less aggregate orientation than rolling wheel compaction, and little or no orientation in aggregates that do not have a flaky shape. Image analysis also reveals that the outer periphery of as-compacted specimens has a different air-void and aggregate structure than that found in the specimen interior. Other results from air-void content measurements of gyratory and rolling wheel specimens at different stages of cutting and coring showed that there is little air-void content gradient in specimens that have been cored and cut from larger compacted masses. In addition, it was learned that RSST-CH results for as-compacted and cut and cored specimens cannot be compared because of problems with air-void content measurement and cut and uncut aggregates' different responses to shear stress at the specimen surface.

The main objective of asphalt-aggregate mix laboratory specimen preparation is to duplicate, as closely as possible, compacted mix in the field. Earlier research (*1,2*) indicates that gyratory, rolling wheel, and kneading compaction produce specimens with significantly different permanent deformation responses to repeated shear loading, which indicates that each compaction method causes a particular type of aggregate structure and binder-aggregate film. It also has been shown that fatigue behavior of a compacted mix is influenced by the mixing and compaction viscosities of the binder (*2*).

Air-void content is one of the most important variables affecting the permanent deformation and fatigue performance of a compacted mix (*1–3*). One of the properties desired in laboratory-prepared specimens is a homogenous air-void and aggregate structure. It is therefore important that air-void content be measurable in an accurate and repeatable manner.

The purpose of this study was to investigate the following aspects of laboratory specimen preparation:

1. Effects of laboratory compaction method and binder viscosity at compaction on aggregate orientation, air-void size, air-void shape, and air-void distribution within the specimen;
2. Extent to which compaction mold surfaces change the aggregate structure at the interface between specimen and mold;
3. Differences in measured air-void content between specimens with as-molded surfaces and specimens with all cut surfaces; and
4. Effects of using specimens with all cut surfaces, instead of specimens with as-molded surfaces, on repeated simple shear test-constant height (RSST-CH) and permanent deformation.

J. Harvey, J. Sousa, C. Monismith, Institute of Transportation Studies, University of California at Berkeley, 1301 S. 46th Street, Building 452, Richmond, Calif. 94804. K. Eriksen, Danish National Road Laboratory, Postbox 235, Elisagaardsvej 5, Roskilde, DK4000, Denmark.

MATERIALS AND SPECIMEN PREPARATION

Materials and methods of specimen preparation used for various experiments related to this study are listed below. The Strategic Highway Research Program (SHRP) code is indicated also, as applicable.

Binders:

- Boscan AC-30 (SHRP code AAK-1);
- California Valley AR-4000 (SHRP code AAG-1); and
- Rubberized asphalt or California Coastal asphalt (SHRP code AAD-1) and crumb rubber from vehicle tires.

Aggregates:

- Pleasanton gravel (SHRP code RH), semi-rounded, partially crushed;
- Watsonville granite (SHRP code RB), semi-angular, completely crushed;
- Maryland limestone (SHRP code RD), completely crushed, very flaky; and
- Texas chert (SHRP code RL), rounded, partly crushed.

Gradations:

- Low fines content gradation (2.5 percent fines), and
- Normal fines content gradation (5.5 percent fines), both within ASTM D 3515 specifications and Caltrans standard specifications.

Compaction Method:

- Texas gyratory, 5 degree angle of gyration, 17.5-cm (7-in.) diameter mold;

- University of California at Berkeley (UCB) rolling wheel; and
- California kneading, 10- and 18.75-cm (4- and 7.5-in.) diameter molds.

Mixing Viscosities:

- 1.7 (optimal) and 6 Poise (high) for conventional binders (virgin asphalt), and
- 177°C (350°F) (optimal) and 149°C (300°F) (high viscosity) mix temperatures for rubberized asphalt binder.

Compaction Viscosities:

- 1.7 (low), 6 (optimal), and 20 Poise (high) for conventional binders (virgin asphalt); and
- 149°C (300°F) (optimal) and 135°C (275°F) (high viscosity) compaction temperatures for rubberized asphalt binder.

EXAMINATION OF AGGREGATE AND AIR-VOID STRUCTURE

The investigation was performed by the Danish National Roads Laboratory (DNRL), using image analysis of plane sections of specimens prepared at UCB using gyratory and rolling wheel compaction. DNRL takes vertical and horizontal plane sections, impregnates them with epoxy, to fill all air voids, applies ultra-violet light to make the epoxy stand out from the asphalt-concrete, and then uses a computer image-scanning and analysis system to measure the percentage of the scanned section that is air voids. In addition to revealing air-void content, such images of the plane sections also allow qualitative examination of the degree of aggregate orientation within a specimen (*4*).

A set of 36 specimens was prepared at UCB and sent to DNRL as part of this project. Specimens were prepared following a balanced full-factorial design with no replicates, using Pleasanton gravel, Watsonville granite, and Maryland limestone aggregates; gyratory and rolling wheel compaction; three compaction temperatures (low, optimum, and high viscosities); and two air-void contents (approximately 4 and 8 percent). DNRL evaluated the extent of aggregate orientation, average air-void section size, and air-void structure homogeneity (*5*).

Aggregate Orientation

The following conclusions were drawn from the investigation regarding aggregate orientation:

- Pronounced orientation of the aggregate was found in mixes containing Maryland aggregate that had been compacted with a rolling wheel. Air voids were oriented and flattened for the Maryland limestone mixes under rolling wheel compaction.
- Less aggregate orientation was observed for the Pleasanton gravel and Watsonville granite mixes compacted with the rolling wheel than was observed for the Maryland limestone mixes.
- Among the mixes compacted using gyratory compaction, only the flaky Maryland limestone mixes showed signs of aggregate orientation. The Maryland limestone mixes compacted using the gyratory compactor showed less orientation than the same mixes compacted using the rolling wheel compactor.

DNRL's analysis confirms the hypothesis that a greater degree of aggregate orientation results from rolling wheel compaction, as compared with that produced by the Texas gyratory compactor. The minimal aggregate orientation observed in the very flaky and enlongated Maryland limestone mixes compacted using the gyratory compactor may have been caused as much by rodding when being placed in the mold, as by the gyratory action that followed. Reducing the angle of inclination used for gyration, as is done by some machines, may result in a compaction method closer to static compaction (although the specimen is spinning), considering that the side-to-side motion caused by the inclination angle is responsible for the shear forces imparted to the mix.

These findings support the hypothesis that Texas gyratory specimens' lower resistance to permanent deformation under repetitive shear loads (*1*) is at least partly related to the lack of a strong, oriented aggregate structure. It is not known how much the static leveling load placed on gyratory specimens after gyration affects aggregate-to-aggregate contact and, therefore, permanent shear deformation resistance.

The rolling wheel specimens' greater resistance is a result of aggregate orientation and interparticle contact caused by the forces induced by the rolling alone because, unlike gyratory and kneading methods, rolling wheel compaction does not include any static leveling load that might increase particle-to-particle contact by crushing aggregates together.

Aggregate orientation and aggregate-to-aggregate contact caused by kneading action are the primary reasons California kneading specimens have greater resistance (*1*), not the leveling load.

Air-Void Structure Homogeneity and Air-Void Section Size

DNRL evaluated the homogeneity of the aggregate structures both among as-compacted gyratory specimens and cut and cored rolling wheel specimens.

Homogeneity of air voids in vertical and horizontal directions was evaluated on the basis of image analysis and examination of the plane sections under ultraviolet light. Aggregate orientation and segregation phenomena, as well as the influence of mold walls on the aggregate structure, (as-compacted gyratory specimens only), were evaluated and described for each specimen.

Average air-void section size within specimens differed for the three aggregates, irrespective of their air-void content, compaction temperature, or method of compaction.

Aggregate	*Gyratory*	*Rolling Wheel*
Maryland	0.32–0.62 mm^2 (496–961 $\times 10^{-6}$ $in.^2$)	0.24–0.97 mm^2 (372–1504 $\times 10^{-6}$ $in.^2$)
Pleasanton	0.14–0.42(217–651)	0.11–0.38 (171–589)
Watsonville	0.08–0.23 (124–357)	0.04–0.25 (62–388)

The more flaky and difficult to compact Maryland limestone specimens had the largest air-voids. Larger air-void sizes also were found in most specimens with higher air-void contents and with increasing compaction temperatures. It is obvious that less compaction would result in larger air-voids as well as higher air-void contents, because the aggregates and binder are not subjected to much orientation and particle arrangement.

Greater homogeneity of air voids was found in specimens with higher air-void contents, indicating that applying compaction energy results in some portions of the specimen having more air voids than others. In the as-compacted gyratory specimens larger air-voids were found along the mold surface, both at the top and bottom, and at the sides. The effect was found to be greater at the top and bottom of the specimens than around the horizontal perimeter. The outer 10 mm to 20 mm (0.4 in. to 0.8 in.) were affected by the mold surface at the top and bottom of the specimens, and the outer 2 mm to 5 mm (0.1 in. to 0.2 in.) were affected around the circumference of the as-compacted gyratory specimens.

Further evidence of the effects of the mold wall on the aggregate at the circumference of a 15-cm (6-in.) diameter Texas gyratory specimen with as-compacted surfaces can be seen in Figure 1. The low air-void content specimen accidently was placed in axial tension while at 60°C (140°F), which separated it into two pieces. The aggregate at the periphery is crushed, and the interior of the specimen broke at the asphalt interface, indicating that an annulus of broken aggregate, or aggregate with no asphalt film between them, exists near the mold wall of at least some as-compacted gyratory specimens. The crushing or grinding together probably is caused by the specimens' inability to become oriented by the gyratory compactor's low shear stresses while under axial compressive stress.

The rolling wheel specimens, which were cored and cut from a larger compacted mass, did not show the effect of mold surfaces on air-void distribution.

Segregation occurs much more frequently in gyratory specimens than in rolling wheel specimens. The effect usually occurs in discrete areas and less frequently in specimens compacted at higher temperatures.

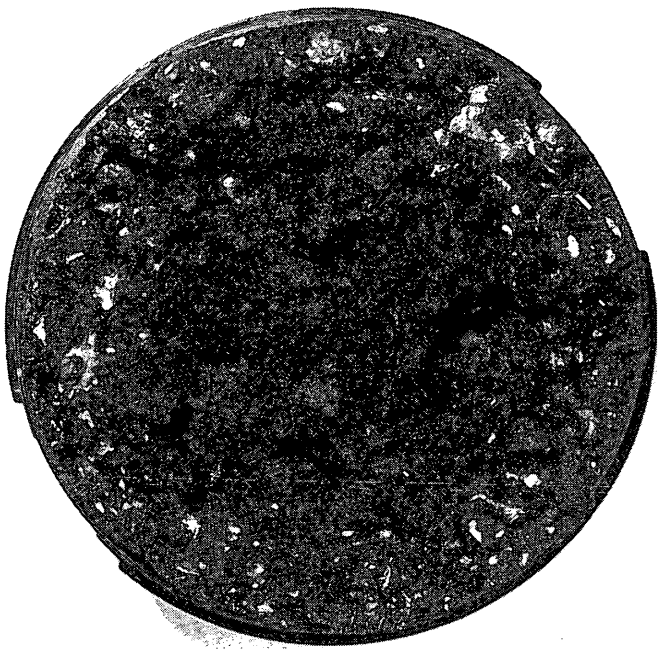

FIGURE 1 Gyratory specimen broken by axial tension, showing aggregates crushed during compaction around mold wall.

EFFECTS OF COMPACTION METHOD AND CUT AND UNCUT SURFACES ON AIR-VOID CONTENT MEASUREMENT

The following questions exist regarding the testing of specimens with as-compacted surfaces versus specimens with cut or cored surfaces:

- What is the relative ability to accurately and repeatably measure air-void content?
- What is the presence of air-void content gradients?
- Is aggregate structure the same in the interior and near the mold wall for specimens with as-compacted surfaces? and
- What are the interactions of two air-void content measurement methods with cut and uncut aggregates?

The difficulties of measuring air voids using parafilm, a waxy elastic paper (*6,7*), and other methods in specimens with uncut surfaces have been documented elsewhere (*7*). Most of these problems have to do with bridging the parafilm or membrane over gaps in the uncut surface, or determining which portions of a rough uncut surface are air voids and which are gaps in the specimen surface caused by rough aggregates.

In addition, it is often difficult to separate the effects of a measurement technique from the additional problem of air-void content gradients between different areas of a compacted specimen. Asphalt-aggregate mixes compacted in the field usually have increasing air-void contents from the top of the lift to the bottom. The reason for air-void gradients can be easily explained by the distribution of forces under a field compaction wheel, which decrease with depth. Laboratory-compacted specimens also often have air-void content gradients, which can be explained primarily by the distribution of stresses during compaction and the effects of the mold wall on aggregate structure.

Rolling wheel specimens would be expected to have increasing air-void contents from the top to the bottom of the lift, as do field-compacted specimens. Kneading compaction would be expected to have a similar gradient, possibly more pronounced than that of the rolling wheel because of the large localized shear force placed on the aggregates near the surface. The presence of cracked aggregates near the surface of kneading specimens, caused by high shear stresses directly under and at the edges of the kneading foot, have been noted previously (*4*). Air-void contents are expected to be fairly homogenous in the horizontal plane for rolling wheel and kneading specimens, except near the mold walls, assuming uniform distribution of passes or tamps over the entire specimen. The aggregate structure and air-void content near the mold wall are expected to be different than that of the interior because aggregate in those areas would become oriented parallel to the wall.

Gyratory specimens are subjected to a high axial compressive stress, a side-to-side shear stress, and a torsional shear stress. The combined effects of these stresses are more difficult to visualize than are the effects of stresses on the rolling wheel and kneading specimens, and they would depend on the relative magnitudes. During kneading and rolling wheel compaction, the material is able to move out from under the shearing force of the compactor, whereas in the gyratory compactor complete confinement of the material prevents this from occurring, and aggregate is primarily forced down.

Under high axial compressive stresses and many gyrations, it is expected that the interior of the specimen becomes better compacted. The torsional shear stress, and the inability of aggregate to become oriented, is thought to reduce compaction near the vertical

walls of the specimen. In lightly compacted specimens, torsional shear stress probably produces most of the compaction. It is likely to produce a lower air-void content around the perimeter than in the interior of the specimen. Our observations confirm those of other researchers: large aggregates near the surface have a tendency to "pop out," because tension is introduced by the mold wall.

As is the case with the other compaction methods, aggregate near the mold surface has a tendency to become aligned with the mold wall. The tendency was observed by DNRL upon examining a limited number of kneading and gyratory specimens (*4*).

Air-Void Content Measurement Problems

In order to investigate differences in air-void content measurements for as-compacted and cut surfaces and the possible existence of air-void content gradients, a variety of rolling wheel and gyratory specimens were subjected to air-void content measurements at various stages of coring and cutting.

Gyratory Specimens

Gyratory specimens compacted to a 17.5-cm (7-in.) diameter and 10-cm (4-in.) height, and measured dry (never exposed to water from coring or cutting), had similar air-void contents after first being submerged in water and then brought to the surface dry condition, which involves removal of all surface water with a 207 kPa (30 psi) air nozzle (*7*), as indicated in Table 1. The large mold and ram are standard features with the large Texas gyratory compactor used by the Texas Department of Transportation. After specimens were cored to a 15-cm (6-in.) diameter, and their top and bottom were trimmed 5 mm to arrive at the cored and cut surface condition, they generally had an air-void content 1 to 2 percent lower than they did before. Measured using parafilm, this drop in air-void content can be attributed partly to the change in surface types, which reduced bridging of the parafilm over surface irregularities, and partly to the removal of the outside 1-in. of the specimen. It is in the outer portion of the specimen removed by coring that the aggregate particles are generally vertically oriented along the mold wall, instead of horizontally oriented as they are in the interior of the specimen.

After cutting the remaining top and bottom portions (Face A and Face B) to arrive at a 5-cm (2-in.) height, no similar drop in measured air-void content occurred when measured with parafilm, as data in Table 1 indicate. Note that the measurements without-parafilm (unsealed condition) remain essentially the same. Upper and lower faces of the specimens have higher air-void contents than the interiors, indicating that they are less compacted. After coring to a 10-cm (4-in.) diameter, the measured air-void contents generally remained the same. The compacted specimen with a 15-cm (6-in.) diameter and 22.5-cm (9-in.) height showed an increase in measured air-voids when cut to a 5-cm (2-in.) height [while maintaining an uncut 15-cm (6-in.) diameter], with the upper and lower surfaces having lower air-void contents than the interior. When cored to 10 cm (4 in.), the specimen had a lower air-void content in its interior.

Statistical *t*-tests were made of the null hypothesis that the sample means are the same for a 5 percent single-tail level of significance for several paired data samples in Table 1. The null hypothesis was acceptable for the dry-with parafilm (dwp, Column A), and wet-with parafilm (wwp, Column B), as-compacted measurements. The null hypothesis was rejected for the wet-with parafilm as-compacted specimens and for the wet-with parafilm cored and trimmed measurements (Columns B and C). It was also rejected for the wet-with parafilm as-compacted and wet-with parafilm cored and cut measurements (Columns B and D).

TABLE 1 Comparison of Air-Void Content Measurements for Gyratory Specimens at Different Stages of Coring and Cutting

Comparison of Air-Void Content Measurements
Different Stages of Coring and Cutting

		as compacted (uncored and uncut)				cored to 6 in. and trimmed		cored to 6 in. and cut to 2 in.						cored to 4 in.	
								center		face a		face b			
Specimen	Agg	dwp	dnp	wwp	wnp	wwp	wnp	wwp	wnp	wwp	wnp	wwp	wnp	wwp	wnp
Texas Gyratory Compactor															
Stages of Cutting and Coring (compacted as 7 x 4 inches)															
t-Test Column:		A		B		C		D							
FMG20-2	M	7.0	4.7	6.9	4.8	5.5	4.8	5.4	4.3	7.4	5.1	8.3	6.0	6.0	4.7
FMG20-1	M	7.1	5.0	7.1	5.1	6.4	4.9	5.7	4.4	9.3	5.6	8.0	5.3	6.4	4.7
FMG10	M	7.3	5.1	6.5	5.4	6.1	5.1	5.5	4.6	11.8	6.2	8.7	5.4	5.8	4.5
FMG00-1	M	7.8	5.0	8.0	5.2	6.0	5.1	6.0	4.4	7.7	5.9	10.6	6.4	5.5	4.4
FPG11-1	P	2.2	1.1	2.3	1.1	0.9	0.5	1.4	0.7	2.4	0.7	2.1	0.7	2.3	1.2
FPG00	P	4.9	2.9	5.0	2.9	3.6	2.5	3.2	2.4	5.2	3.0	5.2	3.1	3.6	2.9
V0W0-G1	W	5.7	3.6	5.2	3.6	4.3	3.3	4.8	3.9	5.6	3.7	4.7	3.1	5.3	4.5
V0W1-G1	W	6.9	4.2	7.1	4.6			5.3	4.2	7.8	3.5		4.6	6.6	4.6
average		*5.5*	*3.4*	*5.5*	*3.5*	*3.7*	*2.9*	*4.1*	*3.1*	*5.7*	*3.4*	*5.6*	*3.6*	*4.7*	*3.5*
Stages of Cutting and Coring (compacted 6 x 9 inches, cut 6 x 2 inches, uncored perimeter)															
VWOSU-5C	W*	3.8	2.3	3.8	2.5	na	na	5.1	3.5	3.2	1.6	2.2	1.5	4.2	2.6

W* is Watsonville granite with a 1/2 in. top size gradation similiar to high fines gradation

Key: M - Maryland limestone P - Pleasanton gravel W - Watsonville granite
dwp - dry with parafilm; dnp - dry no parafilm; wwp - wet with parafilm; wnp - wet no parafilm

The sum of the results in Table 1 indicates that air-void contents measured on as-compacted gyratory specimens cannot be compared with those with cut and cored surfaces because of the effects of the uncut aggregates on parafilm measurements, and the different aggregate structure present near the mold wall. The results indicate that there is little horizontal air-void content gradient in the specimens once they have had the outer as-compacted ring of material removed. There also appears to be little vertical air-void content gradient.

A second set of 27 gyratory specimens, compacted as 15-cm (6-in.) diameter by 15-cm height cylinders with generally high air-void contents, was also evaluated for air-void gradients (*8*). This set included both modified and conventional binders, with Watsonville granite and Texas chert aggregates. Air-void contents were measured by SHRP A-004 (without parafilm), UCB (without parafilm), and UCB (with parafilm); and average air-void contents were 6.8 percent, 6.7 percent, and 12.1 percent, respectively. It was observed that when air-void contents of completely as-compacted specimens were measured without parafilm they were substantially lower than when using parafilm.

After cutting the top and bottom but not coring to create three specimens, 15 cm (6 in.) in diameter and 5 cm (2 in.) high, air-void contents were measured by UCB (without parafilm) and UCB (with parafilm); and average air-void contents were 8.9 percent and 11.9 percent, respectively. It was observed that the parafilm air-void contents remain consistently high and the without-parafilm air-void contents increase compared with the air-void contents of the as-compacted original specimens.

This indicates, first of all, that when parafilm is not used many air-voids are connected to the surface, allowing water to enter the specimen and resulting in unrealistically low air-void content measurements. The fact that the high parafilm measurements are similar both before and after cutting indicates that the bridging of the parafilm is not responsible. The fact that the without-parafilm air-void contents are also higher after cutting indicates that in lightly compacted specimens the top and bottom have lower air-void contents than does their center. This confirms other data presented here and elsewhere (*7*) indicating that heavily compacted gyratory specimens have higher air-void contents at the periphery than within the interior, whereas the opposite holds true for lightly compacted specimens.

Rolling Wheel Specimens

A similar study of rolling wheel specimens is summarized in Table 2. All rolling wheel specimens were cut and cored from a large compacted mass before use. When cut in half horizontally, the 10-cm in diameter by 5-cm high (4 by 2 in.) cylindrical shear specimens showed little difference in air-void content between their upper and lower portions. Similarly, fatigue beams, 5 cm high by 7.5 cm wide by 37.5 cm long (2 by 2.5 by 15 in.), showed little or no difference in air-void content between upper and lower halves. Cylindrical shear specimens (5-cm tall) also showed little or no change in air-void content from the 15-cm diameter specimens and the 10-cm diameter specimens cored out of them.

Statistical *t*-tests were made of the null hypothesis that the sample means are the same for a 5 percent single-tail level of significance for several paired data samples in Table 2. The null hypothesis was accepted for the Face A and Face B measurements (Columns A and B), as well as for the measurements of specimens cored to 15 cm (6 in.) and 10 cm (4 in.) (Columns C and D).

The results indicate that there is little or no vertical or horizontal air-void content gradient in UCB rolling wheel specimens compacted in 7.5 cm (3 in.) lifts.

Comparison of Measured Air-Void Contents for Different Specimens

Air-void content data for as-compacted and cut and cored specimens measured with and without parafilm (unsealed) are plotted in Figures 2 and 3. The permanent deformation cylinder specimens were prepared for a balanced full-factorial experiment design with the following variables and factor levels: Boscan, California Valley, and rubberized asphalt binders; Pleasanton gravel and Watsonville granite aggregates; low and normal fines contents; 4 and 8 percent target air-void contents (measured with parafilm); high and optimal mixing viscosities; and high and optimal compaction viscosities.

Differences in air-void content between the as-compacted specimens and the same specimens cut and cored to their final dimensions as measured using parafilm exist for cylindrical shapes compacted using gyratory and kneading compaction, as shown in Figure 2. The as-compacted specimen usually has a higher air-void content because of the different aggregate structure near the surface, and bridging of the parafilm over the large aggregates and other irregularities at the surface.

Differences in measured air-void content are not only found when parafilm is used. Specimens measured without-parafilm (unsealed condition) in both the as-compacted and cut and cored condition also showed marked differences, as are represented in Figure 3 for cylindrical shear specimens compacted using gyratory and kneading compaction. Well compacted specimens have lower measured air-void contents when cut and cored, which can probably be attributed to the asphalt film that often forms at the surface of these specimens during compaction. Asphalt is forced out of the aggregate matrix by compaction and bleeds to the surfaces. For most specimens with asphalt contents designed by the Hveem Method (as were those described here), there is not much flushed asphalt; however, flushed asphalt is observable and probably plays a role in sealing the outside of the as-compacted specimen to water. For well compacted specimens, the periphery probably has a higher air-void content; aggregate must become oriented vertically to fit the mold wall at the same time it is being pushed to orient horizontally by the shear forces of compaction. The result is a specimen with more air-voids near the surface, partially sealed with asphalt to prevent water from entering. In general, there is a higher measured air-void content for as-compacted specimens.

Poorly compacted specimens do not flush much asphalt to the surface, and differences in aggregate structure between the interior and periphery are probably not as pronounced. Therefore, there is less difference in measured air-void content between as-compacted and cut and cored specimens, as indicated in Figure 3. If a specimen is not sealed with parafilm, higher air-void contents cannot be measured because water is able to pass into the surface-connected pores.

EFFECTS OF COMPACTION AND AS-MOLDED SURFACES ON RSST-CH RESULTS

The possibility of cut and uncut aggregate at a specimen's surface having different mechanical responses to shear loading has been

TABLE 2 Comparison of Air-Void Content Measurements for Rolling Wheel Specimens at Different Stages of Coring and Cutting

Comparison of Air-Void Content Measurements
Different Stages of Coring and Cutting

Rolling Wheel Specimens

Specimen	agg	Whole Specimen AV wwp	Whole Specimen AV wnp	Face A AV wwp	Face A AV wnp	Face B AV wwp	Face B AV wnp
t-Test Column:				A		B	
cut to 4 x 2 in.							
AM0-3-8	M	3.1	1.7	2.6	0.8	2.7	1.8
B1W0-N2-7C	W	4.2	3.0	5.2	2.6	5.6	3.6
B1W0-N2-8T	W	4.6	3.5	5.0	3.4	4.7	3.7
V1T0-N2-7C	T	4.7	3.5	5.1	3.5	4.9	3.4
B1T1-N2-7T	T	7.9	4.8	7.9	5.3	10.1	7.0
V0T1-N1-6T	T	9.9	7.8	11.8	7.4	14.1	9.0
V0W1-N3-8C	W	10.2	8.8	9.8	6.0	8.3	4.6
V0T1-N1-7C	T	11.6	8.3	12.9	7.4	15.0	9.2
VM1-1-6	M	12.6	8.1	13.7	6.9	15.4	7.5
V0W1-N3-9C	W	13.2	6.9	15.2	7.2	13.2	8.6
average		*8.2*	*5.6*	*8.9*	*5.0*	*9.4*	*5.8*

Specimen	agg	Whole Specimen AV wwp	Whole Specimen AV wnp	Top AV wwp	Top AV wnp	Bottom AV wwp	Bottom AV wnp
cut to 2 x 2.5 x 15 in. fatigue beams							
NA2-A5	N	3.4	1.2	3.1	1.4	2.5	0.7
NA1-A3	N	4.8	3.8	4.9	4.0	5.5	3.7
NA1-A4	N	6.1	4.0	6.4	4.9	5.4	3.9
average		*4.8*	*3.0*	*4.8*	*3.5*	*4.5*	*2.8*

Specimen	agg	cut to 6 x 2 in. AV wwp	cut to 6 x 2 in. AV wnp	Cored to 4 x 2 in. AV wwp	Cored to 4 x 2 in. AV wnp
t-Test Column:		C		D	
VP0-C7A	P	1.2	0.6	1.8	1.0
VP0-2-1	P	2.7	1.9	3.0	1.7
VP1-2-1	P	4.4	3.5	4.9	3.6
V0W0-N35-C1	W	4.8	4.0	4.4	3.1
FWR21-3	W	5.1	4.0	4.8	3.9
FWR20-3	W	5.1	4.1	5.8	4.5
VMR20-A2	M	5.3	4.2	6.3	5.0
VMR01-3	M	7.1	5.9	7.2	6.1
V0W1-N5-A	W	9.7	6.6	10.3	7.4
VMR21-A2	M	9.9	7.9	9.9	8.4
VMR21-A1	M	10.1	8.6	10.5	9.0
FPR21-B3	P	12.6	9.6	11.9	9.9
average		*6.5*	*5.1*	*6.7*	*5.3*

Key: M - Maryland limestone N - Nantes limestone P - Pleasanton gravel
T - Texas Gulf Coast Chert W - Watsonville granite

raised also (*7*). Actual effects presumably depend on the aggregate shapes and the relationship of the maximum aggregate size to the specimen size.

To investigate the effects of cut versus as-compacted surfaces on constant height shear testing results, a set of kneading compaction specimens was prepared. The specimens were made using Valley AR-4000 asphalt and Watsonville granite and Pleasanton gravel aggregates. Half were compacted to a shape 10 cm in diameter and 5 cm tall (4 by 2 in.) whereas the other half were compacted to a shape 18.75 cm in diameter and 7.5 cm tall (7.5 by 3 in.) and then cored and cut to the same dimensions as the as-compacted specimens. Specimens were tested at 60°C (140°F) using the repetitive simple shear test-constant height (RSST-CH) (*3,9*) at a stress of 41.4 kPa (6.0 psi).

Permanent deformation results for the cut and as-compacted Pleasanton gravel specimens are plotted in Figure 4. Results for the cut and as-compacted Watsonville granite specimens are plotted in Figure 5. The graphs indicate that the cut specimens following the expected trend of lower air-void content (measured using parafilm) specimens generally perform better than higher air-void content specimens. The peak permanent deformation resistance usually occurs at an air-void content of approximately 3 percent (*9*). The ranking of the as-compacted specimens by number of repetitions to 2 percent permanent shear strain follows the order of air-void contents.

Permanent deformation results for the as-compacted (uncut) specimens, and the rankings of the uncut specimens do not follow the order of air-void content quite as well as the cut specimens. The presence in some uncut specimens of large aggregates, near the in-

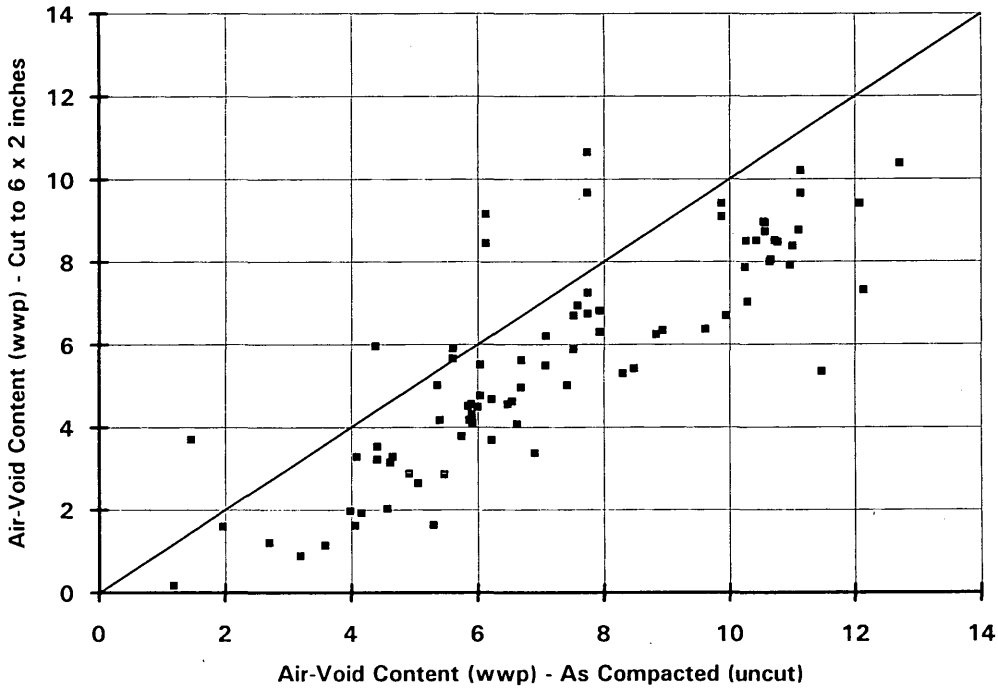

FIGURE 2 Comparison of parafilm air-void contents for permanent deformation specimens, as-compacted versus cut/cored.

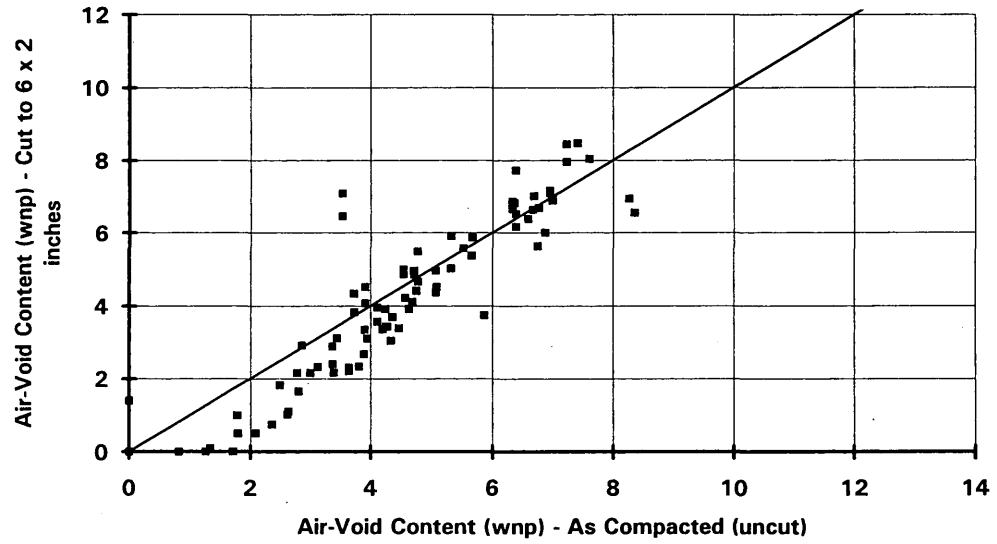

FIGURE 3 Comparison of unsealed (no parafilm) air-void contents for permanent deformation specimens, as-compacted versus cut/cored.

terface with the platens or near the mold wall, and not in others, may be partly responsible for the unexpected rankings of the uncut specimens. Segregation in some specimens may be responsible, as could the inability to precisely measure air-void contents in as-compacted specimens using parafilm.

At low air-void contents, as-compacted and cut and cored Pleasanton gravel specimens with similar air-void contents perform about the same. It can be seen in Table 3 and Figures 4 and 5 for these specimens, the two air-void content measurements show similar air-void contents with parafilm (wwp) and without parafilm (wnp), or unsealed. As air-void contents increase, the as-compacted specimens perform increasingly better compared with the cut and cored specimens of similar air-void content and measured with parafilm. However, when comparing the air-void contents measured without parafilm for these same specimens, the differences in performance are more reasonable.

Combined results from the air-void content measurement and RSST-CH results indicate that, in combination, problems with mea-

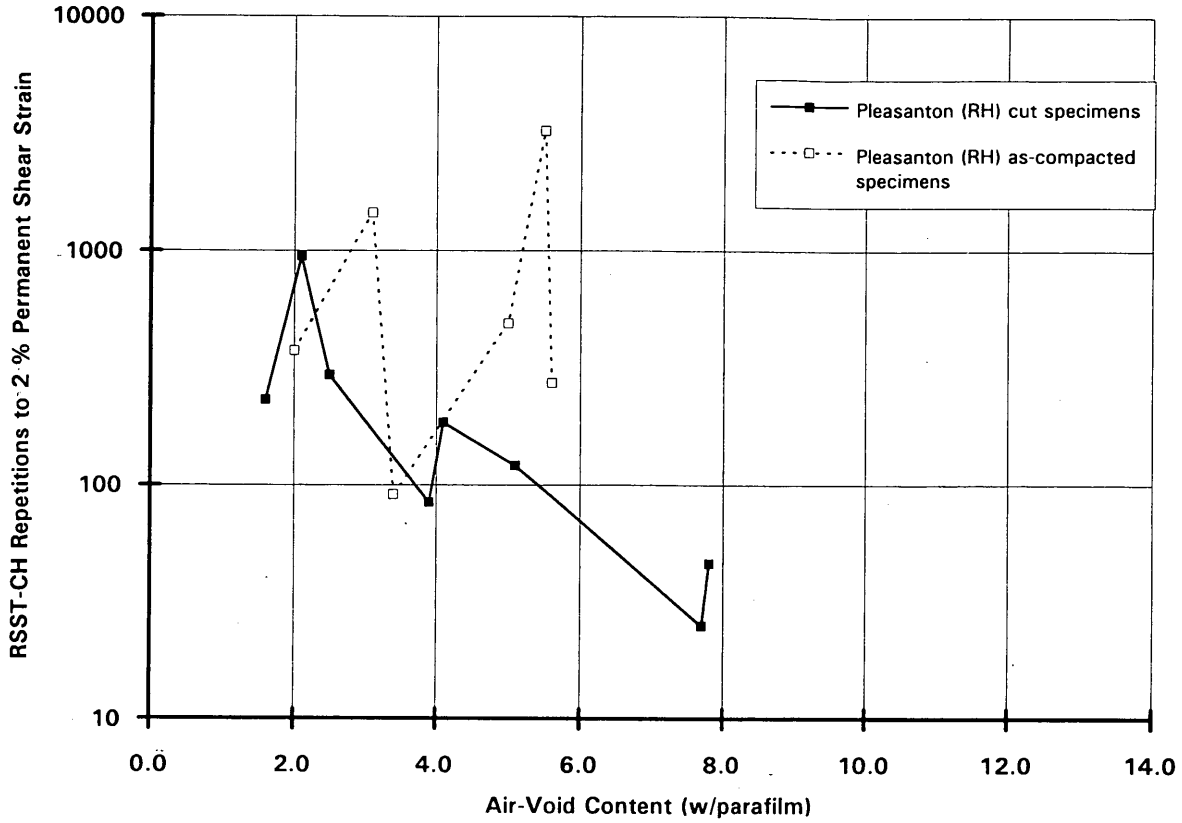

FIGURE 4 Plot of permanent deformation and air-void content for cut/cored and as-compacted Pleasanton gravel specimens.

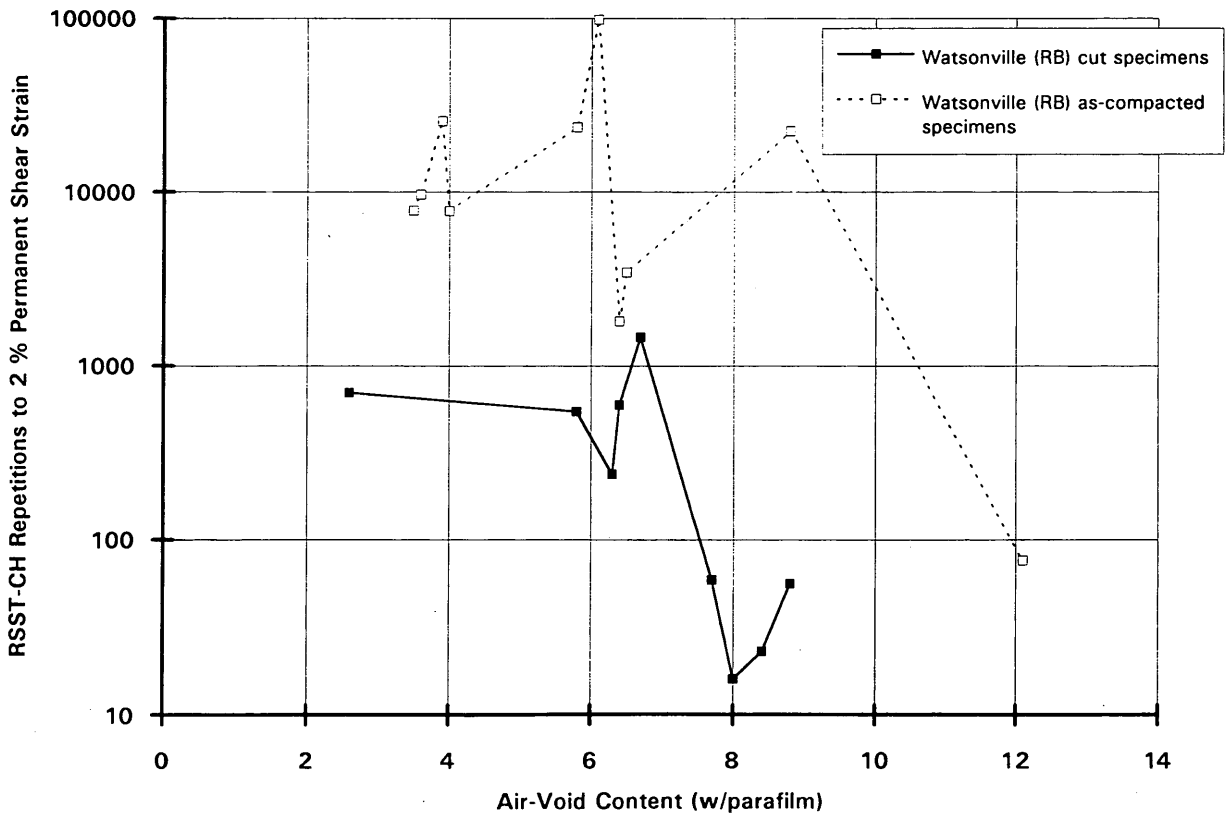

FIGURE 5 Plot of permanent deformation and air-void content for cut/cored and as-compacted Watsonville granite specimens.

TABLE 3 RSST-CH Results for As-Compacted and Cut and Cored Specimens

60 C (140 F) Aggregate	Air-Void Content with parafilm	Air-Void Content unsealed	Cut/ As-Compacted	RSST-CH Repetitions to 2 % shear strain
RH	1.6	1.2	Cut	232
RH	2.1	1.8	Cut	953
RH	2.5	2.2	Cut	295
RH	3.9	3.4	Cut	84
RH	4.1	2.5	Cut	185
RH	5.1	3.7	Cut	121
RH	7.7	6.9	Cut	25
RH	7.8	5.7	Cut	46
RH	2.0	1.1	As-Compacted	376
RH	3.1	1.6	As-Compacted	1449
RH	3.4	1.9	As-Compacted	91
RH	5.0	2.2	As-Compacted	490
RH	5.5	3.1	As-Compacted	3245
RH	5.6	2.9	As-Compacted	273
RB	2.6	1.7	Cut	701
RB	5.8	5.2	Cut	544
RB	6.3	5.6	Cut	238
RB	6.4	5.6	Cut	595
RB	6.7	5.9	Cut	1459
RB	7.7	6.1	Cut	59
RB	8.0	7.0	Cut	16
RB	8.4	7.4	Cut	23
RB	8.8	7.6	Cut	56
RB	3.5	1.8	As-Compacted	7782
RB	3.6	2.5	As-Compacted	9655
RB	3.9	2.4	As-Compacted	25506
RB	4.0	2.3	As-Compacted	7773
RB	5.8	3.4	As-Compacted	23526
RB	6.1	2.9	As-Compacted	98238
RB	6.4	3.9	As-Compacted	1798
RB	6.5	4.2	As-Compacted	3443
RB	8.8	4.6	As-Compacted	22416
RB	12.1	7.5	As-Compacted	76

suring air-void contents, and possible differences affected by cut or uncut aggregates at the interface between the platen and the specimen, make comparison of the performance of as-compacted and cut and cored specimens nearly impossible. Specimens cored from the field cannot be compared to laboratory-compacted specimens that either have not been cored and cut from a larger compacted mass or do not have all cut surfaces.

CONCLUSIONS

As-compacted Texas gyratory and kneading specimens appear to have different aggregate and air-void structures near the mold surface than in their interior. Texas gyratory specimens may have little air-void content gradient if the specimen is cored and cut from a larger compacted mass; note that removal of the outer inch is recommended by UCB for specimens with a 2.5-cm (1-in.) maximum aggregate size. The top and bottom 2.5 cm (1 in.) and outer 1.25 cm (0.5 in.) of gyratory specimens are recommended for cutting and coring, based on image analysis by the DNRL.

Rolling wheel specimens cut and cored from larger masses have little air-void content gradient, compacted in 7.5 cm (3 in.) lifts.

RSST-CH results for cut and cored and as-compacted specimens cannot be compared because of difficulty comparing air-void content measurements and the presence of a different air-void and aggregate structure at the outside edge of as-compacted specimens.

For the same reasons, RSST-CH results for laboratory-compacted specimens with as-compacted surfaces cannot be compared with those from field cores.

DNRL's image analysis showed that the rolling wheel compactor produced aggregate orientation in the mixes containing all three aggregates (completely crushed granite; partially crushed gravel; and completely crushed, flaky limestone). The most aggregate orientation was produced in the mixes containing the flaky limestone. Image analysis showed that the Texas gyratory compactor produced aggregate orientation only in the mixes with flaky aggregate and that even for the flaky aggregate it produced less aggregate orientation than did the rolling wheel compactor. Further, DNRL image analysis showed that average sizes of air-voids are dependent primarily on the aggregate used.

The influence of the mold walls on the exterior structure of gyratory compacted samples is seen as segregation of larger aggregate particles entrapping larger air-voids and the crushing of aggregates or removal of the asphalt between them. The segregation phenom-

enon is most pronounced at the top and bottom surfaces, typically extending 10 mm to 20 mm (0.4 in. to 0.8 in.) inward; it is less pronounced at the vertical mold walls, where the effect typically extends 2 mm to 5 mm (0.08 in. to 0.2 in.) inward. This phenomenon obviously influences the measurement of an air-void content, resulting in one that is too high and not representative of the mix. Crushing of aggregates, or lack of asphalt between aggregates caused by crushing, results in a difference in permanent deformation resistance properties between the interior and the annulus of the specimen.

ACKNOWLEDGMENTS

The work reported here was conducted as part of a doctoral research program at the University of California at Berkeley supported by International Surfacing, Inc.; the Texas Department of Transportation; and the Strategic Highway Research Project, particularly Rita Leahy. Financial assistance was provided for two years by the UCB Transportation Center and the U.S. Department of Transportation. The authors would like to thank Akhtar Tayebali, Maggie Paul, and the University's Asphalt Research Program laboratory staff, for their help.

REFERENCES

1. Harvey, J., and C. L. Monismith. Effects of Laboratory Asphalt Concrete Specimen Preparation Variables on Fatigue and Permanent Deformation Test Results Using Strategic Highway Research Program A-003A Proposed Testing Equipment. In *Transportation Research Record 1417,* TRB, National Research Council, Washington, D.C. 1994, pp. 38–48.
2. Sousa, J., J. Harvey, L. Painter, J. A. Deacon, and C. L. Monismith. *Evaluation of Laboratory Procedures for Compacting Asphalt-Aggregate Mixtures.* Technical Memorandum TM-UCB-A-003A-90-5. Institute of Transportation Studies, University of California at Berkeley, July 1991.
3. Sousa, J., A. Tayebali, J. Harvey, P. Hendricks, and C. L. Monismith. Sensitivity of Strategic Highway Research Program A-003A Testing Equipment to Mix Design Parameters for Permanent Deformation and Fatigue. In *Transportation Research Record 1384,* TRB, National Research Council, Washington, D.C., 1993, pp. 69–79.
4. Eriksen, K., V. Wegan, and J. Krarup. *Air Void Content and Other Air Void Characteristics of Asphalt Concrete by Image Analysis.* Strategic Highway Research Program, National Research Council, Washington D.C., March 1992.
5. Eriksen, K. *Homogeneity of Air Voids in Asphalt-Aggregate Mixtures Compacted by Different Methods at Different Temperatures.* Strategic Highway Research Program, National Research Council, Washington D.C., Sept. 1992.
6. del Valle, H. *Procedure: Bulk Specific Gravity of Compacted Bituminous Mixtures Using Parafilm Coated Specimens.* Chevron Research Company, Richmond, Calif. 1985.
7. Harvey, J., J. Sousa, J. Deacon, and C. L. Monismith. Effects of Sample Preparation and Air-Void Measurement on Asphalt Concrete Properties. In *Transportation Research Record 1317,* TRB, National Research Council, Washington, D.C., 1991, pp. 61–67.
8. J. Sousa. *Evaluation of the Effects of Modifiers on Asphalt-Aggregate Mix Permanent Deformation Performance Using the CHRSST.* Technical Memorandum, Institute of Transportation Studies, University of California at Berkeley, February 1993.
9. Sousa, J. Asphalt-Aggregate Mix Design Using the Simple Shear Test (Constant Height). Presented at the Association of Asphalt Paving Technicians Annual Meeting, 1994.

Publication of this paper sponsored by Committee on Characteristics of Bituminous Paving Mixtures To Meet Structural Requirements.

Evaluation of Fatigue and Permanent Deformation Properties of Several Asphalt-Aggregate Field Mixes Using Strategic Highway Research Program A-003A Equipment

JOHN HARVEY, TINA LEE, JORGE SOUSA, JIMMY PAK, AND CARL L. MONISMITH

Use of fatigue and permanent shear deformation tests, equipment, and analysis procedures developed by the Strategic Highway Research Program (SHRP) A-003A project, are investigated for their applicability for to stone matrix asphalt, recycled asphalt pavement, asphalt-rubber concrete, and large stone gradation as well as conventional asphalt-concrete mixes. Materials were collected in the field and compacted in the laboratory following SHRP A-003A rolling wheel procedures. Mixes were tested for fatigue life and flexural stiffness using controlled-strain equipment. Their permanent shear deformation resistance was evaluated using the repetitive simple shear test-constant height (RSST-CH). Results show that the tests and equipment were sensitive to each of the materials tested, and also confirm engineering expectations. Rut depth predictions were made on the basis of the RSST-CH results and a proposed method for translating the permanent shear strains and load repetitions measured by the test to field rut depths and equivalent single axle loads (ESALs). When the measured ESALs and in situ rut depths were compared with test results, the method proved to be a good predictor, although resulting predictions were often somewhat conservative because mixes in the field had aged. Analysis of fatigue and stiffness data for several hypothetical pavement cross sections applying elastic layer theory showed that ranking of mixes for fatigue life depends on the fatigue curve developed from testing, measured flexural stiffness, and properties of the underlying pavement.

Performance testing and analysis methods designed under Strategic Highway Research Program (SHRP) Project A-003A provide the means to determine the relationship between fatigue life and tensile strain, flexural stiffness, and permanent shear deformation resistance of asphalt-aggregate mixes. The most important distress mechanisms and conditions that cause fatigue cracking and permanent shear deformation now can be duplicated in the laboratory, allowing direct comparisons of the performance characteristics of various mixes for mix and pavement design, measured in fundamental engineering units, (*1–3*). Rapid evaluation of the potential of various new products and mix types can be completed in the laboratory, either, before or as a substitute for field test-section construction. This is a significant improvement because field test sections require years of monitoring before their performance can be analyzed and are subject to uncontrollable variables related to construction and the environment. The enhanced testing capability provided by SHRP A-003A equipment is especially important when asphalt modifiers such as asphalt rubber or new mix types such as stone-matrix asphalt (SMA) are outside the experience of the evaluating agency, and traditional mix evaluation testing does not provide adequate information.

At this time, elements of the SHRP A-003A permanent deformation analysis system are being considered for inclusion in Super-Pave.

Institute of Transportation Studies, University of California, Berkeley, Richmond Field Station, 1301 South 46th Street, Building 452, Richmond, California 94804.

STUDY OBJECTIVES

The first objective of the study was to test a variety of conventional and new materials under similar conditions for fatigue, flexural stiffness, and permanent shear deformation, to demonstrate the sensitivity of the SHRP A-003A equipment and its ability to directly compare each material's relative performance. The second objective was to use permanent shear deformation test results, together with a proposed method for predicting field rut depth, for comparison with rut depths and ESALs measured in the field. The third objective was to demonstrate the use of strain-fatigue-life relationships developed from testing in predicting fatigue life for several pavement cross sections.

MATERIALS AND TEST METHODS

Field mixes were collected during construction from two test section locations: Interstate 40, approximately 40 mi east of Barstow, California, and Interstate 45, in Waukesha County, Wisconsin. Field cores were collected on some sections both inside and outside the wheel path at times ranging from 5 to 22 months after construction.

Barstow Test Section Descriptions

Barstow sections were constructed in April 1992, and field cores were taken in September 1992. A total of 520,000 equivalent single axle loads (ESALs) was measured at the test sections during the 5 months between construction and coring.

Surface materials, including virgin asphalt concrete, asphalt-rubber concrete (RAC), and a blend of virgin and recycled asphalt pavement (RAP), were constructed in layers 60 mm (0.2 ft) thick. A large stone material was used in a 120 mm (0.4 ft) base layer

below a surface 60 mm (0.2 ft) thick. Two SMA materials, with asphalt-rubber and polyolefin-modified binders, were placed as 45-mm (0.15-ft) surface layers.

Wisconsin Test Section Descriptions

One SMA mix was constructed with a polyolefin-modified binder at the Wisconsin test section. This section was constructed in June 1991 and cored in April 1993. Approximately 128,000 ESALs passed across the design lane during those 22 months.

Materials Descriptions

A partially crushed gravel was used for the Barstow mixes, whereas a completely crushed limestone was used for the Wisconsin SMA. Job mix formulas for all mixes are shown in Table 1. Typical quality assurance results for some mixes are shown in parentheses.

Specimen Preparation

The rolling wheel compaction method of University of California at Berkeley was used for the preparation of all laboratory specimens (*3,4*). Mixes were collected in the field directly in front of the paver. They were compacted in the laboratory in 20-kg (44-lb) ingots, which provided either three permanent deformation cores or one core and two fatigue beams (*1*).

After compaction, the ingots were allowed to cool overnight. Cylinders for permanent deformation testing were cored and cut to cores 15 cm (6 in.) in diameter by 5 cm (2 in.) high. Fatigue beams were cut to 5 cm by 5.25 cm by 38 cm (2 in. by 2.5 in. by 15 in).

Air-void contents were measured with parafilm (*5*). Specimens were compacted to the field air-void contents, which were measured at the time of construction and at the time of coring. Air-void contents ranged between 2 and 13 percent, depending on the mix.

Test Methods

To evaluate the specimens, two types of tests were performed: the repetitive simple shear test—constant height (RSST-CH), and the controlled-strain flexural beam fatigue test. Both tests use computer-operated, closed-loop, digital systems that control hydraulic actuators.

Repetitive Simple Shear Test—RSST-CH

All RSST-CH results were obtained with the universal testing machine (*1,6*). Tests on the laboratory specimens were performed at 60°C (140°F). Tests on field cores were performed at the maximum average 7-day pavement temperature at a depth of 50 mm (2 in.) and calculated using the method of Solaimanian and Kennedy (*7*). The temperatures were 57°C (135°F) for Barstow, California, and 43°C (109°F) for Waukesha County, Wisconsin.

For the RSST-CH, one LVDT is attached to the top and bottom platens along the vertical axis to allow the machine to maintain a constant specimen height and another is attached to the side of the core so that horizontal (shear) displacement can be measured. The shear stress was 68.9 kPa (19 psi), applied as a haversine wave with a 0.1-sec load time and a 0.6-sec rest period. Failure was defined as 5.0 percent permanent shear strain. Results for cores that did not reach failure because of time constraints were extrapolated.

Flexural Beam Fatigue Test—Controlled Strain

To determine the fatigue and stiffness characteristics of each mix, a controlled-strain flexural beam test with a third-point loading system was used (*2*). All tests were performed at 20°C (68°F) using a 10 Hz frequency sine wave. During the test, stiffness was recorded at various time intervals. Initial stiffness was defined as that occurring at the fiftieth load repetition. Fatigue failure was defined as a 50 percent reduction in stiffness.

TABLE 1 Job Mix Formulas and In Situ Quality Control Data

Section:	503	504,507	513,514	519	521	522	WIS
Material:	30% RAP 70 % Virg AC	19 mm MSA Virgin AC	19 mm MSA Asph-Rubber	38 mm MSA Base	SMA Asph-Rubber	SMA Polyolefin	SMA Polyolefin
% Passing Sieve (mm)	Job Mix Formulas (Actual in parentheses)						
38	-	-	-	100 (100)	-	-	-
25	100 (100)	100 (100)	100	95 (87)	100 (100)	100	-
19	98 (97)	99 (97)	98	75 (86)	99 (100)	99 (100)	100
9.5	63 (71)	67 (71)	64	62 (64)	74 (80)	75 (80)	70
4.75	46 (53)	50 (54)	36	48 (47)	31 (37)	29 (31)	28
2.36	36 (42)	40 (42)	20	-	23 (25)	24 (23)	20
0.60	20 (24)	21 (22)	13	21 (20)	12 (13)	16 (14)	14
0.075	4.1 (8)	4.8 (5)	4.0	5.0 (4)	4.0 (6)	8.8 (6)	10.0
Binder Content*	3.8	5.3 (5.2)	7.5	5.1 (5.1)	6.8 (5.0)	6.0 (5.2)	6.0
	*percent by wt of aggregate						
Binder	AR-4000	AR-4000	AR-4000 plus rubber	AR-8000	AR-4000 plus rubber	AR-4000 plus polyolefin	85/100 pen plus polyolefin

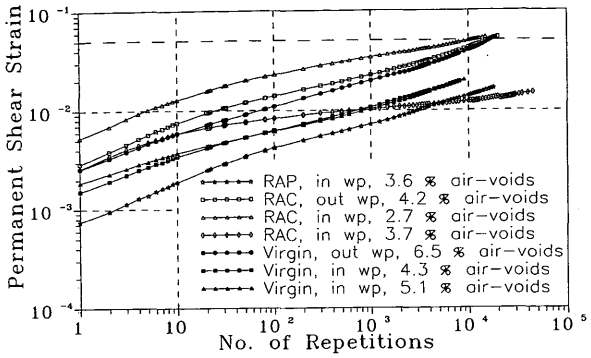

FIGURE 1 Barstow field cores RSST-CH plots, 57°C (135°F).

RSST-CH with Confinement

To evaluate the effects of confining pressure on RSST-CH, results were also obtained for field cores of two mixes from Oregon, one open graded and the other dense graded. The only difference in test method was the application of a 68.9 kPa (10 psi) confining pressure, which was applied using a membrane.

DISCUSSION OF RESULTS

Permanent Shear Deformation

Field Cores

The set of Barstow field core test results performed at 57°C (135°F) is plotted in Figure 1, and the number of RSST-CH repetitions to a 5.0 percent permanent shear strain (pss) are presented in Table 2. It can be seen that the cores from inside the wheel path had slightly lower air-void contents than those taken from outside the wheelpath and had much more permanent deformation resistance. This indicates that besides aging, which doubled the stiffness of the conventional binder in the first 5 months after construction (*8*), densification and aggregate orientation induced by traffic greatly improved permanent shear deformation resistance. Results from the limited number of cores indicate that traffic compaction improved the performance of the RAC more than it did the virgin asphalt concrete.

The Wisconsin field core test results, performed at 43°C (109°F), did not follow the expected pattern of better permanent shear deformation resistance and lower air-void contents inside the wheel path, as can be seen from the plotted results in Figure 2 and related data presented in Table 2. High air-void content and the resultant lower permanent shear deformation resistance of the core taken from within the wheelpath may not be typical.

Laboratory Specimens

RSST-CH results for all laboratory specimens tested at 60°C (140°F) are presented in Figure 3 and Table 3.

Note that the Wisconsin SMA performed very well when compacted to approximately 4.8 percent air voids but did considerably worse when compacted to 6.3 percent. The latter air-voids content was approximately the lowest air-void content achieved in the field on that project. All of the laboratory SMA specimens had a wide range of performance, depending on material type and air-void con-

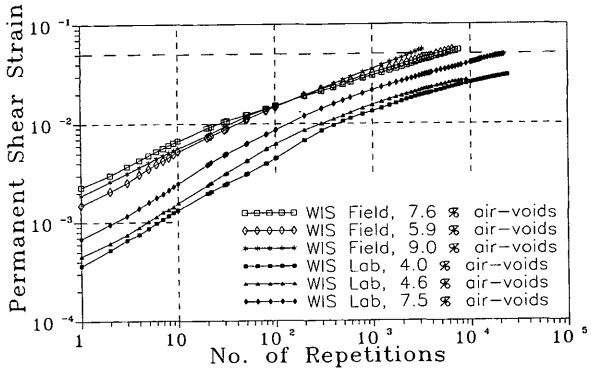

FIGURE 2 Wisconsin SMA field cores and laboratory specimens RSST-CH plots, 43°C (109°F).

TABLE 2 Repetitions to 5 Percent RSST-CH Shear Strain, Field Cores

Specimen	Material	AV	Wheelpath Location	Age	ESALS at Coring	RSST-CH Reps to 5 % Shear Strain
Barstow, Tested at 57 C (134 F)						
B60	Virgin AC	5.1	in	5 mos	520,000	176,523
B59	Virgin AC	4.3	in	5 mos	520,000	151,910
B58	Virgin AC	6.5	out	5 mos	520,000	16,578
B48	RAC	3.7	in	5 mos	520,000	42,539,242
B45	RAC	4.2	out	5 mos	520,000	16,132
B4	RAP	3.6	in	5 mos	520,000	903,134
Wisconsin, Tested at 43 C (109 F)						
WISF6	SMA polyolefin	9.0	in	22 mos	128,000	2,504
WISF5	SMA polyolefin	5.9	out	22 mos	128,000	4,621
WISF3	SMA polyolefin	7.6	out	22 mos	128,000	5,515

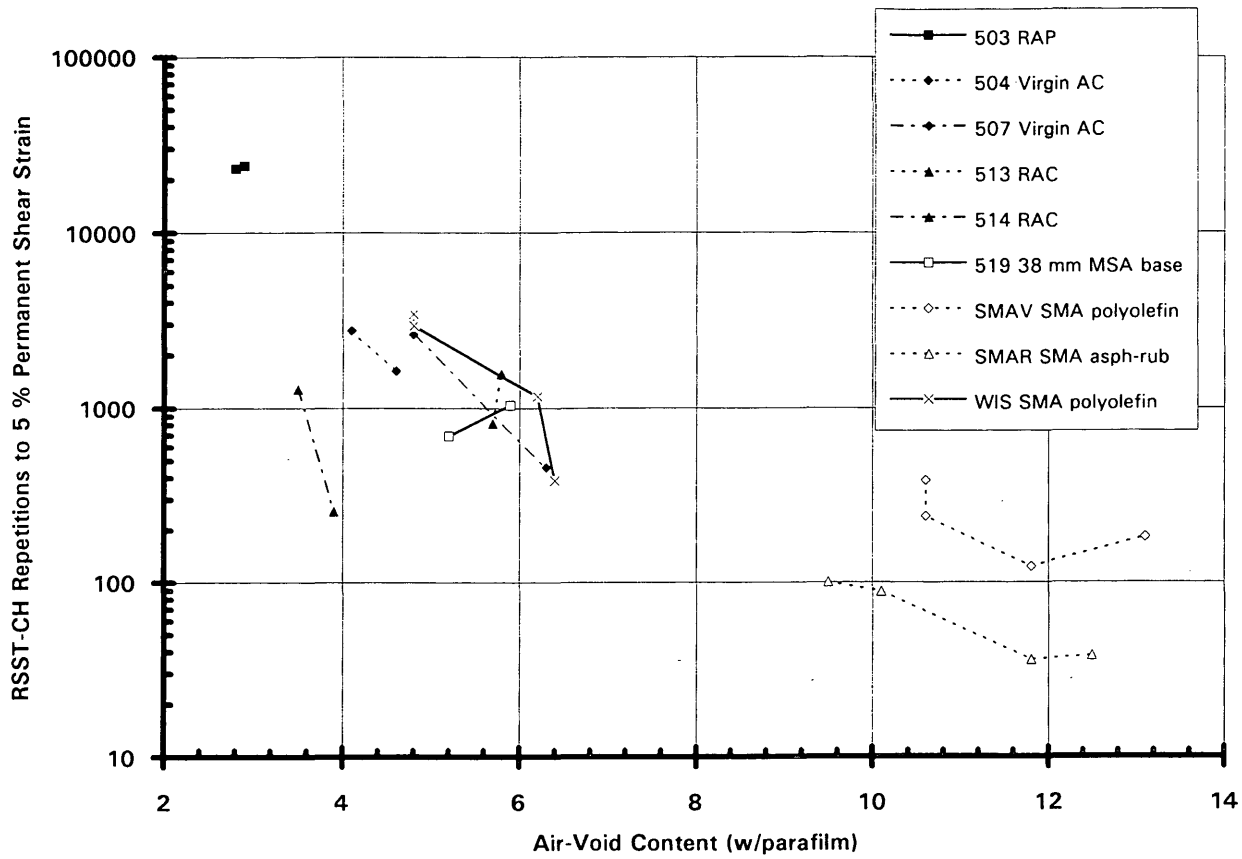

FIGURE 3 Laboratory specimens, RSST-CH repetitions to 5 percent permanent shear strain and air-void content for all mixes, 60°C (140°F).

tent. The Wisconsin SMA, which had lower air-void contents, performed better than did the Barstow SMAs, both of which had relatively low fines contents for this type of mix.

For the Barstow mixes, performance ranking followed the air-void contents, with the exception of the RAC from Section 514. This indicates the tremendous importance of compaction in achieving good permanent shear deformation resistance. Compaction can come from either construction or trafficking, but better compaction in construction will reduce the rut depth caused by densification and also reduce the susceptibility to fatigue and environmental damage before traffic densification. The study results also indicate that at 60°C (140°F) the various mixes used at the Barstow sections were not considerably different from each other with respect to the permanent shear deformation performance of non–long-term aged and laboratory-compacted mixes. However, binders may have different aging rates and varying responses to traffic compaction, which can produce larger differences in performance, such as those seen in the limited field core data already presented, and in a broader comparison of field core data from the Barstow test sections (*8*).

Several Wisconsin SMA laboratory specimens were also tested at 43°C (109°F). It can be seen in Figure 2 and Table 3 that at this temperature permanent shear deformation performance was much better than at the higher temperature. It can also be seen that the laboratory specimens performed better than the field cores. This may be in part the result of the somewhat lower air-voids contents of the laboratory cores. Aging of the binder should not have been significant in Waukesha County, Wisconsin, and little increase in permanent shear deformation resistance from aging was expected in the field cores.

Effect of Confinement on RSST-CH

Comparison of RSST-CH results, unconfined and with 68.9 kPa (10 psi) confining pressure, on duplicate cores of open-graded and dense-graded asphalt-concrete showed virtually no difference between the two testing conditions. On the basis of these tests, it was decided that confinement would not be used for the RSST-CH.

The confinement that resists permanent shear deformation during the RSST-CH is developed within the material by interparticle contact. Because the specimen is maintained at a constant height, aggregate within specimens with good interparticle contact develop dilation pressures as the aggregates attempt to move past each other under 68.9 kPa (10 psi) shear stress. This mechanism appears to be more important than the confining stress applied. Confining pressures greater than 68.9 kPa (10 psi) may influence RSST-CH results, but they were not investigated in this study.

Some lateral densification of the open-graded specimens was observed after the confining stress was applied, but maintenance of a constant height prevented axial densification, and the epoxy fastening the specimen to the platens prevented lateral densification at the ends of the specimens.

TABLE 3 Repetitions to 5 Percent RSST-CH Shear Strain, Laboratory Specimens

Specimen	Material	AV	RSST-CH Reps to 5 % Shear Strain
Tested at 60 C (140 F)			
503-N1	RAP	2.8	23064
503-N3	RAP	2.9	24030
average		*2.9*	*23547*
504-N1-3	Virgin AC	4.1	2780
504-N1-1	Virgin AC	4.6	1632
average		*4.4*	*2206*
507-N1	Virgin AC	4.8	2635
507-N2	Virgin AC	6.3	457
average		*5.6*	*1546*
513-N1C	RAC	5.7	817
513-N1-A	RAC	5.8	1569
average		*5.8*	*1193*
514-N4-B	RAC	3.5	1281
514-N3-A	RAC	3.9	257
average		*3.7*	*769*
519-N1	38mm MSA base	5.2	691
519-N4	38mm MSA base	5.9	1033
average		*5.6*	*862*
SMAV-2-1	SMA polyolefin	10.6	385
SMAV-6	SMA polyolefin	10.6	240
SMAV-1-1	SMA polyolefin	11.8	123
SMAV-4	SMA polyolefin	13.1	182
average		*11.5*	*233*
SMAR-6	SMA rubber	9.5	101
SMAR-2-1	SMA rubber	10.1	89
SMAR-4	SMA rubber	11.8	36
SMAR-7	SMA rubber	12.5	38
average		*11.0*	*66*
WIS 2-1	SMA polyolefin	4.8	3457
WIS 2-2	SMA polyolefin	4.8	2953
WIS 4	SMA polyolefin	6.2	1163
WIS 3-1	SMA polyolefin	6.4	385
average		*5.6*	*1990*
Tested at 43 C (109 F)			
WIS 1-1	SMA polyolefin	4.0	71250
WIS 2-3	SMA polyolefin	4.6	312666
WIS 5	SMA polyolefin	7.5	24062
average		*5.4*	*135993*

Fatigue and Flexural Stiffness

Flexural Stiffness

Initial flexural stiffness results are summarized in Table 4. The RAP material had the highest stiffness, most likely because of the air-void content, the presence of very hard binder material from the recycled pavement, and the addition of only 3.8 percent virgin asphalt cement (by weight of aggregate). Note that the 1.5 Maximum-Size Aggregate (MSA) base material contained a nominally stiffer asphalt, AR-8000, but still exhibited less stiffness than the virgin asphalt mix that contained AR-4000. This is most likely because of

TABLE 4 Fatigue Beam Test Results, All Materials

Tested at 20 C (67 F)						Nf Repetitions to Failure (50 percent initial stiff.)	Total Dissipated Energy (psi)	Regression Equation Nf = k1(strain)^k2		
Material	Specimen	AV	Strain (micro-strain)	Initial (MPa)	Stiffness (psi)			k1	k2	R^2
503 RAP	503-N1-A	2.6	500	6,136	890,495	36,622	1,900			
	503-N1-3	3.9	400	6,323	917,705	73,053	2,414			
	503-2B	2.6	250	6,370	924,559	431,764	5,708			
	503-N3-B	2.8	250	6,083	882,840	459,878	4,985			
average		*3.0*		*6,228*	*903,900*		constants:	2.86E-08	-3.66	0.998
507 Virgin	507-N1-A	5.2	400	3,910	567,521	350,068	14,943			
	507-N2-A	5.1	350	3,318	481,579	149,999	2,520			
	507-N1-B	3.7	550	4,054	588,333	26,298	1,471			
	507-N2-B	5.8	600	3,132	454,553	39,494	2,020			
average		*5.0*		*3,603*	*522,997*		constants:	8.45E-09	-3.90	0.697
514 RAC	514-N1-A	3.5	350	2,957	429,157	190,562	5,166			
	514-N3-B	3.6	300	2,989	433,835	574,923	11,798			
	514-N1-B	3.1	600	2,809	407,672	48,341	4,282			
	514-N3-A	3.9	400	2,746	398,494	183,289	6,985			
average		*3.5*		*2,875*	*417,290*		constants:	1.04E-06	-3.30	0.939
519 38mm MSA base	519-N2-A	7.3	300	3,696	536,375	3,308,566	15,570			
	519-N4-B	6.3	250	3,207	465,468	1,008,293	7,155			
	519-N3-A	7.2	400	2,316	336,176	43,139	673			
	519-N4-A	6.3	400	3,141	455,904	49,169	1,123			
average		*6.8*		*3,090*	*448,481*		constants:	3.29E-23	-8.03	0.724
SMAV polyolefin	SMAV-4A	11.0	400	1,986	288,268	150,000	3,756			
	SMAV-4B	10.8	400	2,537	368,212	97,047	1,649			
	SMAV-5A	11.0	200	2,724	395,424	1,003,047	4,903			
	SMAV-7A	10.6	250	2,845	412,921	2,629,080	10,974			
	SMAV-2B	11.1	300	2,411	349,915	175,000	2,051			
average		*10.9*		*2,501*	*362,948*		constants:	8.21E-09	-3.87	0.681
SMAR a-rubber	SMAR-1B	10.4	450	1,512	219,439	15,000	487			
	SMAR-4A	10.6	400	1,745	253,336	75,923	913			
	SMAR-2A	10.8	300	2,014	292,283	316,536	4,726			
	SMAR-2B	10.2	300	2,052	297,782	227,992	1,813			
average		*10.5*		*1,831*	*265,710*		constants:	7.54E-18	-6.41	0.920
WIS SMA polyolefin	WIS-3-2	5.0	700	5,401	783,864	25,000	5,020			
	WIS-4A	5.4	250	6,541	949,371	1,134,037	23,846			
	WIS-4B	7.1	400	5,278	766,045	262,957	9,598			
average		*5.8*		*5,740*	*833,093*		constants:	4.97E-08	-3.72	0.993

the lower air-void contents of the virgin asphalt specimens, although the two asphalt cements may have different temperature susceptibilities and therefore similar stiffness at 20°C (67°F). The inclusion of rubber in the AR-4000 asphalt used for the asphalt rubber material reduced stiffness by approximately 20 percent compared with the virgin asphalt material, despite somewhat lower air-void contents.

Fatigue

The relationships of controlled-strain fatigue versus strain are plotted in Figure 4, and test results are included in Table 4. The equations were obtained from least-squares regression of the fatigue beam test data and are of the form

$$Nf = k1 * (\text{strain})^{k2}$$

where

Nf = repetitions to a 50 percent reduction in stiffness,
strain = average strain used throughout the test, and
$k1$ and $k2$ = constants.

Although three to five beams were tested for each material, four being the minimum recommended for defining a fatigue curve (*9,2*), the results provide insight into the behavior of the various materials. In particular, it can be seen that the Barstow large-stone base and SMA with asphalt rubber had higher exponent values ($k2$). The plotted fatigue equations cross each other and reverse the fatigue-life rankings of the mixes between 200 and 500 microstrain.

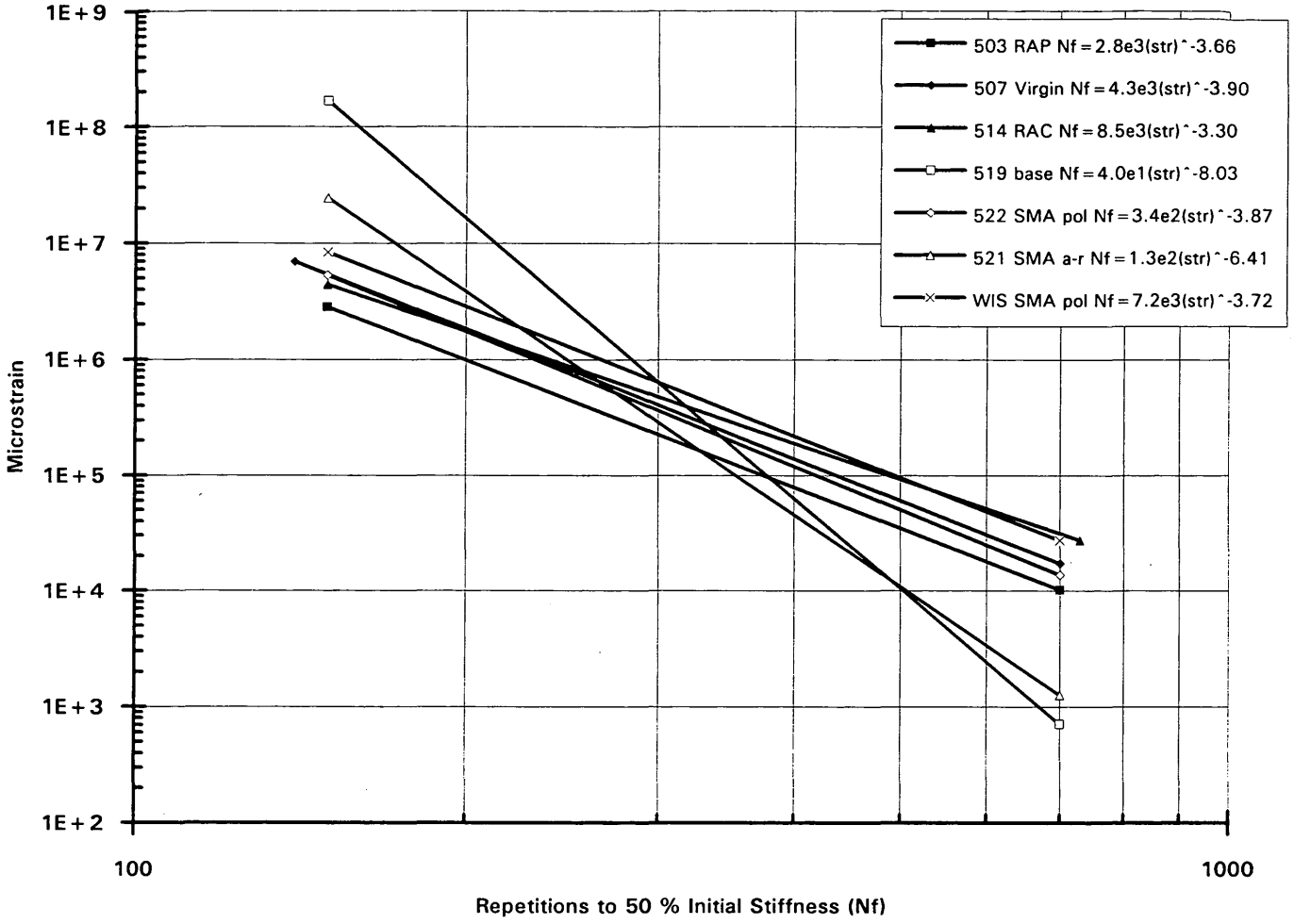

FIGURE 4 Controlled-strain fatigue life equations for all materials, 20°C (67°F).

It can be seen that total dissipated energy for each mix follows fatigue life (Table 4). Evaluation of fatigue performance in terms of total dissipated energy offers no advantages at this time.

PERFORMANCE PREDICTION ANALYSIS

To examine possible uses for the mix performance test data presented above, beyond performance ranking, performance prediction analyses were executed. The methods presented here are still being developed and require further validation; however, results are indicative of the information that can be obtained.

Permanent Deformation Performance Prediction

The following equations presented in a paper by Sousa and Solaimanian (*10*) were used to predict rut depths based on test data previously presented.

$$\text{Field Rut Depth (in.)} = 11 * \text{pss} \quad (1a)$$

$$\text{Field Rut Depth (mm)} = 280 * \text{pss} \quad (1b)$$

where pss is the permanent shear strain measured using the RSST-CH.

$$\log(\text{RSST-CH reps}) = -4.36 + 1.240 \log(\text{ESAL}) \quad (2)$$

where RSST-CH reps is the number of 68.9 kPa (10 psi) load repetitions to a given shear strain (pss) using the RSST-CH, and ESAL is the corresponding equivalent single axle loads.

Using Equation 1, a 5 percent permanent shear strain (pss) selected as failure for comparison of the relative performance of the materials corresponds to a 14-mm (0.55-in.) rut depth (Table 3). Other rut depths can be selected, depending on performance specifications for a given project.

The RSST-CH repetitions to ESALs shift factor are based on correlation of results from SHRP General Pavement Sections that were 1 to 10 years old and account for traffic wander (*10*). The permanent shear strain to field rut depth shift factor is based on finite element analysis (*11*). Additional data, including that presented in this

paper, are in agreement with this performance prediction analysis method; additional field validation data may further refine the two shift factors.

For comparison with field rut depth measurements, ESALs measured using weigh-in-motion equipment at the test sections between construction and rut depth measurement were converted to RSST-CH repetitions using Equation 2. The results were: Barstow, 520,000 ESALs corresponding to 534 RSST-CH repetitions, and Wisconsin, 128,000 ESALs corresponding to 94 RSST-CH repetitions. Permanent shear strain for the appropriate RSST-CH repetitions for each test then was found. Permanent shear strains study for the field cores included in this are found (in Figures 1 and 2). Equation 1 was used to convert permanent shear strains to corresponding rut depths; results of these calculations are in Table 5 for the field cores and in Table 6 for the laboratory specimens.

For the Barstow specimens, rut depths predicted using field cores are lower than those predicted using laboratory specimens and are closer to the actual field rut depths. This can be attributed to binder hardening (aging) caused by extreme temperatures at the Barstow site that the in situ pavement and field cores both were subjected to. Long-term oven-aging of the laboratory specimens before testing would provide a less conservative estimate of field performance.

The Wisconsin section, which was subjected to lower temperatures and therefore less binder aging than the Barstow site, had field rut depths similar to those predicted from the field and laboratory specimens.

A previous study (*3*) indicates that Texas gyratory compaction specimens have less permanent shear deformation resistance, as measured using the RSST-CH, than do rolling wheel specimens. Thus, it would be expected that the predicted rut depths obtained from rolling wheel specimens in this study would be greater, and therefore even more conservative, if the field mixes had been compacted using a gyratory device.

Although large rut depths are predicted by the test results for the Barstow SMAs, the fact that the lift thickness is only about 45 mm (1.8 in.) means that this material will not be subjected to critical shear forces in the field. Critical shear forces have been found by finite element analysis to generally occur near the edge of the tire, at a depth of approximately 50 mm (2 in.). The effects of confining forces from the underlying, less rut-susceptible material just below the SMA on these sections will tend to reduce the actual shear deformations (S. Weissman and C. L. Monismith, unpublished data). For this reason, little or no permanent shear deformation should occur in these materials in the field, as was observed by the field crew during coring.

ANALYSIS OF FATIGUE TEST RESULTS

To evaluate the anticipated fatigue performance of a mix, the effects of both stiffness and the strain-fatigue life curve must be included in a mechanistic analysis of the pavement. For the mixes included in this study, eight pavement cross sections were used that cover a fairly wide range of cases. Cross sections included 50 mm and 100 mm (2 in. and 4 in.) overlays, thick and thin underlying pavement structures, and cracked and uncracked underlying asphalt-concrete layers, as is illustrated in Figure 5.

For each cross section and mix stiffness, the principal tensile strain at the bottom of the overlay was calculated using ELSYM5 elastic layer analysis. The anticipated repetitions to failure for each case were then determined using the calculated principal tensile strain and the strain-fatigue relationships that resulted from testing, as represented in Figure 4 and Table 4. These results, and the ranking of the mixes for fatigue life for each pavement cross section, are summarized in Table 7.

The ranking of the mixes varies widely, depending on the combination of the strength of the underlying pavement, stiffness of the overlay material, and fatigue life-strain equation found for each overlay material from beam testing. For example, for all pavements with uncracked underlying asphalt-concrete, those with a 100-mm

TABLE 5 Comparison of Predicted and Measured Field Rut Depths, Field Cores

Spec	Material	AV	Wheelpath Location	Age at Coring	Rut Depth Predicted from RSST-CH (mm)	Average Field Rut at Coring * (mm)	Maximum Field Rut at Coring * (mm)
Tested at 57 C (134 F)							
B60	Virgin AC	5.1	in *	5 mos	2.5	0.7	1.2
B59	Virgin AC	4.3	in *	5 mos	2.6	0.7	1.2
B58	Virgin AC	6.5	out	5 mos	4.7	0.7	1.2
B48	RAC	3.7	in *	5 mos	2.7	1.0	1.8
B45	RAC	4.2	out	5 mos	5.5	1.0	1.8
B4	RAP	3.6	in *	5 mos	1.7	0.6	0.9
					* After 520,000 ESALs, equiv. to 534 RSST-CH reps		
Tested at 43 C (109 F)						**	**
WISF6	SMA polyolefin	9.0	in **	22 mos	4.1	1.0	2.3
WISF5	SMA polyolefin	5.9	out	22 mos	4.0	1.0	2.3
WISF3	SMA polyolefin	7.6	out	22 mos	4.1	1.0	2.3
					** After 128,000 ESALs, equiv. to 94 RSST-CH reps		

TABLE 6 Comparison of Predicted and Measured Field Rut Depths, Laboratory Specimens

Tested at 60 C (140F) Spec	Material	AV	Rut Depth Predicted from RSST-CH (mm) *	Average Field Rut at Coring (mm) *	Maximum Field Rut at Coring (mm) *
503-N1	RAP	2.8	3.8	0.6	0.9
503-N3	RAP	2.9	4.5	0.6	0.9
504-N1-3	Virgin AC	4.1	8.3	0.7	1.2
504-N1-1	Virgin AC	4.6	9.5	0.7	1.2
507-N1	Virgin AC	4.8	9.6	0.7	1.2
507-N2	Virgin AC	6.3	14.9	0.7	1.2
513-N1C	RAC	5.7	12.8	1.0	1.8
513-N1-A	RAC	5.8	10.8	1.0	1.8
514-N4-B	RAC	3.5	11.9	1.0	1.8
514-N3-A	RAC	3.9	17.2	1.0	1.8
519-N1	1.5 inch	5.2	13.0	na	na
519-N4	1.5 inch	5.9	11.6	na	na
SMAV-2-1	SMA polyolefin	10.6	16.2	na	na
SMAV-6	SMA polyolefin	10.6	17.0	na	na
SMAV-1-1	SMA polyolefin	11.8	22.2	na	na
SMAV-4	SMA polyolefin	13.1	19.6	na	na
SMAR-6	SMA a-rubber	9.5	25.1	na	na
SMAR-2-1	SMA a-rubber	10.1	24.2	na	na
SMAR-4	SMA a-rubber	11.8	42.7	na	na
SMAR-7	SMA a-rubber	12.5	33.2	na	na
			* After 520,000 ESALs, equiv. to 534 RSST-CH reps		
Tested at 43 C (109 F)					
WIS 2-3	SMA polyolefin	4.8	1.2	1.0	2.3
WIS 1-1	SMA polyolefin	4.8	1.7	1.0	2.3
WIS 5	SMA polyolefin	6.4	2.3	1.0	2.3
			* After 128,000 ESALs, equiv. to 94 RSST-CH reps		

(4-in.) overlay on thick pavements with cracked underlying asphalt-concrete, and those in which lower tensile strains would be expected at the bottom of the overlay, the 38-mm (1.5-in.) MSA base material had the greatest fatigue life. It can be seen in Figure 4 that this material has the best fatigue performance for low strain levels (below 300 microstrain). The same mix ranked fifth or sixth for the less substantial pavement structures. The Wisconsin SMA material was ranked first or second for all cases in which the underlying asphalt-concrete was cracked, which would be expected from its high stiffness (Table 4), which would tend to limit strains, and good fatigue performance at high strain levels (Figure 4).

The reliability of the fatigue curves presented must be considered when evaluating the rankings of the mixes for this study. In general, regression coefficients are high (Table 4), indicating good reliability. For those mixes with low regression coefficients, more beams would have been tested if sufficient material had been available.

Evaluation of the variance and the associated calculation of reliability for the experiment designs used here (three to five beams at two or three strain levels) has been presented by Deacon et al. (*9*). In the same report, data are presented indicating preliminary shift factors for converting fatigue beam repetitions to ESALs for different levels of in situ pavement cracking.

CONCLUSIONS AND RECOMMENDATIONS

The following conclusions and recommendations were drawn from the results presented in this paper:

- The kind of performance prediction analysis performed for this paper cannot be obtained using traditional mix design testing and analysis (i.e., Marshall and Hveem methods). In particular, tradi-

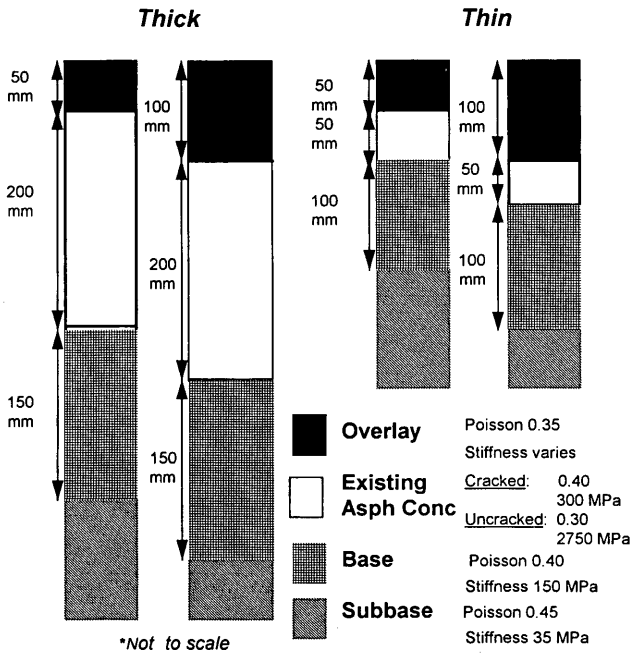

FIGURE 5 Pavement cross sections used for analysis of fatigue life.

tional mix design testing and evaluation methods allow little analysis beyond checking for minimum air-void content under standard compaction for non-conventional mixes, such as RAC and SMAs, let alone comparisons of predicted performance for conventional and nonconventional mixes.

The SHRP A-003A performance-based mix tests used in this study to evaluate permanent deformation and fatigue properties, the RSST-CH, and fatigue beam test, respectively, are sensitive to and reproducible for both conventional and nonconventional asphalt-aggregate mixes. In this study, the tests were sensitive to SMA mixes with polyolefin-modified binders and asphalt-rubber binder, dense-graded, asphalt-rubber mixes, conventional asphalt-concrete, RAP, and 38-mm (1.5-in.) MSA base material. All results followed engineering expectations and past experience and correlated with applicable field results.

- Inclusion of three different SMA mixes, all from field test sections, permitted evaluation of the sensitivity of SMA performance to several mix variables. In particular, it showed that SMA performance for both permanent shear deformation and fatigue depends on both the design and construction of the mix, and that SMA performance can be better (Wisconsin SMA) or worse (Barstow SMAs) than alternative mixes. The same can be said for any mix, including all of those evaluated in this study. There is no mix type, binder or aggregate, that cannot be made very good or very bad by the mix design or construction.

TABLE 7 Ranking of Mixes for Fatigue Life for Various Pavement Structures

Rank	Thick Pavement Uncracked Existing AC 50 mm Overlay	Thick Pavement Uncracked Existing AC 100 mm Overlay	Thin Pavement Uncracked Existing AC 50 mm Overlay	Thin Pavement Uncracked Existing AC 100 mm Overlay
1	519 38mm MSA base	519 38mm MSA base	519 38mm MSA base	519 38mm MSA base
Nf	6.05E+10	1.57E+12	1.76E+08	1.51E+09
2	503 30 % RAP	507 Virgin AC	WIS SMA polyolefin	507 Virgin AC
Nf % of # 1	0.39	0.07	12.3	1.2
3	WIS SMA polyolefin	SMAR SMA asph-rubber	507 Virgin AC	SMAR SMA asph-rubber
Nf % of # 1	0.32	0.06	7.9	1.1
4	507 Virgin AC	WIS SMA polyolefin	503 30 % RAP	SMAV SMA polyolefin
Nf % of # 1	0.29	0.04	7.5	0.9
5	SMAR SMA asph-rubber	503 30 % RAP	514 Asphalt-rubber	514 Asphalt-rubber
Nf % of # 1	0.19	0.03	2.0	0.7
6	SMAV SMA polyolefin	SMAV SMA polyolefin	SMAV SMA polyolefin	WIS SMA polyolefin
Nf % of # 1	0.10	0.02	1.4	0.6
7	514 Asphalt-rubber	514 Asphalt-rubber	SMAR SMA asph-rubber	503 30 % RAP
Nf % of # 1	0.07	0.01	0.5	0.4

Rank	Thick Pavement Cracked Existing AC 50 mm Overlay	Thick Pavement Cracked Existing AC 100 mm Overlay	Thin Pavement Cracked Existing AC 50 mm Overlay	Thin Pavement Cracked Existing AC 100 mm Overlay
1	SMAV SMA polyolefin	519 38mm MSA base	WIS SMA polyolefin	WIS SMA polyolefin
Nf	6.78E+05	2.35E+06	1.52E+05	7.48E+05
2	WIS SMA polyolefin	WIS SMA polyolefin	514 Asphalt-rubber	503 30 % RAP
Nf % of # 1	75.4	84.0	56.0	63.8
3	507 Virgin AC	503 30 % RAP	507 Virgin AC	507 Virgin AC
Nf % of # 1	48.7	57.8	51.6	44.7
4	503 30 % RAP	507 Virgin AC	503 30 % RAP	514 Asphalt-rubber
Nf % of # 1	43.7	48.9	51.4	32.4
5	514 Asphalt-rubber	514 Asphalt-rubber	SMAV SMA polyolefin	519 38mm MSA base
Nf % of # 1	42.2	30.1	24.1	23.1
6	519 38mm MSA base	SMAV SMA polyolefin	519 38mm MSA base	SMAV SMA polyolefin
Nf % of # 1	33.6	20.1	7.8	15.8
7	SMAR SMA asph-rubber	SMAR SMA asph-rubber	SMAR SMA asph-rubber	SMAR SMA asph-rubber
Nf % of # 1	11.3	10.0	5.2	3.6

- From the previous conclusions, the critical need for performance-based tests and analysis, such as those used for this study, is obvious. Without them, there are too many possible combinations of aggregate, binder, modifier, gradation and binder content, and in situ conditions (temperature, existing pavement, etc.) to estimate in situ mix performance with adequate precision to be able to determine the most cost-effective mix for a given project.
- Effects of aging and traffic densification on permanent shear deformation resistance were demonstrated. To improve the rut depth and fatigue life predictions developed in this study, a better understanding of the effects of in situ aging and moisture damage on the stiffness, fatigue, and permanent deformation properties of the mix is needed.
- The desirability of compacting specimens in the laboratory using methods that duplicate in situ aggregate orientation, aggregate interparticle contact, and asphalt-aggregate interfaces is acknowledged. The rolling wheel compactor used in this study allowed the preparation of both fatigue beams and RSST-CH specimens with performance characteristics similar to those produced by field compaction.
- The permanent deformation analysis procedure demonstrated in this study produced results that follow engineering expectations and correlated well with available field data. In all cases, results were somewhat conservative.
- The fatigue analysis procedure demonstrated in this study showed that fatigue life and flexural stiffness must be evaluated together within a mechanistic analysis of the pavement in order to determine the best mix for a project. The mechanistic analysis used in this study, linear elastic layer theory, can be improved upon, but the need for mechanistic analysis to determine the best mix for a given project is clear.
- Confining pressures of up to 68.9 kPa (10 psi) have little or no effect on RSST-CH results. To evaluate permanent shear deformation for the mix design of dense-graded mixes, it is recommended that specimens be compacted to the minimum air-void content expected in the field after traffic densification, approximately 3.0 percent (measured using parafilm) for most dense-graded mixes. Little data have been evaluated regarding critical air-void contents for open-graded mixes. It is recommended that specimens for these mixes be compacted to the air-void content expected after densification caused by initial trafficking.

ACKNOWLEDGMENTS

The authors thank the Institute of Transportation Studies, University of California at Berkeley (UCB) for its support of this study. The kind help of the following agencies, companies, and individuals is also greatly appreciated: California Department of Transportation (TransLab and District 8 Laboratory and Maintenance crews), Wisconsin Department of Transportation, Joseph Vicelja, the Strategic Highway Research Program, Nichols Consulting Engineers, Akhtar Tayebali, Daniel Sosnovske, and the laboratory staff at the UCB Asphalt Research Program.

REFERENCES

1. Sousa, J., A. Tayebali, J. Harvey, P. Hendricks, and C. L. Monismith: Sensitivity of SHRP A-003A Proposed Testing Equipment to Mix Design Parameters for Permanent Deformation and Fatigue. In *Transportation Research Record 1384,* TRB, National Research Council, Washington, D.C., 1993.
2. Tayebali, A., J. Deacon, J. Coplantz, J. Harvey, and C. L. Monismith. Mixture and Mode-of-Loading Effects on Fatigue Response of Asphalt-Aggregate Mixtures. Presented at the Annual Meeting of the Association of Asphalt Paving Technologists, 1994.
3. Harvey, J., and C. L. Monismith. Effects of Laboratory Asphalt-Concrete Specimen Preparation Variables on Fatigue and Permanent Deformation Test Results Using SHRP A-003A Proposed Testing Equipment. In *Transportation Research Record 1417,* TRB, National Research Council, Washington, D.C., 1993.
4. *Standard Practice for Preparation of Bituminous Mixture Test Specimens by Means of Rolling Wheel Compactor.* Interim Proposed Standard Practice Specification. SHRP A-003A, Washington, D.C., May 12, 1992.
5. Harvey, J., J. Sousa, J. Deacon, and C. L. Monismith. Effects of Sample Preparation and Air-Void Content on Asphalt Concrete Properties. In *Transportation Research Record 1317,* TRB, National Research Council, Washington, D.C., 1991.
6. Sousa, J. Asphalt-Aggregate Mix Design Using the Simple Shear Test (Constant Height). Presented at the Association of Asphalt Paving Technicians Annual Meeting, 1994.
7. Solaimanian, M., and T. Kennedy. Predicting Maximum Pavement Surface Temperature Using Maximum Air Temperature and Hourly Solar Radiation. In *Transportation Research Record 1417,* TRB, National Research Council, Washington, D.C., 1993.
8. Harvey, J., C. L. Monismith, and J. Sousa. An Investigation of Field- and Laboratory-Compacted Asphalt-Rubber, SMA, Recycled and Conventional Asphalt-Concrete Mixes Using SHRP A-003A Equipment. Presented at the Association Annual Meeting of Asphalt Paving Technicians 1994.
9. Deacon, J. A., A. A. Tayebali, J. S. Coplantz, F. N. Finn, and C. L. Monismith. *Fatigue Response of Asphalt-Aggregate Mixtures, Part III—Mixture Design and Analysis.* Prepared for Strategic Highway Research Program, Project A-003A. Institute of Transportation Studies, University of California, Berkeley, May 1993.
10. Sousa, J., and M. Solaimanian. Abridged Procedure to Determine Permanent Deformation of Asphalt Concrete Pavements. Presented at the 73rd Annual Meeting of the Transportation Research Board, Washington, D.C., 1994.
11. Sousa, J., et al. *Permanent Deformation Response of Asphalt-Aggregate Mixes.* Prepared for Strategic Highway Research Program, Project A-003A. Institute of Transportation Studies, University of California, Berkeley, March 1994.

The views expressed in this paper are those of the authors and do not necessarily reflect those of the agencies, companies, or individuals who supported the study.

Publication of this paper sponsored by Committee on Characteristics of Bituminous Paving Mixtures To Meet Structural Requirements.

Five-Year Evaluation of HMA Properties at the AAMAS Test Projects

DOUGLAS I. HANSON, RAJIB BASU MALLICK, AND ELTON RAY BROWN

To evaluate the process of densification in hot mix asphalt (HMA) pavements and its effect on laboratory properties, the National Center for Asphalt Technology at Auburn University initiated a performance study. It was to be a follow-up study to the Asphalt-Aggregate Mixture Analysis System (AAMAS), developed in the late 1980s. The first phase involved collection and analysis of data from 5-year-old pavements on AAMAS projects. Changes in HMA properties with time were evaluated. Pavement densification was found to continue after 2 years of traffic. Sections with higher initial voids showed greater changes in properties with time. For the first 2 years after construction, properties of HMA mixes were found to be affected significantly by changes in air voids; values of tensile strength and resilient modulus increased with a decrease in voids. Tensile-strain-at-failure values decreased continuously with time. In a majority of cases, 5-year in-place voids were found to be less than mix design voids. Densification generally increased with traffic during the 5-year investigation.

Several studies (*1–3*) indicate that air-void content substantially affects other properties of hot mix asphalt (HMA). To design HMA properly and to avoid distresses in pavements, it is necessary to understand and evaluate changes in air voids under actual field conditions. Changes in other engineering properties of mixes should be evaluated also, as these can be affected by air voids.

This study is a follow up of a larger, overall study that was developed by Von Quintas et al. (4) in the late 1980s the Asphalt-Aggregate Mixture Analysis System (AAMAS). The authors present the changes of properties of pavement mixes as noted from five different projects over a period of 5 years.

BACKGROUND

Part of the broad-based AAMAS study was to establish field-paving projects in different parts of the country and observe changes in the properties of HMA mixes for a period of 2 years. Properties of initial in-place mixes were compared with laboratory-compacted mixes to evaluate laboratory compaction devices. Laboratory specimens were prepared by compactive efforts to match the air-void levels measured in the field immediately after construction. By excluding the effect of difference in air voids between the laboratory specimens and the field cores, the difference in engineering properties between the specimens and the cores was related to the type of compaction device used. By statistical analysis of results from tests on cores and specimens, the earlier study concluded that the Texas gyratory compactor specimens best matched the field cores (*4*). However, one question remained: How do a mixture's properties change as the mix approaches refusal air-void content or density? The AAMAS study evaluated (*4*) changes in mix properties for 2 years. A longer time frame may be required to evaluate changes of mix properties that occur with time.

National Center for Asphalt Technology, 211 Ramsay Hall, Auburn University, Ala. 36849-5354.

OBJECTIVE AND SCOPE

The objective of this paper is to evaluate the changes in HMA properties with time. To achieve that purpose, we obtained field data from 5 AAMAS projects 5 years after their construction.

Field cores were obtained after 5 years of traffic from test sections in the five projects that comprised the AAMAS study. Air voids, indirect tensile strength, tensile strain at failure, and resilient modulus properties of the cores were measured. Data from the 5-year-old cores were compared with the 0 and 2-year data related to cores taken from the same test sections by AAMAS (*4*).

TEST SECTIONS

Table 1 provides a summary of each of the AAMAS test projects including traffic data. Type, depth, and thickness of each of the pavement sections are shown. Detailed discussions are found elsewhere (*4*). Twenty-one cores were taken at random from each of the sections, which were about 300 ft long. Cores were extracted in the same manner they were for the original AAMAS study. The same number of cores was taken from inside, outside, and between the wheel paths. Two sections in each project site were compacted by different rollers at construction. Air-void data from both of the test sections are presented in Table 2. Designated as the standard test sections by AAMAS, other properties were evaluated for those sections only. The breakdown roller used on the standard section was the same as that used over the entire project.

TEST PLAN

Field cores were obtained from the five projects originally used for the AAMAS study (*4*). Cores of 4 and 6 in. were obtained using diamond core barrels from two test sections at each site. Cores were obtained randomly from three lines parallel to the centerline from three locations: inside, outside, and between the wheel paths. The difference in air-void contents of cores from different wheel paths was not found significant, and hence the cores were combined into a single lot for tests. Twenty-one cores were taken from each section: fifteen 4-in. and 6-in. cores were taken. Only the 4-in. cores were used for this part of the study, however.

Figure 1 shows the laboratory test plan. In the laboratory, the cores were used for various tests according to applicable standard ASTM procedures. The Virginia cores were sawed to 50.8 mm (2 in.) thicknesses before testing. Air voids were determined from tests for bulk gravity (ASTM D726) and theoretical maximum density

TABLE 1 Description of AAMAS Test Sections

State Project	Colorado CO-009	Michigan MI-0021	Texas TX-0021	Virginia VA-0621	Wyoming WY-0080
Type of Section	Lower Surface Course	Surface course	Base course	Base Course	Lower Surface Course
Average Thickness of Section (mm)	34.2	45.7	71.6	96.5	55.3
Depth from Surface (mm)	57.1	0.00	76.2	>100.0	50.8
Roller Compaction					
Section VB/SS	Vibratory roller breakdown, static steel wheel roller finish	Vibratory roller breakdown, static steel wheel roller finish	Vibratory roller breakdown, static steel wheel roller finish	Vibratory roller breakdown, static steel wheel roller finish	Vibratory roller breakdown, static steel wheel roller finish
Section PB/SS	Pneumatic rubber-tired roller breakdown, static steel wheel roller finish	Pneumatic rubber-tired roller breakdown, static steel wheel roller finish	------	------	Pneumatic rubber-tired roller breakdown, static steel wheel roller finish
Section SB/PS	------	------	Static steel wheel roller breakdown, rubber-tired roller and static steel wheel roller finish	-------	------
Section SB/SS	------	------	------	Static steel wheel roller breakdown and finish	------
Standard Section	VB/SS	PB/SS	SB/PS	VB/SS	VB/SS
Average Annual Daily Traffic (AADT) (1991 data)	1700	11,100	11,410	680	9630
Percent Commercial Vehicle	3.5	6	10	10	44
Estimated Total ESAL (in millions)					
2 year	0.01	0.16	0.26	0.01	0.96
5 year	0.03	0.42	0.69	0.04	2.57

------ Section not used in project
ESAL - 18-kip single axle load
1 inch = 25.4 mm

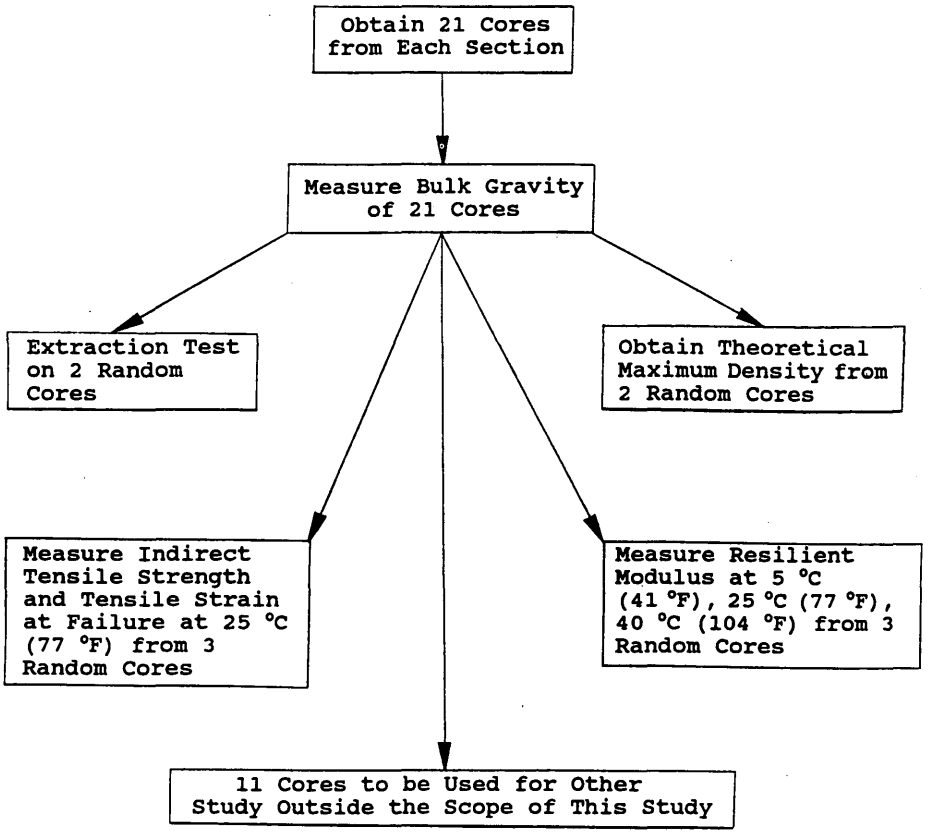

FIGURE 1 Laboratory test plan.

(ASTM D2041). Three random samples were then used to determine indirect tensile strength and tensile strain at failure (ASTM D4123) at 25°C (77°F). Another set of three samples was used to determine resilient modulus (ASTM D4123) at 5°C (41°F), 25°C (77°F), and 40°C (104°F). Other tests included gradation and asphalt content determination by extraction. Because of a shortage of materials, resilient modulus testing was not done on the Michigan cores. Test results were compared with those obtained at construction from in-place samples and after 2 years of traffic (*4*).

RESULTS

A summary of the results from tests on pavement cores at different times after construction is provided in Tables 2–6. Results of air voids, indirect tensile, and resilient modulus properties are compiled in Tables 2–4. Table 6 shows the asphalt content and aggregate gradations measured from the cores recovered at different times after construction. The results on 0- and 2-year cores were obtained from the AAMAS study.

ANALYSIS AND DISCUSSION

Change of HMA Properties with Time

Mix properties include air voids, indirect tensile strength at 25°C (77°F), tensile strain at failure at 25°C (77°F), and resilient modulus at 5°C (41°F), 25°C (77°F), and 40°C (104°F). Because the cores were tested at a different laboratory, interlaboratory variation and the use of different apparatus account for at least some of the difference in properties. Discussed are changes in such mix properties with time.

Air Voids

A summary of air voids data obtained 0, 2, and 5 years after construction is presented in Table 2. The AAMAS study (*4*) reported significant differences between the voids of 0- and 2-year sections. In the present study, *t* tests were performed (with an alpha value of 0.05) with the 2- and 5-year core data to observe any significant difference in voids. Table 7 shows a summary of the *t* test results. In 20 out of 30 cases analyzed, the air voids of the 5-year sections were found to differ significantly from those of the 2-year sections. As expected, in 16 out of the 20 cases, the voids after 5 years were found to be lower than those after 2 years.

Figure 2 shows the change in air voids of different sections with time. The Texas SB/PS and Virginia VB/SS sections showed the highest void changes with time. These two sections were also located in warmer parts of the country where climate might facilitate quicker compaction. The Colorado and Wyoming sections show an increase in voids. The observed difference in voids may be related to a difference in theoretical maximum density values used for calculation of voids at 2 and 5 years. Absorption of asphalt, as suggested by a decrease in asphalt content from extraction results, and

TABLE 2 Summary of Air Voids Data

Type of Specimens	AIR VOIDS (%)				
	PROJECT				
	COLORADO	MICHIGAN	TEXAS	VIRGINIA	WYOMING
MIX DESIGN	4.20	2.80	6.00	5.00	5.00
Initial In-Place	(2.4759)	(2.4748)	(2.4393)	(2.7361)	(2.4516)
VB/SS	8.19	3.74	10.17	5.85	5.77
PB/SS	8.98	4.21	—	—	8.37
SB/PS	—	—	8.75	—	—
SB/SS	—	—	—	7.44	—
Two Year In-Place	(2.4759)	(2.4748)	(2.4343)	(2.7361)	(2.4516)
VB/SS	6.18	2.33	9.38	5.25	4.66
PB/SS	6.26	2.88	—	—	6.50
SB/PS	—	—	7.07	—	—
SB/SS	—	—	—	5.91	—
Five Year In-Place	(2.487)	(2.487)	(2.399)	(2.694)	(2.447)
VB/SS	7.48	2.55	5.55	3.64	4.71
PB/SS	7.47	2.76	—	—	6.51
SB/PS	—	—	3.84	—	—
SB/SS	—	—	—	3.07	—

— Sections not used in project

*NOTE: Numbers in parentheses indicate respective theoretical maximum specific gravities.

TABLE 3 Summary of Indirect Tensile Strength (kPa) Data (25°C)

TYPE OF SPECIMENS	INDIRECT TENSILE STRENGTH (kPa)				
	PROJECT				
	COLORADO	MICHIGAN	TEXAS	VIRGINIA	WYOMING
Mix Design	----	----	----	----	----
Initial In-Place					
VB/SS	621	---	---	1545	986
PB/SS	---	621	---	---	---
SB/PS	---	---	821	---	---
SB/SS	---	---	---	---	---
Two Year In-Place					
VB/SS	483	---	---	1262	1269
PB/SS	---	600	---	---	---
SB/PS	---	---	1718	---	---
SB/SS	---	---	---	---	---
Five Year In-Place					
VB/SS	462	---	---	600	1159
PB/SS	---	600	---	---	---
SB/PS	---	---	1531	---	---
SB/SS	---	---	---	---	---

--- Section not used in project or not a standard section

1 ksi = 6.89 KPa

TABLE 4 Summary of Tensile Strain at Failure Data (25°C)

TYPE OF SPECIMENS	TENSILE STRAIN AT FAILURE (MILS/MM)				
	PROJECT				
	COLORADO	MICHIGAN	TEXAS	VIRGINIA	WYOMING
Mix Design	---	---	---	---	---
Initial In-Place					
VB/SS	15.4	---	---	6.9	6.4
PB/SS	---	14.5	---	---	---
SB/PS	---	---	9.0	---	---
SB/SS	---	---	---	---	---
Two Year In-Place					
VB/SS	1.2	---	---	1.5	1.4
PB/SS	---	5.9	---	---	---
SB/PS	---	---	2.2	---	---
SB/SS	---	---	---	---	---
Five Year In-Place					
VB/SS	1.7	---	---	1.8	2.4
PB/SS	---	3.5	---	---	---
SB/PS	---	---	2.5	---	---
SB/SS	---	---	---	---	---

--- Section not used in project or not a standard section

1 MILS/INCH = 1 MILS/MM

TABLE 5 Summary of Resilient Modulus (10^3MPa) Data

TYPE OF SPECIMENS	RESILIENT MODULUS (10^3 MPa)														
	PROJECT														
	COLORADO			MICHIGAN			TEXAS			VIRGINIA			WYOMING		
TEMPERATURE	5°C	25°C	40°C	5°C	25°C	40°C	5°C	25°C	40°C	5°C	25°C	40°C	5°C	25°C	40°C
Mix Design	---	---	---	---	---	---	---	---	---	---	---	---	---	---	---
Initial In-Place															
VB/SS	11.0	4.0	2.3	---	---	---	---	---	---	23.0	6.4	1.7	14.0	4.9	1.4
PB/SS	---	---	---	16.0	3.1	1.1	---	---	---	---	---	---	---	---	---
SB/PS	---	---	---	---	---	---	30.0	8.9	1.6	---	---	---	---	---	---
SB/SS	---	---	---	---	---	---	---	---	---	---	---	---	---	---	---
Two Year In-Place															
VB/SS	25.0	3.9	1.9	---	---	---	---	---	---	14.0	8.6	2.5	22.0	7.5	2.1
PB/SS	---	---	---	12.0	3.0	1.0	---	---	---	---	---	---	---	---	---
SB/PS	---	---	---	---	---	---	28.0	10.3	3.0	---	---	---	---	---	---
SB/SS	---	---	---	---	---	---	---	---	---	---	---	---	---	---	---
Five Year In-Place															
VB/SS	4.0	1.9	0.3	---	---	---	---	---	---	16.0	2.6	0.5	12.0	3.5	0.8
PB/SS	---	---	---	---	---	---	---	---	---	---	---	---	---	---	---
SB/PS	---	---	---	---	---	---	37.0	9.9	1.2	---	---	---	---	---	---
SB/SS	---	---	---	---	---	---	---	---	---	---	---	---	---	---	---

--- Section not used in project or not a standard section

1 ksi = 6.89 MPa

TABLE 6 Summary of Aggregate Gradation and Asphalt Content Data

Aggregate property	Colorado JMF	Colorado EX1	Colorado EX2	Michigan JMF	Michigan EX1	Michigan EX2	Texas JMF	Texas EX1	Texas EX2	Virginia JMF	Virginia EX1	Virginia EX2	Wyoming JMF	Wyoming EX1	Wyoming EX2
Sieve Size															
2	---	---	---	---	---	---	---	---	---	---	---	---	---#	---	---
1 1/2	---	---	---	---	---	---	---	---	---	100	---	---	---	---	---
1	---	---	---	---	---	100	100	100	---	---	98.8	100	---	100	100
3/4	100	100	100	100	100	92.4	94.1	96.5	100	85.0	85.6	93.1	---	95.6	91.2
1/2	93.4	90.0	93.9	92.2	88.8	81.2	77.1	81.6	89.2	---	68.3	74.4	---	72.0	76.7
3/8	68.	75.0	83.8	79.9	75.8	72.3	67.6	70.0	77.4	---	60.2	69.2	---	63.3	66.3
No. 4	45.5	53.0	61.2	60.9	53.2	52.6	51.9	54.2	63.0	46.0	46.5	50.4	---	40.0	46.1
No. 8	32.2	38.0	44.0	47.4	48.6	37.6	33.7	40.0	51.9	34.0	35.6	38.8	---	29.0	32.6
No. 16	23.8	---	32.8	---	37.0	30.4	---	34.3	42.1	---	---	29.8	---	22.0	25.0
No. 30	17.5	---	24.7	24.9	26.0	25.5	23.0	30.8	33.0	---	19.4	21.6	---	17.6	20.2
No. 50	11.2	14.0	17.5	---	14.0	18.6	19.2	27.8	23.1	---	12.1	13.3	---	13.2	15.8
No. 100	7.7	---	10.9	---	7.0	9.4	---	15.3	16.3	---	---	8.3	---	9.0	11.3
No. 200	4.9	6.0	6.7	5.3	4.0	3.7	2.7	6.8	13.6	5.5	5.6	5.7	---	5.5	7.3
Asphalt Content	5.5	5.0	4.6	4.9	5.3	5.1	5.5	5.5	5.0	4.5	4.5	4.9	2.7*	4.7*	3.6*
Placement Temperature, °C	137			137			154			137			135		

JMF Job Mix Formula from State Highway Agency

EX1 Extraction done by AAMAS (4) from bulk mixture samples at the plant during production of mix

EX2 Extraction done in the present study from five year old pavement cores

Data not available

* JMF indicates new asphalt added to recycled mix, EX1 and EX2 show total asphalt content

1 °C = 0.55 (°F-32)

stripping may also be responsible for this increase in voids. A substantial amount of stripping was observed in the cores from Colorado and Wyoming. The average density of the 2-year Colorado cores was found to be slightly higher than that of the 5-year cores. This difference may be the result of differences in sampling patterns or reflect actual loss in density between 2 and 5 years. As expected, the rate of change in voids is seen to be higher in the first 2 years (Figure 2).

Indirect Tensile Strength at 25°C (77°F)

A summary of indirect tensile strength at 25°C (77°F) from cores obtained at different times after construction is presented in Table 3; Figure 3 shows the changes with time.

In the case of Texas and Wyoming, the values increased for the first 2 years and then decreased slightly for the next 3 years. The increase may be related to the significant decrease in voids with time. However, the voids decreased rapidly with time in Michigan, and the indirect tensile strength of those cores did not change significantly with time. This indicates that mixes with higher initial voids had greater tendency for mixture properties to change with time, considering that the initial voids in the Texas and Wyoming cores were considerably higher than those from Michigan. In the cases of the Colorado and Virginia cores, indirect tensile strength decreased with time. Moisture damage may be the reason for this decrease. The AAMAS study observed that aggregates used in the Colorado and Virginia projects were susceptible to moisture damage, and that, during construction of the Colorado project, the mixture became wet when rain fell before and during the compaction process (*4*). A plot of average tensile strength with time is presented in Figure 3. After 2 years, a slight decrease occurred. Because densification and oxidation slow down after 2 years, the change in indirect tensile strength is expected to be less.

Tensile Strain at Failure at 25°C (77°F)

A summary of tensile strain at failure at 25°C (77°F) from cores obtained at different times after construction is presented in Table 4.

A significant decrease in values was observed for the first 2 years. The Colorado and the Texas sections, which had the highest initial voids, showed the greatest change with time. This was expected because a greater number of voids result in greater hardening of asphalt. Despite low initial voids, the Michigan section showed a considerable decrease in tensile strain values also. The combined effect of voids and aging binder may be responsible for the decrease in tensile-strain-at-failure values with time. As may be noted from Figure 4, the values remained almost constant between the second and fifth years after construction.

Resilient Modulus at 5°C (41°F)

A summary of resilient modulus at 5°C (41°F) from cores obtained at different times after construction is presented in Table 5. Five-year resilient modulus data are not presented for Michigan cores; testing was not done because of a shortage of materials.

TABLE 7 Summary of T Tests on Air Voids from 2- and 5-Year Cores

Project	Section	Wheelpath	Results of T Tests Between Air Voids of 2 and 5 Year Old Cores		
			DF	P	Result
Colorado	VB/SS	RWP	14.0	0.2596	NOT DIFFER
		LWP	12.0	0.0000	DIFFER
		BWP	8.0	0.4584	NOT DIFFER
	PB/SS	RWP	7.5	0.0106	DIFFER
		LWP	12.0	0.0001	DIFFER
		BWP	10.0	0.0119	DIFFER
Michigan	VB/SS	RWP	12.0	0.1519	NOT DIFFER
		LWP	12.0	0.8664	NOT DIFFER
		BWP	7.4	0.9392	NOT DIFFER
	PB/SS	RWP	12.0	0.1749	NOT DIFFER
		LWP	12.0	0.0284	DIFFER
		BWP	12.0	0.0305	DIFFER
Texas	VB/SS	RWP	6.4	0.0012	DIFFER
		LWP	13.0	0.0024	DIFFER
		BWP	13.0	0.0001	DIFFER
	SB/PS	RWP	15.0	0.0000	DIFFER
		LWP	14.0	0.0000	DIFFER
		BWP	15.0	0.0001	DIFFER
Virginia	VB/SS	RWP	11.0	0.0240	DIFFER
		LWP	10.0	0.0000	DIFFER
		BWP	9.0	0.0011	DIFFER
	SB/SS	RWP	9.0	0.0001	DIFFER
		LWP	10.0	0.0000	DIFFER
		BWP	7.0	0.0141	DIFFER
Wyoming	VB/SS	RWP	12.0	0.3525	NOT DIFFER
		LWP	12.0	0.1285	NOT DIFFER
		BWP	12.0	0.2264	NOT DIFFER
	PB/SS	RWP	12.0	0.0243	DIFFER
		LWP	12.0	0.0301	DIFFER
		BWP	12.0	0.4243	NOT DIFFER

RWP right wheel path
LWP left wheel path
BWP between wheel path
DF Degree of freedom
P Probability
Alpha = 0.05

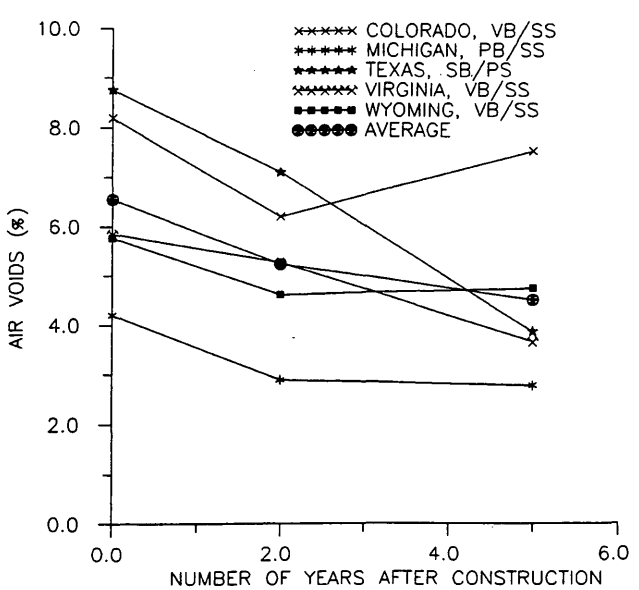

FIGURE 2 Change in percentage air voids with time.

In Colorado and Wyoming, resilient modulus values increased for the first 2 years and then decreased considerably. The pattern in Colorado may be related to change in air voids, which decreased for the first 2 years and then increased. In Texas, the values remained constant for the first 2 years despite a decrease in voids during that period. In the next 3 years, the modulus values increased considerably with a corresponding decrease in voids. In the case of Virginia, the modulus values decreased for the first 2 years, possibly because of damage to the asphalt mixture caused by moisture-susceptible aggregates. Greater changes are observed in the first 2 years than in the later 3 years.

Resilient Modulus at 25°C (77°F)

A summary of resilient modulus at 25°C (77°F) from cores obtained at different times after construction is presented in Table 5; Figure 5 shows the changes of values with time.

In all cases, the values either increased or remained constant during the first 2 years. In the case of Colorado, the values remained constant for the first 2 years despite a decrease in voids. In the next

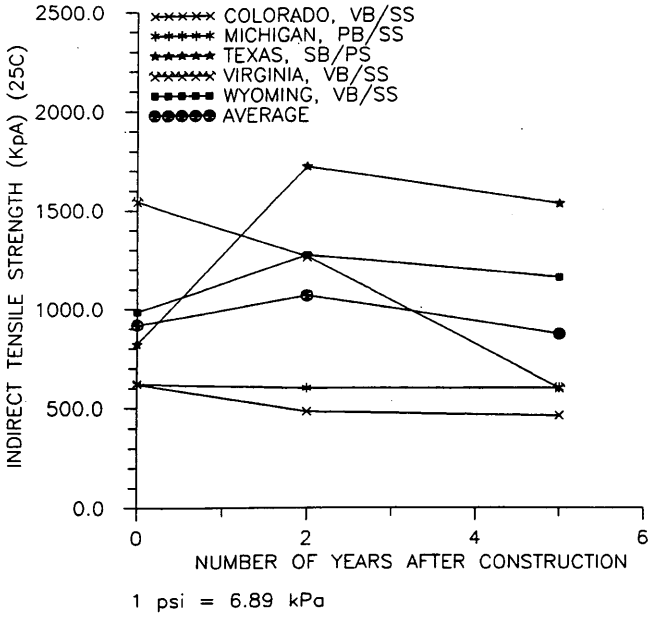

FIGURE 3 Change in indirect tensile strength with time.

3 years, the values dropped considerably with a simultaneous increase in voids. The reason for the decrease may be the use of moisture-susceptible aggregates in the mix. In Texas, the values increased considerably, with an accompanying decrease in voids, and then decreased slightly for the next 3 years, even though the decrease in voids continued. The decrease may be related to a decrease of air voids below optimum and a corresponding decrease in indirect tensile strength during that period. In Virginia, the values increased considerably in the first 2 years and then dropped below the original values in the next 3 years. Use of moisture-susceptible aggregates may have some influence on the decrease of modulus values. In Wyoming, the values increased considerably in the first 2 years with a corresponding decrease in voids. However, for the next 3 years the values dropped considerably, with a simultaneous drop in tensile strength values. A lowering of asphalt content from absorption or stripping may be the reason for this decrease. A plot of average values with time is presented in Figure 5. The pattern of change in resilient modulus is similar to that of indirect tensile strength.

Resilient Modulus at 40°C (104°F)

A summary of resilient modulus at 40°C (104°F) data obtained from cores recovered at different times after construction is provided in Table 5; Figure 5 shows the changes in values with time.

All the sections except Colorado showed an increase in values for the first 2 years, with a corresponding decrease in voids. The mixes having higher initial voids had higher changes with time. In the next 3 years, the values dropped in all the cases. This decrease may be the result of mixture damage caused by a combined action of moisture and aging.

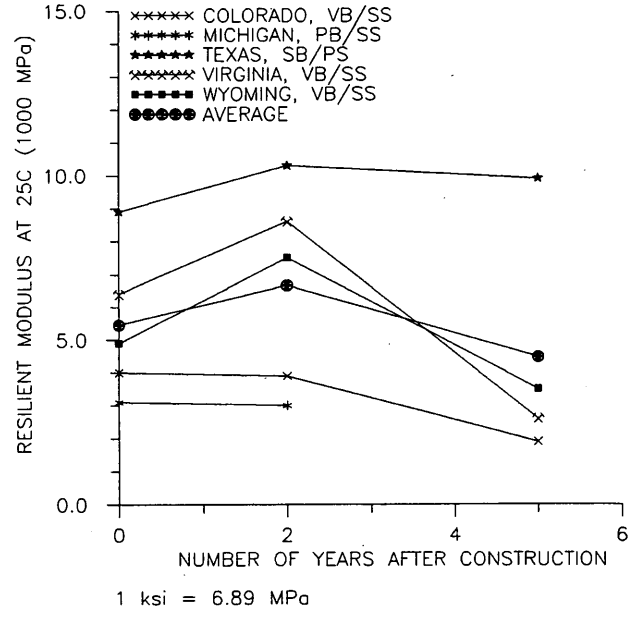

FIGURE 4 Change in resilient modulus at 25°C with time.

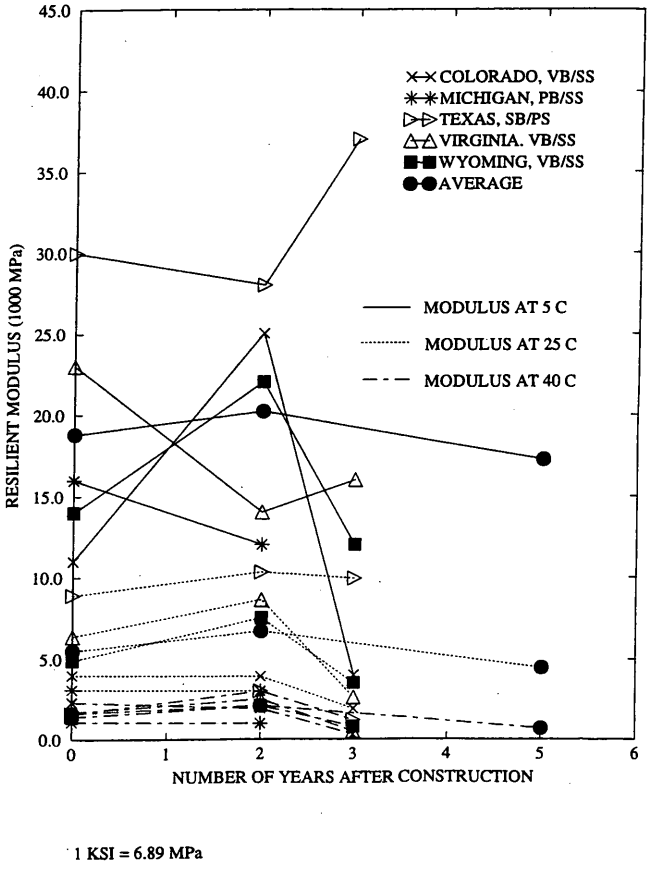

FIGURE 5 Change of resilient modulus with time.

Comparison of Five-Year In-Place Air Voids with Mix Design Voids

A summary of mix-design and 5-year in-place air voids is presented in Table 2; a graphic comparison is presented in Figure 6. Table 1 shows the average annual daily traffic on the different sections. In most cases, the in-place voids are found to be lower than the mix design voids. In Michigan, which had the lowest initial voids, the 5-year voids are found to be equal to the mix design voids. In Colorado, the 5-year voids were greater than mix-design voids, possibly because of moisture damage and related stripping of mixes. It may also be related to very low traffic. As may be observed from the figure, the Texas and Virginia sections have considerably lower air voids than the corresponding mix-design voids. Such high densification may be the result of high temperature in areas in which those sections are located. It may also be caused by changes in mixtures or improper compactive effort in mix design.

Changes of Air Voids with Traffic

Traffic compaction is an important part of the densification process in HMA pavements. Plots of changes in air voids with traffic between 0 and 2 years and between 0 and 5 years are presented in Figures 7 and 8. Traffic is expressed as total equivalent 18-kips single-axle loads in millions, and pavement densification is represented by a ratio of the difference between in-place (2 or 5 year) and original voids and the difference between original and mix design voids. The denominator is the estimated potential change in voids, and the numerator is the actual change in voids to date. A number of 100 percent would mean that the in-place voids were equal to the mix-design voids. Figure 7 shows an increase in densification with an increase in traffic. In a work by Brown and Cross (*5*) similar correlations were obtained. Figure 8 shows a wide scatter in the data, however, even though the trend for increase in densification with increase in traffic is clearly visible.

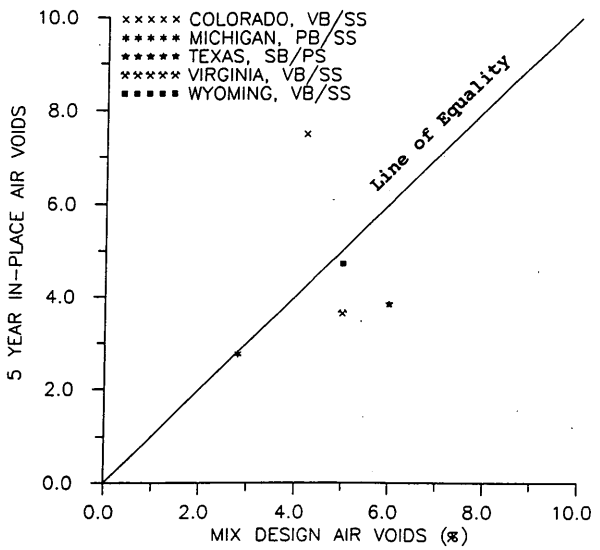

FIGURE 6 Comparison of 5-year in-place and mix design air voids.

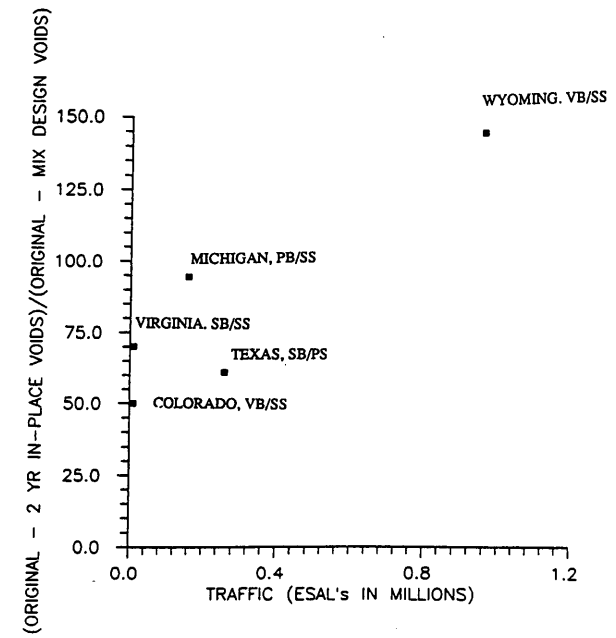

FIGURE 7 Plot of densification versus traffic 2 years after construction.

CONCLUSIONS

On the basis of this study the following conclusions can be made:

- Densification of pavements continues beyond 2 years after construction. In this study, substantial differences in air voids were found between the 2- and 5-year sections.

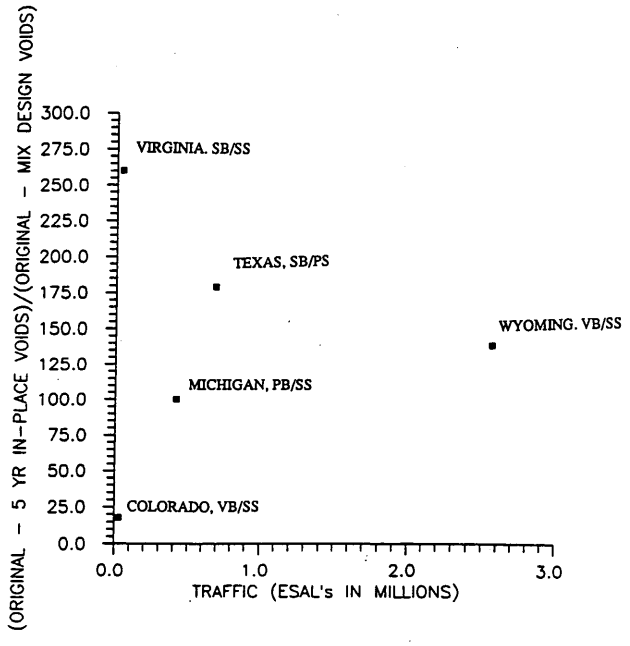

FIGURE 8 Plot of densification versus traffic 5 years after construction.

- Sections with higher initial (at construction) voids have higher rates of void change.
- Tensile strength values increase as air voids decrease; however, the increment may be dependent on initial air voids. Mixes with moisture-susceptible aggregates may suffer a decrease in strength with time.
- Tensile strain at failure values (77°F) for HMA mixes decreases with time, with a sharp decrease within 2 years of construction, and little change between 2 and 5 years.
- There is an increase in resilient modulus at 41F°, 77F°, and 104°F values, with a corresponding decrease in air voids within the first 2 years of construction. After 2 years, the pattern of changes of modulus values is not clear, and it is possibly influenced by a combination of factors like change in voids, moisture damage, and aging.
- In most cases, after 5 years, in-place voids were less than the mix design voids.
- Densification of HMA pavements is substantially influenced by traffic. As traffic increases, the HMA continues to densify—but at a slower rate with time.

RECOMMENDATIONS

On the basis of this study the following recommendations are made regarding further research:

- Densification studies should be carried out with surface courses and heavy traffic-volume pavements for a period of 3 to 4 years to determine changes in various properties of HMA with time and to evaluate the effects of various factors on such changes.
- Available SHRP binder equipment should be used to observe changes in binder properties with time, and to correlate changes in binder properties with changes in HMA properties.

REFERENCES

1. Tunnicliff, D. G., and R. E. Root. *NCHRP Report 274: Use of Antistripping Additives in Asphaltic Concrete Mixtures—Laboratory Phase.* TRB, National Research Council, Washington, D.C., 1984.
2. Powell, W. D., N. W. Lister, and D. Leech. Improved Compaction of Dense Graded Bituminous Macadams. *Proc. Association of Asphalt Paving Technologists,* Vol. 50, St. Paul, Minn., 1981.
3. Huber, G. A., and G. H. Heiman. Effects of Asphalt Concrete Parameters on Rutting Performance: A Field Investigation. *Proc., Association of Asphalt Paving Technologists,* Vol. 57, St. Paul, Minn., 1987.
4. Von Quintas, H. L., J. A. Scherocman, C. S. Hughes, and T. W. Kennedy. *NCHRP Report 338, Asphalt-Aggregate Mixture Analysis System (AAMAS).* TRB, National Research Council, Washington, D.C., 1991.
5. Brown, E. R., and S. A. Cross. Comparison of Laboratory and Field Density of Asphalt Mixtures. In *Transportation Research Record 1300,* TRB, National Research Council, Washington, D.C., 1991.

Publication of this paper sponsored by Committee on Characteristics of Bituminous Paving Mixtures To Meet Structural Requirements

Rational Method for Laboratory Compaction of Hot-Mix Asphalt

PHILLIP B. BLANKENSHIP, KAMYAR C. MAHBOUB, AND GERALD A. HUBER

The study *Gyratory Compaction Characteristics: Relation to Service Densities of Asphalt Mixtures* was initiated by the Asphalt Institute for the Strategic Highway Research Program (SHRP), contract A001. N_{Design} is defined as the compactive effort (number of gyrations at a specific pressure) at which air-void level is measured for volumetric design. To determine the number of gyrations (N_{Design}) required to represent various traffic levels in different climates, an experiment was conducted. Once it is shown that gyrations (N_X) must relate to traffic levels (E_X) and once the design gyrations are known, one simply can enter the design gyration (N_{Design}), representing 20-year design traffic, into the compaction curve of the new mix design to obtain the final percent compaction (C_X) of that mix; the target is 96 percent of maximum theoretical specific gravity (MSG). Thus, one can say, at that specific traffic level (gyration) and climate, the mix will compact to C_X of the given MSG.

Asphalt mixture design has been evolving since the early 1900s, from a rule-of-thumb approach to the mixture design system developed under the Strategic Highway Research Program (SHRP). One of the first rule-of-thumb tests for choosing an asphalt cement (AC) content was the Pat Test. It consisted of placing the asphalt concrete mixture on a piece of brown manila paper and determining the optimum AC content from the residual stain (*1*). Since the earliest attempt at mixture design, the objective has always been to mix, compact, and test asphalt mixture in the laboratory to determine its expected performance in service.

Designing an asphalt concrete mixture consists of selecting the proper aggregate blend and the optimum AC content, such that the mix is as durable as possible, yet stable (*2*). The most critical factor is the AC content, because a deviation from the optimum AC of 0.5 percent could result in either too much or too little AC. Too much asphalt produces a mixture with low air voids that is susceptible to rutting and flushing. Low AC content produces a mixture that under-compacts (has high air voids) and is likely to ravel. Indeed, the optimum AC content is the most difficult variable to set in a mix design.

Compaction of an asphalt concrete mixture is defined as ". . . a stage of construction which transforms the mix from its very loose state into a more coherent mass, thereby permitting it to carry traffic loads . . . the efficiency of the compactive effort will be a function of the internal resistance of the bituminous concrete. This resistance includes aggregate interlock, friction resistance, and viscous resistance" (*3*). Another reason for compacting the asphalt pavement is to make it watertight and impermeable to air (*4*). An increase in the mix's density usually will result in a stronger mix but not necessarily a stronger pavement. However, there is a point of optimum density that correlates with the best combination of strength and durability.

Pavements are compacted in two stages: during construction and as they are trafficked (*5*). Hot mix initially is compacted to about 8 percent air voids during construction. After construction, traffic loads densify the asphalt layer, especially during hot months, until it reaches ultimate density.

In one publication it was stated that " . . . an increasing number of bituminous concrete pavements in Texas as well as other states are not stabilizing at a density equal to that obtained in the laboratory design of a companion paving mixture" (*6*). This is evidence that current methods of laboratory compaction are not sufficient to simulate field conditions. The properties of the asphalt and aggregate based upon the long-term densification of a pavement must be taken into account; that is, consider the resistance of the paving mixture to compactive effort (*6*). If the resistance to compactive effort is weak, the pavement will be sufficient only for low traffic; if the resistance is strong, the pavement will be sufficient for higher traffic.

Pavements densify with an increased volume of traffic until they stabilize. Traffic will compact pavement to ultimate density, which is usually achieved after the third summer's traffic (*7*). A laboratory compactor needs to be able to simulate final density. The heavier the traffic (number of axle loads), the more the density of the pavement increases. Thus, equivalent single (18 kip) axle load (ESAL) is a convenient way to account for the effects of the traffic volume (*6*) on pavement density. Traffic load was measured in ESALs for this experiment.

SHRP, a $150-million research program authorized by the U.S. Congress (1988–1993), provided funds to produce new asphalt binder and mix design specifications to improve pavement performance. The design life of pavements is usually 20 years. Typically, if a pavement is not placed with the optimum AC content and gradation, it could show extensive damage after a few years of traffic. Current methods of asphalt mix design must be improved.

Ideally, a pavement must have the ability to resist vertical and shear forces that are applied by traffic. Indeed that is the basis for mix design criteria today. Factors such as aggregate size, shape, orientation, gradation, and asphalt content may cause premature failure in pavement.

The most widely accepted definition of optimum AC content is ". . . the highest asphalt content that can be used without having so much that it prevents the pavement from developing strength from the applied loads" (*8*). The loads referred to are traffic. Pavement density is a function of traffic and climate (temperature) (*8*). For pavements to be designed correctly, traffic and climate must be simulated in the laboratory for the mix design. Rational traffic simulation has been lacking in current practice.

The heart of all mixture design methods is the laboratory compaction method. From the Hubbard Field Method of mix design to

P.B. Blankenship, Kentucky Transportation Cabinet, Division of Materials, 1227 Wilkinson Boulevard, Frankfort, Ky. 40622; K.C. Mahboub, Department of Civil Engineering, University of Kentucky, 533 South Limestone Street, Transportation Research Building, Lexington, Ky. 40506; G.A. Huber, Heritage Research Group, 7901 West Morris Street, Indianapolis, Ind. 46231.

the SHRP SUPERPAVE method, attempts have been made to select a compaction device that achieves a density similar to that of the actual pavement.

This paper documents development of laboratory gyratory compaction criteria for use in the SUPERPAVE mix design system. Data from in-service pavements were used to determine an appropriate gyratory compaction protocol. Results are presented as well as the method for use in SUPERPAVE.

BACKGROUND

Historically, there have been three compaction methods that have been used in routine asphalt concrete mixture design—impact compaction, kneading compaction, and gyratory compaction.

Impact Compaction

Impact compaction is the oldest method of laboratory compaction. In the 1920s, Hubbard and Field used a Proctor hammer, borrowed from the geotechnical field, to compact asphalt mixtures (*1*).

In the 1930s, Marshall began developing the Marshall method of mixture design. Impact compaction from the Hubbard field method was adopted, except that the compactor face was made equal to the mold diameter. Subsequently, the Marshall method was adopted for highway design. The number of blows applied to each face of the specimen (35, 50, and 75 blows) was tied to general traffic levels. Higher energy levels (blows) were used for higher traffic levels. Unfortunately, different densities, because of the variability in Marshall hammers (mechanical, rotating, and manual hammers), will result when these compaction blows are applied (*9*).

Some variation of Marshall mixture design has been adopted by 75 percent of the highway agencies; it is the predominant method of mix design used today (*1*). However, in simulating field compaction properties the Marshall hammer ranked third out of five compactors tested in the AAMAS study (*10*).

Kneading Compaction

Independent of the Marshall mix design development, Hveem developed a mix design method in the 1930s and 1940s. The compaction method Hveem selected is referred to as kneading compaction. Kneading compaction applies force through a roughly triangular-shaped foot that covers only a portion of the specimen face. Tamps are applied uniformly on the specimen face to achieve compaction.

The objective of kneading compaction, like other compaction methods, is to achieve specimen density that matches postconstruction mixture density under traffic. Mixtures applied to high volume traffic are subjected to more and higher pressure tamps.

Kneading compaction has been adopted by several states in the western United States, where the Hveem mix design is commonly used. Outside this region, kneading compaction is not common practice.

Gyratory Compaction

Gyratory compaction was developed in the 1930s in Texas (*11*). The process involves applying a vertical load while gyrating the mold in a back-and-forth motion. Gyratory compaction, like California kneading compaction, produces a kneading action on the specimen. The kneading action is caused by gyrating the specimen through a horizontal angle. The angle of gyration of various compactors ranges from 1.00 to 6.00.

Gyratory compaction, as it developed in Texas, is used in a few states but has not gained wide acceptance. Compaction using gyratory action has been further developed and applied by the Army Corps of Engineers as well as the Central Laboratory for Bridges and Roads (LCPC) in France (*12,13*).

In a recent study of the AAMAS (*10*), sponsored by NCHRP, which preceded SHRP, the Texas gyratory shear compactor proved to simulate field compaction, when compared to other compactors (*10*), Five compaction devices were compared. They are listed in descending order beginning with those that best simulated field cores in various engineering properties.

- Texas gyratory shear compactor,
- California kneading compactor,
- Mobile steel wheel simulator,
- Arizona vibratory kneading compactor, and
- Marshall mechanical hammer.

In the 1940s, the U.S. Army Corps of Engineers began to develop a compactor by applying the principle of gyratory movement. The goal was to develop a new method of asphalt mix design for service under extreme traffic conditions (*14*). Development of the compactor continued though the 1950s, and by the early 1960s its use had been demonstrated (*15*). However, the gyratory testing machine gained little acceptance as a routine mix design tool. Outside the Corps of Engineers it has been used primarily as a research tool.

In the late 1950s, a delegation from France visited the United States and studied the Texas gyratory method (G. Huber, unpublished data). The LCPC evaluated parameters affecting gyratory compaction; in 1972 it finalized a gyratory protocol. Angle of gyration, speed of rotation, and vertical pressure were the three major variables studied. In the French application of gyratory compaction, the compactor is used to simulate density at the end of construction instead of during service. Today, gyratory compaction is used routinely in France for part of the mix design process. More recently, gyratory compaction has been introduced in several countries, including Sweden, Switzerland, and Australia. The SHRP protocol for gyratory compaction is a workable compromise between various approaches to gyratory compaction, such as the French LCPC, U.S. Army Corps of Engineers, and Texas methods.

Selection of SHRP Compaction Protocol

The gyratory and Hveem methods of asphalt mix design generate higher densities than a mix design using the Marshall hammer (*16*). The reason for the higher densities is the kneading action each method produces. The kneading action simulates field particle orientation of the aggregate better than Marshall compaction does. One of the primary reasons for using a gyratory compactor is its ability to reproduce the high densities that are encountered in the field (*17*). McRae and Foster suggest that the "gyratory compactor is producing specimens with stress-strain properties comparable to those of the actual pavement" (*17*).

A decision was made to evaluate a Texas-type gyratory compaction for application in the SUPERPAVE program on the basis of

compaction studies that predated SHRP. In particular, the NCHRP study as part of AAMAS as well as other studies within SHRP were to be used in this evaluation.

SHRP decided to evaluate gyratory compaction as the potential method of compaction for the SUPERPAVE mixture design system. Work by LCPC provided insights into compaction characteristics of mixtures but did not establish a relationship between gyratory compaction and pavement density at the end of its service life. The purpose of this study is to establish that relationship.

EXPERIMENT BACKGROUND

The study, *Gyratory Compaction Characteristics: Relation to Service Densities of Asphalt Mixtures,* was conducted by the Asphalt Institute. It defined N_{Design} as the compactive effort (number of gyrations at a specific pressure) at which the air void level is measured for volumetric design. In other studies, such as experiments on the Army Corps of Engineers' gyratory testing machine or the Texas gyratory, gyration pressure had been varied as a function of tire pressure and traffic levels (*17,18*). It was decided that the SHRP compaction protocol would maintain a constant gyration pressure and a specified number of gyrations to define two levels of compaction: (a) construction compaction [92 percent of maximum theoretical specific gravity (MSG)] and (b) traffic compaction (96 percent of MSG), as shown in Figure 1. Also, gyrations at 89 and 98 percent densities were defined as threshold limits for an acceptable mix. Percent compaction is defined as the ratio of bulk specific gravity (BSG) to MSG.

Design specifications of the SHRP Gyratory Compactor are as follows:

- Angle of gyration, 1.00 degree;
- Speed, 30 rpm;
- Vertical pressure, 0.6 MPa (87 psi); and
- 100-mm (3.94-in.) and 150-mm (5.91-in.) diameter molds.

The purpose of the experiment was to determine the number of gyrations (N_{Design}) required to represent various traffic levels in different climates. Thus, gyrations (N_X) must relate to traffic levels (E_X). This is compatible with information reported in the literature, which indicates that the asphalt layer under traffic increases in density linearly with the logarithm of the number of traffic passes until it reaches its ultimate density (*7*).

The main concern of those conducting the experiment was relating gyrations to traffic. Initial air voids of GPS sites were unknown, historical traffic was a guess, and the original materials were unavailable. Some assumptions had to be made, increasing the variability and margin of error of the experiment. Such is the challenge SHRP faces with large-scale experimental plans.

A more desirable process would have been a "controlled" field experiment to determine N_{Design} as a function of traffic level, tire pressure, and pavement structure. However, such a project was not feasible within the limited time and resources available. It was decided that the use of uncontrolled GPS sites might provide a reasonable determination of N_{Design}, as long as a number of sites were used to average out the error caused by individual project variations. Scatter in the data was expected to be significant.

The final objective of the experiment was to provide the ability to produce compaction curves for various mix gradations at different asphalt cement contents (percent AC). When N_{Design} is entered into the compaction curves, this will allow the pavement design to have the optimum mix gradation at the optimum percent AC for a desired level of traffic in a specific climate. Thus, we can fulfill the SHRP objective of being able to produce rut-resistant mixtures with adequate durability (*19*).

Two gyration levels were studied: (a) gyrations (N_{Const}) representing compaction (C_{Const}) resulting from initial pavement construction and (b) gyrations (N_{Design}) representing compaction (C_{Design}) from current traffic in the wheel path. N_{Const} is the gyration that represents field compaction at the end of construction as the result of rolling. Neither C_{Const} densities nor out-of-wheel-path densities were available. The out-of-wheel-path data would not have provided usable densities, because the out-of-wheel-path pavement areas densify to some degree from wandering traffic. The only data available were from cores that were in the wheel path. The construction compaction was assumed to be 92 percent of the max-

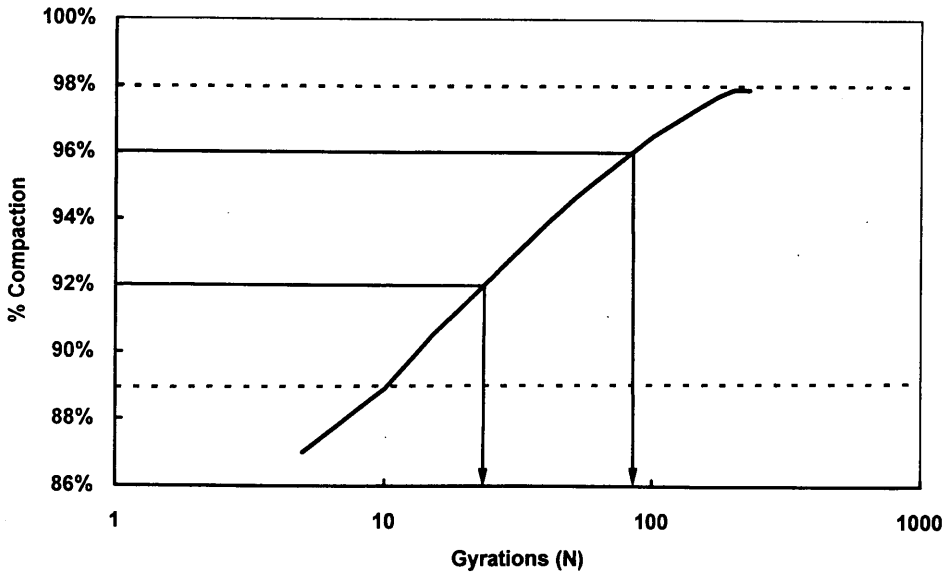

FIGURE 1 Schematic to define construction and traffic compaction.

imum specific gravity, and an assumption was made in order to complete the design curves. Without this assumption, there would have been no data available at zero ESALs (i.e., postconstruction information). The 92 percent of MSG is a reasonable assumption, because these pavements most likely were designed to have an in-place density of 92 percent of solid density, and 8 percent air voids (*8,20*).

N_{Design} EXPERIMENT

The experiment was conducted following these steps:

- Select site of cores,
- Collect cores and core data (layer description, gradation, density, percent AC, BSG, MSG) from the SHRP Material Reference Library (MRL),
- Separate core layers and lifts,
- Measure BSG of each layer and lift,
- Extract asphalt binder and salvage aggregate,
- Compact specimens using salvaged aggregate,
- Measure the BSG and MSG of each compacted specimen,
- Plot densification data,
- Tabulate N_{Const} and N_{Design} for each site,
- Complete statistical analysis, and
- Determine design gyrations (N_{Design}).

The experiment involved extracting the aged asphalt, and then remixing the salvaged aggregate with AC-20 grade asphalt cement and compacting it to achieve compaction curves. The original testing matrix included asphalt concrete cores representing three ages, three climates, three traffic levels, and upper and lower layers. This required 27 pavement sites with 54 mixtures. The goal was to provide sufficient data that would represent the majority of roads that are traveled today and reduce potential error in the analysis. Later, it was decided that only old pavements, older than 12 years, would be used. Pavements at old sites already would be densified to their ultimate density, because most pavements reach their ultimate density after the third summer's traffic (*8*). Table 1 indicates 18 pavement sites in the testing matrix, only 15 of which were available. There are only single sites for hot climates. The 305-mm (12-in.) diameter cores were collected from various SHRP road test sections and stored in the MRL until needed for testing purposes.

Cores from pavements with more than 12 years of traffic exposure represent pavements that have densified to their design percent air voids [100 percent − percent Compaction (percent C_X)]. One assumption made in this experiment is that pavements were designed to have final air voids of 3 to 5 percent and the pavements were placed at 7 to 9 percent air voids. This is a reasonable assumption because most pavements are required to have these densities. Some pavements have higher or lower air voids than 7 to 9 percent at construction. Overall, 7 to 9 percent air voids at construction is a reasonable air-void range (*8,20*).

TABLE 1 Core Site Selection Matrix

TEMPERATURE		HOT			WARM			COOL		
TRAFFIC		*L o w*	*M e d i u m*	*H i g h*	*L o w*	*M e d i u m*	*H i g h*	*L o w*	*M e d i u m*	*H i g h*
CORES	Original	✓	✓	✓	✓	✓	✓	✓	✓	✓
	Replicate				✓	✓	✓	✓	✓	✓

When the cores and core data were received from the MRL, they were verified and marked for cutting. The BSG of each layer and lift to be compacted was measured in accordance with ASTM-D2726-90 and compared with BSG from SHRP core information gathered from various independent contractors. The asphalt binder was extracted from the layers and lifts by the quantitative extraction of bituminous paving mixtures method (ASTM-D2172). Extraction provided the recovered aggregate and indicated the required asphalt cement content (percent AC) needed for remixing. All the aggregate was recovered, including the dust fraction that was removed from the extraction solvent by centrifuge.

Next, the salvaged aggregate was remixed with fresh asphalt binder at the amount percent AC, as determined from the extraction. The laboratory standard asphalt cement (AC-20) was used for mixing all specimens. Because the viscosity of asphalt is directly related to temperature, all the specimens were prepared according to the proper mixing and compacting temperatures as specified by the asphalt grade (*21*).

The most critical time of the bitumen life is the time it is exposed to high temperatures at the hot-mix plant (*22*). Thus, the asphalt concrete mixture was allowed to cure for 4 hr at 135°C in loose form. SHRP determined that this served as the short-term aging process that simulates curing from the plant mixing of asphalt concrete. The mixture was then loaded into a preheated mold for compaction. The size of mold depended upon the nominal maximum aggregate size of the mixture; nominal maximum aggregate size being defined as one sieve size larger than the first sieve to retain more than 10 percent. The 100-mm mold was used for 19.0-mm (¾-in.) and less nominal mixtures, whereas the 150-mm mold was used for greater than 19.0-mm (¾-in.) nominal mixtures. The mold was then placed into an SHRP gyratory compactor, and the vertical ram was lowered into the mold. As the specimen gyrated, specimen heights were recorded at 5, 10, 15, 20, 30, 40, 50, 60, 80, 100, 125, 150, 175, 200, and 230 gyrations. Even though the mix density of most probably occurred at a lower gyration than 230, this end gyration ensures complete densification of the mix. Finally, the specimen was extracted from the mold and allowed to cool overnight. Afterwards, BSG and MSG of each compacted specimen were measured.

Compaction data were then entered into a spreadsheet that produced densification curves for two specimens of the same selected layers and lifts. The two densification curves were averaged and used for further analysis.

The next step was to determine the number of gyrations that corresponded to the in-place density at the time of coring and at the time of construction. The measured density, expressed as percent maximum theoretical density (C_X), of the cores was matched to the compaction data and the corresponding number of gyrations (N_X) was noted. For density at the time of construction, no measured data were available; therefore, an assumption of 92 percent MSG was made. Thus, the construction densities (92 percent) were also entered into the compaction curves to produce the corresponding gyration (N_{Const}).

The corresponding field gyrations (N_X) and construction gyrations (N_{Const}), which achieved the required field and construction densities during laboratory compaction, produced two data points (N_X and N_{Const}) for each specimen's layer and lift. Hence, 30 data points (2 data points × 15 cores) were produced for the upper layers. There was only one upper layer from each core used in the analysis. The upper layers [less than or equal to 102-mm (4-in.) from the surface] analyzed were the uppermost layers tested.

Analysis

It was hypothesized that there was some relation between gyrations (N_X) and traffic (E_X). It has been shown in this experiment that a linear relation exists between percent compaction (C_X) and the logarithmic function of gyrations (Log N_X). It has also been shown that a linear relation exists between percent compaction (C_X) and the logarithmic function of traffic (Log E_X) (*5*). Therefore, a linear relation should exist between the logarithmic function of gyrations (Log N_X) and the logarithmic function of traffic (Log E_X).

Determination of the Design Gyrations (N_{Design})

Three lines were regressed through the data points at a confidence level of 95 percent. This produced curves for the three climates (hot, warm, and cool). By using these design curves, one can enter the graph with a known traffic level and specific climate and obtain the corresponding design gyration (N_{Design}).

Figure 2 shows a plot of these design curves. It should be noted that the experiment includes design traffic up to 3.2×10^7 ESALs. Thus, as represented on the graph, values greater than 3.2×10^7 ESALs were extrapolated.

For the above model to be used in SUPERPAVE, the temperature zones (hot, warm, and cool), which were determined from monthly mean maximum air temperature (°F), had to be converted to weekly mean maximum air temperature (°C).

Next, these temperatures in weekly mean maximum air temperature (°C) were plotted against the design gyrations at designated traffic levels. The design traffic levels to be used in SUPERPAVE are defined in Table 2. The design gyrations (N_{Design}) to represent each of these ESAL limits, which will correspond to a design air voids of 4 percent, are compiled in Figure 3.

One now has the ability to use the design gyrations (N_{Design}), obtained from the design curve, Figure 3, to acquire the design 4 percent compaction (C_x) from compaction curves of future mixes. For instance, to design a mixture for Traffic Level 4 and a weekly mean maximum air temperature of 39°C, the N_{Design} would be 103 gyrations. To achieve the optimum aggregate blend and asphalt content for this mix design, the designer simply would enter the design gyration (N_{Design}), representing design traffic, into the compaction curve of the new mix design to obtain the final percent compaction (C_x) of that mix (target is 96 percent MSG).

CONCLUSIONS AND RECOMMENDATIONS

The purpose of the N_{Design} experiment was to determine the number of gyrations (N_{Design}) required to represent mixture densification that will occur under various traffic levels in different high-temperature climates. Thus, gyrations (N_X) must relate to traffic levels (E_X). This

TABLE 2 SUPERPAVE Traffic Levels

Traffic Level	ESAL Limits	Design %Air Voids
1	<3x10^5	4
2	<1x10^6	4
3	<3x10^6	4
4	<1x10^7	4
5	<3x10^7	4
6	<1x10^8	4
7	<3x10^8	4

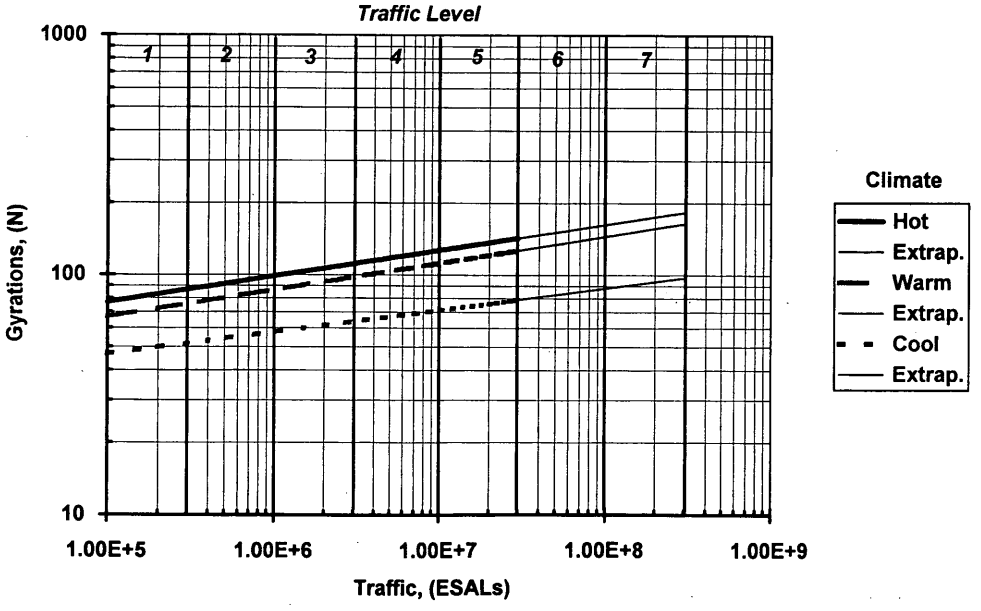

FIGURE 2 Design gyrations versus traffic.

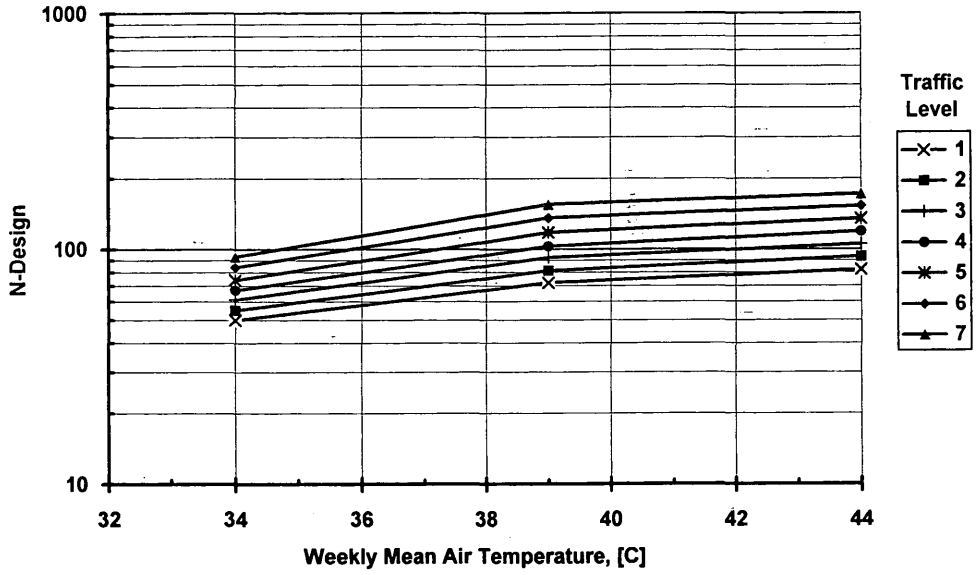

FIGURE 3 Design gyrations.

relationship was proven to exist. This relationship provides a method of choosing a mix design to have the blended aggregate gradation and percent asphalt binder matched to a desired traffic level in a specific climate.

Data for sites with hot climates were limited because there were no replicate specimens. However, design gyrations graph (Figure 3) could be reasonably plotted because the hot-climate design curve requires more gyrations than the cool-climate design curve at the same level of traffic.

The number of gyrations representing construction density (no traffic) is called N_{Const}. N_{Const} was calculated to be 22, 18, and 16 for hot, warm, and cool climates, respectively. Although reasonable, the numbers were based on the assumption that the construction compaction (C_{Const}) of the tested pavements was 92 percent of the maximum specific gravity. N_{Const} will produce a target density that should be generated during initial construction.

The relationship between number of gyrations and traffic would not have been possible if a construction compaction (C_{Const} = 92.0 percent) had not been assumed. Even though the relation is an assumption, which has been proven reasonable, the results may be in error because the traffic data were separated by a large margin. For example, data points were located at 0.001 kESALs (1 ESAL). The rest of the data was located at 600 to 28,713 kESALs. There were no data available for the gap from 0 to 600 kESALs. Hence, error introduced as a result of this gap in traffic data may affect the exact gyration-traffic relation.

The results of the N_{Design} experiment are acceptable at this early stage in the development of the SHRP gyratory compactor. The linear relation of the logarithmic function of gyrations (Log N_X) versus the logarithmic function of traffic (Log E_X) was proven to exist, although, more research is required to increase the precision of the gyration versus traffic model. The SHRP gyratory compactor was used in the mix design of various new SHRP road test sections. Thus, more data will be available soon to check and adjust SHRP gyratory compactor design gyrations (N_{Design}). Certainly, more research needs to be completed to increase the precision of N_{Design}.

In the authors' preliminary studies with a modified Texas 6-in. gyratory compactor, specimens similar to SHRP gyratory specimens have been made (M. Anderson, unpublished data). Therefore, it may be possible for the Texas 6-in. gyratory compactor, with its similarities to the SHRP gyratory, to be modified into a SHRP gyratory compactor.

Degradation of the aggregate, as in any type of compaction method, is a concern that needs to be addressed. Degradation must be simulated in laboratory compaction because aggregate degradation occurs naturally in the field. Laboratory impact compaction causes too much degradation, cracking, and exposing the aggregate faces. However, it has been found that gyratory compaction, which produces proper orientation of the aggregate and has low initial pressures, closely simulates the degradation found in field compaction (*11*).

More research is needed to monitor the long-term pavement performance of experimental pavements that are currently being designed with this new methodology. For example, the long term pavement performance program, designed to generate a large data base in the next 20 years, is being managed by FHWA. Compaction models developed for the FHWA study should be calibrated as soon as long-term pavement performance data become available.

ACKNOWLEDGMENTS

First we thank SHRP for funding this contract (A001, Task F). We also thank Gerald Huber, at the Heritage Research Group, for sharing his knowledge of asphalt mix design and allowing us to conduct such a large and intensive research project. We also thank Michael Anderson and Robert McGennis and everyone at the Asphalt Institute, Lexington, Kentucky, for their assistance and guidance with this experiment, in particular the Asphalt Institute's laboratory technicians and technologists, Raymond Warren, David Ross, Daniel Quire, Carmela Chapelle, Philip Creamer, and Robert Bosely. We thank Teri Cook of the Kentucky Transportation Cabinet for her

assistance in editing this paper. We also want to thank the University of Kentucky Civil Engineering Department for the assistance it provided. P. Blankenship offers thanks to his parents, Bennie and Wanda Blankenship, for encouraging him to set his goals high. The study was part of Phillip Blankenship's Master's thesis in civil engineering at the University of Kentucky (May 1993).

REFERENCES

1. Roberts, K., L. Brown, and T. Kennedy. *Hot Mix Asphalt Materials, Mixture Design and Construction.* NAPA Education Foundation, Lanham, Md., 1991.
2. Kumar, A., and W. H. Goetz. The Gyratory Testing Machine as a Design Tool and as an Instrument for Bituminous Mixture Evaluation. *Asphalt Paving Technology* Vol. 43, 1974, pp. 351–371.
3. Swanson, R. C., J. Nemec, Jr., and E. Tons. Effect of Asphalt Viscosity on Compaction of Bituminous Concrete. In *Highway Research Record* 117, HRB, National Research Council, Washington, D.C., 1966, pp. 23–52.
4. Smith, R. W. Purposes and Reasons for Compacting Asphalt Mixtures. In *Improved Asphalt Pavement Performance Through Effective Compaction.* 1979, pp. 9–11.
5. Paterson, W. D. O., A. Williman, and J. S. Pollard. *Traffic Compaction of Asphalt Surfaces.* RR176-5, National Institute for Road Research, 1974.
6. Epps, J. A., B. M. Gallaway, and W. M. Scott, Jr. Long-Term Compaction of Asphalt Concrete Pavements. In *Highway Research Record* 313, HRB, National Research Council, Washington, D.C., 1970, pp. 79–90.
7. Foster, C. R. *Selecting Proper Marshall Procedures for Optimum Asphalt Content of Dense Graded Paving Mixtures.* Information Series 85, 1992.
8. Foster, C. R. *Development of Marshall Procedures for Designing Asphalt Paving Mixtures.* 1992.
9. Achieving and Verifying Specified Compaction. *Improved Asphalt Pavement Performance Through Effective Compaction* 7. Asphalt Institute, 1981, pp. 1–6.
10. Consuegra, A., D. N. Little, H. L. Von Quintus, and J. Burati. Compaction Evaluation of Laboratory Compaction Devices Based on Their Ability to Produce Mixtures with Engineering Properties Similar to Those Produced in the Field. In *Transportation Research Record* 1228, TRB, National Research Council, Washington, D.C., 1989, pp. 80–87.
11. Ortolani, L., and H. A. Sandberg, Jr. The Gyratory-Shear Method of Molding Asphaltic Concrete Test Specimens; Its Development and Correlation with Field Compaction Methods. *Proc., Association of Asphalt Paving Technologists.* Vol. 21, St. Paul, Minn., 1952, pp. 280–297.
12. McRae, J. L., and A. R. McDaniel. Progress Report on the Corps of Engineers' Kneading Compactor for Bituminous Mixtures. *Proc., Association of Asphalt Paving Technologists.* Vol. 27, St. Paul, Minn., 1958, pp. 357–382.
13. Moutier, F. *Prévision de la Compactabilité des Enrobés Bitumineux à L'aide de la Presse à Cisaillement Giratoire (PCG).* 1973.
14. Maxwell, A. A., and W. H. Larson. Use of Gyratory Compactor in the Design of Bituminous Pavement by the U.S. Army Corps of Engineers. *Australian Road Research Board.* Vol. 2–2, 1964, pp. 787–798.
15. Kimble, F. W., and W. B. Gibboney. Control of Field Density of Bituminous Concrete with a Gyratory Compactor. *Proc., Association of Asphalt Paving Technologists.* Vol. 30, St. Paul, Minn., 1961, pp. 1–46.
16. Adam, V., S. C. Shah, and P. J. Arena Jr. *Compaction of Asphalt Concrete Pavement with High Intensity Pneumatic Roller.* Research Report 10–1, Research Project 61–7B, 1963.
17. McRae, J. L., and C. R. Foster. Theory and Application of a Gyratory Testing Machine. *Bituminous Paving Mixtures.* Baltimore, Md., 1960, pp. 9–21.
18. Design of Bituminous Mixtures. *Manual of Testing Procedures.* Texas State Department of Highways and Public Transportation. 1983.
19. Brown, S. F., J. N. Preston, and K.E. Cooper. Application of New Concepts in Asphalt Mix Design. *Asphalt Paving Technology.* Vol. 60, 1991, pp. 264–265.
20. *Density Specifications for Hot-Mix Asphalt.* Asphalt Institute, TB-9, 1992.
21. *Mix Design Methods for Asphalt Concrete and Other Hot-Mix Types.* Asphalt Institute, MS-2, 1988.
22. Green, D. G., and D. Steenkamp. Hardening of Bitumen During Hot-Mixing and In Service on Roads in South Africa. *Fourth Conference on Asphalt Pavements for Southern Africa.* Vol. 1, 1984, pp. 490–500.

DISCUSSION

JOHN I. MCRAE
CEO Engineering Developments Co., Inc.

This SHRP procedure using a fixed pressure of 0.6 MPa (87 psi) fails to consider the requirement of an increase in density and reduction in bitumen as traffic load increases. Increasing density by increasing the number of cycles of kneading at the same vertical pressure can be empirically related to traffic, but when contact pressures exceed the pressure used in the test, the method will reach its limitations and become out of phase with the ultimate density. Out-of-phase compaction tests are the primary reason for the rutting failures experienced to date.

A rational method of compaction should introduce the tire contact pressure and compact to an equilibrium condition, that is, effect a balance between the applied load and internal resistance. Based upon the Army Corps of Engineers' experience, this has been defined as a rate of densification of 1 lb/ft^3/100 revolutions.

Another tenet of mix design is to accept the maximum permissible bitumen content as that at the peak of the bitumen content versus unit weight aggregate-only curve (minimum VMA).

Figure 4 illustrates a gyratory testing machine (GTM) mix design test using the plot of unit weight aggregate only versus bitumen content, along with the associated gyratory stability index (GSI), GTM shear modulus (*Gg*), and GTM compression modulus (*Eg*).

The authors are to be commended for their extensive literature review. The following articles offer related material:

> From the preceding discussions, it is evident that a procedure that is not dependent upon voids would be desirable. The flexible Pavement Laboratory of the Corps of Engineers has recognized this and is now studying a mix design procedure based on a very direct approach to the problem. Specifically, an attempt is being made to develop a laboratory compaction procedure which will simulate prototype compaction not only as to compactive effort but also as to compactive action and thus allow direct selection of the optimum condition independent of specific gravity and voids considerations.
>
> The compaction phenomenon, when properly controlled, is by its very nature the most direct indicator of optimum asphalt content since what is generally desired in a pavement is a mix that is fully compacted and at a desired equilibrium condition under the imposed traffic. . . .
>
> In the current program, the Flexible Pavement Laboratory is developing a kneading-type laboratory compactor based on the "Texas Gyratory" principle. Field data of density versus asphalt content, mainly from test sections built for other specific purposes, are being collected which will be used as a basis for establishing a laboratory procedure to duplicate the field compaction asphalt-density curve. It is believed that this test method will make it possible to select the optimum bitumen content independent of voids consideration (*1*).

> In an effort to develop improved procedures for the design and control of hot-mix bituminous pavements, the Waterways Experiment Station developed the gyratory testing machine, a laboratory compaction and

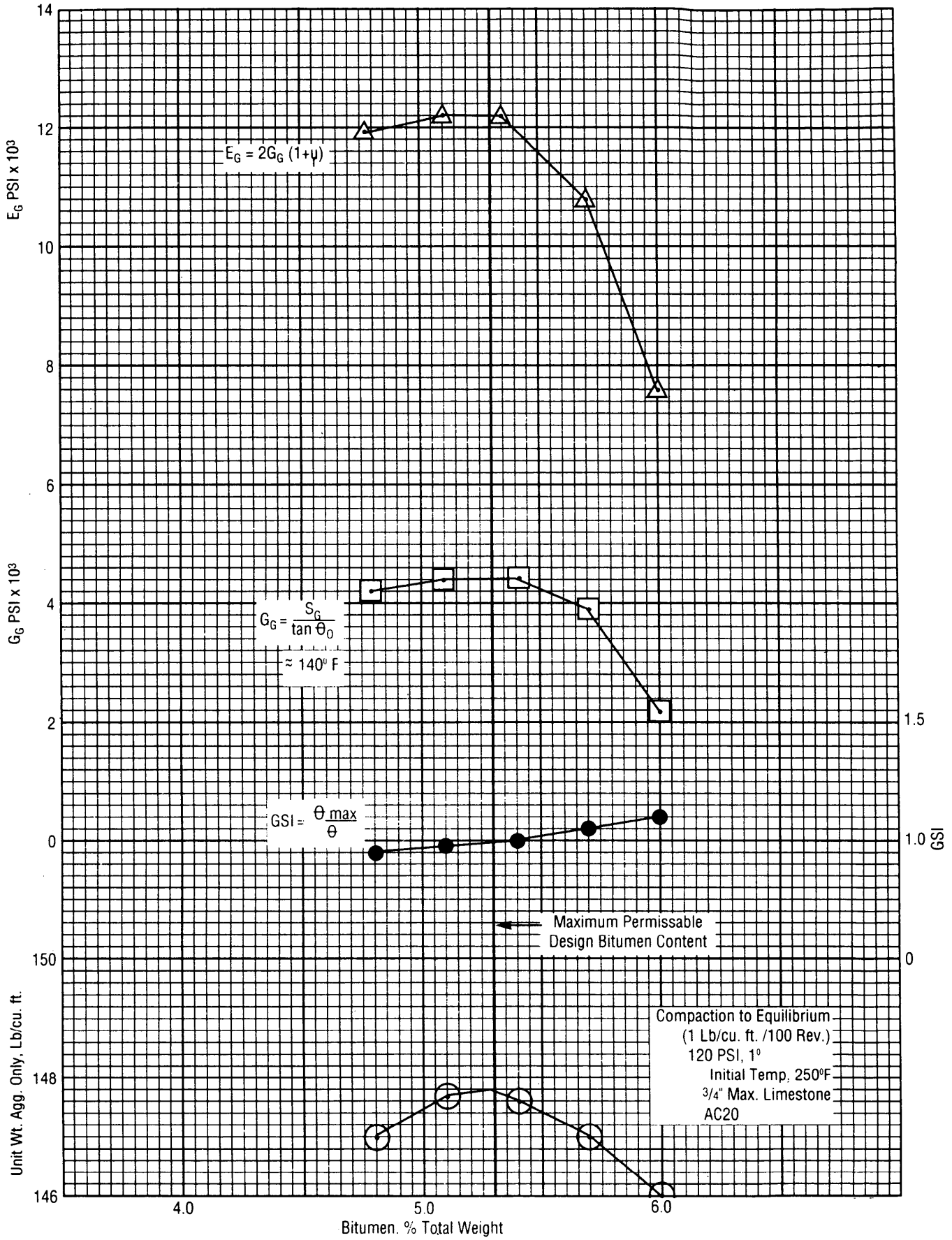

FIGURE 4 Gyratory testing machine mix design test.

testing device believed capable of (*a*) producing high densities equal to those that develop under channelized traffic of heavy wheel loads; (*b*) producing specimens with stressstrain characteristics similar to those of actual pavement sample of equal density and bitumen content; (*c*) predicting the number of load applications a paving mixture can withstand before failure; (*d*) predicting the design bitumen content independently of voids criteria; and (*e*) providing a more positive and faster plant-control test. Extensive laboratory and field tests proved the principle of the gyratory testing machine to be sound and its predictions to be more accurate than those of other previously established test methods (*2*).

The U.S. Army Corps of Engineers' GTM (ASTM D 3387) was evaluated along with the Texas Shear Compactor (ASTM D 4013), which was modified to produce the SHRP (Rainhart) gyratory compactor pictured in Figure 2 of the paper under discussion. The following excerpts from the study apply:

> The Corps of Engineers gyratory testing machine (GTM) was used to study the effects of traffic densification. The GTM is the only device that can monitor the mixtures's behavior during the densification process. Using the other compaction devices, test specimens must be initially compacted and then tested separately (p. 122).
>
> The Corps of Engineers GTM provides an indication of this shearing resistance of asphaltic concrete mixtures. Those mixtures included in this study that are known to be susceptible to shoving and lateral distortion were identified as such with the GTM. Thus use of the GTM is recommended in the AAMAS procedure (p. 166).
>
> Thus it is suggested that additional projects be added or coordinated effort between the states be used to evaluate a more diverse range of mixtures (p. 179).
>
> Gyratory shear strength or the use of the Corps of Engineers GTM was found to provide a reasonable evaluation of asphaltic concrete mixtures that were known to be "sensitive" mixtures or mixtures that are susceptible to a reduction in shear strength with traffic. However, this parameter is not used in any mechanistic model nor is it commonly used to evaluate mixtures. Thus additional mixtures should be evaluated and designed with the GTM and then monitored to gain the critical performance data to validate its results (*3*).

REFERENCES

1. McRae, J. L. *Specific Gravity and Voids Relationships in Bituminous Pavement Mix Design.* Presented at Symposium on Specific Gravity of Bituminous Coated Aggregate, STP No. 191, ASTM, 1956.
2. McRae, J. L. *Development of the Gyratory Testing Machine and Procedures for Testing Bituminous Paving Mixtures.* WESTR No. 3–595, U.S. Army Corps of Engineers, Feb. 1962.
3. Von Quintus, H. L., J. A. Scherocman, C. S. Hughes, and T. W. Kennedy. *NCHRP Report 338: Asphalt-Aggregate Mixture Analysis System (AAMAS).* TRB, National Research Council, Washington, D.C., 1991.

Authors' Closure

We would like to reemphasize the point made in the paper that the SHRP gyratory compactor is not a testing device but is a laboratory compaction device. Mr. McRae raises several points concerning laboratory compaction. The first regards vertical pressure and load.

1. *Vertical pressure and load.* The SHRP gyratory compactor uses a vertical pressure of 0.6 MPa, the same used by LCPC in development of the French gyratory compactor. The pressure is similar to though somewhat lower than highway tire pressures. Ad hoc testing has indicated that SHRP gyratory densification curves, although sensitive to vertical pressure, are highly sensitive to angle of gyration. Additional research would be necessary to confirm use of the SHRP gyratory for airport applications, where tire pressures are three to five times those of highway vehicles.

Mr. McRae's suggestion that compaction continue to an equilibrium condition is an interesting idea, but the definition of equilibrium is unclear. The parameter he proposed, 1 lb/ft^3/100 gyrations, is an empirical value related to mixtures at an air base, under aircraft tires using the gyratory testing machine. The gyratory testing machine can not be compared with the SHRP gyratory compactor.

The densification curve of a mixture under gyratory compaction is very sensitive to angle of gyration. SHRP requires the angle to be specified within a tolerance of ± 0.02 degrees. Mr. McRae's data indicate the angle of the gyratory testing machine varies by as much as 0.10 degrees during specimen compaction—five times the tolerance allowed by SHRP. Furthermore, the angle does not remain constant during specimen compaction. Hence, the variable angle of the gyratory testing machine produces confounded densification curves that cannot be compared with SHRP gyratory compactor data.

2. *Selection of asphalt binder at minimum voids in mineral aggregate.* As Mr. McRae noted, one of the tenets of mixture design is to select asphalt content near the minimum VMA for specimens produced with a compactor that has been calibrated to the application. Figure 5 illustrates the relationship of air voids, voids in mineral aggregate, voids filled with asphalt, and specimen density with asphalt content for a 19-mm nominal, maximum size mixture. This mixture was designed using the SHRP gyratory compactor and was subsequently constructed on Interstate 43 outside Milwaukee, Wisconsin, in August 1992. The mixture has shown excellent performance to date.

Volumetric property data for the I 43 mixture shown in Figure 5 is typical for a SHRP designed mixture. The design asphalt content, 4.8 percent, was selected at 4.0 percent air voids, slightly less than the asphalt content that produces the minimum VMA. Hence, the SHRP gyratory meets this basic tenet of mix design.

3. *Selected Quotes from Literature.* Mr. McRae quotes from three sources. The first paper (I) is a discussion of specific gravity measurement methods and calculation of air voids. The quoted portion of the paper is an opinion of the author based on his belief that air voids inside porous aggregates should be considered part of the specified air-void content. The scientific community has found no evidence to support this opinion and has adopted as standard practice the definition of air voids outside asphalt-coated aggregate particles.

The AAMAS report evaluated the gyratory test machine and recommended it for the AAMAS method of mixture design, with a caveat: because insufficient data exist regarding mixtures designed with the gyratory testing machine, additional pavements must be designed, built, and monitored to provide validation of the machine.

The AAMAS method of mix design was a precursor to the SHRP method; it was intended to set the stage and act as a pilot program. Various portions of the SHRP research plans, including determination of a laboratory compactor, were designed based on results of the AAMAS study. Hence, the gyratory test machine and its limitations were considered by SHRP.

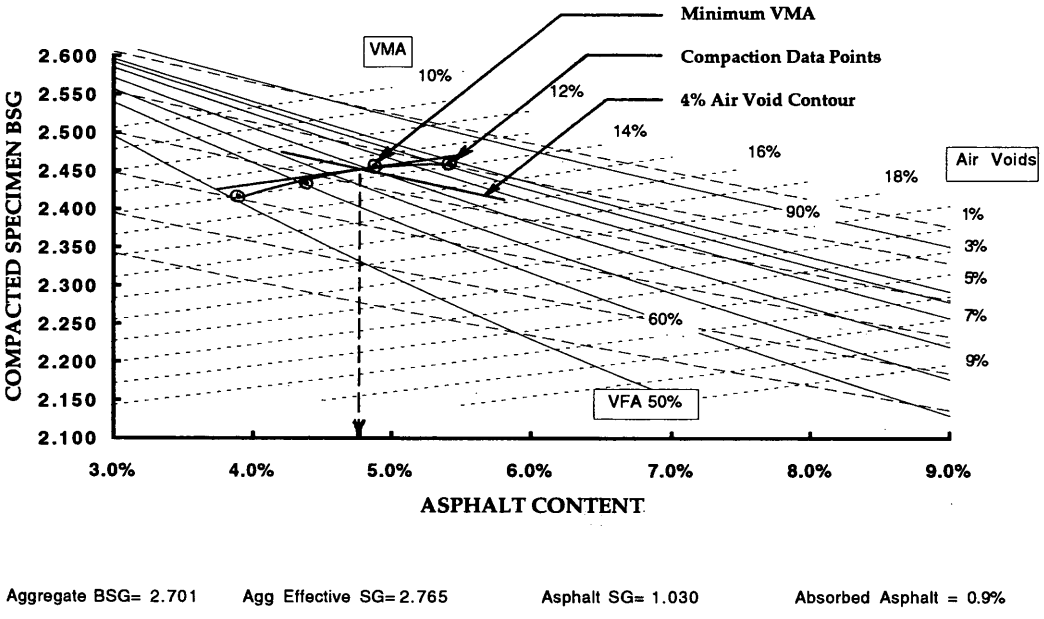

FIGURE 5 Relationship of air voids, VMA, and voids filled with asphalt for Interstate 43 (19-mm nominal maximum size mixture).

Mr. McRae's discussion focuses on promoting the Army Corps of Engineers' gyratory testing machine. The authors believe the SHRP gyratory compactor, complete with validation including the study reported in this paper, is the device that best meets the requirements for a laboratory compactor within the context of the SHRP SUPERPAVE mixture design system.

This paper represents the views and opinions of the authors and not necessarily SHRP, Asphalt Institute, or University of Kentucky.

Publication of this paper sponsored by Committee on Characteristics of Bituminous Paving Mixtures To Meet Structural Requirements.

Application of SHRP Mix Performance-Based Specifications

JORGE B. SOUSA, JOHN T. HARVEY, MARK G. BOULDIN, AND CONCEIÇÃO AZEVEDO

The Strategic Highway Research Program project, SHRP-A003A, has introduced new test methods and procedures that can be easily implemented in pavement design and in the development of performance-based specifications. The basic concepts behind the design of a high traffic, high performance pavement are presented, and the concept of the performance point as a methodology to develop site-specific contract specifications is introduced. This permits a connection between performance observations, structural pavement design, and mix design. This project is the first application of performance-based specifications based on fatigue tests and repetitive simple shear tests at constant height.

In the past few years considerable knowledge has been gained about structural and material behavior of asphalt concrete pavements. The Strategic Highway Research Program (SHRP) in the United States has provided new specifications for binders and mixtures, which permit better materials characterization. Furthermore, validation of asphalt concrete fatigue laws and experience with design of asphalt concrete pavements subjected to high traffic volumes have produced more reliable structural pavement designs.

The authors summarize a pavement design analysis for the Tagus Bridge Crossing between Lisbon and Montijo, Portugal. The project was executed by CONSULPAV for MottConsult, PONTEJO's consultant. The contractor is expected to maintain the pavement for 35 years. At the end of that period, it is expected that no major rehabilitation would be needed for another 5 years.

The pavement sections were designed based on the traffic, geotechnical, and climate data presented (*1,2*). New mechanistic design concepts and recent developments in mix characterization were applied in the project. Rehabilitation strategies proposed for the project are not part of this paper, however. This was a preliminary project. Final performance can only be predicted on the basis of laboratory fatigue, permanent deformation, water sensitivity, and aging tests performed on actual mixes. Redesign is likely to be necessary based on actual values obtained from such tests.

PROJECT DATA

Traffic

Truck traffic estimates were obtained elsewhere (*1,2*). Because no estimates were given for the 40-year life cycle, design life predictions were made by extrapolating the data based on the best fit of the data presented.

J. B. Sousa and Conceição Azevedo, CONSULPAV, Rua Actor Isidoro 3, Lisbon 1900, Portugal; J.T. Harvey, Institute of Transportation Studies, University of California at Berkeley, 1301 So. 46 St., Berkeley, Calif. 94720; M.G. Bouldin, Applied Pavement Technology, 1339 Alston, Houston, Tex. 77008.

Geotechnical Information

Available data (*1*) suggest that the pavement will be resting either on clays or sands on the left bank and possibly better soils along the right bank. In the design of the flexible pavement, three cases were evaluated. The following moduli were assumed: clay, 40 MPa (5.8 ksi); sands, 60 MPa (8.7 ksi); and better soils, 80 MPa (11.6 ksi).

Weather and Temperature

Pavements will be placed between Lisbon and Montijo. The average annual precipitation in the region is about 700 mm (27.6 in.), and average annual temperature is about 17°C (63°F) (*3*). Maximum air temperatures can reach 42°C (108°F), and minimum temperatures may drop as low as −5°C (23°F). Thus, in the design, consideration should be given to water sensitivity of the materials, and materials should be selected carefully to prevent premature failure from rutting at high temperatures. Finally, temperature variations should be accounted for in the fatigue design.

Design Elements

The design approach was as follows:

1. Selection of structural cross section, using stiffness of the asphalt concrete and fatigue cracking as the criteria;
2. Verification of acceptable permanent deformation in the underlying layers;
3. Verification of acceptable permanent deformation in the asphalt concrete from shear deformation; and
4. Definition of performance-based specifications.

STRUCTURAL PAVEMENT DESIGN

The fatigue analysis system developed by SHRP-A003A researchers (*4*) recognizes that mixture performance in situ depends on critical interactions between mixture properties and in situ conditions (e.g., pavement structure, traffic loading, or environmental conditions). The analysis system thus provides not only sensitivity to mixture behavior but also sensitivity to the in situ traffic, climatic, and structural environment as well. It seeks to judge, with

predetermined reliability, whether a mix design would perform satisfactorily in service. If it would not, the designer can opt to redesign the mix, strengthen the pavement section, or repeat the analysis using more refined measurements and estimates. The steps in the analysis system (*4*) are as follows:

1. Determine design requirements for reliability (probability of avoiding the acceptance of a deficient mixture) and performance (extent of permissible fatigue cracking);
2. Determine the expected distribution of in situ pavement temperatures;
3. Estimate design traffic demand in terms of equivalent single axle loads (ESALs);
4. Select trial mixture;
5. Prepare test specimens and condition as required;
6. Measure stiffness of trial mixture;
7. Design pavement structural section;
8. Determine design strain under standard axle load;
9. Determine the resistance of the trial mixture to fatigue (N_{supply}) in the laboratory or by regression estimate;
10. Apply a shift factor to the travel demand (ESALs) to account for differences between laboratory and in situ conditions (such as traffic wander and crack propagation) to determine N_{demand};
11. Compare traffic demand (N_{demand}), including reliability, with mixture resistance (N_{supply}); and
12. If N_{demand} exceeds N_{supply}, reanalyze current trial mixture with procedures that yield greater accuracy, or alter trial mixture or structural section and iterate.

The preceding concepts generally were followed for this project. At the preliminary design level generally accepted fatigue laws were adopted. However, mix performance varies considerably and more reliable predictions can only be made on the basis of results from fatigue tests on actual mixes. The specification section in this paper contains the actual performance specifications required for each mix.

Determination of Temperature Distribution

The new methodology proposed by SHRP-A003A (*4*) proposes limiting fatigue tests to one temperature and expressing the destructive effects of the anticipated traffic in the field as equivalent ESALs at that temperature. This is accomplished through use of temperature equivalency factors. The approach simplifies testing, which increases productivity and reduces costs.

Determination of the Design Traffic

The heavy traffic was converted into ESALs using previously established conversion factors. The British conversion to 80 kN (17.9 kips) of 3.5 (based on a daily traffic of more then 3,000 vehicles) (*5*) was used to convert heavy traffic into ESALs.

It was further assumed that the critical right lane would sustain 70 percent of the traffic. The cumulative variation of ESAL was computed on the basis of these two assumptions.

Selection of Material Properties

Experience has shown (*6,7*)that the most cost effective design of flexible pavement design for high traffic pavements is generally a full-depth asphalt concrete pavement. In this type of pavement significant improvement in performance can be obtained if stiff mixes are used. On the other hand, the most significant benefit of stiff layers is reduction of vertical compressive strains in the subgrade. In general, a reduction in stiffness of the mix, for a given tensile strain, increases fatigue life. However, when stiff mixes are used in a full-depth asphalt concrete pavement, the reduction in tensile strain offsets the propensity of stiffer mixes to fatigue, while providing the benefit of reduced vertical compressive strains in the subgrade.

It is known that temperature variations differ greatly with depth. Furthermore, asphalt concrete mixes are generally susceptible to temperature. Therefore, the structural section can be designed with materials that exhibit different temperature susceptibilities, by placing them at the appropriate depth to match their advantageous properties.

Materials selected for the bottom asphalt concrete layers should be very stiff and may be temperature sensitive. The material properties for the mix (M-3) are presented in the specification section.

The material present in the top layer should have the combined properties of low temperature susceptibility and a high shear stress resistance. Shear stresses occurring under the edge of the truck tires are known to cause rutting. The development of critical shear strains is limited to the upper 10 to 12 cm (3.9 to 4.7 in.) of the pavement section. A mixture placed in this layer (M-1) should be stiff at high temperatures with good aggregate interlock and not very temperature sensitive. This can not usually be easily achieved by normal binders and it is necessary to add modifiers. To satisfy all of these requirements the mix usually has lower stiffness at low temperatures than the materials selected for the underlying layers. For the material placed between those two layers (M-2) an intermediate behavior is desirable.

Traditionally in Europe thin stone mastic asphalt (SMA) layers are used on the upper layer of a pavement section. In this project a gap-graded friction course layer (SMA) was designed to resist permanent deformation but no structural value was given for fatigue design.

To ensure proper compaction of the mixes in situ, it is necessary to provide a stable platform. A 20-cm (8-in.) granular base was selected for placement on the subgrade. The estimated stiffness of this layer (A-1) depends on the moduli of the subgrade. It is generally accepted that the moduli are twice that of the underlying layer. A sensitivity study was made on the use of thick granular bases in an effort to investigate possible cost reductions. For this material a modulus of 180 MPa (26.1 ksi) was assumed. The additional granular base was named A-2.

Determination of Strains in Each Pavement Section

The maximum principal tensile strain at the underside of the asphalt layer usually governs the initiation of fatigue cracking in situ. Mixtures will perform adequately only if they can sustain the necessary repetitions of this strain without cracking. For mixture-analysis purposes, multilayer elastic theory provides a convenient and sufficiently accurate means for estimating the maximum in situ strain at 2°C under the axle load.

In the investigation of the optimal pavement sections several pavement cross sections were evaluated (see Table 1). The asphalt bound layers vary in thickness between 30 and 50 cm (11.8 and 19.7 in.). The performance of these full-depth sections over the three types of soils was evaluated. Two conventional sections with

TABLE 1 Schematic Representation of Structural Sections

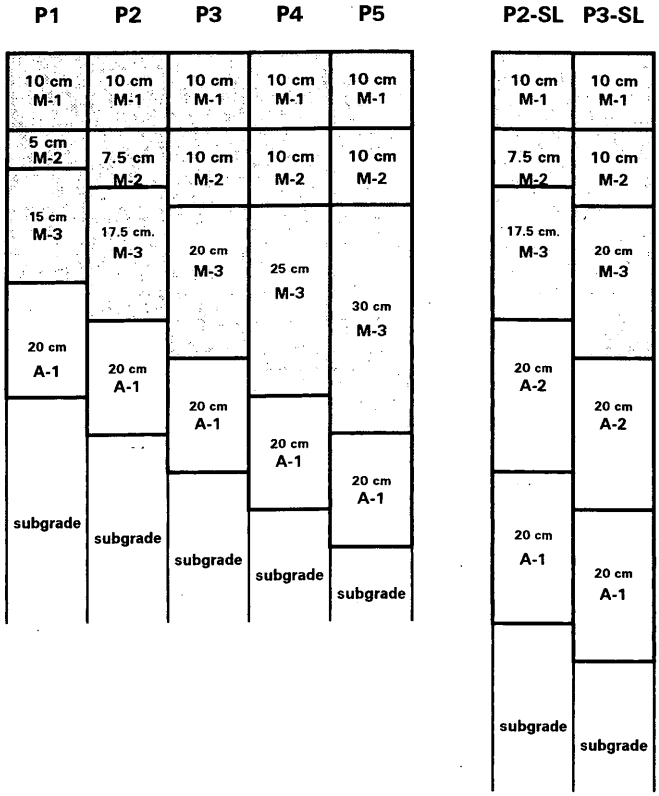

two layers of granular bases were named P2-SL and P3-SL (see Table 1).

For each case the maximum tensile stress and strain on the bottom of the asphalt layer and the maximum compressive vertical strain on the subgrade were determined using linear elastic analysis. Two runs were executed for a pavement section with the same binder thicknesses as P2 and P3 and after adding 20 cm of granular base. These two runs were named P3-CSL and P2-CSL. One run was executed with reduced stiffness of all the binder layers. This run was named P3-CS. The results are presented in Table 2.

Determination of the Fatigue Life of the Pavement Section

The fatigue lives (N_f) of the 33 pavement sections analyzed were computed from the critical principal tensile strain using the newly developed SHRP-A003A model, which accounts for mix void content, mix stiffness, and strain level (*8*).

$$N_f = 2.5263 * 10^5 * e^{(-0.2007 * V_0)} * (\epsilon_0)^{-3.4134} * (S_0)^{-2.1239} \quad (1)$$

where

V_0 = Void content as percent (i.e., 4, 5, or 7);
ϵ_0 = Tensile strain (in./in.);
S_0 = Mix stiffness in psi; and
e = natural logarithm base.

It is considered that this equation, which applies for stress control conditions such as those present in thick pavements, is more likely to yield accurate estimates than any other presented thus far.

Laboratory estimates (N_{supply}) can be compared with service requirements ESAL@20°c only after the application of a suitable shift factor.

$$\text{ESAL@20°C} = SF * N_{demand} \quad (2)$$

where

ESAL@20°C = design ESALs adjusted to a constant temperature of 20 °C,
SF = empirically determined shift factor, and
N_{demand} = design traffic demand (laboratory-equivalent repetitions of standard load).

SHRP-A003A (*4*) reanalyzed previously reported shift factors proposed by NCHRP (*9*) and concluded that a shift factor of 10 would likely correspond to 10 percent field fatigue cracking, whereas a shift factor of 14 would likely correspond to 45 percent field fatigue cracking. These values were used in this analysis. Table 2 presents the fatigue life expected from the pavement sections, using the assumptions presented thus far. Note that the 10 and 45 percent fatigue cracking criteria identify significantly different levels of traffic.

Figure 1 presents the variation of fatigue life for the various pavement sections. It also presents the desired design lives of 20, 30, 35, and 40 years.

The effect on fatigue life of adding an additional 20 cm of aggregate base to pavement types P2 and P3 over a clay subgrade was also evaluated. It was found that the added aggregate layer corresponds to only 2.5 cm of asphalt concrete layer. Based on these results, the use of aggregate base as a structural layer was not recommended; instead, a 20-cm layer is recommended, mainly to provide a good working platform.

By comparing P3-C with P3-CS in Table 2, it can be seen that, with softer asphalt layers, the tensile strain rose from 0.304 E-4 to 0.165 E-4, whereas the vertical compressive strain increased to 1.07E-4 from 0.735E-4. The fatigue life of the pavement section did not change, because stiffness of the mix plays an important role in the fatigue equation (softer mixes can withstand higher strains). If the critical criterion was axial compressive strain on the subgrade, then the pavement with softer asphalt would last a shorter time. It is desirable to have a stiff mix to minimize problems that might emerge from the subgrade.

Recommended Pavement Section

On the basis of these results, pavement type P3 was recommended. This pavement would probably last 20 years (given the predicted traffic pattern), at the end of which, it would only exhibit 10 percent cracking. Before cracking became too extensive, the wearing course would be removed and an overlay placed.

SUBGRADE PERMANENT DEFORMATION VERIFICATION

Permanent deformation of asphalt concrete pavements generally has two major causes

1. Excessive subgrade deformation from high stresses at the subgrade level, and
2. Plastic shear flow in the upper 10 cm (3.9 in.) of the asphalt concrete layer caused by shear stresses near the edge of the tires.

TABLE 2 Results from ELSYM for Structural Pavement Section Analysis and Corresponding Lifetime Predictions for 10 and 45 Percent Fatigue Cracking

Pavement Type	Soil		Tensile Stress (MPa)	AC Tensile Strain	Subgrade Vertical Strain	Nf 10% cracking Fatigue (5%voids) $S_E = 10$	Nf 45% cracking Fatigue (4%voids) $S_E = 14$
P1	A		0.67	2.37E-05	8.91E-05	1.07E+08	1.83E+08
P2	A		0.51	1.79E-05	6.69E-05	2.79E+08	4.77E+08
P3	A		0.41	1.43E-05	5.63E-05	6.00E+08	1.03E+09
P4	A		0.34	1.17E-05	4.58E-05	1.19E+09	2.04E+09
P5	A		0.29	9.76E-06	3.77E-05	2.21E+09	3.78E+09
P1	B		0.70	2.47E-05	1.02E-04	9.28E+07	1.59E+08
P2	B		0.55	1.89E-05	7.93E-05	2.31E+08	3.96E+08
P3	B		0.44	1.52E-05	6.32E-05	4.87E+08	8.33E+08
P4	B		0.39	1.24E-05	5.09E-05	9.76E+08	1.67E+09
P5	B		0.30	1.03E-05	4.18E-05	1.84E+09	3.15E+09
P1	C		0.77	2.65E-05	1.22E-04	7.30E+07	1.25E+08
P2	C		0.60	2.06E-05	9.38E-05	1.73E+08	2.95E+08
P3	C		0.48	1.65E-05	7.35E-05	3.68E+08	6.30E+08
P4	C		0.39	1.34E-05	5.91E-05	7.49E+08	1.28E+09
P5	C		0.32	1.11E-05	5.02E-05	1.42E+09	2.44E+09
P2	C	SL		1.84E-05	7.49E-05	2.54E+08	4.34E+08
P3	C	SL		1.56E-05	6.65E-05	4.46E+08	7.63E+08
P3	C	S		3.06E-05	1.07E-04	3.50E+08	5.99E+08

The first cause can be addressed by increasing the stiffness or thickness of the pavement layers. The Shell design manual (*10*) provides guidelines for this purpose. For a 20-year design life, the limiting vertical compressive strain in the subgrade is 1.37E-4. At 20°C (67°F), the maximum vertical compressive strain for structural pavement type P3 is 7.35E-5. If a conservative value was used in the analysis corresponding to the softer binder, the vertical compressive subgrade strain would be 1.07E-04. This value is still within the limiting criteria.

On hot summer days it is likely that lower stiffness values might occur, thus increasing the vertical compressive subgrade strains. However, only a small percentage of the total truck traffic, less than 10 percent, would be present under those conditions.

MIX DESIGN

The second cause for permanent deformation is loss of shear stability of the mixture, which can only be controlled by proper mix design. Rutting in asphalt-concrete layers develops gradually with increasing load applications. It usually appears as longitudinal depressions in the wheelpaths accompanied by small upheavals at the sides. Rutting is caused by a combination of densification (decrease in volume and increase in density) and shear deformation. For properly compacted pavements, shear deformations, caused primarily by large shear stresses in the upper portions of the asphalt-aggregate layers, are dominant. Repetitive loading in shear is required to accurately measure in the laboratory the influence of mixture composition on resistance to permanent deformation. Because the rate at which permanent deformation accumulates increases rapidly with higher temperatures, laboratory testing must be conducted at temperatures simulating the highest levels expected for the paving mixture in service. In the development of the rut depth it is also necessary to recognize the evolution of the air void content. When air void contents drop below approximately 2 to 3 percent, the binder acts as a lubricant between the aggregates and thus reduces point to point contact.

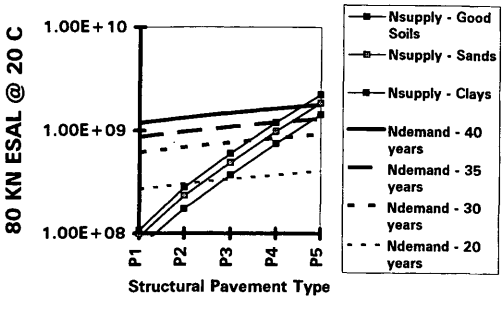

FIGURE 1 80 kN design (SHRP fatigue law, 10 percent cracking) design ESALs at 20°C critical lane.

Procedure to Evaluate the Rutting Propensity of a Mix

A procedure to estimate permanent deformation of asphalt concrete pavements was presented elsewhere (*11,12*). Figure 2 presents a nomograph of the procedure composed of four quadrants; it should be followed clockwise starting in Quadrant 1.

Quadrant 1: Esal versus Rut Depth

Step 1. Determine the number of ESALs for the design life
Step 2. Select maximum allowable rut depth

In the example, a 1,000,000 ESAL design life was selected, and the maximum acceptable rut depth was selected as 0.5 in (1.27 cm).

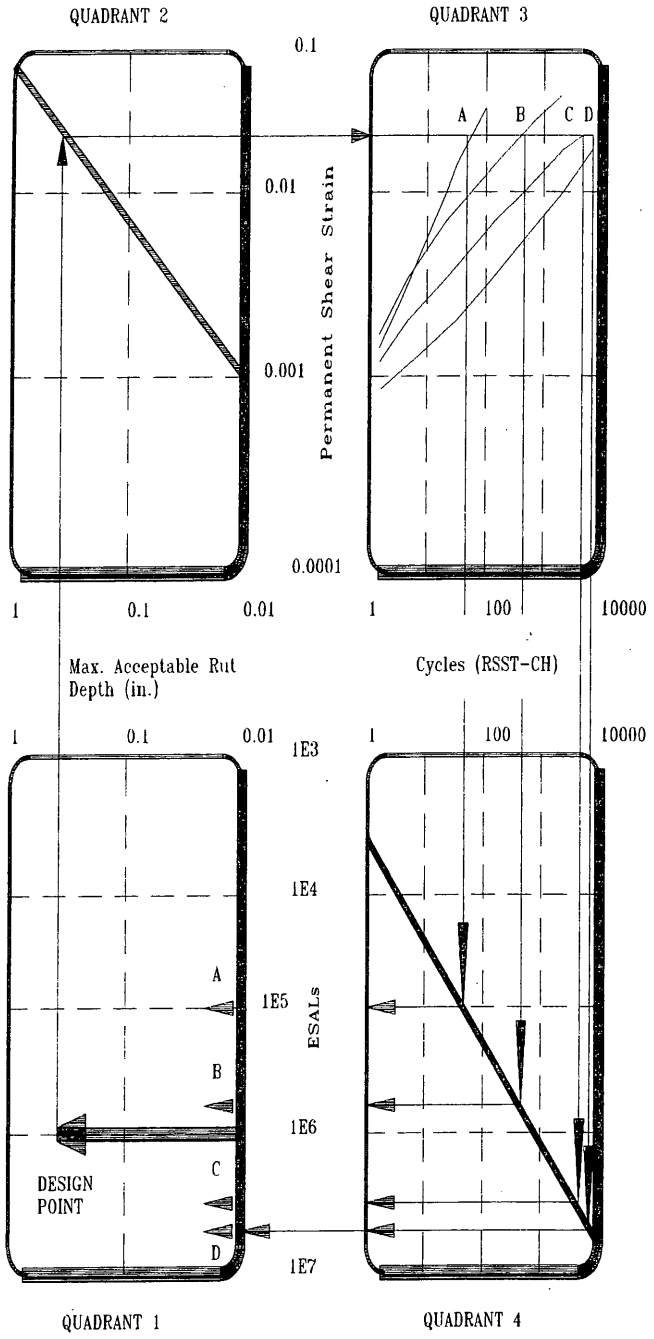

FIGURE 2 Asphalt-aggregate mix design concept (*12*).

Quadrant 2: Rut Depth versus Permanent Shear Strain

Step 3. By using the maximum allowable rut depth, the maximum allowable permanent shear strain is determined on the basis of a relationship between rut depth and maximum shear strain.

This relationship is given by

$$\text{Rut depth (cm)} = 28 * \text{maximum permanent shear strain} \quad (3)$$

Quadrant 3: Permanent Shear Strain versus Cycles

Step 4. Determine mean highest 7-day pavement temperature on site at a depth of 5 cm (2 in.).

Step 5. Execute the repetitive simple shear test at constant height (RSST-CH) test at 69 kPa (10 psi) at that temperature.

Step 6. Determine the number of cycles in RSST-CH that yields maximum allowable shear strain given the relationship between shear strain and the number of cycles obtained from the RSST-CH.

The RSST-CH on a section 15 cm (6 in.) in diameter and 5 cm (2 in.) high was used to evaluate the rutting propensity of the mixes. Three typical graphs of permanent shear strain obtained from the simple shear test at constant height obtained are presented in Quadrant 3 (Figure 2). This graph permits the determination of the number of cycles in RSST-CH required to reach a given permanent shear strain level (in this case shear strain = 0.04545 = 1.25 cm rut depth/28; see Equation 3). It can be seen that Mix D performs better than Mix A.

Quadrant 4: Cycles (RSST-CH) versus ESAL

Step 7. The number of ESALS that can be carried by that mix before the maximum allowable rut depth of 1.25 cm is reached is determined by using the relationship between ESALs and RSST-CH number of cycles.

The equation is given by

$$\log(\text{cycles}) = -4.36 + 1.24 \log(\text{ESAL}) \quad (4)$$

Equation 5 is an empirical equation relating the number of RSST-CH cycles in the laboratory to the number of ESALs in the field. This equation was obtained from SHRP general pavement section sites and has an $R^2 = 0.80$ (*11*).

With results obtained from the analysis which of the mixes would satisfy the design conditions can be identified. In the example, only Mix C and D would satisfy the requirements. Considerations should be given to reliability; adjustments might have to be made. For example, with reliability considerations, perhaps only Mix D would satisfy the requirements.

Determination of Mean Highest 7-Day Maximum Air Temperature

Maximum pavement temperature for a site usually varies within a wide range. To calculate the maximum pavement temperature for the site, data from the two or three nearest weather stations should be selected. Weather stations with more than 20 years of records should be included. For this preliminary project, only 10 years have been used. For each year, the average 7-day maximum temperature is calculated on the basis of the procedure elsewhere (*11*). For the temperatures obtained from the site at Lisbon Airport, which is very close to the location of the future bridge, that value was 31.7°C (89.1°F).

Determination of Surface Pavement Temperature

The pavement surface temperature was calculated using the procedure presented in a work by Sousa and Solaimanian (*11*). By using

this iterative procedure, the surface temperature was calculated to be 56.1°C (133°F). Once the maximum pavement temperature at the surface is found through the preceding formula, the maximum pavement temperature for any depth less than 20 cm (7.8 in.) is found through an empirical equation (11). By using that equation, the following values were obtained for various depths: SMA, 2.5 cm depth, 51.9°C; M-1, 5.0 cm depth, 48.6°C; M-2, 14.0 cm depth, 41.2°C; M-3, 20.3 cm depth, 36.8°C. The temperatures in the table also correspond to the testing temperatures in the permanent shear deformation test (RSST-CH) for each of the mixtures in the pavement layers.

Most of the permanent deformation from shear stresses developing near the edge of the tires takes place at depths of less than 10 cm (3.9 in.). For this reason, special care should be given the mix design of layers SMA and M-1. The mixes should be stable at high temperatures and derive their stability from aggregate interlock.

Rutting Design Requirements

In situ aging of the mixes should also be considered; therefore, they should be tested after being exposed to an aging procedure that best corresponds to the design life that is expected.

Four levels of aging were considered for this project.

1. Short-term oven aging, 4 hr at 135°C (loose mix). The design ESALs expected during the first year should be used in the analysis. Predicted rut depth should not be more than 0.6 cm (0.2 in.).
2. Long-term oven aging, 2 days at 85°C (compacted specimens). The design ESALs expected during the first 3 years should be used in the analysis. The predicted rut depth should not exceed 1.0 cm (0.4 in.).
3. Long-term oven aging, 4 days at 85°C (compacted specimens). The design ESAL expected during the first 6 years should be used in the analysis. The predicted rut depth should not exceed 1.20 cm (0.5 in.).
4. Long-term oven aging 6 days at 85°C (compacted specimens). The design ESAL expected during the first 10 years should be used in the analysis. The predicted rut depth should not exceed 1.25 cm (0.55 in.).

It is known that as a mix ages it stiffens, thereby providing better resistance to permanent shear deformation. It is therefore important to take the age mix into account in the test protocol. Table 3 presents a worksheet for the determination of the parameters for the testing procedures.

Maximum design rut depth at the end of 10 years is 12.5 mm (0.5 in.) This is an acceptable value for pavements with a transverse slope of 2.5 percent. At that time, the first layer should be removed and replaced therefore eliminating any rut.

In Table 3, Column B contains the design ESALs at 80 kN. Column C shows the equivalent laboratory aging level, and Column D contains the cumulative number of ESAL until the corresponding aging level. Column E was determined using Equation 4, and Column F is a design requirement proposed by the authors that can be changed to fit any requirement. Column G was determined using Equation 3.

RSST-CH performance points, reported in Columns E and G for mixes SMA, M-1, M-2, and M-3—at the maximum pavement temperatures encountered at each depth—are presented in the following section.

SPECIFICATIONS

Specifications have been prepared for a preliminary design stage only and provide a general indication of the requirements needed to execute the project. During the execution design stage, more discriminating, accurate, and exact statements must be made. Although several specifications may be presented, only those related to the performance of the mixes in terms of stiffness, fatigue, and permanent deformation (with and without the effect of aging and water sensitivity) are crucial to the behavior of pavement. Penalties and bonuses might be awarded to the contractor on the basis of these values. Gradations and aggregate types and asphalt contents and types can vary as long as performance specifications are satisfied. If any of the performance specifications are not met by a mix, the mix has to be rejected or a new section redesigned to accommodate the new specification if possible. During the execution project level, testing of actual asphalt concrete mixtures is performed.

Specifications have been developed on the basis of new concepts of mix and pavement design. The study is a departure from the Marshall and Hveem empirical methodologies of mix design in that it stresses the determination of fundamental material properties known to affect pavement performance. Fatigue, permanent defor-

TABLE 3 Determination of Permanent Deformation Performance Points for Mix Design

A	B	C	D	E	F	G
Year	LANE (DESIGN) T=(ESAL/2)*0.7	Aging Proced.	Cumm. ESALS to Aging Level	Equivalent Cycles RSST-CH	Total Rut Depth (cm) Acceptable in period	Equivalent Permanent Shear Strain RSST-CH
1	2.84E+06	STOA	2.84E+06	4,389	0.60	2.14E-02
2	5.92E+06	2 Day				
3	9.26E+06	LTOA	1.80E+07	43,362	1.00	3.57E-02
4	1.29E+07					
5	1.69E+07	4 Days				
6	2.12E+07	LTOA	6.89E+07	228,898	1.20	4.29E-02
7	2.59E+07					
8	3.10E+07	6 Days				
9	3.65E+07	LTOA				
10	4.25E+07		2.05E+08	883,134	1.25	4.46E-02

mation, and thermal cracking (although the last one was not considered for this project) are the primary causes of distress in asphalt concrete pavements. These properties are affected by aging and moisture. Protocols have been developed to condition the mixes before testing to determine their fundamental properties. The project specifications require fatigue life and RSST-CH values for conditioned specimens above the minimal 85 percent found for the unconditioned specimens. The moisture conditioning is referred to as "ECFat" and "ECShear" for fatigue beams and RSST-CH specimens, respectively. Moisture conditioning for fatigue and permanent deformation is performed by vacuum saturation of the specimens, followed by immersion for three cycles of 6 hr at 60°C. Between cycles they remain immersed for at least 4 hr at 25°C (75°F).

Specifications for Determination of Fatigue Properties

1. All fatigue testing will be performed at 20°C (67°F), and according to the SHRP A-003A beam fatigue protocol. For each material the following fatigue beam testing program will be performed to determine acceptance.

–The design strain level is the maximum tensile strain at the bottom of the asphalt concrete layer. At this strain level the mix is expected to last N_{demand} cycles. For each material, the mix must reach the required number of repetitions at a given maximum strain. The procedure for determining whether the required number of repetitions is reached is detailed in items immediately following. A reliability factor of 90 percent is applied to the project fatigue life.

–Beam specimens will be fabricated at 4 percent air-void content (with parafilm method), ±0.5 percent air-voids. Beams will be prepared by using rolling wheel compaction and will be mixed and compacted at the specified construction temperatures.

–Two tests, one at 300 microstrain and the other at 700 microstrain, will be conducted to provide a preliminary fatigue curve (relation of $N_f = k_1 * \text{strain}^{k_2}$). From this curve, two strain levels will be selected for further testing, those that result in N_f equal to 50,000 and 500,000 repetitions. The approximate testing time is 24 hr.

–A minimum of four fatigue tests is required (two tests at each of the two strain levels). A least-squares regression fatigue curve must be fitted through the test points. More than four beams can be used to reduce the required number of fatigue load repetitions (N_r). The following equation (*4*) is used to calculate N_r:

$$N_r = N_{demand} * \text{EXP}(Z \times SDn) \quad (5)$$

where

EXP = natural log base, *e;*
Z = coefficient that varies with the confidence levels (Z = 0.84 for 80 percent, 1.28 for 90 percent, 1.64 for 95 percent), and
SDn = standard deviation for the number of beam tests at two strain levels (4) and is given by
= SQRT [0.006903 * $(N_{supply})^{0.2988}$] for 1 replicate per strain level,
= SQRT [0.009653 * $(N_{supply})^{0.2455}$] for 2 replicate per strain level,
= SQRT [0.013450 * $(N_{supply})^{0.2086}$] for 3 replicate per strain level, and
= SQRT [0.017640 * $(N_{supply})^{0.1817}$] for 4 replicate per strain level.

The following two examples illustrate the options that exist for testing to determine acceptance of the material, assuming $N_{demand} = 3.38 * 10^7$ repetitions.

Option 1. Four tests must be performed, two at each strain level. A least-squares regression fatigue curve fitted through the four points plus the two preliminary points must result in a calculated N_r of at least $8.4 * 10^7$ cycles at the design strain [$(N_r = 3.38 * 10^7 * \text{EXP}(1.28 * 0.707)$]. The approximate testing time is 48 hr.

Option 2. Eight tests must be performed, four at each strain level. Following the procedure in Option 1, the calculated N_f must be at least $7.7 * 10^7$ cycles at the design strain [$N_r = 3.38 * 10^7 * EXP(1.28 * 0.645)$]. The approximate testing time is four days.

Figure 3 illustrates the specification concept and identifies a performance point in fatigue corresponding to the design level

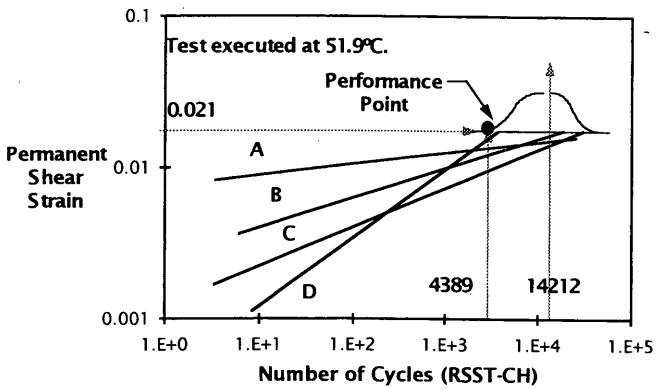

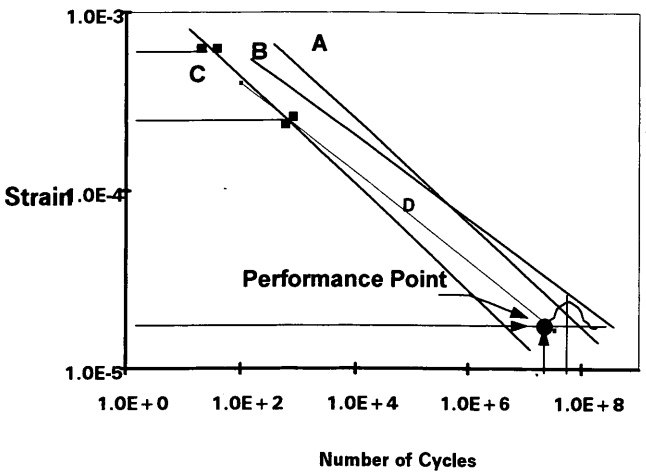

FIGURE 3 Illustration of performance point concept for permanent deformation and fatigue.

computed by ELSYM. Mix A and B would satisfy the requirements, whereas Mix C and D would be rejected (or the pavement section designed).

On the basis of these concepts, fatigue performance points for the mixes are presented in Table 4. Maximum tensile strain is encountered at the bottom of the M3 layer, although it was expected that the top mix, M1, should obey the same criteria, because fatigue cracks can be initiated on the top of the asphalt concrete layer. Given the reduced stiffness of the top mix, it is likely that in some cases aging might harden the mix and therefore reduce its fatigue characteristics. For this reason, fatigue tests after long-term oven aging were recommended .

M3 fatigue resistance basically will control the fatigue life of the pavement. As moisture can affect fatigue performance, a fatigue-life requirement after moisture conditioning is recommended.

For the M2 mix, no fatigue requirement is recommended because tensile strain levels are likely to be very low (except during crack propagation).

During fatigue testing, measurements of stiffness can be made. Table 4 presents the stiffness performance points for the mixes. Requirements after moisture conditioning are recommended for critical mixes.

Specifications for Determination of Permanent Shear Deformation Properties

All permanent shear deformation testing will be performed at the permanent shear deformation design temperature and according to the SHRP A-003A testing protocol. RSST-CH tests will be executed at 69 kPa (10 psi) shear stress (0.1 sec loading with a 0.6 sec rest period).

Cylindrical specimens, 15 cm in diameter by 5 cm high, will be fabricated to a target 3.2 percent air-void content (with parafilm method), ± 0.4 percent air voids. If air-void contents of the specimens are not exactly 3.2 percent, it is acceptable to interpolate or extrapolate the results from specimens with void contents between 2.9 and 3.8 percent with a linear relationship between log of cycles to the required strain with a linear variation of the voids. Specimens will be prepared using rolling wheel compaction and will be mixed and compacted at the specified construction temperatures.

Two RSST-CH tests carried out for at least 4,000 repetitions will be conducted at the specified testing temperature to provide a preliminary rutting curve relation of [Log (permanent shear strain) = A + B * log (cycles)]. A least-squares regression rutting curve must be fitted through the test points for data that begin after 1,000 cycles. This relationship can be extrapolated to any strain level. The approximate testing time is 2 hr.

The number of cycles N_{demand} to reach the required permanent shear strain has to be adjusted to account for reliability based on the variance of the test. The required number (N_r) of cycles is calculated by

$$N_r = N_{demand} * EXP\ (Z \times SDn \tag{6}$$

where

EXP = natural log base e;

TABLE 4 Permanent Deformation, Fatigue, and Stiffness Performance Points for Mixes

MIX	CONDITIONING PROCEDURE	TESTING TEMPERATURE (°C)	PERMANENT SHEAR STRAIN	N (demand) cycles RSST-CH(1)
SMA	STOA	51.9	0.0214	4389
	2 days LTOA	51.9	0.0357	43362
	4 days LTOA	51.9	0.0429	228898
	6 days LTOA	51.9	0.0446	883134
	STOA+ECShear	51.9	0.0214	3730 (2)
M1	STOA	48.6	0.0214	4389
	2 days LTOA	48.6	0.0357	43362
	4 days LTOA	48.6	0.0429	228898
	6 days LTOA	48.6	0.0446	883134
	STOA+ECShear	48.6	0.0214	3730 (2)
M2	STOA	41.2	0.0446	883134
M3	STOA	36.8	0.0446	883134

1- From Table 3
2- From Table 3 requiring 0.85% resistance after moisture conditioning

			FATIGUE		STIFFNESS	
MIX	CONDITIONING PROCEDURE	TESTING TEMPERATURE (°C)	DSL-TENSILE STRAIN	N(demand)(1)	TENSILE STRAIN	STIFFNESS GPa
M1	STOA	20	1.65E-06	3.38 E7	700E-06	>8
	STOA + ECFat	20	1.65E-06	2.87 E7	700E-06	>7
	4 LTOA	20	1.65E-06	2.87 E7		
M2	STOA	20	Not Required	Not Required	700E-06	>10
M3	STOA	20	1.65E-06	3.38 E7	700E-06	>20
	STOA + ECFat	20	1.65E-06	2.87 E7(2)	700E-06	>16

1 - Demand traffic dividing by 10 (shift factor)
2 - Accepting a reduction of 85% in fatigue life due to moisture effects

Z = coefficient that varies with the confidence levels (Z = 0.84 for 80 percent, 1.28 for 90 percent, 1.64 for 95 percent); and
SDn = standard deviation for the RSST-CH for two replicates (= 0.918).

Example: If the N_{demand} is equivalent to 4389 RSST-CH cycles, then the test results should be higher than

$$[N_r = 4389 * EXP (1.28 * 0.918) = 14212$$

The test should be executed at the required testing temperature within ± 0.5°C. Figure 3 illustrates the concept of the performance point in permanent deformation for the SMA mix. Note that either Mix A, B, or C would satisfy the criteria, but Mix D would not.

On the basis of these testing procedures, the performance points for permanent deformation of all mixes are presented in Table 4. Only SMA and M1 mixes have performance requirements after aging and moisture conditioning. If the mix satisfies the N_{demand}, the 6 day long-term aging requirement with short-term oven aging only, then there is no need to execute the 2-4- or 6-day oven-aging process and corresponding testing. Although mixes M2 and M3 will not be subjected to the same shear stress levels in the pavement as those imposed on mixes SMA and M1, the same testing procedure (RSST-CH) was recommended, but at lower testing temperatures.

SUMMARY

The authors present new concepts for asphalt-aggregate mix evaluation based on the findings of the SHRP-A003A project. With new methodologies, it is now possible to tie together pavement performance, structural pavement design, and mix design. The key that links all these concepts together is performance-related mix specifications.

A new pavement was designed in Portugal by CONSULPAV for the new crossing of the Tagus river between Lisbon and Montijo. Asphalt-aggregate mixes were specified based on the results from four-point bending beam fatigue tests, flexural stiffness, and RSST-CH. The specifications constitute a departure from Marshall and Hveem mix design concepts and permit definition of performance points for mixes that are truly site specific.

The concept of performance point has been introduced to facilitate development of specifications. This powerful new approach can be easily implemented at any project level.

ACKNOWLEDGMENTS

The authors express appreciation to the following consultants and advisors for their collaboration and efforts: Bernard Vallerga of B.A. Vallerga Inc., Shmuel Weissman of Symplectic Engineering Corporation Inc., Carl L. Monismith of the University of California at Berkeley, and Lurdes Antunes of the National Laboratory of Civil Engineering, Portugal.

REFERENCES

1. *Nova Travessia Sobre o Rio Tejo em Lisboa—Estudo Geologico e Geotecnico.* Laboratorio Nacional de Engenharia Civil, Departamento de Geotecnia, Nucleo de Prospeccao, Relatorio Sintese, Relatorio 43/93, Lisbon, Portugal, March 1993.
2. *Nova Travessia Rodoviaria sobre o Tejo em Lisboa.* Programa de Concurso 2nd Phase, March 1993.
3. *O Clima de Portugal.* Servico Metereologico Nacional. Fasciculo XIII, 2nd ed. Lisbon, Portugal. 1970.
4. Deacon, J., A. Tayebali, J. Coplantz, F. Finn, and C. L. Monismith, *Fatigue Response of Asphalt-Aggregate Mixtures Part III, Mixture Design and Analysis.* Report prepared for Strategic Highway Research Program A-003A. University of California at Berkeley, May 1993.
5. Powell, W. D. et al. *The Structural Design of Bituminous Roads.* Transport and Road Research Laboratory, Report 1132, Crowthorne, England, 1984.
6. Shook, J. F., F. N. Finn, M. W. Witzack, and C. L. Monismith. Thickness Design of Asphalt Pavements: The Asphalt Institute Method. *Proc., Fifth International Conference on the Structural Design of Asphalt Pavements,* Vol. 1, Delft, the Netherlands, 1982.
7. Monismith, C. L., F. Finn, G. Ahlorn, and N. Markevich. A General Analytical Based Approach to the Design of Asphalt Concrete Pavements. *Proc., Sixth International Conference on the Structural Design of Asphalt Pavements,* Vol. 1, Ann Arbor, Mich., 1978.
8. Tayebali, A., J. Deacon, J. Coplantz, J. Harvey, and C. L. Monismith. *Mixture and Mode-of-Loading Effects on Fatigue Response of Asphalt-Aggregate Mixtures.* Presented at the Annual Meeting of the Association of Asphalt Paving Technologists, St. Louis, Mo., March 1994.
9. Finn, F., C. L. Saraf, R. Kulkarni, K. Nair, W. Smith, and A. Abdullah. *NCHRP Report 291: Development of Pavement Structural Subsystems.* TRB, National Research Council, Washington, D.C., 1986.
10. *Shell Pavement Design Manual,* Asphalt Pavements and Overlays for Road Traffic. In Shell International Petroleum Company Limited, 1978.
11. Sousa, J. B, and M. Solaimanian. *Abridged Procedure to Determine Permanent Deformation of Asphalt Concrete Pavement.* Presented at the Annual Meeting of the Transportation Research Board, Washington, D.C. 1994.
12. Sousa, J. B. *Asphalt Aggregate Mix Design using the Simple Shear Test (Constant Height).* Accepted for presentation at the Association of Asphalt Paving Technologists annual meeting, St. Paul, Minn. 1994.

Publication of this paper sponsored by Committee on Characteristics of Bituminous Paving Mixtures To Meet Structural Requirements.

Development and Evaluation of the Strategic Highway Research Program Measurement and Analysis System for Indirect Tensile Testing at Low Temperatures

WILLIAM G. BUTTLAR AND REYNALDO ROQUE

The indirect tensile testing mode is a practical method for obtaining tensile properties of bituminous mixtures from cylindrical specimens. An indirect tensile creep testing and analysis system is shown analytically to be superior to conventional methods in obtaining fundamental properties of asphalt mixtures at low temperatures in a previous study. Before extensive testing of a wide range of mixtures, however, the ability of the system to obtain accurate, reliable results was unknown. Since the introduction of the new measurement and analysis system, hundreds of field cores and laboratory compacted specimens have been tested and analyzed. Improvements to the system resulting from the testing experience are described, including how analyses of data collected from these tests were used to evaluate the accuracy of the system. Poisson's ratio values obtained with the new system were found not only to be reasonable but also necessary for the accurate determination of creep compliance of the asphalt mixtures tested—a result consistent with analytical findings. In addition, creep compliances obtained from mixtures of well-known components were found to agree with expected values and trends. Input of properties measured on 20 field sections with the new system into a mechanics-based thermal cracking model resulted in accurate predictions of thermal cracking in the field. The measurement and analysis system presented is part of the test selected by the Strategic Highway Research Program to support new mixture specifications for thermal cracking; it has been incorporated into the SUPERPAVE software.

A measurement and analysis system was developed by Roque and Buttlar (*1*) to obtain accurate, fundamental mixture properties at low temperatures in the indirect tensile testing mode (Figure 1). Finite element analyses of diametrally loaded cylindrical specimens have indicated that properties cannot be accurately determined from measurements obtained on the perimeter of the specimen. Stress concentrations near loading heads do not allow the accurate determination of Poisson's ratio, which is required for accurate interpretation of the deformation response. This and other problems were overcome by obtaining vertical and horizontal measurements in the center of flat faces of cylindrical specimens (Figure 1). This measurement system is an extension of the system developed by Anderson [see Hussain (*2*)]. Other advantages of the system include (*a*) reduction or elimination of measurement errors caused by specimen rotation and (*b*) nearly uniform stresses in the measurement zone.

It was determined that analyses of stresses and deformations within the specimen are clearly needed to interpret accurately deflections obtained from the test. Finite element analyses showed that deformations and stresses on flat faces of cylindrical specimens are dependent upon specimen thickness and Poisson's ratio. Roque and Buttlar (*1*) developed a set of correction factors to perform a pseudo–three-dimensional analysis based upon conventional, two-dimensional plane-stress solutions.

The final step in developing the system was to evaluate its practicality and accuracy by testing a broad range of asphalt mixtures. This paper describes the results of testing and analyzing hundreds of field cores and laboratory-compacted specimens, from efforts associated with the thermal cracking validation work of the Strategic Highway Research Program (SHRP) A005 research program.

OBJECTIVES

- To report developments in specimen preparation, testing, and data reduction procedures for the SHRP measurement and analysis system for indirect tensile testing at low temperatures.
- To determine whether reasonable and accurate values of creep compliance and Poisson's ratio can be obtained using this system.

SCOPE

- Four mixtures were tested and analyzed by using materials having well-known properties from the SHRP Materials Reference Library (MRL). Measurements taken from these mixtures were used to compare measured properties with expected trends.
- Cores from 20 test sections across the United States were tested and analyzed as part of the SHRP A005 project to validate the SHRP binder and mixture tests for thermal cracking.
- The present study is limited to procedures and analysis methods related to creep testing, even though the system is often used to obtain the creep and strength properties of bituminous mixtures.

Because of the wide range of properties represented by the mixtures described, it was possible to develop and refine universal testing protocols for the new measurement and analysis system. In addition, measured properties were used in a mechanics-based model developed at Pennsylvania State University (PSU) to predict

Pennsylvania Transportation Institute, Pennsylvania State University, Research Office Building, University Park, Pennsylvania 16802.

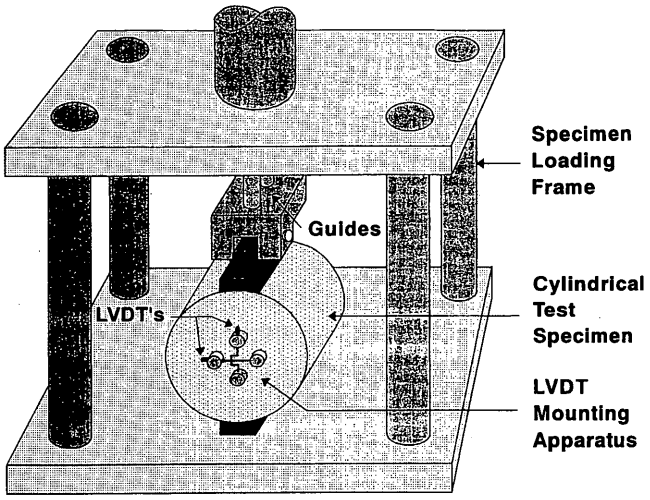

FIGURE 1 Testing arrangement of the new measurement and analysis system.

thermal cracking pavement performance. Comparisons between predicted and observed cracking were used to help evaluate the quality of properties obtained by the new system.

DEVELOPMENT OF TEST EQUIPMENT AND TESTING METHODS

Since its introduction in 1991, the measurement and analysis system developed at PSU has been used to test and analyze hundreds of field cores and laboratory compacted specimens. The test experience has led to substantial developments in test equipment, test procedures, and analysis methods. Such developments, in turn, have led to a system that is more accurate, reliable, and practical.

Development of Test Equipment

The following modifications to test equipment have led to enhanced testing efficiency, longer equipment life, and superior measurements.

1. Round gauge points help produce a simpler, more effective mounting system. Gauge points are small, brass pieces that are glued symmetrically about the centers of both flat faces of test specimens, at a spacing of one-fourth of the diameter. The function of the linear variable differential transformers (LVDT) mounting apparatus (Figures 1 and 2) is to secure LVDT coils and cores onto gauge points at 6.4 mm (0.25 in.) above the surface of the specimen, in such a manner that LVDT core alignment can be manually adjusted to avoid scraping against the inner surface of the coil.

Square gauge points were used originally; however, it was found that they had two disadvantages: (*a*) any substantial misalignment of gauge points makes it difficult to center LVDT cores within the coil, and (*b*) square gauge points do not allow an LVDT mounting apparatus to pivot upon specimen rupture in a failure test, thus increasing the potential for bending or even breakage of the core assembly. Round gauge points, 7.9 mm in diameter by 3.2 mm 5/16 in. in diameter by 1/8 in. now are being used effectively to alleviate these problems.

2. A specimen loading frame should be used inside the testing frame. A specimen load frame (Figure 1) should be used to help deliver loads that are in good alignment, with minimal friction in guides or bearings—22.2 N (5 lb) or less—even when eccentric loads occur because of slightly uneven specimens or temperature changes, for example.

3. A transducer mounting station can be used to expedite testing. Because creep testing often allows time for the operator to perform other tasks during each test, a separate temperature-controlled container can be used to mount and "zero" LVDTs during this free time. As a result, tests can be run consecutively without the additional time required to mount and align LVDTs safely within their linear range before each test.

4. A transducer diagnostics program can help ensure proper LVDT operation. Before deflection data are collected, a diagnostics program should be used to examine the electrical signals of all LVDTs. Checking signals before each test will greatly reduce prob-

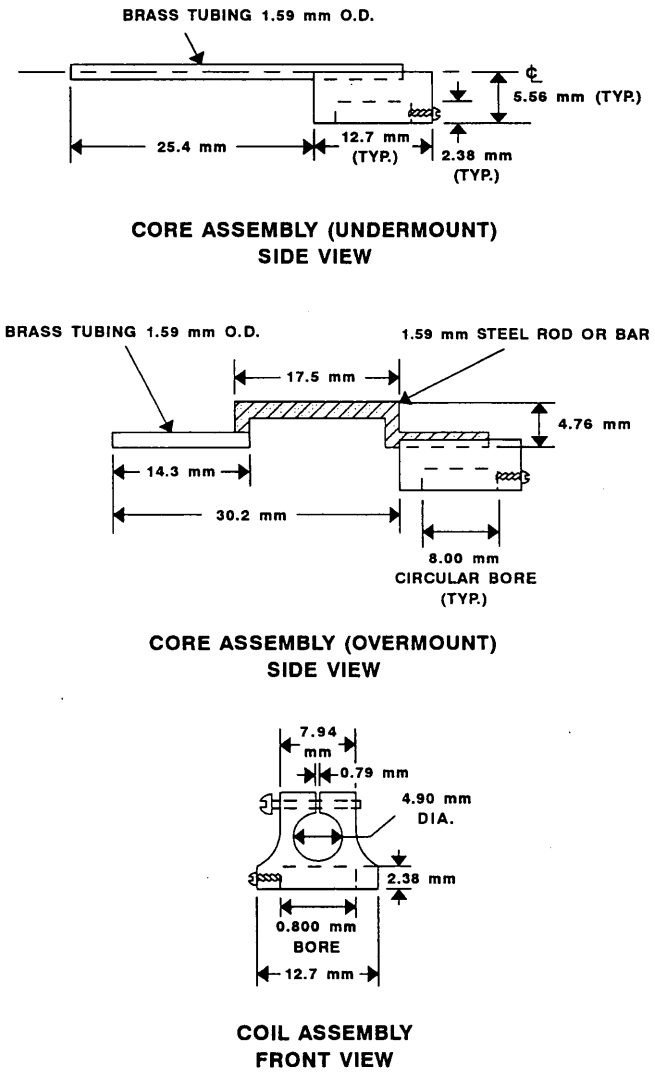

FIGURE 2 New LVDT mounting apparatus.

lems associated with substandard transducers, cables, or connections, as well as help identify temperature or electrical drift. Such monitoring is especially critical because transducers and cables are subject to wear and tear as a result of the explosive nature of failure testing at low temperatures. Signals should be checked for noise levels and signal stability (drift) and to verify that LVDTs have remained safely within their linear range after the specimen is moved into the test chamber. Signal noise should be no greater than $\pm 125 * 10^{-6}$ mm, and signal drift should be negligible. In addition, the diagnostics program should alert the operator if any of the four LVDTs are connected out of order in the test chamber.

5. Use of a data acquisition system is recommended. Because the new measurement and analysis system involves collecting and analyzing large amounts of data, the use of a data-acquisition system to collect deflections and loads is highly recommended and preferable to simply using a chart recorder. One system successfully used in this study collected conditioned LVDT signals using a personal computer with an A/D board and a data-acquisition program. To minimize the size of data files, a 10 Hz sampling rate should be used for the first 10 sec to permit accurate determination of the beginning of the test, followed by a slower rate for the remainder of the test. For example, a 100-sec creep test might consist of 10 Hz for 10 sec and 1 Hz for 90 sec.

Developments in Testing Methods

Strain Limits Established To Keep Specimens in the Linear Range

The analysis system presented later in this study is valid only for specimens tested at temperatures and loading times at which the material exhibits linear elastic or linear viscoelastic behavior. Testing experience indicates that specimens tested at 0°C or lower generally exhibit linear behavior for tests up to 1,000 sec in duration, if creep loads are kept low enough. Additional research is underway, and one finding indicates that choosing loads that limit horizontal tensile strains to 300 microstrains or less helps to keep asphalt mixture behavior safely within the linear range.

Although keeping strains low is desirable, a lower limit on strains must be imposed to ensure the signal to noise ratio is high enough. A lower limit of 50 microstrains has been used successfully with equipment in this study. Because choosing the correct loads to keep strains within these limits requires some trial and error (material properties are not known a priori), a deflection window can be set at some specified time near the beginning of the test. One window that has been used successfully requires that horizontal strains remain within 40 and 120 microstrains at $t = 30$ sec for a 1,000-sec creep test. An operator should stop a test immediately if strains exceed these limits. Specimens should be allowed to recover for at least 3 min before they are reloaded at a different level. Although deflections are not converted into corrected strains until a three-dimensional analysis is performed, for this purpose, strains can be approximated as measured deflection divided by the gauge length.

Specimen Conditioning Recommendations

As with any test method, observing consistent specimen conditioning techniques leads to more accurate and repeatable results. The most critical concerns for this test with respect to specimen conditioning are temperature, humidity, and preloading or seating loads.

Specimens should be cooled at test temperature for 3 to 12 hr before testing. The minimum cooling time recommended is 3 hr, which is determined by embedding thermocouples in the middle of Marshall-sized test specimens and cooling them from room temperature (20°C) to very low test temperatures (−25°C). The maximum recommended cooling time has been established to avoid the effects of low-temperature physical hardening, a phenomenon observed by Bahia (*3*) in asphalt cements. The effects of this phenomenon on the properties of asphalt mixtures are not thoroughly understood at this time.

Tests have clearly shown that variation in moisture within specimens may have a dramatic effect on low-temperature mixture compliance. Thus, humidity conditioning of specimens is highly recommended. A humidity-conditioning procedure that has been used successfully at Pennsylvania State University requires storing specimens at 30 percent relative humidity and 20°C for at least 3 days before testing to ensure uniform and consistent moisture content.

To reduce problems associated with incompatibility between the specimen and loading heads, seating loads should be applied to all specimens before creep tests are performed. A procedure was developed to seat specimens at room temperature (20°C) without introducing large permanent deformations. The procedure involves applying 100 cycles of load pulses and rest periods. Each cycle consists of a 0.1 sec inverted haversine load pulse, with an amplitude of approximately 70 kPa tensile stress (Equation 1), followed by a rest period of 0.9 sec.

$$P_{SEAT} = 0.110(D)(t) \quad (1)$$

where

P_{SEAT} = target seating load (kN),
D = specimen diameter (mm), and
t = specimen thickness (mm).

Test Chamber Temperature Tolerance

Because asphalt concrete properties are particularly temperature-dependent, careful control of test chamber temperatures is required to obtain accurate material properties. A test chamber temperature tolerance of ± 0.5°C is practical and generally acceptable. However, because low temperature measurements on asphalt concrete are extremely small, large temperature fluctuations within this range during testing can lead to significant drift in deflection measurements. Thus, it is recommended that once a test is initiated (where the actual temperature is within ± 0.5°C of the target temperature) the test chamber should not fluctuate more than 0.2°C from this initial test temperature during the entire test.

DEVELOPMENTS IN ANALYSIS PROCEDURES

Simplified Analysis Procedures

Review of Existing Analysis Procedures

A brief review of the measurement and analysis system as presented elsewhere (*1*) aids understanding of newer analysis methods. A finite element study of diametrally loaded cylindrical specimens indicated that measurements obtained with the new system needed to

be corrected to account for three-dimensional effects. Bulging of specimens, as illustrated in Figure 3 (top), affects horizontal and vertical measurements. Bulging correction factors dependent on Poisson's ratio and specimen geometry were developed to account for this phenomenon. In addition, three-dimensional stress states differ dramatically from those predicted by conventional two-dimensional plane-stress theory, as illustrated in Figure 3 (bottom). Stress correction factors, also dependent on Poisson's ratio and specimen geometry, were presented in tabular form. Finally, it was found that horizontal and vertical deformations measured over finite gauge lengths were related to point strains at the center of the flat face by a constant. After two-dimensional stresses and strains were corrected to account for three-dimensional effects, creep compliance was obtained by applying Hooke's law. Because several correction factors were functions of Poisson's ratio, which is not known a priori, the original analysis scheme involved a somewhat tedious iterative solution scheme.

The following sections present a simple set of equations that can be used to obtain creep compliance directly, as well as Poisson's ratio and other quantities of interest. These equations were obtained by presolving the iterative analysis scheme and fitting simple functions through the results.

Creep Compliance

Tensile creep compliance, $D(t)$, is usually the primary quantity to be obtained from the creep test. Poisson's ratio is indirectly very important because it strongly influences the three-dimensional behavior of the specimen and thus plays an important role in the calculation of creep compliance. Poisson's ratio, by definition, is a function of X/Y, where

X/Y = absolute value of ratio of measured horizontal deflection to measured vertical deflection (2)

The absolute value is taken for convenience to avoid the negative ratio that occurs because x and y deflections are always of opposite sign (tensile deflections versus compressive deflections). Thus, creep compliance adjusted for three-dimensional effects can be expressed as a function of X/Y. A method for calculating a representative X/Y from the creep test will be presented later.

Creep compliance for the biaxial stress state that exists on the specimen face ($\sigma_z = 0$) is obtained through Hooke's law.

$$D(t) = \frac{\epsilon_x}{\sigma_x - \upsilon\sigma_y} \tag{3}$$

Substituting correction factors to account for three-dimensional effects (*1*).

$$D(t) = \frac{\frac{H_M^{(t)}}{GL} * 1.071 * C_{BX}}{\frac{2P}{\pi tD}(C_{SX} + 3\upsilon\, C_{SY})} \tag{4}$$

where

ϵ_x = horizontal strain,
σ_x = horizontal stress,
σ_y = vertical stress,
υ = Poisson's ratio,
$H_M(t)$ = measured horizontal deflection at time t,
GL = gauge length (25.4 mm for 101.6 mm diameter, 38.1 mm for 152.4 mm diameter),
C_{BX} = horizontal bulging correction factor,
P = creep load,
C_{SX} = horizontal stress correction factor,
C_{SY} = vertical stress correction factor, and
t,D = as defined before.

Rearranging Equation 4, we obtain Equations 5 and 6.

$$D(t) = \frac{H_m^{(t)} * D * t}{P * GL} * (C_{CMPL}) \tag{5}$$

where

$$C_{CMPL} = \frac{1.071 * \pi * C_{BX}}{2(C_{SX} + 3\upsilon C_{SY}} \tag{6}$$

C_{CMPL} is a nondimensional creep compliance factor that varies linearly with $(X/Y)^{-1}$, as illustrated in Figure 4. This relationship is given by Equation 7.

$$C_{CMPL} = 0.6354\left(\frac{X}{Y}\right)^{-1} - 0.332 \tag{7}$$

This factor is restricted to the following limits (Equations 8 and 9):

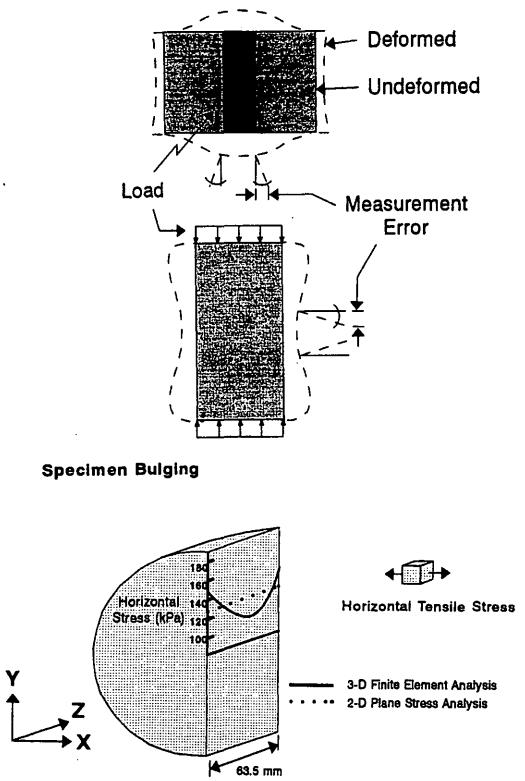

FIGURE 3 Three-dimensional behavior of indirect tensile specimens.

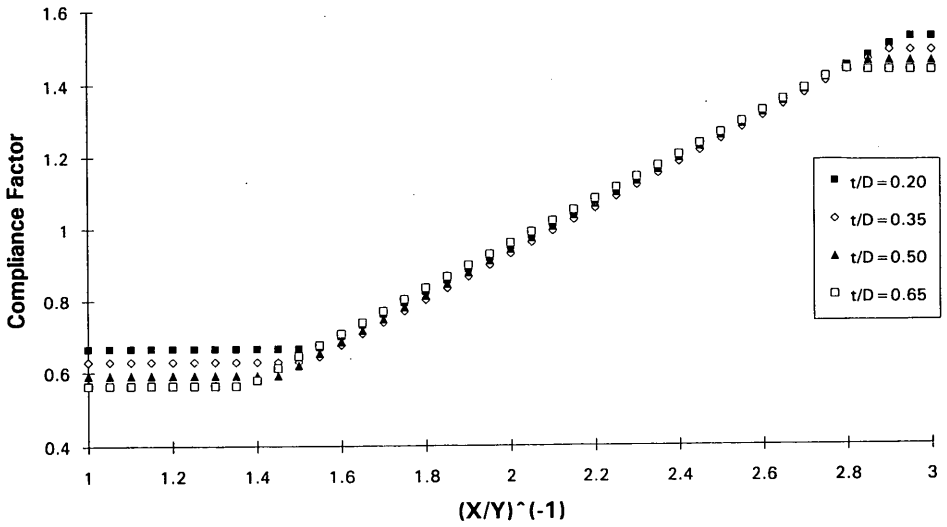

FIGURE 4 Compliance factor versus $(X/Y)^{-1}$ and t/D.

$$\left[0.704 - 0.213\left(\frac{t}{D}\right)\right] \leq C_{CMPL} \leq \left[1.566 - 0.195\left(\frac{t}{D}\right)\right] \quad (8)$$

$$0.20 \leq \frac{t}{D} \leq 0.65 \quad (9)$$

The above limits define the horizontal portions of the data in Figure 4. These limits are a direct consequence of the limits imposed on Poisson's ratio, as described in the following section.

Poisson's Ratio

The calculation of creep compliance presented in the previous section had Poisson's ratio inherently built into the solution via the $(X/Y)^{-1}$ term and did not require the direct solution of Poisson's ratio. However, if a measure of Poisson's ratio of the mixture is desired, it can be easily computed through a family of curves (Figure 5). Poisson's ratio was determined to be related to X/Y and specimen aspect ratio (t/D). The curves were fit with a single function (Equation 10) using linear regression and least squares estimators.

$$\upsilon = -0.10 + 1.480\left(\frac{X}{Y}\right)^2 - 0.778\left(\frac{t}{D}\right)^2\left(\frac{X}{Y}\right)^2 \quad (10)$$

where

$$0.05 \leq \upsilon \leq 0.50 \quad (11)$$

Here, the regression variables reflect the quadratic form of the relation between X/Y and Poisson's ratio and account for the effect of t/D on the relation.

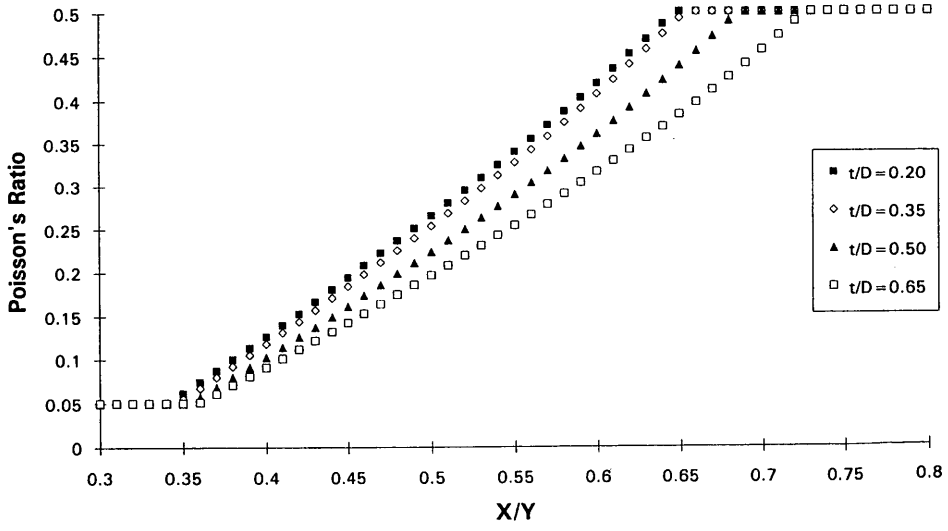

FIGURE 5 Poisson's ratio versus X/Y and t/D.

As seen in the previous limits (Equation 11), Poisson's ratio is restricted between 0.05 and 0.50. These limits were imposed to prohibit unrealistic values of Poisson's ratio from entering into other computations. The upper limit of 0.50 was selected to coincide with the upper bound of Poisson's ratio for elastic materials. Although the lower bound of 0.05 is seldom approached, it was instituted to help keep compliance factors within reasonable limits for unrealistic *X/Y* values. An analysis method aimed at using replication to arrive at a more statistically stable estimate of Poisson's ratio is presented later in this section.

Other Quantities

Other quantities that may be useful in other pavement-response or prediction models are presented in the following equations. The maximum tensile stress, corrected to account for three-dimensional effects, can be obtained by Equations 12 and 13.

$$\sigma_X = \frac{2 * P}{\pi * t * D} (C_{SX}) \tag{12}$$

where

$$C_{SX} = 0.948 - 0.01114\,(t/D) - 0.2693(\upsilon) + 1.436(t/D)(\upsilon) \tag{13}$$

The maximum compressive stress, also corrected for three-dimensional effects is where

$$\sigma_Y = -\frac{6 * P}{\pi * t * D} (C_{SY}) \tag{14}$$

$$C_{SY} = 0.901 + 0.138(\upsilon) + 0.287(t/D) - 0.251(\upsilon)(t/D) - 0.264\,(t/D)^2 \tag{15}$$

Finally, maximum tensile strain, corrected for specimen bulging and conversion to point strain, is obtained by Equations 16 and 17.

$$\epsilon_X = \frac{H_M}{GL} * 1.072 * C_{BX} \tag{16}$$

where

$$C_{BX} = 1.03 - 0.189(t/D) - 0.081(\upsilon) + 0.089(t/D)^2 \tag{17}$$

The advantage of the new analysis system is readily apparent. For example, if creep compliance is the only parameter to be obtained from the creep test (as in SUPERPAVE), it can be easily obtained through Equations 7–9. The new system does not involve an iterative set of equations or require interpolation of tables to obtain correction factors. Instead, the iterative solution is presolved and correction factors are built into the simple relations.

Obtaining Reliable Measures of Poisson's Ratio and Creep Compliance

Accurate measures of Poisson's ratio are necessary to obtain reasonable values of creep compliance (*1*). However, because of variability in asphalt mixtures, unreliable measures of Poisson's ratio may be obtained when using measurements from a single face. Several approaches that use replication to arrive at more reliable values were considered. Of all methods considered, the most reliable results were obtained by taking a trimmed mean of deflections measured on replicate specimens and calculating a single Poisson's ratio and creep compliance for the mixture.

The trimmed mean involves ranking observations numerically, that is, "trimming" the highest and lowest values and averaging the remaining observations. Trimmed observations, although not directly used to calculate the mean, influence the mean and should not be considered wasted data. By using the trimmed mean technique to obtain average horizontal and vertical strains for the mixture, a single, representative Poisson's ratio is determined for the mixture on the basis of measured deflections from all the replicate specimens.

Because replicate specimens may have different thicknesses, creep loads, and possibly diameters, deflections must be normalized so that they can be ranked and trimmed properly. The first step is to find the average thickness, diameter, and creep load of the specimens (Equations 18–20), in which the summation for i varies from 1 to the n number of specimens.

$$t_{AVG} = \frac{\sum t_i}{n} \tag{18}$$

$$D_{AVG} = \frac{\sum D_i}{n} \tag{19}$$

$$P_{AVG} = \frac{\sum P_i}{n} \tag{20}$$

Where n equals the number of specimens.

Each of the ith horizontal and vertical deflection arrays are then multiplied by the following normalization factor (Equation 21) to obtain normalized deflections (Equations 22 and 23).

$$C_{NORM_i} = \left(\frac{t_i}{t_{avg}}\right) * \left(\frac{D_i}{D_{avg}}\right) * \left(\frac{P_{avg}}{P_i}\right) \tag{21}$$

$$H(t)_{NORM_i} = H_M(t)_i * C_{NORM_i} \tag{22}$$

$$V(t)_{NORM_i} = V_M(t)_i * C_{NORM_i} \tag{23}$$

The trimmed mean of the normalized deflection arrays is then obtained by ranking each of the horizontal and vertical arrays according to its normalized deflection values in a window around the middle of the test. For example, consider a 1,000 sec creep test with three replicates and horizontal and vertical measurements taken on both sides of each specimen (Figure 6). Because the data arrays contain measurements taken every 10 sec, and some small level of noise is present in the data, a "noise-insensitive" approximation of the normalized deflection at t = 500 sec is obtained by averaging the nine values in a window between t = 460 and t = 540 sec. These "mid-test" averages of the six horizontal and six vertical deflection arrays are then ranked numerically to identify the middle four horizontal and middle four vertical deformation arrays (the trimmed mean discards the upper and lower observations) to be used in subsequent steps.

The horizontal and vertical deflection arrays remaining after trimming are averaged to obtain the trimmed mean deflection arrays (Equations 24 and 25), where the summation on j

$$H(t)_{TRIM} = \frac{\sum H(t)_{NORM_j}}{2n - 2} \tag{24}$$

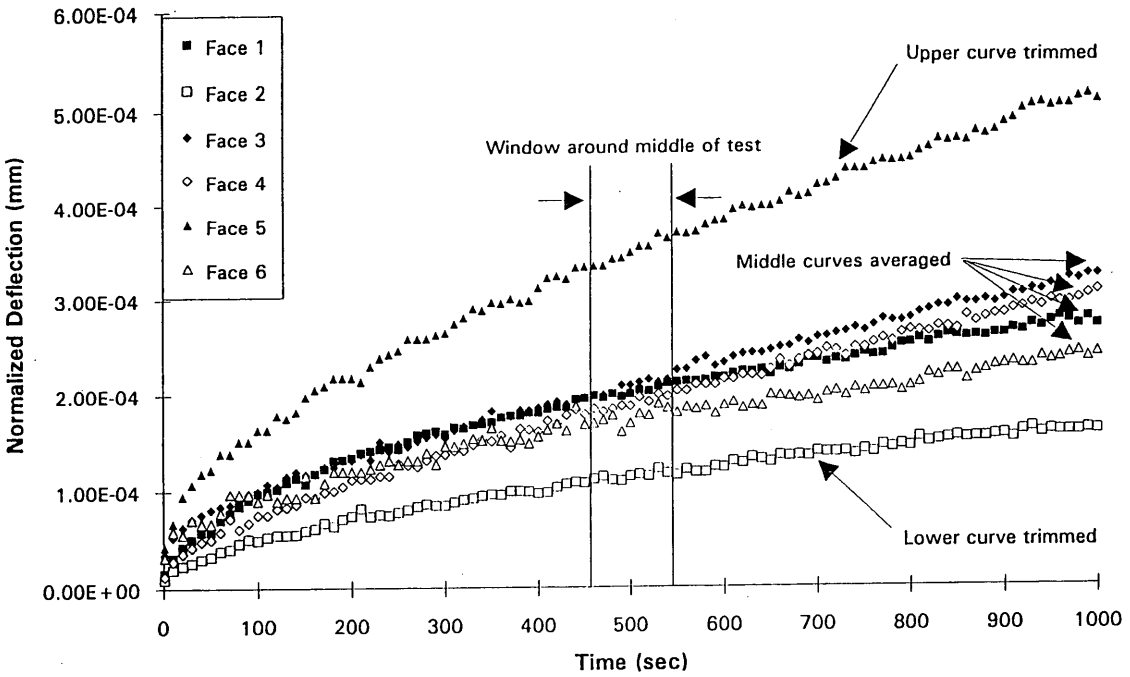

FIGURE 6 Trimmed mean approach for obtaining $H(t)_{AVG}$ and $V(t)_{AVG}$.

$$V(t)_{TRIM} = \frac{\sum V(t)_{NORM_j}}{2n - 2} \tag{25}$$

varies from 1 to the $2n - 2$ sorted deflection arrays.

The scalar quantity $(X/Y)_{TRIM}$ is then calculated for the entire test (Equation 26),

$$\left(\frac{X}{Y}\right)_{TRIM} = \frac{\sum H(t)_{TRIM}}{\sum V(t)_{TRIM}} \tag{26}$$

where the summation is taken over all elements in the array. The remainder of the analysis can be performed using Equations 1 through 17, after making the following substitutions:

$$t = t_{AVG}$$
$$D = D_{AVG}$$
$$P = P_{AVG}$$
$$X/Y = (X/Y)_{TRIM}$$
$$H_M(t) = H(t)_{TRIM}$$

SYSTEM EVALUATION

Although the previous sections described the evolution of the testing and analysis system in terms of test protocols, equipment, and analysis methods, there is one major issue that must still be addressed, namely: Does the new system give reasonable values of creep compliance and Poisson's ratio? There is no simple answer to this because fundamental properties of asphaltic mixtures at low temperatures are not thoroughly documented. In the following section, two separate experiments will show that (*a*) the Poisson ratio values obtained from the new system are reasonable and necessary if creep compliances are to be computed correctly and (*b*) creep compliances obtained from the new system were used successfully to predict thermal cracking performance of field sections when used in a mechanics-based model developed for SHRP at PSU.

MRL Materials Testing Program

Specimens were prepared by using rolling wheel compaction and MRL materials at Oregon State University. Four mixtures were prepared, consisting of two binders (AAG-1 and AAK-2), two air-void levels (approximately 4 percent and 8 percent, and one aggregate (RB). The two binders selected are known to have extremely different properties. The AAG-1 binder is very hard (low compliance), whereas the AAK-2 binder is very soft (high compliance).

Because well-known values of Poisson's ratio for the selected mixtures do not exist, one way to evaluate the reasonableness of values obtained was to compare measured values against expected trends. It is clear that measured Poisson's ratios (Table 1) for mixtures with low air voids (about 4 percent) are higher than those obtained from mixtures with high air voids (about 8 percent). Values range from 0.18 to 0.33 for low-void mixtures, whereas high-void

TABLE 1 Measured Poisson's Ratios in Study on MRL Mixtures

Mixture	Temp. (°C)	Air Voids	
		High	Low
Hard Asphalt (AAG-1)	-5	0.20	0.46
	-15	0.30	0.50
Soft Asphalt (AAK-2)	-5	0.18	0.49
	-15	0.33	0.50

mixtures range from 0.46 to 0.50, following the expected trend. Poisson's ratio is a measure of compressibility, where $\upsilon = 0.5$ for incompressible materials and $\upsilon \leq 0.5$ for compressible materials. A less significant difference is seen between Poisson's ratios obtained at −5°C and those obtained at −15°C for specimens having similar air-void levels. For mixtures with high voids, the differences in Poisson's ratios at the two temperatures range from 0.10 and 0.15; whereas for low-void mixtures the differences range from 0.01 to 0.04.

The importance of using these values of Poisson's ratio measured directly from the specimen, as opposed to the commonly accepted practice of using default values (e.g., $\upsilon = 0.35$), can be seen by comparing compliances obtained using measured Poisson's ratios with those obtained using a default value (Table 2). For mixtures with identical constituents, specimens compacted to a lower level of air voids logically should exhibit lower compliance than specimens compacted to a higher level of air voids. This trend is observed to be true for all four mixtures by comparing compliances computed using measured values of Poisson's ratio (Table 2). In contrast, when a default value of Poisson's ratio ($\upsilon = 0.35$) was used in computing compliances, the expected trend was less prominent. In fact, in two of the four mixtures the expected trend was reversed when the default value of Poisson's ratio was used.

Therefore, measured values of Poisson's ratio appear both reasonable and necessary for the accurate computation of creep compliance. This confirms the analytical findings of Roque and Buttlar (*1*). Other expected trends, such as higher compliance at higher temperatures and higher compliances for the mixture containing the softer AAK-2 binder were also observed (Table 2).

Comprehensive Field Core Testing Program

The new system can be used to obtain fundamental mixture properties at low temperatures that appear to be reasonable. The advantage of obtaining fundamental mixture properties is that the measured values can be used directly in mechanics-based performance prediction models. Such models can be used to predict pavement response and performance for a broad range of conditions and assist efforts to control thermal cracking in performance-based mixture specifications. Additional details on this subject were reported by Lytton et al. (*4*).

A mechanics-based thermal cracking model was developed at PSU under the SHRP A-005 contract. This model was incorporated into the SUPERPAVE software, which was designed to support the new SHRP binder and mixture specification (*5*). A complete description of this model is beyond the scope of this paper. However, the strong correlation between cracking predicted by the mechanics-based model using properties measured from the new system with thermal cracking observed in the field also provides evidence that the method presented here provides reasonable and accurate estimates of low-temperature mixture properties.

In the final calibration of the PSU thermal cracking model, 20 GPS sections from around the United States were used. Site-specific environmental and pavement structure data were used along with information obtained from field-cored specimens using the new testing and analysis system. Rheological properties (i.e., compliances) were obtained by testing each section at three temperatures with three replicates; thus, 180 specimens were tested and analyzed.

Predicted and observed cracking for this comparison were categorized as follows:

- *Zero cracking:* 0 to 7.6 m of cracking per 152-m section (< 1 crack per 76 m) [0 to 25 ft of cracking per 500-ft section (< 1 crack per 250 ft)],
- *Low cracking:* 7.6 to 23 m of cracking per 152-m section (from 1 crack per 76 m to 1 crack per 26 m) [25 to 75 ft of cracking per 500-ft section (from 1 crack per 250 ft to 1 crack per 85 ft)],
- *Medium cracking:* 23 to 46 m of cracking per 152-m section (from 1 crack per 26 m to 1 crack per 12 m) [75 to 150 ft of cracking per 500-ft section (from 1 crack per 85 ft to 1 crack per 40 ft)], and
- *High cracking:* greater than 46 m of cracking per 152-m section (> 1 crack per 12 m) [greater than 150 ft of cracking per 500-ft section (> 1 crack per 40 ft)].

The development of this grouping system is described elsewhere (*4*).

Predicted and observed cracking of the 20 sections were correlated fairly strongly ($R^2 = 0.84$). These results were arranged (Table 3) so that accurate predictions would fall on a diagonal line. As displayed, only one prediction was off the diagonal by two cells and no prediction deviated by three cells. Of the other 19 predictions, 16 were on the diagonal, indicating an excellent prediction, and only three were off the diagonal by one cell, suggesting a fairly good prediction. Thus, the correspondence between predicted and observed cracking was excellent or good for 19 of the 20 test sections. Additional details concerning these predictions may be found elsewhere (*4,5*).

TABLE 2 Compliances from Measured and Assumed Poisson's Ratios in Study on MRL Mixtures

		Compliance @ 1000 sec (1/mPa) x 10^6			
		Measured Poisson's Ratio		Poisson's Ratio = 0.35	
		Air Voids		Air Voids	
	Temp °C	High	Low	High	Low
Hard Asphalt (AAG-1)	-5	251	147	190	231
	-15	60	41	55	55
Soft Asphalt (AAK-2)	-5	3220	1260	2350	1600
	-15	432	247	425	353

TABLE 3 Observed Versus Predicted Cracking Using PSU Thermal Cracking Model and Properties Obtained with New Measurement and Analysis System

		Observed Cracking			
		Zero	Low	Med	High
Predicted Cracking	Zero	4	2	1	
	Low		1		
	Med			3	
	High			1	8

Considering the inherent variability of bituminous mixtures and the potential problems in obtaining properties from field-cored specimens, the quality of measurements obtained with the new system appears to be suitable for use with a mechanics-based thermal cracking model in a performance-based specification test.

SUMMARY AND CONCLUSIONS

Suitable test methods, test equipment, and analysis procedures for the new indirect tensile creep measurement and analysis system were presented in this paper. Developments in test methods help keep specimen behavior in the linear range and allow for consistent temperature, humidity, and load conditioning of specimens. Round gauge points led to an improved transducer mounting system, and the use of a transducer diagnostics program improved the quality of data acquired. Simplified analysis equations were developed that incorporate the solutions of more complicated iterative equations. A trimmed mean data-reduction approach was presented that can be used to obtain more reliable estimates of Poisson's ratio and creep compliance by using data from replicate tests.

It appears that reasonable and accurate estimates of creep compliance and Poisson's ratio can be obtained using the new measurement and analysis system presented. Tests on four MRL mixtures showed the importance of obtaining Poisson's ratio for each mixture. Expected trends between the mixtures were detected by the new system. Performance of 20 field sections was predicted with good accuracy ($R^2 = 0.84$) when properties obtained with the new system were used in a mechanics-based thermal cracking prediction model developed at PSU.

REFERENCES

1. Roque, R., and W. G. Buttlar. Development of a Measurement and Analysis Method to Accurately Determine Asphalt Concrete Properties Using the Indirect Tensile Mode. *Proc., Association of Asphalt Paving Technologists,* Vol. 61, 1992.
2. Hussain, S. R. *Evaluation of Low Temperature and Pavement Deformation Characteristics of Some Polymer Modified Asphalts.* Master of science thesis, Department of Civil Engineering, University of Alberta, Edmonton, Alberta, Canada, spring 1990.
3. Bahia, H. *Low Temperature Isothermal Physical Hardening of Asphalt Cements.* Ph.d. thesis, Pennsylvania State University, University Park, Pa., 1991.
4. Lytton, R. L., R. Roque, J. Uzan, D. R. Hiltunen, E. Fernando, and S. M. Stoffels. *Performance Models and Validation of Test Results.* Draft Final Report to Strategic Highway Research Program, Project A-005, Washington, D.C. 1993.
5. Roque, R., D. R. Hiltunen, and S. M. Stoffels. *Field Validation of SHRP Asphalt Binder and Mixture Specification Tests to Control Thermal Cracking Through Performance Modeling.* Presented at the Annual Meeting of the Association of Asphalt Paving Technologists, 1993.

Publication of paper sponsored by Committee on Characteristics of Bituminous Paving Mixtures To Meet Structural Requirements.

Comparative Performance of Pavement Mixes Containing Conventional and Engineered Asphalts

NABIL I. KAMEL AND LAVERNE J. MILLER

Results of a comprehensive laboratory evaluation of asphalt and pavement mixes containing conventional and engineered paving binders are presented. Model pavement structures were constructed and tested under full-scale dynamic loads and high temperatures simulating field conditions for rutting evaluation. Pavement rutting was monitored over hundreds of thousands of load cycles simulating long-term performance. Comparative results on pavement temperature susceptibility and low-temperature behavior of various conventional and engineered asphalt mixes are presented. Pavement temperature susceptibility is evaluated by determination of resilient moduli (M_R) at various test temperatures. Low-temperature performance is evaluated by determination of pavement stiffness values derived from direct tension tests carried out at very slow speeds. Conventional physical properties and the Strategic Highway Research Program's performance characteristics on test asphalts are presented and discussed in relation to actual measured performance. Analysis of test results identified three asphalt characteristics of particular importance for good performance; all are measured on the aged thin-film oven test residue including asphalt viscosity at 60°C, low-temperature penetration at 4°C, and asphalt temperature susceptibility.

Rutting of asphalt pavements is a problem that many roadway authorities face North America. Pavement rutting can be affected by many factors, including the quality of materials used in terms of aggregates, quality of asphalt cement, and the resultant properties of the selected mix. The mix performance will be affected by the volume of commercial traffic, axle weights and configuration, tire type, tire pressures, and climatic conditions, particularly warm summer temperatures (*1, 2*).

During the past decade, not only has the number of commercial transports and buses increased significantly, but also axle loads and the use of higher tire pressures, and radial and super-single tires by truckers have resulted in widely observed pavement-rutting problems on many highways and arterial roads. Rehabilitation of premature rutting damage not only depletes available maintenance dollars but also inconveniences travelers.

In recent years, highway engineers and researchers have developed alternative mixes to be used in situations of severe loading or when conventional paving materials perform inadequately. Such asphalt mixes may contain large stones, higher percentages of coarse aggregate, or higher percentages of crushed particles—up to 100 percent of the total aggregate mixture. Ontario Ministry of Transportation (MTO), for example, developed new dense-graded asphalt concrete pavement mixes, such as heavy duty binder and heavy duty surface course mixes. Specifications for these heavy duty mixes require the use of 100 percent crushed quarry materials, both in the coarse and the fine aggregates. Use of large stone mixes (*3*) and stone mastic (*4,5*) are other examples of heavy duty pavement mixtures that are expected to attain a higher degree of aggregate interlock, improved load-carrying properties, and enhanced resistance to pavement rutting.

The use of such heavy duty, high stone content, high stability mixes, however, poses performance questions, particularly about long-term durability. Field observations indicate that compaction of such mixes is difficult, and attainment of a 95 percent minimum compaction level, required in dense-graded mixes for good durability, is difficult or, in some cases impractical to achieve.

Other materials have received considerable attention from various highway and road authorities, such as asphalt modifiers (*6,7*), premium grade asphalts (*8,9*), and polymer modified materials (*10,11*). The presence of asphalt cement in the mix can significantly affect pavement performance (*12, 13*). Physical properties and temperature susceptibility characteristics of the asphalt binder influence pavement stiffness, both at high and low field-operating temperatures, and thereby can dramatically affect final performance of the mix. Such modified or engineered asphalts have been used with conventional and with high-stability heavy duty mixes to control rutting, improve low-temperature behavior, and enhance overall pavement durability.

PAVEMENT TEST PROGRAM

The purpose of this investigation was to conduct a comparative test program on pavement mixes containing conventional and engineered asphalts and assess the effects of asphalt properties on pavement performance. Asphalt characteristics were evaluated both by conventional testing and according to the Strategic Highway Research Program SHRP asphalt-binder specifications.

Four commercial asphalt binders were included in the test program: two engineered asphalts and two conventional binders. The two conventional materials were 85–100 pen and 150–200 pen grades. The two engineered asphalts were both 85–100 pen and included an SBS polymer modified asphalt (Styrelf) as well as an asphalt produced by a modified refining process without use of polymer, "premium asphalt." These two engineered asphalts are well-known materials that have been used in many paving projects in various parts of Canada and the United States The premium and the conventional asphalts were obtained from Petro-Canada Lake Ontario Refinery, Mississauga, Ontario. The Styrelf polymer modified material was obtained from Polymac Engineered Asphalts Inc. of Oshawa, Ontario.

The aggregate mixture used conformed to the MTO's requirements for HL3 mix. The HL3 mix is a dense-graded asphalt con-

Petro-Canada Lubricants, Research and Development Centre, 2489 North Sheridan Way, Mississauga, Ontario, Canada L5K 1A8.

crete mix with a 13-mm (0.5-in.) top aggregate size, and typically is used in Ontario for surface course paving on highways carrying up to 5,000 AADT per lane. In all comparisons, the mix design employed was kept the same, the asphalt cement type being the test variable.

Pavement evaluations carried out included determinations of pavement resistance to rutting, low-temperature cracking, and pavement temperature susceptibility. Rutting resistance evaluations were performed at Petro-Canada Asphalt Research Lab in Sheridan Park, Ontario, on full-scale pavement structure models tested under full-scale heavy dynamic loading. Hundreds of thousands of load cycles were applied at high temperatures to simulate long-term permanent deformation response.

Low-temperature stiffness evaluations were carried out on pavement samples using a direct tension test performed at very slow speeds. Pavement temperature susceptibility was determined by measurements of pavement resilient moduli (M_R) on standard pavement briquettes at various temperatures, using dynamic, indirect tension testing.

CHARACTERISTICS OF TEST ASPHALTS AND MIXES

Physical Characterization of Test Asphalt

Physical characteristics of the four test asphalts were determined and are presented in Table 1. Physical properties of the conventional asphalts are typical of high quality 85–100 pen and 150–200 pen asphalt cements used in eastern Canada and the northeastern United States. These materials meet all ASTM and AASHTO specifications for penetration-graded asphalts as well as the requirements for Group A asphalt cement specified by the Canadian General Standards Board (CGSB) as well as all MTO asphalt specifications.

As compared with the 85–100 pen conventional product, both the premium and the Styrelf asphalts provided significantly higher viscosity values, both at 60°C and 135°C, higher low-temperature (4°C) penetration, and superior temperature susceptibility parameters in terms of the penetration-viscosity number (PVN) and the penetration index (PI). The test results on the residue from the thin-film

TABLE 1 Physical Characteristics of Test Asphalts

	ASTM Reference Test	Conventional Asphalts		Engineered Asphalts	
		85-100 Pen	150-200 Pen	Premium	Polymer Modified
Viscosity, poise, 60°C (140°F)	D2171	1453	584	3092	4372
Viscosity, cSt, 120°C (248°F)	D2170	760		1165	1918
Viscosity, cSt, 135°C (275°F)	D2170	350	230	612	835
Pen, 25°C (77°F), 100 g, 5 s	D5	91	168	91	88
Pen, 4°C (39°F), 200 g, 60 s	D5	27	47	38	34
Pen, 4°C (39°F), 100 g, 5 s	D5	7	12	12	10
Ductility, 4°C, cm	D113	60	>150	12	49
Flash Point, C O C, °C (°F)	D92	306 (583)	308 (586)	274 (525)	318 (604)
Pen-Vis No. (PVN), 25-60		-0.5	-0.4	+0.3	+0.6
Pen-Vis No. (PVN), 25-135		-0.5	-0.5	+0.3	+0.7
Penetration Index (PI), 25-4		-1.8	-1.95	-0.3	-0.8
Thin Film Oven Test (TFOT)	D1754				
Mass, % Loss		0.047	0.02	0.14	0.16
Pen, 25°C, 100 g, 5 s	D5	56	100	54	55
% of Original Pen		62	60	59	63
Pen, 4°C, 200 g, 60 s	D5	20	35	30	26
Pen, 4°C, 100 g, 5 s	D5	6	10	9	8
Viscosity, poise, 60°C (140°F)	D2171	2,999	1,215	13,124	11,133
Viscosity, cSt, 135°C (275°F)	D2170	460	325	1,117	1,240
PVN (25-60)		-0.5	-0.6	+0.9	+0.7
PVN (25-135)		-0.6	-0.5	+0.5	+0.7
PI (25-4)		-0.9	-1.1	+0.5	0.0
Solubility in $ClCHCCl_2$	D2042	99.9	99.9	99.9	99.9

oven test (TFOT) also confirm these improved qualities of the engineered asphalt products. Asphalt viscosity at 60°C (high pavement operating temperatures) increased several times over, suggesting that these engineered asphalts should significantly improve rutting resistance more than conventional 85–100 pen grade material.

Again, a significant increase in low-temperature asphalt penetrations measured at 4°C, 200 g, 60s on the TFOT residues is obtained with the engineered products. With improved temperature susceptibility for these asphalts, they should yield superior low-temperature pavement performance. The 150–200 pen asphalt was also evaluated for its low-temperature pavement performance.

By comparing the low-temperature penetrations (4°C, 200 g, 60s) of the engineered and conventional asphalts, it would appear that these engineered asphalts should provide low-temperature pavement performance equivalent to an asphalt grade between 85–100 and 150–200 pen materials. But, because of the improved temperature susceptibility of the engineered asphalts, one may expect their low-temperature performance to approach that of the softer grade 150–200 pen materials at temperatures below 4°C.

In summary, analysis of the physical test data suggests that both engineered asphalts included in this test program should improve pavement rutting, as well as improve low-temperature pavement performance relative to the conventional 85–100 pen control materials.

SHRP Binder Tests and Analysis

A summary of the results on SHRP asphalt binder tests is given in Table 2. These test data were developed through a testing program carried out at Pennsylvania State University. The SHRP test data were obtained on three of the four test asphalts as illustrated in Table 2. A detailed description of the SHRP performance specifications is given in a work by Anderson and Kennedy (*13*).

By comparing the engineered asphalt with the 85–100 pen and 150–200 pen conventional materials, the SHRP test results indicated the following:

TABLE 2 Summary of SHRP Binder Test Results

SHRP Test	Conventional Asphalts (AC-5) 150-200 Pen	Conventional Asphalts (AC-15) 85-100 Pen	Engineered Asphalt Premium	SHRP Binder Specifications
		Tests on Original Binder		
Flash Point, °C	308	306	274	230 min.
Viscosity, Pa.s @ 135°C	0.212	0.338	0.560	3 Pa.s max.
Dynamic Shear, SHRP B-003				
Temp. at which G*/sin δ = 1.0 kPa	56.9	63.5	68.4	52 to 70+ depending on grade
Physical Hardening Index, h	1.71	1.61	1.45	Report
		Tests on Rolling Thin Film Oven Test Residue		
Mass Loss, %	0.007	0.056	0.119	1.0 max.
Dynamic Shear, SHRP B-003				
Temp. at which G*/sin δ = 2.2 kPa	56.4	64.5	70.9	52 to 70+ depending on grade
		Tests on Pressure Aging Vessel Residue, SHRP B-005		
PAV Aging Temperature, °C	100	100	100	90 to 110 depending on grade
Dynamic Shear, SHRP B-003				
Temp at which G*sin δ = 5.0 MPa	13.6	20.3	13.5	7 to 34 depending on grade
Creep Stiffness, SHRP B-002				
Temp. at S(t) = 300 MPa	-22.0	-19.5	-24.8	0 to -36 depending on grade
Temp at which m = 0.3	-23.3	-18.0	-20.0	
Direct Tension, SHRP B-006				
Temp. at which Failure Strain = 1.0%	-16.2	-11.6	-14.5	0 to -36 depending on grade
SHRP Binder Classification	PG 52-28	PG 58-22	PG 64-28	

1. Engineered asphalt should provide a higher rutting resistance performance, as indicated by the B-003 test on RTFOT residue. The temperature at which $G^*/\sin\delta$ reaches 2.2 kPa is about 7°C (12°F) higher for the engineered product than for the conventional 85–100 pen asphalt.

2. Engineered asphalt also should provide superior cold-temperature performance as indicated by the creep stiffness, SHRP B-002, and the direct tension SHRP B-006 test results. SHRP tests rated the engineered asphalt cold-temperature performance between the two conventional asphalts. The limiting temperature at which the *m* value is equal to 0.3 for the 85–100 pen conventional asphalt is −18.0°C (0°F) compared with −20.0°C (−4°F) for the engineered asphalt and −23.3°C (−10°F) for the conventional 150–200 pen materials. The limiting temperature at which the binder stiffnesses are equal to 300 MPa is −24.8°C (−12°F) for the engineered asphalt versus −19.5°C (−2°F) for the 85–100 pen and −22.0°C (−8°F) for the 150–200 pen conventional asphalts.

3. SHRP test results indicate superior fatigue performance for the engineered asphalt. The temperature at which $G^*/\sin\delta$ is equal to 5.0 MPa is 7°C (12°F) lower for the engineered product if compared with that of the control 85–100 pen conventional product. Note that the limiting temperature for fatigue performance of the engineered asphalt is equivalent to that displayed by the softer 150–200 pen (AC-5) conventional product.

4. For design purposes, the SHRP test results rated the engineered product in the same low temperature classification as the 150–200 pen (AC-5) materials, [i.e., a minimum pavement design temperature of −28°C (−18°F)], and in a classification higher than the 85–100 pen (AC-15) conventional product for high temperature performance, [i.e., an average 7-day maximum pavement temperature of 64°C (147°F) versus 58°C (136°F) for the conventional material].

5. In the final analysis, according to the SHRP test results, the engineered asphalt is a superior asphalt that has higher resistance to rutting and tenderness; has superior fatigue, low-temperature, and physical hardening characteristics; and meets requirements for ten SHRP performance grades versus only four grades for each of the conventional materials 85–100 pen and 150–200 pen consecutively, as shown in Table 3. According to the SHRP classification, the engineered asphalt has a useful temperature span of 92°C; whereas each of the conventional asphalts tested has a 80°C span.

Characteristics of Asphalt Test Mixtures

Marshall design characteristics for the HL3 test mixes were determined and are presented given in Table 4. The HL3 mix contained 40 percent coarse aggregate, 60 percent fine aggregate, and 5.4 percent asphalt cement. The coarse aggregate is a crushed quarry limestone material, and the fine aggregate is a 2:1 blend of sand and washed screenings. All the three test mixes provided excellent stability and overall Marshall properties exceeding the HL3 requirements in the MTO specifications (Table 2).

Note that the HL3 test mix used is a high-quality mix; it contains large amounts of crushed quarry materials for good interlock, and high-stability properties to optimize the effects of the aggregate on final performance. No significant differences in Marshall properties are noted between conventional and engineered asphalts.

TABLE 3 Comparative Compliance to SHRP PG-Grades for Asphalts Tested

Grade	Conventional Asphalts		Engineered Premium Asphalt
	85-100 Pen (AC-15)	150-200 Pen (AC-5)	
PG 52-10	YES	YES	YES
PG 52-16	YES	YES	YES
PG 52-22	No	YES	YES
PG 52-28	No	YES	YES
PG 52-34	No	No	No
PG 52-40	No	No	No
PG 52-46	No	No	No
PG 58-16	YES	No	YES
PG 58-22	YES	No	YES
PG 58-28	No	No	YES
PG 58-34	No	No	No
PG 58-40	No	No	No
PG 64-16	No	No	YES
PG 64-22	No	No	YES
PG 64-28	No	No	YES
PG 64-34	No	No	No
PG 64-40	No	No	No
PG 70-10	No	No	No
PG 70-16	No	No	No
PG 70-22	No	No	No
PG 70-28	No	No	No

TABLE 4 Marshall Characteristics for Various HL3 Test Mixes

	Conventional Asphalt 85-100 Pen	Engineered Asphalts		Ontario MTO, HL3 Specifications
		Premium	Polymer Modified	
Voids, %	3.1	3.3	3.6	3-5
Stability, N	13,967	13,580	14,975	8,900 min.
(lb)	(3,140)	(3,055)	(3,366)	(2,000 min.)
Flow, 0.25 mm	11	11.3	12.5	8 min.
VMA, %	15.0	15.7	15.4	15.0 min.

PAVEMENT PERFORMANCE EVALUATIONS

Various test mixes were evaluated for pavement rutting resistance, low-temperature stiffness, and pavement resilient modulus.

Pavement Rutting Resistance

Test pavements were constructed in the Petro-Canada Research and Development pavement performance simulation test pit and then tested under full-scale repeated loadings simulating heavy trucks. The pavement structure was built in layers from the subgrade and under controlled conditions to attain required thickness, moisture, and density. The total structure was tested with a 40 kN (9 kips) dynamic load at 9 cps frequency and at a loading pressure of 552 kPa (80 psi), simulating a fully loaded truck axle traveling at 50 km/hr (30 mph). The pavement structure consisted of 600 mm (24.0 in.) of sand subgrade, 225 mm (9.0 in.) of granular base, and 75.0 mm (3.0 in.) of asphaltic concrete mix. A detailed description of the test is given elsewhere (*12*).

Pavement permanent deformation is monitored continuously with various load cycles. The test is run for 1,000,000 load cycles at the desired test temperature. At the end of the test, the pavement surface profile is recorded and pavement rutting under the centerline of the load is measured.

Three test pavements were evaluated using the two engineered asphalts and the conventional 85–100 pen material as a control. Rutting resistance evaluation testing was carried out at 50°C (122°F) using a specially designed environmental chamber placed on top of the pavement in the test pit.

Test results for the three HL3 pavements are plotted in Figure 1. In terms of performance, both the premium and the polymer modified asphalts provided superior rutting resistance when compared with the pavement with conventional asphalt. At the start of the test, the rutting performance was excellent for each of the three test pavements. Differences in performance began to be observed after passes of 10,000 to 20,000 load cycles, when the conventional pavement section started to show deterioration at an accelerated rate. As more loads were applied, the superior performance of the premium and the polymer modified asphalts became clear. These quality pavements performed equally well throughout the test.

After 100,000 load cycles, pavement permanent deformation in the HL3 mix with conventional asphalt amounted to 19.8 mm (0.8 in.) versus 10.8 mm (0.4 in.) and 11.9 mm (0.5 in.) for the premium and polymer modified asphalt pavements, respectively. These values represent a 45 percent reduction in pavement rutting with premium asphalt and a 40 percent reduction with the polymer modified materials.

Because excessive rutting occurred in the pavement test section with the conventional asphalt, the test was terminated after 300,000 load cycles. Tests for the other two pavement sections continued to 900,000 load cycles (Figure 1).

Comparing the number of 40 kN (9.0 kips) load cycles needed to cause 26.0 mm (1.0 in.) deformation in each of the three pavement test sections, it is clear that the premium and the polymer modified asphalt pavements provided a significant increase in load-carrying capacity. As illustrated in Figure 1, the number of accumulated heavy load cycles carried out by these pavements is more than 300 percent of that carried out by the pavement with conventional asphalt.

Figure 2 shows a schematic diagram for pavement surface profiles taken before and after the test for the conventional and premium asphalt sections. The total pavement rutting in the mix with conventional asphalt amounted to 37.7 mm (1.5 in.) versus 18.4 mm (0.7 in.) for the mix with premium asphalt. This represents a 51 percent reduction in the total pavement rutting. Note that lateral displacement of the mix under the combined effects of repeated heavy loadings and high test temperature is substantial in the conventional asphalt pavement section. Lateral displacement of the paving material is significantly reduced with use of the premium asphalt, substantially reducing total pavement rutting as indicated in Figure 2.

In summary, the results of the rutting resistance evaluations demonstrated clearly that the quality of the asphalt cement in the mix greatly influences the final rutting performance. Pavement permanent deformation reduction of up to 50 percent was obtained with the use of the engineered asphalts tested.

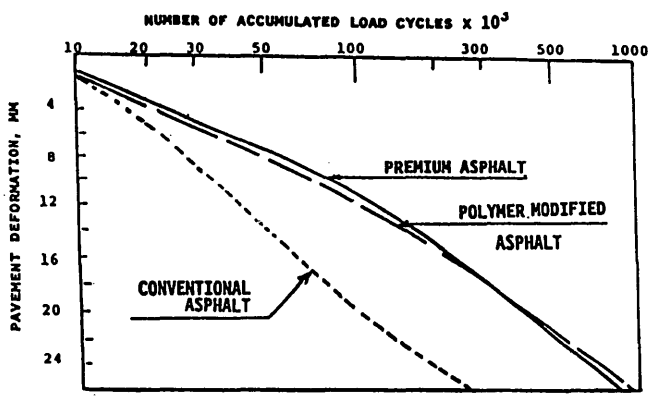

FIGURE 1 Pavement permanent deformation versus load cycles for various HL3 test mixes, 50°C (122°F).

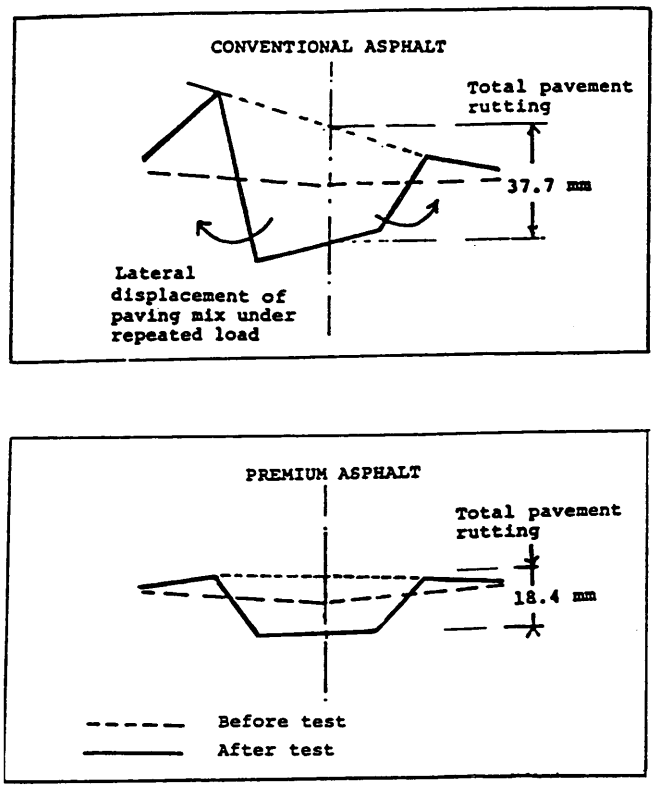

FIGURE 2 Pavement surface profiles before and after 100,000 load cycles, 50°C (122°F).

Pavement Low-Temperature Stiffness

Low-temperature pavement stiffness evaluations using a direct tension testing were carried out on samples cut from standard pavement briquettes. The pavement briquettes were tested at the University of Waterloo cold temperature facility (*14*) using a constant rate of extension, 0.004 mm/min (0.00016 in./min), at a temperature of −18°C (0°F).

The testing included conventional, premium, and polymer modified asphalts. For comparison, a sample of the same HL3 mix with the 150–200 pen conventional asphalt cement was also included in the study, as shown in Table 5. The test results shown represent an average for a minimum of five test samples.

The effects of asphalt cement on low-temperature stiffness is significant and is well demonstrated in these tests. On comparing mix stiffness for premium and conventional asphalts, it is clear that the mixes with engineered asphalts provide substantial reductions in low-temperature pavement stiffness, 42 and 45 percent at −18°C (0°F). The reductions observed with premium asphalt appear to approach the levels experienced with the control mix containing the 150–200 pen asphalt. These results suggest that pavements constructed with such engineered asphalts will not only provide substantial reductions in pavement permanent deformation but also significantly improve low-temperature pavement performance.

Pavement Temperature Susceptibility Evaluations

Pavement resilient modulus determinations were carried out on standard pavement briquettes at three test temperatures (5°C, 25°C, and 40°C) using indirect tension testing, ASTM D4123 (*15*). The test results on HL3 mixes for both conventional and premium asphalts are shown in Table 6. Test results confirm the superior temperature susceptibility properties of the pavement mixtures with premium asphalt. Improved resilient modulus was obtained at both low and high temperatures with the engineered asphalt. Pavement mix moduli at 5°C were 15 percent lower and at 40°C were 25 percent higher with the engineered asphalt as compared with the same mix with conventional asphalt. These results confirm the superior pavement rutting performance and the improved low-temperature behavior observed with premium asphalt pavements.

Temperature susceptibility performance of the various test mixes is directly related to temperature susceptibility of the asphalt in the mix. Note that both test asphalts exhibit the same 85–100 pen consistency at 25°C; however, the superior temperature susceptibility of premium asphalt as indicated by the PVN and PI parameters (Table 1) is directly responsible for the superior performance of the mixes containing this material. To attain good pavement performance under a wider range of field operating conditions, the asphalt binder must have superior temperature susceptibility properties.

INFLUENCE OF ASPHALT PHYSICAL PROPERTIES ON PAVEMENT PERFORMANCE

Although all three test asphalts used in the pavement rutting evaluation were of the same grade (i.e., 85–100 pen) their relative performance was quite different. The superior pavement rutting per-

TABLE 5 Summary of Low-Temperature Pavement Stiffness

Test Speed 0.004 mm/minute
Test Temperature -18°C (0°F)
Test Samples measured 40 mm x 40 mm x 75 mm

	Conventional Asphalts		Engineered Asphalts	
	85-100 Pen	150-200 Pen	Premium	Polymer Modified
Mean Failure Stress, KPa (psi)	4461(647)	4026(584)	3585(520)	4716(684)
Mean Stiffness Modulus, MPa(psi x 10^3)	6.1(884)	2.77(401)	3.38(490)	3.52(510)
Stiffness as a % of Conventional Mix	100	45	55	58
% Stiffness Reduction at -18°C	-	55	45	42

TABLE 6 Pavement Resilient Moduli Test Results

	Conventional Asphalt 85-100 Pen	Engineered Asphalt Premium
Modulus of Elasticity (M_R)		
5°C, MPa (psi x 10^3)	4.72 (684)	4.13 (598)
25°C, MPa (psi x 10^3)	1.86 (270)	1.78 (258)
40°C, MPa (psi x 10^3)	0.61 (88)	0.75 (108)

formance of the pavements made with the engineered asphalts can be attributed to the rheology of these materials. Both the Styrelf and premium asphalts have significantly higher viscosity values at 60°C than the conventional 85–100 pen asphalt, and their deformation resistance corresponds with such properties.

Absolute viscosity at 60°C (140°F) is particularly important because it represents the asphalt consistency at a high operating temperature range in which pavement mix is generally softer and weaker. The higher the absolute viscosity of the binder at 60°C, the stiffer and the more resistant the pavement mix to permanent deformation.

But, because different asphalt materials, depending upon chemical composition and other factors, would age during mixing at the hot mix plant at different rates, the viscosity of the virgin asphalt may not be the best indicator of long-term performance. One must examine the characteristics of the residue from the TFOT or RTFOT, which simulate the aged asphalt after mixing at the hot mix plant. This is quite apparent from the data on physical characteristics presented in Table 7. Comparing the TFOT viscosity at 60°C (140°F) for the three asphalts tested in the rutting evaluations, both the premium and the polymer modified products show consistencies in the range of 11,000 to 13,000 poise in comparison to 3,000 poise for the conventional asphalt. The three- to fourfold increase in asphalt viscosity at 60°C produced the significant reductions noted in pavement rutting for the mixes tested with these materials.

SHRP performance testing predicted the improved rutting resistance of the engineered product tested, premium asphalt. The temperature at which the dynamic shear measurement of $G^*/\sin\delta$ on the RTFOT residue reached 2.2 kPa was 7°C to 8°C higher in the case of the engineered product, as compared with the control asphalt. Improved rutting performance of the engineered product is also consistent with the higher moduli values obtained on the pavement samples containing this material.

The low-temperature pavement stiffness behavior of the various test mixes is affected primarily by the asphalt binder in the mix. Mixes with the engineered asphalts provided substantial reductions in low-temperature pavement stiffness. The asphalt physical property that may best describe asphalt consistency at low temperature is the low-temperature penetration (4°C, 200 g, 60s) measured on the aged TFOT residue as shown in Table 7. The higher the value of the low-temperature penetration, the more flexible and less stiff is the pavement mix, and the better the pavement performance at low temperature. Note that the Pen Ratio (4°C/25°C), Table 7, fails to differentiate between the low-temperature performances of the

TABLE 7 Asphalt Physical Characteristics Influencing Rutting, Low-Temperature Stiffness, and Pavement Temperature Susceptibility

Pavement Performance Concern	Asphalt Properties	Conventional Asphalts		Engineered Asphalts	
		85-100 Pen	150-200 Pen	Premium	Polymer Modified
Rutting Resistance	Absolute Viscosity @ 60°C, P				
	Original	1453	584	3092	4372
	TFOT Residue	2999	1215	13,124	11,133
Low Temperature Thermal Cracking	TFOT Residue				
	Pen @ 25°C, 100 g, 5 s	56	100	54	55
	Pen @ 4°C, 100 g, 5 s	6	10	9	8
	Pen @ 4°C, 200 g, 60 s	20	35	30	26
	Pen Ratio (4°C/25°C)	36	35	56	47
Temperature Susceptibility	TFOT Residue				
	PVN (25-60)	-0.5	-0.6	+0.9	+0.7
	PVN (25-135)	-0.6	-0.5	+0.5	+0.7
	PI (25-4)	-0.9	-1.1	+0.5	+0.0

two conventional asphalts. The parameter essentially measures asphalt temperature dependence instead of low-temperature behavior.

The engineered asphalts provided approximately a 50 percent increase in low-temperature penetration (4°C, 200 g, 60s) over that of conventional asphalt; this improved property, coupled with improved temperature susceptibility of the asphalt, produced the significant reductions noted in pavement low-temperature stiffness for the test mixes incorporating these materials.

SHRP performance tests on thermal cracking performed on the aged residue from the pressure aging vessel predicted improved low-temperature performance of the engineered asphalt and rated it closer to the performance of the 150–200 pen asphalt. These results were confirmed by low-temperature pavement stiffness tests carried out on the pavement samples containing these asphalts.

Asphalt temperature susceptibility, as indicated by PVN, PI, and pen ratio measurements, is another critical parameter; it influences pavement temperature susceptibility, pavement stiffness, and pavement performance over the entire range of field-operating temperatures. To attain good pavement performance for heavy loading conditions at extremely warm and cold temperatures, the asphalt cement must have good temperature-susceptibility properties. The requirement now has been recognized in the CGSB asphalt specifications (i.e., grouping A, B, C asphalts according to their temperature susceptibility). New SHRP performance-based asphalt specifications also recognize the importance of this property and classify various asphalts according to their temperature susceptibility. The engineered asphalts evaluated provided superior temperature susceptibility parameters, with positive PVN and PI values and pen ratios around 50 percent—significantly higher parameters than were established for the conventional asphalts.

Other asphalt physical characteristics such as kinematic viscosity at 135°C and flash point will affect handling of asphalt at the hot mix plant as well as mixing temperatures and final field compaction of the product.

SUMMARY AND CONCLUSIONS

A comprehensive asphalt test program on pavement mixes containing conventional and engineered asphalts evaluated pavement performance in terms of pavement rutting, low-temperature stiffness, and pavement temperature susceptibility.

Pavement samples were tested under full-scale dynamic, heavy loadings to hundreds of thousands of load repetitions to simulate the long-term pavement permanent deformation response. Low-temperature pavement stiffness evaluations were carried out on pavement samples using a direct tension testing at very slow speeds. Pavement temperature susceptibility tests were conducted by determining test pavement resilient modulus for a temperature range, 5°C to 40°C, using dynamic indirect tension tests on standard pavement briquettes.

It is well established that substantial improvements in pavement rutting performance can be achieved by using asphalt mixtures containing maximum amounts of crushed aggregates, which provide good interlocking properties and higher load-carrying characteristics. Results of this investigation show that the use of high-quality asphalt cement in the mix may be equally important. The use of premium and polymer modified asphalts provided rutting reductions of up to 50 percent and an increase in pavement load-carrying capacity of more than 300 percent. Mixes with these engineered asphalts also exhibited superior low-temperature behavior and reduced low-temperature pavement stiffness by as much as 45 percent. Mixes containing premium asphalt exhibited superior temperature-susceptibility characteristics and provided improved pavement moduli values at both the highest and lowest test temperatures, further confirming the improved rutting and low-temperature performance results.

The authors identified three important asphalt physical characteristics affecting pavement performance: absolute viscosity at 60°C, low-temperature penetration at 4°C, and asphalt temperature susceptibility, all measured on aged TFOT residue. Substantial improvement in pavement rutting, low-temperature stiffness, and temperature susceptibility performance resulted when test pavements incorporated asphalts that were characterized by high viscosity, high low-temperature penetration, and low-temperature susceptibility.

When the test asphalts were characterized according to SHRP binder specifications, the engineered premium asphalt showed significant performance improvements at high, intermediate, and low temperatures in contrast with unmodified control asphalts. SHRP test results rated the engineered premium asphalt in an improved class for both rutting and low-temperature cracking. The engineered asphalt also showed significant improvement in the limiting temperature for fatigue performance. It satisfied requirements for 10 SHRP asphalt grades whereas the conventional asphalt product met requirements for only four. The final SHRP classification suggests that the engineered asphalt has a useful service temperature span of 92°C as compared with a span of 80°C for conventional asphalt.

ACKNOWLEDGMENTS

The authors express their appreciation to R.C.G. Haas and others at the University of Waterloo for performing low-temperature stiffness testing on the pavement samples, to H. Bahia and the Pennsylvania Transportation Institute for performing the SHRP binder characterization, and to Polymac Engineered Asphalt Corp. of Oshawa, Ontario, and Petro-Canada Lake Ontario Refinery, Mississauga, for providing the asphalt materials used in this work.

REFERENCES

1. Tam, K. K., and D. F. Lynch. *Ontario Freeway Rutting Investigation.* Ontario Ministry of Transportation and Communications. Presented at the Roads and Transportation Association of Canada Annual Conference Workshop on Rutting, Toronto, Ontario, Canada, Sept. 1986.
2. Robberts, F. L. et al. *Effects of Tire Pressures on Flexible Pavements.* Research Report 372-1F. Texas Transportation Institute, Texas A&M University, College Station, Aug. 1986.
3. Mahboub, K., and D. L. Allen. Characterization of Rutting Potential of Large-Stone Asphalt Mixes in Kentucky. In *Transportation Research Record 1259,* TRB, National Research Council, Washington, D.C., 1990.
4. *Stone Mastic Asphalt: SMA Technology Synopsis and Work Plan,* Draft Report, Office of Technology Applications, Engineering Applications Division. FHWA, U.S. Department of Transportation, Feb. 1991.
5. Kennepohl, G. J., and J. K. Davidson. *Introduction of Stone Mastic Asphalts in Ontario.* Presented at the Annual Meeting of Association of Asphalt Paving Technologists, Charleston, S.C., Feb. 24–26, 1992.
6. Little, D. N. et al. *Mechanistic Evaluation of Selected Asphalt Additives.* Texas Transportation Institute, Texas A&M University, College Station, Dec. 1988.
7. Hicks, R. G. et al. *Evaluation of Asphalt Additives: Lava Butte Road—Fremont Highway Junction.* Presented at the 66th Annual Meeting of the Transportation Research Board, Washington, D.C., 1987.

8. Joseph, P. E., and G. J. Kennepohl. *Trial Sections with Polymer-Modified Asphalts on Highway 400.* Report PAV-91-03 Research and Development Branch, Ontario Ministry of Transportation, Ottawa, Ontario, Canada, June 1991.
9. Kamel, N. I., and L. J. Miller. Premium Asphalt: Influence of Asphalt Properties on Pavement Performance, Vol. 1. *1992 Proc., Transportation Association of Canada Annual Conference* Transportation Association of Canada.
10. Kennepohl, G. J. *Trial Sections with Polymer-Modified Asphalt Cement at Port Hope.* Report PAV-88-04, Research and Development Branch, Ontario Ministry of Transportation, June 1988.
11. J. Ponniah, et al. *Evaluation of Polymer-Modified Asphalts in Ontario.* Presented at the Canadian Technical Asphalt Association Annual Meeting, Victoria, British Columbia, Canada, 1992.
12. Kamel, N. I. and L. J. Miller. Asphalt Properties and Compaction Effects on Pavement Performance. *Proc., of the Canadian Technical Asphalt Association,* Canada, 1988.
13. Anderson, D., and T. W. Kennedy. *Development of SHRP Binder Specifications.* Presented at the Annual Meeting of the Association of Asphalt Paving Technologists, Austin, Tex. 1993.
14. Haas, R. C. G. *A Method for Designing Asphalt Pavements to Minimize Low-Temperature Shrinkage Cracking.* RR-73-1. Asphalt Institute, 1973.
15. *Bituminous Materials Characterization Manual.* Report ISBN 0-7729-39225. Ontario Ministry of Transportation, Ottawa, Ontario, Canada, Dec. 1987.

Publication of this paper sponsored by Committee on Characteristics of Bituminous Paving Mixtures To Meet Structural Requirements.

Evaluation of Three Polymer Modified Asphalt Concretes

HAIPING ZHOU, SCOTT E. NODES, AND JAMES E. NICHOLS

In 1989, the Oregon Department of Transportation initiated a research study to evaluate the field performance of three polymer modified asphalts. The polymer modified asphalts evaluated included (*a*) Styrelf, a polymerized binder with a thermoplastic styrene-butadiene block copolymer (*b*) AC–20R, a polymerized binder with a thermosetting styrene-butadiene latex anionic polymer, and (*C*) CA(P)–1, a polymerized binder with a thermoplastic ethylene-vinyl-acetate random copolymer. The three polymer modified asphalt concretes were constructed in five separate test sections adjacent to each other. In addition to the use of polymer modified asphalt, two control sections with a conventional AC–20 asphalt were also constructed for comparison of the performance. A comprehensive evaluation of the materials used on this project and their performance up to June 1993 is presented. Various laboratory tests on binders and mixtures were performed and the results are discussed. Field surveys were conducted annually, and survey results indicate that primary surface distress on all sections is transverse cracking with varying spacing. The level of severity ranged from low to medium. The AC–20 (control) sections showed a more noticeable loss of aggregate than the polymer modified AC sections. In general, both the AC–20 (control) sections and polymer modified (test) sections have been performing well. There is no clear distinction as to which section is superior. As of today, all sections of pavement have carried over 1.5 million equivalent axle loadings.

The use of additives to improve the performance of asphalt cement and asphalt concrete mixtures has increased in recent years (*1*). Polymer additives to asphalt materials are being advocated as having high potential for improving long-term pavement performance through their ability to enhance the properties of the asphalt binder and of the resulting asphalt concrete mix (*2*). Advantages of polymer additives to asphalt include improved adhesion and cohesion, temperature susceptibility, modulus, resistance to fatigue, resistance to rutting, and durability (*3*).

In 1989, the Oregon Department of Transportation (ODOT) initiated a research study to evaluate the field performance of three polymer modified asphalts (*4*). The polymer modified asphalts evaluated included

- Styrelf, a polymerized binder that met Elf Acquitan's PAC–20 specifications. The additive was a thermoplastic styrene-butadiene block copolymer (SB). Asphalt from Montana was used as a base stock, and the polymer content was 3 percent of the binder weight.
- AC–20R, a polymerized binder that met Asphalt Supply and Service's AC–20R specifications. The additive was a thermosetting styrene-butadiene latex anionic polymer (SBR). The base stock was penetration graded asphalt from Montana, and the polymer content was 2 percent of the binder volume.
- CA(P)–1, a polymerized binder that met Chevron's CA(P)–1 specifications. The additive was Elvax 150W, a thermoplastic ethylene-vinyl-acetate random copolymer produced by DuPont Company. The polymer content was 3 percent of the binder weight.

In addition to the use of polymer modified asphalt, two control sections with a conventional AC–20 asphalt were also constructed for comparison of the performance.

This paper presents a comprehensive evaluation of the materials used on this project and their performance as of June 1993.

H. Zhou and J.E. Nichols, Nichols Consulting Engineers, Chtd., 1885 S. Arlington Avenue, Suite 111, Reno, Nev. 89509; S. Nodes, Oregon Department of Transportation, 2950 State Street, Salem, Oreg. 97310.

PROJECT DESCRIPTION

Project Location

This project is located on the Dalles-California Highway (U.S. Route 97) south of the city of Bend, Oregon, between mile point 141.5 and 150.8. The project is a region with severe climate: cold winters, hot summers, frequent freeze-thaw cycles, frequent snowfalls in the winter, and dramatic temperature swings daily. In the winter, the average daily low temperature is about −6°C (21°F) in January. In the summer, the average daily high temperature is about 28°C (82°F) in July. An average of 11 days with highs over 32°C (90°F) occur annually. There are over 150 freeze-thaw cycles annually. The area also receives an annual average of 305 mm (12 in.) of rain and 991 mm (39 in.) of snow. Daily temperature variations are typically in a range of 17°C (30°F) to 22°C (40°F). In August, a daily temperature swing of 31°C (56°F) has been recorded in the past.

Project Layout

The project consists of seven sections. Sections 1 and 3 were paved with Styrelf mixture. Sections 2 and 5 were paved with AC–20 mixture and are the control sections. Sections 4 and 7 were paved with AC–20R mixture. Section 6 was paved with CA(P)–1 mixture.

The wearing course is 51 mm (2 in.) of ODOT Class F open-graded asphalt concrete (*5*), with or without the aforementioned polymer additives. The base course is 51 mm of ODOT Class B dense-graded asphalt concrete (*5*) with conventional AR–4000 grade asphalt. Both mixes have a maximum stone size of 19 mm (¾ in.). Typical tests such as bulk specific gravity, absorption, soundness, and degradation were performed on the aggregate material, and all results were within the limits of the specifications.

Before construction, the existing pavement had two 3.7-m (12-ft) travel lanes and consisted of varying thicknesses of asphalt concrete (AC), oil mat, and cinder base. To accommodate traffic needs, some

locations were widened to four travel lanes. The widened sections were constructed with 356 mm (14 in.) of cement treated base and then paved with 51 mm of AC base course and 51 mm of AC wearing course, with or without the polymer additives. The subgrade is powdered pumice soil, basalt boulders, and volcanic cinders.

Condition of the Existing Pavement

Before construction of new AC materials, an extensive survey was conducted to evaluate the type and extent of distress along the existing pavement. Within each section, a 76.2-m long segment that represented conditions of the entire section was selected. For each segment, distress type and severity, including a map of all cracks, was recorded. There was considerable alligator and thermal transverse cracking in all sections. The overall condition rating for the project was poor.

Traffic

Traffic data provided by ODOT indicate that the equivalent axle loading (EAL) in 1988 was approximately 314,000. In the last few years (since the construction of the overlay), the pavements have carried over 1.5 million EALs.

PRECONSTRUCTION ENGINEERING

Binder Properties

Laboratory tests on both original and residue asphalt were performed in 1989. The tests included penetration, viscosity, ring and ball softening point, Fraass point, ductility and elastic recovery, force ductility, and toughness and tenacity.

Table 1 presents a summary of the test results. The consistency tests followed ASTM standard testing procedures. The ductility test was used to measure "extension" properties of the binders and was also used in this project to determine elastic recovery property of the binders. Force ductility is a nonstandard test and is a modification of the conventional ductility test. The test has been described as a means to measure tensile load-deformation characteristics of asphalt and asphalt-rubber binders (*6, 7*). The toughness and tenacity test was also used to measure tensile strength of the binders. The Fraass test was used to assess the cold temperature flexibility of an asphalt.

Consistency Tests

Figure 1 shows the consistency test results for original asphalt and residue asphalt on a single diagram, which has been used by ODOT as a means of assessing temperature susceptibility of a binder. The binder with a steeper viscosity-temperature slope is predicted to be more temperature susceptible than a binder with a flatter viscosity-temperature slope. In Figure 1, it is apparent that the AC–20 asphalt binder has a steeper slope than those polymer modified binders. The same trend may be seen for residue asphalt.

Temperature susceptibility of a binder may also be evaluated in terms of Penetration Index (PI) and Penetration Viscosity Number (PVN). PI is calculated by the following equation (*8*):

$$PI = \frac{30}{1 + 90 \times PTS} - 10$$

where PTS is penetration-temperature-susceptibility and is expressed as follows:

$$PTS = \frac{\log 800 - \log Pen_{25}}{T_{RB} - T_{pen25}}$$

where

Pen_{25} = penetration at 25°C (77°F),
T_{RB} = softening point, and
T_{pen25} = 25°C.

The above relationship indicates that an increase in the PI number is an indication of decrease in temperature susceptibility of a binder.

PVN is another way to evaluate the temperature susceptibility of a binder. It is expressed by the following Equation (*9*):

$$PVN = \frac{4.285 - .7967 (\log P) - \log V}{.7591 - .1858 (\log P)} \times (-1.5)$$

where P is the penetration at 25°C and V is Kinematic viscosity at 135°C (275°F). A high value of PVN indicates a binder that has a low-temperature susceptibility.

The calculated PI and PVN values are presented in Figure 2. The AC–20 binder has the lowest PI and PVN, indicating this binder is more temperature susceptible than polymer modified binders.

Ductility and Elastic Recovery Tests

Ductilities were determined in accordance with ASTM D111 testing procedures. At 4°C (39.2°F), ductilities for polymer modified binders were higher than the conventional AC–20 asphalt. There was no noticeable difference for ductility tested at 25°C.

Elastic recovery test results indicate similar characteristics; binders with polymer additives had considerably higher elastic recovery than conventional AC–20 binder. Among the polymer modified binders, Styrelf and AC–20R appeared more ductile and had higher elastic recovery than CA(P)–1.

Force Ductility Tests

Force ductility tests were conducted in accordance with the conventional ductility test with several changes. Two force cells were added to the loading chain and the mold was modified to produce a specimen with constant cross-sectional area through the gage length. The force ductility test data were used to determine the maximum engineering stress, engineering strain, and engineering work. A majority of researchers seem to believe that this test is a significant binder test and an improvement over the conventional ductility test (*2.*) However, other findings (*10*) reported that force ductility test results did not correlate well with low-temperature creep or with fatigue test results for the binder-aggregate mixture.

The force ductility tests were conducted at 4°C and 25°C. The maximum engineering stress was obtained by dividing the maximum load by the original cross-sectioned area. Maximum engineering strain was calculated by dividing the length at failure of the

TABLE 1 Binder Properties (Original and Residue)

Test	AC-20		Styrelf		AC-20R		CA(P)-1	
	Original	Residue	Original	Residue	Original	Residue	Original	Residue
Pen @ 39.2°F, 200g, 60s (dmm)	30	23	50	37	48	34	43	25
Pen @ 77°F, 100g, 5s (dmm)	70 50 min	37	111 60 min	67	105	58	112 85 min	50
Abs Vis @ 140°F (p)	2150 1600-2400	6420	2008 1600-2400	5675	1890 1600-2400	5058	1857 1600-2400	5000
Kin Vis @ 275°F (cSt)	395 230 min	665	572 300 min	960	649 325 min	877	607 325 min	1100
R&B Softening Point (°F)	125	144	130	140	133	140	124	142
Ductility @ 39.2°F 5cm/min (cm)	7	0	47	24	50+ 50 min	45+	42+ 25 min	22
Ductility @ 77°F 5cm/min (cm)	150+	100+	150+	54	100+ 100 min	100+	100+ 100 min	100+
Elastic Recovery @ 50°F (%)	10	-	68 58 min	68	58 58 min	53	35	35
Force-Ductility @ 39.2°F								
Max. Engr. Stress (lb/in^2)	100	220	34	77	49	77	51	100
Max. Engr. Strain (in/in)	33+	6.5	33	19	47+	26	21	15
Max. Engr. Work (lb-in)	54	92	81	130	130	130	130	150
Force-Ductility @ 77°F								
Max. Engr. Stress (lb/in^2)	0.8	4.2	0.4	1.3	1.1	1.5	0.2	2.9
Max. Engr. Strain (in/in)	47+	47+	47+	47+	47+	47+	47+	47+
Max. Engr. Work (lb-in)	0.5	1.7	1.3	5.1	6.7	1.5	0.2	3.9
Toughness (lb-in)	76	138	174	119	216 100 min	164	165 75 min	196
Tenacity (lb-in)	37	52	152	68	197 75 min	115	141 50 min	147
Fraass Point (°F)	19	23	-1	3	3	4	9	17

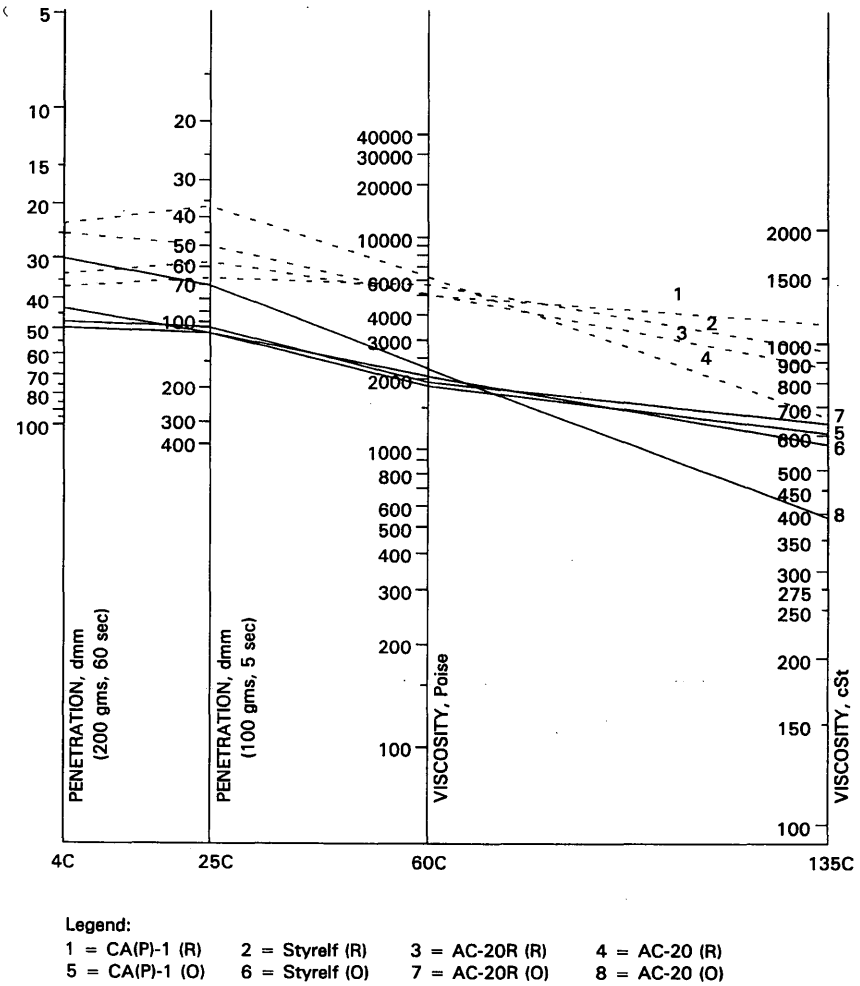

FIGURE 1 Consistency test results on binders.

specimen by the original length. Maximum engineering work is the area under the stress-strain curve and could be considered as energy required to produce failure. For binders containing polymer additives, marked increases at 4°C in energy required to produce failure were noticed. This characteristic may be useful in predicting mixture tensile strength when polymer additives are used in binders.

Toughness and Tenacity Tests

The toughness and tenacity tests were performed by placing a tension head into a standard 3-oz penetration tin containing 36 g of binder; the tension head was then pulled at 508mm/min while the force versus extension plot was recorded (*2,11*). The total area under the force-extension curve (typically a bell shaped) was calculated and reported as Toughness. The declining side of the curve was extended to the horizontal axis in a straight line and the area to the right of this line was reported as tenacity. Figure 3 illustrates a comparison of the results of the toughness and tenacity tests. The original binders with polymer additives have higher toughness and tenacity values than the conventional AC–20 asphalt. The polymer modified residue asphalt also exhibits the similar characteristics, except for Styrelf. These test results imply that the binders with polymer additives have a higher tensile strength than the binder without.

Fraass Test Results

The Fraass test measures the cold-temperature flexibility of an asphalt (*2,12*). The test results indicate that all polymer modified binders had lower Fraass points than the conventional AC–20 asphalt, which suggests that the polymer modified asphalts are more flexible at cold temperatures than is the conventional AC–20 binder.

Mix Design

Separate mix designs were made for each binder using the ODOT version of the Hveem method (*13*). The design mix characteristics at design binder content for each mix are listed in Table 2. For open-graded mixes, the mix design criteria are slightly different from those of dense-graded mixes. The criteria used to evaluate the mix properties are binder film thickness, voids, and stability at first com-

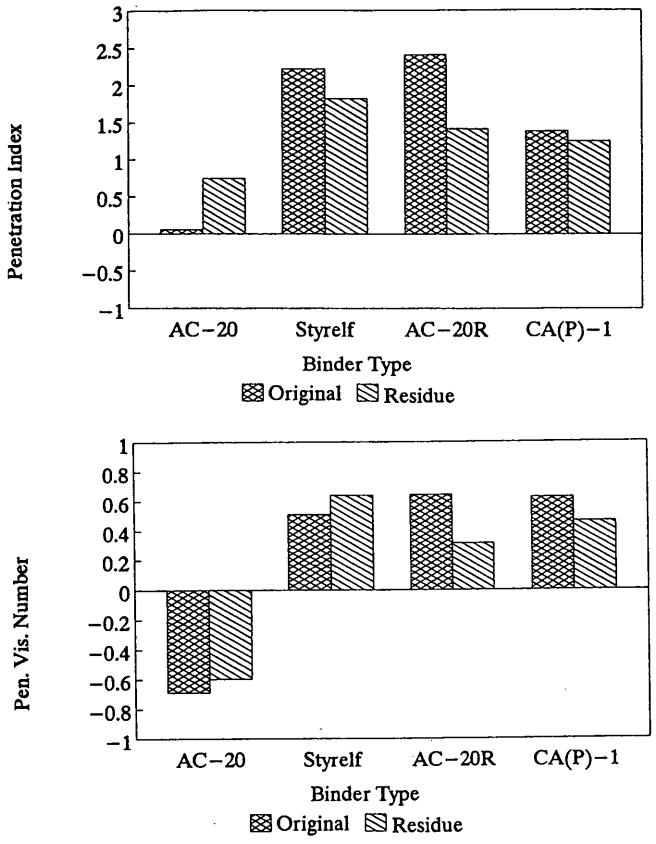

FIGURE 2 Calculations of PI and PVN.

paction, stability at second compaction, and index of retained strength.

CONSTRUCTION

Placement

The AC–20 mix was used for the construction of the control sections. No unusual problems were reported for this conventional asphalt.

The Styrelf binder mixed easily with the aggregate in the pugmill. Unlike the conventional asphalt, this binder tended to cling to the surfaces of the equipment. Observations indicated that the buildup was moderate and that plant operation was not affected. However, when the binder temperature was at 135°C, the Styrelf binder became very viscous and caused pumping problems that slowed down the batching of the mix production. Consequently, the pumping temperature was raised to range from 149°C (300°F) to 182°C (360°F).

Two other observations on the Styrelf binder were that (a) the binder migrated through the mix to the bottom of the silo when the mix was stored for an extended period, and (b) the binder was especially sensitive to paver speed and screed setting compared with other mixes. For any screed setting, there was a definite maximum paver speed. If the paver exceeded this speed, the screen would rapidly lift. In general, this mix was easy to place.

The AC–20R binder was somewhat similar to Styrelf: easily mixed with the aggregate, tended to cling to the surfaces of the equipment, and was more viscous than AC–20. This binder built up heavier coatings on the surfaces of the equipment than Styrelf, and the buildup was very hard to remove. Migration problems were noticed during construction. In addition, this mix was not smoothly finished by the passage of the screed. There was a minor amount of rolling and picking as the screed passed over the mix. These surface irregularities were not seen after compaction. The mix tended to harden quicker upon cooling than the conventional AC–20, causing difficulty in raking. In general, placement went smoothly and no unusual problems were noticed.

The CA(P)–1 mix is very much like the conventional AC–20 mix except that the smell of fumes from the CA(P)–1 binder were noxious. The placement went easily and otherwise no problems were encountered.

Various quality control tests were conducted during the construction. The test results indicated that the asphalt content and mix gradation were within the specification ranges for all mixes and the average mix placement temperatures generally conformed to or were close to the specifications.

Costs

For a compacted mix 51-mm (2 in.) thick, the Styrelf mix cost $26.75/ton, about 15 percent more than conventional AC–20 mix. Both the AC–20R and CA(P)–1 mixes cost $29.50/ton, about 27 percent more than conventional AC–20 mix. These unit bid prices are for small quantities of binders. The cost would decrease as larger

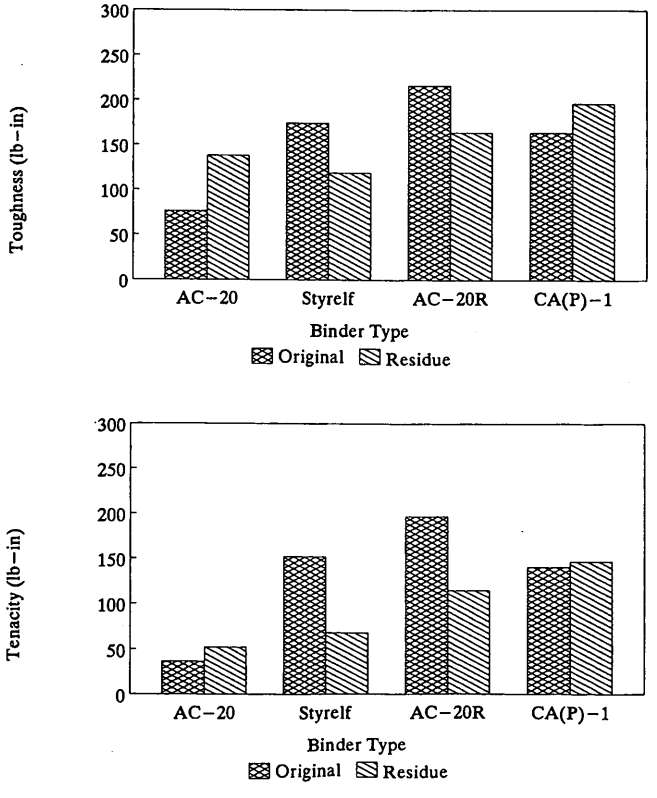

FIGURE 3 Toughness and tenacity test results.

TABLE 2 Design Mix Characteristics at Design Binder Content

Item	AC−20	Styrelf	AC−20R	CA(P)−1	ODOT Class F mix design criteria
Percent passing sieve:					
1"	100	100	100	100	99-100
3/4"	100	98	98	98	95-100
1/2"	76	75	75	75	66-80
3/8"	57	56	56	56	
1/4"	28	25	25	25	18-30
#10	11	10	10	10	5-19
#40	6	6	6	6	
#200	3.6[a]	3.6[a]	3.5[a]	3.5[a]	1.5-6.5[b]
Mineral filler (%)	1[c]	1[c]	1[c]	1[c]	.5-1.5
Voids in mineral agg (%)	19.8	21	21	20	
Binder content (%)	5.2	5.5	5.5	5.5	4-8
Binder film thickness	Suff.	Suff.	Suff.	Suff.	Suff.
SG @ 1st compaction	2.29	2.26	2.27	2.30	
Voids @ 1st comp. (%)	9.0	11.1	9.5	8.7	6-9
Stability @ 1st comp.	24	26	22	21	≥26
SG @ 2nd compaction	2.35	2.36	2.37	2.38	
Voids @ 2nd comp. (%)	6.6	7.2	5.5	5.6	
Stability @ 2nd comp.	37	39	33	32	≥26
Rice Specific Gravity	2.518	2.542	2.509	2.52	
Index of Retained Strength (%)	83	73	84+	76	≥75

[a] Includes loose lime from treated aggregate and 1% fly ash mineral filler.
[b] Includes .5% allowance for loose lime from treated aggregate.
[c] Estimated.

quantities of mix were used, especially if placed by contractors with more experience with the polymer modified AC.

POSTCONSTRUCTION ENGINEERING

Mix Sampling

Mix samples were taken from the discharge chute of the pugmill and sent to the ODOT Materials Laboratory for the determination of asphalt content and aggregate gradation. Some of the observations regarding the mix sampling were that when the mix was hot, the binder would migrate to the bottom of the mix sample; when the mix was cold, it was very difficult to remove all of the binder from the container for testing. In addition, the polymer modified mixes were very tenacious.

Binder Properties

The asphalt in the mixes was extracted to conduct consistency, force ductility, and toughness and tenacity tests. The consistency tests were also performed on recovered asphalt from core samples obtained in 1991, 2 years after construction.

Consistency Tests

The same consistency tests performed on the original binders were conducted on the recovered binders in 1989 and 1991. These tests included penetration and viscosity tests. In addition to tests at 4°C, 200 g, 60 s and at 25°C, 100 g, 5 s, a penetration test was also run at 4°C, 100 g, 5 sec on the binders extracted from core samples obtained in 1991; this test was intended to evaluate the binders' ability to resist low-temperature cracking.

Table 3 summarizes the consistency test results of recovered asphalts for both 1989 and 1991. These results are illustrated in Figure 4 for comparison.

In 2 years the binders' properties had changed considerably: viscosities at 60°C (140°F) changed from approximately 5000 p to over 10000 p; at 135°C (275°F), viscosities also increased—but at different rates, depending on the binders. These changes indicate that the asphalt binders become more viscous after 2 years of road service. The penetration test results also reflect these changes: at

TABLE 3 Binder Properties (Recovered)

Test	AC-20		Styrelf		AC-20R		CA(P)-1	
	1989	1991	1989	1991	1989	1991	1989	1991
Pen @ 39.2°F, 200g, 60s (dmm)	22	17	35	24	26	22	25	14
Pen @ 39.2°F, 100g, 5s (dmm)	N/T	5	N/T	8	N/T	7	N/T	3
Pen @ 77°F, 100g, 5s (dmm)	41	29	63	43	50	35	48	25
Abs Vis @ 140°F (p)	5790	10200	4850	10680	5210	11000	5240	11500
Kin Vis @ 275°F (cSt)	598	811	861	970	964	1040	1090	1380
R&B Softening Point (°F)	144	N/T	140	N/T	136	N/T	140	N/T
Force-Duct @ 39.2°F Max. Engr. Stress (lb/in^2) Max. Engr. Strain (in/in) Max. Engr. Work (lb-in)	 150 7.2 64	N/T	 64 16 110	N/T	 77 19 110	N/T	 110 14 160	N/T
Force-Duct @ 77°F Max. Engr. Stress (lb/in^2) Max. Engr. Strain (in/in) Max. Engr. Work (lb-in)	 2.5 47+ 1.3	N/T	 1.5 47+ 7.0	N/T	 1.6 47+ 2.1	N/T	 2.4 47+ 3.0	N/T
Toughness (lb-in)	80	N/T	87	N/T	124	N/T	219	N/T
Tenacity (lb-in)	18	N/T	48	N/T	56	N/T	101	N/T

N/T = Not Tested

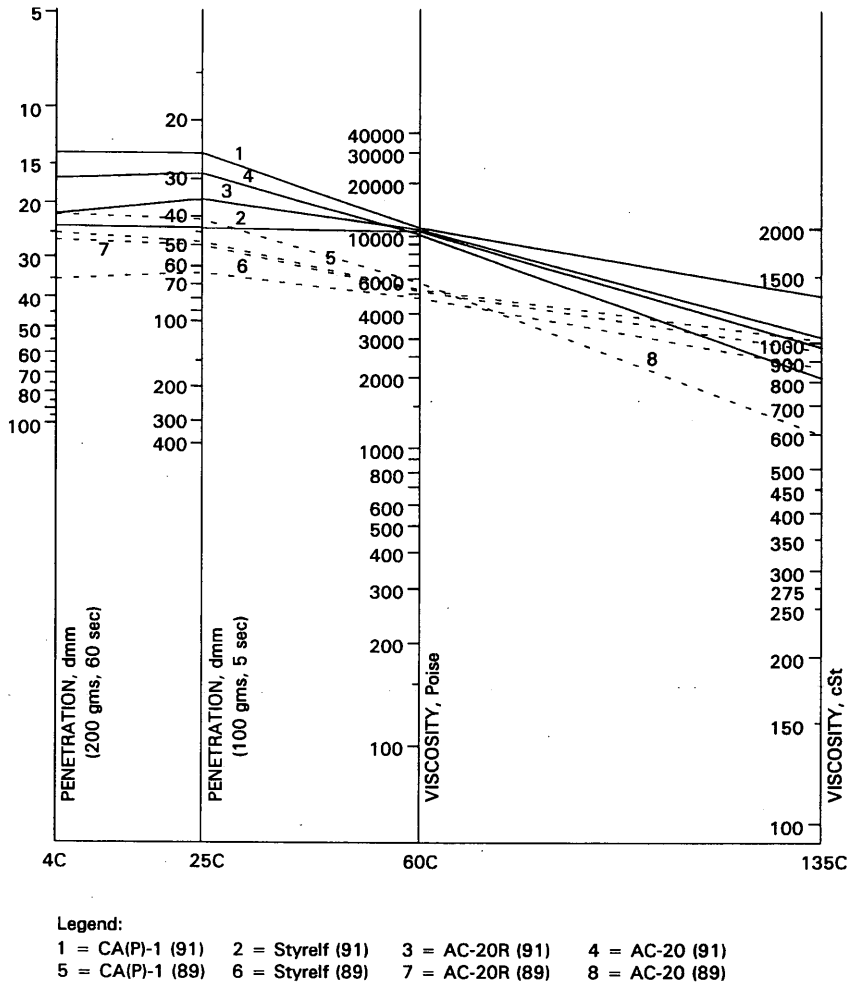

FIGURE 4 Consistency test results on recovered asphalt.

two temperature levels, 4°C and 25°C, the penetration values had decreased nearly proportionally, indicating the binders were much harder in 1991 than they were in 1989.

These test results permitted the reevaluation of temperature susceptibility of the binders. Figure 5 shows a comparison of the calculated PI and PVN for each recovered binder. Based on the PI calculations, the 1989 results indicate the AC–20R binder is the most temperature susceptible. However, the 1991 results indicate the CA(P)–1 binder is the most susceptible to temperature change. PVN calculations present a different picture: calculated PVNs indicate AC–20 has the lowest PVN and is therefore the most susceptible to temperature change.

One additional penetration test at 4°C, 100 g, 5 s was performed in 1991 on binders that were used in the wearing course as well as in the base course. The test was intended to evaluate the binders' ability to resist low-temperature cracking. The test applies a procedure developed by Gaw (*14*) which uses penetration values tested at 4°C and 25°C to predict the temperature at which binder will crack. Based on the Gaw procedure, the predicted cracking temperatures for the binders are

- −40°C (−40°F) for AC–20;
- −45°C (−49°F) for Styrelf;
- −45°C (−49°F) for AC–20R; and
- −30°C (−22°F) for CA(P)–1.

Force Ductility and Toughness and Tenacity Tests

Force ductility and toughness and tenacity tests were conducted on recovered binders in 1989, and the test results are shown in Table 3.

Considerable differences in engineering work at 4°C may be noted: The recovered AC–20 asphalt has the lowest value, meaning that this binder requires the least energy to produce failure. At 25°C, the differences are not significant.

The toughness and tenacity test results show a similar tendency. The AC–20 binder has the lowest toughness and tenacity and the polymer modified binders all have higher toughness and tenacity values, which suggests that they are tougher and more tenacious than conventional AC–20 asphalt.

Mixture Properties

Mixture properties were measured on core samples obtained from the site. The laboratory tests included measurements of bulk specific gravity, Rice specific gravity, Hveem stability, resilient mod-

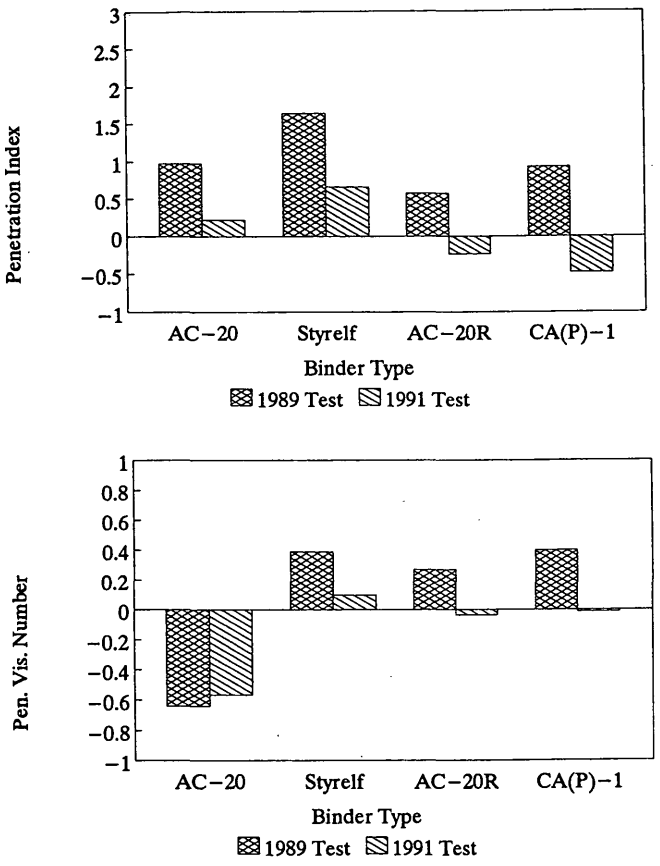

FIGURE 5 Comparison of temperature susceptibility.

ulus, and fatigue life. All tests were performed following ASTM or ODOT standard testing procedures. Table 4 presents the results of various tests.

Bulk and Rice Specific Gravity

The bulk and Rice specific gravity tests were conducted on cores for 3 consecutive years, thus allowing an examination of the change in in-place density and in-place voids of each mixture. Bulk specific gravities of all mixes had been increasing from 1989 to 1990. The rate of change slowed or decreased from 1990 to 1991. As expected, the voids had been decreasing except for the Styrelf and CA(P)–1 mixtures, which show an increase in voids. The determination of voids was based on the test results of both bulk specific gravity and Rice specific gravity, which were determined using recompacted samples. It is possible that samples obtained from two different locations may have slightly different bulk-specific gravities.

Hveem Stability

Hveem stability tests were performed on cores obtained in-place and recompacted mixes and tested in accordance with ODOT Test Method 305-86 (*15*). Two general observations may be concluded from the test results: polymer modified mixes have a similar or slightly higher Hveem stability than the conventional AC–20 mix, and recompacted samples have much higher Hveem stability than in-place cores.

Resilient Modulus

Resilient modulus tests were conducted on cores obtained in-place in 1989, following ASTM D4123 test procedures. The test results indicate that the AC–20R mixture has the lowest resilient modulus; the AC–20 and CA(P)–1 mixtures have a similar resilient modulus; whereas the Styrelf mix has a resilient modulus between those of AC–20 and AC–20R mixtures.

Fatigue

The fatigue tests followed the same procedures as those of resilient modulus tests. The total repetitions of the load to cause failure of the sample was recorded as the fatigue life of the sample. Although these test results may have little meaning to the field performance of each mixture, the AC–20R mixture does show a relatively longer life to resist repeated loading than other mixtures in the controlled laboratory environment. The CA(P)–1 mix, on the other hand, shows a much shorter fatigue life, even shorter than the conventional AC–20 mix.

When the fatigue test results are compared to the resilient modulus test results, it is found that mixes with higher resilient modulus would have lower fatigue life and vice versa.

PERFORMANCE EVALUATION

1989 Survey

Visual Inspection

The visual inspection conducted in 1989 shortly after the construction indicated that the new wearing course of all materials was in an excellent condition. There were no cracks or other types of surface distress. However, it was noticed that before the wearing course was placed, there were 1.6-mm (1/16 in.) to 3.2 mm (1/8 in.) wide transverse cracks completely across the roadway at a frequency of 90 cracks per mile in the new base course, which was constructed directly on the existing pavement in the fall of 1988. There were three possible causes for these cracks: (a) reflective cracking from the existing pavement, (b) shrinkage cracking caused from the cement treated base, and (c) binder's inability of resisting lower temperature cracking. As mentioned earlier, the base course was constructed with AR-4000 asphalt which, from the laboratory test result, had a penetration value of 1 at 4°C, 100 g, 5 s. Based on Gaw's procedure (*14*), the binder with this penetration value would crack at a temperature below −15°C (5°F) by extrapolation. Temperatures in the project area are generally below −18°C (0°F).

Regardless of what caused the cracks in the base course, they could have a considerable effect on the performance of the wearing course.

Friction

The pavement surface friction was measured before construction in 1988 and shortly after construction. All testing was done in accordance with AASHTO T242-84 and was performed at speeds near 40 mph in the left wheel path of the outer lane. The test data was adjusted to standard 40-mph friction number (FN_{40}) using correlation equations. The FNs of the various sections after construction were typical of other new open-graded AC pavements.

TABLE 4 Summary of Core Sample Mix Properties

Test	AC−20	Styrelf	AC−20R	CA(P)−1
a) In-Place				
Bulk Specific Gravity	2.12 (89) 2.26 (90) 2.25 (91)	2.16 (89) 2.26 (90) 2.26 (91)	2.17 (89) 2.24 (90) 2.29 (91)	2.17 (89) 2.25 (90) 2.22 (91)
Voids (%)	14.9 (89) 12.0 (90) 10.7 (91)	17.6 (89) 10.5 (90) 11.3 (91)	14.5 (89) 12.3 (90) 9.4 (91)	14.5 (89) 10.9 (90) 11.6 (91)
Hveem Stability	N/A (89) 11 (90) 15 (91)	13 (89) 16 (90) 22 (91)	14 (89) 15 (90) 15 (91)	13 (89) 16 (90) 14 (91)
Resilient Modulus (ksi)	715[1]	613[2]	339[1]	761[2]
Fatigue (repetitions)	7190[1]	18400[2]	32100[1]	3220[2]
b) Recompacted				
Bulk Specific Gravity	2.33 (89) 2.31 (90) 2.39 (91)	2.29 (89) 2.38 (90) 2.37 (91)	2.30 (89) 2.36 (90) 2.38 (91)	2.29 (89) 2.39 (90) 2.37 (91)
Rice Specific Gravity	2.492 (89) 2.568 (90) 2.519 (91)	2.540 (89) 2.525 (90) 2.550 (91)	2.549 (89) 2.553 (90) 2.525 (91)	2.537 (89) 2.525 (90) 2.516 (91)
Voids (%)	6.5 (89) 10.0 (90) 5.1 (91)	9.8 (89) 5.8 (90) 6.9 (91)	9.8 (89) 7.6 (90) 5.7 (91)	9.7 (89) 5.3 (90) 5.4 (91)
Hveem Stability	17 (89) 32 (90) 30 (91)	25 (89) 28 (90) 50 (91)	23 (89) 51 (90) 37 (91)	24 (89) 29 (90) 31 (91)

Number in parentheses is year.
N/A = Not Available.
[1] Average of two samples. Tested in 1989.
[2] Average of three samples. Tested in 1989.

Roughness

The pavement roughness was measured using a May's ride meter soon after construction in 1989. For all test sections, the roughness values are in a range of 30 to 56 in./mi. Therefore, all test sections were classified as smooth under the ODOT paving award criteria (*4*).

Surveys Since 1990

Visual Inspection

From 1990 to 1993, four separate pavement condition surveys were conducted. Table 5 summarizes the survey results. General observations from these surveys include the following:

1. In 1990, there were no transverse cracks in Sections 1 to 4. There was an average of 10 cracks per mile in Section 5 (AC–20); 2 cracks per mile in Section 6 (Styrelf); and 2 cracks per mile in Section 7 (AC–20R). There was no rutting in Section 1 (Styrelf), approximately 3.2 mm (⅛ in.) ruts in section 2 (AC–20), and about 1.6mm (1/16 in.) ruts in all other sections.

2. In 1991, all sections had transverse cracks at varying spacing and with a low level of severity. Section 1 (Styrelf) had more transverse cracks per mile than other sections. Section 4 (AC–20R) had the least amount of transverse cracks per mile. All transverse cracks were low level in severity. Rut depths on all sections were generally the same as measured the previous year. No stripping was observed from visual examinations of the cores.

3. The survey results from 1992 and 1993 indicate that there were no new transverse cracks. Some of the existing ones extended slightly towards the pavement edge. The level of severity of the cracks increased on most of the sections from low to medium, particularly on the AC–20 and CA(P)–1 sections. Rut depths on most of the sections also increased slightly from 1992 to 1993.

Friction

Additional friction tests were performed in the summer of 1991. The FNs were slightly higher for all sections compared to FNs measured in 1989. The FNs are typical of other relatively new AC pavements.

TABLE 5 Summary of Condition Survey Since 1990

Sect.	Mix Type	Average Crack Spacing (ft)	Severity	Rutting (inch)	Remarks
1990					
1	Styrelf	No cracks	N/A	0	All sections were in an excellent condition.
2	AC−20	No cracks	N/A	1/8	
3	Styrelf	No cracks	N/A	1/16	
4	AC−20R	No cracks	N/A	1/16	
5	AC−20	~530	L	1/16	
6	CA(P)−1	~2640	L	1/16	
7	AC−20R	~2640	L	1/16	
1991					
1	Styrelf	~80	L	1/16	Cores were taken from all sections for examination of stripping. No stripping was found.
2	AC−20	~140	L	1/8	
3	Styrelf	~135	L	1/16	
4	AC−20R	~165	L	1/16	
5	AC−20	~115	L	1/16	
6	CA(P)−1	~120	L	1/16	
7	AC−20R	~110	L	1/16	
1992					
1	Styrelf	~80	L	1/6	No new transverse cracks were observed. Some of the existing ones extended towards the pavement edge.
2	AC−20	~140	L	1/4	
3	Styrelf	~135	L	1/8	
4	AC−20R	~165	L	1/8	
5	AC−20	~115	L	1/8	
6	CA(P)−1	~120	L	1/8	
7	AC−20R	~110	L	1/8	
1993					
1	Styrelf	~80	L to M	1/6	No new transverse cracks were observed. There were noticeable losses of aggregate on the AC−20 sections.
2	AC−20	~140	M	1/4	
3	Styrelf	~135	L to M	1/6	
4	AC−20R	~165	L to M	1/6	
5	AC−20	~115	M	1/6	
6	CA(P)−1	~120	M	1/6	
7	AC−20R	~110	L	1/6	

N/A = Not Applicable: L = Low, M = Medium.

Roughness

Roughness tests performed in 1990 indicated that the pavement surfaces are slightly rougher than they were in 1989. The roughness values were in a range of 41 to 55 in./mi for all sections. Percent of increase from 1989 to 1990 varies for each section. The two AC–20 sections showed greatest increase (> 30 percent) in roughness. However, all sections of pavement surface were considered smooth based on ODOT paving award criteria.

Discussion of Results

Comparing the laboratory test results to field performance, it appears that force-ductility, and toughness and tenacity tests may be able to assess the binder's tensile and tenacious properties. In the 1993 survey, the loss of coarse aggregate in the wheel path in the AC–20 sections was more noticeable than the loss from the polymer modified AC sections. This seems to support the force-ductility, and toughness and tenacity test results, which all indicated that AC–20 asphalt had lowest values among all binders.

The Gaw procedure predicted a much lower cracking temperature than those measured in the laboratory Fraass test. Based on the Gaw procedure, all binders should be able to resist low-temperature cracking up to at least −30°C (−22°F). In the last few years, the lowest temperature recorded at the project site was not less than −30°C (−22°F). Therefore, the transverse cracks that are in all sections of the pavement may have resulted from either reflective cracking of the existing pavement or shrinkage cracking of the cement treated base; or the Gaw procedure may have overestimated the temperature at which the binder would crack.

CONCLUSIONS

1. The laboratory test results indicate polymer modified asphalt [Styrelf, AC–20R, and CA(P)–1] could be less temperature susceptible than the conventional AC–20 asphalt.

2. The polymer modified binders are much tougher and more tenacious and ductile than the conventional AC–20 asphalt.

3. Fraass test results show the Styrelf, AC–20R, and CA(P)–1 asphalts have lower cracking temperatures than the conventional AC–20 asphalt.

4. Conventional construction processes are suitable to the construction of the Styrelf, AC–20R, and CA(P)–1 modified asphalt mixtures. The Styrelf and AC–20R asphalt tended to migrate to the bottom of the mix. Therefore, appropriate control of mixing temperature is important.

5. The laboratory test results showed that the conventional AC–20 had a higher resilient modulus than the Styrelf and the AC–20R modified AC, and a similar resilient modulus to that of the CA(P)–1 modified AC. The conventional AC–20 AC had a lower fatigue life than the Styrelf and the AC–20R modified AC but had a slightly higher fatigue life than that of CA(P)–1 modified AC.

6. The primary surface distress in all sections is transverse cracking. The level of severity ranged from low to medium. The AC–20 sections showed a more noticeable loss of aggregate than the polymer modified AC sections.

7. The roughness test results showed the Styrelf sections are slightly rougher than other sections, but the AC–20 sections had the greatest increase in roughness, from 1989 to 1990.

8. In general, both the AC–20 (control) sections and polymer modified (test) sections have been performing well. There is no clear distinction as to which section is superior. As of today, all sections of pavement have carried over 1.5 million EALs.

RECOMMENDATIONS

If funding is available, the performance of both the test and control sections should be monitored periodically until the pavement sections fail. Resilient modulus and fatigue tests on core samples, consistency tests on recovered asphalt from both conventional and polymer modified AC, and the friction and roughness tests should be performed every 2 years. Analysis of the above recommended tests will allow ODOT to determine the cost-effectiveness of the three polymer modified asphalt concrete pavements.

ACKNOWLEDGMENTS

The authors gratefully acknowledge the funding provided by FHWA and the ODT, and the laboratory testing work performed by the latter's materials unit staff.

REFERENCES

1. Carpenter, S. H. and T. VanDam. Laboratory Performance Comparisons of Polymer-Modified and Unmodified Asphalt Concrete Mixtures. In *Transportation Research Record 1115,* TRB, National Research Council, Washington, D.C., 1987, pp. 62–74.
2. Rogge, D. F., C. Ifft, R. G. Hicks, and L. G. Scholl. *Laboratory Study of Test Methods for Polymer Modified Asphalt in Hot Mix Pavement.* Final Report, FHWA-OR-RD-90-06. FHWA, U.S. Department of Transportation, Nov. 1989.
3. Terrel, R. L. and J. L. Walter. "Modified Asphalt Pavement Materials: The European Experience," *Proc., Association of Asphalt Paving Technologists,* Clearwater, Fla., Feb. 1986, pp. 482–518.
4. Miller, B. and L. G. Scholl. *Field Test of Polymer Modified Asphalt Concrete: Murphy Road to Lava Butte Section.* Construction Report FHWA-OR-RD-90-07. FHWA, U.S. Department of Transportation, Dec. 1990.
5. Oregon State Highway Division. *Standard Specifications for Highway Construction.* Salem, Oreg., 1991.
6. Salam, Y. *Characterization of Deformation and Fracture of Asphalt Concrete.* Institute of Transportation and Traffic Engineering Series No. 1971:1. University of California, Berkeley, Jan. 1971.
7. Way, B. "Prevention of Reflective Cracking Minnetonka-East," Appendix B (1979 Addendum Report) August 1979.
8. Pfeiffer, *The Properties of Asphalt Bitumen.* Elsevier Science Publishing Company, New York, 1950.
9. McLeod, N.W. Asphalt Cements: Pen-Vis Number and Its Application to Moduli of Stiffness. *ASTM Journal of Testing and Evaluation,* Vol. 4, No. 4, July 1976.
10. Goodrich, J.L. Asphalt and Polymer Modified Asphalt Properties Related to the Performance of Asphalt Concrete Mixes. *Proc., Association of Asphalt Paving Technologists,* Williamsburg, Va., Feb. 1988.
11. Reinke, G. and T. O'Connell. Use of the Toughness and Tenacity Test in the Analysis of Polymer Modified Binders. *Proc., Asphalt Emulsion Manufacturers Association,* New Orleans, La. March 1985, 25 pp.
12. Thenoux, G., G. Lees, and C. Bell. Laboratory Investigation of the Fraass Brittle Test. *Proc., Association of Asphalt Paving Technologists,* San Antonio, Tex., 1985, pp. 529–550.
13. Quinn, W.J. et al., Mix Design Procedures and Guidelines for Asphalt Concrete, Cement Treated Base, and Portland Cement Concrete. Oregon Department of Transportation, Salem, Oreg., April 1987.
14. Gaw, W.J. The Measurement and Prediction of Asphalt Stiffness at Low and Intermediate Pavement Service Temperatures. *Proc., Association of Asphalt Paving Technologists,* 1978.
15. Oregon State Highway Division. *Laboratory Manual of Test Procedures.* Oregon Department of Transportation, Salem, Oreg., 1986.

Publication of this paper sponsored by Committee on Characteristics of Bituminous Paving Mixtures to Meet Structural Requirements.

Correlation of Selected Laboratory Compaction Methods with Field Compaction

JOE W. BUTTON, DALLAS N. LITTLE, VIDYASAGAR JAGADAM, AND OLGA J. PENDLETON

It is well established that method of compaction affects the physical properties of compacted asphalt concrete specimens. When evaluating asphalt concrete mixtures in the laboratory, it is desirable to fabricate compacted specimens that closely duplicate the properties of the actual road pavement. The goal was to determine which of four laboratory compaction methods (Exxon rolling wheel, Texas gyratory, rotating base Marshall hammer, and the Elf linear kneading compactor) most nearly simulate field compaction. Field cores were obtained from five different highway pavements. Laboratory specimens were fabricated using materials and mixture designs identical to those used in the pavement cores. Where achievable, they were expected to have the same air-voids range as the pavement cores. Various physical properties of pavement cores as well as the laboratory specimens were measured. The test results were compared and statistically analyzed to determine similarity. From the statistical analysis of the test data, the Texas gyratory compactor simulated pavement cores most often. The Exxon rolling wheel and Elf compactor simulated pavement cores with equal frequency. The rotating base Marshall hammer was similar to the pavement cores least often. From an overall statistical standpoint, however, it cannot be stated with confidence that any one compaction method more closely simulated field compaction than any one of the other three methods tested. The rolling wheel compactor exhibited difficulties in controlling the air voids of the compacted specimens to such an extent that the desired range of air void contents was never attained with this compactor.

Highway researchers and paving engineers recognized many years ago that different compaction techniques produce asphalt concrete specimens with different particle orientations and thus differing physical properties. When evaluating asphalt concrete mixtures in the laboratory, it is desirable to produce test specimens that duplicate, as nearly as possible, the compacted mixture as it exists (or will exist) in an actual pavement layer.

OBJECTIVE AND SCOPE

The requirement of this research study was to determine which of four compaction devices most closely simulates actual field compaction and to make a recommendation to the Strategic Highway Research Program (SHRP). Detailed studies were conducted to compare the properties of specimens made using the Texas gyratory compactor and the Exxon rolling wheel compactor with pavement cores. An abbreviated study was performed using selected test procedures to evaluate mixtures compacted using the rotating base Marshall hammer. The Elf linear kneading compactor was evaluated for only two types of mixtures.

Paving mixtures from five different locations and made up of different aggregates and asphalts were used in the study. These materials provided a wide range of engineering properties and test values for the compacted mixtures. The experiment was designed to determine the extent to which the method of laboratory compaction affects certain fundamental and commonly measured properties of asphalt concrete. Statistical analyses of the test results were performed to determine whether significant differences existed between the field cores and the different compaction methods.

This report is an abridged version of the original research report (*1*) prepared for the National Research Council in partial fulfillment of SHRP project A-005. All of the data are contained in a complete report, compiled in 21 tables and presented graphically in 40 figures.

RELATED RESEARCH

Several significant studies have been performed that focus on comparing the properties of mixtures compacted with different laboratory compaction devices. These studies include: Vallerga (*2*), Fields (*3*), Epps et al. (*4*), Nunn (*5*), Huschek (*6*), Van Grevenynghe (*7*), Aunan et al. (*8*), Von Quintus et al. (*9*), and Sousa et al. (*10*). The consensus of these studies is that the response of a mixture to loading (mixture property) is affected by the type of laboratory compaction method used to prepare the specimen. Perhaps the most extensive and most relevant studies are the two most recent (*9, 10*).

In the NCHRP study, *Asphalt-Aggregate Mixture Analysis System,* by Von Quintus et al. (*9*), the effects of five different laboratory compactors on the selected properties of the compacted mixtures are investigated. Field cores and lab compacted samples were subjected to indirect tensile testing (strength, strain at failure, resilient modulus, and creep) and aggregate particle orientation evaluation. On the basis of the pooled results of mechanical tests performed at three different temperatures, Von Quintus et al. reported the relative similarity between laboratory compaction technique and field compaction (Table 1).

The study by Sousa et al. (*10*), performed under SHRP contract A-003A at the University of California at Berkeley, evaluated three compaction devices: Texas gyratory, kneading, and rolling wheel. The purpose of the study was to determine the extent to which method of laboratory compaction affects fundamental mixture properties (permanent deformation and fatigue) related to pavement

Texas Transportation Institute, TTI/CE Building, Texas A&M University, College Station, Tex. 77843–3135.

TABLE 1 Summary of Findings from NHCRP AAMAS Study (*9*)

Compaction Device	Percent of Cells with Properties, Closest to the Field Cores	Indifferent from the Field Cores
Texas Gyratory	45	63
Rolling Wheel Compactor*	25	49
Kneading Compactor	23	52
Arizona Vibratory/Kneading	7	41
Standard Marshall Hammer	7	35

*The rolling wheel compactor was the Mobil Steel Wheel Simulator

performance. Perhaps the most important findings of the study were the following:

1. Samples prepared with the Texas gyratory compactor are expected to be more sensitive to asphalt type (and perhaps to binder content) than samples prepared by the kneading compactor.
2. Samples prepared using the kneading compaction device are more resistant to permanent deformation, primarily because of the development of a more complete interparticle contact "structure," at least for densely graded aggregates; mixtures prepared under kneading compaction are more sensitive to aggregate angularity and surface texture.
3. Specimens prepared using the rolling wheel compactor were ranked between specimens prepared by kneading and gyratory methods in terms of their resistance to permanent deformation. However, they were stiffer under transient (dynamic) loading and more fatigue resistant than either gyratory or kneading specimens.

On the basis of these findings, Sousa et al. (*10*) stated that the compaction method had a profound impact on fundamental mixture properties and summarized their recommendations by stating that among the methods investigated, the rolling wheel appears to best duplicate field-compacted mixtures.

A criticism of this study is that it is not correlated to field results. Although Sousa et al. performed mixture property tests that have been shown to be related to field performance, the link between laboratory compacted and field compacted mixture properties is absent.

It should be noted that the Von Quintus et al. (*9*) and Sousa et al. (*10*) studies are consistent in that both concluded that the kneading compactor produced specimens with the greatest resistance to rutting, as compared with the rolling wheel compactor and the Texas gyratory compactor. Specimens produced by the Texas gyratory compactor were found to have properties most susceptible to rutting. It may be argued that, because the Texas gyratory compactor is the most sensitive to asphalt type and asphalt cement properties, it is an appropriate device for mixture analysis under the SHRP concept, which clearly identified the importance of the ability to discriminate among asphalts with various physical properties.

DESCRIPTION OF EXPERIMENTAL PROGRAM

Experiment Design

Five pavement sites were selected from the SHRP SPS-5 and SPS-6 field tests as a foundation for the analysis. Approximately thirty 102-mm (4-in.) diameter cores from each of these pavement sections provided the basis for the evaluation of the laboratory compaction devices. The experiment design is summarized in Table 2.

Aggregate and asphalt identical to that used in the production of these test sections were used to prepare the laboratory compacted specimens using the same mixture design (same proportions of same materials) as in the pavement. Laboratory-fabricated specimens from each compaction device were tested to characterize the material response of each mixture in tensile and compressive shear modes of loading. Test results were compared to corresponding results from field cores and statistically analyzed.

Average air-voids content of the cores among the different sites varied from about 3 to 8 percent; within a given site, they typically had a range of 2 to 5 percent. Laboratory samples for each mixture were compacted to simulate the range of field air voids. This was accomplished by varying the compactive effort. Compaction energy variation was achieved with the Texas gyratory compactor by varying the number of gyrations and the applied pressure. Controlling the compaction energy with the Exxon rolling wheel compactor was more difficult than originally believed; therefore, air-voids content of the resulting specimens was not ideal. Mean air-void contents for the initial set of Exxon compacted samples were too low. A second set of samples was prepared with the hope of achieving a higher air-void content. However, they also had lower air voids than desired.

More work than this study permitted is needed to do a satisfactory comparative evaluation of the Exxon rolling wheel compactor. Compaction energy applied by the Marshall device was varied by simply changing the number of blows of the drop hammer. The Elf compactor can essentially guarantee a particular average air-void content because it compresses a known weight of material into a predetermined volume.

TABLE 2 Compaction Experiment Design

Mixture Type	Compaction Method	Testing Program[1]	
		Test Type	No. Tests
Casa Grande, Az Flagstaff, Az Michigan DOT Alberta, Canada Manitoba, Canada	Field, Tex Gyratory,[2] Exxon Rolling Wheel	Indirect Tension, 25°C Resilient Modulus, 0° + 25°C Marshall Stability Hveem Stability Cyclic Creep, 40°C Direct Compression, 40°C	5 5 5 5 5 5
Casa Grande, Az Flagstaff, Az Michigan DOT Alberta, Canada Manitoba, Canada	Marshall Hammer[3]	Indirect Tension, 25°C Resilient Modulus, 0° + 25°C Marshall Stability	5 5 5
Casa Grande, Az Alberta, Canada	Elf Linear Kneading Compactor	Indirect Tension, 25°C Resilient Modulus, 0° + 25°C Marshall Stability Hveem Stability Cyclic Creep, 40°C Direct Compression, 40°C	5 5 5 5 5 5

[1] Test results from all laboratory compacted specimens were compared with results from field cores.

[2] The Texas gyratory compactor uses a tilt angle of three degrees, a contact pressure varying from 50 psi to a maximum of 150 psi, and a leveling load of 2500 psi.

[3] Marshall compacted samples were not tested for cyclic creep and direct compression, as only an abbreviated study was performed on Marshall Compaction.

Four commonly used laboratory tests and two specialized tests were used in comparing specimens from the different compaction devices. These tests included indirect tension at 25°C (77°F), resilient modulus at 0°C (32°F) and 25°C, Marshall stability, Hveem stability, and uniaxial repetitive compressive creep followed by compression to failure. These tests may not be ideal for evaluating the effect of compaction method on asphalt concrete, but they were selected because they can be performed on 100-mm (4-in.) core samples from thin pavement layers. The pavement layers sampled were seldom thicker than 64 mm (2.5 in.) and hence were usually not thick enough for tests such as unconfined compressive strength, repeated load triaxial resilient modulus, or compressive creep.

The uniaxial repetitive compressive creep test can be performed on samples that are 76 to 203 mm (3 to 8 in.) in height. A uniaxial compressive load of 2.76×10^5 Pascals (40 psi) was applied to the specimen for 60 sec at a temperature of 40°C (104°F), while the deformation in vertical and horizontal directions was measured. After the 60-sec load period, the sample was allowed to relax for 60 sec while creep recovery data was acquired. Each test consisted of eight such cycles followed by compressive load to failure. Indirect tension and resilient modulus tests were used to categorize the fracture and fatigue characteristics of the compacted mixtures.

Materials Tested

Pavement cores, aggregates, and asphalt cements from five pavement test sites were obtained and tested (Table 3).

Sample Preparation

Immediately before mixing the asphalt and aggregate, both were heated to the mixing temperature specified for the particular compaction method. Then the ingredients were mixed in accordance with the procedures specified for the particular compaction method. Compaction effort was varied to produce specimens with a range of air voids similar to that found in the different pavements.

Mixing and compaction temperatures for the gyratory compactor were 135°C (275°F) and 121°C (250°F), respectively, as required by the standard procedure. Mixing and compaction temperatures for the Marshall method were determined in accordance with ASTM D 1559 and were as follows: Casa Grande, 152°C and 143°C (306°F and 290°F); Flagstaff, 146°C and 138°C (295°F and 280°F); Alberta, 143°C and 132°C (290°F and 270°F); and Manitoba, 143°C and 132°C.

For the Exxon rolling wheel, the mixing process starts with the aggregate at 163°C (325°F) and ends with it at about 144°C (291°F). The Exxon compactor used the equivalent of 10 complete passes at increasing loads up to 714 kg (1,570 lb) on each tire of the dual pneumatic wheel roller. Compaction typically starts when the mix is at about 138°C (280°F) and ends with it at about 105°C (221°F). Approximately 100 kg (220 lb) of mix was used to prepare a single 180-mm (7-in.) thick slab from which 100-mm (4-in.) diameter cores were drilled.

For the Elf compactor, the Casa Grande material was mixed at 149°C (300°F) and compacted at 135°C (275°F), whereas the Alberta material was mixed at 135°C and compacted at 121°C

TABLE 3 Description of Materials Tested

Specimen Identification	Aggregate Type	Asphalt Grade	Content[1]	Admixture	Average Air Void Content of Cores[2] percent	Range of Air-Void Content of Cores[2], percent
Casa Grande	Gravel, Sand, Crushed Fines	AC-40	4.7	1% Cement	5.6	4.5-7.0
Flagstaff	Crushed Basalt w/ Sand + 1.5% Lime	AC-20	4.6	1.5% Lime	8.8	6.0-12.0
Alberta	Crushed Stone and Sand	150-200 Pen	5.1	None	3.9	2.6-5.6
Manitoba	Crushed Gravel w/ Sand	150-200 Pen High Viscosity	5.9	None	3.8	2.8-5.6
Michigan	Crushed Stone and manuf. sand	AC-10	5.1	None	3.0	1.8-5.5

[1] Asphalt content is given in percent by weight of total mix.

[2] Air void data is for pavement cores received.

(250°F). Approximately 17 kg (38 lb) of mix was used to prepare a 75-mm (3-in.) thick slab from which cores were drilled.

Field Cores

Cores drilled from the test pavements were shipped to Texas Transportation Institute. All cores were 102 mm (4 in.) in diameter. The layer of interest typically ranged from 25 mm (1 in.) to 152 mm (6 in.) in depth.

FINDINGS

Pavement cores were drilled within and between the wheel paths in an attempt to obtain samples with low and high air voids. Measurements showed that in many cases there were no significant differences in air voids of cores taken between the wheel paths and those from within the wheel paths. That is likely because these pavements were fairly new and had not been exposed to enough traffic to cause differences in densification.

The Exxon compactor experienced extreme difficulty in producing specimens with the desired air-void content. Because a limited supply of the paving materials was available, the large quantity of material required for repeated operations with the Exxon compactor precluded more than two attempts to obtain the desired level of air voids.

Statistical Analysis of Standard Tests

The statistical approach used in this portion of the study was to fit linear regression lines using ordinary least squares and comparing the slopes and intercepts of these lines for each laboratory compaction method to field compaction. This was done using a dummy variable regression model that allowed a separate intercept and slope term for each line for a given site. Hypotheses about the model parameters were tested, to compare each compaction method's terms to the field terms. When necessary, a line with a realistic slope was fitted through the Exxon data to complete the statistical analysis using the available data. Results of the statistical analyses are given in the following subsections. To understand the following statistical discussion, see Figures 1–6.

Resilient Modulus At 25°C (77°F)

For the Casa Grande mix (Figure 1), gyratory, Elf, and Marshall methods had resilient moduli equivalent to the field. The Exxon method, though decreasing with increasing air voids at the same rate as the field cores, yielded consistently lower modulus values at any given air-void content than did the other methods.

In summary, the Exxon method yielded lower levels of resilient moduli at 25°C (77°F) than the field cores at three of the four sites tested. The gyratory compacted samples were similar to pavement cores at four sites, Marshall compacted samples were similar to the field cores at two sites, and the Elf specimens were similar to the pavement cores at both of the sites tested.

Resilient Modulus At 0°C (32°F)

For the Flagstaff mixture (Figure 2), there was no difference between any of the laboratory compaction methods and the field cores.

Indirect Tension Tests

For the Flagstaff mixture (Figure 3), three of the four compaction methods (pavement cores, Marshall, and gyratory) showed a significant decrease in indirect tension (IDT) strength as percent air

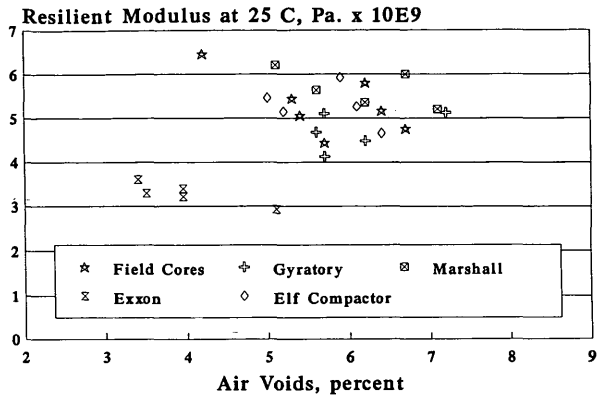

FIGURE 1 Resilient modulus at 25°C for mixture from Casa Grande, Arizona.

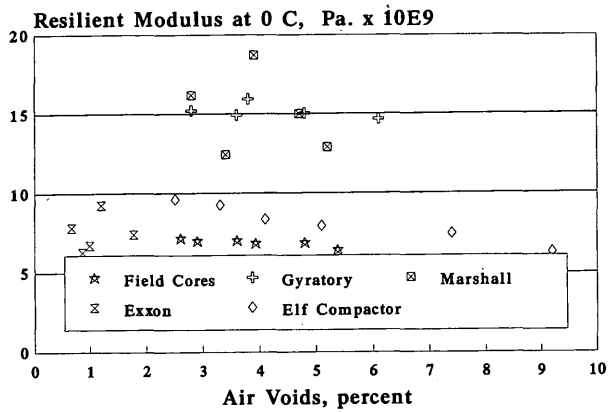

FIGURE 2 Resilient modulus at 0°C for mixture from Alberta, Canada.

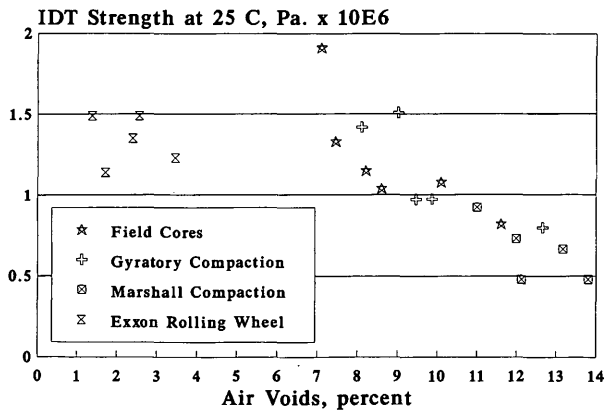

FIGURE 3 Indirect tensile strength at 25°C for mixture from Flagstaff, Arizona.

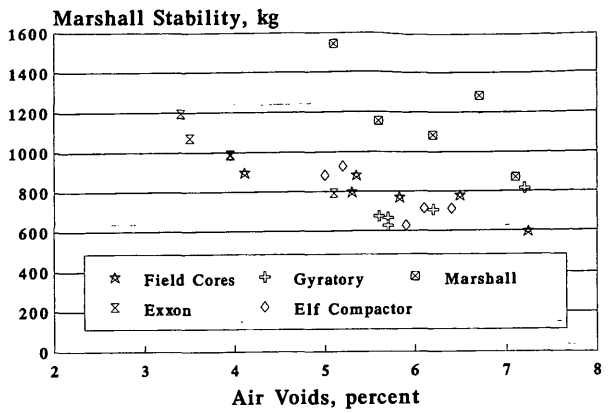

FIGURE 4 Marshall stability at 60°C for mixture from Casa Grande, Arizona.

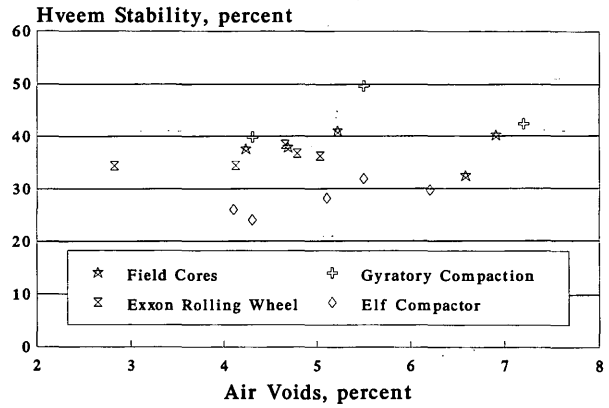

FIGURE 5 Hveem stability at 60°C for mixture from Casa Grande, Arizona.

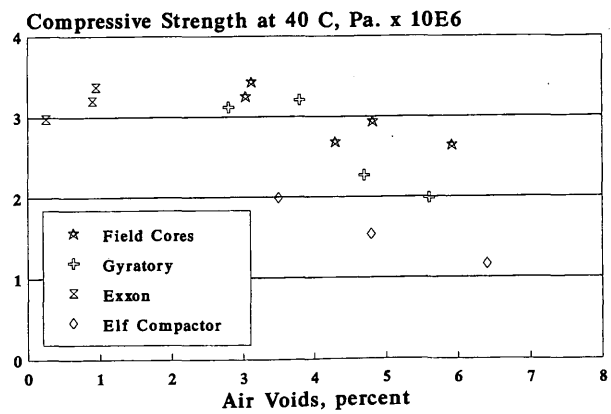

FIGURE 6 Compressive strength at 40°C for mixture from Alberta, Canada.

voids increased and the rate of decrease was equal for the three compaction methods. The Exxon method apparently yielded lower IDT strengths than did the other three methods. Both the Marshall and gyratory methods were equivalent to the field compaction.

In summary, only the Flagstaff site showed a statistically significant decrease in IDT strength as air voids increased and all three compaction methods were equal to the field. Exxon, Marshall, and gyratory methods were equivalent to field at two sites each, and Elf was equivalent to field at the two sites it was tested (Casa Grande and Alberta).

Marshall Stability

For both the Casa Grande (Figure 4) and Alberta sites, Marshall stability for all four laboratory compaction methods was statistically equivalent to the pavement cores. For the Casa Grande mix, there was no significant relationship between Marshall stability and air voids for any of the compaction methods, and the average stability was equal to the field for all four laboratory compaction methods and at all air-void levels. For Alberta mix, the Marshall stability decreased with increase in air voids and the rate of decrease was the same for all methods.

In summary, the Exxon and Marshall methods were equivalent to the field compaction at three sites, the Elf method was equivalent to the field at both the sites tested, and the gyratory method was equivalent to the field at four of five sties.

Marshall Flow

All compaction methods produced Marshall flows statistically equivalent to field compaction, except for the Michigan mix, for which Marshall compaction yielded higher values than the other compaction methods.

Hveem Stability

For the Casa Grande mixtures (Figure 5), none of the compaction methods showed a significant relationship between Hveem and level of air voids and all methods yielded statistically equivalent Hveem stabilities over all air-void levels. Both the Exxon and gyratory methods were equal to the field cores, and the Elf method yielded consistently lower Hveem stability values. (Note: Hveem stability was not measured on Marshall compacted specimens.)

In summary, as with IDT, only the Flagstaff mixture showed a significant decrease in Hveem stability with increasing air voids; this was shown only for the field and gyratory methods. Three of four sites concurred that the Exxon method yielded significantly lower Hveem stability. The gyratory method was equal to the field at four sites, and the Exxon method was equivalent to the field at only one site.

Statistical Analysis of Compressive Creep Tests

Data from the repetitive compressive creep tests were reduced to vertical stress as well as vertical and horizontal strains. Because some of the specimens failed before the end of the test, the first of eight repetitive load cycles was taken as the basis for comparison. Dilation ratio, defined as the ratio of horizontal radial strain to vertical strain, and the ultimate compressive strength were determined for each of the samples. The Marshall compactor was not used in this element of work. Compaction method was considered to be the main effect and air-void content was considered the covariate. The two properties, dilation ratio and compressive strength, were the dependent variables. A multifactor analysis of variance, at a confidence level of 95 percent, was performed on each mix separately.

For the Casa Grande mix, analysis of the data indicated that neither air-void content nor compaction method had a statistically significant effect on dilation ratio. Compressive strength was affected significantly both by air voids and by compaction method. With respect to the compressive strength, the Elf compaction was statistically different from the other three methods, which were not different from one another.

The Flagstaff data suggested that neither the air voids nor the compaction method had a significant effect on the dilation ratio. Compaction method had a significant effect on the compressive strength, whereas air voids had no significant effect. All three compaction methods were statistically different from one another.

The Alberta data indicated that air voids had a significant effect on the dilation ratio, whereas the effect of the compaction method was not significant. Compressive strength (Figure 6) was significantly affected both by air voids and compaction method, with the effect of air voids more profound. However, only the Elf compaction method was statistically different from the other three (field, Exxon, and gyratory) methods, which were not different from one another.

For the Manitoba mix, data was used only from field-cores and Exxon compacted specimens (gyratory compacted samples were tested but no meaningful data were obtained). Compaction method showed no significant effect on dilation ratio, whereas the air voids showed a statistically significant effect. Both air voids and compaction method had a significant effect on the compressive strength.

For the Michigan mix, only field cores and gyratory compacted specimens were tested. The dilation ratio was not significantly affected by either air voids or compaction method; although, compaction method had a statistically significant effect on the compressive strength and the air voids did not.

In summary, the statistical analyses showed that for all five test sites (Casa Grande, Flagstaff, Alberta, Manitoba, and Michigan) the compaction methods evaluated (field, Exxon rolling wheel, Texas gyratory, and Elf linear kneading compactor) were not statistically different from each other with respect to their effect on the dilation ratio. Similarly, compressive strength data indicated the compaction methods were not significantly different from each other except for the Flagstaff mix, and that Elf compacted samples exhibited lower compressive strengths than the other methods.

Overall Summary of Statistical Analysis

Results from the statistical analyses are summarized in Table 4. The results are tabulated according to the source of the paving mixture and method of compaction for each site. For each set of tests performed, the test values as a function of air voids (slope/intercept) for the laboratory compacted specimens were compared statistically to the corresponding test values as a function of air voids for the pavement cores. Results of the comparisons are described in Table 4 by the following statistically significant categories: equivalent to (E), less than (L), higher than (H), or different from (D) the field

TABLE 4 Consolidated Results from Statistical Analysis

Site/ Compaction Method	Resilient Modulus, 25°C	Resilient Modulus, 0°C	IDT Strength	Marshall Stability	Hveem Stability	Compressive Dilation Ratio	Creep Test Compressive Strength
Casa Grande							
Gyratory	E	H	H	E	E	E	E
Marshall	E	H	E	E	-	-	-
Exxon	L	E	E	E	E	E	E
Elf	E	H	E	E	L	E	L
Flagstaff							
Gyratory	D	E	E	D	E	E	H
Marshall	H	E	E	E	-	-	-
Exxon	L	E	L	E	L	E	D
Alberta							
Gyratory	E	H	D	E	E	E	E
Marshall	E	H	H	E	-	-	-
Exxon	E	E	E	E	L	E	E
Elf	E	E	E	E	L	E	L
Manitoba							
Gyratory	E	E	H	E	H	-	-
Marshall	H	E	H	H	-	-	-
Exxon	L	L	L	E	L	E	E
Michigan							
Gyratory	E	E	E	E	E	E	E
Marshall	H	E	H	H	-	-	-

E = Equivalent to
L = Less than
H = Higher than
D = Different from
} the Field Compaction

All four compaction methods were not used to prepare specimens from all five locations.

cores. To clarify the category "different", the following is given: certain values measured on the laboratory specimens had a different relationship (slope) with air voids, and thus some values were higher and some were lower than the corresponding values for the field cores.

The total number of Es determined for each laboratory compaction method from all the five locations was summed and compared with the maximum possible number of Es and was expressed as a percent. Gyratory compaction was equivalent to the field cores 24 times out of a possible 33 times (or 73 percent). Exxon rolling wheel compaction was equivalent to the field cores 18 times out of a possible 28 times (64 percent). Elf linear kneading compaction was equivalent to the field 9 times out of a possible 14 (64 percent). Rotating base Marshall compaction was similar to the field 10 times out of 20 (50 percent). A statistical test of significance (with $\alpha = 0.05$) of these percentages indicated that, although the gyratory compactor is equivalent to field compaction more often than the other methods, the differences between these percentages is not statistically significant.

Other interesting observations can be made from this comparison. The Exxon and Elf compacted specimens were either equal to or less than the field cores in all properties tested. The Marshall method yielded specimens that were higher than the field whenever they were not similar. The gyratory compacted specimens were equal to, higher than, or different from the field cores but never lower.

STUDY OF AIR VOID STRUCTURE

One specimen each representing selected mixtures and compaction methods was sent to the Road Directorate of the National Road Laboratory in Denmark, where they used special microscopy and imaging techniques to study the air-void structure (*1,11*). The objective of the investigation was to analyze and characterize air voids visible in a cut section of the compacted mixtures. The voids in an exposed plane section of a compacted sample were filled with epoxy containing fluorescent dye. Fluorescent image analysis of the

two-dimensional section was used to determine size, shape, and distribution of the air-void intersections as well as to estimate volume percent voids in the specimen.

The image analysis technique provides valuable information that improves the understanding of air-voids distribution in hot-mix asphalt compacted by different methods. Unfortunately, this was a very limited study, and no firm conclusions were made about the various compaction devices.

Generally, the pavement cores and the Exxon rolling wheel compactor exhibited better homogeneity of air-void distribution than the gyratory compactor. The Casa Grande mixture, which contained a relatively hard asphalt (AC-40), was essentially unaffected by compaction method.

CONCLUSIONS AND RECOMMENDATIONS

The research reported herein was designed primarily to compare specimens compacted using the Exxon rolling wheel compactor and the gyratory compactor with field cores. Additional limited work was performed to compare specimens prepared using the rotating base Marshall compactor and the Elf linear kneading compactor with field cores.

Conclusions

1. Analyses indicated that the gyratory method most often produced specimens similar to pavement cores (73 percent of the tests performed). Exxon and Elf compactors had the same probability of producing specimens similar to pavement cores (64 percent of the tests performed). The Marshall rotating base compactor had the least probability of producing specimens similar to pavement cores (50 percent of the tests performed). These differences are not statistically significant (at $\alpha = 0.05$).
2. When all the data, as reflected by the mixture properties measured, are considered collectively, the differences between field cores and the specimens produced by the four laboratory compaction methods compared in this study are relatively small. The types of tests selected to evaluate mixture properties were not ideal but were dictated by the small size of many of the field cores.
3. The Exxon rolling wheel compactor exhibited much more difficulty in controlling air voids in the finished specimens than the other compaction methods. The Exxon compactor requires about 100 kg (220 lb) of mix to prepare one set of specimens (one slab) at one air-void level, making it a very labor-intensive and material-intensive operation to prepare samples with various air-void contents. The comparatively low air-void level of the Exxon specimens renders conclusions about similarity or lack of similarity to the pavement specimens questionable.
4. For producing small samples of specific air-void contents, as in this study, the gyratory compactor was much more convenient, faster, and cheaper than the Exxon compactor. This is because much less material is required and no coring is necessary to produce laboratory specimens.
5. Elf compactor easily produces a 17 kg (38 lb) slab with a predictable air-void content. It is convenient and offers a great deal of versatility because the mold can be constructed to almost any plane geometric shape.
6. When compared with the Exxon rolling wheel compactor, the Texas gyratory compactor is more convenient for preparing laboratory specimens for routine mixture design testing of asphalt concrete.
7. On the basis of other studies, air-void distribution of gyratory compacted specimens may be less similar to pavement cores than rolling wheel compacted specimens; however, this difference did not adversely affect the mixture properties measured for this study.
8. Based solely on the findings of this comparative study, the Texas gyratory compactor was recommended to SHRP for use in preparing routine laboratory test specimens.

Recommendations

1. Additional research is needed to investigate in detail the size and distribution of air voids within hot-mix asphalt specimens compacted by different methods, as compared with field compaction, and to determine the resultant effect on fundamental engineering properties.
2. Testing in this study was limited to dense graded mixtures. Stone mastic or other nonconventional mixtures were not evaluated. Therefore, an evaluation of laboratory compactibility of nonconventional mixtures, including stone mastic and open-graded mixtures, is needed.

ACKNOWLEDGMENTS

This research was sponsored by the SHRP of the National Research Council.

Elf Asphalt of Terre Haute, Indiana, furnished all test specimens that were prepared using the Elf linear kneading compactor, without cost to the project, and also funded all testing associated with its compactor. The assistance and advice of Michael L. Hines was of significant value to this portion of the work.

Exxon Research and Engineering Company of Linden, New Jersey, furnished all specimens that were prepared using the Exxon rolling wheel compactor, without cost to the project. Nicholas C. Nahas coordinated the work at Exxon and was of particular aid to this study.

The generous contributions of these companies and individuals are acknowledged and appreciated.

REFERENCES

1. Button, J. W., D. N. Little, V. Jagadam, and O. J. Pendleton. Correlation of Selected Laboratory Compaction Methods with Field Compaction, Research Report 7157–1 for Strategic Highway Research Program. Texas Transportation Institute, Texas A&M University, College Station, Tex., May 1992.
2. Vallerga, B. A. Recent Laboratory Compaction Studies of Bituminous Paving Mixtures. *Proc., Association of Asphalt Paving Technologists,* Vol. 20, St. Paul, Minn., 1951, pp. 117–153.
3. Fields, F. Correlation of Laboratory Compaction with Field Compaction for Asphaltic Concrete Pavements. *Pro., Canadian Technical Asphalt Association,* Vol. 3, 1958.
4. Epps, J. A., B. M. Gallaway, W. J. Harper, W. W. Scott, Jr., and J. W. Sealy. Compaction of Asphalt Concrete Pavements. Research Report 90-2F, Texas Transportation Institute, Texas Highway Department, July, 1969.

5. Nunn, M. E. *Deformation Testing of Dense Coated Macadam: Effect of Method of Compaction.* Report No. TRRL 870, Transportation Roads and Research Laboratory, 1978.
6. Huschek, S. The Deformation Behavior of Asphaltic Concrete Under Triaxial Compression. *Proc., Association of Asphalt Paving Technologists,* Vol. 54, St. Paul, Minn., 1985.
7. Van Grevenynghe. Effect of Compaction Method on the Mechanical Properties of Asphalt-Aggregate Mixtures. *Proc., International Symposium, RILEM, France.* Laboratoires Central des Ponts et Chaussées, Paris, France, Sept. 1986.
8. Aunan, R. B., R. Luna, A. G. Altschaefel, and L. E. Wood. Reproduction of Thin Bituminous Surface Course Fabric by Laboratory Compaction Procedures. Presented at the Annual Meeting of the Transportation Research Board, Washington, D.C., 1988.
9. Von Quintus, H. L., J. A. Scherocman, C. W. Hughes, and T. W. Kennedy. *Development of Asphalt-Aggregate Mixture Analysis System: AAMAS, Phase II: Volume I, Preliminary Draft Final Report.* Brent Rauhut Engineering Inc., Austin, Tex., 1988.
10. Sousa, J. B., J. Harvey, L. Painter, J. A. Deacon, and C. L. Monismith. *Evaluation of Laboratory Procedure for Compacting Asphalt-Aggregate Mixtures.* TM-UCB-A-003A-90-S, Institute of Transportation Studies, University of California, Berkeley, Aug. 1990.
11. Eriksen, K. *Air Void Characteristics in Asphalt-Concrete Samples from the Compaction Study.* Contract SHRP-88-AIIR-13, National Road Laboratory, Denmark, for Strategic Highway Research Program, National Research Council, April 1992.

Publication of this paper sponsored by Committee on Characteristics of Bituminous Paving Mixtures To Meet Structural Requirements.